Treatise on Invertebrate Paleontology

Part B

Prokaryota

Bacteria and Archaea

by Anthony Bouton, Brendan P. Burns, Flavia Callefo, Hugo Beraldi-Campesi, Noelia Carmona, Diana G. Cuadrado, Erika J. Espinosa-Ortiz, Kimberley L. Gallagher, Robin Gerlach, Adriana Heimann, Keyron Hickman-Lewis, Martin Homann, Ria Mitchell, Nora Noffke, R. S. Shapiro, Nathan Sheldon, Qing Tang, Christophe Thomazo, Emmanuelle Vennin, Pieter T. Visscher, Francis Westall, D. T. Wilmeth, Richard A. White III, and Shuhai Xiao

Nora Noffke
Coordinating Author

Prepared under Sponsorship of

The Paleontological Society
The Palaeontographical Society
SEPM (*Society for Sedimentary Geology*)
The Palaeontological Association

Raymond C. Moore
Founder

William I. Ausich and Paul A. Selden
Editors

Elizabeth Black, Michael Cormack, Denise Mayse
Assistant Editor and Editorial Staff

The University of Kansas
Paleontological Institute
Lawrence, Kansas
2023

Library of Congress Catalogue Card Number 53-12913
ISBN 978-0-99003621-4-2

Distributed by the Paleontological Institute, The University of Kansas, 1475 Jayhawk Blvd., Room 119, Lawrence, Kansas 66045-7594, USA, www.paleo.ku.edu, from which current price lists of parts in print may be obtained and to which all orders and related correspondence should be directed. Editorial office of the *Treatise:* Paleontological Institute, The University of Kansas, 1475 Jayhawk Blvd., Room 119, Lawrence, Kansas 66045-7594, USA, www.paleo.ku.edu.

Citation information: Paul William I. Ausich and Paul A. Selden, eds. 2023. Treatise on Invertebrate Paleontology. Part B, Prokaryotes (Bacteria and Archaea). The University of Kansas Paleontological Institute. Lawrence, Kansas. xxvi + 178 p., 48 fig., 3 tables.

The *Treatise on Invertebrate Paleontology* has been made possible by (1) funding principally from the National Science Foundation of the United States in its early stages, from The Geological Society of America through the bequest of Richard Alexander Fullerton Penrose, Jr., and from The Kansas University Endowment Association through the bequest of Raymond C. and Lillian B. Moore; (2) contribution of the knowledge and labor of specialists throughout the world, working in cooperation under sponsorship of the Paleontological Society, the SEPM (Society for Sedimentary Geology), the Palaeontographical Society, and the Palaeontological Association; (3) acceptance by The University of Kansas of publication without any financial gain to the University; and (4) generous contributions by our individual and corporate sponsors.

PART B
PROKARYOTA
Bacteria and Archaea

Nora Noffke, Coordinating Author

CONTENTS

INFORMATION ON TREATISE VOLUMES

The *Treatise on Invertebrate Paleontology* is published by the University of Kansas Paleontological Institute, www.paleo.ku.edu. The *Treatise* is organized in lettered Parts (A–W) to indicate their systematic sequence but also allowing publication of units in whatever order each is finalized. It is published in three formats. Individual chapters are published when completed in the *Treatise Online* series. When a volume is complete, it is published both as a book and as an online volume in the *Digital Treatise* series. In addition, *Paleontological Institute Special Publications* series are published periodically. The web address above provides information for ordering *Treatise* publications. Please encourage academic libraries to subscribe to all Paleontological Institute publications.

PUBLISHED VOLUMES

Part A. Introduction: Fossilization (Taphonomy), Biogeography, and Biostratigraphy, xxiii + 569 p., 169 fig., 1979.

Part B. Protoctista 1 (Charophyta), xvi + 170 p., 79 fig., 9 tables, 2005.

Part C. Protista 2 (Sarcodina, Chiefly "Thecamoebians" and Foraminiferida), Volumes 1 and 2, xxxi + 900 p., 653 fig., 1964.

Part D. Protista 3 (Protozoa: Chiefly Radiolaria, Tintinnina), xii + 195 p., 92 fig., 1954.

Part E. Archaeocyatha and Porifera, xviii + 122 p., 89 fig., 1955.

Part E, Revised. Archaeocyatha, Volume 1, xxx + 158 p., 107 fig., 1972.

Part E, Revised. Porifera, Volume 2 (Introduction to the Porifera), xxvii + 349 p., 135 fig., 10 tables, 2003.

Part E, Revised. Porifera, Volume 3 (Demospongea, Hexactinellida, Heteractinida, Calcarea), xxxi + 872 p., 506 fig., 1 table, 2004.

Part E, Revised. Porifera, Volumes 4 and 5 (Hypercalcified Porifera), liii + 1223 p., 665 fig., 42 tables, 2015.

Part E, Revised. Porifera, Volume 5 (Demospongea, Hexactinellida, Heteractinida, Calcarea), xxxi + 872 p., 506 fig., 1 table, 2004.

Part F. Coelenterata, xx + 498 p., 358 fig., 1956.

Part F. Coelenterata, Supplement 1 (Rugosa and Tabulata), Volumes 1 and 2, xl + 762 p., 462 fig., 1981.

Part G. Bryozoa, xiii + 253 p., 175 fig., 1953.

Part G, Revised. Bryozoa, Volume 1 (Introduction, Order Cystoporata, Order Cryptostomata), xxvi + 625 p., 295 fig., 1983.

Part H. Brachiopoda, Volumes 1 and 2, xxxii + 927 p., 746 fig., 1965.

Part H, Revised. Brachiopoda, Volume 1 (Introduction), xx + 539 p., 417 fig., 40 tables, 1997.

Part H, Revised. Brachiopoda, Volumes 2 and 3 (Linguliformea, Craniiformea, Rhynchonelliformea [part]), xxx + 919 p., 616 fig., 17 tables, 2000.

Part H, Revised. Brachiopoda, Volume 4 (Rhynchonelliformea [part]), xxxix + 768 p., 484 fig., 3 tables, 2002.

Part H, Revised. Brachiopoda, Volume 5 (Rhynchonelliformea [part]), xlvi + 631 p., 398 fig., 2006.

Part H, Revised. Brachiopoda, Volume 6 (Supplement), l + 906 p., 461 fig., 38 tables, CD of compiled references from volumes 1–6, 2007.

Part I. Mollusca 1 (Mollusca General Features, Scaphopoda, Amphineura, Monoplacophora, Gastropoda General Features, Archaeogastropoda, Mainly Paleozoic Caenogastropoda and Opisthobranchia), xxiii + 351 p., 216 fig., 1960.
Part K. Mollusca 3 (Cephalopoda General Features, Endoceratoidea, Actinoceratoidea, Nautiloidea, Bactritoidea), xxviii + 519 p., 361 fig., 1964.
Part L. Mollusca 4 (Cephalopoda: Ammonoidea), xxii + 490 p., 558 fig., 1957.
Part L, Revised. Mollusca 4, Volume 2 (Carboniferous and Permian Ammonoidea), xxix + 258 p., 139 fig., 1 table, 2009.
Part L, Revised. Mollusca 4, Volume 4 (Cretaceous Ammonoidea), xx + 362 p., 216 fig., 1996.
Part N. Mollusca 6 (Bivalvia), Volumes 1 and 2 (of 3), xxxvii + 952 p., 613 fig., 1969; Volume 3, iv + 272 p., 153 fig., 1971.
Part O. Arthropoda 1 (Arthropoda General Features, Protarthropoda, Euarthropoda General Features, Trilobitomorpha), xix + 560 p., 415 fig., 1959.
Part O, Revised. Arthropoda 1 (Trilobita: Introduction, Order Agnostida, Order Redlichiida), xxiv + 530 p., 309 fig., 1997.
Part P. Arthropoda 2 (Chelicerata, Pycnogonida, Palaeoisopus), xvii + 181 p., 123 fig., 1955 [1956].
Part Q. Arthropoda 3 (Crustacea, Ostracoda), xxiii + 442 p., 334 fig., 1961.
Part R. Arthropoda 4, Volumes 1 and 2 (Crustacea Exclusive of Ostracoda, Myriapoda, Hexapoda), xxxvi + 651 p., 397 fig., 1969.
Part R. Arthropoda 4, Volumes 3 and 4 (Hexapoda), xxii + 655 p., 265 fig., 1992.
Part S. Echinodermata 1 (Echinodermata General Features, Homalozoa, Crinozoa, exclusive of Crinoidea), Volumes 1 and 2, xxx + 650 p., 400 fig., 1967 [1968].
Part T. Echinodermata 2 (Crinoidea), Volumes 1–3, xxxviii + 1,027 p., 619 fig., 1978.
Part T. Revised. Echinodermata 2 (Crinoidea), Volume 3, xxix + 261 p., 112 fig., 2011.
Part U. Echinodermata 3 (Asterozoans, Echinozoans), xxx + 695 p., 534 fig., 1966.
Part V. Graptolithina, xvii + 101 p., 72 fig., 1955.
Part V, Revised. Graptolithina, xxxii + 163 p., 109 fig., 1970.
Part V, Second Revision. Hemichordata (incl. Graptolithina), xxx + 548 p., 310 fig., 2023.
Part W. Miscellanea (Conodonts, Conoidal Shells of Uncertain Affinities, Worms, Trace Fossils, Problematica), xxv + 259 p., 153 fig., 1962.
Part W, Revised. Miscellanea, Supplement 1 (Trace Fossils and Problematica), xxi + 269 p., 110 fig., 1975.
Part W, Revised. Miscellanea, Supplement 2 (Conodonta), xxviii + 202 p., frontis., 122 fig., 1981.

THIS VOLUME

Part B. Prokaryota (Bacteria and Archaea), xxvi + 178 p., 48 fig., 3 tables, 2023.

VOLUMES IN PREPARATION

Part B. Protista 1 (Chrysomonadida, Coccolithophorida, Diatomacea).
Part E, Revised. Porifera (additional volumes).
Part F, Revised. Cnidaria (Scleractinia).
Part G, Revised. Bryozoa (additional volumes).
Part K, Revised. Mollusca 3 (Nautiloidea).
Part L, Revised. Mollusca 4 (Ammonoidea) (additional volumes).

Part M. Mollusca 5 (Coleoidea).
Part N. Revised. Mollusca 6 (Bivalvia), Volume 1
Part O, Revised. Arthropoda 1 (Trilobita) (additional volumes).
Part P, Revised. Arthropoda 2 (Chelicerata).
Part Q, Revised. Arthropoda 3 (Ostracoda).
Part R, Revised. Arthropoda 4 (Crustacea Exclusive of Ostracoda).
Part T, Revised. Echinodermata 2 (Crinoidea) (additional volumes).

ORIGINAL PUBLICATION IN *TREATISE ONLINE*

All content in this volume was originally published online. Below are the relevant *Treatise Online* chapters with their original titles in the order reflected in this volume (not in date order). Color illustrations can be found in these online versions. Authors wishing to cite the online published material, may follow the suggested citations below.

Biofilms:
Espinosa-Ortiz, Erika J. and Robin Gerlach. 2021. Part B, Chapter 2: Biofilms. Treatise Online 147: 1–12, 3 fig.

Microbial Mats:
Visscher, Pieter T., Kimberley L. Gallagher, Anthony Bouton, Emmanuelle Vennin, Christophe Thomazo, Richard A. White III, Brendan P. Burns. 2022. Part B,-Chapter 3: Microbial mats. Treatise Online 163:1–32, 5 fig.

Microfossils of Prokaryotes:
Xiao, Shuhai, & Qing Tang. 2021. Part B, Chapter 7: Microfossils of Prokaryotes (Bacteria and Archaea): Research History, Taphonomy, and Paleobiology. Treatise Online 160:1–37, 9 fig., 1 table.

Microbialites:
Shapiro, R. S. & D. T. Wilmeth. 2020. Part B, Chapter 8: Microbialites. Treatise Online 134:1–24, 10 fig.

Microbially induced sedimentary structures (MISS):
Noffke, Nora, Hugo Beraldi-Campesi, Flavia Callefo, Noelia Carmona, Diana G. Cuadrado, Keyron Hickman-Lewis, Martin Homann, Ria Mitchell, Nathan Sheldon, Frances Westall, & Shuhai Xiao. 2022. Part B, Chapter 5: Microbially induced sedimentary structures (MISS). Treatise Online 162: 1–29, 17 fig.

Banded iron formations:
Heimann, Adriana. 2021. Part B, Chapter 6: Banded iron formations. Treatise Online 158:1–48, 4 fig., 2 tables.

EDITORIAL PREFACE

William I. Ausich

From the outset, the aim of the *Treatise on Invertebrate Paleontology* has been to present a comprehensive and authoritative, yet compact, statement of knowledge concerning groups of invertebrate fossils. Typically, preparation of early *Treatise* volumes was undertaken by a small group with a synoptic view of the taxa being monographed. Two, or perhaps three, specialists worked together, sometimes co-opting others for coverage of highly specialized taxa. Recently, however, both new *Treatise* volumes and revisions of existing ones have been undertaken increasingly by teams of specialists led by a coordinating author. This volume, Part B, Prokaryotes has been nurtured and guided by Coordinating Author Nora Noffke. The planning began during the editorship of Paul Selden. Most of the text was submitted after I took up the mantle as interim editor. Editorial matters specific to this volume are discussed near the end of this editorial preface.

Because of the nature of its subject matter, this volume does not include the usual *Treatise* systematic information, as is explained in the Coordinating Author's Introduction (p. xxii–xxiii). Nevertheless, it is important to discuss systematic requirements herein for those preparing other *Treatise* volumes.

ZOOLOGICAL NAMES

Questions about the proper use of zoological names arise continually, especially questions regarding both the acceptability of names and alterations of names that are allowed or even required. Regulations prepared by the International Commission on Zoological Nomenclature (ICZN) and published in the *International Code of Zoological Nomenclature* (4th edition, 1999), hereinafter referred to as the *Code,* provide procedures for answering such questions. The prime objective of the *Code* is to promote stability and universality in the use of the scientific names of animals, ensuring also that each generic name is distinct and unique, while avoiding unwarranted restrictions on freedom of thought and action of systematists. Priority of names is a basic principle of the *Code;* but, under specified conditions and by following prescribed procedures, priority may be set aside by the Commission. These procedures apply especially where slavish adherence to the principle of priority would hamper or even disrupt zoological nomenclature and the information it conveys.

The Code is updated periodically and is now available online [www.iczn.org/the-code/the-international-code-of-zoological-nomenclature/the-code-online]. A significant recent change to nomenclatoral practice is that new nomenclatoral acts must be registered on Zoobank [zoobank.org] for recognition by the ICZN. Zoobank is the offical register of the ICZN and includes registry of nomenclatoral acts of genera and species, authors, publications, and type specimens.

Among other requirements, the revised *Code* is clear that the type genus of family-level taxa must be specified. In this volume we have continued the practice that has characterized most previous volumes of the *Treatise*, namely that the type genus of all family-level taxa is the first listed and diagnosed. In spite of the revisions, the nomenclatorial tasks that confront zoological taxonomists are formidable and have often justified the complaint that the study of zoology and paleontology is too often merely the study of names rather than the study of animals. It is incumbent on all systematists, therefore, at the outset of their work to pay careful attention to the *Code* to enhance stability by minimizing the number of subsequent

changes of names, too many of which are necessitated by insufficient attention to detail. To that end, several pages here are devoted to aspects of zoological nomenclature that are judged to have chief importance in relation to procedures adopted in the *Treatise*. Terminology is explained, and examples are given of the style employed in the nomenclatorial parts of the systematic descriptions.

GROUPS OF TAXONOMIC CATEGORIES

Each taxon belongs to a category in the Linnaean hierarchical classification. The *Code* recognizes three groups of categories, a species-group, a genus-group, and a family-group. Taxa of lower rank than subspecies are excluded from the rules of zoological nomenclature, and those of higher rank than superfamily are also not regulated by the *Code.* It is both natural and convenient to discuss nomenclatorial matters in general terms first and then to consider each of these three, recognized groups separately. Especially important is the provision that within each group the categories are coordinate, that is, equal in rank, whereas categories of different groups are not coordinate.

FORMS OF NAMES

All zoological names can be considered on the basis of their spelling. The first form of a name to be published is defined as the original spelling (*Code,* Article 32), and any form of the same name that is published later and is different from the original spelling is designated a subsequent spelling (*Code,* Article 33). Not every original or subsequent spelling is correct.

ORIGINAL SPELLINGS

If the first form of a name to be published is consistent and unambiguous, the original is defined as correct unless it contravenes some stipulation of the *Code* (Articles 11, 27 to 31, and 34) or unless the original publication contains clear evidence of an inadvertent error in the sense of the *Code,* or, among names belonging to the family-group, unless correction of the termination or the stem of the type genus is required. An original spelling that fails to meet these requirements is defined as incorrect.

If a name is spelled in more than one way in the original publication, the form adopted by the first reviser is accepted as the correct original spelling, provided that it complies with mandatory stipulations of the *Code* (Articles 11 and 24 to 34).

Incorrect original spellings are any that fail to satisfy requirements of the *Code,* represent an inadvertent error, or are one of multiple original spellings not adopted by a first reviser. These have no separate status in zoological nomenclature and, therefore, cannot enter into homonymy or be used as replacement names. They call for correction. For example, a name originally published with a diacritical mark, apostrophe, dieresis, or hyphen requires correction by deleting such features and uniting parts of the name originally separated by them, except that deletion of an umlaut from a vowel in a name derived from a German word or personal name unfortunately requires the insertion of *e* after the vowel. Where original spelling is judged to be incorrect solely because of inadequacies of the Greek or Latin scholarship of the author, nomenclatorial changes conflict with the primary purpose of zoological nomenclature as an information retrieval system. One looks forward with hope to further revisions of the *Code* wherein rules are emplaced that enhance stability rather than classical scholarship, thereby facilitating access to information.

SUBSEQUENT SPELLINGS

If a subsequent spelling differs from an original spelling in any way, even by the omission, addition, or alteration of a single letter, the subsequent spelling must be defined as a different name. Exceptions include such changes as an altered termination of adjectival specific names to agree in gender with associated generic names (an unfortunate impediment to stability and retrieval

of information); changes of family-group names to denote assigned taxonomic rank; and corrections that eliminate originally used diacritical marks, hyphens, and the like. Such changes are not regarded as spelling changes conceived to produce a different name. In some instances, however, species-group names having variable spellings are regarded as homonyms as specified in the *Code* (Article 58).

Altered subsequent spellings other than the exceptions noted may be either intentional or unintentional. If "demonstrably intentional" (*Code,* Article 33), the change is designated as an emendation. Emendations may be either justifiable or unjustifiable. Justifiable emendations are corrections of incorrect original spellings, and these take the authorship and date of the original spellings. Unjustifiable emendations are names having their own status in nomenclature, with author and date of their publication. They are junior, objective synonyms of the name in its original form.

Subsequent spellings, if unintentional, are defined as incorrect subsequent spellings. They have no status in nomenclature, do not enter into homonymy, and cannot be used as replacement names.

AVAILABLE AND UNAVAILABLE NAMES

Editorial prefaces of some previous volumes of the *Treatise* have discussed in appreciable detail the availability of the many kinds of zoological names that have been proposed under a variety of circumstances. Much of that information, while important, does not pertain to the present volume, in which authors have used fewer terms for such names. The reader is referred to the *Code* (Articles 10 to 20) for further details on availability of names. Here, suffice it to say that an available zoological name is any that conforms to all mandatory provisions of the *Code.* All zoological names that fail to comply with mandatory provisions of the *Code* are unavailable and have no status in zoological nomenclature. Both available and unavailable names may be classified into groups that have been recognized in previous volumes of the *Treatise,* although not explicitly differentiated in the *Code.* Among names that are available, these groups include inviolate names, perfect names, imperfect names, vain names, transferred names, improved or corrected names, substitute names, and conserved names. Kinds of unavailable names include naked names (see *nomina nuda* below), denied names, impermissible names, null names, and forgotten names.

Nomina nuda include all names that fail to satisfy provisions stipulated in Article 11 of the *Code,* which states general requirements of availability. In addition, they include names published before 1931 that were unaccompanied by a description, definition, or indication (*Code,* Article 12) and names published after 1930 that (1) lacked an accompanying statement of characters that differentiate the taxon, (2) were without a definite bibliographic reference to such a statement, (3) were not proposed expressly as a replacement (*nomen novum*) of a preexisting available name (*Code,* Article 13.1), or (4) for genus-group names, were unaccompanied by definite fixation of a type species by original designation or indication (*Code,* Article 13.2). *Nomina nuda* have no status in nomenclature, and they are not correctable to establish original authorship and date.

VALID AND INVALID NAMES

Important considerations distinguish valid from available names on the one hand and invalid from unavailable names on the other. Whereas determination of availability is based entirely on objective considerations guided by articles of the *Code,* conclusions as to validity of zoological names may be partly subjective. A valid name is the correct one for a given taxon, which may have two or more available names but only a single correct, hence valid, name, which is also generally the oldest name that it has been given. Obviously, no valid name can also be

an unavailable name, but invalid names may be either available or unavailable. It follows that any name for a given taxon other than the valid name, whether available or unavailable, is an invalid name.

One encounters a sort of nomenclatorial no-man's land in considering the status of such zoological names as *nomina dubia* (doubtful names), which may include both available and unavailable names. The unavailable ones can well be ignored, but names considered to be available contribute to uncertainty and instability in the systematic literature. These can ordinarily be removed only by appeal to the ICZN for special action. Because few systematists care to seek such remedy, such invalid but available names persist in the literature.

NAME CHANGES IN RELATION TO GROUPS OF TAXONOMIC CATEGORIES

SPECIES-GROUP NAMES

Detailed consideration of valid emendation of specific and subspecific names is unnecessary here, both because the topic is well understood and relatively inconsequential and because the *Treatise* deals with genus-group names and higher categories. When the form of adjectival specific names is changed to agree with the gender of a generic name in transferring a species from one genus to another, one need never label the changed name as *nomen correctum.* Similarly, transliteration of a letter accompanied by a diacritical mark in the manner now called for by the *Code,* as in changing originally *bröggeri* to *broeggeri,* or eliminating a hyphen, as in changing originally published *cornu-oryx* to *cornuoryx,* does not require the designation *nomen correctum.* Of course, in this age of computers and electronic databases, such changes of name, which are perfectly valid for the purposes of scholarship, run counter to the requirements of nomenclatorial stability on which the preparation of massive, electronic databases is predicated.

GENUS-GROUP NAMES

Conditions warranting change of the originally published, valid form of generic and subgeneric names are sufficiently rare that lengthy discussion is unnecessary. Only elimination of diacritical marks and hyphens in some names in this category and replacement of homonyms seem to furnish basis for valid emendation. Many names that formerly were regarded as homonyms are no longer so regarded, because two names that differ only by a single letter or in original publication by the presence of a diacritical mark in one are now construed to be entirely distinct (but see *Code,* Article 58).

As has been pointed out above, difficulty typically arises when one tries to decide whether a change of spelling of a name by a subsequent author was intentional or unintentional, and the decision has to be made often arbitrarily.

FAMILY-GROUP NAMES

Family-Group Names: Authorship and Date

All family-group taxa having names based on the same type genus are attributed to the author who first published the name of any of these groups, whether tribe, subfamily, or family (superfamily being almost inevitably a later-conceived taxon). Accordingly, if a family is divided into subfamilies or a subfamily into tribes, the name of no such subfamily or tribe can antedate the family name. Moreover, every family containing differentiated subfamilies must have a nominate subfamily (*sensu stricto*), which is based on the same type genus as the family. Finally, the author and date set down for the nominate subfamily invariably are identical with those of the family, irrespective of whether the author of the family or some subsequent author introduced subdivisions.

Corrections in the form of family-group names do not affect authorship and date of the taxon concerned, but in the *Treatise,* recording the authorship and date of the correction is desirable, because it provides

a pathway to follow the thinking of the systematists involved.

Family-Group Names: Use of *nomen translatum*

The *Code* (Article 29.2) specifies the suffixes for tribe (-ini), subfamily (-inae), family (-idae) and superfamily (-oidea), the formerly widely used ending (-acea) for superfamily having been disallowed. All these family-group categories are defined as coordinate (*Code*, Article 36.1): "A name established for a taxon at any rank in the family group is deemed to have been simultaneously established for nominal taxa at other ranks in the family group; all these taxa have the same type genus, and their names are formed from the stem of the name of the type genus (Art. 29.3] with appropriate change of suffix [Art. 34.1]. The name has the same authorship and date at every rank." Such changes of rank and concomitant changes of endings as elevation of a subfamily to family rank or of a family to superfamily rank, if introduced subsequent to designation of the original taxon or based on the same nominotypical genus, are *nomina translata*. In the *Treatise,* it is desirable to distinguish the valid alteration in the changed ending of each transferred family-group name by the term *nomen translatum,* abbreviated to *nom. transl.* Similarly for clarity, authors should record the author, date, and page of the alteration, as in the following example.

Family HEXAGENITIDAE Lameere, 1917

[*nom. transl.* Demoulin, 1954, p. 566, *ex* Hexagenitinae Lameere, 1917,p. 74]

This is especially important for superfamilies, for the information of interest is the author who initially introduced a taxon rather than the author of the superfamily as defined by the *Code.* For example:

Superfamily AGNOSTOIDEA M'Coy, 1849

[*nom. transl.* Shergold, Laurie, & Sun, 1990, p. 32, *ex* Agnostinae M'Coy, 1849, p. 402]

The latter is merely the individual who first defined some lower-ranked, family-group taxon that contains the nominotypical genus of the superfamily. On the other hand, the publication that introduces the superfamily by *nomen translatum* is likely to furnish the information on taxonomic considerations that support definition of the taxon.

Family-Group Names: Use of *nomen correctum*

Valid name changes classed as *nomina correcta* do not depend on transfer from one category of the family group to another but most commonly involve correction of the stem of the nominotypical genus. In addition, they include somewhat arbitrarily chosen modifications of endings for names of tribes or superfamilies. Examples of the use of *nomen correctum* are the following.

Family STREPTELASMATIDAE Nicholson, 1889

[*nom. correct.* Wedekind, 1927, p. 7, *pro* Streptelasmidae Nicholson inNicholson & Lydekker, 1889, p. 297]

Family PALAEOSCORPIDAE Lehmann, 1944

[*nom. correct.* Petrunkevitch, 1955, p. 73, *pro* Palaeoscorpionidae Lehmann, 1944, p. 177]

Family-Group Names: Replacements

Family-group names are formed by adding combinations of letters, which are prescribed for all family-group categories, to the stem of the name belonging to the nominotypical genus first chosen as type of the assemblage. The type genus need not be the first genus in the family to have been named and defined, but among all those included it must be the first published as name giver to a family-group taxon. Once fixed, the family-group name remains tied to the nominotypical genus even if the generic name is changed by reason of status as a junior homonym or junior synonym, either objective or subjective. Seemingly, the *Code* requires replacement of a family-group name only if the

nominotypical genus is found to have been a junior homonym when it was proposed (*Code,* Article 39), in which case ". . . it must be replaced either by the next oldest available name from among its synonyms [Art. 23.3.5], including the names of its subordinate family-group taxa, or, if there is no such synonym, by a new name based on the valid name . . . of the former type genus." Authorship and date attributed to the replacement family-group name are determined by first publication of the changed family-group name. Recommendation 40A of the *Code,* however, specifies that for subsequent application of the rule of priority, the family-group name ". . . should be cited with its original author and date (see Recommendation 22A.2.2), followed by the date of its priority as determined by this Article; the date of priority should be enclosed in parentheses." Many family-group names that have been in use for a long time are *nomina nuda,* because they fail to satisfy criteria of availability (*Code,* Article 11.7). These demand replacement by valid names.

The aim of family-group nomenclature is to yield the greatest possible stability and uniformity, just as in other zoological names. Both taxonomic experience and the *Code* (Article 40) indicate the wisdom of sustaining family-group names based on junior subjective synonyms if they have priority of publication, for opinions of the same worker may change from time to time. The retention of first-published, family-group names that are found to be based on junior objective synonyms, however, is less clearly desirable, especially if a replacement name derived from the senior objective synonym has been recognized very long and widely. Moreover, to displace a widely used, family-group name based on the senior objective synonym by disinterring a forgotten and virtually unused family-group name based on a junior objective synonym because the latter happens to have priority of publication is unsettling.

A family-group name may need to be replaced if the nominotypical genus is transferred to another family group. If so, the first-published of the generic names remaining in the family-group taxon is to be recognized in forming a replacement name.

SUPRAFAMILIAL TAXA: TAXA ABOVE FAMILY-GROUP

International rules of zoological nomenclature as given in the *Code* affect only lower-rank categories: subspecies to superfamily. Suprafamilial categories (suborder to kingdom) are either not mentioned or explicitly placed outside of the application of zoological rules. The *Copenhagen Decisions on Zoological Nomenclature* (1953, Articles 59 to 69) proposed adopting rules for naming suborders and higher taxa up to and including phylum, with provision for designating a type genus for each, in such manner as not to interfere with the taxonomic freedom of workers. Procedures were outlined for applying the rule of priority and rule of homonymy to suprafamilial taxa and for dealing with the names of such taxa and their authorship, with assigned dates, if they should be transferred on taxonomic grounds from one rank to another. The adoption of terminations of names, different for each category but uniform within each, was recommended.

The Colloquium on Zoological Nomenclature, which met in London during the week just before the 15th International Congress of Zoology convened in 1958, thoroughly discussed the proposals for regulating suprafamilial nomenclature, as well as many others advocated for inclusion in the new *Code* or recommended for exclusion from it. A decision that was supported by a wide majority of the participants in the colloquium was against the establishment of rules for naming taxa above family-group rank, mainly because it was judged that such regulation would unwisely tie the hands of taxonomists. For example, a class or order defined by an author at a given date, using chosen morphologic characters (*e.g.,* gills of bivalves), should not be allowed to freeze nomenclature, taking precedence over

another class or order that is proposed later and distinguished by different characters (*e.g.,* hinge teeth of bivalves). Even the fixing of type genera for suprafamilial taxa would have little, if any, value, hindering taxonomic work rather than aiding it. Beyond mere tidying up, no basis for establishing such types and for naming these taxa has yet been provided.

The considerations just stated do not prevent the editors of the *Treatise* from making rules for dealing with suprafamilial groups of animals described and illustrated in this publication. Some uniformity is needed, especially for the guidance of *Treatise* authors. This policy should accord with recognized general practice among zoologists; but where general practice is indeterminate or nonexistent, our own procedure in suprafamilial nomenclature needs to be specified as clearly as possible. This pertains especially to decisions about names themselves, about citation of authors and dates, and about treatment of suprafamilial taxa that, on taxonomic grounds, are changed from their originally assigned rank. Accordingly, a few rules expressing *Treatise* policy are given here, some with examples of their application.

1. The name of any suprafamilial taxon must be a Latin or Latinized, uninominal noun of plural form or treated as such, with a capital initial letter and without diacritical mark, apostrophe, diaeresis, or hyphen. If a component consists of a numeral, numerical adjective, or adverb, this must be written in full.

2. Names of suprafamilial taxa may be constructed in almost any manner. A name may indicate morphological attributes (*e.g.,* Lamellibranchiata, Cyclostomata, Toxoglossa) or be based on the stem of an included genus (*e.g.,* Bellerophontina, Nautilida, Fungiina) or on arbitrary combinations of letters (*e.g.,* Yuania); none of these, however, can end in -oidea,-idae or -inae, which terminations are reserved for family-group taxa. No suprafamilial name identical in form to that of a genus or to another published suprafamilial name should be employed (*e.g.,* order Decapoda Latreille, 1803, crustaceans, and order Decapoda Leach, 1818, cephalopods; suborder Chonetoidea Muir-Wood, 1955, and genus *Chonetoidea* Jones, 1928). Worthy of notice is the classificatory and nomenclatorial distinction between suprafamilial and family-group taxa that, respectively, are named from the same type genus, because one is not considered to be transferable to the other (*e.g.,* suborder Bellerophontina Ulrich & Scofield, 1897 is not coordinate with superfamily Bellerophontacea McCoy, 1851 or family Bellerophontidae McCoy, 1851).

3. The rules of priority and homonymy lack any force of international agreement as applied to suprafamilial names, yet in the interest of nomenclatorial stability and to avoid confusion these rules are widely applied by zoologists to taxa above the family-group level wherever they do not infringe on taxonomic freedom and long-established usage.

4. Authors who accept priority as a determinant in nomenclature of a suprafamilial taxon may change its assigned rank at will, with or without modifying the terminal letters of the name, but such changes cannot rationally be judged to alter the authorship and date of the taxon as published originally. A name revised from its previously published rank is a transferred name (*nomen translatum*), as illustrated in the following.

Order CORYNEXOCHIDA Kobayashi, 1935

[*nom. transl.* Moore, 1959, p. 217, *ex* suborder Corynexochida Kobayashi, 1935, p. 81]

A name revised from its previously published form merely by adoption of a different termination without changing taxonomic rank is a *nomen correctum.*

Order DISPARIDA Moore & Laudon, 1943

[*nom. correct.* Moore in Moore, Lalicker, & Fischer, 1952, p. 613, *pro* order Disparata Moore & Laudon, 1943, p. 24]

A suprafamilial name revised from its previously published rank with accompanying change of termination, which signals the change of rank, is recorded as a *nomen translatum et correctum.*

Order HYBOCRINIDA Jaekel, 1918

[*nom. transl. et correct.* Moore in Moore, Lalicker, & Fischer, 1952, p. 613, *ex* suborder Hybocrinites Jaekel, 1918, p. 90]

5. The authorship and date of nominate subordinate and supraordinate taxa among suprafamilial taxa are considered in the *Treatise* to be identical because each actually or potentially has the same type. Examples are given below.

Subclass ENDOCERATOIDEA Teichert, 1933

[*nom. transl.* Teichert in Teichert & others, 1964, p. 128, *ex* order Endoceroidea Teichert, 1933, p. 214]

Order ENDOCERIDA Teichert, 1933

[*nom. correct.* Teichert in Teichert & others, 1964, p. 165, *pro* order Endoceroidea Teichert, 1933, p. 214]

TAXONOMIC EMENDATION

Emendation has two distinct meanings as regards zoological nomenclature. These are alteration of a name itself in various ways for various reasons, as has been reviewed, and alteration of the taxonomic scope or concept for which a name is used. The *Code* (Article 33.1 and Glossary) concerns itself only with the first type of emendation, applying the term to intentional, either justified or unjustified changes of the original spelling of a name. The second type of emendation primarily concerns classification and inherently is not associated with change of name. Little attention generally has been paid to this distinction in spite of its significance.

Most zoologists, including paleontologists, who have emended zoological names refer to what they consider a material change in application of the name such as may be expressed by an importantly altered diagnosis of the assemblage covered by the name. The abbreviation *emend.* then must accompany the name with statement of the author and date of the emendation. On the other hand, many systematists think that publication of *emend.* with a zoological name is valueless because alteration of a taxonomic concept is introduced whenever a subspecies, species, genus, or other taxon is incorporated into or removed from a higher zoological taxon. Inevitably associated with such classificatory expansions and restrictions is some degree of emendation affecting diagnosis. Granting this, still it is true that now and then somewhat more extensive revisions are put forward, generally with a published statement of the reasons for changing the application of a name. To erect a signpost at such points of most significant change is worthwhile, both as an aid to subsequent workers in taking account of the altered nomenclatorial usage and to indicate where in the literature cogent discussion may be found. Authors of contributions to the *Treatise* are encouraged to include records of all especially noteworthy emendations of this nature, using the abbreviation *emend.* with the name to which it refers and citing the author, date, and page of the emendation. Examples from *Treatise* volumes follow.

Order ORTHIDA Schuchert & Cooper, 1932

[*nom. transl. et correct.* Moore in Moore, Lalicker, & Fischer, 1952, p. 220, *ex* suborder Orthoidea Schuchert & Cooper, 1932, p. 43; *emend.,* Williams & Wright, 1965, p. 299]

Subfamily ROVEACRININAE Peck, 1943

[Roveacrininae Peck, 1943, p. 465; *emend.,* Peck in Moore & Teichert, 1978, p. 921]

STYLE IN GENERIC DESCRIPTIONS

CITATION OF TYPE SPECIES

In the *Treatise,* the name of the type species of each genus and subgenus is given immediately following the generic name with its accompanying author, date, and page reference or after entries needed

for definition of the name if it is involved in homonymy. The originally published combination of generic and trivial names of this species is cited, accompanied by an asterisk (*), with notation of the author, date, and page of original publication, except if the species was first published in the same paper and by the same author as that containing definition of the genus of which it is the type. In this instance, the initial letter of the generic name followed by the trivial name is given without repeating the name of the author and date. Examples of these two sorts of citations follow.

Orionastraea SMITH, 1917, p. 294 [**Sarcinula phillipsi* MCCOY, 1849, p. 125; OD].

Schoenophyllum SIMPSON, 1900, p. 214 [**S. aggregatum;* OD].

If the cited type species is a junior synonym of some other species, the name of this latter is given also, as follows.

Actinocyathus D'ORBIGNY, 1849, p. 12 [**Cyathophyllum crenulate* PHILLIPS, 1836, p. 202; M; *=Lonsdaleia floriformis* (MARTIN), 1809, pl. 43; validated by ICZN Opinion 419].

In some instances the type species is a junior homonym. If so, it is cited as shown in the following example.

Prionocyclus MEEK, 1871b, p. 298 [**Ammonites serratocarinatus* MEEK, 1871a, p. 429, *non* STOLICZKA, 1864, p. 57; *=Prionocyclus wyomingensis* MEEK, 1876, p. 452].

In the *Treatise,* the name of the type species is always given in the exact form it had in the original publication except that diacritical marks have been removed. Where other mandatory changes are required, these are introduced later in the text, typically in the description of a figure.

Fixation of Type Species Originally

It is desirable to record the manner of establishing the type species, whether by original designation (OD) or by subsequent designation (SD). The type species of a genus or subgenus, according to provisions of the *Code,* may be fixed in various ways in the original publication; or it may be fixed subsequently in ways specified by the *Code* (Article 68) and described in the next section. Type species fixed in the original publication include (1) *original designation* (in the *Treatise* indicated by OD) when the type species is explicitly stated or (before 1931) indicated by n. gen., n. sp. (or its equivalent) applied to a single species included in a new genus; (2) defined by use of *typus* or *typicus* for one of the species included in a new genus (adequately indicated in the *Treatise* by the specific name); (3) established by *monotypy* if a new genus or subgenus has only one originally included species (in the *Treatise* indicated as M); and (4) fixed by *tautonymy* if the genus-group name is identical to an included species name not indicated as the type.

Fixation of Type Species Subsequently

The type species of many genera are not determinable from the publication in which the generic name was introduced. Therefore, such genera can acquire a type species only by some manner of subsequent designation. Most commonly this is established by publishing a statement naming as type species one of the species originally included in the genus. In the *Treatise,* such fixation of the type species by subsequent designation in this manner is indicated by the letters SD accompanied by the name of the subsequent author (who may be the same person as the original author) and the publication date and page number of the subsequent designation. Some genera, as first described and named, included no mentioned species (for such genera established after 1930, see below); these necessarily lack a type species until a date subsequent to that of the original publication when one or more species is assigned to such a genus. If only a single species is thus assigned, it becomes automatically the type species. Of course, the first publication containing assignment of species to the genus that originally lacked any included species is the one concerned in fixation of the type species, and if this

publication names two or more species as belonging to the genus but did not designate a type species, then a later SD designation is necessary. Examples of the use of SD as employed in the *Treatise* follow.

Hexagonaria GURICH, 1896, p. 171 [**Cyathophyllum hexagonum* GOLDFUSS, 1826, p. 61; SD LANG, SMITH, & THOMAS, 1940, p. 69].

Mesephemera HANDLIRSCH, 1906, p. 600 [**Tineites lithophilus* GERMAR, 1842, p. 88; SD CARPENTER, herein].

Another mode of fixing the type species of a genus is through action of the International Commission of Zoological Nomenclature using its plenary powers. Definition in this way may set aside application of the *Code* so as to arrive at a decision considered to be in the best interest of continuity and stability of zoological nomenclature. When made, it is binding and commonly is cited in the *Treatise* by the letters ICZN, accompanied by the date of announced decision and reference to the appropriate numbered opinion.

Subsequent designation of a type species is admissible only for genera established prior to 1931. A new genus-group name established after 1930 and not accompanied by fixation of a type species through original designation or original indication is invalid (*Code,* Article 13.3). Effort of a subsequent author to validate such a name by subsequent designation of a type species constitutes an original publication, making the name available under authorship and date of the subsequent author.

HOMONYMS

Most generic names are distinct from all others and are indicated without ambiguity by citing their originally published spelling accompanied by name of the author and date of first publication. If the same generic name has been applied to two or more distinct taxonomic units, however, it is necessary to differentiate such homonyms. This calls for distinction between junior homonyms and senior homonyms. Because a junior homonym is invalid, it must be replaced by some other name. For example, *Callophora* HALL, 1852, introduced for Paleozoic trepostomate bryozoans, is invalid because Gray in 1848 published the same name for Cretaceous–Holocene cheilostomate bryozoans. Bassler in 1911 introduced the new name *Hallophora* to replace Hall's homonym. The *Treatise* style of entry is given below.

Hallophora BASSLER, 1911, p. 325, *nom. nov. pro Callophora* HALL, 1852, p. 144, *non* GRAY, 1848.

In like manner, a replacement generic name that is needed may be introduced in the *Treatise* (even though first publication of generic names otherwise in this work is generally avoided). An exact bibliographic reference must be given for the replaced name as in the following example.

Mysterium DE LAUBENFELS, herein, *nom. nov. pro Mystrium* SCHRAMMEN, 1936, p. 183, *non* ROGER, 1862 [**Mystrium porosum* SCHRAMMEN, 1936, p. 183; OD].

Otherwise, no mention is made generally of the existence of a junior homonym.

Synonymous Homonyms

An author sometimes publishes a generic name in two or more papers of different date, each of which indicates that the name is new. This is a bothersome source of errors for later workers who are unaware that a supposed first publication that they have in hand is not actually the original one. Although the names were published separately, they are identical and therefore definable as homonyms; at the same time they are absolute synonyms. For the guidance of all concerned, it seems desirable to record such names as synonymous homonyms. In the *Treatise,* the junior of one of these is indicated by the abbreviation *jr. syn. hom.*

Not infrequently, identical family-group names are published as new names by different authors, the author of the name that was introduced last being ignorant of previous publication(s) by one or more other workers. In spite of differences in taxonomic concepts as indicated by diagnoses and grouping of genera and possibly in assigned rank, these family-group taxa, being based on the same

type genus, are nomenclatorial homonyms. They are also synonyms. Wherever encountered, such synonymous homonyms are distinguished in the *Treatise* as in dealing with generic names.

A rare but special case of homonymy exists when identical family names are formed from generic names having the same stem but differing in their endings. An example is the family name Scutellidae RICHTER & RICHTER, 1925, based on *Scutellum* PUSCH, 1833, a trilobite. This name is a junior homonym of Scutellidae GRAY, 1825, based on the echinoid genus *Scutella* LAMARCK, 1816. The name of the trilobite family was later changed to Scutelluidae (ICZN, Opinion 1004, 1974).

SYNONYMS

In the *Treatise,* citation of synonyms is given immediately after the record of the type species. If two or more synonyms of differing date are recognized, these are arranged in chronological order. Objective synonyms are indicated by accompanying designation *obj.,* others being understood to constitute subjective synonyms, of which the types are also indicated. Examples showing *Treatise* style in listing synonyms follow.

Mackenziephyllum PEDDER, 1971, p. 48 [**M. insolitum;* OD] [=*Zonastraea* TSYGANKO in SPASSKIY, KRAVTSOV, & TSYGANKO, 1971, p. 85, *nom. nud.;* =*Zonastraea* TSYGANKO, 1972, p. 21 (type, *Z. graciosa,* OD)].

Kodonophyllum WEDEKIND, 1927, p. 34 [**Streptelasma Milne-Edwardsi* DYBOWSKI, 1873, p. 409; OD; =*Madrepora truncata* LINNE, 1758, p. 795, see SMITH & TREMBERTH, 1929, p. 368] [=*Patrophontes* LANG & SMITH, 1927, p. 456 (type, *Madrepora truncata* LINNE, 1758, p. 795, OD); =*Codonophyllum* LANG, SMITH, & THOMAS, 1940, p. 39, obj.].

Some junior synonyms of either the objective or the subjective sort may be preferred over senior synonyms whenever uniformity and continuity of nomenclature are served by retaining a widely used but technically rejectable name for a genus. This requires action of the ICZN, which may use its plenary powers to set aside the unwanted name, validate the wanted one, and place the concerned names on appropriate official lists.

OTHER EDITORIAL MATTERS

BIOGEOGRAPHY

Purists, *Treatise* editors among them, would like nothing better than a stable world with a stable geography that makes possible a stable biogeographical classification. Global events of the past few years have shown how rapidly geography can change, and in all likelihood we have not witnessed the last of such change as new, so-called republics continue to spring up around the globe. One expects confusion among readers in the future as they try to decipher such geographical terms as USSR, Yugoslavia, or Ceylon. Such confusion is unavoidable, as books must be completed and published at some real time. Libraries would be limited indeed if publication were always to be delayed until the political world had settled down. In addition, such terms as central Europe and western Europe are likely to mean different things to different people. Some imprecision is introduced by the use of all such terms, of course, but it is probably no greater than the imprecision that stems from the fact that the work of paleontology is not yet finished, and the geographical ranges of many genera are imperfectly known.

Other geographic terms can also have varying degrees of formality. In general, *Treatise* policy is to use adjectives rather than nouns to refer to directions. Thus, we use *southern* and *western* in place of *South* and *West* unless a term has been formally defined as a geographic entity (e.g., South America or West Virginia). Note that we have referred to western Texas rather than West Texas, which is said to be not a state but a state of mind.

NAMES OF AUTHORS: TRANSLATION AND TRANSLITERATION

Chinese scientists have become increasingly active in systematic paleontology in the past two decades. Chinese names cause anguish among English-language bibliographers

for two reasons. First, no scheme exists for one-to-one transliteration of Chinese characters into roman letters. Thus, a Chinese author may change the roman-letter spelling of his name from one publication to another. For example, the name Chang, the most common family name in the world reportedly held by some one billion people, has been spelled more recently Zhang. The principal purpose of a bibliography is to provide the reader with entry into the literature. hat Chinese authors have used in each of their publications rather than attempting to adopt a common spelling to be used in all citations of their work. It is entirely possible, therefore, that the publications of a Chinese author may be listed in more than one place under more than one name in the reference section.

Second, most but by no means all Chinese list their family name first followed by given names. People with Chinese names who study in the West, however, often reverse the order, putting the family name last as is the Western custom. In the *Treatise,* authors' names are generally used in the text and listed in the references as they appear in the source being cited.

In previous *Treatise* volumes, traditional Chinese name order was followed when citing a Chinese language publication, in an attempt to list authors as they appear in the source being cited. However, the increasingly global nature of scientific publishing has rendered this past *Treatise* policy cumbersome and prone to error. Therefore, starting with this volume, *Treatise* is using the Western name order style for all authors, regardless of country of origin or language of publishing. The aim is for consistency and should not imply disrespect for any tradition.

In this volume, we also use the full given name for Chinese authors rather than initials when the name is known (Yuandong Zhang instead of Y.-D. Zhang).

Several systems exist for transliterating the Cyrillic alphabet into the roman alphabet. On the recommendation of skilled bibliographic librarians, we have adopted the American Library Association/Library of Congress romanization table for Russian and other languages using the Cyrillic alphabet.

MATTERS SPECIFIC TO THIS VOLUME

Authorship entails both credit and responsibility. As the knowledge of paleontology grows and paleontologists become more specialized, preparation of *Treatise* volumes must necessarily involve larger and larger teams of researchers, each focusing on increasingly narrow aspects of the higher taxon under revision. In this volume, we have taken special pains to acknowledge authorship of small subsections. Readers citing the volume are encouraged to pay close attention to the actual authorship of a section or subsection.

Stratigraphic nomenclature in the *Treatise* follows that recommended by the International Commission of Stratigraphy, which updates their International Chronostratigraphic Chart periodically (www.stratigraphy.org).

All sections in this volume first appeared as chapters in *Treatise Online,* published between 2021 and 2022 and uploaded as they were finished. This presented new dilemmas. For instance, credits for previously published figures are identified by publication and date at the end of figure captions; "new" is used if a figure is being published for the first time. In that regard, we treat *Treatise Online* and *Treatise* (the printed volume) as the same entity, therefore "new" will appear herein, even if technically published online earlier.

Color versions of many of the illustrations in this volume are available in *Treatise Online*. A reference to the color version is included in captions when color contributes vital information.

Authors who wish to cite *Treatise* material may choose to cite the online publication, which is the earliest date—often referred to in the text as "originally published as..." A listing of all Part B *Treatise Online* chapters is on p. ix. Please note that editorial changes

have been made subsequent to *Treatise Online* versions. Therefore, the printed volume represents the most accurate and up-to-date information.

ACKNOWLEDGMENTS

Discussions about the increasing interest in Precambrian paleontology and whether prokaryotes could fit into the traditional framework of the *Treatise* began under the supervision of the late assistant editor Jill Hardesty, editor and director Paul Selden, and Nora Noffke. Assistant editor Elizabeth Black took on the task in 2016 in the early stages of submission of manuscripts. As chapters were finished, they were made available to the community in *Treatise Online*. As interim director, I provided editorial guidance, moving this volume through early manuscripts through the various stages of final editing and into production. In this, able assistance was provided by other members of the editorial team, including Denise Mayse, office Manager and copy editor, with her excellent attention to detail while proofing, checking the references, and various other tasks, and Mike Cormack with his outstanding computer skills and management of subscriptions and *Treatise Online*. Three months before this volume went to the printer, Bruce Lieberman became Director and Editor, and his input was invaluable in the last stages.

This editorial preface and other, recent ones are extensive revisions of the prefaces prepared for previous *Treatise* volumes by former editors, including the late Raymond C. Moore, the late Curt Teichert, Richard A. Robison, and the late Roger L. Kaesler, and most recently, Paul A. Selden. I am indebted to them for preparing earlier prefaces and for the leadership they have provided in bringing the *Treatise* project to its present status.

William I. Ausich

REFERENCES

International Commission on Zoological Nomenclature. 1999. International Code of Zoological Nomenclature, 4th edition. International Trust for Zoological Nomenclature. London. 306 p.

Moore, R. C., and Curt Teichert. 1978. Treatise on Invertebrate Paleontology. Part T, Echinodermata 2(1). The Geological Society of America and The University of Kansas. Boulder & Lawrence. 401 p.

Robison, R. A., and Curt Teichert. 1979. Treatise on Invertebrate Paleontology. Part A, Introduction. The Geological Society of America and The University of Kansas. Boulder & Lawrence. 569 p.

CONTRIBUTORS

[Email addresses are provided for lead authors of sections.]

Nora Noffke
Coordinating Author
Old Dominion University, Department of Ocean, Earth and Atmospheric Sciences, Norfolk, Virginia, 23529, USA
nnoffke@odu.edu

Anthony Bouton[1, 2]
[1]Department of Marine Sciences, University of Connecticut, Groton, Connecticut, 06340, USA
[2]Biogeosciences, Université de Bourgogne Franche-Comté, 21000 Dijon, France

Brendan P. Burns[1, 2]
[1]Australian Centre for Astrobiology, University of New South Wales, Sydney, NSW 2052, Australia;
[2]School of Biotechnology and Biomolecular Sciences, University of New South Wales, Sydney, NSW 2052, Australia

Flavia Callefo
Brazilian Synchrotron Light Laboratory, Giuseppe Máximo Scolfaro Street, 10000, Campinas, 13083-100, Brazil

Hugo Beraldi-Campesi
SOMA, Universidad Naciona l Autonoma de Mexico, Cuiadad Universitaria, 04510, CDMX, Mexico

Noelia Carmona[1, 2]
[1]Universidad Nacional de Río Negro, Instituto de Investigaciones en Paleobiología y Geología, Río Negro, Av. Roca 1242, General Roca, Argentina,

Diana G. Cuadrado
Instituto Argentino de Oceanografía, Departamento de Geología, Universidad Nacional del Sur, Bahía Blanca B8000CPB, Buenos Aires, Argentina

Erika J. Espinosa-Ortiz
Department of Chemical and Biological Engineering, Center for Biofilm Engineering, Montana State University, 366 Barnard Hall Building, Bozeman, Montana, 59717, USA
erika.espinosaortiz@montana.edu

Kimberley L. Gallagher
Department of Marine Sciences, University of Connecticut, Groton, Connecticut, 06340, USA

Robin Gerlach
Department of Chemical and Biological Engineering, Center for Biofilm Engineering, Montana State University, 366 Barnard Hall Building, Bozeman, Montana, 59717, USA
robin_g@montana.ed

Adriana Heimann
East Carolina University, Department of Geological Sciences, Graham 101, Greenville, North Carolina, 27858, USA
heimanna@ecu.edu

Keyron Hickman-Lewis
Department of Earth Sciences, The Natural History Museum, South Kensington, London, SW7 5BD, UK

Martin Homann
University College London, Department of Earth Sciences, 5 Gower Place, London WC1E 6BS, UK

Ria Mitchell
Sheffield Tomography Center, University of Sheffield, Sheffield, S3 7HQ, UK

R. S. Shapiro
Department of Earth and Environmental Sciences
California State University Chico,
400 W. First Street, Chico, California, 95929, USA
rsshapiro@csuchico.edu

Nathan Sheldon
Department of Earth and Environmental Sciences, University of Michigan, Ann Arbor, Michigan, 48109, USA

Qing Tang
Department of Earth Sciences, University of Hong Kong, Pokfulam Road, Hong Kong, China
qingt@hku.hk

Christophe Thomazo[1, 2]
[1]Biogeosciences, Université de Bourgogne Franche-Comté, 21000 Dijon, France
[2] Institut Universitaire de France, Paris, France

Emmanuelle Vennin
Biogeosciences, Université de Bourgogne Franche-Comté, 21000 Dijon, France

Pieter T. Visscher[1, 2, 3]
[1]Department of Marine Sciences, University of Connecticut, Groton, Connecticut, 06340, USA
pieter.visscher@uconn.edu
[2]Biogeosciences, Université de Bourgogne Franche-Comté, 21000 Dijon, France
[3]Australian Centre for Astrobiology,University of New South Wales, Sydney, NSW 2052, Australia

Francis Westall
Centre de Biophysique Moleculaire, CNRS CBM, 45071 Orleans Cedex 2, France

Dylan T. Wilmeth
Grand Valley State University
1 Campus Drive, Allendale, Michigan, USA 49401, USA
wilmethd@gvsu.edu

Richard A. White III[1, 2]
[1]Australian Centre for Astrobiology, University of New South Wales, Sydney, NSW 2052, Australia
[2]College of Computing and Informatics, University of North Carolina Charlotte, Charlotte, North Carolina, 28223, USA

Shuhai Xiao
Department of Geosciences,
Virginia Tech, Blacksburg, Virginia, 24061, USA
xiao@vt.edu

INTRODUCTION

Nora Noffke and Paul Selden

In 2012, we began discussing the problems associated with prokaryote fossil systematics in paleontology and whether this subject belonged in the *Treatise on Invertebrate Paleontology*. With Precambrian paleontology gaining increasing traction in novel analytical studies, we agreed it would be timely for the *Treatise* to publish a volume dedicated to prokaryotes. One of the problems we encountered was how to categorize prokaryotes and fit this organismic group into the traditional systematic framework of the *Treatise*. In the prokaryote world, speciation in the Darwinian sense does not exist, and, more so, prokaryotes commonly assemble into highly complex communities called biofilms. Microbial cells are rarely preserved, and sedimentary structures arising from prokaryote activity constitute biofilm expressions. Biofilms, however, are complex assemblages of microorganisms and a dominant group cannot always be of geological significance in the sense of causing a visible fossil, texture, or structure. For these reasons, it seemed prudent to explore the topic of Prokaryota in the fossil record by presenting a volume that would include a general overview on the main fossil types that constitute this indisputably largest group of organisms on Earth. Future work may contribute to categorizing taphonomic groups and testing biostratigraphic application, which may well result in additional volumes on Prokaryota.

This volume begins with an introduction into biofilms that have mostly been the subject of medical research before moving into the limelight of geosciences. Biofilms are assemblages of microbes that organize into a three-dimensional structure with the single cells attached to a substrate by their extracellular polymeric substances (EPS)—in colloquial terms also called slime. Traditional sedimentology and paleontology are not familiar with biofilms but are definitively familiar with microbial mats (algal mats) that are basically large-scale biofilms occurring in aquatic settings. Such mats are well known as producers of microbialites, of which the carbonate buildups (stromatolites) in shallow coastal zones are prominent examples. Such buildups form through the metabolic activity of the biofilm/mat community in which each member is interacting with the next, as well as with environmental parameters. Biofilms and mats also contributed to the enormous quantities of Banded Iron Formations (BIFs), to date the most important ore deposits in the world. Where mats develop in clastic settings of little to no mineral precipitation, microbially induced sedimentary structures (MISS) represent the microbialite spectrum. Microbial mats, microbialites, and BIFs constitute large structures, but they may include myriads of microfossils of the ancient structure-formers. However, the paleontological spectrum of prokaryotes also includes deposits of fossils of cells and filaments preserved *in situ* as carbonaceous matter in rapidly precipitated mineralogies, such as glass-like chert. In some examples, the organic matter had been replaced by minerals such as pyrite.

Prokaryote fossils and structures have modern counterparts that can be studied. Typically, the record spans from the early Archean (perhaps Hadean) to the modern. Indeed, the modern serves as the key to the past and is instrumental for the exploration of Earth history, especially that of the Precambrian.

Compiling a volume such as this requires many colleagues working together. We are most grateful to the diligent staff at the *Treatise* editorial office—editor Jill Hardesty, who guided the project in the beginning; Elizabeth Black, who edited chapters as our team produced them; and interim director William Ausich who oversaw the final stages. We thank our authors for putting their

chapters together despite the daily pressure of research and teaching activities, and we are grateful for the many timely reviews provided by experts in the field. Thank you all!

We look forward to the continuation of this initiative regarding the organismic group Prokaryota in the future of the *Treatise on Invertebrate Paleontology*.

GLOSSARY OF IMPORTANT TERMS

General Terms

Active continental margin: a continental margin with a subduction zone.

Alteration: change.

Amorphous: disordered atomic arrangement of a mineralic substance.

Analog: a model for.

Authigenic: formed in place, typically referring to mineralization.

Banding: horizontal layers in a rock, differentiated by color or material but not by bedding planes.

Biofilm: a layer of microbial cells and their extracellular polymeric substances (EPS).

Biogenicity: characteristics of biological origin.

Biomineralization: process of minerals formed by biotic processes.

Biosignature: a sedimentary structure, texture, or chemical signal in a rock bed that has a biological origin.

Bioturbation: structure caused by an organism in a sediment.

Calcification: calcite mineralization of the organic substance of an organism.

Cement: minerals precipitated in void space surrounding sedimentary grains in a sedimentary rock such as a sandstone.

Chert: rock formed of microcrystalline silica.

Crystalline: comprised of mineral crystals.

Diagenesis: post-burial chemical and physical changes of sediments and organisms within.

Ediacara: name of a formation of terminal Neoproterozoic age; also name of a fauna occurring in this stratigraphic section.

Fe-Fenton reaction: catalytic process that forms hydroxyl free radicals from ferrous Fe.

Fischer-Tropsch processes: chemical reactions that convert a mixture of carbon monoxide and hydrogen into hydrocarbons.

Fluvial: riverine.

Graywacke: type of sandstone that is poorly sorted and comprised of a variety of minerals including quartz.

Hiatus: pause in sedimentation, causing a gap in a stratigraphic rock succession

Hydrothermal vent: an opening in the Earth's crust where hot and chemical-laden water emerges.

Intertidal: zone along the coast affected by daily tides.

Lacustrine: in a lake.

Lamina: layer in a sediment or sedimentary rock, typically less than a millimeter thick.

Lithology: type of rock.

Micritic: calcite crystals less than 4 microns in diameter.

Platform: a shallow shelf covered by carbonate sediment in a tropical ocean.

Precipitation: crystalization of minerals.

Pustular: covered with a pimple-like texture.

Metamorphic facies: degree of metamorphosis.

Metamorphism: change of a rock due to high temperature and pressure.

Microbialite: build-up caused by microorganisms.

Microbial mat: benthic assemblage of microorganisms on the sedimentary surface in an aquatic or moist setting, commonly resembling a soft tissue or carpet.

Microfossil: fossil of a microscopic organism, either prokaryotic or eukaryotic.

Mold and cast: type of preservation, in which a cast is a positive mineralogical infill of an organism and a mold is an imprint.

Passive-margin continental shelf: a continental margin without a subduction zone.

Peritidal: along an intertidal flat, landward.

Quartzite: rock comprised of quartz minerals, often white in color.

Rayleigh oxidation: distillation, kinetic or non-equilibrium oxidation.

Shale: slightly metamorphic mudstone.

Silicification: process of permeation by silica.

Snowball Earth: hypothesis of Earth being completely covered in ice, originally defined for the terminal Neoproterozoic.

Taphonomy: process of fossilization.

Commonly Used Acronyms

BIF: banded iron formation.

DIR: dissimilatory iron reduction.

DSR: dissimilatory sulfate reduction.

EPS: extracellular polymeric substances, mucilages, of microbial cells.

GIF: granular iron formation.

GOE: great oxidation event.

GSB: green sulfur bacteria.

LIP: large igneous province.

MAGs: metagenome-assembled genomes.

MISS: microbially induced sedimentary structure.

MIST: microbially induced sedimentary texture.

MSD: massive sulfide deposit.

PDB: Pee Dee Belemnite, a standard used for C isotope analysis, based on the Cretaceous marine fossil *Belemnitella americana* from the Peedee Formation in South Carolina.

REE: rare earth element.

TOS: textured organic surfaces.

SRB: sulfate-reducing bacteria.

BIOFILMS

Erika J. Espinosa-Ortiz and Robin Gerlach

INTRODUCTION

Most microorganisms found in natural, clinical, and industrial environments prevail associated with surfaces rather than as free-living (planktonic) organisms (Costerton & others, 1995; Flemming & Wuertz, 2019). These communities can develop as biofilms in a diverse range of environments (e.g. living tissues, indwelling medical devices, water distribution systems, natural aquatic and sediment systems, rocks, surfaces of buildings, stromatolites, etc.). Biofilms are "aggregates of microorganisms in which cells that are frequently embedded within a self-produced matrix of extracellular polymeric substances (EPS) adhere to each other and/or to a surface" (Vert & others, 2012, p. 383). The aggregation of cells can result in highly structured microbial communities that allow for cell-to-cell contact. This proximity of the cells, the intra- and intercellular interactions within the microbial community, and the properties of the EPS matrix can confer distinct emergent properties upon the biofilm substantially different from planktonic communities (Flemming & others, 2016). Biofilms are characterized by their unique: 1) physicochemical and biological heterogeneity, which provides habitat diversity; 2) services provided by the EPS matrix, which provides architecture and stability to the biofilm and acts as a protective barrier; 3) physical and social interactions, which in conjunction determine the survival strategies for the community, such as quorum sensing, gene exchange, EPS production, or coordination of metabolic action; and 4) increased tolerance and/or resistance to survive environmental stress (Costerton, Stewart, & Greenberg, 1999; Flemming & others, 2016). The biological and physicochemical characteristics of biofilms (e.g., structure, EPS production, and cell biomass) are the result of the environment, the nutritional and physical conditions in which the biofilm develops (Nielsen, Jahn, & Palmgren, 1997).

The significance of biofilms in the geological record of life was recognized by Noffke (2010). Examples of the manifestation of biofilms in the geological record include microbially induced sedimentary structures (MISS) and stromatolites (Astafieva, 2013; Noffke, 2010). These structures suggest that biofilms have existed throughout the geological record of life (Costerton & Stoodley, 2003; Noffke, 2010). Considering that cells within a biofilm can exhibit different phenotypes and change their metabolic activities compared to their planktonic counterparts, it is possible that biofilms induce distinct characteristics (e.g., structures, textures, chemical signatures) in the consolidated rock record. Thus, a better understanding of the biofilm way of life can aid in reconstructing the evolution of prokaryotes throughout Earth history.

BIOFILM FORMATION AND DEVELOPMENT

Biofilm formation follows a number of progressive steps including initial microbial attachment to a surface, microcolony formation, development of a three-dimensional community structure, maturation, and detachment.

ATTACHMENT OF MICROORGANISMS

The first step in biofilm formation is microbial attachment, which includes planktonic cells being able to find, interact with, and adhere to a surface. Microbial attachment is influenced by several factors, including the type of substratum (e.g. an inert surface or living tissue), hydrodynamics

of the aqueous medium, physicochemical characteristics of the medium (e.g., pH, nutrient levels, temperature), and properties of the cell surface and cell motility (Bouwer & others, 2000; Donlan, 2002; Palmer, Flint, & Brooks, 2007). Attachment is more likely to occur on surfaces that are rough, hydrophobic, and coated by conditioning films (i.e., surfaces in nature and industry are often at least partially coated by compounds—including polymers—from the liquid medium) (Donlan, 2002; Palmer, Flint, & Brooks, 2007).

FORMATION OF MICROCOLONIES

With the initial attachment of cells, microbial association to the surface (substratum) begins and—given appropriate growth conditions—becomes suitable for microcolony formation. During this stage of biofilm development, microbial cells undergo growth, which is usually accompanied by the excretion of EPS, resulting in the formation of aggregates or microcolonies. EPS production aids in promoting the irreversible attachment of cells to a substratum (Flemming & Wingender, 2010). Microbial aggregation also occurs as a result of the interaction of already attached cells and the recruitment of planktonic cells from the surrounding medium (McLean & others, 1997). Initial EPS production can be a response to attachment and environmental conditions such as osmotic pressure, pH, temperature, starvation and likely other factors (Flemming & others, 2016).

FORMATION OF THREE-DIMENSIONAL STRUCTURE AND MATURATION

Given suitable growth conditions, microcolonies develop into an organized structure over time and differentiate into true biofilms. Mature biofilms are typically comprised of multilayered microcolonies encased in EPS and separated by interspersed water channels. The EPS matrix has an active role in microbial attachment to surfaces, acts as a glue that keeps cells together, and allows for the development of a three-dimensional structure (Flemming & Wingender, 2010).

DETACHMENT

As the biofilm matures, detachment or dispersal occurs, which is crucial to the biofilm life cycle. Detachment of microbial cells occurs due to multiple factors including the lack of nutrients, competition, hydrodynamic stresses, among others (Stewart, 1993). The release and dispersion of microbial cells can lead to the formation of new biofilms (Stewart, 1993). Detachment can occur as a rapid, extensive loss of parts of the biofilm known as sloughing, or as continuous loss of single cells (small fractions of the biofilm) known as erosion (Bryers, 1988; Stewart, 1993). Detachment can influence the competition in biofilms (Morgenroth & Wilderer, 2000) and the biofilm morphology (Picioreanu, van Loosdrecht, & Heijnen, 2001). For instance, erosion can result in smoother biofilms, whereas sloughing usually increases the morphological heterogeneity of the biofilm (Picioreanu, van Loosdrecht, & Heijnen, 2001).

THE BIOFILM MATRIX

The biofilm matrix is a conglomeration of different extracellular biopolymers in which the biofilm cells are embedded. The microbial extracellular material, known as extracellular polymeric substances or EPS, typically accounts for ~90% of the biofilm, and the rest corresponds to biomass as well as minor components such as particulates, gas bubbles, etc. (Flemming & Wingender, 2010). EPS are comprised mostly of water (up to ~97%) (Zhang, Bishop, & Kupferle, 1998) and are usually a mixture of polysaccharides, proteins, lipids, nucleic acids, and other organic compounds (Flemming & Wingender, 2010; More & others, 2014). The EPS composition within a biofilm can vary greatly; it can be strain-dependent but can also be affected by the nutritional and physical conditions in which the biofilm develops (Nielsen, Jahn, &

Palmgren, 1997). It has also been suggested that the presence of microenvironments within biofilms may lead to the production of various mixtures of polysaccharides by specific subpopulations (Sutherland, 2001).

The presence of EPS does not seem to be key for the initial attachment of microbial cells to surfaces (Gaylarde & Gaylarde, 2005). However, EPS production is essential for the development of the architecture of any biofilm (Flemming & Wingender, 2010; Sutherland, 2001). EPS production appears to begin after the initial attachment of the microbial cells and the formation of the first microcolonies; production of EPS is often associated with the so-called irreversible attachment of cells (Flemming & Wingender, 2010).

Although the production of EPS can also occur during planktonic growth (e.g., microbial aggregates) (More & others, 2014), EPS provide biofilms with many of their unique physical characteristics. The EPS matrix has different functions in biofilms, including: 1) adhesion, cohesion, and aggregation of microbial cells—the EPS immobilize cells and keep them close allowing for cell-cell communication; 2) architecture and stability of the biofilm—formation of the structural support of the biofilm is a continuous and dynamic process that results in the spatial organization of biofilms; 3) protective barrier for cells and retention of water to prevent desiccation, which increases the tolerance and/or resistance to antimicrobials and other stressors; 4) resource capture (nutrients, organic compounds and inorganic ions) by sorption; 5) enzyme retention, which provides digestive capabilities; 6) exchange of genetic information; 7) function as electron donor or acceptor; 8) export of cell components; 9) sink for excess energy; and 10) binding of enzymes (Flemming & Wingender, 2010; Flemming & others, 2016). For excellent reviews summarizing the possible services the EPS matrix can provide to biofilms, see Flemming and Wingender, 2010; More and others, 2014; and Sutherland, 2001.

CHARACTERISTICS OF BIOFILMS

HETEROGENEITY

Biofilms are comprised of dense clusters of microbial cells (microcolonies) held together by the EPS matrix with fluid channels formed within the biofilm through which nutrients circulate. This structural organization leads to the formation of numerous microenvironments within the biofilm with different microbial composition, activity, cell density, pH, EPS production, water content, presence of channels, and solute concentrations (Stewart & Franklin, 2008). As a result, biofilms are physically, chemically, and biologically heterogeneous.

Mature biofilms are characterized by the presence of concentration gradients of metabolic substrates and products, resulting in chemical heterogeneity within the biofilm matrix. Specific patterns of chemical heterogeneity can be observed within biofilms due to reaction-diffusion interactions for metabolic substrates, metabolic products, and metabolic intermediates (Stewart & Franklin, 2008) (Fig. 1). As biofilms grow, the microbial cell density often increases, leading to an increase in the demand of nutrients (metabolic substrate). In general, cells located closest to the substratum are more limited for nutrients, whereas cells closest to the surrounding environment (e.g., farthest from the substratum) have higher availability of nutrients (Stewart & Franklin, 2008). Opposite to nutrients, metabolic products are usually present at higher concentrations inside the biofilm with decreasing concentrations in the outer layers. Metabolic intermediates can be produced and consumed in the biofilms, leading to concentration profiles with maxima somewhere within the biofilm; for instance, in a multi-species biofilm, the waste product of one species can serve as substrate for another species (Fig. 1) (Stewart & Franklin, 2008).

Under well-mixed conditions, planktonic microorganisms show fairly uniform physiological activity, whereas the chemical

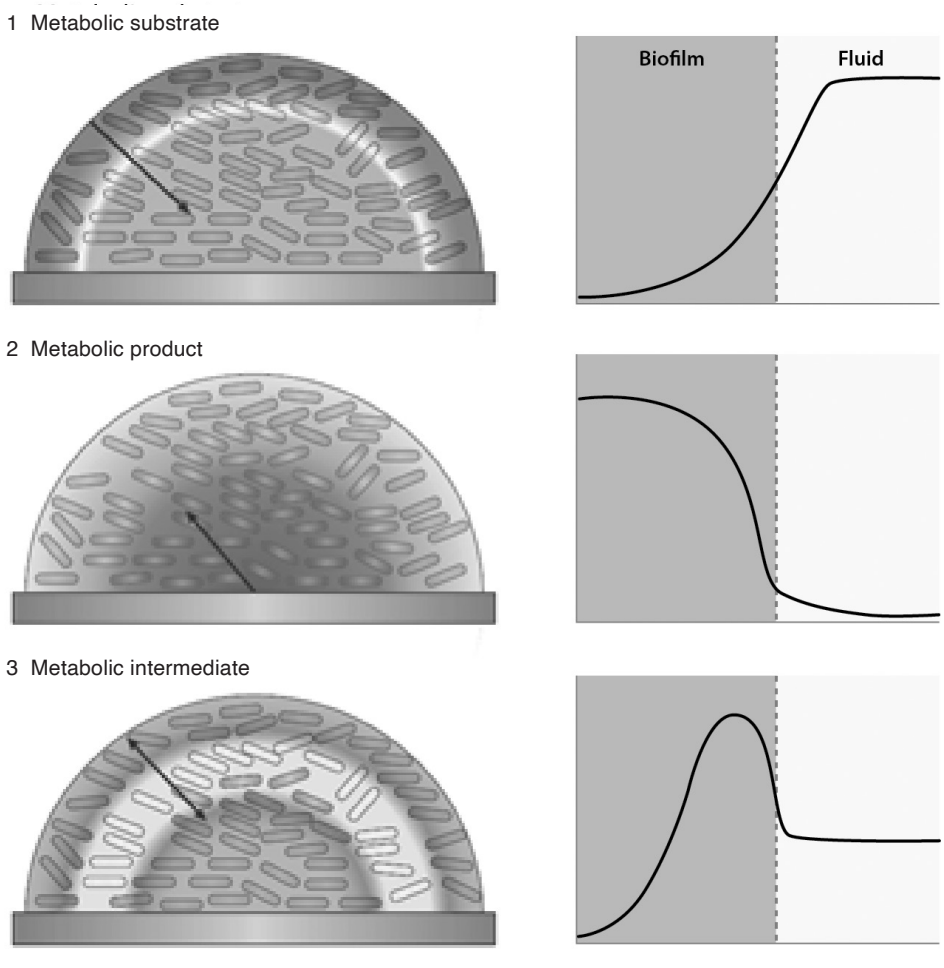

FIG. 1. Chemical heterogeneity in biofilms. Three qualitatively distinct patterns of chemical heterogeneity arise in biofilms owing to reaction-diffusion interactions for a metabolic substrate, *light gray* (*1*); a metabolic product, *medium gray* (*2*); and a metabolic intermediate, *darker gray* (*3*). *1,* The concentration of a substrate that is consumed inside the biofilm decreases with depth into the biofilm and distance away from the bulk fluid. *2,* Conversely, a metabolic product is more concentrated inside the biofilm. *3,* A metabolic intermediate that is both consumed and produced within the biofilm can exhibit concentration profiles that have local maxima (reprinted by permission from Springer Nature Customer Service Center, Nature Reviews Microbiology, Stewart & Franklin, 2008, fig. 2). Color version available in *Treatise Online* 147 (paleo.ku.edu/treatiseonline).

gradients within biofilms are commonly accompanied by physiological heterogeneity (GU & others, 2013; JENSEN & others, 2017). Due to limitations in metabolic substrates and oxygen (or other electron acceptor) availability, there are usually regions of slow microbial growth and activity within a biofilm. Furthermore, as a response to microenvironments inside a biofilm, microorganisms can modify gene expression patterns and physiological activities, favor the growth of particular microbial species, and select for fitter strains that can adapt to and survive in particular conditions (STEWART & FRANKLIN, 2008).

As an illustration of the various biogeochemical gradients that can be found in a biofilm, consider a mixed-species microbial mat, which may be viewed as complex biofilms (STOLZ, 2000) growing in (and producing)

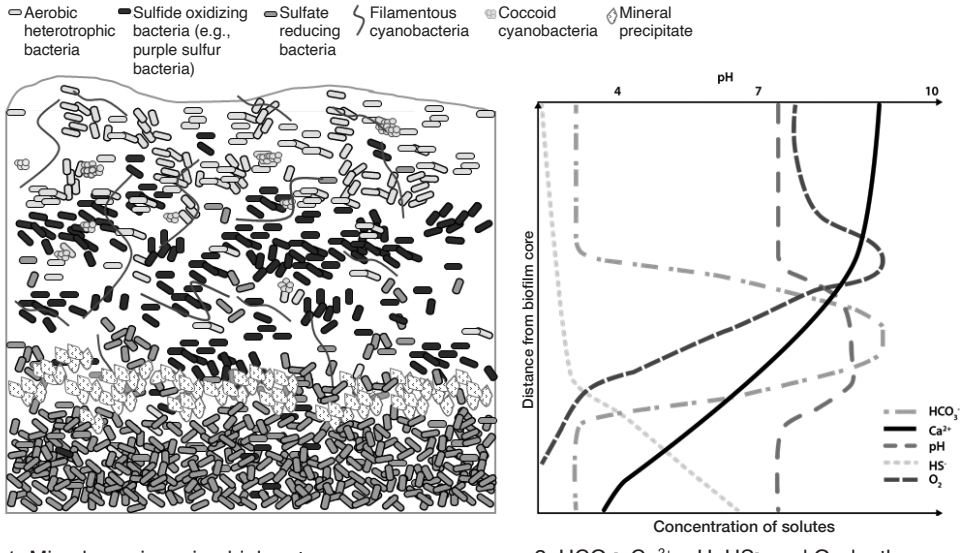

FIG. 2. Microbial diversity in biofilms. *1,* Conceptual representation of the microbial diversity observed in a mat similar to the one in the superficial layer of the stromatolite in the Cayo Coco Lagoonal Network described by Pace and others (2018); various groups of microorganisms are distributed within the mat and are located based on their physiological preferences, including photosynthetic microorganisms (filamentous and coccoid cyanobacteria), aerobic heterotrophic bacteria, and sulfate-reducing and sulfide-oxidizing bacteria. *2,* Sketch of chemical microenvironments developing within the mat indicated by the HCO_3^-, Ca^{2+}, pH, HS^-, and O_2 depth profiles. Mineral precipitation is observed in the oxygenic-anoxygenic photosynthetic interface as a result of a pH maximum induced by the microbial activity. (adapted from Pace & others, 2018, fig. 3 and fig. 8). Color version available in *Treatise Online* 147 (paleo.ku.edu/treatiseonline).

a lithifying stromatolite (Fig. 2) (PACE & others, 2018). Stromatolite growth can be the result of dynamic and successive cycles of sedimentation and microbial lithification in which the metabolism of microbial mats plays a key role (REID & others, 2000). Early studies reported the formation of chemical micro-gradients within microbial mats due to the metabolic activity of various microbial groups (VISSCHER & VAN GEMERDEN, 1993; STAL, GEMERDEN, & KRUMBEIN, 1985; JØRGENSEN, REVSBECH, & COHEN, 1983; JØRGENSEN & REVSBECH, 1983). PACE and others (2018) collected an actively growing microbial mat from a lithifying stromatolite in the hypersaline Cayo Coco Lagoonal Network (Fig. 2.1–2.2). Based on confocal laser scanning microscopy, microbial community analysis, dissolved oxygen (O_2), sulfide (H_2S/HS-/S^{2-}) concentration, and pH profiles, various chemical microenvironments were observed along a vertical profile in the stromatolite (Fig. 2.2). Microbial activity in the upper layers of the stromatolite is indicated by the O_2 and bicarbonate profiles (Fig. 2.2); and within the first few millimeters from the surface, O_2 concentration peak and bicarbonate concentrations are low due to oxygenic photosynthesis by, most likely, cyanobacteria. Below ~3 mm depth, bicarbonate concentrations increase and O_2 decreases rapidly due to reduced photosynthetic activity and increased net-aerobic respiration creating an oxic-anoxic interface at about 5 mm depth. Sulfide appears below the oxic-anoxic interface.

TOLERANCE AND RESISTANCE TO ENVIRONMENTAL STRESS

One of the unique properties of biofilm-grown cells is their enhanced tolerance

and/or resistance to antimicrobials (e.g. disinfectants, toxic compounds, antibiotics) and stresses compared to their planktonic counterparts. Flemming and others (2016) described biofilms as fortresses due to the ability of biofilm-grown cells to survive exposure to antimicrobials as well as desiccation. We refer here to resistance as the inherited ability of microorganisms to survive exposure to concentrations of antimicrobials that can be lethal (Sholar & Pratt, 2000) and that remains even when cells in the biofilm are dispersed. The term tolerance is described as the ability of the cells to survive transient exposure to compounds or stresses that could be lethal (Kester & Fortune, 2014), a phenomenon that is uniquely observed when cells grow as biofilms (Olsen, 2015).

Tolerance in biofilms is often attributed to the role of the EPS matrix acting as a protective barrier as well as to the development of regions with low metabolic activity created as a result of the intrinsically heterogeneous nature of biofilms. The EPS matrix acts as a protective barrier by: 1) quenching the activity of antimicrobials that diffuse through the biofilms via diffusion-reaction inhibition (Daddi Oubekka & others, 2012); this could involve the binding of the antimicrobials to components of the biofilm matrix or to microbial membranes (Chiang & others, 2013) as well as degradation of antimicrobials by enzymes contained in the EPS (Høiby & others, 2010), and 2) acting as a hydrogel that holds water protecting the organisms from desiccation (Flemming & Wingender, 2010). The intrinsic heterogeneity of the biofilms promotes the creation of zones of low metabolic activity and dormancy, which can decrease the susceptibility of the biofilm to harmful substances and increase the resistance of the biofilm to changing environmental conditions (Brown, Allison, & Gilbert, 1988; Stewart & Franklin, 2008). Cells in these zones of low metabolic activity and dormancy have reduced susceptibility to antimicrobials that depend on the microbial metabolism for their activities (Amato & others, 2014). Furthermore, biofilms can contain inactive microbial subpopulations (up to 1%) known as persisters that appear to exhibit unique phenotypic traits that make them more tolerant to antimicrobials (Wood, Knabel, & Kwan, 2013).

Microbial diversity within biofilms is a factor that can further increase the tolerance of biofilm-grown cells. Biofilms comprised of multiple species are affected by cross-species interactions, which can influence the development and structure of the microbial species within the biofilms and, in turn, provide an increased tolerance to stresses compared to their single-species biofilms (Lee & others, 2014; Moons, Michiels, & Aertsen, 2009).

DIVISION OF LABOR

Biofilm-grown cells can demonstrate division of labor (Armbruster & others, 2019; Dragoš & others, 2018; van Gestel, Vlamakis, & Kolter, 2015; Vlamakis & others, 2008), which refers to the specialization of subpopulations of cells to perform different tasks within a microbial community. Division of labor appears to be based on three conditions: 1) development of different microbial phenotypes (task allocation); 2) associated microorganisms having a cooperative interaction; and 3) all partners involved in the interactions gaining inclusive fitness benefits (West & Cooper, 2016).

An example of division of labor can be found in *Bacillus subtilis* biofilms, which have subpopulations that are genetically similar but are able to perform different specialized activities including motility, matrix production, and sporulation, which in conjunction are key for the successful development of the biofilm (Dragoš & others, 2018; van Gestel, Vlamakis, & Kolter, 2015; Vlamakis & others, 2008). In *B. subtilis* biofilms, flagellum-independent migration is achieved by two different cell types: surfactin-producing cells that aid lubricating the substratum and matrix-producing cells, which agglomerate as bundles (van

Gogh bundles) that are able to move away from the colony; these bundles can migrate greater distances compared to what would be possible without the division of labor (van Gestel, Vlamakis, & Kolter, 2015).

BIOFILMS AS COMPLEX MICROBIAL COMMUNITIES

Biofilms in the environment typically consist of complex microbial communities that host multiple species. Subaerial biofilms, biofilms that grow on solid mineral surfaces exposed to the atmosphere (e.g., rocks, surface of buildings, stromatolites), are perfect examples of complex communities with different cross-species interactions. A diverse community of microorganisms is usually present in subaerial biofilms, including algae, bacteria, fungi, protozoa, and even microscopic animals such as mites and insects (Gaylarde & Gaylarde, 2005; Gorbushina & Petersen, 2000). Interactions among different microbial species in mixed-biofilm communities seem to influence the development, structure, and functions of these communities (Moons, Michiels, & Aertsen, 2009). Cross-species interactions in mixed biofilms can range from synergistic (cooperative) to antagonistic (competitive) (Elias & Banin, 2012), and they can lead to a number of microbial adaptations by promoting horizontal gene transfer events, cell-cell communication (quorum-sensing abilities) (Davies & others, 1998; Parsek & Greenberg, 2005), and can induce protein secretion systems resulting in phenotypic changes that can affect the survival, dynamics, spatial distribution, and coexistence of the microbial communities (Elias & Banin, 2012).

Cross-species interactions can influence the development and structure of microbial species within the biofilms, which can provide an increased resistance to stresses compared to their single-species biofilms (Lee & others, 2014; Moons, Michiels, & Aertsen, 2009). Lee and others (2014) tested the response of mixed-species biofilms, comprised of *Pseudomonas aeruginosa, Pseudomonas protegens,* and *Klebsella pneumoniae* to their exposure to two antimicrobials—sodium dodecyl sulfate and tobramycin. Compared to single-species biofilms, the mixed-species biofilm was more adept at maximizing and optimizing the use of nutrients to enhance their growth and persistence, which made it more resilient to these antimicrobials. Furthermore, the increased tolerance observed in the mixed-species biofilm was suggested to be a result of a cross protection effect provided by the resistant species to all other members of the microbial community, rather than selecting for the least sensitive species in the biofilm (Lee & others, 2014). The way microorganisms interact within biofilms can indeed influence the spatial organization of the biofilm (see Fig. 3). Liu and others (2016), for instance, described that 1) species exhibiting strong cooperation appear to develop intermixed distributions or layered structures without patchy patterning; 2) in the absence of nutrient or space limitation, species with weak interdependence tend to interspecifically segregate; 3) exploitation by one of the species can result in the formation of layered structures with patchy patterning; and 4) competition appears to lead to an overall decrease in biomass with patchy patterning or interspecific segregation (Fig. 3.1–3.4) (Liu & others, 2016).

Whereas biofilms in the environment can be dominated by a particular species, other secondary species are almost always present. Dominance by one species in a biofilm is determined by: 1) the particular location within the biofilm; 2) the environmental conditions; and 3) the specific stage in the development of the biofilm. In the example of the microbial mat studied from the lithifying stromatolite in the hypersaline Cayo Coco Lagoonal Network, dominance of a particular species varied according to the specific location within the biofilm. The green lamina of the stromatolite (top layer of the biofilm) was dominated by cyanobacteria, whereas deeper layers (mineralized lamina)

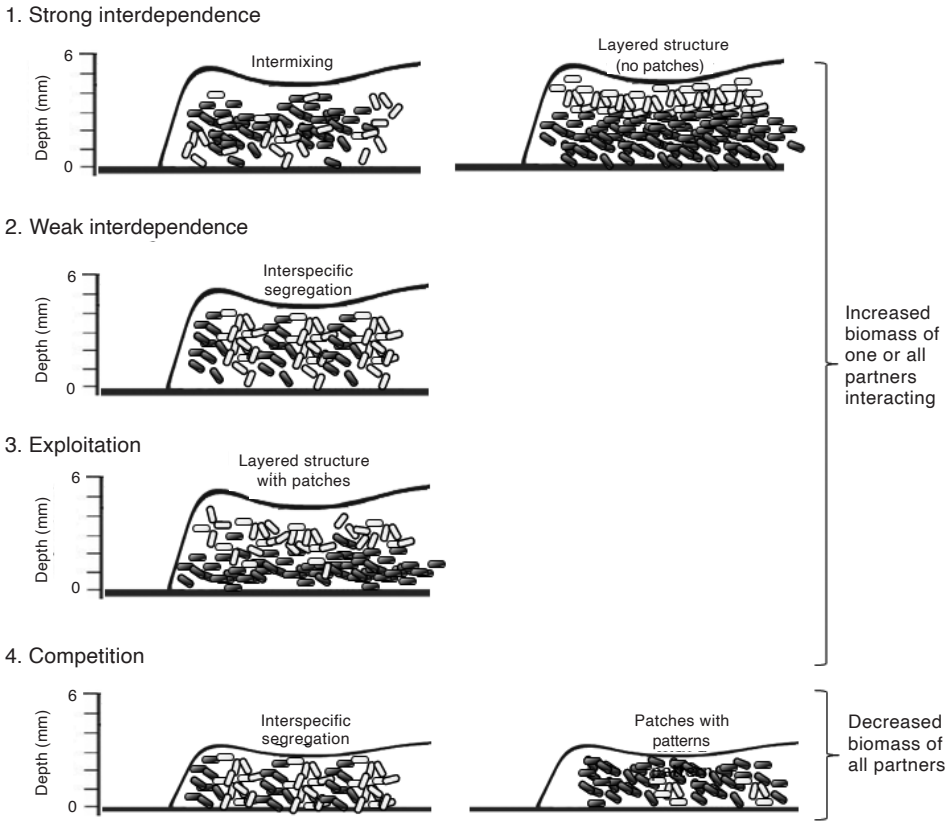

FIG. 3. Cross-species interactions influence the spatial organization of mixed-species biofilms. *1,* Strong interdependence (cooperation) leads to the formation of intermixing or layered structures. *2,* Weak interdependence results in interspecific segregation. *3,* Exploitation results in layered structures with patches. *4,* Competition can lead to species segregation and the formation of patches with patterns. Negative interactions (competition) can result in the overall decrease of biomass (new; based on information in Liu & others, 2016). Color version available in *Treatise Online* 147 (paleo.ku.edu/treatiseonline).

were dominated by purple sulfur (sulfide-oxidizing) bacteria (PACE & others, 2018) (see Fig. 2.1). The development of freshwater phototrophic biofilms can also be influenced by environmental conditions, such as the presence of light (ROESELERS, VAN LOOSDRECHT, & MUYZER, 2007). For instance, under high light conditions, initial colonizers can predominantly consist of green algae, whereas under low light intensities, heterotrophic bacteria tend to colonize. Moreover, over time, as the biofilm matures, filamentous cyanobacteria can become predominant in these phototrophic biofilms (ROESELERS, VAN LOOSDRECHT, & MUYZER, 2007).

BIOFILMS AND MINERAL PRECIPITATION

Microbially induced precipitation of minerals (biomineralization) is a relevant process in various biological, geological, medical, and engineered systems (PHILLIPS & others, 2013). Of importance for the study of the evolution of prokaryotes throughout Earth history, is the understanding of carbonate biomineralization. The formation of carbonate sediments in

different environments (e.g., marine reefs, fluviatile tufas, hot springs, travertines, etc.) seems to be influenced by microbial mineralization.

Various microbial metabolic processes, including photosynthesis, sulfate reduction, urea hydrolysis, ammonification, denitrification, and methane oxidation, affect the solution chemistry of the surrounding environment (e.g., increase carbonate alkalinity, pH values, or dissolved inorganic carbon), which in turn can induce carbonate or other mineral precipitation (Dupraz & others, 2009; Zhu & Dittrich, 2016).

Biomineralization is a common event in microbial mats or biofilms (Braissant & others, 2003; Handley & others, 2008; Shiraishi & others, 2008). Chemical heterogeneity in biofilms can lead to the formation of microenvironments that create gradients of alkalinity and/or supersaturation, which can facilitate mineral precipitation within the biofilm. Furthermore, the presence of EPS in biofilms can influence the biomineralization process by providing nucleation sites for mineral precipitation, regulating the patterns of mineralization and the types of minerals produced (Braissant & others, 2003; Decho, 2010). Certain functional groups in the EPS can inhibit carbonate precipitation: negatively charged groups can bind with mineral ions such as Ca^{2+} and Mg^{2+}, thus, a high binding capacity of the EPS can potentially inhibit carbonate precipitation (Flemming, 1995). Release of cations from the EPS can occur due to EPS degradation or after release from the binding sites through an external trigger (e.g., change in ionic strength, salinity), which can lead to carbonate and other mineral precipitation (Decho, 2010; Dupraz & others, 2009).

As an illustration of the various metabolic processes that can promote mineral precipitation, consider again the example of the stromatolite in the Cayo Coco Lagoonal Network described by Pace and others (2018) (see Fig. 2). As mentioned earlier, stromatolites result from successive cycles of microbial mineralization triggered by the metabolism of biofilm forming microbiota. Pace and others (2018) suggested that mat formation starts with the development of biofilms comprised of coccoid and filamentous cyanobacteria-fixing CO_2, leading to the formation of biomass and the production of O_2 through oxygenic photosynthesis. Oxygenic photosynthesis also consumes CO_2 and increases the pH, which can result in the precipitation of (calcium) carbonates. In the top layer of the microbial mat, aerobic heterotrophs consume O_2; in the anoxic depths, sulfate-reducing bacteria produce HS^- from sulfate. Sulfate reduction can increase carbonate alkalinity (in the form of bicarbonate, HCO_3^-). In an intermediate zone, both sulfide and O_2 are present. Purple sulfur (sulfide-oxidizing) bacteria are involved in recycling the sulfide back to sulfate, and other microbes are involved in this process as well. The microbial activity of cyanobacteria, sulfate-reducing and sulfide-oxidizing bacteria creates a daytime pH maximum, which promotes the precipitation of magnesium calcite from dissolved ions in the lagoon. Mineral precipitates are mostly located at the oxygenic-anoxygenic photosynthetic interface. Figure 2.2 shows the different chemical profiles in the microbial that can be created due to the different microbial activities. The repetition of these series of physicochemical and biological steps along with the upward growth of the biofilm led to the formation of stromatolites in the studied lagoon (Pace & others, 2018).

Pace and colleagues suggested a role of the EPS in the different mineralization steps, hypothesizing that cyanobacterial EPS acts as a binding agent for calcium, thus inhibiting carbonate precipitation in the green lamina of the stromatolite (upper layer of the mat). EPS in the oxic-anoxic zone appears to have a decreased cation-binding capacity, which would make Ca^{2+} more available for carbonate precipitation or indicate that the EPS in these layers is saturated with multivalent cations.

SUMMARY

Most microorganisms persist associated with surfaces in the natural environment, most likely in the form of biofilms. Biofilms are complex microbial communities attached to surfaces and embedded in a matrix of extracellular polymeric substances (EPS). The presence of EPS provides architecture, stability, and protection to the microbial communities within the biofilm. Furthermore, these microbial communities typically contain multiple species that interact with each other and with the environment.

Due to the spatial arrangement of the microbial communities, biofilms develop microenvironments, which result in highly physically, chemically, and biologically heterogeneous arrangements. Biofilm-grown cells can exhibit different phenotypes and change their metabolic activities compared to their planktonic counterparts.

Considering that biofilm-grown cells exhibit characteristics distinct from their corresponding planktonic communities, it is possible that biofilms produce specific marks in the consolidated rock record. Thus, a better understanding of the biofilm way of life can aid in the reconstruction of the evolution of prokaryotes throughout Earth history.

ACKNOWLEDGEMENTS

This work was supported by the Montana University System Research Initiative (51040-MUSRI2015-03), a grant from Montana NASA EPSCoR Research Infrastructure Development, and by the National Science Foundation under Grant #1736255 (BuG ReMeDEE).

MICROBIAL MATS

Pieter T. Visscher, Kimberley L. Gallagher, Anthony Bouton, Emmanuelle Vennin, Christophe Thomazo, Richard A. White III, and Brendan P. Burns

INTRODUCTION

Microbial mats are laminated organosedimentary structures that develop as benthic biofilms in a wide range of aquatic environments (Fig. 4). They are robust, complex ecosystems, primarily comprised of bacteria and archaea, semi-isolated from their immediate environment by a self-constructed matrix of extracellular polymer substances (EPS) (Nicholson, Stolz, & Pierson, 1987). Understanding present-day microbial mat development and preservation is valuable for interpreting signs of life through geologic time. Microbial mats stabilize sediments, precipitate minerals, and typically include remnants of organisms, making them important to the paleontology field. Several processes, such as binding and trapping and *in situ* precipitation of minerals, can lead to complete lithification of microbial mats, forming microbialites,

Microbial mat populations exhibit large metabolic diversities, driven by the availability of various electron donors and acceptors and mediated by environmental controls. Their diverse biochemical pathways convey an extraordinary capacity to fill every available niche. Because the microbial rates utilizing metabolites are higher than the limited diffusion rate afforded by the polymer matrix, elements are recycled rapidly (Des Marais, 2003), and nutrients are contained within the mat.

The difference between microbial mats and biofilms is somewhat indistinct. Although some biofilms are referred to as microbial mats, they do not fit the definition of mats as described here. Microbial mats, while often considered a type of biofilm, are generally thicker, more developed and complex; they host a more diverse microbial community yet exhibit a relatively high degree of structure and permanence, whereas the simplest biofilm could consist of a single bacterial species colonizing any surface, even temporarily (Decho & Gutierrez, 2017; Flemming & Wingender, 2010). The focus of this review is on photosynthetic microbial mats, their composition, diversity, geochemistry, preservation, and significance for paleontological studies.

MICROBIAL MAT DISTRIBUTION

Photosynthetic microbial mats develop in a wide variety of environmental conditions and settings. Modern mat environments include hypersaline lagoons, hot springs, alkaline lakes, open marine, shallow intertidal sediments, salt marshes, and mine tailings (Seckbach & Oren 2010) (Fig. 5). Coherent microbial biofilms also exist in aphotic coastal marine environments (Gallardo, 1977; Schulz & others, 1999), permanently dark environments such as caves (Summers Engel & others, 2004), and deep-sea methane seeps (Paul & others, 2017) and vents (Jørgensen & Boetius, 2007; Crépeau & others, 2011).

A wide range of physicochemical conditions support development of microbial mats. Prior to the evolution of multicellular life, microbial mats developed in the photic zone of shallow aquatic environments (Stal, van Gemerden, & Krumbein, 1985; Dupraz, Reid, & Visscher, 2011; Knoll, 2016), such as hot springs, streams, rivers, and lakes and in the marine environment (Walter, 1976; Grotzinger & Knoll, 1999; Nisbet & Fowler, 1999;

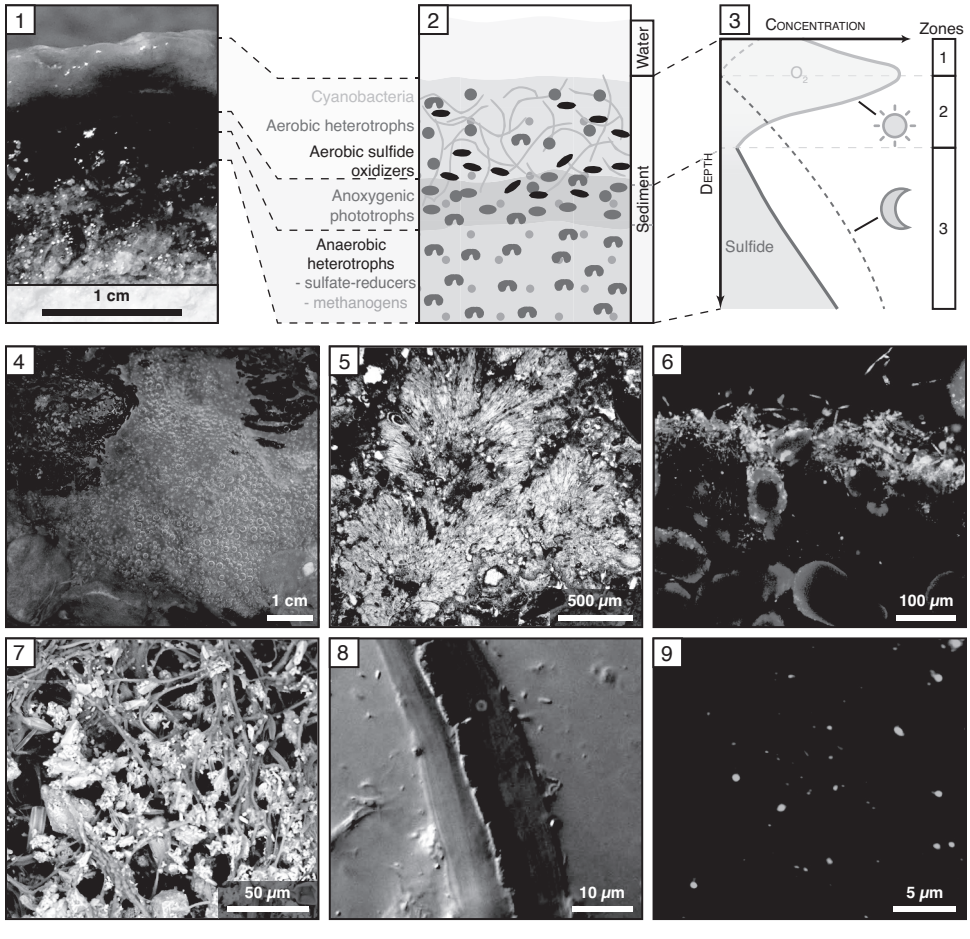

Fig. 4. Typical photosynthetic microbial mat characteristics. *1–3,* Properties of marine photosynthetic mats shown in cross section. *1,* Hand sample of a typical mat, showing exopolymeric substances near the surface. Top surface layer is dominated by cyanobacteria, the red (in color version) layer underneath by anoxygenic purple sulfur bacteria, and the deeper dark-colored sediment at the bottom is the anoxic part of the mat. *2,* Schematic representation showing the depth distribution of the major guilds of mat microbes. These are the key groups involved in element cycling. Note the presence of both sulfate-reducing bacteria and methanogenic bacteria in the oxic surface layer of the mat. *3,* Typical daytime (*solid lines*) and nighttime (*dashed lines*) depth profiles of oxygen (*green in color version*) and sulfide (*purple* in color version). Zones indicated on the right. Zone 1: Permanently oxic during a light-dark cycle; Zone 2: Oxic during the day and anoxic (and sulfidic) during the night; Zone 3: Continuously anoxic. The bottom and top of Zone 2 are defined by the oxic-anoxic (O_2/HS^-) interface during the day and night, respectively (new). *4–9,* Various imaging techniques used to study microbial mats and microbialites. *4,* Top view of a submerged lithifying microbial mat, showing oxygen bubbles at the surface; Great Salt Lake, Utah, USA. *5,* Polarized light petrographic thin section of a fossil microbialite (~14,500–12,500 cal ^{14}C BP) showing bundles of filamentous cyanobacteria (*Gloetrichia*/*Rivularia*-like nitrogen fixing cyanobacteria); pluvial Lake Bonneville; Stansbury Terrace, Oquirrh Mountains, Utah, USA. *6,* Confocal scanning laser microscopic image of a surface mat from a modern marine stromatolite (Highborne Cay, Bahamas) showing autofluorescent cyanobacteria (red; note the endoliths in the lower left of the image), sulfate-reducing bacteria, SRB385 probe (green), $CaCO_3$ ooids (blue) (image courtesy of Alan W. Decho, University of South Carolina, USA, see color image in *Treatise Online* 163. *7,* Scanning electron microscope image of filamentous cyanobacteria precipitating carbonate minerals; Green Lakes, NY, USA. *8,* Filamentous cyanobacterium *Oscillatoria* sp., surrounded by sheath of exopolymer (parallel to the filament) using Nomarski light microscopy; Cabo Rojo, Puerto Rico. *9,* Fluorescence microscopic image of viruses (*small dots*) and coccoid cyanobacteria (*larger dots*), *Synechococcus* spp. from a lithifying microbial mat; Green Lake, New York, USA. All images new. Color images available in *Treatise Online* 163 (paleo.ku.edu/treatiseonline).

Tice & Lowe, 2004; Dupraz & others, 2009; Djokic & others, 2017). The first microbial mats in the early Archean were most likely built by anoxygenic phototrophs (Guitiérrez-Preciado & others, 2018; Visscher & others, 2020). Oxygenic photosynthesis that evolved later, likely in microbial mats, resulted in the Great Oxidation Event (GOE) and allowed the development of multicellular life. Ironically, although the GOE created an opportunity for microbial life to develop and diversify beyond benthic biofilms (Knoll, 2016), it ended hundreds of million years of mats' dominance on Earth. Newly evolved multicellular life forms using aerobic respiration outcompeted mats for resources, such as space and nutrients. This and the burrowing activity and predation of animals (Walter & Heys 1985; Knoll 2016; Bosak, Knoll, & Petroff, 2013) forced mats to extreme environments (Seckbach & Oren, 2010; Dupraz, Reid, & Visscher, 2011). The physicochemical and geochemical conditions that define environments where mats develop today include:

1) *salinity*—0 to >300 ppt (Des Marais, 1995; Roche & others, 2019; Visscher & others, 2010; Preisner, Fichot, & Norman, 2016; Perillo & others, 2019);

2) *temperature*—from below zero (de los Ríos & others, 2015; Peeters & others, 2012; Sumner & others, 2015) to ~72–73°C, possibly short term up to 75°C (Meeks & Castenholz, 1971; Van der Meer & others, 2005; Beam & others, 2016; Bennett, Murugapiran, & Hamilton, 2020);

3) *specific chemical composition of the water and sediments*—iron, arsenic, zinc, copper, mercury, tungsten, sulfide (Pierson, Parenteau, & Griffin, 1999; Härtig & Planer-Friederich, 2012; Méndez-García & others, 2014; Visscher & van Gemerden, 1993; Beam & others, 2016; Fernández & others, 2016; Visscher & others 2020);

4) *hydrodynamics*—quiescent pools to rapidly flowing rivers (Cuadrado, Perillo, & Vitale, 2014; Roche & others, 2019;

5) pH—pH <1 to >9 (Visscher & others, 2010; Härtig & Planer-Friederich, 2012; Méndez-García & others, 2014; Bernstein & others, 2013; Prieto-Barajas, Valencia-Cantero, & Santoyo, 2017;

6) *desiccation* (Potts, 1999; Noffke, 2008; Dupraz, Reid, & Visscher, 2011; Perillo & others, 2019);

7) *light regime*—intensity of photosynthetically active radiation, <1 to >2000 $\mu E.m^{-2}.s^{-1}$ (Jørgensen, Cohen, & Des Marais, 1987; Visscher & others, 1998; Fernández & others, 2016);

8) *UV radiation*—<1 to 64 $W.m^{-2}$ (Farias & others 2017; Visscher & others, 2020);

9) *nutrient availability*—eutrophic to oligotrophic (Paerl, Joye, & Fitzpatrick, 1993; Pinckney, Paerl & Fitzpatrick, 1995; Rejmankova & Komárková, 2000; Smith & others, 2010; Varin & others, 2011; Kohler & others, 2016).

In summary, contemporary microbial mats have adapted to exist in many diverse environments where they often cope with multiple extremes such as alkaline and hypersaline conditions, elevated heavy metals concentrations and low pH, high UV radiation, arsenic and sulfide concentrations, and permanent anoxia. They have been successful in adapting to environments inhospitable to most multicellular life in many different geographic settings, thriving in early Earth environments and changing over time for billions of years.

THE ROLE OF SUBSTRATE IN MAT DEVELOPMENT

The development of microbial mats is influenced by physical and chemical properties of the substrate, which has major implications for their preservation (Roche & others, 2019). Some physical properties that affect mat development are grain size and sediment stability. For example, filamentous cyanobacteria form mats faster on the fine fraction (<125 μm) than on larger particle sizes (Rozenstein & others, 2014). The absence of microbialites developing on mud, silt, or sand in streambeds of rivers is due to a low lithification potential of microbial mats in these conditions (Roche & others, 2019). Harder and more extensive substrates

result in more stable microbialites (Moore & Burne, 1994). Increasing roughness of the substrate enhances the growth rate of microbial mats and microbialites (Tuchman & Stevenson, 1980). Turbulence and flow velocity over the microbialite surface affect the colonization of grazers, such as ciliates (Primc-Habdija, Habdija, & Plenkovic-Moraj, 2001). In addition, the chemical composition of the substrate may affect the colonization by microbial communities, the ability to mineralize, and preservation potential (Gradzinski, 2010; Chafetz, Rush, & Utech, 1991; Parsiegla & Katz, 2000). For example, microbial deposits grow faster on a limestone substrate than on elemental copper, due to the toxicity of the metal (Parsiegla & Katz, 2000). However, the effects of physical (roughness) and chemical properties of the substrate on mat adherence are often difficult to separate (Diaz & others, 2007).

BIOGEOCHEMISTRY

Chemical and physical environmental conditions determine the initial composition of the microbial community (Baas Becking, 1934). The metabolisms of this pioneer microbial community in turn change the microenvironmental conditions. This creates a feedback that likely affects the community metabolism and/or composition, possibly leading to a predictable oscillation (Dupraz & others, 2009). In a photosynthetic microbial mat lacking major disturbances, this results in a community adapted to extreme diel fluctuations (between daylight and nighttime conditions) of oxygen, sulfide, and pH (see Fig. 4.3).

THE MICROBIAL MAT COMMUNITY

Within microbial mats, biogeochemical processes can be described by a small number of functional groups or guilds, including oxygenic and anoxygenic phototrophs, aerobic chemoorganoheterotrophs, chemolithoautotrophic sulfur oxidizers, fermenters, and anaerobic chemoorganoheterotrophs (notably sulfate reducers and methanogens; see Fig. 4) (van Gemerden 1993; Ward & others, 1998; Decker & others 2005; Taffs & others, 2009; Pace & others, 2018). Their actual diversity is extremely high, exceeding 4,000 operational taxonomic units (OTUs) (Ley & others, 2006; Baumgartner, Dupraz, & others, 2009; Baumgartner, Spear, & others, 2009; Armitage & others, 2012; Bolhuis, Cretoiu, & Stal, 2014; Wong, Ahmed-Cox, & Burns, 2016). Interactions between mat-inhabiting organisms have been described in detail in several laboratory studies (e.g., De Wit & van Gemerden, 1987; Visscher & others, 1992; Caumette, 1993; Van den Ende, Laverman, & van Gemerden, 1996; Massé, Pringault, & de Wit, 2002; Müller & Overmann, 2011), and the effect of their combined metabolic activities on geochemistry of the mat has been measured *in situ* (e.g., Revsbech & others, 1983; Visscher, Taylor, & Kiene, 1995; Visscher & others, 1998, 2003, 2010, 2020; Ferris & others, 1997; Jonkers & others, 2003; Wieland & others, 2005, Pace & others, 2018; Maegaard, Nielsen, & Revsbech, 2017). Field measurements using microelectrodes demonstrate the dynamic nature of photosynthetic mats (Jørgensen, Cohen, & Revsbech, 1986; De Wit & others, 1989; Kühl, Lassen, & Jørgensen 1994; Visscher & van Gemerden, 1993), and oxygen and sulfide concentrations and depth distribution fluctuate vastly over a diel cycle (see Fig. 4.3).

EFFECT OF LIGHT REGIME AND PHOTOTROPHY

Layering within the microbial mat is a consequence of the changes in available light with depth (Jørgensen, Cohen, & Des Marais, 1987). Light of longer wavelengths penetrates deeper into the sediment, with near infrared penetrating the deepest, typically >1 cm (Kühl & Fenchel, 2000). This differential irradiance penetration accommodates a discrete vertical distribution of oxygenic and anoxygenic photosynthetic

organisms with light harvesting pigments that absorb different parts of the light spectrum. For example, cyanobacteria near the surface are oxygenic phototrophs with chlorophylls, phycobilins, carotenoids, xanthophyll pigments absorbing light between ~500 nm and 700 nm. Some cyanobacteria in microbial mats contain chlorophyll *d* and *f*, absorbing light in the far-red spectrum and are able to survive in environments with little photosynthetically active radiation (Ohkubo & Miyashita, 2017). Green and purple (non)sulfur bacteria are anoxygenic phototrophs constrained to deeper layers and use bacteriochlorophyll pigments (green bacteria: ~680–820 nm; purple bacteria: 820–150 nm) and carotenoids (absorbing around 500–600 nm) (van Gemerden & Mas, 1995). Some anoxygenic phototrophs contain bacteriochlorophyll *b*, which can absorb infrared light of 1050 nm. The extracellular polymer substances (EPS) themselves typically do not absorb visible wavelengths and even promote the downward (i.e., forward) scattering of light into a mat, which is the so-called biofilm gel effect (Decho & others, 2003).

Oxygenic photosynthesis occurs in the upper layers and is accompanied by a strong peak of oxygen production during daylight (Fig. 4.1–4.3). It uses two photosystems and electrons from water. In contrast, anoxygenic photosynthesis generally occurs deeper in the mat. It depends on one photosystem and utilizes other electron donors, typically sulfide and other reduced sulfur compounds, although H_2, Fe(II), NO_2^- or As(III) may also be used to supply electrons for photosynthesis (Hamilton, 2019). Because water is not the electron donor, oxygen is not produced.

Oxygenic and anoxygenic phototrophs, as well as chemolithoautotrophs (e.g., sulfide oxidizing bacteria), are the primary producers of the microbial mat ecosystem, fixing CO_2 carbon and producing biomass. In most contemporary mats, benthic cyanobacteria are the dominant phototrophs. Cyanobacteria in microbial mats can photosynthesize under extremely low light intensities, as low as 1 $\mu E.m^{-2}.s^{-1}$ (Jørgensen, Cohen, & Des Marais, 1987). Consequently, the peak of photosynthetic activity during the early afternoon is not at the surface, but just beneath it, typically at 1–2 mm depth (van Gemerden, 1993; Dupraz, Reid, & Visscher, 2011). Microbial filaments, typically cyanobacterial, weave together to form a coherent organic sediment, for which the designation mat is given. Biomass produced during autotrophy fuels a community of heterotrophic organisms that recycle the organic carbon (cellular material, EPS, and exudates of photorespiration like glycolate; Fründ & Cohen, 1992; Bateson & Ward, 1988) to yield metabolic energy and, to a lesser extent, provide building blocks for biomass. In marine and hypersaline microbial mats, the two major pathways of organic carbon oxidation are aerobic respiration and sulfate reduction (O_2 and SO_4^{2-} respectively, as electron acceptors; Fründ & Cohen, 1992; Visscher & others, 1998; Pace & others, 2018; Wong & others, 2018). Sulfate reduction (discussed in detail later) yields hydrogen sulfide as a metabolic product, which is used by anoxyphototrophs and colorless sulfide-oxidizing bacteria. Depth profiles of oxygen and sulfide concentrations fluctuate over a diel cycle (Fig. 4) (De Wit & van Gemerden, 1987; Dupraz & Visscher, 2005) as oxygen is only produced during daylight, and sulfide production continues in the dark (provided there is sufficient electron donor, e.g., organic carbon or H_2). The deeper mat layers are permanently anoxic, an intermediate depth zone is oxic during the day and anoxic during the night, and a thin surface layer is mostly oxic due to O_2 diffusion from the overlying water or atmosphere and, in daylight, from production by oxygenic photosynthetic organisms below (De Wit & others, 1989; Visscher, Beukema, & van Gemerden, 1991, Visscher & others, 1998). The vertical compartmentalization of the different types of phototrophy results in different availabilities of

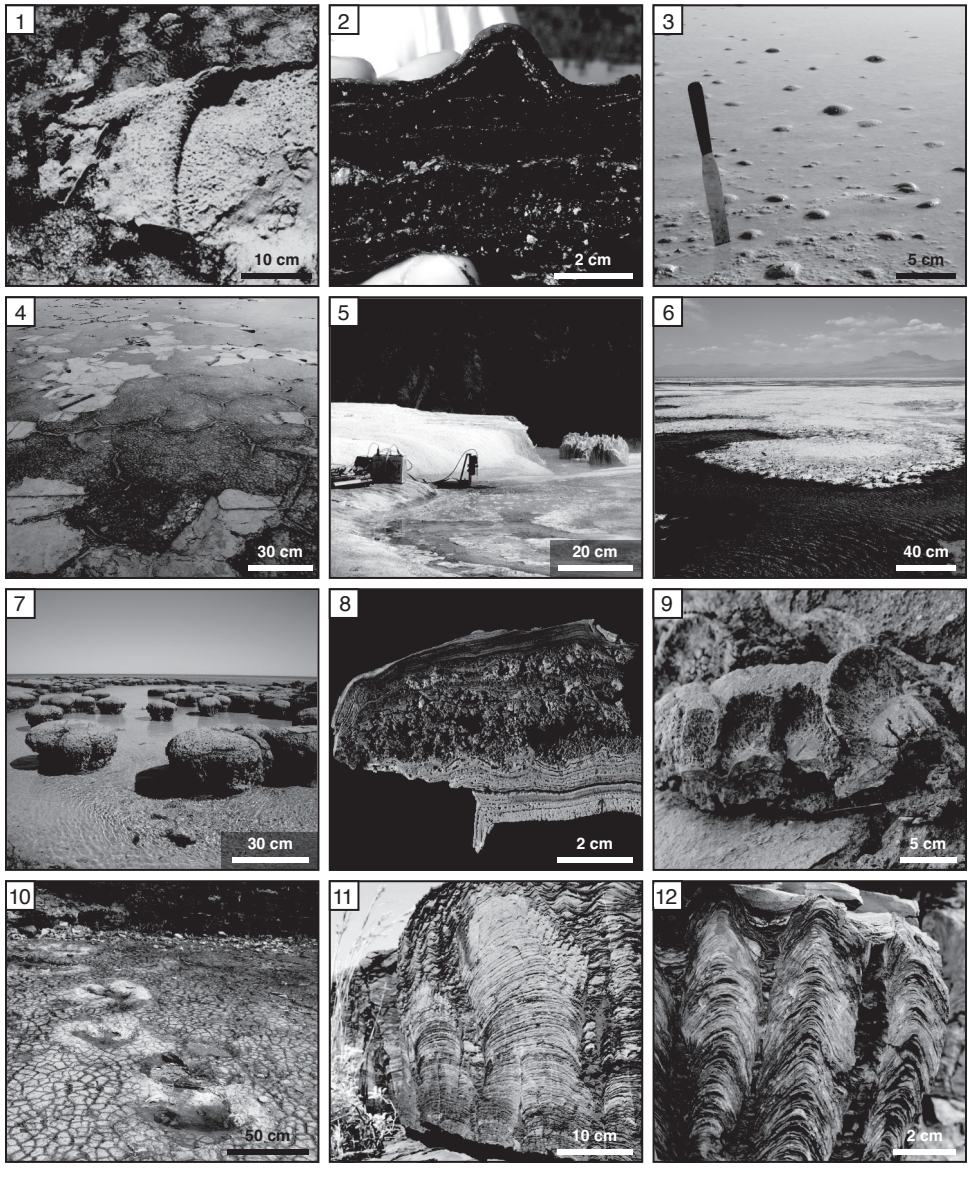

FIG. 5. Examples of contemporary (living) microbial mats (*1–6*), surface mats associated with microbialite structures (*7–8*), and recent and fossil microbialites of various ages (*9–12*) in diverse habitats. *1,* Top view of a temperate intertidal microbial mat showing the green cyanobacterial (*Microcoleus* sp.) surface with trapped sand and purple sulfur bacteria (*Thiocapsa* sp.) underneath; Orkney Islands, Scotland, UK. *2,* Cross section of a hypersaline, gelatinous mat with trapping and binding and *in situ* precipitation of carbonate minerals; Big Pond, Eleuthera, Bahamas. *3,* Microbial mat surface showing gas bubbles, in this particular case of trapped methane. The mat is lifting, showing the filamentous nature of the mats. Trapped sediment and extracellular polymer substances provide a gas-tight seal. This mat undergoes frequent salinity fluctuations from 35 ppt to 350 ppt; Cabo Rojo, Puerto Rico. *4,* Hypersaline mat that experiences wetting-drying (desiccation) cycles. During extensive dry periods, polygonal cracks form that often fill with exopolymeric substances. Recolonization and regrowth following wetting takes place within hours to days; James Pond, Eleuthera, Bahamas. *5,* Mats associated with a hydrothermal spring (72°C, the maximum temperature supporting photosynthesis) near a travertine platform; Mammoth Hot Spring, Montana, USA; image taken during microelectrode measurements. *6,* Permanently anoxic high-altitude microbial mats,

(*continued on facing page*)

FIG. 6. Global distribution of microbial mats and microbialites. Both living and fossil photosynthetic microbial mats and microbialites are present in terrestrial and marine settings across the planet within the shallow aquatic environments (including hot springs, lakes, rivers, the intertidal and subtidal zone of coastal marine environments). This is not meant to be a complete survey but merely to show the extensive geographic dispersal pattern of mats and microbialites.

electron donor, primarily low-molecular weight carbon and H_2, and electron acceptors. This generates characteristic steep geochemical gradients of O_2, sulfide, and pH that fluctuate depending on the available light (Fig. 4).

ELEMENT CYCLING

Microbial mats are among the most productive ecosystems on Earth, with extremely high rates of element cycling (JØRGENSEN, 2001), especially the major elements—carbon (C), oxygen (O), and sulfur (S) (CANFIELD & DES MARAIS, 1993) and, depending on the environment, nitrogen (N), arsenic (As), iron (Fe), and hydrogen (H) (EMERSON & REVSBECH, 1994; JOYE & PAERL, 1994; VISSCHER & others, 1998, 2020; DESNUES & others, 2007). The carbon cycle in microbial mats is coupled to other element cycles, such as O, S, N, Fe, and As (Fig. 7.1–7.3). Reduction of CO_2 is coupled to phototrophic oxidation of H_2O, HS^-, NO_2^-, Fe^{2+}, or As^{3+}. In turn, oxidation of organic carbon, including methane, is coupled to reduction of O_2, SO_4^{2-}, NO_3^- (producing mainly N_2), Fe^{3+} or As^{5+}. In most modern marine mats, sulfate is abundant relative to other electron acceptors, and respiratory processes rely mainly on O_2 and SO_4^{2-} as electron acceptors (Fig. 7.1) (VAN GEMERDEN, 1993). In non-marine environments, other available electron acceptors may be used preferentially. Iron cycling (Fig. 7.3) is abundant in some hot-spring mats (PIERSON, PARENTEAU, & GRIFFIN, 1999)

(*continued from facing page*) comprising purple-sulfur bacteria (anoxygenic phototroph *Ectothiorhodospira* sp.), cycling sulfur and arsenic; La Brava, Atacama, Chile. *7,* Intertidal living stromatolites; Hamelin Pool, Shark Bay, Australia. *8,* Cross section of a living hypersaline microbialite; Great Salt Lake, Utah, USA. The surface fabric is laminated (stromatolitic) with a clotted (thrombolitic) fabric underneath. *9,* Fossil microbial crust capping Cambrian rocks, (30,000–28,000 cal ^{14}C BP); Buffalo Terrace, Lake Bonneville, Utah, USA. The fabric of the inner part is laminated while the outer part depicts a clotted mesofabric. The microbialite displays a cauliflower-like macrofabric. *10,* Fossilized microbial mat showing mud cracks and dinosaur tracks, Late Jurassic; Loulle section, France. *11,* Outcrop showing fossil stromatolites (2.72 Ga), Meentheena Member, Tumbiana Formation, Australia; *12,* Fossil egg carton-like stromatolites; Meentheena Member, Tumbiana Formation, Australia. All images new, contributed by authors. Images *11* and *12,* courtesy of Dr. David Flannery, Queensland Institute of Technology, Australia. Color images available in *Treatise Online* 163 (paleo.ku.edu/treatiseonline).

and seeps (Emerson & Revsbech, 1994). Denitrification contributes to respiration in some mne and hypersaline mats (Joye & Paerl, 1994; Bouton & others, 2020), and arsenic cycling (Fig. 7.3) occurs in mats surrounding alkaline lakes (Hoeft & others, 2010; Visscher & others, 2020).

The distribution of aerobic and anaerobic chemoorganoheterotrophs depends on availability of reactants for their redox reactions. Both types of heterotrophs prefer to be in close proximity to cyanobacteria, which are typically the main carbon-fixing organisms in the mat. There they compete for organic carbon and hydrogen electron donors. Fermentation and other partial degradation pathways of complex carbon molecules support methanogens, acetogens, and sulfate reducers (Megonigal, Hines, & Visscher, 2003). A common misconception is that methanogens and sulfate reducers are confined to deeper anoxic layers. In fact, they frequently display maximum metabolic rates in the oxic zone of the mat (Canfield & Des Marais, 1991; Fründ & Cohen, 1992; Visscher, Prins, & van Gemerden, 1992; Hoehler, Bebout, & Des Marais, 2001; Buckley, Baumgartner, & Visscher, 2008). These anaerobes require physiological adaptations or formation of consortia to survive in the presence of oxygen. For example, sulfate-reducing bacteria (SRB) form microcolonies (Postgate, 1979; Petrisor & others, 2014), the center of which could be anoxic; or they form consortia with sulfide-oxidizers that remove the toxic oxygen by reaction with sulfide (Decho, Norman, & Visscher, 2010). Alternatively, some SRB can actually use oxygen or nitrate (Dilling & Cypionka, 1990; Sigalevich & others 2000; Baumgartner & others, 2006) or disproportionate intermediate sulfur compounds independent of O_2-sensitive enzymes (Bak & Pfennig, 1987). SRB can also survive by forming spores (Cypionka, Widdel, & Pfennig, 1985). Sulfate reducers and methanogens are at an energetic disadvantage compared to aerobes but can compete where organic carbon is in abundance (near cyanobacteria) and have an advantage at night when anoxic conditions prevail.

Chemolithoautotrophy is another metabolic strategy important to element cycling, notably through organic carbon production, and is common in microbial mats. It is supported by high concentrations of reduced sulfur compounds (thiosulfate, polysulfides, polythionates, zero-valent sulfur, etc.; Steudel & others, 1990; Visscher & van Gemerden, 1993; Findlay, 2016) and to some extent by H_2, NH_4^+, and Fe^{2+} (Visscher & Stolz, 2005; Fan, Bolhuis, & Stal, 2015; Chan & others, 2016). Sulfide oxidizing bacteria perform chemolithotrophic sulfide oxidation at the interface of O_2 and S^{2-}, but they can also use a range of intermediate sulfur compounds, including organosulfur compounds with oxygen and alternatively nitrate as electron acceptor (Kelly, 1982; Visscher & van Gemerden, 1993; Van den Ende & van Gemerden, 1993). Some purple sulfur bacteria can grow as chemolithotrophic sulfur oxidizers (De Wit & van Gemerden, 1987), thereby enhancing their competitive position in the mat ecosystem and even outcompete colorless sulfur bacteria (Visscher & others, 1992). H_2 is sometimes produced to release excess reducing equivalents (Burrow, Chaplen, & Ely, 2011), especially under anoxic conditions. Most of this is rapidly scavenged by sulfate reducers (Nielsen, Revsbech, & Kühl, 2015), but methanogens and acetogens can also use H_2 (Megonigal, Hines, & Visscher, 2003). Both hydrogen- and sulfur-oxidizing chemolithotrophs are generally autotrophs and, thus, can contribute to the primary production in the mats.

Other sulfur compounds have a role in microbial mats and are important in global sulfur cycling and climate regulation. Dimethylsulfoniopropionate (DMSP) is a non-competitive solute that also acts among others as an osmolyte and cryoprotectant. DMSP is present in some cyanobacteria and is the precursor to dimethyl sulfide (DMS)

in microbial mats (Fig. 7.1) (Visscher & van Gemerden, 1991; Vogt & others, 1998). DMS is further consumed by aerobic heterotrophs (methylotrophs), sulfate reducers, colorless sulfur bacteria, and methanogens (Visscher & Kiene, 1994; Visscher, Taylor, & Kiene, 1995; De Zwart & Kuenen, 1997). DMS and several thiols can be used as electron donors for photosynthesis in purple sulfur bacteria (Visscher & van Gemerden, 1991; Visscher & Taylor, 1993). DMS photooxidation yields dimethylsulfoxide, which is a common electron acceptor in marine mats (Taylor & Kiene, 1989). Importantly, the emission of volatile methylated sulfur compounds to the atmosphere has a significant role in climate regulation (Lovelock, Maggs, & Rasmussen, 1972; Kiene & others, 1996) by producing a cloud of condensation nuclei. Through the production and consumption of methylated sulfur compounds, methane, and carbon dioxide, microbial mats may therefore have played an important role in climate regulation through geologic time.

The nitrogen cycle (Fig. 7.2) provides metabolic energy but also has a critical role in biomass production. Nitrogen is typically a growth-limiting nutrient in the marine environment, and by fixing atmospheric N_2, various microorganisms in the mat enhance nitrogen supply (Steppe & others 1996; Paerl, Fitzpatrick, & Bebout, 1996; Steppe & Paerl, 2002; Olson, Litaker, & Paerl, 1999). The breakage of the triple bond of N_2 is energetically costly, and thus the capacity for nitrogen fixation is most prevalent in oxygenic and anoxygenic phototrophs. However, heterotrophs, including some clostridia, hyphomicrobia, azotobacters, sulfate reducers, and methanogens are also capable of nitrogen fixation in microbial mats (Fan, Bolhuis, & Stal, 2015; Finke & others, 2019). As biomass is degraded, ammonia can be released and either assimilated or used as an electron donor in energy metabolism. Chemolithotrophic oxidation of ammonium takes place during a two-step nitrification process, which has been found in coastal microbial mats (Fan, Bolhuis, & Stal, 2015; Bonin & Michotey, 2006). Under anoxic conditions, ammonium can be oxidized to N_2 with NO_2^- (anammox) (Jaeschke & others, 2009) or with sulfate (sulfammox) (Rios-Del Toro & others, 2018). However, the sulfammox reaction may be carried out by a consortium of different microbes (Bi & others, 2020). Nitrate can be assimilated into cell material or used as an electron acceptor for respiration with organic carbon and reduced sulfur. Based on ^{15}N-labeled isotope experiments, anammox is thought to be insignificant in intertidal mats (Bonin & Michotey, 2006), but may be prevalent in hot spring mats (Jaeschke & others, 2009). Nitrogen-containing compounds glycine betaine and ectoine are among common osmolytes in hypersaline mats (Oren, 1990; Stal & Reed, 1987; Welsh & others, 1996; Karsten, 1996; Wong & others, 2018). Ectoine transformations yield various amino acids, and ultimately ammonium as a degradation product (Reshetnikov & others, 2020). Glycine betaine catabolism produces trimethylamine (Oren 1990), a non-competitive compound that supports methanogenesis in mats (King, 1988; Orphan & others, 2008).

Concentrations of arsenic in microbial mats have been associated with biogenic metals: zinc (Zn), manganese (Mn), and copper (Cu) following early diagenesis (Sforna & others, 2017), indicating a biological role for this metalloid. In fact, arsenic provides a biogeochemical alternative to sulfur and iron (Fig. 7.3). Arsenite (As(III)) can be used as an electron donor for photosynthesis by some purple and green (non)sulfur bacteria (Kulp & others, 2008; Summers Engel, Johnson, & Porter, 2013; Hoeft McCann & others, 2016) and anaerobic denitrifying microbes (Oremland & Stolz, 2003). Arsenate (As(V)) is a product of As(III) oxidation, and can be used as an electron acceptor for the oxidation of organic carbon, H_2 or H_2S (Oremland & others, 2000; Hoeft & others, 2004). The

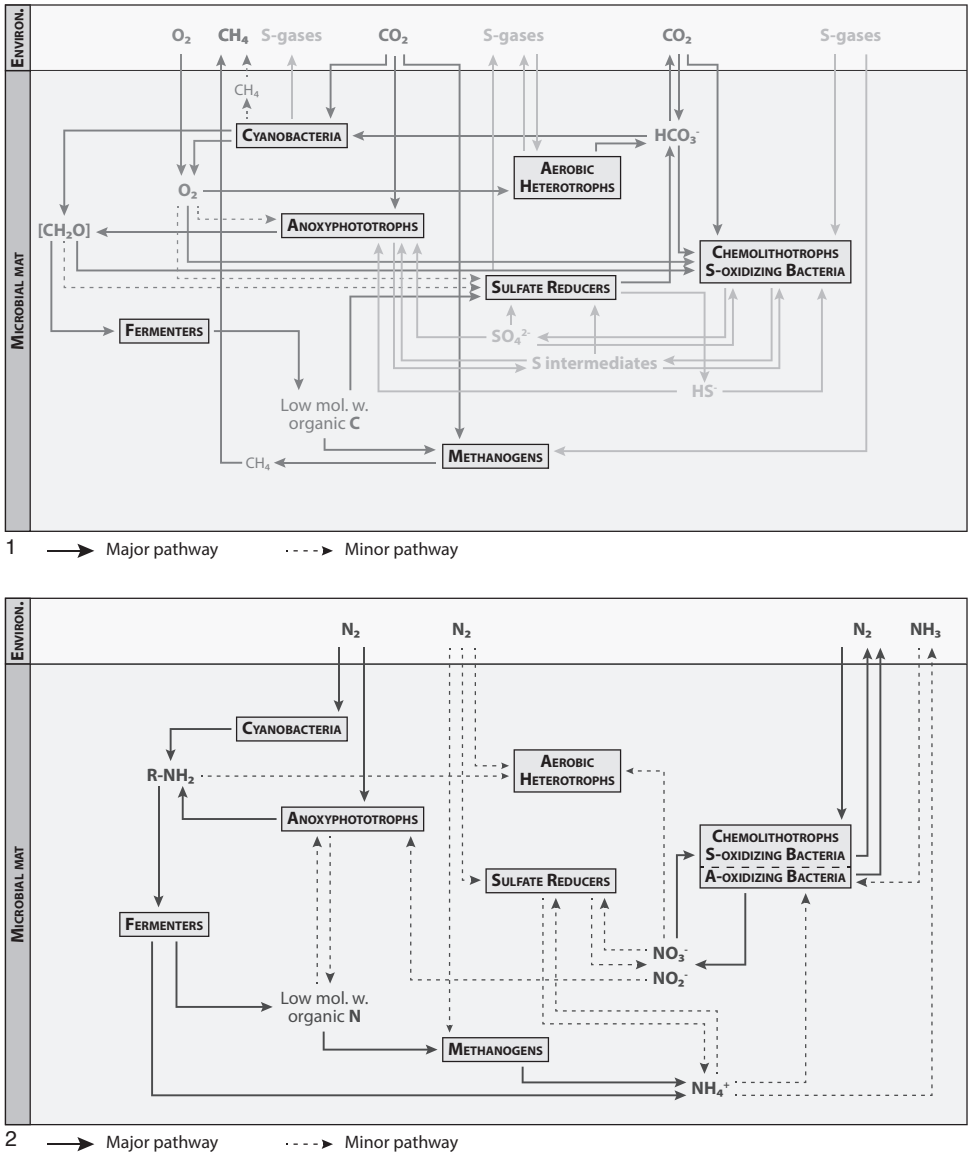

FIG. 7. Major element cycles in microbial mats showing intimate interactions between key guilds of microbes. *Solid lines* depict major biogeochemical transformations, *dashed lines* are minor pathways and *dot/dashed lines* are detoxification mechanisms (*3*). *1,* Cycles of oxygen and sulfur, the main elements supporting carbon cycling in modern photosynthetic microbial mats. *2,* Nitrogen cycling. *3,* Iron and arsenic cycling (on facing page).

presence of both As(III) and As(V) oxidation states in microbialites suggests that complete arsenic cycling could be involved in the lithification of these structures in Laguna Diamante, Argentina (SANCHO-TOMÁS & others, 2020). Arsenotrophic photosynthesis and arsenate-supported respiration may have existed before the GOE, supported by the association of arsenic with organic carbon globules in the 2.72-billion-year-old domal stromatolite laminae in the Tumbiana Formation in Australia (SFORNA & others, 2014).

At Laguna La Brava Atacama, Chile, mats proliferate under permanent anoxic condi-

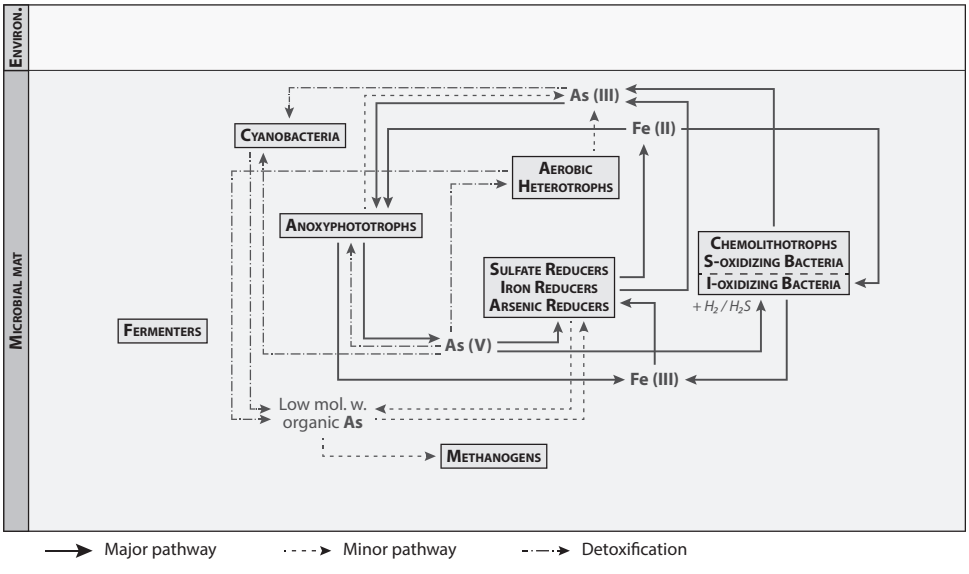

Fig. 7. (*continued*).

tions, using arsenic and sulfur cycling instead of oxygen (Visscher & others, 2020). Arsenic and sulfur cycles may have co-evolved. Several strains of phototrophs (e.g., *Ectothiorhodospira* sp.; Hoeft McCann & others, 2016; Visscher & others, 2020) that can use arsenite also use reduced sulfur compounds as electron donors. Similarly, known arsenate-respiring bacteria also use sulfate as an electron acceptor.

MICROBIAL DIVERSITY

Microbial mats are considered as functionally (van Gemerden, 1993) or biogeochemically simple ecosystems (Des Marais, 1995; Prieto-Barajas, Valencia-Cantero, & Santoyo, 2017), yet are very complex in their diversity and function at the genomic level (Kunin & others, 2008; Varin & others, 2011; Bonilla-Rosso & others, 2012; Khodadad & Foster, 2012; Bolhuis, Cretoiu & Stal, 2014; Ruvindy & others, 2015; White III & others, 2016; Babilonia & others, 2018; Wong & others, 2018, 2020). Over past decades, microbial diversity based on 16S rDNA sequencing has been studied extensively in a variety of microbial mats (Ley & others, 2006; Baumgartner, Dupraz & others, 2009; Bolhuis & Stal, 2011; Armitage & others, 2012; Farias & others, 2014, 2017; Cardoso & others, 2017; Louyakis & others, 2017; Greco & others, 2020) and estimates of operational taxonomic units (OTUs) typically present confirm that these ecosystems are in fact quite complex. In addition to diversity studies at the taxonomic level, several metagenomes of mats have also been assembled, providing a wealth of functional information. Previous metagenome-based studies may have targeted only specific ecophysiological responses (Varin & others, 2011, Lopéz-Lopéz & others, 2013; Mendes-Monteiro & others, 2019; Aubé & others, 2020) or had limited sequencing depth (Bolhuis, Cretoiu & Stal, 2014; Wong, Ahmed-Cox, & Burns, 2016). Furthermore, these studies generally lacked a clear biogeochemical context (Breitbart & others, 2009; Mobberley & others, 2015; Paul & others, 2017).

With advances in taxnomics, studies linking microbial diversity to mat function are beginning to develop. The spatial and/or temporal resolution of microbial diversity (i.e., species composition) in relation to selective geochemical data has been investigated at a few specific sites (Ley & others,

2006; Baumgartner, Dupraz & others, 2009, Baumgartner, Spear, & others, 2009; Visscher & others, 2010; Farias & others, 2014, 2017; Louyakis & others, 2017; Fernández & others, 2016), yet only a few metagenome studies with a similar focus exist (Breitbart & others 2009; Mobberley, Khodadad, & Foster, 2013; Wong & others, 2018; Paul & others, 2017). Metatranscriptomes of mats are even more sparse and suffer from the same shortcomings as those for metagenomes (Liu & others, 2011; Mobberley & others, 2015; Louyakis & others, 2017; Hörnlein & others, 2018; Campbell & others, 2020). However, studies at the metagenomic/metatranscriptomic level have the potential to delineate key microbial interactions and the role of gene transfer as well as identify novel organisms and pathways in microbial mat systems.

One intriguing area opened up through omic studies in microbial mats is that of understanding so-called microbial dark matter in these systems. Microbial dark matter is defined as the many unculturable community members in an ecosystem, and represents a huge untapped resource of biological information (Rinke & others, 2013). In the case of microbial mats, understanding the ecological roles of this dark matter is crucial for a complete understanding of the functioning of these systems through space and time. The only in-depth study on microbial dark matter in mats was undertaken in Shark Bay in Australia (Wong & others, 2020), with 115 potentially novel metagenome-assembled genomes affiliated with dark matter described. Detailed analyses of metabolic pathways allowed putative inferences about the roles of these microbes in recycling organic carbon and the potential for H_2, ribose and CO/CO_2 to become major energy currencies. Understanding these metabolic pathways may even provide key insights into the origin of eukaryotes (Wong & others, 2020). Indeed, a novel group of archaea—the Asgard archaea—represents the closest lineage of the archaeal ancestor of eukaryotes (Spang & others, 2015). The highest abundances of Asgard archaea found so far anywhere in the world are in microbial mats (Wong & others, 2018; Wong & others, 2020).

Viruses are another crucial component of microbial mats. Although modern sequencing approaches have helped our understanding of viral diversity and metabolisms in modern microbial mats and microbialites, their role through geologic time remains elusive. The virome of modern microbialites was first described by comparing viral communities in marine (Highborne Cay, Bahamas) and freshwater (Pozas Azules II and Rio Mesquites, Mexico) microbialites (Desnues & others, 2008). This study suggested some viruses appeared to be endemic to a given microbialite system, indicating biogeographical variability from one microbialite to another (Desnues & others, 2008). In a study on Pavillion Lake (British Columbia, Canada) microbialites (White III & others, 2016), most of the viruses within the microbialites were unclassified, consistent with earlier observations (Desnues & others, 2008). Interestingly, although the water column of Pavillion Lake had a great abundance of viruses, predominantly comprised of T4-like cyanophage (e.g., *Myoviridae*) and large algal viruses (e.g., *Phycodnaviridae*), few viral sequences were found within the microbialites. Instead, large numbers of antiviral phage genes were present (e.g., CRISPR-cas and phage shock proteins), suggesting that microbialites inhibit viral infection from the water column and surrounding sediments (White III & others, 2016). Similarly, a study of viruses in Shark Bay (Australia) stromatolites (White III & others, 2018), revealed few viral sequences and abundant antiviral genes (BREX, CRISPR-cas, DISARM).

The precise role of viruses in microbial mats is not known, although it is thought they may modulate microbial diversity or affect ecosystem function through the recycling of essential nutrients. Most recently, some have proposed that viruses may be key players in regulating the transition from

soft microbial mat to hard stromatolite (White III, Visscher, & Burns, 2021), including through mechanisms affecting carbonate precipitation and possibly also mineral composition (Perri & others, 2017; Slowakiewicz & others, 2021). Similarly, viruses may have influenced, transformed, and manipulated ancient microbial communities. Understanding the role of viruses in microbialites is needed to fully understand key biological processes and pathways relevant to early life on Earth, as well as to better interpret mineral biosignatures.

THE EXOPOLYMERIC MATRIX

All mats, including photosynthetic ones, typically form a slimy biofilm matrix. Large amounts of extracellular polymeric substances (EPS) excreted by cyanobacteria (Klock & others, 2007; Rossi & De Philippis, 2015) and other mat inhabitants (Braissant & others, 2007) make the microbial mat gelatinous and sticky. These EPS consist of polysaccharides, proteins, with small amounts of extracellular DNA, exoenzymes, trace metals and minerals. EPS facilitate adhesion to surfaces such as sediments (Grant & Gust, 1987; Yallop & others, 1994), protect the cells against desiccation and UV radiation, sequester nutrients such as essential trace metals, localize and facilitate cell-to-cell communication (quorum sensing) (Decho, 2015), and support gliding motility within the mat for phototaxis in cyanobacteria, and chemotaxis in sulfide-oxidizing bacteria. The EPS matrix also protects the organisms within by reducing predation and trapping viruses (Decho & Gutierrez, 2017; White III, Visscher, & Burns, 2021). The chemical composition of EPS varies with environmental conditions, microbial community, and biofilm maturity. Some EPS components such as uronic acids provide binding sites for calcium and other ions, potentially enhancing carbonate mineral precipitation (Dupraz & others, 2004; Decho, Visscher, & Reid, 2005; Braissant & others, 2007; Gallagher & others, 2011). The presence of authigenic minerals within the EPS matrix indicates its pivotal role in carbonate precipitation.

LITHIFICATION

Some microbial mats trap and bind sediments and skeletal grains and precipitate minerals directly within the polymer matrix (Dupraz & Visscher, 2005) or intracellularly (Couradeau & others, 2012). Over time, these minerals cement together, resulting in lithification, and enhanced potential for preservation of the mat morphology in the fossil record (Dupraz & others, 2009; Riding, 2011a; Finke & others, 2019). The oldest lithified examples of mats are stromatolites (Walter, Buick, & Dunlop, 1980), some arguably ~3.7 billion years old (Fig. **5**) (Nutman & others, 2016; Allwood & others, 2018; Shapiro & Wilmeth, 2020, see p. 56–60).

Another type, microbially-induced sedimentary structures (MISS), develop as a response of microbial mats to sediment dynamics (Noffke & Awramik, 2013; see p. 71–90). Carbonate precipitation and silicification of MISS can result in long term preservation of these sedimentary structures (Noffke, 2008; Fischer & Fralick, 2020), some dating back to 3.48 (Noffke & others, 2013) and 3.47 billion years (Hickman-Lewis & others, 2018), respectively.

CARBONATE SYSTEMS

Lithification of microbial mats can lead to formation of biogenic carbonate rocks, also known as microbialites (see *Precipitated Microbiolites*, p. 55–70). Of these, stromatolites have layers that are often compared with the lamination of microbial mats. This is deceiving; with only a few exceptions (Marin-Carbonne & others, 2018), a single layer in a stromatolite is more likely produced by an entire mat community, rather than by a single mat layer (Visscher & others, 1998; Reid & others, 2000). The precipitation of minerals within certain mats contributes to eventual mat lithification as does trapping and binding of sediment in the sticky extracellular polymer substances. Therefore, it is

generally accepted that microbial mats are the progenitors of microbialites.

Within mats, the precipitation of carbonate minerals is mediated by 1) the interaction of the EPS with calcium and magnesium ions, and 2) by the effect of combined microbial metabolisms on the carbonate saturation index. First, freshly produced EPS inhibits carbonate precipitation by binding cations such as calcium and magnesium. The maximum calcium binding capacity can reach 280–380 mg/g EPS (Braissant & others, 2007, 2009; Pace & others, 2018), which is about the amount present in six liters of water. The magnesium binding capacity of EPS is typically much lower (~5 times in Pace & others 2018), possibly because magnesium has a much larger hydration shell than calcium (Freytet & Verrecchia, 1998). EPS concentration decreases with depth in the mat (Braissant & others, 2009; Pace & others, 2018; Sforna & others, 2017) as it is consumed by aerobic and anaerobic heterotrophs (Braissant & others, 2009; Visscher & others, 1998; Decho, Visscher, & Reid, 2005). Anaerobic degradation of EPS, facilitated by fermenters and sulfate reducers, is about four to six times slower than aerobic consumption. Maximum potential consumption rates of EPS do not seem to change with depth in the upper four cm of the mat (Braissant & others, 2009).

Microbial degradation of EPS releases Ca^{2+} ions and, in case of microbial decomposition, locally produces dissolved inorganic carbon. This increases the saturation index of $CaCO_3$, thus favoring carbonate precipitation. Cryo SEM images of mat materials clearly show mineral precipitation associated with the organic matrix of the EPS, which acts as nucleation site for initial mineral growth (Dupraz & others, 2004; Dupraz & Visscher, 2005). In addition, intracellular carbonate precipitation found in several strains of cyanobacteria can add to the carbonate production in microbial mats (Benzerara & others, 2014).

SILICATE SYSTEMS

Similar to carbonate precipitation, silicate mineralization can also be facilitated by microbial mats (Ericksson & others, 2010; Zeyen & others, 2015; Pace & others, 2016). An increase of the pH through photosynthesis facilitates nucleation of a poorly crystallized Mg-Si phase in the EPS of Great Salt Lake (USA) mats. Silica formation within a mat involves the formation and dissolution of carbonate mineral phases. Below the photic zone in these mats, aragonite precipitates first during anaerobic degradation of EPS (Pace & others, 2016). Subsequently, this aragonite dissolves in acidic pockets deeper in the mat, where partially degraded EPS binds calcium (Ca) and magnesium (Mg), ultimately forming dolomite. Some of the liberated Ca and Mg may also form a complex silicon (Si). This sequential formation of aragonite followed by precipitation of a Mg-Si phase has been observed in Lake Clifton (Western Australia) thrombolites (Burne & others, 2014) and in Mexican lakes (Zeyen & others, 2015). Amorphous Ca-Mg-Si-Al nanoparticles, presumably permineralized viruses, formed in the surface of sabkha mats (Perri & others, 2017). These amorphous phases were the precursor of the Mg-rich clay palygorskite.

Micrometer-sized calcite, pyrite nanocrystals and framboids also precipitated in the sabkha mat. These mineral precipitation processes were interpreted as induced organomineralization, and may be a common feature in silica precipitation. However, this active organomineralization process differs from the silicification of microbial mats associated with some silicon-rich hot springs, which can produce stromatolite-like features (Schultze-Lam & others, 1995; Jones, Renaut, & Rosen, 1997; Berelson & others, 2011). In these systems, the EPS of the microbial sheath material may act as passive nucleation site, but microbial metabolisms do not have a role in mineralization (Konhauser & others, 2004; Yee &

others, 2013). Regardless of the mechanism, silicification of microbial mats was important in the preservation of early life (Awramik & Barghoorn, 1977; Walter & Awramik, 1979; Lowe, 1980; Manning-Berg & others, 2019), some as old as 3.5–3.3 billion years (Hickman-Lewis, Westall, & Cavalazzi, 2020).

Microbial activities can enhance mineral precipitation by increasing the alkalinity in the microbial mat on a microscale (Dupraz & Visscher, 2005; Petrisor & others, 2014). Some metabolic reactions, such as oxygenic and anoxygenic photosynthesis, certain types of sulfate and methanogenesis increase alkalinity (Visscher & others, 1998, 2020; Visscher & Stolz, 2005; Dupraz & Visscher, 2005; Gallagher & others, 2012; Gallagher, Dupraz, & Visscher, 2014) (Fig. 5). Other metabolic reactions decrease the alkalinity, e.g., aerobic respiration, fermentation, denitrification, and other types of sulfate reduction (Visscher & Stolz, 2005; Gallagher & others, 2012; Gallagher, Dupraz, & Visscher, 2014). In the case of sulfate reduction, the nature of the electron donor can drastically alter alkalinity—the use of hydrogen and formate increases alkalinity and mineral saturation more than other donors (Gallagher & others, 2012; Gallagher, Dupraz, & Visscher, 2014). So, if the community produces excess hydrogen (Skyring, Lynch, & Smith, 1988), the sulfate-reducing bacteria are more likely to increase the local mineral saturation leading to precipitation (Gallagher & others, 2012; Gallagher, Dupraz, & Visscher, 2014). It should, however, be noted that the metabolic reaction rates of all members of the microbial mat community determine the overall change in alkalinity and the dynamic balance between mineral precipitation and dissolution (Visscher & Stolz, 2005; Pace & others, 2018). In biofilm surface mats of modern stromatolites in the Bahamas, microcolonies—likely clusters of sulfate reducers (Petrisor & others, 2014)—can have a pronounced impact on the local alkalinity and could produce microcrystalline carbonates (Visscher, Reid, & Bebout, 2000; Reid & others 2000). Significant changes in microbial community metabolisms over a light-dark cycle need to be considered when assessing a potential precipitation or dissolution effect on carbonate minerals (Visscher & others, 1998; Dupraz & Visscher, 2005). In this, it is critical to combine actual *in situ* activity measurements at a micrometer scale with fabrics (Visscher, Reid, & Bebout,, 2000) and, when possible, metagenomic information (Mobberley, Khodadad, & Foster, 2013; Mobberley & others, 2015; Louyakis & others, 2017; Wong, Ahmed-Cox, & Burns, 2016; Preisner, Fichot, & Norman, 2016). Multiple analytical techniques are needed to determine the microbial origin of carbonate minerals. For example, the use of stable isotopes ($\delta^{13}C$) alone can easily lead to misinterpretations due to the extremely high and variable rates of photosynthesis, changing ratio of autotrophic versus heterotrophic carbon cycling or changes in surrounding chemical parameters such as salinity that influence inorganic carbon speciation (Arp & others, 2012; Chagas & others, 2016).

Precipitation of minerals associated with mats is merely the onset of lithification. Complete lithification of microbial mats yields microbialites and may involve physicochemical processes, such as evaporation, or influx of alkaline water, in addition to the microbial metabolisms described (Dupraz & others, 2009). Although widely varied in shape and origin, ooids, peloids, and oncolites can possibly be used as structural biomarkers (Chafetz, 1986; Riding 1991; Diaz & others, 2017), but further work is needed. Lithification can either be microbially induced (when the microbial mat community increases the alkalinity through the combined metabolisms) or microbially influenced (when environmentally-driven processes change the alkalinity). In both scenarios, the extracellular polymer matrix

acts as a nucleation site (Dupraz & others, 2009).

MICROBIALITE MORPHOLOGIES THROUGH TIME

Stromatolites formed in the early Paleoarchean (3.6–3.2 Ga; Allwood & others, 2006), but a biotic origin of the earliest formations is still being debated (Grotzinger & Knoll, 1999). During the Late Mesoarchean-Early Neoarchean (2.94–2.5 Ga), the fossil record shows more diverse stromatolite morphologies that were biogenic (Bosak, Knoll & Petroff, 2013; Lepot, 2020). For example, aragonite spheroids associated with organic globules were present in 2.72-billion-year-old Archean stromatolites (Lepot & others, 2008). Thrombolites appeared later, after approximately 2.3–1.9 billion years ago (Barlow & others, 2016; Kah & Grotzinger, 1992).

Several mechanisms for transition from a laminated (stromatolitic) to a clotted (thrombolitic) fabric have been proposed: 1) the dominance of coccoid cyanobacteria relative to filamentous morphologies (Moore & Burne, 1994); 2) a typical fan-shaped distribution of cyanobacterial filament in open marine thrombolites in the Bahamas (Planavsky & others, 2009), consecutively modified by early diagenesis with secondary cement deposition (Planavsky & Ginsburg, 2009); 3) infaunal boring (Tarhan & others, 2013); 4) disruption of a laminated fabric by animals and/or eukaryotic macrophytes (Walter & Heys, 1985); or 5) grazing by reticulopodia (Bernhard & others, 2013). A combination of the above mechanisms may be at play. Interestingly, modern thrombolites in open marine (Bahamas), hypersaline bay (Hamelin Pool, Western Australia), hypersaline (Lake Clifton, Western Australia, Great Salt Lake, USA, Lake Alchichica, Mexico) and freshwater (Green Lake, New York, USA) lacustrine environments all have a stromatolitic crust overlying a thrombolitic fabric. This transition from a laminated surface to a clotted fabric at depth observed in modern settings suggests that a revision of the macroscale terminology of microbialites is needed.

Also worth noting, diagenetic overprinting of mineral precipitates can significantly alter and sometimes erase the micro- to macrostructure and mineral composition (Freytet & Verrecchia, 1998; Pace & others, 2018).

MICROBIAL MAT TAPHONOMY

Mats preserve more than just layers of carbonate or silicate minerals. They may contain microfossils or chemical remnants of cellular structures, such as membrane lipids or rare earth elements (Awramik & Barghoorn, 1977; Walter & Awramik, 1979; Oehler & others, 2009; Benzerara & Menguy, 2009; Pawlowska, Butterfield, & Brocks, 2012; Knoll, 2016; Javaux & Lepot, 2018). Their preserved morphology may also include biological imprints and sediment features like ripples, roll-up structures, and cracks because of the stabilizing influence of cyanobacterial filaments on sediment structure (Noffke & Awramik, 2013).

Preservation of prokaryotes as microfossils is not widespread, and their interpretation is challenging (Knoll, 2016; Schopf & others, 2017; Manning-Berg & others, 2019). However, a variety of chemical or molecular fossils aid in the interpretation of lithifying and non-lithifying mats (lipids, such as hopanes, isoprenoids, etc.; Didyk & others, 1978; Allen & others 2010; Briggs & Summons, 2014; Pagès & others, 2014; Knoll, 2016; Hickman-Lewis, Cavalazzi, & others, 2020). Lipids are excellent biomarkers specific to groups of bacteria and archaea, both in modern (Jahnke & others, 2008) and in fossil microbial mats (Summons & Walter, 1990). These complex branched and/or cyclic hydrocarbons are resistant to microbial degradation during early diagenesis. Thus, membrane-associated polar lipid

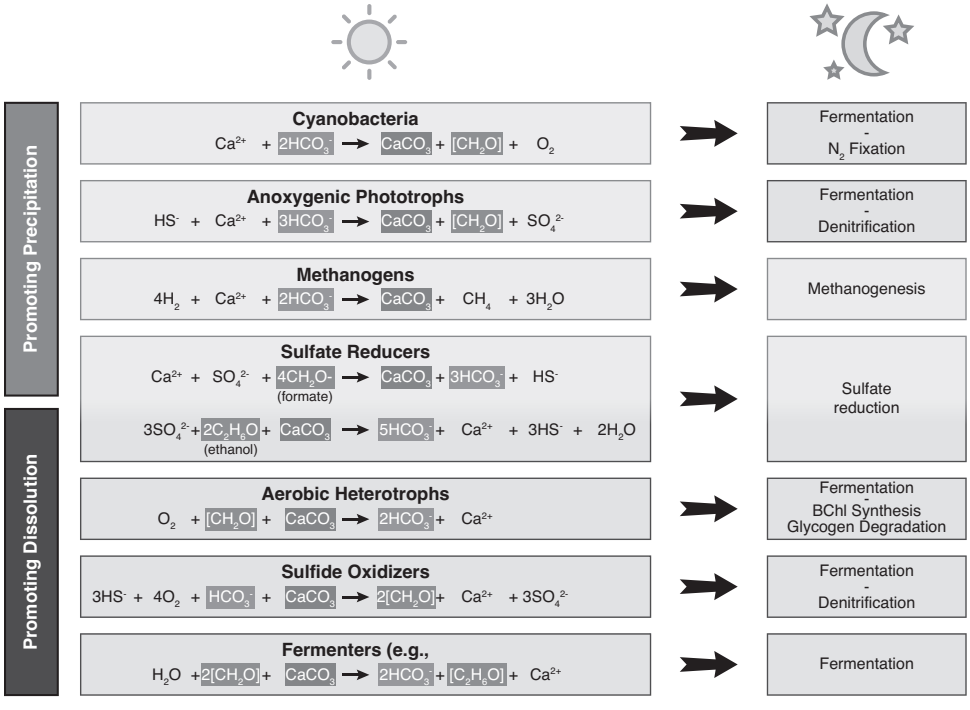

FIG. 8. Key metabolic reactions in a modern photosynthetic microbial mat combined with the precipitation/dissolution of carbonates: $HCO_3^- + Ca^{2+} \leftrightarrow CaCO_3 + H^+$ (for details, see VISSCHER & STOLZ, 2005; DUPRAZ & VISSCHER, 2005; and DUPRAZ & others, 2009). Reactions (in light gray-shaded boxes) promote precipitation of carbonates; reactions in darker-shaded boxes result in conditions favoring dissolution of carbonates. Note that depending on the electron donor type, sulfate reduction can either promote precipitation or dissolution (GALLAGHER & others, 2012). Photosynthetic microbial mats depend on light for carbon fixation, and several metabolic activities within guilds vary between light (boxes on the left) and dark (boxes on the right) conditions. The actual precipitation potential depends on the sum of actual metabolic activities for each group at each depth during a diel cycle.

biomarkers can be used to identify specific functional groups of microbes, notably those of phototrophs, sulfate reducers (having ester-bound lipids), and methanogens (with ether-linked lipids). Protists and other eukaryotes also contain specific lipids that can be used as diagnostic biomarkers (SUMMONS & WALTER, 1990; JAVAUX & LEPOT, 2018). However, prior to the onset of bioturbation in the Ediacaran (635–542 Ma) microbial mats may have formed a barrier to inclusion of planktonic biomass in sediments where heterotrophic activity fueled by cyanobacterial oxygen largely degraded the freshly deposited biomass (PAWLOWSKA, BUTTERFIELD, & BROCKS, 2012). Most Archean and Proterozoic samples that have been investigated with respect to lipid biomarkers originated in shallow sediments that were most likely colonized by microbial mats (GEHLING, 1999; EIGENBRODE, FREEMAN & SUMMONS, 2008; HICKMAN-LEWIS, & others, 2018). The presence and specific distribution of Rare Earth Elements (REE), i.e., specific REE anomalies, has also been used to interpret microbial mats and the paleoenvironmental conditions in which they developed (TAKAHASHI & others 2005; LAWRENCE & KAMBER 2006; CENSI & others, 2015; COFFEY & others, 2013; HICKMAN-LEWIS, GOURCEROL, & others, 2020). REE Yttrium (Y) and Thorium (Th) have been used to discriminate between trapping and binding and *in situ* precipitation of minerals in Precambrian stromatolites (CORKERON & others 2012),

but results can be ambiguous (Nutman & others, 2016; Allwood & others, 2018). High-resolution stable isotopes of carbon and nitrogen in organic remains and of sulfur in sulfide biominerals provide insight in ancient microbial mat metabolisms (Marin-Carbonne & others, 2018; Lepot & others, 2019).

Precipitation of minerals alone does not guarantee lithification of the mat. Some mats may lithify (Tice & Lowe, 2004; Duda & others, 2016), but the majority do not and are not preserved or easily recognized in the rock record. Certain surface features of soft mats are found in the fossil record (Hagadorn & Bottjer, 1997; Schieber, 1999; Gerdes, 2007; Noffke, 2008; Noffke & others 2001, 2013; Noffke & Awramik, 2013). So-called microbially-induced sedimentary structures (MISS), typically siliciclastic in composition, capture the sediment dynamics in shallow-marine, lacustrine, and riverine settings. Some MISS date to the Archean, such as the 2.9 Ga Pongola Supergroup in South Africa and the 3.5 Ga Dresser Formation in Western Australia. These fossilized surface structures resemble contemporary intertidal ripple marks and erosion pockets, polygonal crack features, gas domes, pinnacles and pustular mat fabrics (Gerdes, 2007; Harwood & Sumner, 2011; Visscher & others, 2010; McMahon, Davies, & Went, 2017; Morris & others, 2020). For more details, see p. 71–90). Also, a large number of preserved siliciclastic mats and MISS images are in an atlas of microbial mat features (Schieber & others 2007). Particularly well-preserved microbial mats from the Bhander Formation, Vindhyan Supergroup, India, have features that typically only occur in siliciclastic rocks (ripples, wrinkle marks, cracks) also preserved in carbonates (Sarkar & others, 2016).

Microbial mats stabilize sediments through their combined network of filamentous microorganisms and sticky, somewhat plastic EPS (Noffke, Decho, & Stoodley, 2013; Decho & Gutierrez, 2017). This matrix facilitates preservation of both vertebrates and invertebrates, which occurs by molding morphological features (Iniesto & others, 2016). Typically, successful fossilization occurs during rapid burial in non-cohesive sediments, but the slow incorporation in the mat matrix provides a similarly efficient alternative in low-depositional environments. Soft tissue, such as skin and scales, dating back to the Neoproterozoic, are particularly well preserved in microbial mats (Darroch & others, 2012). The cohesiveness of microbial mats prevents erosion and, consequently, many fossilized mats from the Ediacaran, Triassic, and Cretaceous that were thriving in hot and humid conditions hold excellent examples of fossils, including *Dickinsonia* sp., *Parvancorina* sp., and burrowing *Yichnus* sp. (Gehling, 1999; Chen & others, 2013; Xiao & others, 2019). Other fossils of interest include dinosaur tracks, tetrapods, crustaceans, fish, and possibly plants (Iniesto & others, 2018).

Thick, moist mats have the best preservation potential, sometimes showing exquisite detail (Marty, Strasser, & Meyer, 2009), biostabilizing, and preventing reworking by wind or currents (Bouougri & Porada, 2012. Cuadrado, Perillo, & Vitale, 2014; Kvale & others, 1995). A hot climate and high evaporation rates may further enhance the preservation potential of mats, supported by increased microbially-influenced organo-mineralization and elevated saturation indices (Nemati & Voowdouw, 2003).

CONCLUSION

Life began during the Archean eon, potentially as prebiotic gels associated with minerals. These transitioned to life that may have formed primitive microbial mats (Trevors, 2011) 3.7–3.4 billion years ago, either in fluvial, shallow tidal, or hot spring environments. Some of these mats may have lithified, forming the first stromatolites preserved in the fossil record. Although microbial mats have undoubtedly evolved through geological time in response to changing environmental conditions, their presence throughout the past 3.5 billion years

makes contemporary mats a potential analog for the past. The appearance of oxygenic photosynthesis and potential to fix atmospheric nitrogen—important milestones in the evolution and diversification of life—is ascribed to microbial mats. Early eukaryotes may have even emerged in these systems via endosymbiosis. The cohesive properties of these laminated organosedimentary ecosystems are most often based on filamentous microorganisms and exopolymeric substances.

Microbial mats are consummate survivors unequaled in Earth's history, and they possess an astonishing array of adaptive metabolisms enabling them to thrive in the harshest of environments. Their preserved remains, billions of years old, provide insight into the origins of life on Earth. The study of living mats is key to understanding these remains and how processes of mineral precipitation may have led to their preservation. Microbial mat ecosystems have played a pivotal role in the preservation of soft and hard tissue and provide a wealth of diverse trace and chemical fossils, making these benthic biofilms crucial paleontological phenomena.

In addition to having many other roles, microbial mats and microbialites are critical biogeomorphological agents on coastlines that in the near future will aid in the protection of nearshore environments (Morris & others, 2020), as they have done from the onset of life on our planet. Their long presence in geologic time makes microbial mats potential targets for the search for evidence of extraterrestrial life (Dupraz & Visscher, 2005).

ACKNOWLEDGEMENTS

The authors thank Professors Malcolm R. Walter and Alan W. Decho for their helpful comments on the manuscript. This work was supported by a grant from the National Science Foundation NSF grant OCE 1561173 (USA) to P.T.V. and ISITE project UB18016-BGS-IS (France) to P.T.V., E.V., and A.B.

MICROFOSSILS OF PROKARYOTES

Shuhai Xiao and Qing Tang

INTRODUCTION

Bacteria and archaea make up the paraphyletic group of prokaryotes, and together with eukaryotes they form the three major domains of life. One can easily envision a world without eukaryotes, but it is difficult to imagine a biosphere without prokaryotes. Today prokaryotes colonize virtually every corner of the surface Earth system, from human guts to oceanic gyres to hydrothermal vents. Earth is home to millions of prokaryote species (Schloss & others, 2016), which amount to a staggering number of individuals (Whitman, Coleman, & Wiebe, 1998; Flemming & Wuertz, 2019; Locey & Lennon, 2019) and account for ~14–50% of carbon in the biosphere (Whitman, Coleman, & Wiebe, 1998; Bar-On, Phillips, & Milo, 2018). In fact, the biochemical capability to fix carbon and to produce oxygen can be evolutionarily traced to prokaryotes (cyanobacteria to be exact), and nitrogen fixation in nature is exclusively carried out by prokaryotes. Thus, it is safe to say that there would not be a biosphere without prokaryotes.

There are no credible reasons to doubt that prokaryotes were as abundant and important in the geological past as they are today. Yet, the fossil record of prokaryotes is extremely poor. This poor record is largely related to the fact that most prokaryotes—with the prominent exception of magnetotactic bacteria (Bazylinski & Frankel, 2003) and some cyanobacteria (Benzerara & others, 2014)—do not perform biologically controlled mineralization. Thus, the preservation of prokaryotes as fossils requires specific taphonomic conditions. Furthermore, the microscopic size and simple morphology of prokaryotic fossils means that they are difficult to study because of potential problems related to contamination from younger microbes, conflation with abiotic structures, and convergence with eukaryotic microbes. Despite these challenges, there have been many reports of fossil prokaryotes since the late ninteenth century. This chapter is an overview of fossil prokaryotes, with a focus on bacteria, particularly cyanobacteria, preserved in Precambrian rocks.

HISTORY OF THE STUDY OF BACTERIAL FOSSILS

More detailed accounts of the history of fossil prokaryote research can be found in Fenton (1946), Banks and others (1967), Schopf (1992a), and Taylor, Taylor, and Krings (2009). Prokaryotic fossils had been reported in the literature by the late nineteenth century, although some were not originally identified as such, others may be eukaryotic, and still others were later proven abiotic. For example, the tubular microfossil *Girvanella* Nicholson & Etheridge, 1878 was first described as a foraminifer from Ordovician strata but later understood as a cyanobacterium (Wood, 1957; Riding, 1991). Renault (1896) described coccoidal and rod-shaped microstructures preserved in Carboniferous-Permian plant fossils under the extant bacterial genera *Micrococcus* Cohn, 1872 and *Bacillus* Ehrenberg, 1835. These structures were originally interpreted and subsequently accepted as bacterial fossils (Pia, 1927; Banks & others, 1967), but many of them probably represent inorganic particles (Taylor & Krings, 2005). During the early twentieth century, definitively biogenic and possibly bacterial fossils were reported in the literature. Worth mentioning are *Gloeocapsomorpha* Zalessky, 1917 from Middle Ordoviclan kukersites of the Baltic Shale Basin in Estonia, as well as the middle Cambrian fossils *Morania* Walcott, 1919 and *Marpolia* Walcott, 1919 from the Burgess Shale in Canada. *Gloeocapsomorpha* was compared with extant chroococcalean

cyanobacteria such as *Gloeocapsa* Kützing, 1843 and *Entophysalis* Kützing, 1843 (Foster, Reed, & Wicander, 1989; Stasiuk & Osadetz, 1990), but a cyanobacterial interpretation remains uncertain (Blokker & others, 2001) and some authors have interpreted *Gloeocapsomorpha* as a eukaryotic organism (e.g., a green alga) on the basis of organic geochemical evidence (Hoffmann & others, 1987; Derenne & others, 1991). The interpretation of *Marpolia* is also uncertain. It is commonly regarded as a cyanobacterium (Walcott, 1919; Steiner & Fatka, 1996), although Walcott (1919) also compared it with modern green and red algae, and fossils described as *Marpolia* may belong to different taxa or indeed different domains (LoDuca & others, 2017). *Morania*, on the other hand, has been generally accepted as a colonial organism consisting of cyanobacterial filaments (Walcott, 1919).

In addition to marine prokaryotes mentioned above, terrestrial cyanobacterial fossils have also been known from Phanerozoic deposits since the twentieth century. Among these, the most famous examples are various coccoidal and filamentous bacterial fossils from the Devonian Rhynie chert (Kidston & Lang, 1921; see also Croft & George, 1959; Edwards & Lyon, 1983; Krings & others, 2007; Krings, 2019; Krings & Harper, 2019).

By the first half of the twentieth century, alleged bacterial microfossils had been reported from Precambrian rocks (Walcott, 1914, 1915; Moore, 1918; Gruner, 1922, 1923, 1924, 1925; Ashley, 1937). Many of these were later confirmed to be pseudofossils. For example, tubular structures illustrated in Gruner (1923) and possibly those in Ashley (1937) are likely ambient pyrite trails (Tyler & Barghoorn, 1963; Knoll & Barghoorn, 1974). Such trails are common in cherts and phosphorites ranging from the Archean (Wacey & others, 2008) to the Ediacaran (Xiao & Knoll, 1999; She & others, 2016), and they were likely produced by pyrite crystal movement related to local build-up of degradational gas and pressure dissolution (Knoll & Barghoorn, 1974). However, some of these early reports likely included *bona fide* Precambrian microfossils from the Proterozoic Belcher Supergroup (Moore, 1918, fig. 14), Gunflint Formation (Gruner, 1922, pl. 7; Gruner, 1924, pl. 11), and Belt Supergroup (Walcott, 1914, pl. 20,*2–6*). In particular, Gruner's reports were from the same stratigraphic unit—the Gunflint Formation—where paradigm-shifting discoveries were reported three decades later (Tyler & Barghoorn, 1954; Barghoorn & Tyler, 1965; Cloud, 1965). But these earlier reports did not spark much interest at the time, perhaps because the quality of photomicrographs was poor (indeed, some reports had only camera lucida drawings), the great antiquity of these fossils was not appreciated, and preservation of bacterial fossils was not expected, as pointed out by Knoll, Barghoorn, and Awramik (1978).

During the second half of the twentieth century, the study of Precambrian prokaryotes opened a new chapter. This was initiated by several high-profile reports of silicified bacterial microfossils from the Paleoproterozoic (~1880 Ma) Gunflint chert in Canada (Tyler & Barghoorn, 1954; Barghoorn & Tyler, 1965; Cloud, 1965). The Gunflint fossils include stromatolite-associated coccoidal and filamentous fossils (Fig. 9.1) (Barghoorn & Tyler, 1965), as well as coccoidal planktonic microbes (Knoll, Barghoorn, & Awramik, 1978). These fossils were compared with extant cyanobacteria, iron-oxidizing bacteria, and fungi (Barghoorn & Tyler, 1965; Cloud, 1965). Serving as a search image in the field and in the laboratory, Gunflint-type stromatolitic cherts and microfossils soon opened the floodgates to numerous discoveries of Precambrian microfossils. Within a decade, Precambrian microfossils had been reported from many Precambrian cherts in North America and Australia, including the Neoproterozoic Bitter Springs Formation in Australia (Fig. 9.7) (Barghoorn & Schopf, 1965; Schopf, 1968;

Schopf & Blacic, 1971), the Neoproterozoic Skillogalee Dolomite in South Australia (Schopf & Barghoorn, 1969; Knoll, Barghoorn, & Golubic, 1975), the Neoproterozoic Beck Springs Formation in eastern California (Cloud & others, 1969), the Paleoproterozoic Belcher Supergroup in Canada (Hofmann, 1974; Hofmann, 1976), Archean strata in South Africa (Schopf & Barghoorn, 1967; Knoll & Barghoorn, 1977), and many other units. These were followed by reports of silicified microfossils, many of which are interpreted as cyanobacteria, from Precambrian cherts around the world (see summary in Schopf, 1983; Schopf & Klein, 1992; Sergeev, Sharma, & Shukla, 2012). Among these, Paleoarchean microfossils from Western Australia are the most contentious (Awramik, Schopf, & Walter, 1983; Buick, 1984; Schopf & Packer, 1987; Schopf, 1993; Brasier & others, 2002; Schopf & others, 2002). The combined geochemical, paleontological, and sedimentological data indicate the existence of a microbial ecosystem on Earth at ~3500 Ma or earlier (Rosing, 1999; Schopf, 2006a), perhaps with diverse microbial metabolic pathways (Schopf & others, 2018).

Since the 1960–1970s, paleontologists have also been investigating Precambrian organic-walled microfossils preserved in fine-grained siliciclastic rocks or shales using hydrofluoric acid maceration techniques (Xing & Liu, 1973; Timofeev, Hermann, & Mikhailova, 1976; Vidal, 1976), and some of these are filamentous microfossils that are interpreted as cyanobacteria (Hermann, 1974). This line of research opened a new taphonomic window onto the Precambrian microbial world (Vidal, 1981; Hofmann & Jackson, 1994; Grey, 2005; Tang & others, 2013). Together, microfossils preserved in cherts and shales provide a broader view of the paleoecology and taphonomy of Precambrian microbes.

MODES OF PRESERVATION

Because most prokaryotic microfossils are preserved in cherts and shales, silicification and carbonaceous compression are the main modes of preservation. However, prokaryotic microfossils can also be replicated by phosphate, pyrite, gypsum, and other minerals; and they have been reported from ambers. These taphonomic modes are briefly described below.

SILICIFICATION

As a major permineralization pathway, silicification is responsible for the preservation of the majority of prokaryotic microfossils (Fig. 9), including those preserved in cherts of the Gunflint Formation (Fig. 9.1–9.3) and Bitter Springs Group in Australia (Fig. 9.7). Generally understood as a taphonomic process through which organisms are replaced by diagenetic silica, silicification of microbes is neither molecule-by-molecule replacement of cellular structures by silica nor wholesale replacement of the entire organism by silica, as sometimes occurs in silicification of animal skeletons (Butts, 2014). Rather, at the microscopic level, silicification is fundamentally a casting and molding process, with silica precipitating on organic substrates, such as cell walls and laminae of cyanobacterial sheaths, through chemical bonds between organic functional groups and silicic acids (Leo & Barghoorn, 1976) and perhaps assisted by the presence of metallic ions (Ferris, Fyfe, & Beveridge, 1988), thus producing molds or casts of microbial cells and sheaths. Thus, the organic substrates are encased within the replicating silica and are subsequently degraded to various degrees. The taphonomic survival of the organic substrates, albeit in degraded forms and in trace amounts, aids the recognition and identification of these fossils in thin section microscopy and is regarded by some geologists as an indispensable criterion for affirmation of biogenicity (Buick, 1990).

A number of taphonomic experiments have been carried out to understand the silicification process. Degradation experiments have demonstrated that cyanobacterial cells degrade over periods of days to months

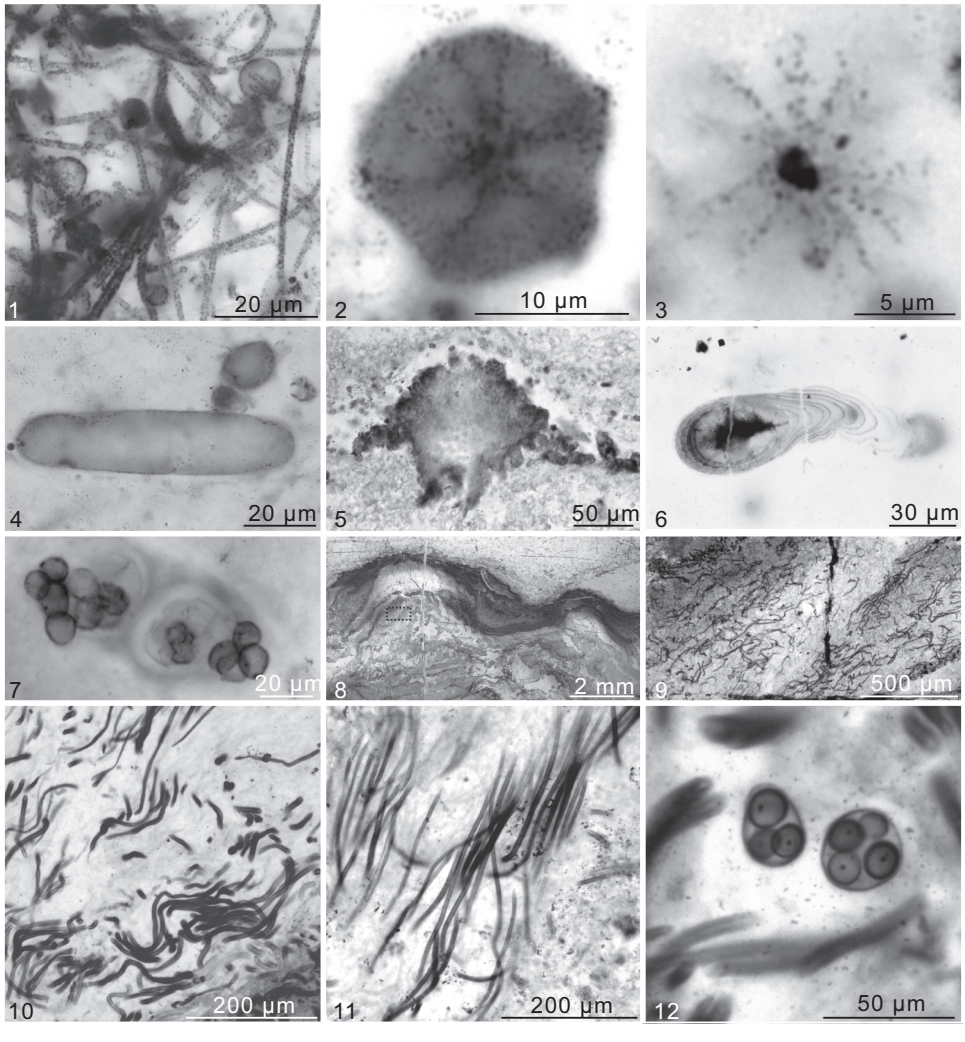

Fig. 9. Thin section photomicrographs of silicified prokaryotic microfossils from the ~1880 Ma Gunflint Formation in Canada (*1–3*), ~1400–1500 Ma Billyakh Group in Siberia (*4–5*), Tonian Draken Formation in Svalbard (*6*), Tonian Bitter Springs Group in Australia (*7*), and Tonian Jiudingshan Formation in North China (*8–12*). *1*, Coccoidal specimens of *Huroniospora* Barghoorn in Barghoorn & Tyler, 1965 and filamentous specimens of *Gunflintia* Barghoorn in Barghoorn & Tyler, 1965. Although *Gunflintia* was described as a multicellular filament (Barghoorn & Tyler, 1965), most specimens do not preserve trichome structure and may be identified as *Siphonophycus*; *2*, *Kakabekia* Barghoorn in Barghoorn & Tyler, 1965; *3*, possibly *Eoastrion* Barghoorn in Barghoorn & Tyler,1965; *4*, *Archaeoellipsoides* Horodyski & Donaldson, 1980; *5*, *Eoentophysalis* Hofmann, 1976; *6*, *Polybessurus* Green & others, 1987; *7*, *Myxococcoides* Schopf, 1968; *8*, stromatolites consisting of filamentous *Siphonophycus* Schopf, 1968; *9–11*, close-up views of *Siphonophycus* filaments, *9* being a magnification of *8* (dotted line box); *12*, *Caryosphaeroides* Schopf, 1968 in the center, with coccoidal cells arranged in tetrads and enclosed in a common envelope. Note intracellular inclusions that were interpreted as degraded nuclei (Schopf, 1968; but see Knoll & Barghoorn, 1975). Also note *Siphonophycus* filaments co-occurring with *Caryosphaeroides.* Fig. *1.1–1.3* and *1.7–1.12,* new; Fig. *1.4–1.6* courtesy of Andrew H. Knoll, previously published as fig. 10,*2* and 17,*4* in Sergeev, Knoll, & Grotzinger, 1995, and fig. 12,*5* in Knoll, Swett, & Mark, 1991, respectively. Color version available in *Treatise Online* 160 (paleo.ku.edu/treatiseonline).

but cyanobacterial sheaths are much more resistant and can remain recognizable over longer time (Golubic & Barghoorn, 1977; Bartley, 1996). These experiments have been borne out by field observations showing the degraded but still recognizable cyanobacterial cells and sheaths in pigment-poor layers of modern microbial mats (Gomes & others, 2020), and they indicate that fossil mineralization must have occurred rapidly during early diagenesis in order to preserve cellular structures. Indeed, field observations of microbial silicification in modern hot spring sinters, which are widely regarded as modern taphonomic analogs of microbial silicification in Precambrian oceans, indicate that cyanobacterial and other microbes can be silicified shortly after death or even *in vivo* (Renaut, Jones, & Tiercelin, 1998), and that cyanobacterial sheaths are preferentially preserved through silica encrustation and permeation (Renaut, Jones, & Tiercelin, 1998; Konhauser & others, 2003). Mineralization experiments have also demonstrated that silica and clay minerals can coat on cyanobacterial sheaths, and silica can permeate cyanobacterial sheaths and cell walls, thus rapidly replicating cyanobacterial morphology in three dimensions (Oehler & Schopf, 1971; Westall, Boni, & Guerzoni, 1995; Toporski & others, 2002; Newman & others, 2017). These encrustation and permeation processes may have been facilitated or accelerated by elevated silica concentrations in Precambrian seawaters and pore waters (Maliva, Knoll, & Simonson, 2005) and photosynthetic activity of cyanobacteria themselves (Moore & others, 2020). Thus, it is not surprising that microbial silicification was common in Precambrian marine environments, but as biosilification (e.g., in sponges, radiolarians, and diatoms) became more important and dissolved silica concentrations declined in Phanerozoic oceans (Conley & others, 2017), this taphonomic mode declined in and throughout the Phanerozoic, not only for bacterial silicification but for silicification in general (Schubert, Kidder, & Erwin, 1997). Nor is it surprising that microbial silicification is common in hydrothermal settings (e.g., modern hot spring and Devonian Rhynie chert) where dissolved silica concentrations are high.

Yet silicification is not ubiquitous in all Precambrian marine environments. Knoll (1985a) identified three sedimentary and geochemical factors that control microbial silicification: 1) sediment permeability, 2) silica availability in pore waters, and 3) local concentration of organic matter. It is possible that these factors can interact with each other to promote silicification. For example, the degradation of organic matter (and the partial degradation of organic substrates) can activate organic functional groups, thus facilitating the nucleation of silica. It can also drive down local pH values, thus promoting the precipitation of silica as the solubility of silica decreases with pH. These sedimentary and geochemical factors mean that silicification of microbes is environmentally restricted. Indeed, although there are notable exceptions (e.g., the Ediacaran Doushantuo Formation Zhang & others, 1998; Muscente, Hawkins, & Xiao, 2015), most silicified microbial assemblages are preserved in either peritidal or hydrothermal environments (Knoll, 1985a; Knoll, 1985b; Trewin, Fayers, & Kelman, 2003). As such, silicification provides a limited and probably biased view of the environmental and ecological ranges of prokaryotic microbes (Knoll, 1985b; Butterfield & Chandler, 1992). Fortunately, this limitation is mitigated to some degree by other taphonomic modes, such as phosphatization and pyritization that are also known to preserve microbial fossils.

PHOSPHATIZATION

Although a different fossil mineralization process, phosphatization is mechanistically similar to silicification, and fossiliferous phosphorites tend to be siliceous (Yao & others, 2005; Dong & others, 2009; Sergeev, Schopf, & Kudryavtsev, 2020). Like silicification, phosphate encrustation

and impregnation of organic substrates are key processes that are responsible for the three-dimensional preservation of microbial cell morphology (Xiao, Zhang, & Knoll, 1998; Xiao & Schiffbauer, 2009). Unlike silicification, however, the phosphatization is largely restricted to subtidal environments (Zhang & others, 1998; Muscente, Hawkins, & Xiao, 2015) and occurs mostly in the Ediacaran and the Phanerozoic (Schiffbauer, Wallace, & others, 2014; Muscente & others, 2017). Phosphatized cyanobacteria, for example, are best known from Ediacaran-Cambrian strata, including the Ediacaran Doushantuo Formation in the South China Craton (Fig. 10) (Zhang & others, 1998; Yuan, Xiao, & Taylor, 2005), the early Cambrian (Terreneuvian) Yurtus Formation in the Tarim Basin of northwestern China (Yao & others, 2005; Dong & others, 2009) and equivalent strata in the South China Craton (Wang & others, 1984; Dong & others, 2009; Guo, Li, & Shu, 2010), and the middle Cambrian (Guzhuangian) Alum Shale Formation in Sweden (Castellani & others, 2018). In addition, many Phanerozoic coprolites and cololites contain micrometer-sized spherical and rod-shaped structures interpreted as bacteria (Lamboy & others, 1994; Cosmidis & others, 2013; Pesquero & others, 2014), although some of these spherical structures may be alternatively interpreted as phosphatic granules that may have been present in the digestive guts of some invertebrate animals (Butterfield, 2002; Hawkins & others, 2018).

Relative to silicification, taphonomic experiments of phosphatization have been less successful and mostly focused on invertebrate degradation and mineralization (Briggs & McMahon, 2016). Degradation experiments indicate that animal cells and tissues can be pseudomorphed by heterotrophic microbes and microbial biofilms (Raff & others, 2008; Raff & others, 2013; Butler & others, 2015), thus helping to stabilize anatomical details to be phosphatized during subsequent fossil mineralization. However, the giant sulfur bacterium *Thiomargarita* Schulz & others, 1999 subjected to similar experiments did not seem to be pseudomorphed by microbial biofilms during degradation (Cunningham & others, 2012). Mineralization experiments thus far are limited and have only been able to partially phosphatize invertebrate animals (Wilby & Briggs, 1997; Martin, Briggs, & Parkes, 2003; Hippler & others, 2011). To our knowledge, no mineralization experiments have been carried out on prokaryotic organisms, and this represents a key gap in the study of prokaryote phosphatization and an area for future research.

Exceptional preservation of microbial fossils through silicification and phosphatization depends on a delicate balance between rapid mineralization and over-mineralization. Over-mineralization results in thick mineral coats that bias and disguise microbial morphologies, making it difficult to recognize mineralized microfossils in microscopy, particularly when organic substrates, such as cell walls and sheaths are completely obliterated. This has been observed in modern hot spring sinters (Jones, Renaut, & Rosen, 2001; Peng & Jones, 2012) as well as phosphatized microbes in the Ediacaran Doushantuo Formation in South China (Xiao & Schiffbauer, 2009).

The inhibition of post-mineralization recrystallization is also an integral part of exceptional preservation through phosphatization (Xiao & Hochella, 2017). The successful fossilization of microscopic prokaryotic organisms, in particular, is critically dependent on the maintenance of fossilization minerals at micrometers or even nanometers in size; this is analogous to the achievement of the highest resolution in digital imaging by the smallest pixels. Exceptionally phosphatized microfossils from the Ediacaran Doushantuo Formation (Fig. 10), for example, are replicated by apatite minerals of tens to hundreds of nanometers in size (Xiao & Schiffbauer, 2009). It is not completely understood why these apatite nanocrystals were prevented from dissolution and then recrystallization to become

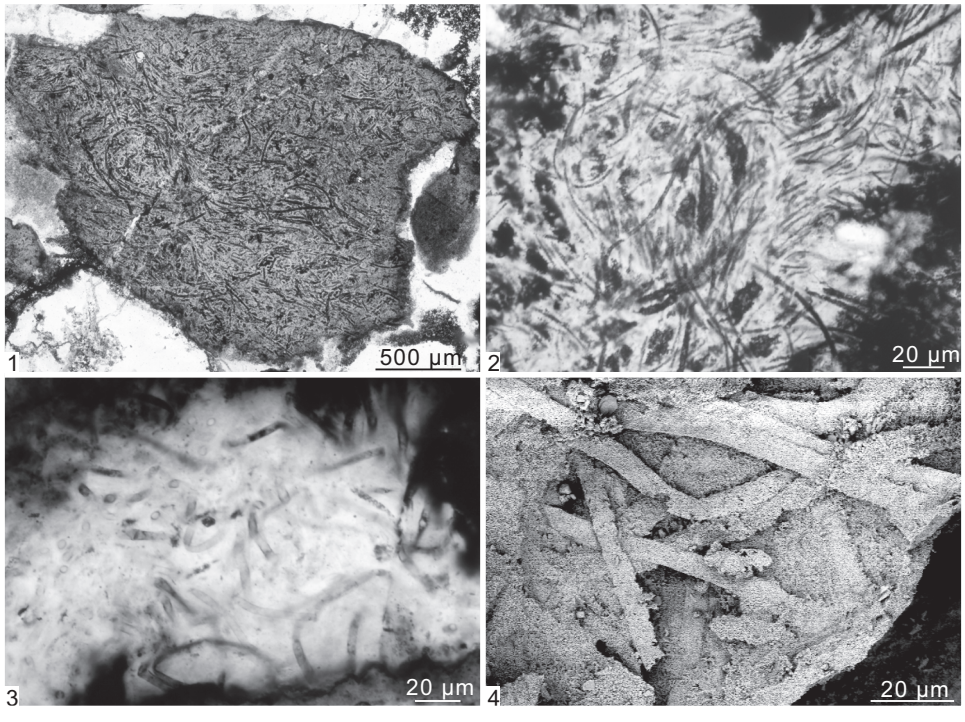

FIG. 10. Phosphatized *Siphonophycus* filaments from the Ediacaran Doushantuo Formation in South China. *1–3*, thin section photomicrographs (new; photos taken by and courtesy of Lei Chen); *4*, scanning electron microscopic (SEM) image (new; image by Shuhai Xiao). Color version of *1–3, Treatise Online* 160 (paleo.ku.edu/treatiseonline).

larger crystals. However, it is possible that the dissolution of phosphate nanocrystals in the size range of tens to hundreds of nanometers is self-suppressed or self-inhibited by the limited formation and growth of dissolution pits, the size of which is constrained by the nanocrystal size (TANG, NANCOLLAS, & ORME, 2001). This may be a fruitful area for future exploration of phosphatization (XIAO & HOCHELLA, 2017).

CALCIFICATION

Microbial calcification can occur as biologically controlled *in vivo* intracellular mineralization, biologically induced *in vivo* extracellular mineralization, or extrinsically induced *in vivo* or post-mortem extracellular mineralization. All three forms of mineralization can be found in cyanobacteria. Some cyanobacteria carry out biologically controlled mineralization and precipitate intracellular carbonates (COURADEAU & others, 2012; BENZERARA & others, 2014), but thus far these cyano-bacterial biominerals are not known to be preserved and identified in the fossil record. More commonly, metabolic activities of cyanobacteria, particularly photosynthesis and carbon dioxide concentration mechanisms, promote an increase in local pH values and induce *in vivo* precipitation of calcium carbonate that impregnate the sheath (RIDING, 2006). This form of biologically induced mineralization results in extracellular sheath calcification and may be responsible for the preservation of the majority of calcified cyanobacterial fossils, such as *Girvanella* NICHOLSON & ETHERIDGE, 1878 (Fig. 11.1–11.2), *Epiphyton* BORNEMANN, 1886 (Fig. 11.3), and *Renalcis* VOLOGDIN, 1932. Finally, microbes can be entombed *in-vivo* or postmortem in carbonate deposits (Fig. 11.4–11.6) (KREMER & others,

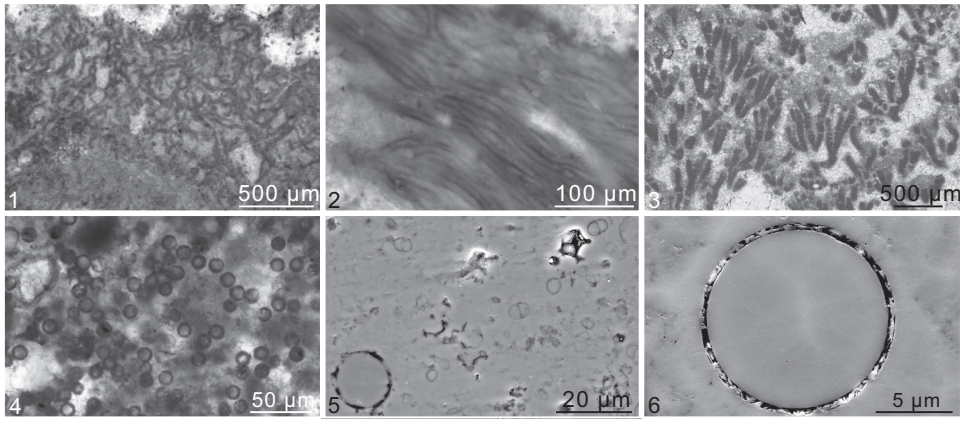

FIG. 11. Prokaryotic microfossils preserved in carbonate rocks. *1–2*, *Girvanella* NICHOLSON & ETHERIDGE, 1878 from the Lower Ordovician Fenhsiang Formation at the Liujiachang section, Songzi, Hubei Province, South China; *3*, *Epiphyton* BORNEMANN, 1886 from Cambrian Stage 3, Zhangxia Formation in Laiwu, Shandong Province, North China. Both *Girvanella* and *Epiphyton* have been interpreted as calcified cyanobacteria (RIDING, 1991); *4–6*, Coccoid microfossils, interpreted as methanogens on the basis of extremely high $\delta^{13}C_{carb}$ values up to 20‰ of the host dolomite concretions from the Middle Permian lacustrine deposits of the Lucaogou Formation in Xinjiang, northwestern China (SUN & others, 2020). Note two size classes in *5*, representing two different taxa. *1–4* are thin section photomicrographs and *5–6* are SEM images. Images *1–3,* new; photos taken by and courtesy of Jianbo Liu; *4–6,* courtesy of Funing Sun and Wenxuan Hu, previously published as fig. 2D, 2G, and 2F, respectively, in Sun & others, 2020. Color version of *1–4* in *Treatise Online* 160 (paleo.ku.edu/treatiseonline).

2012; SUN & others, 2020)—including tufas, travertines, and speleothems whose precipitation is primarily driven by abiotic processes such as CO_2 degassing, although it is not always possible to determine whether biological processes also play a secondary role in facilitating calcification (JONES & PENG, 2012; LI & others, 2013; JONES & PENG, 2014).

Microbial calcification is not uniformly distributed across geological time, sedimentary environments, and taxonomic groups. As calcification is critically dependent on carbonate supersaturation levels, it is not surprising that microbial calcification tends to be focused on tropical shallow marine realms, for example evaporitic, peritidal, and reefal or mud mound environments. In addition, because various microbial metabolisms have different impacts on the precipitation and dissolution of carbonate minerals (CANFIELD & RAISWELL, 1991), it is anticipated that different groups of microbes have different propensities to induce calcification. As mentioned earlier, photosynthesis and carbon dioxide concentration mechanisms of cyanobacteria facilitate fossilization through calcification (RIDING, 2006). But calcified cyanobacterial fossils have a non-uniform distribution in warm shallow marine environments across geological history. Although they range from the Meso-Neoproterozoic (KNOLL, FAIRCHILD, & SWETT, 1993; TURNER, NARBONNE, & JAMES, 1993; KAH & RIDING, 2007) to the Cenozoic (ARP, REIMER, & REITNER, 2001), they are mostly concentrated in the Paleozoic and early Mesozoic (ARP, REIMER, & REITNER, 2001). Geochemical, atmospheric, and biological factors have been implicated as controlling factors for the non-uniform distribution of calcified cyanobacterial microfossils in marine environments. For example, RIDING (2006) proposed that pCO_2 levels fell below ~0.4% (or 10× present atmospheric level) at 750–700 Ma, driving the evolution of CO_2-concentrating mechanisms and facilitating *in vivo* calcification of cyanobacterial sheaths in the Neoproterozoic and Paleozoic. ARP, REIMER, and REITNER (2001)

suggested that the Paleozoic abundance of cyanobacterial calcification may be related to high calcium concentrations in Paleozoic oceans. Biological factors were in play too. Knoll, Fairchild, and Swett (1993), for example, suggested that, whereas the rarity of cyanobacterial calcification in the Precambrian may be attributed to the abundance of micrite (e.g., whiting) that outcompeted cyanobacterial sheaths as nucleation sites for calcite overgrowth in the sediment, the post-Mesozoic decline of cyanobacterial calcification was due to the ecological rise of calcareous phytoplankton.

PYRITIZATION AND RELATED PRESERVATION MODES

Bacteria and archaea are key players in the sulfur cycle (Ehrlich & Newman, 2009). Thus, it is not surprising that they play direct and indirect roles in the precipitation of sulfur-bearing minerals. Some sulfide-oxidizing bacteria (e.g., *Beggiatoa* Trevisan, 1842, *Thiomargarita* Schulz & others, 1999, and *Thioploca* Lauterborn, 1907) produce intracellular sulfur granules (Ehrlich & Newman, 2009; Bailey & others, 2013). Although such sulfur granules are not supposed to be stable in geological time scales, filamentous microfossils from the Ediacaran Doushantuo Formation in South China contain sulfur-rich granules that are interpreted as intracellular sulfur granules produced by sulfide-oxidizing bacteria (Bailey & others, 2013). More commonly, microbial sulfate reduction promotes the precipitation of pyrite, which can replicate microbes in the fossil record through pyritization; often, it is the organisms that are degraded by sulfate reducing microbes, rather than the sulfate reducing microbes themselves, that are pyritized (Schiffbauer, Xiao, & others, 2014). Pyritized microfossils are common in the geological record (Schopf & others, 1965; Rasmussen, 2000; Moore & others, 2017). In some pyritized filamentous microfossils (e.g., those from the Ediacaran Krol Group in India; Fig. 12), pyrite crystals seem to precipitate within a tubular sheath, thus outlining the filamentous morphology but not faithfully replicating the diameter of the filaments until a full internal mold is formed. Thus, pyritization seems to be initiated within partially degraded filamentous microbes (perhaps after the degradation of trichomes but before the complete destruction of the sheath), and can proceed to form pyritic internal mold of microbes. Finally, microbial fossils can be replicated by gypsum (Vai & Lucchi, 1977; Schopf & others, 2012), the precipitation of which is primarily driven by abiotic processes such as evaporation.

PRESERVATION OF BIOMINERALS PRODUCED BY MAGNETOTACTIC BACTERIA

A number of iron bacteria can produce biologically controlled and biologically induced biominerals (Bazylinski & Frankel, 2003; Frankel & Bazylinski, 2003). Magnetotactic bacteria, for example, produce intracellular minerals such as magnetite (Fe_3O_4) and greigite (Fe_3S_4) that can have distinct morphologies and crystallographic features (Fig. 13) (Bazylinski & Frankel, 2003; Li & others, 2013, 2020). These distinct crystals allow their identification in the fossil record, and indeed fossil magnetotactic bacteria have been reported in Mesozoic and Cenozoic sediments (Chang & Kirschvink, 1989; Kopp & Kirschvink, 2008).

Some iron bacteria can also produce biologically induced biominerals with distinct morphologies. For example, the iron bacteria *Gallionella* Ehrenberg, 1838 and *Mariprofundus* Emerson & others, 2007 can produce extracellular ferric-oxyhydroxide stalks that are twisted, branched, or organized into ribbon-like bands (Frankel & Bazylinski, 2003; Chan & others, 2011; Krepski & others, 2013). Morphologically similar stalks have also been identified in the fossil record and interpreted as evidence for iron bacteria

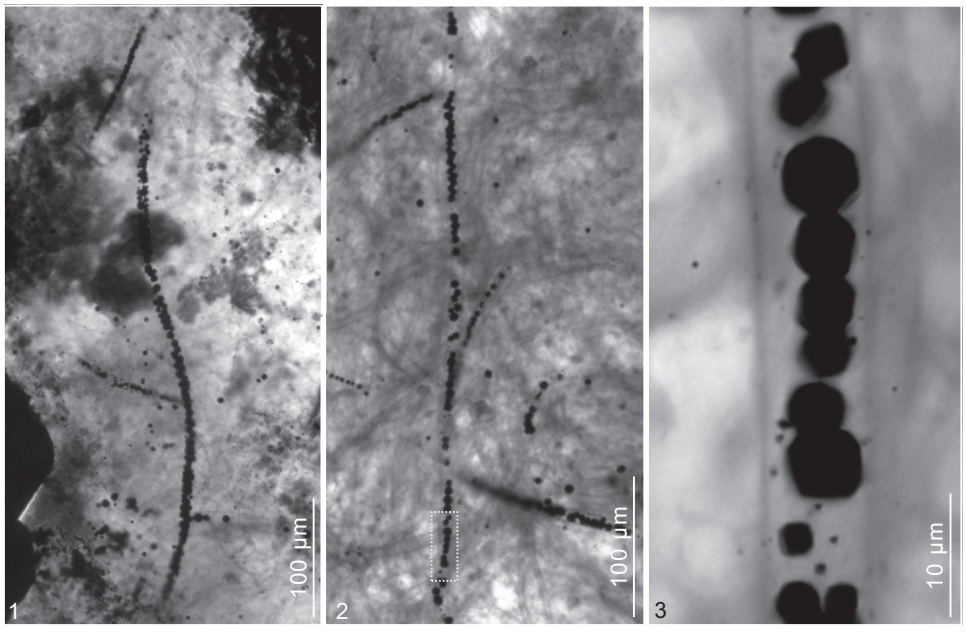

Fig. 12. Thin section photomicrographs of pyritized Siphonophycus filaments from the Ediacaran Krol Group in northern India. 3 is magnified view of 2 (yellow dotted-line box). Note that organic sheath is largely degraded in 1 and well preserved in 2–3. All images are new and were taken by Shuhai Xiao. Color version in *Treatise Online* 160.

(Hofmann & others, 2008; Krepski & others, 2013; Crosby, Bailey, & Sharma, 2014).

CARBONACEOUS PRESERVATION

Although traces of carbonaceous material are commonly found in mineralized prokaryotic fossils, they are typically impregnated or penetrated by replicating minerals such as microquartz and apatite, so that extraction of coherent organic-walled microfossils using hydrofluoric (HF) digestion method is difficult. In contrast, carbonaceous preservation of prokaryotic fossils in fine-grained siliciclastic rocks may manifest as compressed organic-walled structures with little mineral permeation or impregnation (Xiao & others, 2002; Callow & Brasier, 2009), and these fossils can be extracted from the rock matrix using hydrofluoric acid digestion methods without compromising their structural integrity (Fig. 14) (Tang & others, 2013; Tang & others, 2015). In addition to carbonaceous compressions, structurally recognizable organic residues of prokaryotic microbes can also be preserved in ambers (Poinar, Waggoner, & Bauer, 1993; Waggoner, 1994; Dörfelt, Schmidt, & Wunderlich, 2000; Schmidt & Schäfer, 2005). Finally, carbonaceous coccoids, filaments, and sheets have been reported on the basis of scanning electron microscopic observation of fractured rock surface (sometimes after acid etching), and these have been interpreted as fossil microbes or as extracellular polymeric substances (Westall & Folk, 2003; Dai, Song, & Shen, 2004; Rozanov & Astafieva, 2009; Lan & others, 2020), although it is a significant challenge to demonstrate their syngenicity (Altermann, 2001; Edwards & others, 2006).

TRACE FOSSILS

Some prokaryotic micro-organisms, particularly cyanobacteria, can bore into hard substrates and leave a trace fossil record (Golubic, Perkins, & Lukas, 1975; Cockell & Herrera, 2008). Tunnels and galleries of tunnels interpreted as traces of euendolithic cyanobacteria have been reported from many phosphatic small shelly fossils from

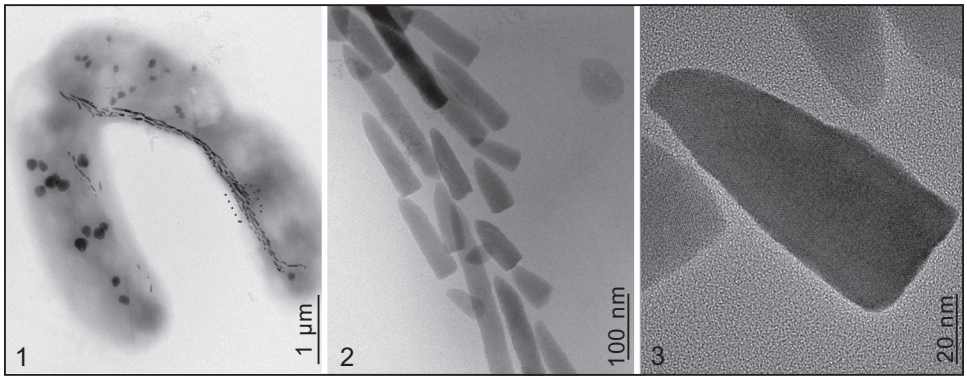

Fig. 13. Bright-field TEM (transmission electron microscopy) images (*1–2*) and high-resolution TEM image (*3*) of chains of straight bullet-shaped magnetite nanocrystals produced by extant magnetotactic deltaproteobacteria (strain WYHR-1) collected from Weiyang Lake, north of Xi'an city, Shaanxi Province, North China (Li & others, 2020). Images are new and courtesy of Jinhua Li.

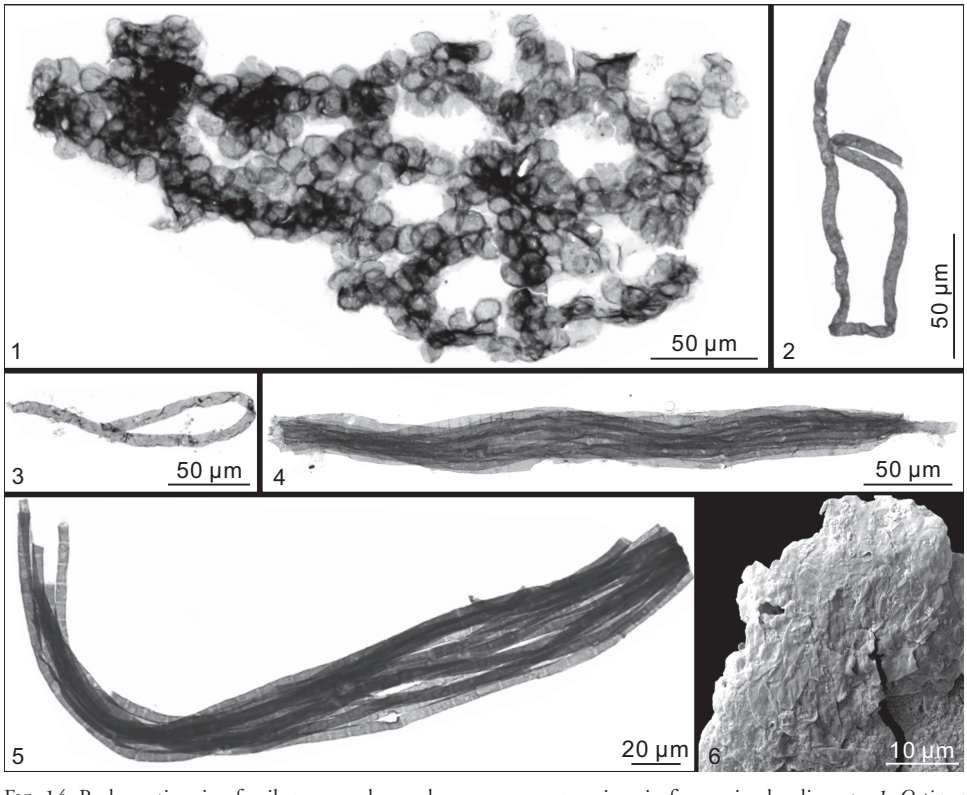

Fig. 14. Prokaryotic microfossils preserved as carbonaceous compressions in fine-grained sediments. *1*, *Ostiana microcystis* Hermann in Timofeev, Hermann, & Mikhailova, 1976, a possible cyanobacterium (Butterfield, Knoll, & Swett, 1994); *2–3*, *Siphonophycus typicum* (Hermann, 1974; transferred to the genus *Siphonophycus* by Butterfield in Butterfield, Knoll, & Swett, 1994); *4–5*, *Polytrichoides lineatus* Hermann, 1974; *6*, ellipsoidal cells of *Eosynechococcus moorei* Hofmann, 1976. All specimens were extracted from shale samples using hydrofluoric acid digestion method. *1–4* are from the Tonian Liulaobei Formation in the North China Craton (Tang & others, 2013, fig. 5G, 13C, 13D, and 14A, respectively), and *5–6* are from the Tonian Gouhou Formation in the North China Craton (Tang & others, 2015, fig. 19E and 5B, respectively). Fig. *1–5* are transmitted light photomicrographs; *6* is an SEM image.

the Cambrian Period (Runnegar, 1985; Li, 1997). These tunnels typically have smooth walls and a constant diameter along their length, but they are otherwise simple in morphology, and the distinction between cyanobacterial, fungal, and green algal borings can be difficult (Golubić, Perkins, & Lukas, 1975). However, they can be easily differentiated from ambient pyrite trails in phosphorites and cherts, which are characterized by striated walls and commonly terminated by a pyrite grain (Xiao & Knoll, 1999; She & others, 2016; Yang & others, 2017). They can also be easily differentiated from tubular structures in Paleoarchean pillow basalts that were controversially interpreted as putative bioerosional structures of early microbes (Furnes & others, 2004; Staudigel & others, 2006).

CHALLENGES IN THE INTERPRETATION OF PROKARYOTIC MICROFOSSILS

To unambiguously demonstrate the syngenicity, biogenicity, and affinity of purported prokaryotic microfossils is a significant challenge, particularly in the study of Precambrian micropaleontology because of the poor age constraints, difficulty in stratigraphic correlation, and simple (and sometimes exotic) morphologies of ancient microorganisms. This challenge is highlighted in the debate on the earliest traces of microbial life on Earth (Buick, 1990; Brasier & others, 2005; Brasier & others, 2006; Javaux, 2019). Below, indigenicity, syngenicity, biogenicity, and affinity are discussed separately for clarity purpose, although these are often intimately related.

INDIGENICITY AND SYNGENICITY

Syngenicity refers to the provenance of the purported microfossils. Syngenetic microfossils must be indigenous; they should be demostrated to be enclosed within and thus have the same age of the host rock, rather than later contaminants. Contaminants can be introduced in the geological past, in the field, or in the laboratory (Cloud & Morrison, 1979). In early studies of Precambrian microfossils, there were numerous cases of contamination. Such examples included modern chasmolithic filaments or extracellular polysaccharide strands, seemingly indigenous as they pass beneath mineral grains in sediment (Cloud & Morrison, 1979). Other examples involved modern fungal spores and hyphae that were introduced in the field and laboratory, particularly when samples were processed using acid digestion methods. Mendelson and Schopf (1992) provided a comprehensive assessment of these contaminants.

An accepted criterion for indigenicity is to demonstrate—typically through petrographic observation of thin sections cut from freshly collected rock samples—that the purported microfossils are encased in rock matrix. In order to confirm syngenicity in thin sections, care must be taken to distinguish whether the purported microfossils were buried in the rock matrix at the time of deposition or are embedded in secondary cements/crystals that fill voids, fractures, veins, dikes, or volcanic vesicles (i.e., amygdales). In the latter case, the secondary cements/crystals should be independently dated because they can be markedly younger than the host rock. This can be achieved through relative dating using cement stratigraphy and cross-cutting relationships (Zhou & others, 2015; Gan & others, 2021), analysis of mineral assemblages tied to dated metamorphic events (Bengtson & others, 2017), or (when carbonaceous material is available) Raman spectroscopic analysis of carbonaceous material to determine maximum metamorphic temperatures (Schopf & others, 2005; Schiffbauer & others, 2007; Javaux, Marshall, & Bekker, 2010).

BIOGENICITY

Biogenicity refers to the biological origin of the purported microfossils. It should be

emphasized that, to prove biogenicity, the morphologies of the microfossils must be shown to be biological in origin. This is a distinction between morphological and chemical biosignatures. For example, a pyrite concretion may preserve chemical biosignatures because its sulfur isotopic composition indicates the involvement of microbial sulfate reduction, but this by itself does not offer evidence for a biological origin of the pyrite concretion.

Cloud (1965, p. 27) argued that the null hypothesis in Precambrian micropaleontology should be that purported microfossils be initially regarded as abiotic in origin. He wrote, "... in considering what we may accept as unequivocal Precambrian fossils, the crucial point is not whether materials observed might conceivably be of vital origin, but whether they could have been produced by non-vital processes; and, if not, whether they are sure endemic to authentic Precambrian rocks." Only after an abiotic origin can be ruled out and syngenicity is confirmed can Precambrian microfossils be accepted. This restrictive approach is necessary because of the possibility of biomorphs that are abiotic in origin but morphologically mimic microfossils (García-Ruiz & others, 2003; Javaux, 2019) and also because of the profound ramifications of false positives in the study of Precambrian (particularly Archean) microfossils.

In early debates on putative microfossils from the Paleoarchean Warrawoona Group in Western Australia, Buick (1990) proposed a seven-point test to assess their syngenicity and biogenicity. He argued that *bona-fide* microfossils should be observed in petrographic thin sections, preserved in sedimentary rocks or low-grade metasediments, no smaller than the smallest extant modern microbes (i.e., >0.01 μm^3), comprised of kerogen, part of a larger population of similar morphologies, hollow structures, and show cellular elaborations. Subsequently, a number of authors proposed additional criteria to assess the morphology, ontogeny, metabolism, behavior, taphonomy, chemistry, and geological context of purported microfossils (Schopf & others, 2010; Brasier & Wacey, 2012; Rouillard & others, 2018; Javaux, 2019; Rouillard & others, 2021). For example, *bona fide* microfossils should have a stable species-specific morphology with a unimodal size distribution and would exhibit evidence of development (e.g., cell division and development of branching filaments), distinct cell wall ultrastructures, taphonomic degradation (e.g., degradation of cytoplasm, deflation of cell vesicles, and deformation of cell walls and sheaths), ecological interactions (e.g., aggregations and attachment to substrates), and metabolic activities (e.g., organic C and N isotope signatures, trace metal enrichment) (Lepot, 2020).

Recent exploration of ancient microfossils have pushed the envelope beyond the preservation of organic-walled structures in sedimentary rocks as stipulated by Buick (1990). Coccoidal, rod-shaped, and filamentous structures preserved in igneous rocks, sometimes with no traces of organic walls, may represent evidence for ancient life, including both prokaryotes and eukaryotes (Fig. 15.1) (Bengtson & others, 2017; Ivarsson & others, 2020). More controversial are micrometer-sized titanite filaments or microtextures in altered volcanic glass of Paleoarchean pillow basalts that have been interpreted as bioerosional structures or trace fossils produced by chasmoendolithic and euendolithic microbes (Fig. 15.2) (Furnes & others, 2004; Staudigel & others, 2006) and micrometer-sized hematitic tubular structures from >3.77 Ga ferruginous sedimentary rocks in the Nuvvuagittuq supracrustal belt in Canada that are regarded as putative microfossils, possibly representing iron-oxidizing bacteria (Fig. 15.3) (Dodd & others, 2017). Given that inorganic and morphologically simple tubes and spheres can be produced abiotically (García-Ruiz & others, 2003; García-Ruiz & others, 2017; McMahon, 2019), extra efforts must be made to affirm the biogenicity of these purported microfossils, and alternative

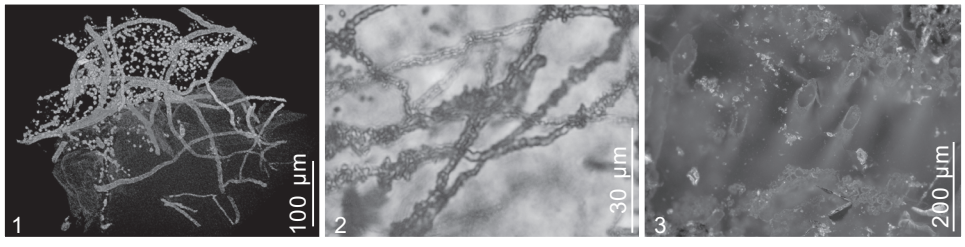

FIG.15. Coccoidal, filamentous, and tubular structures with no preservation of organic walls. *1*, synchrotron-based X-ray tomographic rendition of coccoidal structures (interpreted as unicellular prokaryotes) suspended in filamentous cobweb-like structures (interpreted as fungal hyphae) from Koko Seamount (Ivarsson & others, 2020, fig. 4C); *2*, titanite microtextures from the ~3350 Ma Euro Basalt in Western Australia (see MCLOUGHLIN & others, 2020) (new; image by Nicola McLoughlin); *3*, hematitic tubes in chert from jasper banded iron formation in hydrothermal vent deposits of the Nuvvuagittuq Supracrustal Belt (NSB) in Québec, Canada, constrained between ~3750 and ~4280 Ma (Dodd & others, 2017, fig. 2e). Photographed in a one-cm-thick polished slab under dark-field reflected light. *1* is courtesy of Magnus Ivarsson and Stefan Bengtson; *2* courtesy of Nicola McLoughlin; and *3* courtesy of Matthew Dodd and Dominic Papineau. Color version available in *Treatise Online* 160 (paleo.ku.edu/treatiseonline).

abiotic origins must be ruled out before they can be considered evidence for ancient life (STAUDIGEL & others, 2008; GROSCH & MCLOUGHLIN, 2014; MCMAHON, 2019; MCLOUGHLIN & others, 2020). Controversies notwithstanding, igneous rocks and inorganic preservation may represent underexplored archives of microbes in deep time and deep Earth (IVARSSON & others, 2020).

AFFINITY

With syngenicity and biogenicity established, the next challenge is to assess the affinity of the microfossils—whether they are prokaryotes or eukaryotes, and which group of prokaryotes they belong to. The most common microfossils are filaments, bacilloids, and coccoids, but these morphotypes occur in both eukaryotes and prokaryotes. To complicate interpretations further, subcellular structures such as melanosomes can be superficially similar in size and shape to bacilloidal and coccoidal bacteria (MOYER & others, 2014; VINTHER, 2015), although they are less relevant in the study of Precambrian microfossils. Eukaryotic cells are typically larger than prokaryotic cells, but there is a significant overlap (SCHOPF, 1992b; PANG & others, 2018). Thus, cell size is a suggestive but inconclusive criterion. Other morphological features, such as branching filaments, fused filaments, anastomosed filaments, coccoidal diads and tetrads, cell differentiation, and cell wall ornaments can be useful in distinguishing eukaryotic from prokaryotic microfossils. Typically, eukaryotic cells are morphologically more complex than prokaryotic cells. However, many of the features listed above may occur in bacterial cells. For example, actinobacteria can develop branching filaments and some of them (e.g., *Streptomyces* WAKSMAN & HENRICI, 1943) have been reported to form anastomosis of network (ERIKSON, 1949; GREGORY, 1956). A number of cyanobacteria can develop branching filaments (e.g., *Fischerella* GOMONT, 1895), coccoidal diads and tetrads (e.g., *Chroococcus* NÄGELI, 1849 and *Gloeocapsa* KÜTZING, 1843), and morphologically and functionally differentiated cells (e.g., heterocysts and akinetes in *Anabaena* BORY *ex* BORNET & FLAHAULT, 1886a) (CASTENHOLZ, 2001). Thus, these features are not exclusively eukaryotic, and only more complex features such as spinose cell wall ornaments, differentiated holdfast, apical meristem, and parenchymatous thallus are regarded diagnostic characters for eukaryotes (KNOLL & others, 2006). Cell wall ultrastructures can also be useful. For example, the trilaminar structure with two electron-dense layers around a thicker electron-tenuous layer is said to be characteristic of eukaryotic cell walls (JAVAUX,

Knoll, & Walter, 2004; Moczydłowska, Schopf, & Willman, 2010), although cell wall ultrastructures of modern eukaryotes and prokaryotes have not been thoroughly surveyed. Geochemical evidence can also be used to infer the prokaryotic versus eukaryotic affinities of microfossils. For example, combined micro-FTIR (Fourier-transform infrared spectroscopy) and Raman spectroscopic data—that is, FTIR CH3/CH2 absorbance ratio and Raman I-1350/I-1600 ratio of carbonaceous material—may be useful in distinguishing prokaryotic from eukaryotic microfossils (Igisu & others, 2009; Qu & others, 2015; Qu & others, 2018; Bonneville & others, 2020), although diagenetic and thermal alteration of these parameters has not been completely understood (Igisu & others, 2018). As another example, methanogenic archaea can generate large carbon isotope fractionations that can be preserved in the geological record (Stueken & others, 2017; Lepot, 2020). The assignment of prokaryotic microfossils to the various phylogenetic and physiological groups is another major challenge; but ecological, morphological, and chemical comparison with modern prokaryotic groups can provide some insights. This is discussed below for selected groups of prokaryotic microfossils.

SELECTED GROUPS OF PROKARYOTIC MICROFOSSILS

CYANOBACTERIA

Modern cyanobacteria consist of five morphological groups (Castenholz, 2001). Subsection I includes unicellular/colonial cyanobacteria that reproduce by binary fission (e.g., *Prochlorococcus* Chisholm & others, 1992, *Synechococcus* Nägeli, 1849, *Gloeocapsa*, *Entophysalis* Kützing, 1843, *Chroococcus*). Subsection II includes unicellular/colonial cyanobacteria that reproduce by internal multiple fissions and formation baeocytes (e.g., *Pleurocapsa* Thuret in Hauck, 1885*, Hyella* Bornet & Flahault, 1888). Subsection III (e.g., *Lyngbya* Agardh *ex* Gomont, 1892b*, Microcoleus* Desmazières *ex* Gomont, 1892a*, Oscillatoria* Vaucher *ex* Gomont, 1892b*, Spirulina* Turpin *ex* Gomont, 1892b*, Trichodesmium* Ehrenberg *ex* Gomont, 1892b) and Subsection IV (e.g., *Anabaena, Nostoc* Vaucher *ex* Bornet & Flahault, 1886a, *Calothrix* Agardh *ex* Bornet & Flahault, 1886b) are both characterized by uniseriate and unbranched trichomes produced by binary fission in one plane, but the latter have differentiated cells (e.g., specialized N_2-fixing heterocysts and resting akinetes). Subsection V is characterized by multiseriate or branching trichomes produced by binary fission in more than one plane, with some members having differentiated heterocysts (e.g., *Stigonema* Agardh *ex* Bornet & Flahault 1886c, *Fischerella*). Recent Phylogenetic analyses indicate that Subsections IV and V are monophyletic groups, whereas the other three are paraphyletic (Sánchez-Baracaldo, 2015; Schirrmeister, Gugger, & Donoghue, 2015).

Cyanobacteria play a major role in modern ecosystems and in the global carbon and oxygen cycles. The cyanobacteria *Prochlorococcus* and *Synechococcus* are the most abundant photosynthetic organisms in modern oceans, accounting for about 10% of the total ocean picoplankton cells in the euphotic zone and responsible for as much as 25% of ocean net primary productivity (Flombaum & others, 2013). A single cyanobacterial genus, *Trichodesmium,* is responsible for nearly 50% of global marine N_2 fixation (Sohm, Webb, & Capone, 2011; Bergman & others, 2013). Benthic cyanobacteria are also important sedimentary agents. They build microbial mats and stromatolites (Stal, 2012), stabilize sediments (Noffke, 2010), and perform bioerosion and biodegradation (Golubic, Pietrini, & Ricci, 2015). Cyanobacteria also played a transformative role in Earth history. The origin of oxygenic photosynthesis in a common ancestor of cyanobacteria is the geobiological foundation of the Great Oxidation Event and the origin of photosynthetic eukaryotes (Knoll, 2008). Thus, it is expected that

cyanobacteria should be richly archived in the geological record. Indeed, they are the most common and widespread prokaryotic microfossils in the geological record, and some of the Precambrian microfossils first reported in the literature were compared and identified with cyanobacteria (Barghoorn & Tyler, 1965; Cloud, 1965).

A number of researchers have reviewed Precambrian cyanobacterial microfossils from different perspectives (Knoll & Golubic, 1992; Golubic & Lee, 1999; Schopf, 2012; Sergeev, Sharma, & Shukla, 2012; Knoll, 2016; Schirrmeister, Sánchez-Baracaldo, & Wacey, 2016; Demoulin & others, 2019). The identification of cyanobacterial microfossils is based on their combined morphologic, taphonomic, paleoecological, paleoenvironmental, and behavioral features that are considered with modern counterparts (Knoll & Golubic, 1992; Golubic & Lee, 1999). Relative to other bacteria, cyanobacteria are typically larger in size and more complex in morphologies, some have sheaths, many are associated with stromatolites, and they commonly live in the photic zone or shallow marine environments where silicification occurs, although there are aspects of morphological and ecological convergences between cyanobacteria and some mat-forming sulfide-oxidizing bacteria. Some purported cyanobacterial fossils are morphologically simple. Examples include micrometer-sized coccoids such as *Myxococcoides* Schopf, 1968 (Fig. 9.7) and tubular filaments such as *Siphonophycus* Schopf, 1968 (Fig. 9.9–9.12; Fig. 10.4). Their cyanobacterial interpretation is primarily based on their preservation, sometimes in life position (Fig. 9.8–9.9) in stromatolitic laminae (Golubic & Lee, 1999; Cao, Yuan, & Xiao, 2001). It is assumed that these stromatolites were likely constructed by cyanobacteria. Others have a combination of morphologies and ecologies that support a cyanobacterial interpretation. These include *Eoentophysalis* Hofmann, 1976 with colonial coccoidal cells forming microbial crusts (Fig. 9.5); *Eohyella* Zhang & Golubic, 1987 being euendolithic and psuedofilamentous; and *Polybessurus* Green & others, 1987, with a stalk consisting of stacked cup-like gelatinous material (Fig. 9.6). Still others are character-rich and have distinctive, if not diagnostic, cyanobacterial features such as fossilized akinetes. The co-occurrence of *Archaeoellipsoides* Horodyski & Donaldson, 1980 and *Filiconstrictosus* Schopf & Blacic, 1971—which are interpreted as akinetes and short-trichome germlings, respectively—from the Mesoproterozoic Billyakh Group in Siberia provides a plausible case for fossil akinetes (Golubic, Sergeev, & Knoll, 1995; Sergeev, Knoll, & Grotzinger, 1995). Akinetes also occur in the Tonian fossil *Anhuithrix* Pang & others, 2018, and both akinetes and heterocysts have been reported in the Devonian microfossils *Langiella* Croft & George, 1959 and *Kidstoniella* Croft & George, 1959. These features facilitate morphological comparisons with modern cyanobacteria, where akinetes and heterocysts occur only in Subsections IV–V (Castenholz, 2001; Uyeda, Harmon, & Blank, 2016, fig. S7). Various ecological and morphological comparisons have been proposed for a number of well-known cyanobacterial fossils (Table 1, p. 48–49), many of which were named after their modern counterparts (Schopf, 1994; Knoll, 2016). Accepting the interpretations presented in Table 1, all five cyanobacterial subdivisions are represented in the fossil record.

When did cyanobacteria first evolve? This question can be addressed from the perspectives of molecular clocks, geochemical signatures, and fossils, but currently available data do not provide a tight constraint on this important evolutionary event. Molecular clocks give divergent results, with the estimated divergence time of crown-group cyanobacteria ranging widely from more than 3600 Ma to less than 2000 Ma, with very large error bars (Schirrmeister, Gugger, & Donoghue, 2015; Shih & others, 2017; see summary in Demoulin & others, 2019; Garcia-Pichel & others,

2019). Stable carbon isotope signatures of Archean organic carbon are consistent with but are not uniquely diagnostic of cyanobacterial metabolism (Demoulin & others, 2019), although Lyons, Reinhard, and Planavsky (2014) argue that the total organic carbon content in Archean shales presents strong evidence for oxygenic photosynthesis (and perhaps cyanobacteria) before the Great Oxidation Event at 2320–2450 Ma (Bekker & others, 2004; Holland, 2006; Luo & others, 2016). The report of 2-methylhopanoids—which were regarded as a biomarker of cyanobacteria—from the ~2700 Ma Jeerinah Formation in Western Australia (Brocks & others, 1999) was later shown to be compromised by contaminations (Rasmussen & others, 2008; French & others, 2015), leaving the 1.64 Barney Creek Formation in Western Australia as the oldest known unit to contain appreciable amount of 2-methylhopanoids (Summons & others, 1999; Brocks & others, 2005). More recent studies, however, have brought uncertainty to the interpretation of 2-methylhopanoids as a cyanobacterial biomarker; it seems that 2-methylhopanoids can also be produced by diverse alphaproteobacteria, including the anoxygenic purple nonsulfur phototroph *Rhodopseudomonas palustris* (Rashby & others, 2007) and the nitrifying bacterium *Nitrobacter vulgaris* (Elling & others, 2020). Thus, it is possible that the biochemical capability to synthesize 2-methylhopanoids may have a broader phylogenetic distribution and a deeper evolutionary history than cyanobacteria. More convincing biomarker evidence for cyanobacteria comes from fossil porphyrins, coupled with compound-specific nitrogen isotope data, from the ~1100 Ma El Mreïti Group in the Taoudeni Basin of Mauritania in northwestern Africa (Gueneli & others, 2018).

The Archean micropaleontological record is sparse and intensely debated. Various microfossils have been reported from the ~3400–3500 Ma Warrawoona Group and Strelley Pool Formation in Western Australia (Schopf, 2006a; Schopf, 2006b; Sugitania & others, 2013), and some have been compared with and interpreted as cyanobacteria (Awramik, Schopf, & Walter, 1983; Schopf & Packer, 1987; Schopf, 1993), although their biogenicity is a continual debate (Buick, 1984; Brasier & others, 2002; Wacey, Eiloart, & Saunders, 2019). More convincing Archean and early Paleoproterozoic filamentous microfossils have been known from ~3235 Ma volcanogenic massive sulfide deposit in in Sulfur Spring Group (Rasmussen, 2000) and the 2450–2210 Ma Kazput Formation of the Turee Creek Group in Western Australia (Schopf & others, 2015; Fadel & others, 2017; Barlow & Kranendonk, 2018), but none of these have been interpreted as cyanobacterial filaments. Filamentous microfossils described as *Siphonophycus transvaalensis* Beukes, Klein, & Schopf in Klein, Beukes, & Schopf, 1987 from the ~2500 Ma Gamohaan Formation and the ~2600 Ma Campbellrand Group of the Transvaal Supergroup in South Africa are among the oldest microfossils that have been interpreted as cyanobacteria (Klein, Beukes, & Schopf, 1987; Altermann & Schopf, 1995), but the simple morphology of *Siphonophycus* (see Fig. 9.9–9.12, Fig. 10, Fig. 12, Fig. 14.2–14.3) means that this interpretation is open to scrutiny. Indeed, among the genera listed in Table 1, only *Eoentophysalis* (Fig. 9.5), *Eohyella*, and *Polybessurus* (Fig. 9.6) are regarded as uncontested cyanobacteria (Demoulin & others, 2019), although several others are likely or probable cyanobacteria when additional paleonenvironmental and taphonomic conditions are considered together with morphological features (Knoll, 2016). As such, *Eoentophysalis belcherensis* Hofmann, 1976 from the 2015–2018 Ma Belcher Supergroup in Canada (Hofmann, 1976; Hodgskiss & others, 2019) represents the oldest unequivocal cyanobacterial fossil and provides a minimum age constraint on cyanobacterial divergence (Fig. 16).

Stromatolites have been reported from a number of Archean successions. Putative stromatolites are known from the

Table 1. Selected microfossils that have been interpreted as cyanobacteria. With the exception of *Anhuithrix* Pang & others, 2018, most are a few to a few tens of micrometers in cell/trichome diameter/width. See Demoulin & others (2019) for a more complete list of occurrences.

Fossil genus	Proposed cyanobacterial features	Oldest occurrence	Proposed modern analogs	Cyanobacteria?
Eosynechococcus Hofmann, 1976 (Fig. 6.6)	Rod-shaped cells, no sheath, sometimes two cells attached end-to-end, indicating symmetrical transverse binary fission in a single plane	2015–2018 Ma Belcher Supergroup, Canada (Hofmann, 1976; Hodgskiss & others, 2019)	*Synechococcus,* Subsection I	Probable
Gloeocapsomorpha Zalessky, 1917	Nested planar cell aggregates surrounded by multilaminated sheaths	Middle Ordovician oil shale, Baltic Shale Basin, Estonia (Zalessky, 1917; Foster, Reed, & Wicander, 1989)	*Gloeocapsa* & *Entophysalis,* Subsection I	Possible
Eoentophysalis Hofmann, 1976	Layers or crusts consisting of solitary cells, paired cells, planar tetrads, or irregular clusters of cells embedded in multilaminated sheaths	2015–2018 Ma Belcher Supergroup, Canada (Golubic & Hofmann, 1976; Hofmann, 1976; Hodgskiss & others, 2019)	*Entophysalis,* Subsection I	Likely
Palaeopleurocapsa Knoll, Barghoorn, & Golubic, 1975.	Sheathed pseudofilamentous cell packets	~800 Ma Skillogalee Dolomite, Adelaide Geosyncline, southern Australia (Knoll, Barghoorn, & Golubic, 1975).	*Pleurocapsa,* Subsection II	Probable
Eohyella Zhang & Golubic, 1987	euendolithic pseudofilamentous cyanobacterium	~1625 Ma Dahongyu Formation, North China (Zhang & Golubic, 1987)	*Hyella,* Subsection II	Likely
Polybessurus Green & others, 1987 (Fig. 1.6)	Spherical cell subtended by a cylindrical stalk consisting of stacked cup-like envelopes and may have reproduced by baeocytes	~1200 Ma Avzyan Formation, Ural Mountains, Russia (Sergeev, 1994); ~1050 Ma Uluksan Group (Kah & Knoll, 1996; Gibson & others, 2018); Tonian Eleanor Bay Supergroup in eastern Greenland (Green & others, 1987); Tonian Draken Formation in Svalbard (Knoll, Swett, & Mark, 1991)	*Cyanostylon,* Subsection II	Likely
Palaeolyngbya Schopf, 1968	Cellular trichome singularly enclosed in sheath	Tonian (~825 Ma) Bitter Springs Group, Australia (Schopf, 1968; Normington & others, 2019)	*Lyngbya,* Subsection III	Probable
Oscillatoriopsis Schopf, 1968	Unsheathed uniseriate trichome, cells wider than long, slightly differentiated apical cells	Tonian (~825 Ma) Bitter Springs Group, Australia (Schopf, 1968; Normington & others, 2019)	*Oscillatoria,* Subsection III	Probable
Obruchevella Reitlinger, 1948	Helical tubular filaments	~1560 Ma Gaoyuzhuang Formation, North China (Shi & others, 2017)	*Spirulina,* Subsection III	Possible

Table 1 *continued on next page*

Fossil genus	Proposed cyanobacterial features	Oldest occurrence	Proposed modern analogs	Cyanobacteria?
Siphonophycus Schopf, 1968 (Fig. 1.9–1.12, 2,4)	Tubular filament interpreted as cyanobacterial sheaths; form genus	~2600 Ma Campbellrand Group (Altermann & Schopf, 1995) and ~2500 Ma Gamohaan Formation (Klein, Beukes, & Schopf, 1987), both of Transvaal Supergroup, South Africa	Tubular sheath of Subsection III filaments	Probable
Eoschizothrix	Sheathed multitrichomous filaments	~1560 Ma Gaoyuzhuang Formation, North China Craton (Lee & Golubic, 1998)	*Microcoleus* & *Schizothrix* Subsection III	Probable
Archaeoellipsoides Horodyski & Donaldson, 1980 (Fig. 1.4)	Large (~100 µm) elongate sausage-shaped vesicles interpreted as isolated akinetes, sometimes co-occurring with short trichomes interpreted as germlings (Sergeev, Knoll, & Grotzinger, 1995)	(?) ~2100–2040 Ma Francevillian Group (Amard & Beertrand-Sarfati, 1997); ~1560 Ma Gaoyuzhuang Formation, North China Craton (Shi & others, 2017); 1653–1647 Ma McArthur Group, Australia (Tomtani & others, 2006); 1400–1500 Ma Billyakh Group, Siberia (Golubic, Sergeev, & Knoll, 1995; Sergeev, Knoll, & Grotzinger, 1995; Gorokhov & others, 2019); ~1400 Ma Dismal Lake Group, Canada (Horodyski & Donaldson, 1980)	Akinetes of Member IV cyanobacteria	Likely
Veteronostocale Schopf & Blacic, 1971	Unsheathed uniseriate trichome with rounded cells, no apical attenuation	Tonian (~825 Ma) Bitter Springs Group, Australia (Schopf & Blacic, 1971; Normington & others, 2019)	*Nostoc,* Subsection IV according to Schopf & Blacic (1971)	Probable
Anhuithrix Pang & others, 2018	Unbranched, uniseriate trichomes with sheathed vegetative cells and akinetes	Tonian Liulaobei Formation, North China (Pang & others, 2018)	*Anabaena* & *Nostoc,* Subsection IV	Likely
Langiella Croft & George, 1959 & ***Kidstoniella*** Croft & George, 1959	Branching trichomes with sheathed cells as well as differentiated heterocysts and (in *Langiella*) akinetes	Early Devonian (~400–412 Ma) Rhynie Chert, Scotland (Croft & George, 1959)	*Stigonema,* Subsection V	Likely

~3470 Ma Dresser Formation in Western Australia (Fig. 17.1) (Buick, Dunlop, & Groves, 1981). Conical stromatolites from the ~3430 Ma Strelley Pool Formation in Western Australia (Fig. 17.2) are regarded as biosedimentary structures (Hofmann & others, 1999; Allwood & others, 2006), possibly related to cyanobacterial activities (Schopf, 2012). More convincing evidence for cyanobacterial metabolism comes from disrupted stromatolitic laminae due to bubble formation related to oxygenic photosynthesis (Bosak & others, 2009); such evidence first appears in stromatolites from the ~2700 Ma Tumbiana Formation in Western Australia (Fig. 17.3). Consistent with this inference, limited evidence for Fe and S cycling in strata hosting the Tumbiana stromatolites indicates photoautotrophy using water rather than iron or sulfur as electron donors (Buick, 1992; Stueken & others, 2017). Overall, microfossils and stromatolites indicate that cyanobacteria may have diverged between 2700 Ma and 2000 Ma. If one accepts that the origin of cyanobacteria must predate the Great Oxidation Event (Bekker

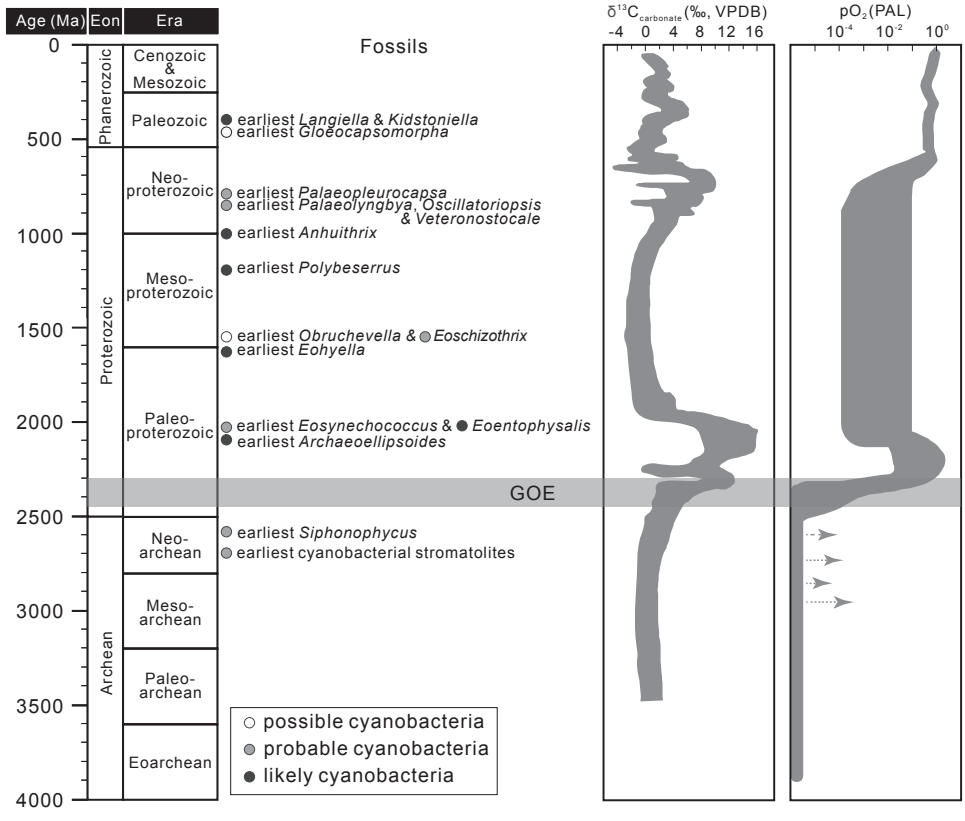

FIG. 16. Geological distribution of cyanobacterial microfossils. Hollow, gray, and solid circles represent the oldest known occurrence of possible, probable, and likely cyanobacterial microfossils. Purple bar represents the Great Oxidation Event (GOE) (adapted from Xiao & Tang, 2018 and Demoulin & others, 2019, and based on data in Table 1).

& others, 2004; HOLLAND, 2006; LUO & others, 2016), this window can be further narrowed to be 2700–2450 Ma (Fig. 16).

NON-CYANOBACTERIAL MICROBES

The identification of non-cyanobacterial microbes in the geological record is usually based only on geochemical data (e.g., carbon, iron, and sulfur isotopes) indicative of specific physiology or metabolism (e.g., STUEKEN & others, 2017; LEPOT, 2020). Thus, unlike cyanobacterial fossils, these inferred physiologies—because of their diverse phylogenetic distributions—do not define monophyletic groups. For example, iron oxidation (EMERSON, FLEMING, & MCBETH, 2010), dissimilatory iron reduction (LOVLEY, 2013), dissimilatory sulfate/sulfur reduction (CANFIELD & RAISWELL, 1999), and methanotrophy (HANSON & HANSON, 1996; KNITTEL & others, 2005) occur in both bacteria and archaea. And methanogensis occurs in multiple archaeal groups (LYU & LIU, 2018). Nonetheless, there are reports of body fossils of non-cyanobacterial prokaryotes, and their interpretations are sometimes based on characteristic morphological features and aided by geochemical data. These are briefly described below.

IRON-METABOLIZING MICROBES

Iron is involved in the metabolism of diverse bacteria and archaea, including dissimilatory Fe^{3+} reducing or Fe^{3+} respiring

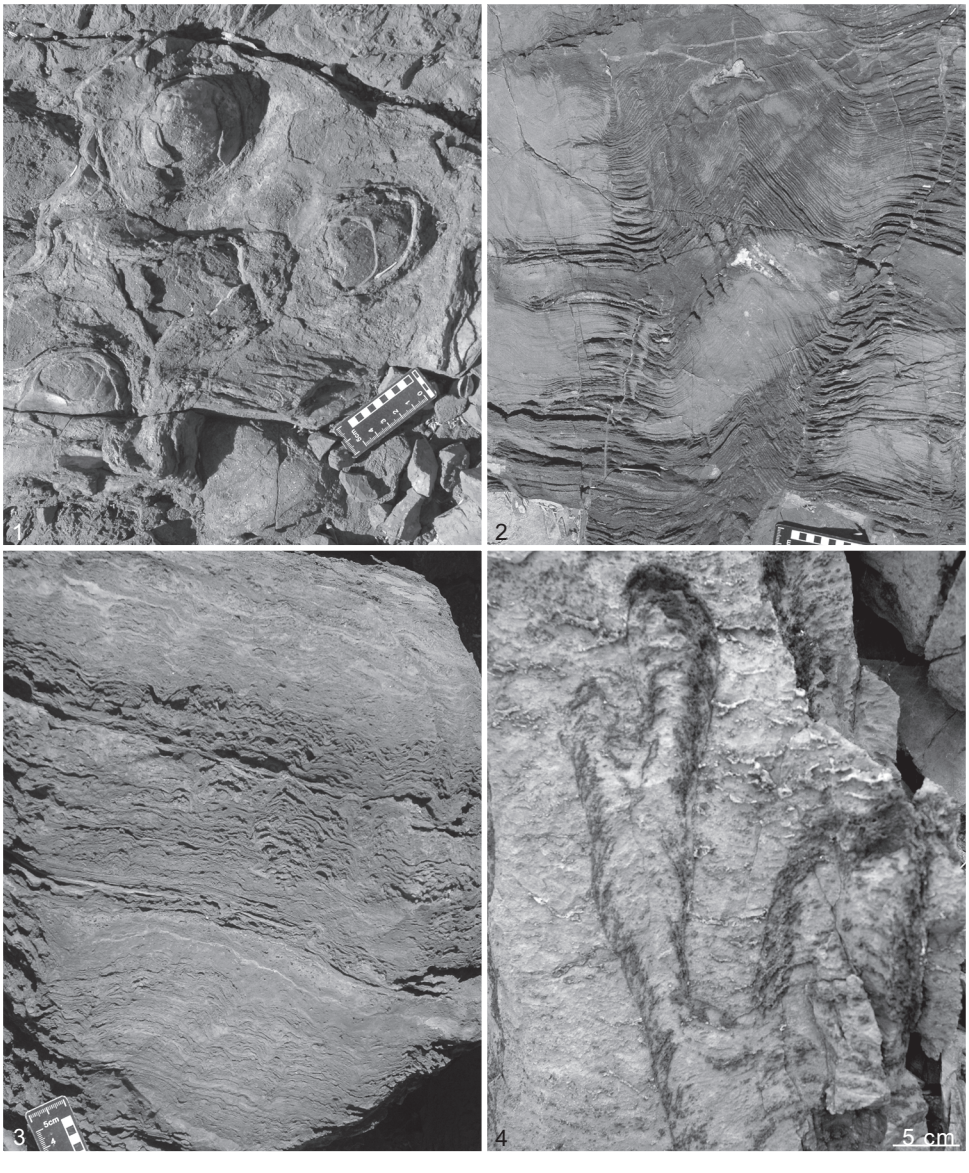

Fig. 17. Field photographs of representative Archean and Paleoproterozoic stromatolites. 1, possible coniform stromatolites (top view) from the ~3470 Ma Dresser Formation, North Pole, Western Australia (Buick, Dunlop, & Groves, 1981); 2, Conical stromatolite (vertical cross-sectional view) from the ~3430 Ma Strelley Pool Formation in Western Australia (Hofmann & others, 1999; Allwood & others, 2006); 3, microbial stromatolites (cross-sectional view) from the ~2700 Ma Tumbiana Formation of the Fortescue Group in Western Australia (Awramik & Buchheim, 2009); 4, branching stromatolites (cross-sectional view) from the ~2450–2210 Ma Kazput Formation of the Turee Creek Group in Western Australia (Martindale & others, 2015). All photos are new and by Shuhai Xiao. Color version available in *Treatise Online* 160.

bacteria (Lovley, 2013) such as *Geobacter* Lovley & others, 1993 and *Shewanella* MacDonell & Colwell, 1985, Fe^{2+} oxiwdizing bacteria (some of which are anoxygenic phototrophs) (Brock & others, 1994), and magnetotactic bacteria (Bazylinski & Frankel, 2003). There are a number of reports of iron-oxidizing microbial fossils. For example, *Frutexites*-like microstromatolites in Cenozoic basaltic seafloor are interpreted as structures produced by biofilms involving iron-oxidizing bacteria (Heim & others, 2017; Ivarsson & others, 2020). Some filamentous microfossils from the Ediacaran Qigebulake Formation in China (Zhou & others, 2015), the ~1880 Ma Gunflint Formation in Canada (Barghoorn & Tyler, 1965; Cloud, 1965), and the ~2450–2210 Ma Kazput Formation of the Turee Creek Group in northwestern Australia(Fadel & others, 2017) were compared with iron-oxidizing bacteria, but these microfossils do not seem to have diagnostic features uniquely characteristic of iron bacteria. Similarly, the Gunflint microfossil *Eoastrion* Barghoorn in Barghoorn & Tyler, 1965 (Fig. 9.3) has been compared with the extant Fe- and Mn-oxidizing bacterium *Metallogenium* Perfilev & Gabe, 1961 (Cloud, 1965; Zavarzin, 1981), although the nature of *Metallogenium* remains enigmatic (Klaveness, 1999), and a recent study of *Eoastrion*-like structures from the ~2100 Ma FC Formation of the Francevillian in Gabon was unable to unequivocally confirm its biogenicity (Lekele Baghekema & others, 2017). Additionally, tubular structures from the >3750 Ma Nuvvuagittuq supracrustal belt in Canada (Fig. 14.3) were tentatively compared with iron-oxidizing bacteria (Dodd & others, 2017), but their biogenicity has been debated (McMahon, 2019). Some extant iron-oxidizing bacteria do produce morphologically distinct stalks (e.g., branching and twisted Fe-oxyhydroxide stalks in *Gallionella*) (Chan & others, 2011) that can be preserved in the fossil record and thus offer promising diagnostic features for this group of bacteria (Johannessen & others, 2020). Morphologically similar stalks have been reported from Jurassic hydrothermal deposits at ODP site 801 in the western Pacific Ocean (Krepski & others, 2013), Pennsylvanian coal beds in Ohio, USA (e.g., Schopf & others, 1965, fig. 12), the late Paleoproterozoic (~1700 Ma) Jhamarkotra Formation in India (Crosby, Bailey, & Sharma, 2014), the late Paleoproterozoic Chuanlinggou Formation in the North China Craton (Lin & others, 2019), and late Paleoproterozoic (1.74 Ga) jasper in the lower Cleopatra Rhyolite in central Arizona, USA (Little & others, 2021). These are intriguing and more convincing evidence for iron-oxidizing bacteria in the fossil record.

Both microaerophilic iron-oxidizing bacteria and anoxygenic photoferrotrophs have been implicated in the deposition of Precambrian banded iron formations (Kappler & others, 2005; Konhauser & others, 2002; Chi Fru & others, 2013; Chan, Emerson, & Luther, 2016). If so, then Archean and Paleoproterozoic banded iron formations can be regarded as indirect evidence for iron-oxidizing bacteria (Heimann, 2021, see p. 91–127). In fact, Chi Fru and others (2013) reported what appears to be anoxygenic photoferrotroph fossils from a Quaternary hydrothermal vent field on Milos Island, Greece.

Magnetotactic bacteria represent a special group of iron bacteria that can uptake complexed ferric iron and, through reduction and partial oxidation of Fe, precipitate intracellular magnetite (Fe_3O_4) or greigite (Fe_3S_4) nanocrystals in membranous magnetosomes (Bazylinski & Frankel, 2003). Magnetite crystals produced by magnetotactic bacteria have distinct morphologies and crystallographic features that allow their identification in the fossil record (see Fig. 13) (Bazylinski & Frankel, 2003; Li & others, 2020). Magnetofossils have been reported from Mesozoic and Cenozoic sediments (Chang & Kirschvink, 1989; Kopp

& Kirschvink, 2008; Roberts & others, 2011) and even Precambrian stromatolites (Chang & others, 1989).

SULFUR-METABOLIZING MICROBES

Sulfur cycling in the water column and sediments can be inferred from geochemical data. For example, sulfate reduction, sulfide oxidation, and sulfur disproportionation can be inferred from sulfur isotope data (Canfield & Raiswell, 1999; Shen & Buick, 2004; Johnston & others, 2005), and anoxygenic photosynthesizers such as green and purple sulfur bacteria can be inferred from biomarker data (Brocks & others, 2005). The body fossil record of sulfur-metabolizing microbes is scarce, primarily because they generally do not have diagnostic morphological features. Nonetheless, sulfur-metabolizing microbial fossils have been reported in the literature. For example, Schopf and others (2015) reported filamentous microbial communities from the Paleoproterozoic Turee Creek Group and Duck Creek Formation in Australia, and interpreted them as sulfureta in which sulfate/sulfur-reducing and sulfide-oxidizing microbes worked together to cycle sulfur species. This interpretation is based on inferred community ecology and the cobweb-like microbial fabrics that are often found in sulfureta. It is possible that these microbes also recycled iron species (Fadel & others, 2017). Additionally, Bailey and others (2013) reported septate filamentous microfossils with sparse intracellular sulfur globules from the Ediacaran Doushantuo Formation and interpreted them as sulfide-oxidizing bacteria analogous to the extant *Beggiatoa*. Finally, Bailey and others (2007) interpreted the animal embryo-like microfossil *Megasphaera* Chen & Liu, 1986 from the Ediacaran Doushantuo Formation in the South China Craton as a giant sulfide-oxidizing bacterium analogous to the extant genus *Thiomargarita*, but this interpretation has been refuted (Xiao, Zhou, & Yuan, 2007; Cunningham & others, 2012).

METHANOGENS AND METHANOTROPHS

Microbial activities of methanogens in the geological record are chiefly inferred from $\delta^{13}C$ data, because they produce a CH_4 pool extremely depleted in ^{13}C and correspondingly a CO_2 pool enriched in ^{13}C (Lepot, 2020). This isotopic signal can be recorded as extremely high $\delta^{13}C_{carb}$ values of carbonate sourced from the CO_2 pool as long as CH_4 is effectively removed from the system (Sun & others, 2020) or as extremely negative $\delta^{13}C_{carb}$ values of carbonate related to anaerobic oxidation of methane (Jiang, Kennedy, & Christie-Blick, 2003; Wang & others, 2008), or as extremely negative $\delta^{13}C_{org}$ values of organic carbon produced by methanotrophs or methylotrophs in general (Stueken & others, 2017; Xiao & others, 2017). Thus, extremely negative $\delta^{13}C_{org}$ values (as low as −57‰) from the ~2700 Ma Fortescue Group in Western Australia indicate that both methanogens and methanotrophs must have evolved by the Neoarchean. Body fossils of methanotrophs or methylotrophs, however, are extremely rare, although Sun and others (2020) recently reported micrometer-sized coccoidal methanogens from dolomite concretions in Permian lacustrine deposits of northwestern China. These coccoids are morphologically indistinct and their interpretation as fossil methanogens was largely based on the extremely positive $\delta^{13}C_{carb}$ values of the host dolomite concretions.

SUMMARY AND FUTURE PROSPECTS

Prokaryotes (bacteria and archaea) are ubiquitous, abundant, and physiologically diverse. They play essential roles in modern Earth systems and were likely as important in the geological past as they are today. Yet, their fossil record is rather sparse, and the prokaryote paleontology is a relatively young science. Since the 1950s, however, we have learned a great deal about prokaryotes in

the geological past and the field continues to grow rapidly. Prokaryotic microfossils are known in a number of taphonomic modes: silicification, phosphatization, calcification, pyritization, carbonaceous compression in fine-grained siliciclastic sediments and in amber, biomineral preservation, and trace fossil preservation. The study of prokaryotic microfossils faces many challenges. Given their microscopic sizes, simple morphologies, and possible confusion with biomorphs and eukaryotic microbes, it is a difficult task to demonstrate the syngenicity, biogenicity, and phylogenetic affinity of purported prokaryotic microfossils. Nonetheless, authentic prokaryotic microfossils are known in the geological record, and they extend as far back as 3200 Ma and perhaps 3500 Ma. Some of these microfossils can be assigned to phylogenetic or physiological groups, including cyanobacteria, iron-oxidizing bacteria, magnetotactic bacteria, sulfur-oxidizing bacteria, and methanogens. Of these, cyanobacteria have the richest record, one that goes back to 2000 Ma and perhaps 2700 Ma, and their identification is aided by ecological association with stromatolites and sometimes diagnostic morphological features.

Despite notable progress in the study of prokaryotic fossils since the 1950s, there remain enormous opportunities for future research. Prokaryotic micropaleontology continues to be a frontier in scientific investigation. The vast majority of prokaryotic groups are poorly (or not at all) represented in the fossil record, including archaea and various nitrogen-metabolizing microbes, which are fundamental in the origin and function of the biosphere. The full spectrum of environmental distribution of prokaryotes is poorly documented in the geological record. This is particularly true for microbes in the terrestrial realm, cryptic spaces, deep-sea settings, deep lithosphere, and other extreme environments.

We know very little about how prokaryotes interacted with the environment and with other organisms in the geological record. It is likely that new advances will be made in the study of prokaryote micropaleontology at the interface with other sciences (e.g., geochemistry, sedimentology, microbiology, big data science) and advanced analytical techniques. Ultimately, the vast phylogenetic, physiological, and ecological diversity of bacteria and archaea evident today must surely have substantial geological and evolutionary roots, and much more awaits discovery.

PRECIPITATED MICROBIALITES

R. S. Shapiro and D. T. Wilmeth

INTRODUCTION

Microbially induced, lithified structures known as microbialites are both geologically and biologically significant, forming extensive sedimentary, geochemical, and microbiological records in modern and ancient environments. Depositional settings range from deep ocean hydrocarbon seeps, hydrothermal vents, and whale falls, to cool water carbonate banks—abundant occurrences within peritidal zones and, finally, to non-marine environments such as lakes, rivers, and springs. More than three billion years of Earth's biosphere is primarily recorded within microbialites, including the oldest macrofossils on the planet (Walter, Buick, & Dunlop, 1980; Van Kranendonk, Webb, & Kamber, 2003; Van Kranendonk, 2006). Even with diminished diversity and abundance during the Phanerozoic, periodic microbialite resurgences after mass extinctions are used as indicators for relative environmental recovery (Mata & Bottjer, 2012). Microbialites are also targeted by astrobiology studies for their ability to form in harsh environments and their capacity to preserve specific biosignatures (Corsetti & Storrie-Lombardi, 2003; Shapiro, 2004a; Ibarra & Corsetti, 2016). Yet, despite the broad scientific significance of microbialites, many authors note a lack of consistent terminology (Riding, 1999), whereas others address the challenges of differentiating microbialites from numerous abiogenic sedimentary deposits (Buick, Dunlop, & Groves, 1981; Grotzinger & Rothman, 1996; Grotzinger & Knoll, 1999; Awramik & Grey, 2005).

The aim, herein, is to provide the reader with a basic working guide for field and laboratory descriptions of microbialites and to synthesize the various terminologies present in the literature. As a guide, this contribution is meant to complement the various review articles that focus more specifically on the fossil record of microbialites (Hofmann, 1973; Awramik & Riding, 1988; Awramik, 1991; Hofmann, 2000; Rowland & Shapiro, 2002; Riding, 2011a, and references therein). For example, Flügel (2004) provided an excellent analysis of microbialite as a carbonate lithologic unit with much discussion on genesis, diagenesis, and terminology. There have also been significant contributions from non-English literature, primarily by Russian workers (e.g., Maslov, 1960; Krylov, 1963; Raaben, 1991) in addition to other international researchers, including the earliest description of stromatolites (Kalkowsky, 1908). The diversity of unique microbialite textures has produced many study-specific nomenclatures in the primary literature, and increases the difficulty of succinct review. Instead, this chapter synthesizes key features of previously published guides over multiple decades of microbialite research. Nomenclature that has gained acceptance by extensive utilization in the literature is given preference herein, with references provided for more detailed discussions beyond the scope of this review.

HISTORICAL PERSPECTIVE AND WORKING DEFINITION OF THE TERM MICROBIALITE

The word microbialite was introduced by Burne and Moore (1987) as a general term for sedimentary deposits created by the actions of microorganisms (see historical discussion in Riding, 2011a). Current researchers employ the term for microbially induced deposits in general, or when specific discrimination of stromatolitic, thrombolitic, or other textures is untenable. An alternative spelling, microbolite (Riding,

1991), while perhaps more accurate, has not gained traction in the literature. In contrast to microbialites, microbial mats (often shortened to mats) are unlithified, macroscopic microbial communities in modern environments, commonly divided into layers with distinct microbial metabolisms. Special care should be taken to use the terms microbialite and microbial mat only for lithified and unlithified communities respectively, especially in modern and Holocene locations where both structures may be present.

Microbial activity preserved in the sedimentary record includes 1) mineral precipitation within mats due to the physico-chemical properties of microbial communities, and 2) the trapping and binding of detrital grains on and within mat layers (Awramik, Margulis, & Barghoorn, 1976; Burne & Moore, 1987; Noffke & Awarmik, 2013). Microbial deposits predominantly formed by trapping, binding, and stabilization of detrital grains are prevalent in siliciclastic environments and have distinct nomenclatures described in greater detail on p. 76–81. Microbialites described herein are primarily formed via mineralization of mat textures, although detrital grains are commonly important components. The vast majority of microbialites are comprised of calcium carbonate, although many examples have been described comprised of primary opaline silica, oxides, sulfides, phosphates, and other minerals (Walter, Bauld, & Brock, 1972; Wallace, Keays, & Gostin, 1991; Martín-Algarra & Sánchez-Navas, 1995; Berelson & others, 2011). Whereas individual microbes are very rarely preserved within microbialites, specific features in macro- and microscopic textures indicate origination via microbial activity, as opposed to abiogenic sedimentation or precipitation. When microfossils are preserved, the lithified microbialite structure on a microscopic scale may be largely comprised of permineralized skeletons or mineralized molds.

Further refinement of microbialites is based on the mesostructure scale of observation (Fig. 18). Mesostructure refers to the millimeter to centimeter scale elements visible with the unaided eye or hand lens (Kennard & James, 1986). In contrast, microstructure encompasses all observations with a light or scanning electron microscope. The macrostructure refers to the larger association of mesostructural elements (Fig. 19, Fig. 20). For instance, laminae (mesostructure) may be stacked to form a cylindrical column (macrostructure). Some authors employ a larger hierarchical stage, megastructure, to describe the bed or overall stratigraphy of the microbialite-bearing units (Kennard & James, 1986). The necessity of using several scales of description of microbialites is one of the distinguishing features of their taxonomy relative to other fossils (Awramik, 1991; Shapiro & Awramik, 2006). Importantly, microbialites are organosedimentary constructions, and all scales of structure need to be studied for both biogenic and sedimentologic signals. The next sections describe five major categories of microbialites based on mesostructure.

STROMATOLITES

Substrate-attached microbialites with laminated fabrics are defined as stromatolites, deriving from the word stromatolith in Kalkowsky (1908). More than a century of successive studies has produced various definitions of the term stromatolite, both genetic and purely descriptive, as recounted in detail by Riding (2000, 2008). Many arguments center on the difficulty of directly identifying biogenicity in laminated deposits, which stems from 1) the removal of specific biosignatures by secondary alteration, and 2) the morphological similarity of laminated abiological structures to biogenic stromatolites (Grotzinger & Rothman, 1996; Grotzinger & Knoll, 1999). For simplicity, this chapter defines laminated microbialites as stromatolites, as opposed to abiogenic structures formed without the mediation of microbial communities. Recommended guides to stromatolite morphologies and textures include Logan, Rezak, and Ginsburg (1964); Walter (1976); Preiss (1976);

Buick, Dunlop, and Groves (1981); Grey (1989); Riding (1999); and Shapiro (2007), to name a select few.

On a macrostructural level, stromatolites vary from stratiform morphologies with low vertical relief, to simple columns, domes, and cones, to complex branching structures (Fig. *20*). Furthermore, individual stromatolites can change morphologies with successive generations of laminae accretion. For example, slight irregularities of stratiform stromatolites can propagate into larger domes or cones with continued growth. A standard stromatolite classification scheme that accounts for vertical changes in structure is provided in Logan, Rezak, and Ginsburg (1964). Changes in stromatolite morphology can arise from shifting depositional environments, biological communities, hydrochemistry, or all of these factors over time. As previously mentioned, many stromatolite macrostructures resemble laminated textures formed by abiogenic mineral precipitation, especially less complex stratiform or domal morphologies (Grotzinger & Knoll, 1999). Branching and conical morphologies have been hypothesized in simulations of abiogenic mineral growth (Grotzinger & Knoll, 1999; Dupraz, Pattisina, & Verrecchia, 2006), but such macrostructures have not been abiogenically replicated in physical experiments. One detailed method to study stromatolite macrostructure involves serially sectioning samples so that true three-dimensional reconstruction can be quantitatively assessed (see discussion in Hofmann, 1973). A number of publications describe serial sectioning techniques (Krylov, 1963; Preiss, 1976), and the capabilities have been significantly enhanced with modern illustration computer programs. A critical aspect is recognizing that one or several two-dimensional planes are insufficient to truly understand the complexity of stromatolite structures.

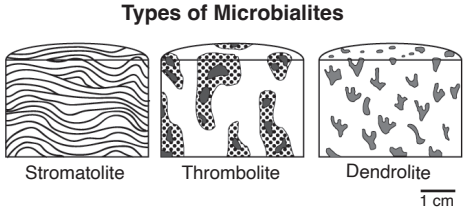

Fig. 18. Main groups of attached microbialites. The different groups are defined based on the mesostructure or constructional elements. Stromatolites are laminated, thrombolites are clotted, and dendrolites are comprised of bushes (new).

Because laminae are the defining mesoscale feature of stromatolites, special detail must be given to describing mesoscale textures. Laminae are typically comprised of light and dark couplets, with darker layers formed

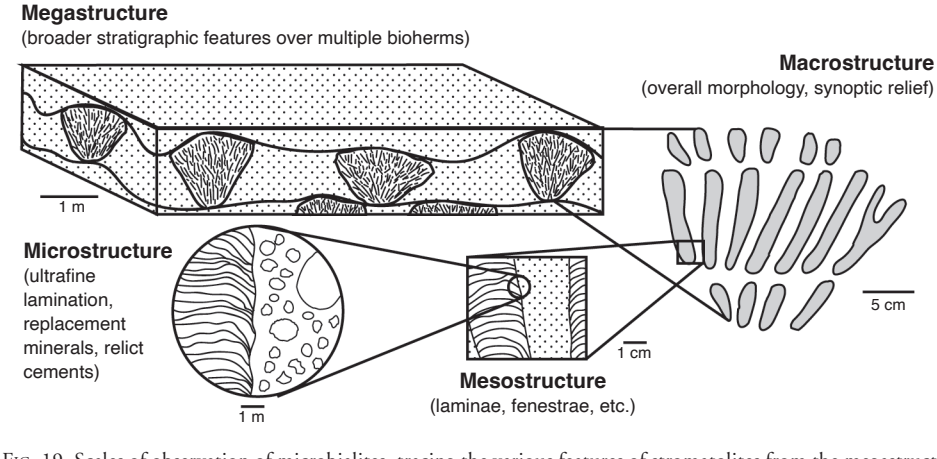

Fig. 19. Scales of observation of microbialites, tracing the various features of stromatolites from the megastructure through the microstructure (adapted from Shapiro & Awramik, 2006, fig. 2).

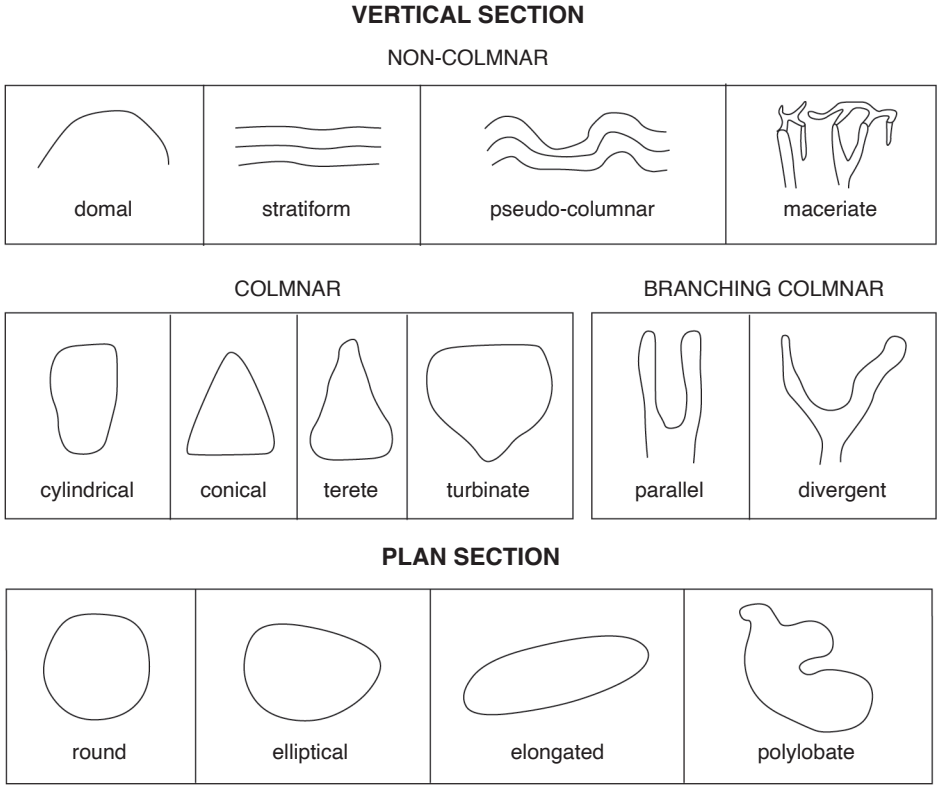

FIG. 20. Descriptive terminology as applied to the macrostructure of all microbialites (new).

by finer-grained, less porous micrite or microspar in carbonates or microcrystalline quartz in cherts (GROTZINGER & KNOLL, 1999). Darker zones can also be attributed to higher concentrations of organic material or insoluble residue such as iron oxides. Lighter laminae are generally defined by higher amounts of cemented interstitial spaces, filled with spar in carbonates or macroquartz in cherts. Microfossils in well-preserved stromatolite laminae have different orientations of filamentous cells, with laminae-parallel filaments in dark layers and laminae-normal or vertical filaments in light layers (GEBELEIN, 1969; WALTER, BAULD, & BROCK, 1972; GOLUBIC & FOCKE, 1978).

Key differences between stromatolites include laminae smoothness or waviness, thickness variation, nature of the laminae over the growth axis (apex), and nature of the laminae against the stromatolite margins (Fig. 21). For example, the height of a stromatolite at a single point in time (synoptical relief) can be established by measuring the vertical distance between the apex of a single layer and the same layer's intersection with the stromatolite margin. Another useful parameter when describing stromatolite textures is inheritance, or how well laminae inherit the shape of preceding layers. For example, a stromatolite that progresses upward from stratiform through domal to conical textures has low inheritance, as laminae over time do not resemble the shapes of lower layers. Conversely, a stromatolite that maintains consistent layer morphologies throughout the structure, whether flat, domal, or conical, has high inheritance.

In well-preserved carbonates, the laminar mesostructure can also help distinguish biogenic stromatolites from abiogenic

precipitates (Grotzinger & Knoll, 1999). Laminae formed within microbial mats are typically comprised of micrite or microspar and have irregular, wavy laminae resulting in low inheritance. In contrast, many laminated abiogenic carbonates are comprised of bladed or acicular needles, maintaining isopachous thicknesses across the stromatolite and extremely high inheritance. There are exceptions to these trends, but a meaningful assessment of biogenicity cannot be accomplished without first analyzing laminae petrography. For example, several lacustrine stromatolites exhibit both styles of lamination, alternating between irregular micritic layers and isopachous bladed fabrics, and have been correlated with changes in lake environments (Frantz & others, 2014; Fedorchuk & others, 2016).

Microstructural attributes vary widely between stromatolites (Fig. 22). The variety of textures observed is due to both depositional heterogeneity and subsequent diagenesis. Original fabrics include detrital grains (micrite, silt to fine sediment, coated grains, skeletal fragments), organic films, and various cements (isopachous rims, bladed fringes, botryoids, etc.). Among the many potential microscopic features within stromatolites, several diagnostic textures can help increase the confidence of stromatolite biogenicity (Buick, Dunlop, & Groves, 1981; Grotzinger & Knoll, 1999). Some Phanerozoic stromatolites preserve microfossils as carbonate permineralized sheaths, such as the filamentous morphotype *Girvanella* (Nicholson & Everidge, 1878), but these are relatively uncommon. Rounded fenestrae, which do not crosscut primary stromatolite textures, represent the preservation of former void spaces within microbial mats, which can be produced either by metabolic gas production or by natural irregularities in microbial mat textures (Sumner, 2000; Bosak & others, 2009, 2010; Mata & others, 2012; Wilmeth & others, 2019). Finally, the presence of detrital grains on sloped laminae that exceed the angle of repose indicate the

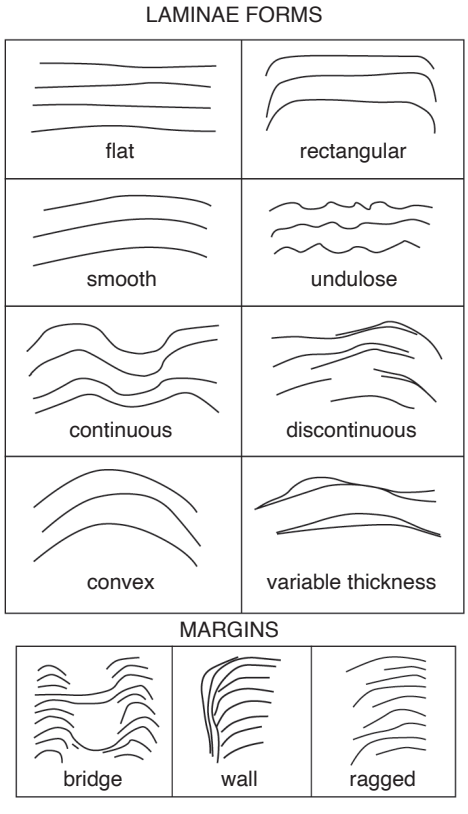

Fig. 21. Descriptive terminology as applied to the mesostructure of stromatolites (new).

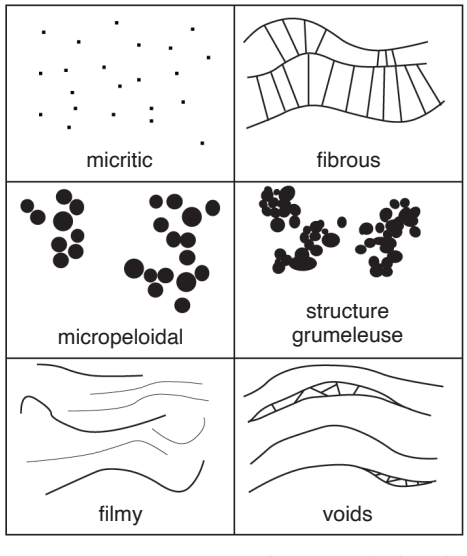

Fig. 22. Descriptive terminology as applied to the microstructure of all microbialites.

presence of adhesive microbial mats rather than pure mineral precipitates (Bailey & others, 2009; Tice, 2009; Frantz, Petryshyn, & Corsetti, 2015).

Early diagenesis in carbonates commonly leads to both micritization and aggrading neomorphic spar, obscuring original textures. Additionally, many stromatolites have destructive replacement of primary fabrics by mosaic dolomite. In some cases, placing a white card underneath a thin section increases the potential to view original textures on a microscope stage (Folk, 1987). Examples indicate that dolomitization is fabric selective, even down to individual laminae (Glumac & Walker, 1997; Riding, 2008). Dolomitization can be accentuated by staining with Alizarin Red to differentiate calcite (stained) from dolomite (unstained). Regardless of the preservation, describing stromatolite microstructure is critical when possible, noting presence or absence of microfossils, and any variation in mineralogy.

ONCOIDS

Oncoids are laminated microbialites that form unattached grains (Heim, 1916; Pia, 1927), in contrast to stromatolites attached to benthic substrates. Oncoids are typically spherical to ellipsoidal in shape, with variably smooth, pustular, or lobate surfaces (Fig. 23) resulting from patterns of primary precipitation and mechanical weathering. Most oncoids are comprised of calcium carbonate, with some siliceous examples surrounding hot springs (Jones & Renaut, 1997; Jones, Renaut, & Rosen, 1999; Konhauser & others, 2001), and several phosphatic and oxide-rich samples are known in ancient lithologies (Krajewski, 1983; Schaefer, Gutzmer, & Beukes, 2001; Gradziński & others, 2004; Sallstedt & others, 2018). For a detailed review of oncoid terminology and sedimentology, including comparisons with other coated grains, see Flügel, 2010.

Internal oncoid mesostructure consists of a nucleus surrounded by a cortex of variously concentric laminae. Nuclei vary depending on depositional environment, and include clastic grains, fossils, or reworked chemical sediments, such as surrounding carbonates or cherts. Nuclei are sometimes absent from samples, depending on diagenetic alteration, the angle of dissection, or an initial particle that was soft and/or featureless (Flügel, 2010). Cortices contain micritic or fine-grained laminae, which vary in thickness and concentricity, in contrast to grains such as ooids and pisoids, which contain radially fibrous, highly concentric laminae. Variable thicknesses of oncoid laminae typically result in low inheritance, leading to asymmetrical shapes including small domes and even cones (Logan, Rezak, & Ginsburg, 1964; Wilmeth & others, 2015). Logan, Rezak, and Ginsburg (1964) included a classification scheme for oncoid morphologies in addition to stromatolite textures. Oncoid laminae are similar in microstructure to biogenic stromatolites, including light and dark couplets, variously oriented microfossils, and rounded fenestrae (Peryt, 1981; Flügel, 2010; Wilmeth & others, 2015; Sallstedt & others, 2018). Microfossils are commonly present as filamentous permineralized sheaths, usually described as the morphotype *Girvanella* (Peryt, 1981; Riding, 1983).

The unattached nature of oncoids, unique among microbialites, provides useful insights into paleoenvironment. An oncoid-rich facies is called an oncolite, as opposed to singular oncoid grains. Oncolites can be described in a similar manner to other grain-dominated facies in terms of sorting, roundness, and grain vs. matrix support. Oncoids and oncolites provide evidence for agitated environments, requiring frequent exposure of fresh surfaces for microbial colonies to grow and eventually mineralize (Dahanayake, 1977; Ratcliffe, 1988). As oncoids grow larger, layers typically become increasingly asymmetrical due to longer periods of quiescence (Wright, 1983; Smith & Mason, 1991; Shapiro, Fricke, & Fox, 2009; Wilmeth & others, 2015). Oncoids

that become too large for continued agitation become the stable base for subseqatolite nucleation (Martín-Algarra & Vera, 1994; Burne & Moore, 1987).

THROMBOLITES

Thrombolites are clotted microbialites (Aitken, 1967). Although the term is nongenetic, the study of thrombolites has indicated that clotted fabrics are largely constructional and not merely secondarily altered stromatolitic textures. Shapiro (2000) addressed the terminological confusion of thrombolites, and further elaboration was provided by Shapiro and Awramik (2006). Because thrombolites lack laminae as a mesostructural fabric, synoptic relief is more difficult to assess. However, column margins and their relationship with surrounding sediments can still hold clues to syndepositional relief, with margins varying between smooth, invaginated, wrinkled, or lobate morphologies. If margin walls are not smooth, it is important to recognize whether surrounding sediments interfinger (low synoptic relief) or truncate against the margin (potentially higher synoptic relief).

The mesostructure of thrombolites is dominated by mesoclots separated by either cements or sediment (Kennard & James, 1986). Mesoclots are millimeter- to centimeter-scale zones of variable texture in both plan and longitudinal sections. Petrographic analysis of the mesoclots reveal them to be comprised of a variety of elements, including coccoid calcimicrobes (Kennard & James, 1986), botryoidal calcimicrobes (Latham & Riding, 1990), filamentous calcimicrobes (Moore & Byrne, 1994), algal-foraminiferal colonies (Toomey & Cys, 1979), dense micrite (Glumac & Walker, 1997), and peloids (Pratt & James, 1982). The distribution of mesoclots across two-dimensional thrombolitic surfaces imparts a clotted composition (see Fig. 24 for a compendium of the more common mesoclot forms as described in the literature).

The term mesoclot was first proposed by Kennard and James (1986) as an emendation for Aitken's (1967) clots, as the latter term was ambiguous and could be mistaken for submillimeter-size clotted microstructures. Other terms employed include fenestrae (Pratt & James, 1982) or thromboids (Kennard, 1994) (see review in Shapiro, 2000). Thromboid is unacceptable because the term is confusing when considering the present non-parallel usage of stromatoid and the multiple, conflicting definitions in the literature. The term fenestrae is not appropriate because it refers to a former void within a rock (Bates & Jackson, 1987) and not all mesoclots were open spaces. As with stromatolite laminae, the morphology and texture of the mesoclots are referred to as the fabric of a thrombolite. Microscopic features of the mesoclots should be described under microstructure. Using the terms macroclots or microclots is not advised, as this will only exacerbate confusion.

The three-dimensional morphology of a mesoclot is referred to as the mesoclot shape. There has not been a quantification scheme proposed for the study of mesoclots;

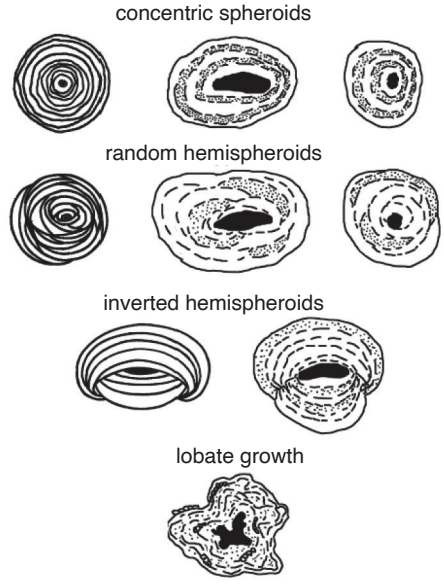

Fig. 23. Descriptive terminology as applied to the macrostructure of all oncoids (adapted from Logan, 1964, as presented in Flüge, 2010).

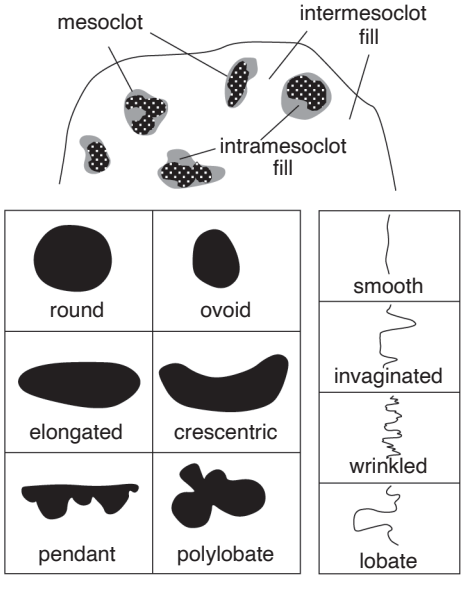

FIG. 24. Descriptive terminology as applied to the mesostructure of thrombolites (new).

the method of geometric study is left up to the discretion of the researcher, with the hopes that clear explanations are given. As with stromatolites, mesostructural aspects of thrombolites are best studied in three-dimensional preparations as their typically polymorphic shapes may present a variety of patterns on two-dimensional surfaces (SHAPIRO & AWRAMIK, 2006). Qualitative description of two-dimensional surfaces are still of great use for field and comparative study and should also be undertaken. To date, most studies have featured longitudinal sections, or mesoclot profiles (e.g., AITKEN & NARBONNE, 1989; KENNARD, 1994). However, much information can be gleaned from plan-view sections or mesoclot outlines. A good practice is to trace the mesoclots physically or digitally to demonstrate clear shapes, and then present patterns in a simple, two-tone scheme. Instead of using vague terms such as irregular or globular, measurements should be made of mesoclot height, length, and width, citing the orientation of the viewing plane relative to the growth axis of the thrombolite. Mention should be made if the mesoclot dimensions vary in different spots within one thrombolite, particularly from the base toward the top of the structure or from the margins toward the center.

The spatial relations of mesoclots can be isolated, interconnected, or coalesced (KENNARD & JAMES, 1986; SHAPIRO & AWRAMIK, 2006). The degree of coalescence can further be qualified as slightly coalesced or highly coalesced. In turn, mesoclots can be arranged in parallel to subparallel patterns within the thrombolite, presenting a horizontal, radial, or vertical mesostructure. Mention should be made of the amount of mesoclots (as percent abundance) within thrombolites.

In addition to mesoclots, the mesostructural analysis should also include descriptions of any voids, inter-mesoclot fill, calcimicrobes, and metazoans. Laminae are extremely rare, but if present should be described following the guidelines set forth for stromatolitic mesostructure. Care should be taken to note the relationship of the laminae to the mesoclots, whether gradational, alternating, or adjacent.

It is common for mesoclots in localized portions or in the entire thrombolite to be oriented in a regular pattern. Although much of the existing literature describes the orientation of thrombolite columns (macrostructure)—often misidentifying the elements as clots or thromboids (see RIDING, 2011a)—the terms here are still applicable to mesoclot orientation. Orientations of the columns should be described under macrostructure. For example, SHAPIRO and AWRAMIK (2006) presented a variety of plan-view shapes of arabesque columns (maceriae) that are macrostructural, as opposed to the mesoclots that comprise the mesostructure of maceriae.

DENDROLITES

Dendrolites are neither laminated nor clotted but are comprised of branching millimeter-scale bushes (RIDING, 1991). The bushes are inferred to be organic in origin, although the exact nature of the biota neces-

sary for the construction is not known. In many structures, bushes can be identified as (inferred genera of) calcimicrobes such as Epiphyton (Bornemann, 1886), *Renalcis* (Vologdin 1932), *Gordonophyton* (Korde, 1973), or *Angusticellularia* (Vologdin, 1962)(Rowland & Shapiro, 2002). The term dendrolite should not be utilized for structures that display branching crystalline growth, which can be easily recognized by clear crystal boundaries and more regular arrangement of the branches (Shapiro, 2004b). Thrombolites and dendrolites may represent end members of a continuum of diagenetic alteration, in which dendrolite bushes recrystallize to amorphic micrite that may then be considered a thrombolitic mesoclot (Riding, 1991).

Dendrolites occur as meter-scale domes, tabular biostromes, and centimeter-scale crusts. It may also be most accurate to refer to the microbial frameworks within archeocyath and lithistid reefs as dendrolite although the term has not been used in that regard. Dendrolites are distinctive but are present alongside and even interfingering with thrombolites and stromatolites. To date, there are few described dendrolites in the literature, although it is likely that some published accounts of thrombolites should more accurately be termed dendrolites. The original papers discussing dendrolites (Riding, 1991; Riding & Zhuravlev, 1995; Turner, James, & Narbonne, 2000; Shapiro & Rigby, 2004) did not propose a formal definition of dendrolite morphology. In a study of three-dimensional dendrolite reconstruction, Howell, Woo, and Chough (2011) proposed terminology for the dendrolite elements. Herein, a model (Fig. 25) is provided that merges the suggestions of that paper with published accounts of other occurrences, including Cambrian and Devonian samples (Riding & Zhuravlev, 1995; Turner, James, & Narbonne, 2000; Kruse & Zhuravlev, 2008). Howell, Woo, and Chough (2011) suggested several tiers of mesostructure based on growth structure of the dendroids, which

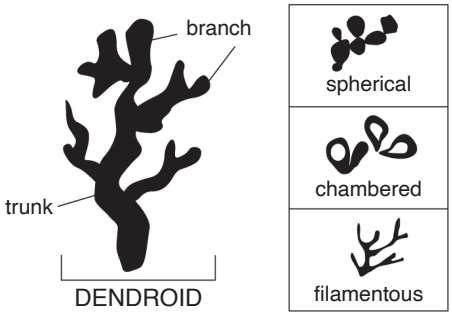

Fig. 25. Descriptive terminology as applied to the mesostructure of dendrolites (new).

may prove to be a valuable level of differentiation in future studies.

LEIOLITES

Braga, Martin, and Riding, 1995 suggested the term leiolite to encompass microbial constructions that lack diagnostic mesoscale structure. There are many pathways to create massive structure (e.g., irregular accretion of microspar, extensive boring or bioturbation, or burial dolomitization), but the term leiolite is valuable as it is non-genetic and does not presume a prior mesostructure. If, however, the microbialite can be shown to have originally been laminated, clotted, or dendrolitic, the pre-alteration terminology should be utilized. It may be possible to recognize pre-alteration original fabrics in dolomitized leiolites using the white card technique of Folk (1987). Leiolites have not received the same amount of descriptive study as other microbialites, although a further short review can be found in Riding (2000).

MODELS OF MICROBIALITE FORMATION

No single model of formation produces the variety of microbialites described above. The mineralization of a microbial mat is the final result of interplay between the physical sedimentary environment, surrounding chemical parameters (temperature, mineral saturation states), and biological processes within microbial communities themselves (Riding, 2000;

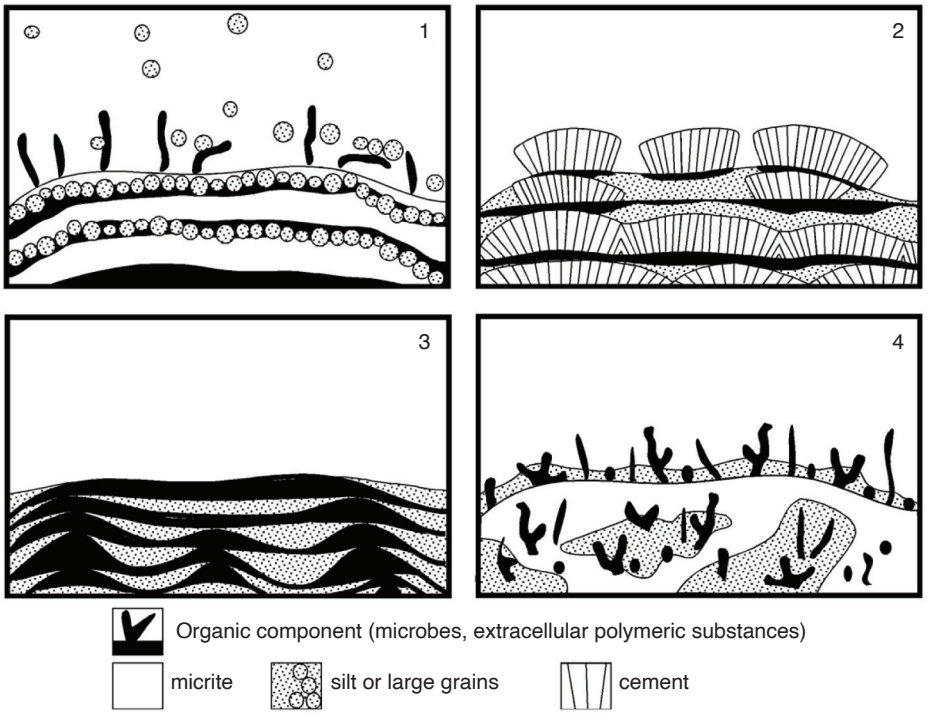

FIG. 26. Models of formation of microbialites. *1,* Trapping and binding of particles; *2,* precipitation of cement layers; *3,* entombing of sediments by mats or extracellular polymeric substances; *4,* skeletal algae or metazoans (adapted from Shapiro, 2007, fig. 3).

SHAPIRO, 2007; DUPRAZ & others, 2009). In contrast, the shells and tests of organisms described in other volumes of the *Treatise,* although influenced by surrounding chemistry, are directly formed from the cellular activity of eukaryotes (WEINER & DOVE, 2003). Microbialites can also be considered as trace fossils, recording the previous activity of localized microbial ecosystems, but only rarely preserving the organisms themselves (SHAPIRO, 2007). A further discussion on the differences between microbial and metazoan biomineralization, as well as modern processes of microbialite formation, is provided in DUPRAZ and others (2009).

Broadly speaking, there are four models that encompass microbialite formation, and any one deposit may have components of all four (Fig. 26). 1) The physical properties of microbial mats commonly result in the trapping and binding of sedimentary particles, either by filamentous cells or adhesive extracellular polymeric substances (EPS) produced by the mat (GEBELEIN, 1969; RIDING, 1991; FRANTZ, PETRYSHYN, & CORSETTI, 2015). Most Phanerozoic and many Proterozoic marine stromatolites preserve detrital material, with grains ranging from clay through sand-sized particles. Further cementation of the grains within mats may be accomplished below the accreting and stabilizing surface by heterotrophic bacteria and other biota. 2) Mineral precipitation within microbial mats is induced by elevated saturation states in surrounding waters, occurring both on cells and on organic compounds such as EPS (ARP, 2001; ARP, REIMER, & REITNER, 1999, 2004; REID & others, 2000; DUPRAZ & VISSCHER, 2005; BRAISSANT &

others, 2007). Mineral saturation states can be altered by metabolic processes of living organisms, such as photosynthesis, respiration, or chemosynthesis (biologically induced mineralization; Dupraz & others, 2009). Alternatively, chemical changes in the surrounding environment can also force mineral precipitation, with mats serving as a nucleation site (biologically influenced mineralization; Dupraz & others, 2009). Many Archean and Paleoproterozoic stromatolites are comprised of precipitated cement layers (Riding, 2008, 2011a), although the role of diagenesis in promoting aggrading neomorphic spar must also be considered. 3) A third model, typified by the Omachta Formation of Siberia, comprises stromatolites that form not from trapping sediments but from microbial mats enclosing sediments that have already been deposited. This construction preserves signatures of mechanical deposition such as crossbeds and ripples (Knoll & Semikhatov, 1998). 4) A fourth model of formation recognizes the importance of skeletal algae, foraminifera, and invertebrates in comprising a significant component of Phanerozoic microbialites (Riding, 1977). There may be secular trends to both abundance and diversity of these skeletal microbialites related to evolutionary patterns of the constructors as well as ocean chemistry (Riding, 1977, 2011a).

Important to note, the vast majority of described microbialites occur in carbonates and thus are susceptible to the myriad of diagenetic processes that affect all carbonate facies (Beukes, 1987; Burne & Moore, 1987; Planavsky & others, 2009; Pace & others, 2016). Such considerations include near-surface void cementation and dissolution in the phreatic and vadose zone, recrystallization or aggrading neomorphism in shallow burial conditions, and significant dissolution and reprecipitation under deeper burial conditions. Replacement by silica is common and can be either fabric retentive or destructive. Therefore, interpreting the model of formation of all microbialites must take into account the effects of secondary diagenesis.

MODERN STRUCTURES

Both microbial mats and subsequently mineralized microbialites are known from many different facies. Rather than attempt to provide a comprehensive list or to fit microbialites into generic facies models, this section will highlight unique attributes of several key modern environments.

Peritidal Open Marine and Reef

Some of the most well-studied modern microbialites are found in the intertidal embayment of Shark Bay, Western Australia (Logan, 1961; Hofmann, 1973; Chivas, Torgersen, & Polach, 1990; Reid & others, 2003) and unrestricted tidal channels of the Bahamas (Dravis, 1983; Dill & others, 1986; Shapiro & others, 1995; Andres & Reid, 2006; Planavsky & Ginsburg, 2009). These microbialites are predominantly stromatolites with laminae comprised of fine- to medium-sized grains and cement, although coarser textures have been diagnosed as thrombolites (Planavsky & Ginsburg, 2009; Riding, 2011a).

Other significant but overlooked modern peritidal microbialites include reef and cryptic crusts (Camoin & others, 1999), which are also well described from Paleozoic and Mesozoic reefs (e.g., Flügel & Steiger, 1981; Leinfelder & others, 1996). Whereas the textures of modern peritidal deposits are fairly uniform, macrostructure varies with respect to current and wave conditions. In particular, modern peritidal stromatolites have very high relief from the seabed (although not necessarily a high synoptic relief within individual laminae), and columns typically have a pronounced elongation of the major axis. In most cases, the elongation is parallel to tidal flow and perpendicular to wave crests. Overall stromatolite size also decreases away from the tidal zone toward the margins of deposits.

Biological studies of peritidal microbialites typically focus on extensive cyanobacterial

communities, both for the ability of cyanobacteria to bind detrital grains and for influence local carbonate saturation states (Gebelein, 1969; Reid & others, 2000). However, many other organisms also contribute to microbialite growth, including diatoms and other algae trapping grains (Awramik & Riding, 1988) and cement precipitation mediated by heterotrophic bacteria (Visscher & others, 1998; Reid & others, 2000). Modern stromatolites also host localized ecosystems of corals and sponges in addition to algae and microbial mats. Similar microbialite-metazoan reefs are well known throughout the Phanerozoic and Neoproterozoic (Riding, 1991; Rowland & Shapiro, 2002; Grotzinger, Adams, & Schröder, 2005). However, the relatively coarse grains and common presence of eukaryotes within modern peritidal microbialites limits their capabilities as faithful analogs for many ancient examples, especially in Precambrian environments.

Lacustrine

Microbialites are present in a number of lacustrine settings across various climates, typically as calcitic thrombolites and stromatolites with distinct micritic or micrite-microspar laminae (Burne & Moore, 1987; Winsborough & others, 1994; Laval & others, 2000; Gischler, Gibson, & Oschmann, 2008). Lacustrine microbialites occur across a greater range of depths than within marine peritidal zones, although most deposits form near lake surfaces (e.g., Kempe & others, 1991). Sharp depth gradients of geochemistry, temperature, and light produce distinct microbialite biofacies. For example, microbial mats within deeper lake waters typically have higher vertical relief for photosynthetic organisms to access more sunlight, forming textures such as pillars or cones (Laval & others, 2000; Andersen & others, 2011). Lake depth profiles and chemistry also change more dramatically during short-term climate fluctuations than in marine peritidal environments, especially in closed basin lakes where evaporation and precipitation dominate water budgets (see *Geological Significance of Microbialites,* p. 69). Relatively rapid depth and climate changes can produce distinct fabrics in lacustrine microbialites, particularly in stromatolites (Frantz & others, 2014; Fedorchuk & others, 2016).

Springs

Both carbonate and silica microbialites are well known from modern hot and cold springs (Weed, 1889; Jones & Renaut, 1997; Turner & Jones, 2005). Modern spring microbialites are of low areal extent compared with peritidal and lacustrine examples, although wetter climates generally lead to increased discharge rates and more extensive deposits (Bargar 1978; Guo & Riding, 1998). Most described spring microbialites are stromatolitic, with macrostructure varying as flow gradients shift from the vent to outflow apron (Walter, Bauld, & Brock, 1972; Jones, Renaut, & Rosen, 1998). Differentiating true biologically mediated microbialites from abiogenic deposits (e.g., tufa, travertine, and sinter) is a continuing challenge, because many spring deposits are thinly laminated without the presence of microbial mats (Konhauser & others, 2003; Riding, 2008). However, recent work on silica-cemented microbial textures has demonstrated exquisite preservation of microbial cells (Schultze-Lam & others, 1995; Konhauser & others, 2001; Mata & others, 2012), although it remains to be shown if this preservation would persist through early diagenesis.

Hydrocarbon Seeps

Both stromatolitic and thrombolitic textures have been described at hydrocarbon seeps, but many deposits are neither laminated nor clotted and would best be termed as leiolites (Greinert, Bohrmann, & Elvert, 2002; Shapiro, 2004a; Lloyd & others, 2010). The microstructure of seep microbialites is noteworthy for abundant non-fecal micropeloids, dissolution surfaces, yellow, bladed calcite cements, and arago-

nitic botryoids (Campbell, Farmer, & Des Marais, 2002), although carbonate fabrics themselves are not conclusive of a hydrocarbon source. Instead, microbial carbonates with substantially depleted $\delta^{13}C$ signatures are a common indicator of hydrocarbon seeps (Aharon, 2000) and reflect either thermogenic or biogenic methane as sources of carbon (Birgel & others, 2006). The co-occurrence of chemosynthetic metazoans alongside localized carbonate deposits within a siliciclastic lithofacies provides additional biological and sedimentary evidence for hydrocarbon seeps.

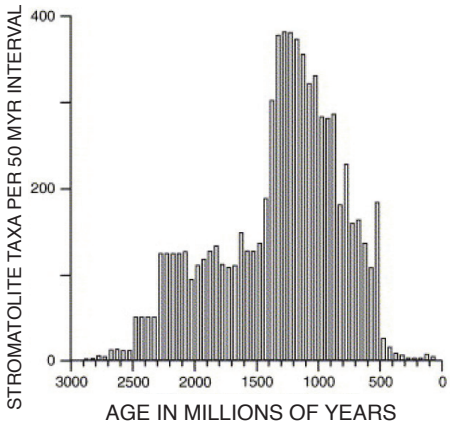

Fig. 27. Stromatolite abundance plot of Awramik and Sprinkle (1999) as presented in Riding (2006).

ANCIENT EXAMPLES

Precambrian

The great antiquity of stromatolites cannot be overstated. Dating back nearly 3.5 billion years (Ga), stromatolites have a sporadic but impressive preserved fossil record through Archean and Proterozoic deposits (Hofmann, 2000; Schopf, 2006b). Nutman and others (2016) recently report stromatolitic textures in 3.7 Ga carbonates from Isua, Greenland, but subsequent studies argue that domal and conical textures are the result of secondary alteration (Allwood & others, 2018). The oldest definitive Archean stromatolites are from the Pilbara Craton of Australia, including the 3.5 Ga Dresser Formation (Walter, Buick, & Dunlop, 1980; Van Kranendonk, 2006; Van Kranendonk, Webb, & Kamber, 2003), and the 3.2 Ga Strelley Pool Chert (Lowe, 1980; Allwood & others, 2006), as well as 2.7–2.5 Ga Fortescue and Hamersley Group deposits (Buick, 1992; Lepot & others, 2008; Hickman, 2012).

The Kaapvaal Craton of South Africa also contains a variety of Archean stromatolites and other microbial textures, including the Buck Reef Chert, Pongola and Ventersdorp Supergroups, and the Campbellrand-Malmani Dolomite (Buck, 1980; Beukes, 1987; Beukes & Lowe, 1989; Sumner, 1997, 2000; Tice & Lowe, 2006; Homann, 2019; Wilmeth & others, 2019). Other Archean stromatolite locations include the Superior and Slave Cratons (Canada), the Dharwar and Singhbhum Cratons (India), the Yilgarn Craton (Australia), and the Zimbabwe Craton (Hofmann, 2000; Schopf, 2006b).

The Precambrian microbialite record is rich and diverse enough to suggest secular variation in stromatolitic attributes (Grotzinger & Knoll, 1999). In general, stromatolites are less common in the Archean (although this is likely a function of lack of preserved suitable facies within greenstone belts) and increase in both diversity and abundance through the Paleoproterozoic, reaching a maximum in the Mesoproterozoic (Awramik & Sprinkle, 1999) (Fig. 27). The Proterozoic increase in microbialite abundance and diversity has been linked to the development of large continents with stable continental shelves where extensive shallow-marine carbonates can form (Eriksson & others, 2006, 2007). Although stromatolites and thrombolites continued to dominate shallow water carbonates during the Neoproterozoic, overall microbialite diversity decreased during this era (Grotzinger, 1990; Awramik & Sprinkle, 1999). Lacustrine and spring microbialites have also been described as early as the Archean, although smaller primary spatial extents limit the number of known locations (Buck,

1980; Buick, 1992; Djokic & others, 2017; Wilmeth & others, 2019). Many researchers have developed biostratigraphic schemes for correlating Precambrian deposits (e.g., Cloud & Semikhatov, 1969; Knoll & Semikhatov, 1998; Semikhatov & Raaben, 2000) although not without controversy.

There are several features of Precambrian stromatolites that segregate them from younger, Phanerozoic counterparts. Precambrian stromatolites are fine grained, with most Archean and Paleoproterozoic forms dominated by crystalline microfabrics (Riding, 2008). Some have argued that Precambrian stromatolites are more likely to host abiotic crystal precipitate layers than their Phanerozoic counterparts (Grotzinger & Knoll, 1999). Precambrian deposits contain extremely large stromatolites, measured in tens of meters in height and diameter, including size ranges that are not known from the Phanerozoic (Beukes, 1987; Fralick & Riding, 2015). In contrast, ministromatolites one to several millimeters across are most common in the Neoarchean and Paleoproterozoic (Hofmann & Jackson, 1987; Medvedev & others, 2005). Upper Paleoproterozoic and Mesoproterozoic marine stromatolites display many diverse macrostructures rarely observed in Phanerozoic deposits, including simple and complexly branching forms (Cloud & Semikhatov, 1969; Awramik & Sprinkle, 1999). In terms of size, fabric, and morphology, uniformitarian principles do not allow for clear correlation from modern marine stromatolites to the vast Precambrian record.

Phanerozoic Marine and Lacustrine

Phanerozoic marine microbialites are noteworthy for their relatively simplistic morphologies compared with Proterozoic forms. Even when comprising kilometer-scale bioherms and biostrome deposits, most Phanerozoic microbialites are dominated by simple centimeter- to meter-scale, unbranched columns comprised of irregular but roughly parallel laminae. Detrital grains become increasingly important fabric components over time, typically as fine- to medium-grained sediments.

Another noteworthy development in Phanerozoic (and Neoproterozoic) microbialites is the addition of algae, foraminifera, poriferans, and other metazoans to the construction. The role of metazoans ranges from passive benthic filter feeders that use the rigid developing microbialite as a base to active constructors (Dupraz & Strasser, 1999; Kershaw, Zhang, & Lan, 1999; Ricardi-Branco & others, 2018). Thrombolites first appear in the Neoproterozoic (although there are reports from the Paleoproterozoic) and are common during the middle Cambrian through Lower Ordovician (Kennard & James, 1986; Kah & Grotzinger, 1992; Rowland & Shapiro, 2002). Thrombolites also increase in abundance during the Devonian, Mesozoic, and locally during the Neogene (Kennard & James, 1986; Shapiro, 2000).

The fossil record of dendrolites is still poorly established, but deposits are abundant in the Cambrian with potential resurgences in the Devonian and Jurassic (Shapiro & Awramik, 2000). It is likely that previously published reports of thrombolites will be revised as dendrolites with further study, because the two forms were not distinguished in the past. Oncoids, which had been present since the Archean, also had an increase in abundance during the Cambrian, as well as the appearance of filamentous *Girvanella* microfossils (Shapiro, 2004b).

It is important to note that Phanerozoic lacustrine and fluvial stromatolites can be quite diverse with respect to macrostructure, with many forms developing columns and pseudocolumns on upper surfaces. In microstructure, lacustrine stromatolites are typified by more regular, repeating couplets of laminae, separated by sharp boundaries. Primary cement fabrics such as botryoids and isopachous bladed calcite are also more common in lacustrine stromatolites than their marine counterparts (Casanova, 1994), and a challenge of lacustrine stromatolite description and terminology is

differentiating organically mediated accretion from presumably abiogenic tufa (Riding 2008; Petryshyn & Corsetti, 2011).

GEOLOGICAL SIGNIFICANCE OF MICROBIALITES

Hofmann (1973) detailed 15 different geological topics where microbialites can be utilized, ranging in scale from geopetal indicators to evidence for the oldest life on Earth. Subsequent studies have further expanded the significance of microbial deposits, particularly in the fields of geochemistry, geobiology, and astrobiology. Rather than cover each topic in detail, this section lists several applications for researchers to consider when studying microbialites. A unifying principle behind many of these applications is that as benthic trace fossils, microbialites can faithfully record *in situ* biological, sedimentary, and geochemical conditions during formation.

MICROBIALITES AS FACIES INDICATORS

For many geologists, a significant value of microbialites is their use as facies indicators. For example, microbialite facies definitions have recently become important after the announcement of vast carbonate reservoirs in the deep pre-salt deposits of offshore Brazil, which may be microbialite or tufa in origin (Awramik & Buchheim, 2012; Muniz & Bosence, 2015). Yet, like most carbonate deposits, there are few generalities that apply to the vast rock record, and uniformitarian principles do not always apply to ancient microbialites. In particular, the utility of stromatolites has been hampered due to what has been termed the Shark Bay Effect. Although Black (1933) described modern stromatolites from the intertidal flats of Abaco Island, Bahamas, the forms were small and the widespread applicability was not realized. The discovery of meter-scale buildups in Shark Bay, Western Australia (Logan, 1961) revolutionized the field and provided a key analog of a restricted marine, hypersaline, intertidal setting. Subsequently, nearly all fossil stromatolite buildups were interpreted—or reinterpreted—as hypersaline and intertidal, even when the deposit lacked additional criteria for recognition such as mudcracks, herring-bone crossbeds, or evaporate molds. Therefore, the discovery of morphologically similar stromatolites in subtidal, normal marine tidal channels of Eleuthera (Dravis, 1983) and the Exuma (Dill & others, 1986) Islands, Bahamas, opened the door to much broader interpretation of microbialite depositional environments.

Although the diversity of microbial forms produces many unique sedimentary facies, there are several trends in the facies applicability of microbialites that are corroborated across multiple studies. A few general observations are listed below, with the volume edited by Riding and Awramik (2000) providing an excellent resource for more detailed comparisons of different facies models. In most deposits, microbialites form on flooding surfaces, with stromatolites occurring in shallower water than thrombolites do. Stratiform deposits are typically indicative of intertidal conditions, as is the case with crinkly microbial mats. In plan view, if a significant major axis develops, it is likely that the axis parallels the dominant current. Branching appears to be related to an increase in sedimentation relative to growth rates. Other models will no doubt be added as additional studies are published.

BIOSTRATIGRAPHY OF MICROBIALITES

The biostratigraphic utility of microbialites remains a debated topic. Because microbialites are produced by microbial ecosystems rather than by individual organisms, biostratigraphic studies are often highly scrutinized (Grotzinger & Knoll, 1999; Bosak, Knoll, & Petroff, 2013). However, even though microbial structures are not subject to the same evolutionary patterns that govern eukaryotic index fossils, Proterozoic deposits typically contain temporally constrained patterns of unique stromatolite

morphologies. Early observations led Soviet scientists to employ a biostratigraphic zonation for the Siberian Platform (see reviews in Cloud & Semikhatov, 1969). Similar patterns have subsequently been described across various Proterozoic basins, most notably in Australia (Grey & Thorne, 1985; Hill, Cotter, & Grey, 2000). Most stratigraphic studies are restricted to intra-basinal deposits, although some have attempted to expand correlations between cratons (Medvedev & others, 2005; Grey, Hill, & Calver, 2011). A few case studies have also employed microbialites for correlation in early Phanerozoic deposits (Shapiro & Awramik, 2000, 2006). The governing forces behind widespread changes in Proterozoic stromatolite morphologies still remain enigmatic, potentially representing large-scale shifts in climate, biology, or geochemical cycles (Semikhatov & Raaben, 2000).

MICROBIALITES AS SIGNALS OF ENVIRONMENTAL CHANGE

Microbialite abundance and diversity broadly decrease across the Phanerozoic, and relatively sudden increases in microbialite deposits appear to be linked to shifts in climate, metazoan ecology, or both. For example, the end-Devonian and end-Permian mass extinctions are associated with increased microbialite abundance, as reviewed in Mata and Bottjer (2012). Many studies note the expansion of microbialites across ramp, platform, and shelf environments after the end-Permian mass extinction, the most devastating in Earth history (Schubert & Bottjer, 1992; Baud, Cirilli, & Marcoux, 1997; Baud, Richoz, & Pruss, 2007; Pruss & others, 2006; Kershaw & others, 2007; Mata & Bottjer, 2011). Even though the end-Devonian event was less severe regarding metazoan diversity, microbialites flourished during the aftermath (Playford, 1980; Wood, 2000; Webb, 2002; Whalen & others, 2002). Various hypotheses exist as to why microbialite abundances are less pronounced during other mass extinctions, including ecospace competition from bioturbating and reef-building organisms, as well as carbonate availability (Mata & Bottjer, 2012).

In addition to providing sedimentary evidence for ecological shifts, microbialites have the potential to record geochemical signatures of climate and environmental change. Stromatolites can contain especially detailed records of local geochemistry over time, with each layer representing a distinct period of microbial growth and mineral precipitation. Strong climate signals are observed from stromatolites within closed lake systems, where concentrations and isotopes of stable elements are controlled by variations in evaporation and precipitation (Talbot, 1990). Studies of lacustrine stromatolites have focused on several Cenozoic climate changes relevant to modern interest, including the Early Eocene Climatic Optimum and Plio-Pleistocene trends (Abell & others, 1982; Frantz & others, 2014; Petryshyn & others, 2016), with occasional studies investigating Mesozoic environments (de Wet & Hubert, 1989; Woo & others, 2004). Geochemical analyses of microbialites from any age or environment need to first analyze diagenetic and/or metamorphic alteration of minerals before collecting data, especially in easily altered carbonate minerals.

CONCLUSION

More than three billion years of interactions between microbial mats and their surrounding environments has produced a staggering diversity of microbialites. Many macroscale morphologies and mesoscale textures are specific to certain times and facies, and a detailed analysis of every form of microbial deposit would require a separate treatise for adequate description. The reader is invited to further investigate specific topics presented by consulting the reviews and primary literature cited herein.

MICROBIALLY INDUCED SEDIMENTARY STRUCTURES (MISS)

Nora Noffke, Hugo Beraldi-Campesi, Flavia Callefo, Noelia Carmona, Diana G. Cuadrado, Keyron Hickman-Lewis, Martin Homann, Ria Mitchell, Nathan Sheldon, Francis Westall, and Shuhai Xiao

INTRODUCTION

To date, microbialites include five groups: stromatolites, thrombolites, leiolites, and dendrolites. All these microbialites occur in carbonate or silica lithologies. However, research during the past 25 years has defined an additional group of microbialites that occurs predominantly in clastic deposits. These structures are called microbially induced sedimentary structures, commonly simply abbreviated to MISS. The morphologies of MISS do not resemble those of precipitated microbialites due to the much different formation and different location of these structural groups. The genesis of the main types of MISS has been elucidated in studies in modern environments. The results were key for the search of such structures in the fossil record. Systematic exploration from youngest to oldest stratigraphic successions has given rise to a data set that allows identification of MISS in respective paleoenvironments. MISS are biosignatures helpful to understanding aspects of prokaryote evolution and the search for life on other planets.

BIOFILMS AND MICROBIAL MATS

Modern sedimentology recognizes that benthic microbiota are (and have always been) part of every sediment and that microbial activities may substantively contribute to sediment formation and lithification (Fig. 28).

In close-up view, sedimentary deposits are widely colonized by a great variety of benthic microorganisms. Most of these microbes organize into aggregates called biofilms, which are attached to a surface. Biofilms are probably the most common organization of life, developing everywhere in nature provided that water molecules and a surface are present (Stoodley & others, 2002; Neu, 1994; Gerbersdorf & others, 2008; Stal, van Gemerden, & Krumbein, 1985; Ramsing, Ferris, & Ward, 2000; Franks & Stolz, 2009; Gerbersdorf & Wieprecht, 2015; Espinoza-Ortiz & Gerlach, 2021). Biofilms include both microbial cells and their extracellular polymeric substances (EPS); (e.g., Decho, 1990, 1994). EPS are cohesive mucilages comprised of complex polysaccharide biomolecules that provide a suitable microenvironment for the microorganisms, buffering against rapid environmental changes, such as desiccation, sudden salinity changes, and other environmental stressors (Decho, 1994; Flemming, Neu, & Wozniak, 2007; Westall & Rince 1994; Westall & others, 2000). These mucilages serve to anchor cells on their substrate or enable the motion of cells within the structure of the biofilm. Biofilms are therefore assemblages of cells working interdependently with each other with the ultimate aim of effective resource exploration. In a biofilm community, cells are arranged in certain positions relative to one other, allowing collaborative nutrient harvesting and consumption (Decho, 1994). Biofilm research, especially in the medical sciences, reveals a complex pattern of communication between cells. Such communication takes place between different groups of prokaryotes and even some eukaryotes. Quorum sensing between members of the biofilm ensures targeted action of the community (Waters & Bassler, 2005; Decho, Norman, & Visscher, 2010; Decho, & Gutierrez, 2017).

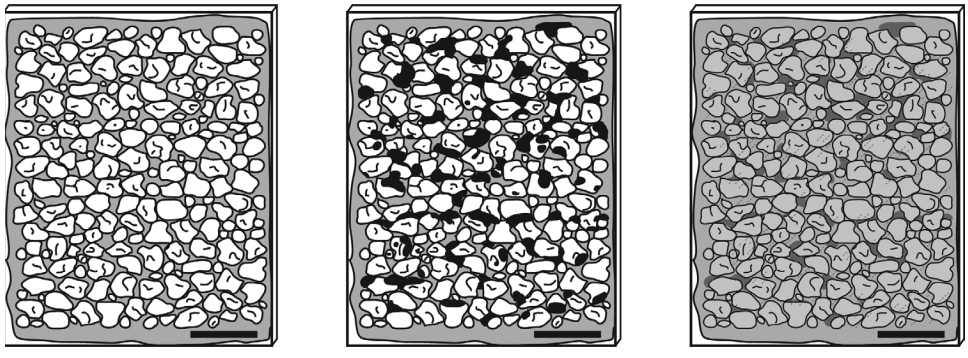

FIG. 28. Biofilms in classic and modern sedimentology. Modern sedimentology understands sediment not as a mere assemblage of mineral grains. Rather, biofilms colonize particles of sediment as long as water molecules are present. *In situ* lithification of the biofilm adds to cementation during diagenesis.

In marine settings, biofilms may merely envelope a sedimentary grain (Fig. 29.1); however, at suitable natural sites, they may develop into large, macroscopically visible layers. Such large-scale organic layers are termed microbial mats (Fig. 29.2–29.3).

In sedimentology, classical and well-studied examples of microbial mats include so-called algal mats in tidal settings, predominantly those constructed by cyanobacteria (BLACK, 1933; HARDIE & GARRETT, 1977; HORODYSKI, BLOESER, & VONDER HAAR, 1977; KRUMBEIN, 1983; GERDES, KRUMBEIN, & REINECK, 1985; COHEN & ROSENBERG, 1989; GERDES & KRUMBEIN, 1987; REINECK & others, 1990; GINSBURG, 1991; VAN GEMERDEN, 1993; STAL & CAUMETTE, 1994; TAHER & others, 1994; REID & others, 1995; STOLZ, 2000; PEARL, PINKNEY, & STEPPE, 2000; GERDES, KRUMBEIN, & NOFFKE, 2000; VASCONCELOS & others, 2006; TAHER, 2014). However, there are many types of microbial mats in a great array of environments including the deep-water marine (e.g. GALLARDO, 1977; HEIJS, SINNINGHE DAMSTE, & FORNEY, 2005; GALLARDO & ESPINOZA, 2007). Despite their impressive sizes—sometimes many square kilometers—microbial mats are still nothing more than biofilms.

A look at the vertical organization of a microbial mat reveals that it is comprised of a stack of horizontal layers, each of which is dominated by a microbial community different to that of the layer above or below (Fig. 30). This arrangement into layered communities has been investigated with the example of the multicolored sand flat (microbial mats in tidal flats) in great detail (STAL, VAN GEMERDEN, & KRUMBEIN,1985; VISSCHER & STOLZ, 2005). The metabolic activities of the community of each layer interlock with the metabolic activities of the communities in the layers directly above and below. This interlocking arrangement results in a complex interactive system best described as a cooperative of microbial groups. It functions as what could be called a "disassembly line" that harvests energy from the environment and transforms it through many steps first into organic matter and then into mineral substances (STAL, VAN GEMERDEN, & KRUMBEIN,1985; DES MARAIS & CANFIELD, 1994; VISSCHER & STOLZ, 2005; DUPRAZ & others, 2009; BLUMENBERG, THIEL, & REITNER, 2015) (Fig. 30).

In modern tidal flats, the top layer of microbial mats comprises photoautotrophic cyanobacteria that, as primary producers, harvest sunlight and store this energy as biomass. The layer immediately beneath the cyanobacteria includes chemoorganotrophic microbes that gain energy by disintegrating

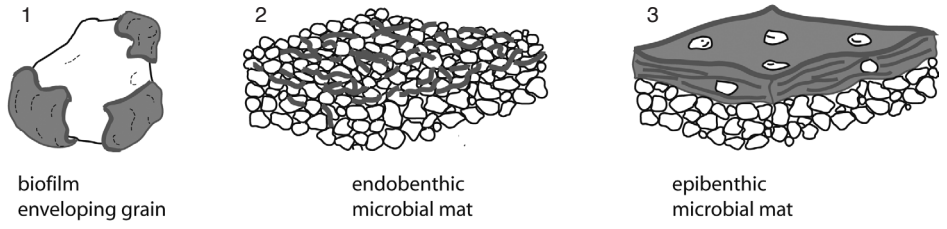

FIG. 29. The three endmembers of microbenthos type in an aquatic setting. A biofilm (*1*) is a microscopic coating around individual mineral grains. A microbial mat (*2–3*) is a macroscopic biofilm covering wide areas of sedimentary surfaces, sometimes square kilometers. Microbial mats can be separated into endobenthic mats, which occur within the uppermost layers of sediment (*2*), and epibenthic mats (*3*), which grow on top of the sediment surface. Sizes of grains, ~0.2 mm.

the complex biomolecules of the primary producers into inorganic compounds. Further beneath, in the third layer, these inorganic compounds are further disassembled by chemolithotrophic microbes. At the base of this stack of layers, small molecules such as methane and ions are released, for example by methanogenic bacteria or archaea (KINSMAN-COSTELLO & others, 2017). The finally released cations and anions at the base of the disassembly line immediately react with chemical compounds suspended in the surrounding water and sediment (SCHULTZE-LAM & others, 1996). The results of these reactions can be nucleation points for mineral precipitates. Because the first mineral precipitates still include water molecules, they are commonly amorphous. In carbonate regimens, early crystalline dolomite or calcite may form, typically directly nucleating in the EPS (VAN LITH & others, 2002; SÁNCHEZ-ROMÁN & others, 2008; DUPRAZ & others, 2009). Later, during diagenesis, larger-scale crystallinity develops. Such processes lead to the replacement of organic matter by inorganic mineral

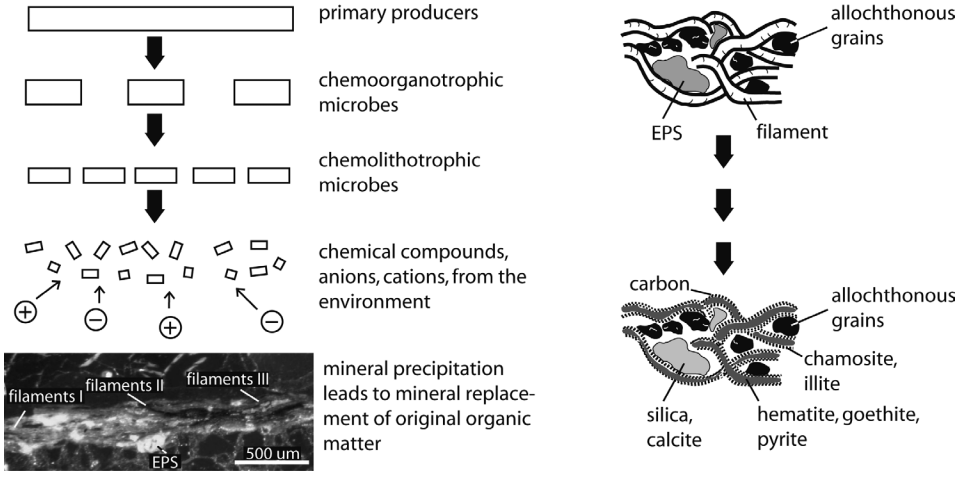

FIG. 30. The microbial energy disassembly line of a microbial mat (*left*) and the resulting formation of minerals (*right*). Left: The primary producers in the top of the mat harvest solar energy via photosynthesis and transform it into organic matter. This organic matter serves as the energy source for various heterotrophic microbial groups in deeper parts of the mat. *In situ* precipitation of minerals is a consequence of this metabolic disassembly line. Right: Dependent on the chemical composition of water in sediment, typical minerals crystallize, replacing the original organic matter. In many fossil microbially induced sedimentary st, the cell walls of filaments still include some of the original carbon, and chamosite and illite may form. Pyrite, goethite, and hematite may have replaced the ancient trichomes, whereas silica and calcite may have replaced fossil extracellular polymeric substances (EPS).

substances and ultimately to the preservation of microbial mats (Ferris, Beveridge, & Fyfe, 1986; Ferris, Fyfe, & Beveridge, 1987, 1988; Schultze-Lam & others, 1996; Konhauser & Riding, 2012). Impressions of mat textures, as known from carbonate microbialites, have to our knowledge not been observed in siliciclastic material. In summary, the cooperative action of this microbial disassembly line transforms and transfers the original amount of solar energy, via several steps, first into organic matter and then into chemical compounds (Schultze-Lam & others, 1996). The microbes work as a cooperative until almost all of the original energy is used up.

The difference between MISS and carbonate/silica microbialites, such as stromatolites, is that in the latter rapid and ubiquitous *in situ* lithification of EPS takes place (Dupraz & others, 2009). The EPS constitute organic matrix, providing a template for nucleation of carbonate minerals (Dupraz & others, 2009). In MISS, such EPS lithification plays only a minor role in structure formation (Noffke & Awramik, 2013). Here, *in situ* replacement of filaments happens very quickly (Schieber & others, 2007; Noffke, 2010; Gomes & others, 2020).

FORMATION OF MISS AND MAIN MORPHOTYPES

In general, three main types sedimentary systems are distinguished: 1) clastic, 2) clastic-evaporitic, and 3) carbonatic (Warren, 1999). Clastic deposits are comprised of mineral grains, bioclasts, and lithoclasts. Such deposits are governed by physical sedimentary dynamics (erosion and deposition). Dynamic events are interrupted by a time period of quiescence called latency. Clastic-evaporitic settings are likewise characterized by such physical sedimentary dynamics but, in addition, also by evaporite mineral crystallization. Carbonate sediments are subject to both physical dynamics and evaporite mineral formation but are dominated by carbonate precipitation. The term sediment, however, cannot be understood as substrate merely comprised of particles that by diagenetic processes turn into a cement-stabilized sedimentary rock. The hydraulic activities are reflected by the wealth of sedimentary structures that are well familiar to sedimentologists (Pettijohn & Potter, 1964). In order to survive, macro- and microbenthos must be able to actively respond to sedimentary dynamics.

Clearly, given the small scales relevant to the microbial world, any instability of the substrate affects microbenthos significantly. In a high-energy setting, strong waves and currents may erode and rip off microbial mats from their substrate, forming meter-scale roll-ups (Cuadrado & others, 2015; Maisano, Cuadrado, & Gómez, 2019). In arid, terrestrial settings, roll-ups form through desiccation of a mat. In a low-energy environment, fine particles may continuously fall out of suspension and bury the microbenthos, potentially altering the physico-chemical properties of the sediment or blocking essential sunlight from reaching the bottom. In the face of such challenges, microbes ensure the survival of the biofilm community by active upward motion and escape from burial (Bebout & García-Pichel, 1995; Paterson & Black, 2000; Shepard & others, 2005; Shepard & Sumner, 2010; Cuadrado, Carmona, & Bournod, 2011; Risgaard-Petersen & others, 2015). That means that microbes respond differently to erosion than to deposition, which results in lessened erosion rates and increased depositional rates. In fact, the microbial activities generate moderate dynamic sedimentary conditions more suitable for microbial colonization of deposits (Noffke, Knoll, & Grotzinger, 2002; Noffke, 2010). The microbenthos, thus, establishes what we've termed a "window of optimal dynamic conditions" for biofilms and microbial mats to form and thrive (Fig. 31).

Physical sedimentary dynamics include erosion, deposition, and latencies. Deformation plays a role once the sediment is deposited. Erosion differs from deposition in its physical sediment dynamics. Microbial activi-

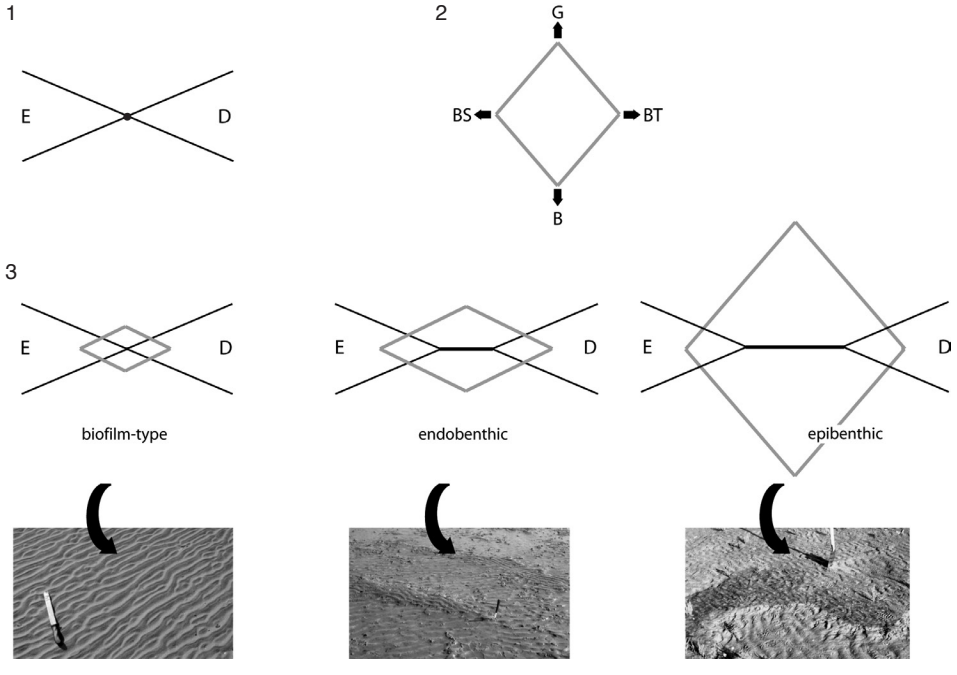

FIG. 31. Overview of the microbial modification of physical sedimentary dynamics. Microbial mats and biofilms influence physical sediment dynamics in such a fashion that the microbenthos constructs its own dynamically suitable habitat, the optimal dynamic window for mat development (see NOFFKE, KNOLL, & GROTZINGER, 2002). *1,* Physical sediment dynamics without microbial influence: E, erosion; D, deposition; *dot* at the crossing point, latency (time of no erosion or deposition). *2,* Physical sediment dynamics affected by microbial influence. The rhombus (*gray*) represents microbial activities: G, growth; BT, baffling and trapping; BS, biostabilization; B, binding. Microbial activities create the window of optimal dynamic conditions biostabilization (BS) acts against erosion, while baffling and trapping (BT) increases the rate of deposition, especially of grains of the silt- to fine-sand fraction. Growth (G) and binding (B) rise the sedimentary surface. *3,* The presence of small biofilms would not affect ripple morphologies (photo, *left*). However, where endobenthic microbial mats establish, biostabilization counteracting erosion (E) and baffling and trapping fostering deposition (D) sets in, and in consequence, the latency (black horizontal line separating E and D and representing time periods of dynamic quietness) increases. Endobenthic microbial mats modify physical sediment dynamics moderately and therefore their erosional remnants and pockets (photo, *middle*) appear as somewhat projecting surface morphologies. Epibenthic microbial mats affect erosion and deposition significantly and in consequence their erosional remnants and pockets are larger structures (photo, *right*). Color version available in *Treatise Online* 162 (paleo.ku.edu/treatiseonline).

ties differ from each other as well. Microbial growth is not the same as biostabilization, and both are distinct from baffling and trapping. Furthermore, binding also differs from the three other activities. Biostabilization is the response to erosion; baffling and trapping is the response to deposition; and growth (cell replication and EPS-production) or binding (organizing a mat fabrics by movement, not growth) is a response to latencies.

The microbiotic-physical interactions produce sedimentary structures (MISS) that, due to the different nature of their formational processes, differ morphologically from the physical sedimentary structures (*sensu* PETTIJOHN & POTTER, 1964) generated by purely physical dynamics.

GROWTH

Sediment affected neither by erosion nor by deposition provides a most suitable substrate for a biofilm or microbial mat to grow. This moment (or time period) of quiescence is called latency. Growth is herein understood as the increase of biomass, both through cell replication and the production

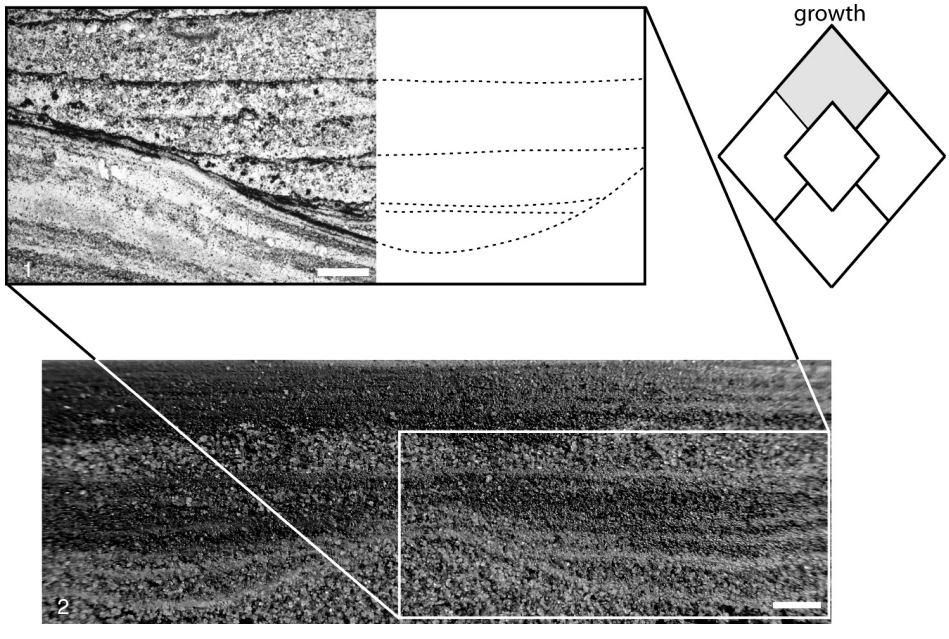

Fig. 32. Examples of microbially induced sedimentary structures formed by growth. A ripple valley is filled-in with layers of sediment (light) alternating with (dark) microbial mat laminae. *1,* Thin section of sample from 3.48 Ga Dresser Formation, Pilbara, Western Australia, scale bar, 0.1 cm. *2,* A scenario similar to (*1*) is visible in this vertical section through a modern sediment sample, Paso Seco coastal area, Argentina, scale bar, 0.5 cm. Color version available in *Treatise Online* 162 (paleo.ku.edu/treatiseonline).

of EPS and the establishment of a fully functioning biofilm community best suited for its specific environmental locale. With continuous growth of a biofilm or microbial mat, its vertical thickness increases. A microbial mat covering a bumpy sedimentary surface will—if the growth remains undisturbed—eventually smoothen this uneven surface relief. Thus, surface becomes level, or planar (Fig. 32). In this context, laminated leveling structures may form (Noffke & others, 2001; Noffke, 2010; Liu & Zhang, 2017).

In microscopic close-up of a growing microbial mat, the biomass surrounding a mineral grain increases in thickness over time. The developing biomass forces grains upward and away from each other until the original grain-grain contact is lost (Fig. 33.2). Such individual grains in the mat matrix may be observed, especially in thin sections of epibenthic microbial mats. Typically, the grains rotate to a position with their long-axes parallel to the sedimentary surface, termed oriented grain (see Noffke & others, 1997) (Fig. 33.3).

BIOSTABILIZATION

Biostabilization includes three types of processes. It may be a response to 1) erosion by horizontally directed water currents, but also to 2) intra-sedimentary gas pressure, or to 3) mechanical stress leading to ductile deformation. Species diversity, EPS structure and adhesiveness, salinity, light conditions, and other factors play a role in the effectiveness of biostabilization (Yallop & others, 1994; Paterson, 1997; Amos & others, 2004; Consalevy & others, 2004; Friend & others, 2008; Taher & Abdel-Motelib, 2014; Gerbersdorf & Wieprecht, 2015; Dick, Grim, & Klatt, 2018).

Biostabilization type 1 is the response of benthic microbiota to erosive forces by a horizontally directed water current passing the mat surface (Fig. 33). The smooth, EPS-rich surface of epibenthic microbial mats

induces a predominantly laminar flow across its surface (BS A in Fig. 33.1). Such laminar flow generally has a far less eroding effect than turbulent flow because of absence of the vertical component of motion (Stoodley & others, 2005; Noffke, 2010; Tice & others, 2011; Hagadorn & McDowell, 2012). Endobenthic microbial mats develop within the upper millimeters of a sedimentary surface such that, in microscopic close-up, individual mineral grains project upward from the surface (BS B in Fig. 33.2). The surface is rough. Thus, passing water currents have a turbulent character with a higher erosive effect. In local areas, where hydrodynamic reworking constantly exceeds mat stability, only limited biofilms can develop. They cover water-suspended grains, sometimes holding a few grains together. Constant water motion keeps such biofilm-grain-aggregates in suspension for a longer time than sterile mineral grains (BS C in Fig. 33.3). The reason for this prolonged suspension is that biofilm-grain aggregates have comparatively larger diameters and lower specific densities than individual sterile grains. It appears that one advantage of this microbially induced suspension mechanism is to prohibit the lethal burial of microbes by light-blocking sediment (Noffke, 2010). This type of biostabilization may also give rise to microsequences (Noffke & others, 1997). Microsequences are vertical successions of graded sediments layers covered by a microbial mat on the top of each bed. As soon as quiet conditions establish, the mat can develop. Each layer is preserved due to the biostabilization effect of the mat, which exceeds the erosion.

Biostabilization type 2 is the sealing of sediment by EPS that prohibit gas exchange between deposits and water or the atmosphere. Consequently, gases (O_2, CO_2, CH_4, H_2S, and others), which accumulate in the pore space of clastic deposits beneath microbial mats cannot escape. Consequently, gas pressure in the sediment may cause millimeter-scale pores visible in vertical section through mat-sealed sediment. Such

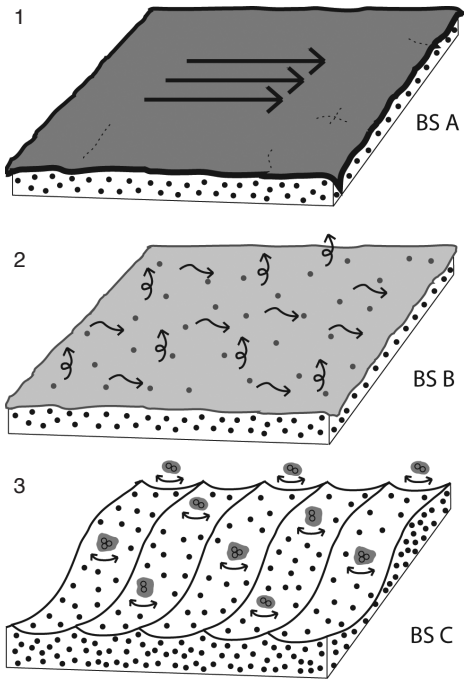

Fig. 33. Biostabilization type 1 by microbial mats and biofilms. Biostabilization BS A (*1*) is observed in epibenthic microbial mats sealing the sedimentary surface; biostabilization BS B (*2*) is observed in endobenthic microbial mats that form organic networks within the upper layers of the sedimentary deposits; biostabilization BS C (3) is observed in microbial-sediment aggregates.

sedimentary textures are termed sponge pore sand (Tebbutt, Conley, & Boyd, 1965; Noffke & others, 1996; Kinsman-Costello & others, 2017) (Fig. 34).

Gas domes are local centimeter-scale upheavals associated with biostabilization type 2, which locally form as a result of gas accumulations immediately beneath a microbial mat (Noffke & others, 1996; Wilmeth & others, 2014) (Fig. 35). Commonly, sponge pore fabrics and gas domes occur together.

Biostabilization type 3 involves the reaction of mat-stabilized sediment in ductile fashion. This biostabilization is typical in areas of vertically oriented water motion, e.g. where oscillating groundwater affects the sedimentary surface. A desiccating, microbial-mat-bound sand layer contracts,

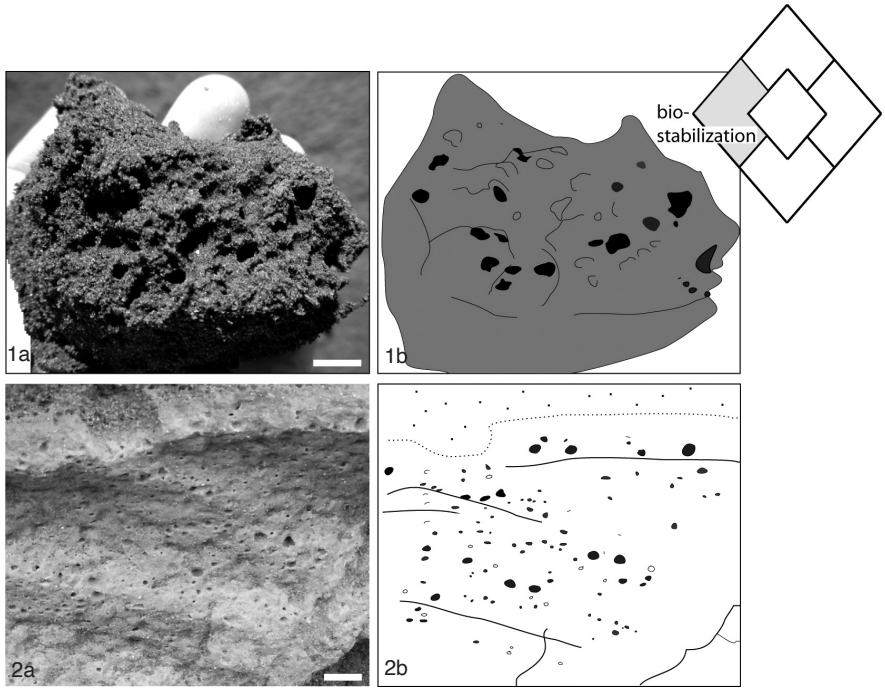

FIG. 34. Examples of microbially induced sedimentary structures caused by biostabilization. *1,* Sponge pore structure in modern sand flats, Paso Seco, Argentina (*a*), with accompanying drawing (*b*), scale bar, 1 cm. *2,* Sponge pore structure in the Rio Negro Formation (Miocene–Pliocene), Argentina (*a*), with accompanying drawing (*b*), scale bar, 1 cm. Color version available in *Treatise Online* 162 (paleo.ku.edu/treatiseonline).

curls up, and loses contact with the sediment beneath (GERDES, KLENKE, & NOFFKE, 2000). Unconsolidated, loose sand in the absence of biology would react to desiccation simply by dispersing into individual grains. However, if a microbial mat holds grains in place, the sediment does not disperse. Rather, the mat-bound sediment layer has deformation properties similar to clay (ductile deformation). Deformation of mats may also result from mechanical dislocation of a microbial mat through transport and lateral shear (PFLÜGER & GRESSE, 1996; SIMONSON & CARNEY, 1999; TICE & LOWE, 2004). MISS such as roll-ups or over-flips are good examples of this (Fig. 36).

In semi-arid climate zones, where significant seasonal changes affect sediments such that the degree of moisture switches periodically between dry and moist, MISS such as polygonal oscillation cracks form. The periodic shrinking and expanding of microbial mat polygons causes their edges to increasingly budge (NOFFKE, GERDES, & KLENKE, 2003). Additionally, the effects of gas pressure are thought to play a role in this process, since seasonally occurring gas domes are frequently associated with polygonal oscillation cracks.

BAFFLING AND TRAPPING

Microorganisms respond to deposition by baffling and trapping (BLACK, 1933), which are two different processes (Fig. 37). Baffling is the response of the microbenthos to sedimentation (NOFFKE, 1997; GERDES, KRUMBEIN, & NOFFKE, 2000; SCHIEBER, 2004). In laboratory experiments, filaments of cyanobacteria are shown to orientate vertically and move upward in accordance with sedimentation rate (GERDES, KRUMBEIN, & REINECK, 1991). Such vertical movement of cyanobacteria (and other photoautotrophic microorganisms) is called phototaxis;

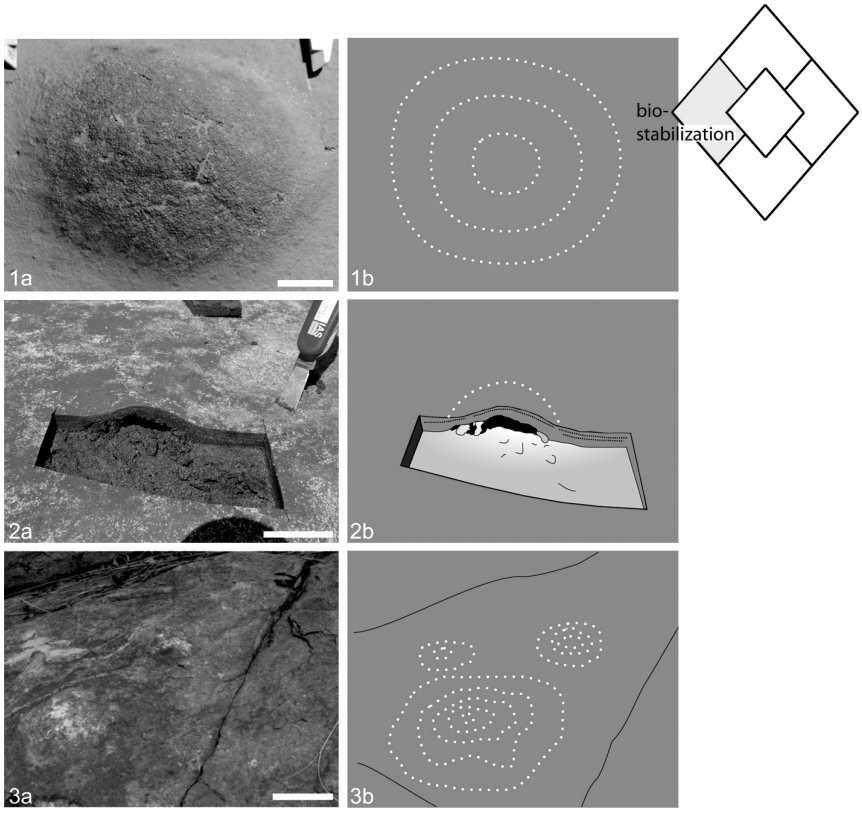

FIG. 35. Examples of microbially induced sedimentary structures caused by biostabilization (*a*), with accompanying drawings (*b*). *1,* gas dome in top view, Paso Seco, Argentina; scale bar, 2 cm. *2,* The cross-section view through a gas dome reveals a hollow cavern beneath the dome, scale bar, 5 cm. *3,* Gas domes *in situ* preserved in the 2.8 Ga Pongola Supergroup, South Africa; scale bar, 5 cm. Color version available in *Treatise Online* 162 (paleo.ku.edu/treatiseonline).

it allows the organisms to position themselves in optimal light conditions. Baffling caused the fall-out of grains of small sizes which, under the same hydraulic conditions but without microbial presence, would remain in suspension. Essentially, microbial baffling increases the rate of deposition of finer-grained material relative to that under ambient hydraulic conditions. This baffling-induced fall-out of suspended particles may clear the water column from fine particles that would otherwise cloud the water, hindering the penetration of light and thus impairing photosynthetic processes (NOFFKE, 2010).

Trapping commonly refers to the adhesive effect of sticky extracellular polymeric substances (EPS) from microbial mats on ambient particles (GEHLING & DROSER, 2009). Mineral particles (commonly of silt size) and other lithic fragments are baffled and trapped, and therefore adher to mat surfaces. Baffling and trapping may be a function of the length of filament protrusion above the mat or sediment surface, grain size and availability, grain weight, frequency and constancy of current transport, as well as the angle of incline of the mat (FRANTZ, PETRYSHYN, & CORSETTI, 2015 for stromatolites; SUAREZ-GONZALEZ & others, 2019). The stickiness or adhesiveness of EPS, which appears to differ between microbial groups, may also play a role in grain trapping (KAWAGUCHI & DECHO, 2000; TICE & others, 2011). Adhesiveness may also be controlled by electrolyte concentration or salinity in the ambient environment (SPEARS & others, 2008). Sometimes, heavy

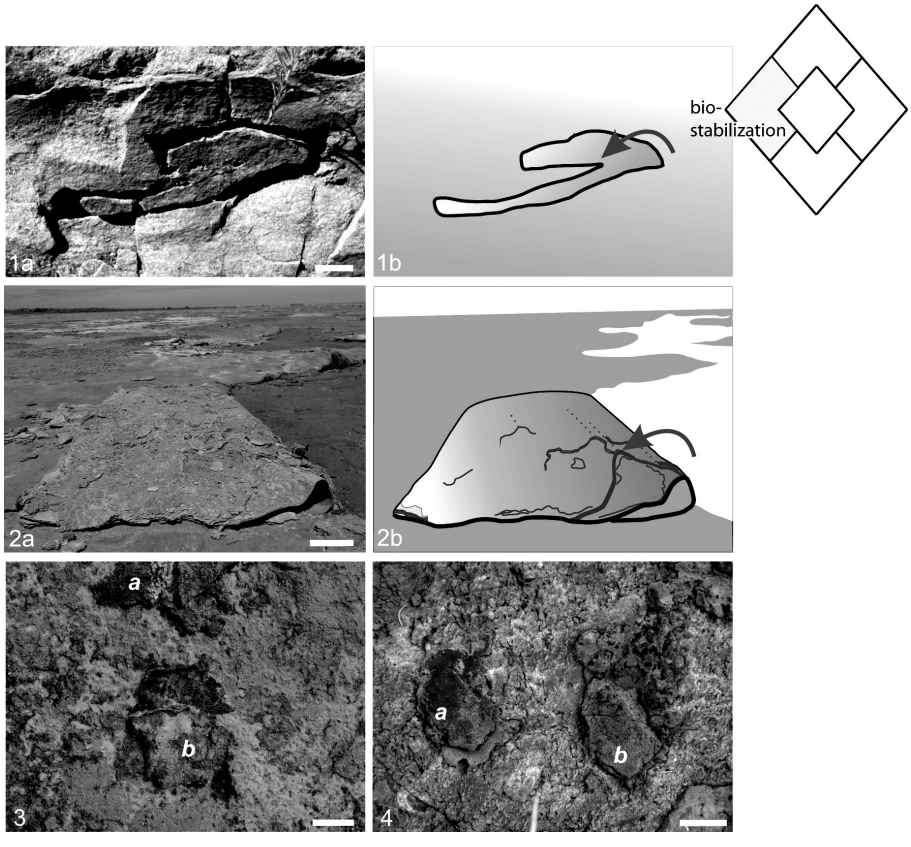

FIG. 36. Examples of microbially induced sedimentary structures caused by biostabilization. *1a,* Large-scale roll-up preserved in the 2.8 Ga Pongola Supergroup, South Africa, scale bar, 5 cm. *1b,* drawing, yellow arrow shows direction of roll-up. *2a,* Modern example of an overflip (roll-up, still connected to the parent mat), Paso Seco, Argentina, scale bar, 5 cm. *2b,* Color-coded drawing showing direction of roll up. *3,* Modern microbial mat chips on the tidal flats of Portsmouth Island, North Carolina, USA. Note that chip (*a*) is turned top-down, whereas chip (*b*) is turned top-up, scale bar, 2.5 cm; *4,* Top-down (*a*) and top-down (*b*) oriented mat chips preserved in the 3.48 Ga Dresser Formation, Pilbara, Western Australia, scale bar, 2.5 cm. Color version available in *Treatise Online* 162 (paleo.ku.edu/treatiseonline).

mineral grains and redox-sensitive metals can be found preferentially enriched in mat layers (GERDES, KRUMBEIN, & NOFFKE, 2000; TAHER & ABDEL-MOTELIB, 2015; TICE, QUEZERGUE, & POPE, 2017; RICO, SHELDON, & KINSMAN-COSTELLO, 2020).

If a biofilm is to function effectively in harvesting energy, each microorganism must place itself into the most suitable position with respect to the other members of the community (STOLZ, 2000; FRANKS & STOLZ, 2009). The coordinated arrangement of filaments into a biofilm or mat fabrics is not possible if the substrate is constantly being reworked. Therefore, as soon as water motion settles down, microbes start to form a biofilm or mat network by actively moving through the sediment.

BINDING

The arrangement of a consortium of microbes into a biofilm or microbial mat is referred to as binding. Examples of active movement by cyanobacteria have been shown in lab experiments (BEBOUT & GARCÍA-PICHEL, 1995; SHEPARD & SUMNER, 2010; BIDDANDA

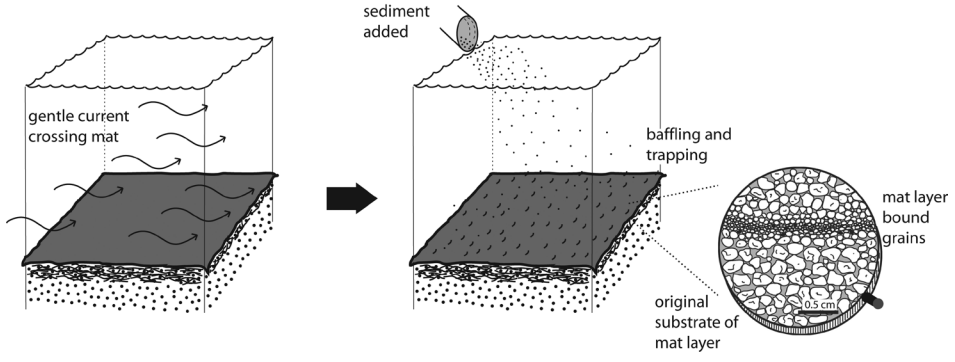

FIG. 37. Baffling and trapping. Left: gentle currents cross an epibenthic microbial mat. Right: When finer-grained sediment is introduced to the system, filaments orientate perpendicularly and promote deposition of the finer grains. The finer-grained sediment forms distinct layers in the deposits (see close-up view on the far right).

& others, 2015) and observed in nature (WALTER, 1976, DECH, NORMAN, & VISSCHER, 2010). Ancient products of binding are described in FLANNERY and WALTER (2011). In contrast to biomass increase (which is largely dependent on nutrient supply, the dynamics of nutrient diffusion through the biofilm, and light availability), binding is controlled only by sedimentary parameters (SHEPARD & SUMMER, 2010). No biomass accumulation is involved. Binding causes structures, such as reticulate patterns comprised of centimeter- to millimeter-scale ridges and tufts, which may cover large areas of microbial mats (GERDES, KRUMBEIN, & NOFFKE, 2000; SHEPARD & SUMNER, 2010) (Fig. 38).

Field observations of modern mats show that such patterns may withstand high energy events (CUADRADO & PAN, 2018). Sinoidal structures are features caused by biofilms covering ripple mark troughs as seen in cross sections through buried sediment (CUADRADO, 2020) (Fig. 39). Fossil examples of such features are also known from the Dresser Formation, Pilbara, Western Australia (NOFFKE & others, 2013).

Field studies monitoring the formation of MISS in modern tidal flats have shown that some MISS form due to an overlap between all of the above-mentioned microbial activities. Good examples of MISS with complex formational histories are multidirectional ripple marks (NOFFKE, 1998; HAGADORN, PFLÜGER, & BOTTJER, 1999) and erosional remnants and pockets (REINECK, 1979; NOFFKE, 1999; NOFFKE & KRUMBEIN, 1999; SCHIEBER, 2007a; NOFFKE, HAGADORN, & BARTLETT, 2019) (Fig. 40).

Highly abundant in the depositional record are wrinkle structures (HAGADORN & BOTTJER, 1997; NOFFKE, 2010; CHU & others, 2015; HOMANN, 2019) (Fig. 41), and several studies have investigated their formation. Wrinkle structures induced by microbes are crinkled surfaces commonly found on the upper bedding planes of fine-grained sandstone beds. They are composed of crests and grooves with irregular directions, with crests generally ranging between 0.1 to 2 mm in height, and a crest-to-crest distance of 0.1 mm to 2 cm. Patterns of crests and valleys vary from specimen to specimen (Fig. 41).

Elephant-skin textures—textured organic surfaces (TOS)—are very common (Fig. 41.4) and well preserved in Ediacaran sandstones (GEHLING, 1999; GEHLING & DROSER, 2009; BOTTJER & HAGADORN, 2007). Fossil impressions have been described as wrinkled surfaces by FEDONKIN (1992). Elephant skin textures are commonly associated with fossils of the Ediacara biota and may have influenced their preservation, according to the iconic death-mask-model (GEHLING, 1999; GEHLING & DROSER, 2009). In both the modern environment and the lab, such

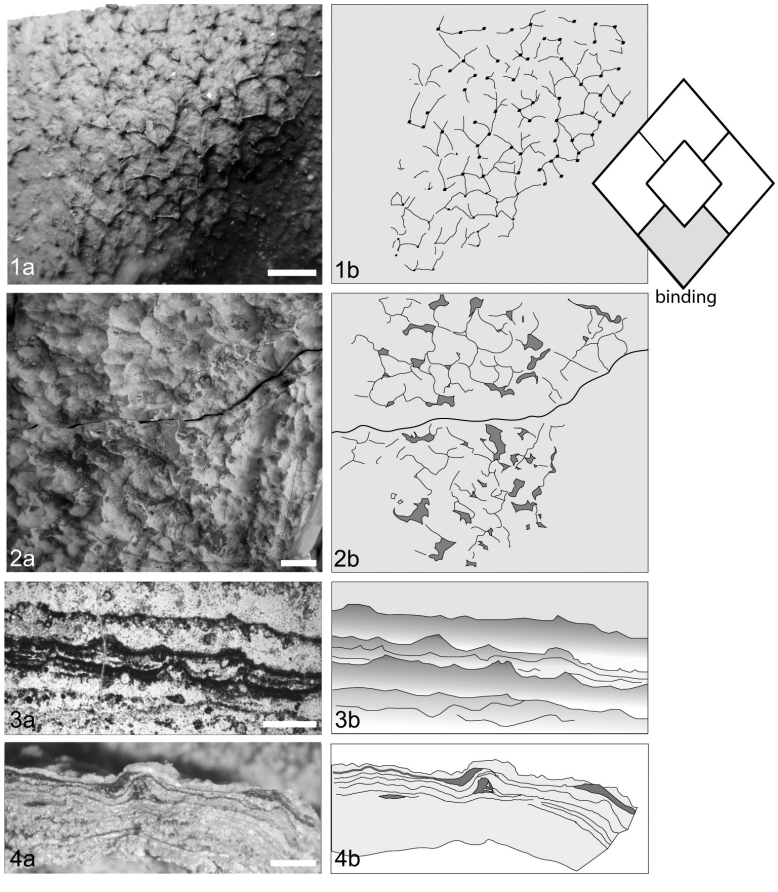

FIG. 38. Examples of microbially induced sedimentary structures caused by binding (*a*), with accompanying drawings (*b*). *1,* Reticulate pattern covering the surface of a modern microbial mat, Paso Seco, Argentina, scale bar, 1 cm. *2,* Reticulate pattern on the surface of a fossil microbial mat from the 3.48 Ga Dresser Formation, Pilbara, Western Australia, scale bar, 1 cm. *3,* Tufts preserved in the 3.48 Ga Dresser Formation, Pilbara, Western Australia, scale bar, 0.1 mm. *4,* Tufts overgrown by microbial mat laminae, Paso Seco, Argentina, scale bar, 1 mm. Color version available in *Treatise Online* 162 (paleo.ku.edu/treatiseonline).

reticulate structures and tufts on sedimentary surfaces result from migrating trichomes (SHEPARD & SUMNER, 2010, CUADRADO & PAN, 2018). The gliding motility and tangling behavior of filaments leads to the formation of tufts resembling centimeter-scale needles on the mat surfaces (GERDES, 2007; STRADER & others, 2009; SIM & others, 2012).

Shearing off a microbial mat from its surface by passing bottom currents (THOMAS & others, 2013) may cause irregularly crinkled surfaces. A microbial mat layer may be arranged into irregular tissue-like folds (Fig. 42.2) and the rapid preservation of such microbial mat fabrics produces crinkled mat surfaces, which sometimes have tears in the originally tissue-like material (fossil examples in NOFFKE, 2000, NOFFKE & others, 2008).

In lab experiments, wrinkle structures (Fig. 42.3) have been shown to form at the sediment-water interface by microbial-mineral aggregates moving back and forth with wave motion creating a *Kinneyia*-like pattern (MARIOTTI & others, 2014). Due to the original fossil *Kinneyi* WALCOTT, 1914 probably being abiotic, the name *Rugalichnus matthewii* was suggested for such *Kinneyiya*-like wrinkle structures, although the trace fossil character of MISS is debatable (STIMSON & others, 2017).

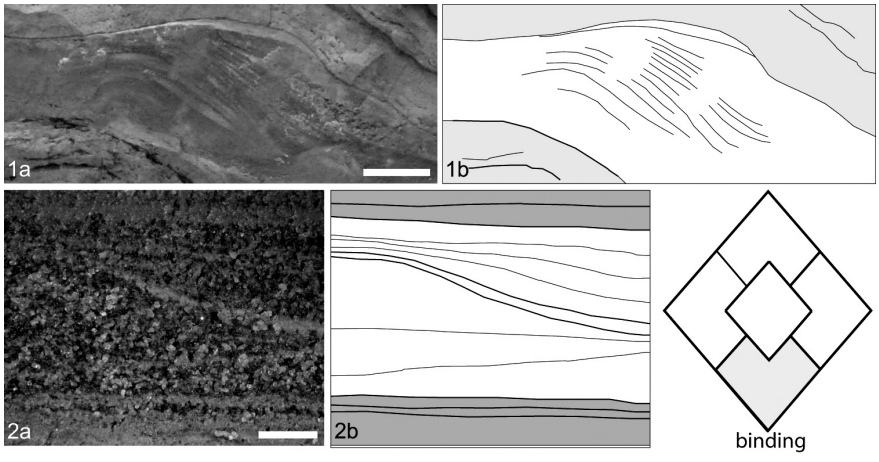

FIG. 39. Example of microbially induced sedimentary structures caused by binding (*a*), with accompanying drawings (*b*). *1,* Biofilms (*black*) overgrow ripple valleys, 3.48 Ga Dresser Formation, Pilbara, Western Australia. Such structures are called sinoidal structures, scale bar, 2 cm. *2,* Similar example for a sinoidal structure in a modern sediment, with mat layers appearing light in color, Paso Seco, Argentina, scale bar, 1 cm. Color version available in *Treatise Online* 162 (paleo.ku.edu/treatiseonline).

Finally, if a microbial mat is suddenly buried by a substantial amount of sediment, the squeezing out of mat-bound water can cause lateral grooves to form in the mat (PFLÜGER, 1999) (Fig. 42.4). Two main types of such wrinkle structures exist: transparent, in which any proceeding (physical) sedimentary structure, such as ripple marks, remain still visible underneath the wrinkles, and non-transparent, in which proceeding surface morphologies are covered completely by wrinkles and are therefore invisible. These two main types reflect endobenthic (transparent) and epibenthic (non-transparent) microbial mats (NOFFKE, 2000). *In situ* preservation of microbial mats occurs in several steps (NOFFKE, KNOLL, & GROTZINGER, 2002). It requires a pause in sedimentation, during which the mat develops and fine-grained material falls out, draping the mat surface and becoming incorporated into the mat fabrics. Subsequently deposited sediment must not be able to erode the mat during placement for *in situ* preservation to occur (NOFFKE, KNOLL, & GROTZINGER, 2002).

It is important to understand that there are different ways to arrive at wrinkled patterns in clastic sediment and that such structures are not always biologically induced patterns (HAGADORN & BOTTJER, 1997; HAGADORN, PFLÜGER, & BOTTJER, 1999; NOFFKE, 2010; see details in DAVIES & others, 2016). Nonbiological mechanisms of formation include, for example, the imprinting of a surface by foam (foam marks), by rapid water motion in very shallow water depths (millimeter ripple marks), or through the deformation of semi-consolidated material by slumping or by ball and pillows formation on the lower bedding plane. Abiotic wrinkle structures may also be caused by tectonic crinkling or biased diagenetic processes (HAGADORN & BOTTJER, 1999).

One last important aspect to consider, if sediment (at least on Earth) always includes biofilms, the question may arise as to whether purely physical sedimentary structures truly exist. Would the presence of biofilms in all deposits not mean that physical sedimentary structures in a natural environment are actually always microbiotic-physical structures? In answering this question, even where biofilms may smother surfaces, they commonly are of too little mechanistic impact to affect a structural representation. However, microbially induced sedimentary structures (MISS) exist, and so the question may be asked, where is the boundary between physical sedimentary

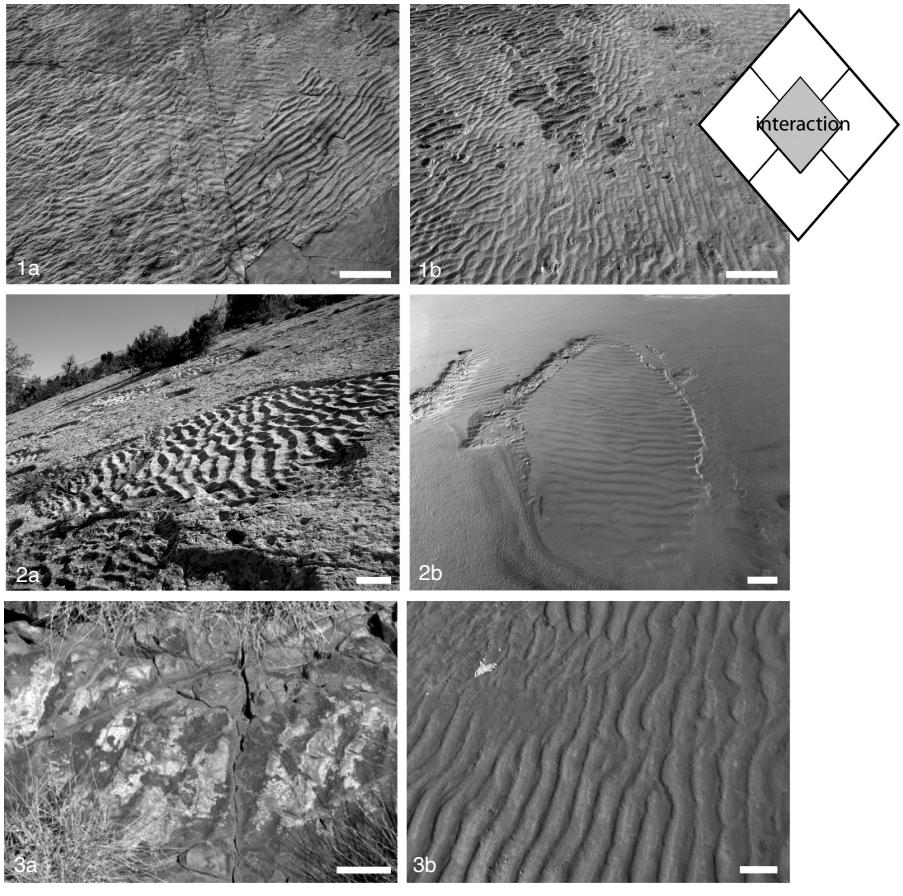

FIG. 40. Examples of microbially induced sedimentary structures produced by the interaction of all microbial activities. *1,* Multidirectional ripple marks in the 2.8 Ga Pongola Supergroup, South Africa (*a*) and in the modern sandflat of Bahia Blanca Estuary, Argentina (*b*), scale bars, 30 cm. *2,* Erosional pocket showing ripple marks in the Cretaceous Dakota Sandstone, USA (*a*), and in a tidal flat, Paso Seco, Argentina (*b*), scale bars, 10 cm. *3,* Rippled surface covered by minute fossil biofilm in the 3.48 Ga Dresser Formation (*a*) and in the modern Paso Seco, Argentina (*b*), scale bars, 10 cm. Color version available in *Treatise Online* 162 (paleo.ku.edu/treatiseonline).

structures and MISS? This question was approached by examining a tidal flat (NOFFKE & KRUMBEIN, 1999). The study developed a modification index (MOD-I) that describes the degree of microbial influence on tidal surface morphologies (erosional remnants and pockets). A MOD-I of 0 would describe sedimentary surface morphologies that show no influence by microbenthos, a MOD-I of 1 describes maximal influence. The boundary between microbially induced or not would be any value >0, with fluctuations of structure-modification in response to seasons being typical. While this study worked well for a local tidal flat with a simple biofilm catena, any conclusion for general sedimentology or even the sedimentology of other planets is unwarranted.

PRESERVATION OF MISS

In thin sections through fossil microbially induced sedimentary structures (MISS), the different components of an ancient microbial mat texture may be visible. Mat textures are fossilized by different minerals depending on the ancient water chemistry providing anions and ions that nucleate into first precipitates.

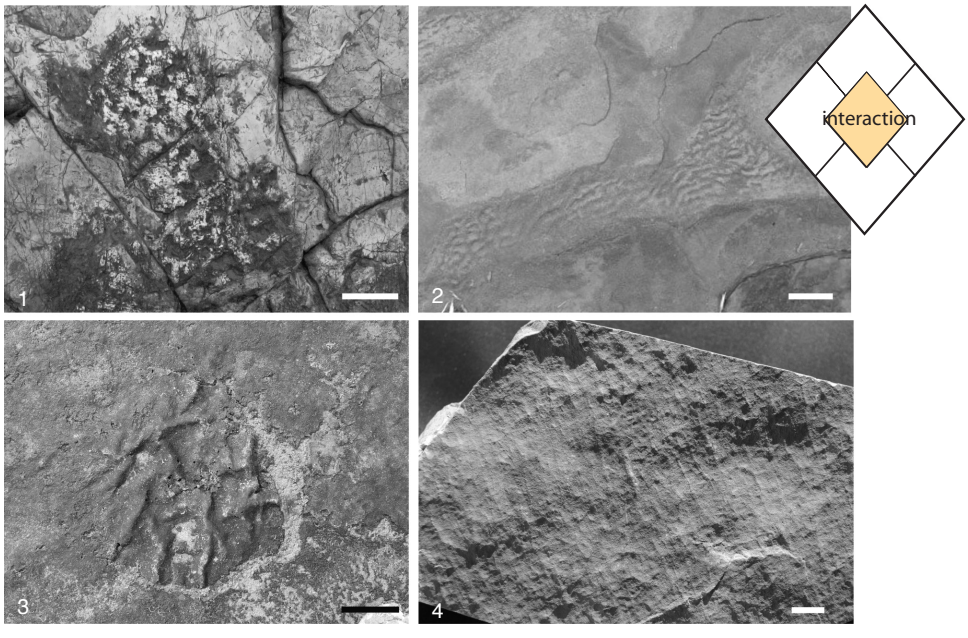

Fig. 41. Biogenic wrinkle structures. *1,* One of the oldest wrinkle structure known in the fossil record is preserved in the 3.48 Ga Dresser Formation, Pilbara, Western Australiam scale bar, 5 cm. *2, Kinneyia*-like wrinkle structure, 2.8 Ga Pongola Supergroup, South Africa, scale bar, 10 cm. *3,* A round piece of microbial mat became detached from its sandy substrate and crinkled. The cause may have been a current crossing the microbial mat in fall, when mats in this area start to compose; Portsmouth Island, North Carolina, USA, scale bar, 10 cm. *4,* Elephant skin texture, Tonian, circa 750 Ma, Qingshuijiangh Formation, South China, scale bar, 1 cm. Color version available in *Treatise Online* 162 (paleo.ku.edu/treatiseonline).

1) Illite or chamosite, pyrite or goethite, and limonite may line the original trichomes of the microbes (Schieber, 1986, 1989, 1999; Pflüger & Gresse, 1996; Hagadorn & Bottjer, 1997, 1999; Logan & others, 1999; Noffke, 2000; Noffke, Hazen, & Nhleko, 2003; Westall & others, 2006; Noffke, Beukes, & others, 2006; Noffke, Eriksson, & others, 2006; Noffke & others, 2013; Heubeck & others, 2016). The formation of clay coats in sandy estuarine and tidal environments can occur as a result of clay-EPS complexes developing along hydroxylated biofilm-clay interfaces or between biofilm proteins and the neutral siloxane surface in quartz sands (Duteil & others, 2020; Worden & others, 2020). Such precipitative clay mineral coatings can develop on microbial biomass surfaces within days as a result of metal ion binding (e.g. Fe, Al), which reduces the nucleation energy of aluminosilicates (Ferris, Fyfe, & Beveridge, 1987; Laflamme & others, 2011; Newman & others, 2016, 2017).

2) Cell walls may still include fragments of the original carbonaceous materials. The organic carbon remains provide opportunity for organic carbon isotope measurements and Raman and infra-red spectroscopic characterization. Anoxic conditions promote the *in situ* preservation of organic carbonaceous matter, as evidenced by the fossilization processes of Burgess Shale macrofossils (Briggs, 2003, Gaines, Briggs, & Zhao, 2008). However, cellular organic matter may also be protected against oxygenation by EPS, which reduces gas exchange between sediment and atmosphere or water significantly.

3) EPS is frequently recorded as silica (Westall & others, 2001, 2011; Noffke & others, 2013). In modern hot springs and also in peritidal sedimentary rocks formed in the silica-rich Archean oceans, rapidly precipitating silica produces an

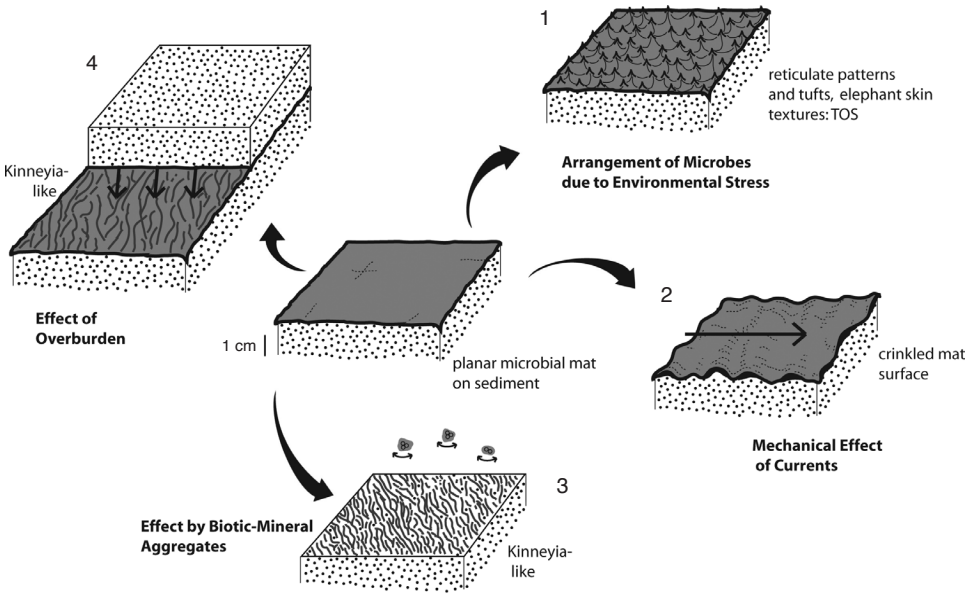

FIG. 42. Various causes and types of microbially induced wrinkle structures. A planar microbial mat is shown in the center of this figure. Variations are shown from *1* to *4. 1,* filamentous microbes form tufts and reticulate patterns in response to environmental stresses causing textured organic surfaces (TOS); *2,* a coherent epibenthic mat is affected by a strong current dislocating the mat and folding it into irregular crinkles resembling folds in a tablecloth, tearing may also occur; *3,* mineral-biofilm-aggregates moved by waves give rise to *Kinneyia*-like structures. *4, Kinneyia*-like structures are caused by jetting water squeezed out of the underlying microbial mat layer when buried by new deposits.

almost impermeable preservational time capsule, resilient even to low-grade metamorphism (TREWIN, 1996; KAH & KNOLL, 1996; MANNING-BERG & others, 2019; HICKMAN-LEWIS, WESTALL, & CAVALAZZI, 2019; HICKMAN-LEWIS & others, 2019; HICKMAN-LEWIS, CAVALAZZI, & others, 2020). The embedding of silica in mat textures has been demonstrated in modern hot spring microbial mats and in lab experiments (TAHER & ABDEL-MOTELIB, 2015; JOHANNESSEN, MCLOUGHLIN, & VULLUM, 2018). Silicification may be microbially mediated within EPS even when silica concentrations within aqueous media are below supersaturation (KAH & KNOLL, 1996; MANNING-BERG & KAH, 2017; MOORE & others, 2020). Calcite formation in EPS has also been studied in great detail in lab experiments and natural settings by DUPRAZ & others (2009) and DECHO (2010).

In most if not all cases of exceptional preservation of microbial mat textures, lithification must have occurred very quickly. In thin sections, fossil MISS may reveal upright tufts (filament bundles) preserved *in situ* (KAH & KNOLL, 1996; NOFFKE, 2000; CAO, YUAN, & XIAO, 2001; HOMANN & others, 2018; HICKMAN-LEWIS, & others, 2018; HICKMAN-LEWIS, WESTALL, & CAVALAZZI, 2019; HICKMAN-LEWIS & others, 2019).

Textures preserved in MISS are essential for determining biogenicity. The example of wrinkle structures is quite frequently debated with respect to their biogenicity. In order to distinguish microbially induced wrinkle structures from abiotic wrinkle structures, thin sections should be examined to reveal the presence or absence of fossil microscopic textures. If a wrinkle structure-bearing specimen is too valuable to be destroyed by thin section analysis, X-ray micro Computed Tomography (X-ray CT) can be used to nondestructively resolve 3D morphologies using density contrasts between the different

materials constituting the internal build-up of such structures (Fig. 43). The primary density contrast comes from the presence of laminated organic matter on top of and inside the rock bed. A number of views of a sample with tufts (Fig. 43) is quite revealing (Sheldon, 2012). Surface mapping (Fig. 43.2) indicates consistent tuft-peak height, which is verified by the 2D- and 3D-segmentation of internal organic-rich laminations (Fig. 43.3). Thus, it can be shown that the example consists of more than just a single microbial mat on the bedding plane surface but rather a series of microbial mats. Each microbial mat may exhibit tufts or evidence of deformation by loading pressure.

CLASSIFICATION OF MISS AND MIST

Conforming to the nomenclature of stromatolites, thrombolites, dendrolites, and leiolites, the overall group of microbially induced sedimentary structures (MISS) constitute the fifth group of microbialites (Riding, 2011b; Noffke & Awramik, 2013; Grey & Awramik, 2020). The main characteristics of MISS that differ from other microbialites are: 1) structure-forming biofilms or microbial mats occur on top or within clastic deposits; 2) only minor to negligible mineral precipitation may occur and is predominantly caused by the biological degradation of organic matter of deceased primary producers and EPS; and 3) as a consequence, the structures are predominantly planar and have, in contrast to most of the other microbialites, low morphological relief.

MISS are divided into five classes, each of which includes individual structures (Fig. 44). These classes are named according to the dominant microbial activity that governs the formation of the structures within the respective class: class 1, structures caused by growth; class 2, structures caused by biostabilization; class 3, structures caused by baffling and trapping; class 4, structures caused by binding (formerly, Noffke & others, 2001, ascribed this class to imprinting); and class 5, structures caused by the interference of all above-mentioned microbial activities (Fig. 44), in center dashed-line diamond). Each structure within each class is named according to its morphological appearance. This enables the surveying geologist to identify a structure even without any knowledge or prejudgment of its genesis. To date, 18 main MISS structures have been distinguished and no

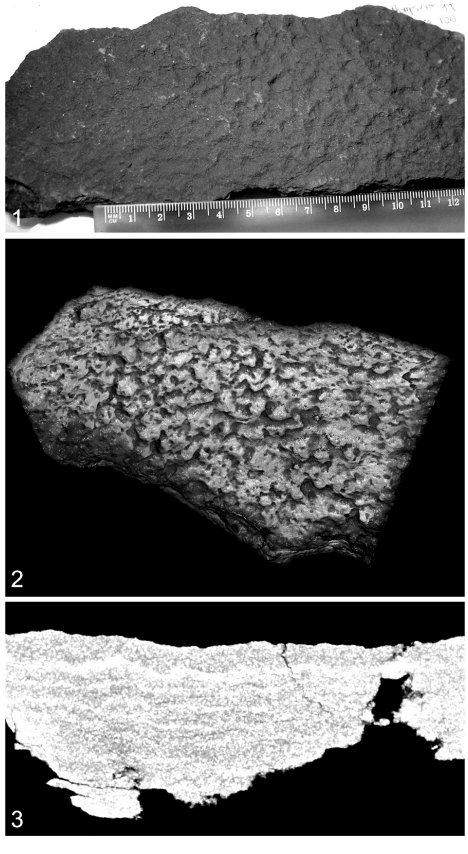

Fig. 43. X-ray CT scans of a microbially induced sedimentary structure sample. *1, Kinneyia*-like wrinkle structure on sandstone slab. *2,* X-ray CT scan of top surface exhibiting *Kinneyia* structure; the corresponding thickness map shows the morphology of the surface peaks. *3,* 2D side-on views of the *Kinneyia* slab, where black microbial-like laminations are visible beneath the surface. Each lamination has been individually segmented to highlight the wavy morphology, which correlated with the peaked surface texture. All images collected with the Advanced Imaging of Materials (AIM) Facility at Swansea University, UK, and rendered using ORS Dragonfly software. Color version available in *Treatise Online* 162 (paleo.ku.edu/treatiseonline).

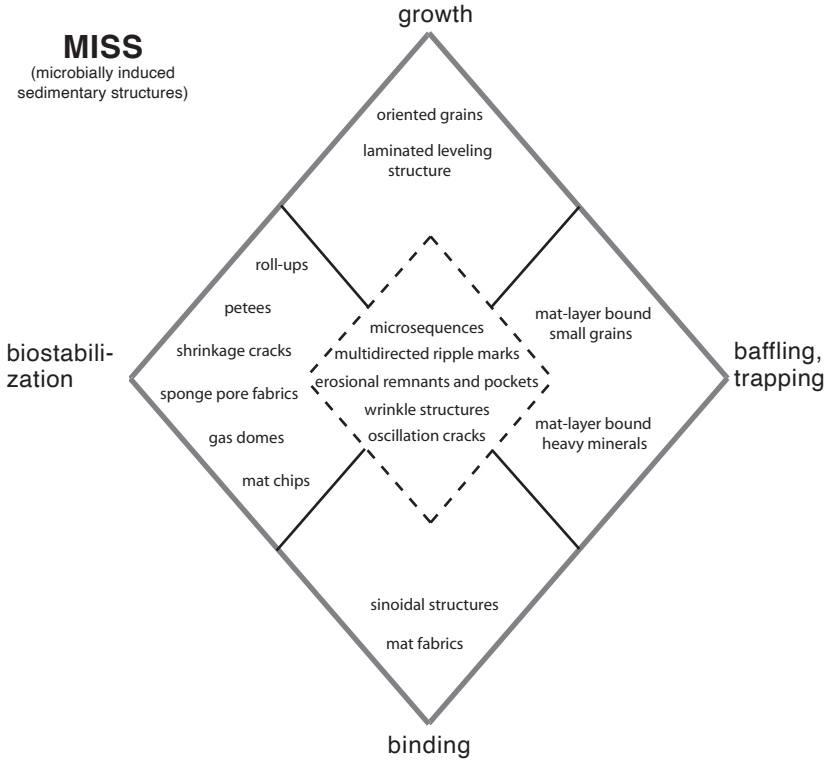

FIG. 44. Classification of MISS and their MIST (on facing page). The classification of both macroscopic and microscopic features each includes five genetic groups related to their means of formation. Descriptive names of individual structures and textures are listed to aid in identification in the field or laboratory.

transitions seem to exist between them (NOFFKE & others, 1996, 2001; NOFFKE, 2010).

MISS include, in thin-section view, a wealth of microscopic microbially induced sedimentary textures (MIST) that witness the former presence of the MISS-producing biofilms or microbial mats (Fig. 44). Textures are divided into five classes according to their genesis: class 1, textures caused by microbial-physical interaction; class 2, textures caused by entombment of carbon; class 3, textures caused by mineralization of organic matter; class 4, textures caused by microbial-chemical interaction; and class 5, textures that rise from the combination of all the four processes. Following the classification of MISS, each MIST within each class is named according to its morphological appearance and pattern of chemical signals. Eleven MIST textures are suggested herein (Fig. 44), but future discussions and contributions will certainly add to this catalog.

SCHIEBER (2004) suggested different groups of mat structures, each categorized according to a leading process: 1) mat growth (comprising binding, baffling and trapping); 2) metabolism (encompassing mineral precipitation); 3) physical destruction (encompassing dehydration, erosion and transport); and 4) mat decay (gas development) and diagenesis (organic matter destruction and mineral precipitation). However, processes that the specific groups cannot be clearly distinguished from each other. For example, (2) metabolism encompassing mineralization overlaps with diagenesis and mineral formation, listed under (4).

Following the broad definition proposed by BURNE and MOORE (1987, p. 241–242)

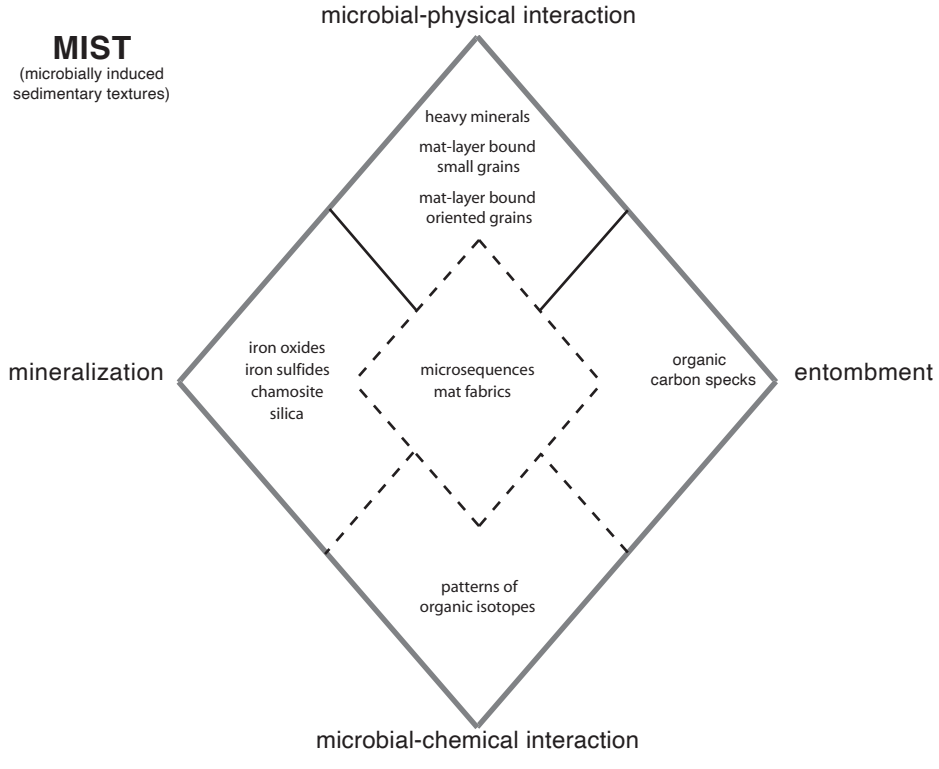

FIG. 44. (continued from previous page). Classification of MISS (facing page) and their MIST. Descriptive names of individual structures and textures are listed to aid in identification in the field or laboratory.

that microbialites are "organosedimentary deposits that have accreted as a result of a benthic microbial community trapping and binding detrital sediment and/or forming the locus of mineral precipitation," RIDING (2011b) and GREY and AWRAMIK (2020) classified MISS in the broad category of microbialites. Overall, MISS constitute the fifth category of microbialites—bedding modified by microbial mats and biofilms—in PETTIJOHN and POTTER's (1964) classification of primary sedimentary structures (NOFFKE & others, 2001).

MISS IN THE COURSE OF EARTH HISTORY

Microbially induced sedimentary structures (MISS) and microbially induced sedimentary textures (MIST) are known in clastic rocks of all Earth ages. Specimen occur in one of the oldest non-metamorphosed sedimentary rock successions, the 3.48 Ga old Dresser Formation in Western Australia (BUICK & DUNLOP, 1990; NOFFKE & others, 2013). Marine stratigraphic successions with Archean MISS once formed by photoautotrophic mats include the 2.9 Ga old Pongola Supergroup and the Witwatersrand Supergroup (BEUKES & LOWE, 1989; NOFFKE, BEUKES, & others, 2006; NOFFKE, ERIKSSON & others, 2006; NOFFKE & others, 2008; TICE, 2009). Fossil microbial mats and biofilms are also widespread in carbonaceous cherts and sandstones of the Paleoarchean Barberton Greenstone Belt in South Africa (see HICKMAN-LEWIS & others, 2018 and HOMANN, 2019 for a review). There, they occur in the 3.472 Ga Middle Marker horizon (HICKMAN-LEWIS & others, 2018); the 3.45 Ga Hooggenoeg Formation cherts (WALSH, 1992; HICKMAN-LEWIS, CAVALAZZI, & others, 2020); the 3.416 Ga Buck Reef

Chert (Walsh & Lowe, 1999; Tice & Lowe, 2004, 2006; Tice, 2009; Tice & others, 2011; Greco & others, 2018); the 3.334 Ga Footbridge Chert (Hickman-Lewis, Cavalazzi, & others, 2020); the 3.33 Ga Josefsdal Chert (Westall & others, 2001, 2006, 2011, 2015); the 3.26 Ga Mendon Formation (Byerly, Lower, & Walsh, 1986; Trower & Lowe, 2016); and sandstones of the 3.22 Ga Moodies Group (Noffke, Eriksson, & others, 2006; Heubeck, 2009, Homann & others, 2015, 2016, 2018). In these deposits, wavy-crinkly laminations have been interpreted as fossil microbial mats based on their laminated structure, sediment trapping and cohesive behavior, carbonaceous and carbon isotopic composition, and the occurrence of eroded and in places rolled-up mat fragments. Wrinkle structures occur but are quite rare. Most fossil mats occur either in carbonaceous banded cherts or interbedded with volcaniclastic sand- and siltstones and quartz-rich sandstones.

The nearly *in situ* preservation of the delicate carbonaceous mat laminae in the Barberton Greenstone Belt show textures such as mat-laminae-bound small grains and oriented grains. Phototactic behavior may be recorded by an increase of mat thickness toward crests in undulating laminae (Tice & Lowe, 2004; Noffke, Gerdes, & Klenke 2003; Homann & others, 2015; Hickman-Lewis & others, 2016, 2018).

Trace and rare earth element data from mat-bearing horizons in cherts up to 3.47 Ga also show strong influences from continental weathering in the form of light rare earth element enrichment, chondritic to sub-chondritic Y/Ho ratios and negligible La and Y anomalies, and it is therefore evident that microbial life inhabited semi-restricted epicontinental basins by this time ~1.09 Ga Mesoproterozoic Copper Harbor Conglomerate (Elmore, 1983; Fedorchuk, 2014). Sheldon (2012) reported 1.1 Ga terrestrial MISS from low-energy fluvial floodplain paleoenvironments preserved in siliciclastic deposits from North America.

Late Neoproterozoic seafloors were widely overgrown by significant microbial mats (Schieber, 1986; Awramik, 1991; Hagadorn & Bottjer, 1997; Hagadorn, Pflüger, & Bottjer, 1999; Bottjer, Hagador, & Dornbos, 2000). Neoproterozoic textured organic surfaces (TOS) record relationships between the Ediacara biota, the earliest macroscopic, multicellular organisms, and contemporaneous microbial mats (Gehling & Droser, 2009; Callow & Brasier, 2009; Laflamme & others, 2011; Darroch & others, 2012; Tarhan, Droser, & Gehling, 2015; Dunn, Liu, & Donogue, 2018). The extraordinary preservation of this soft-bodied biota suggests the extensive presence of microbial mats during this period of time (e.g., Hagadorn & Bottjer, 1999; Gehling, 1999; Seilacher, 1999; Liu & others, 2011; Tarhan, Droser, & Gehling, 2015; Menon & others, 2016; Liu & Dunn, 2020). Terrestrial MISS arising from microbes interacting with aeolian processes are known from the Neoproterozoic Venkatpur Sandstone (Basilici & others, 2020).

Phanerozoic occurrences are known from the Cambrian (Buatois & Mángano, 2003; Seilacher, Buatois, & Mangano, 2005; Mata & Bottjer, 2012; Buatois & others, 2014; Liu & Zhang, 2017; Bayet-Goll & Daraei, 2020); the Ordovician (Gerdes, Klenke, & Noffke, 2000; Noffke, 2000; Buatois & others, 2009; Hints & others, 2014; the Silurian (Hillier & Morrissey, 2010; Calner & Eriksson, 2012); the Devonian (Draganits & Noffke, 2004; Gaillard & Racheboeuf, 2006); the Carboniferous (Mángano & others, 2002; Buatois & others, 2013; Callefo & others, 2019); the Permian (Webb & Spence, 2008); the Triassic (Pruss, Fraiser, & Bottjer, 2004; Pruss, Corsetti, & Bottjer, 2005; Pruss & others, 2006; Mata & Bottjer, 2009; Feng & others, 2019; Wignall & others, 2020); the Jurassic (Porada, Ghergut, & Bouougri, 2008; Peterffy, Calner, & Vajda 2016); the Cretaceous (Gerdes, Krumbein, & Noffke, 2000; Schieber 2007a; Fernández & Pazos, 2014; Noffke, Hagadorn, & Bartlett, 2019); the Neogene (Carmona & others, 2012); and the Quaternary (Kilias & others, 2020).

BANDED IRON FORMATIONS

Adriana Heimann

INTRODUCTION

Banded iron formations (BIFs) are widespread marine chemical sedimentary rocks typical of the Precambrian with no perfect analogs in chemical composition and volume having formed since then. These enigmatic rocks, characterized by banding defined by the alternation of iron-rich minerals and chert, not only are the testimony of a very different young Earth but also the main source of iron worldwide. Extensive BIFs are used as important indicators of the redox state of the ancient oceans, and their characteristics and variations also reflect the evolution of the biosphere-atmosphere-solid Earth system from the Archean to the present. The literature on BIFs is immense and continues to grow. This chapter provides a summary and review of the current knowledge about BIFs, focusing on the hypotheses of BIF formation, both organic and inorganic, recognizing that such an overview will be far from complete. For a conceptual framework for the deposition of BIFs through time, see Bekker and others (2010) and references therein. For an alternative interpretation of the significance of BIFs in the rock record, see Ohmoto and others (2006). The main characteristics of BIFs, including their classification, temporal and geographic distribution, mineralogy, precursor phases, and geochemistry are presented here, followed by the main hypotheses of BIF genesis, including the sources of iron and silica, the genesis of the banding, inorganic hypotheses for their formation, and the ideas and evidence for the likely role of various bacterial processes in their formation. Geochemical (carbon isotopes, iron isotopes, molecular biomarkers), physical (microfossils), experimental, theoretical (cell calculations), and natural (biofilms) lines of evidence that provide insights into the various hypotheses of BIF formation are reviewed. Finally, possible Phanerozoic and modern environmental analogs to Archean–Proterozoic BIFs and their settings are described.

Although BIFs have been the focus of a huge number of studies, their genesis is still a matter of considerable debate. In particular, the origin of the oxidized iron present in BIFs has been debated for decades. Oxidation and precipitation of iron led to the deposition of some BIFs but exactly how this process operated is yet to be fully deciphered. The origin of the negative carbon isotope composition of carbonate carbon in BIFs, whether biotic or abiotic, has also been debated. Because of their age, BIFs are metamorphosed to various degrees and some are highly deformed. However, some BIFs only experienced a very low degree of metamorphism and a low degree of deformation and are beautifully preserved. Banding occurs at diverse scales, from microbanding (micrometric to millimetric laminations), to mesobanding (centimeter-scale), to macrobanding (meter-scale). How this banding originated has also been debated for decades and is still a matter of controversy. The mineralogy of BIFs is defined by various combinations of the main iron phases (magnetite, hematite, siderite, ankerite, and Fe-silicates) and chert.

Large BIFs range in age from the Eoarchean (~3.8 Ga) Isua BIF from Greenland, to the late Paleoproterozoic (~1.8 Ga) Biwabik and Gunflint BIFs from North America (Canada and USA). The abundance of BIFs in the rock record peaked during the late Archean (2.7–2.5 Ga) and early Proterozoic (2.5–1.8 Ga). After a hiatus of at least 1.1 billion years, BIFs briefly appeared again during the Neoproterozoic (~0.8–0.6 Ga), for example as the ~0.6 Ga BIFs of Urucum, Brazil, and the ~0.75 Ga Rapitan BIFs, Canada. BIFs are most commonly classified based on tectonic setting and age. Algoma-type BIFs are

mostly Archean BIFs that formed in active tectonic settings, whereas Superior-type BIFs formed in stable platforms mostly during the Archean–Paleoproterozic. Neoproterozoic BIFs are referred to as Rapitan BIFs and are spatially and temporally associated with Snowball Earth glacial deposits. Snowball Earth refers to a time when Earth's surface is thought to have been entirely or nearly entirely frozen (KIRSCHVINK, 1992). In this chapter, the term BIF is used to refer to all iron formations unless a particular type of BIF is noted. Geographically, BIFs are distributed throughout the planet, but some of the largest and most studied ones include the low metamorphic grade Kuruman BIF from the Transvaal Supergroup in South Africa, the Brockman BIF from the Hamersley Range in Western Australia, and the Biwabik-Gunflint BIF from the Animikie Basin of North America.

The most traditional view holds that BIFs were formed by inorganic chemical and physical processes by which $Fe(II)_{aq}$ emanating from hydrothermal vents would, for example, combine with inorganic bicarbonate dissolved in ocean water and precipitate directly as siderite ($FeCO_3$). Alternatively, after upwelling, $Fe(II)_{aq}$ would become oxidized by small amounts of dissolved O_2 in the upper water column and form hematite (Fe_2O_3) or magnetite (Fe_3O_4) after recrystallization of Fe(III)-hydrated precipitates, such as ferrihydrite. However, based on an increasing body of evidence, other hypotheses have been proposed to explain the formation of BIFs mediated by biological processes. Oxidation of $Fe(II)_{aq}$ and reduction of Fe(III) mediated by various kinds of bacteria, including chemolithoautotrophic iron-oxidizing bacteria, photoferrotrophic bacteria, and dissimilatory iron-reducing bacteria, have been invoked to explain the formation of magnetite, hematite, and siderite.

The disappearance of BIFs from the rock record at ~1.8 Ga, except from the resurgence in the glacial Neoproterozoic successions, is highly debated and has been attributed to various processes. These include the complete oxidation of the atmosphere and oceans after the Great Oxidation Event (GOE) and the increase in seawater sulfate concentration with subsequent expansion of bacterial dissimilatory sulfate reduction and the formation of a sulfidic deep ocean.

Some Phanerozoic ironstones, Phanerozoic iron formations related to massive sulfide deposits (MSDs), and modern siliceous ferric oxide precipitates from marine hydrothermal vents and the Red Sea, are the closest younger equivalents to BIFs. Modern environments that serve as possible analogs to those in which BIF deposition took place in the Precambrian—and where similar processes occur today—include deep ferruginous lakes, such as Lake Matano, Indonesia; iron-rich phototrophic microbial mats, such as those in Yellowstone National Park, USA; and the Iron Mountain acid mine drainage site in California, USA. However, it is important to note that considering size, mineralogy, and environmental conditions together, no real modern analogs of BIFs and their depositional environments occur today on Earth.

See the Glossary, p. xxvi, for terms and common abbreviations used in this chapter.

TYPES OF BANDED IRON FORMATIONS

Various classification schemes have been used to refer to different varieties of banded iron formations (BIFs), variably considering features such as age, tectonic setting, mineralogy, and texture (JAMES, 1954; GROSS, 1965, 1980; KIMBERLEY, 1978; SIMONSON, 1985). The most currently used classification considers mainly age and tectonic setting to divide BIFs into two main classes: 1) Algoma-type BIFs, found in volcano-sedimentary sequences of greenstone belts and typical of Eoarchean age; and 2) Superior-type BIFs, formed in stable platform sedimentary successions and characteristic of late Archean to late Paleoproterozoic age (e.g., GROSS, 1965; BEUKES & GUTZMER, 2008). There are also occurrences of BIFs in the Neoproterozoic

related to Snowball Earth (Kirschvink, 1992) glaciogenic sedimentary rocks, which are commonly referred to as Rapitan BIFs (Gross, 1965; Klein, 2005; Macdonald & others, 2010). In addition, BIFs and exhalites occur spatially associated with massive sulfide deposits (MSDs) (e.g., Spry, Peter, & Slack, 2000; Corriveau & Spry, 2014). Exhalites, however, are chemically different than BIFs because they commonly contain a higher metal content (Pb and Zn, for example) compared to normal, non-MSD-related BIFs, and are not included here. Other iron-rich deposits include the Devonian Lahn-Dill-type iron ores in Germany, which occur as lenses and layers of massive iron associated with bimodal and pyroclastic volcanism and carbonate rocks (e.g., Flick, Nesbor, & Behnisch, 1990). The most likely origin of these iron ores is mobilization and redeposition of iron related to secondary diagenetic alteration of pyroclastic rocks (Flick, Nesbor, & Behnisch, 1990). Because some of these iron ores are different than Archean–Proterozoic BIFs, they are not included here. Many Phanerozoic ironstones are different than BIFs in mineralogy and texture but some can be considered similar; therefore, a brief description of these ironstones is included in *Phanerozoic Ironstones* (p. 122–124). Algoma, Superior, and Rapitan BIFs, as well as those associated with massive sulfide deposits (MSDs), are described in separate sections. However, all other mention of BIFs with no specific reference to a particular type imply Archean–Paleoproterozic BIFs and mostly Superior type, and not those related to MSDs.

Texturally, iron formations have been divided into banded iron formations (BIFs) and granular iron formations (GIFs) (see Klein, 2005 and references therein). BIFs are typical of Archean to early Paleoproterozoic successions and formed prior to the rise of atmospheric oxygen during the great oxidation event, ~2.4 Ga (Holland, 1984), whereas GIFs are clastic sedimentary rocks that became abundant after the GOE and are typical of the late Paleoproterozoic (e.g., Klein, 2005). Based on the lack of structures indicative of wave or storm action, Archean BIFs are generally considered to have been deposited in relatively deep water. In contrast, the granular textures typical of late Paleoproterozoic (1.8 Ga) GIFs indicate that they were deposited in shallow water under the influence of waves, likely close to or above storm and fair-weather wave base (e.g., Klein & Beukes, 1992). Granular iron formations can be slaty and cherty and can also be associated with stromatolites (e.g., Pufahl & Fralick, 2004). Both Algoma- and Superior-type BIFs were deposited in open marine environments during high sea level (Simonson & Hassler, 1996; Krapež, Barley, & Pickard, 2003; Fralick & Pufahl, 2006). However, some Superior-type BIFs contain banded and granular textures, the latter of which represent remobilization, transport, and redeposition of BIFs (Beukes & Gutzmer, 2008). GIFs are mainly restricted to Paleoproterozoic continental basins, such as those surrounding the Superior Craton of North America. Examples of BIFs include the giant Brockman Iron Formation of Western Australia (e.g., Klein, 2005), whereas the type examples of GIFs are those from the Lake Superior Region, USA; Labrador Trough, Canada; and Nabberu Basin of Western Australia (James, 1954; Goodwin, 1956; Simonson, 2003; Klein, 2005).

ALGOMA-TYPE BIFs

Algoma-type banded iron formations (BIFs) occur within Eoarchean to early Paleoproterozoic volcano-sedimentary sequences in greenstone belts, range in age from 3.8 Ga to ~2.6 Ga, and are characterized by currently being relatively small occurrences (lateral extent <10 km, thickness <100 m) (Goodwin, 1973; James, 1983; Isley & Abbott, 1999; Huston & Logan, 2004). These BIFs are typically associated with volcanic rocks and greywackes and formed in tectonically active areas in volcanic arcs and spreading centers (Gross, 1995). Because of this association, scientists have hypothesized

that Algoma-type BIFs formed by exhalative hydrothermal processes during pulses of magmatic and hydrothermal activity coeval with the deposition of the volcano-sedimentary successions of greenstone belts (Barley & others, 1998). Many Algoma-type BIFs are typically intensely deformed and folded, in contrast to Lake Superior BIFs that are commonly undeformed. Mineralogically, Algoma-type BIFs are characterized by iron that occurs in ferric and ferrous states in silicates, siderite, magnetite, and hematite.

The ~3.8 Ga Isua BIF, from the Isua Supracrustal Sequence in West Greenland, is an Algoma-type BIF and possibly the oldest BIF in the world. It is found in association with greenstones with low-K tholeiitic characteristics and turbidites, and experienced medium grade (amphibolite facies) metamorphism (Dymek & Klein, 1988; Komiya & others, 1999; Dauphas & others, 2004; Kato, Yamaguchi, & Ohmoto, 2006). Other Algoma-type BIFs include those in the Nulliak supracrustal sequence in Labrador, Canada, dated at ~3.95 Ga (Shimojo & others, 2013) associated with mafic rocks and metamorphosed to amphibolite facies (e.g., Aoki & others, 2013), and those in the 3.13–2.92 Ga Sargur greenstone belt in India, associated with mafic-ultramafic rocks, quartzites, pelites, and calc-silicate rocks and metamorphosed to upper amphibolite-granulite facies (e.g., Kato, Kano, & Kunugiza, 2002; Kato, Yamaguchi, & Ohmoto, 2006).

SUPERIOR-TYPE BIFs

Superior-type banded iron formations (BIFs) mostly formed in the late Archean to late Paleoproterozoic (3.0 to ~1.8 Ga) on stable, passive-margin continental shelf and slope. They are characterized by great areas and lateral extent (up to hundreds of meters thick, >100,000 km^2), are associated with marine siliciclastic (shale and quartzarenite) and carbonate rocks, and lack direct relationships with volcanic rocks (Trendall & Blockley, 1970; Gross, 1983, 1995; Klein, 2005; Kato, Yamaguchi, & Ohmoto, 2006; Beukes & Gutzmer, 2008; Bekker & others, 2010). They are also thought to have formed during periods of global high sea level and during pulses of enhanced magmatic (mantle plumes) and hydrothermal activity (e.g., Bekker & others, 2010). Mineralogically, Superior-type BIFs are characterized by iron in the ferrous state hosted in silicates, siderite, and magnetite, as well as iron in mixed-state minerals (most commonly magnetite) (e.g., Klein & Ladeira, 2004). Late Paleoproterozoic Superior-type BIFs, which have been studied extensively, commonly exhibit granular textures (e.g., Beukes & Gutzmer, 2008), are generally undeformed, and have been metamorphosed to only very low grades (see Klein, 2005; Beukes & Gutzmer, 2008 and references therein).

Examples of Superior-type BIFs include the giant ~2.5 Ga Brockman Iron Formation (Fig. 45.1, see p. 98); the extensive ~2.6 Ga Marra Mamba Iron Formation, and the smaller Weeli Wolli and Boolgeda BIFs of the Hamersley Range, Western Australia; the ~2.5–2.4 Ga Kuruman-Griquatown-Penge Iron Formations of the Kaapvaal craton, South Africa; the ~2.5 Ga BIFs from the São Francisco craton in Minas Gerais, Brazil; the ~2.4 Ga Kursk BIFs from the Kursk magnetic anomaly, Russia; the ~1.88 Ga Biwabik and Gunflint Iron Formations from the Animikie-Marquette basin, North America; and the ~1.88 Ga BIFs from the Yilgarn craton (Nabberu basin), Australia (see Klein, 2005; Beukes & Gutzmer, 2008; Bekker & others, 2010, and references therein).

RAPITAN BIFs

Neoproterozoic (~0.8–0.6 Ga) Rapitan banded iron formations (BIFs) are found in marginal marine settings, some in broad extensional graben settings, and some are located in mobile belts, such as the Pan African and Brazilian-African belts (Gross, 1995; Trompette, Alvarenga, & de Walde, 1998; Ilyn, 2009). They are typically temporally and spatially associated to Sturtian (~716.5 Ma) and Marinoan (~635 Ma) glacial deposits of global Snowball Earth events (e.g., Kirschvink, 1992; Hoffman

& others, 1998). However, studies based on mapping, stratigraphy, and geochemistry of Neoproterozoic BIFs from Namibia and South Africa suggest that all Neoproterozoic iron formations may be of 716.5 Ma Sturtian age (Macdonald & others, 2010). If this is the case, Rapitan BIFs formed as a result of the secular evolution of the redox state of the ocean, which is considered to have been anoxic at the time of iron concentration (Klein & Ladeira, 2004; Macdonald & others, 2010). Because the oceans were covered by ice, hydrothermal iron was able to accumulate in the water and precipitate as ferric oxyhydroxides when mixed with more oxic waters, either derived from subglacial meltwater plumes (Hoffman & others, 1998) or surface waters at the onset of ice melting (Klein & Beukes, 1993).

Rapitan BIFs are commonly associated with diamictite, are typically succeeded by cap carbonates (usually dolomite and rarely limestone), and may contain dropstones (e.g., Bekker & others, 2010; Macdonald & others, 2010). Texturally, these BIFs are commonly laminated, nodular, and oolitic. Mineralogically, Rapitan BIFs consist almost entirely of iron in the ferric state in hematite, in contrast to Archean and Paleoproterozoic BIFs (Klein & Ladeira, 2004). In addition, these iron deposits sometimes host economic manganese concentrations (Klein & Beukes, 1992; Klein & Ladeira, 2004; Halverson & others, 2011). Examples of Neoproterozoic BIFs, some of them large, include the Rapitan BIFs of the Northwestern Territories, Canada; the Urucúm region of Brazil; the Arroyo del Soldado Group, Lavalleja, in Uruguay; the Damara orogen in Namibia; and the Serranía de Mutum in Bolivia (Gross, 1983; Bühn, Stanistreet, & Okrusch, 1992; Klein & Ladeira, 2004; Klein, 2005; Pecoits & others, 2008).

BIFs RELATED TO MASSIVE SULFIDE DEPOSITS

Banded iron formations (BIFs) are commonly associated with metamorphosed base metal (Pb, Zn, Cu) massive sulfide deposits (MSDs) in sedimentary sequences and in felsic volcanic belts (Spry, Peter, & Slack, 2000; Slack, Grenne, & Bekker, 2009; Corriveau & Spry, 2014). These BIFs generally form below, above, in, or along strike from stratiform, exhalative, or volcanogenic ore deposits (e.g., Spry, Peter, & Slack, 2000). Less commonly, they form lateral to the ore deposits and extend for kilometers. Typically, the BIFs form layers less than two meters thick, although they can also reach tens of meters in thickness. They are also normally laminated with varying mineralogy from layer to layer. Geochemical data and diagrams, including those of Al/Al+Fe+Mn vs. Fe/Ti and ternary Al-Fe-Mn, indicate that the BIFs have variable amounts of hydrothermal and detrital components, but usually the detrital content is less than 30 wt% (Corriveau & Spry, 2014). BIFs related to MSDs tend to have a higher detrital component than non-MSD related BIFs but are very similar in most other aspects. Most BIFs associated with sulfide mineralization are chemical sedimentary rocks similar to Algoma-type iron formations and likely formed by venting of hydrothermal fluids into submarine basins (Stanton, 1972, 1976; Spry, Peter, & Slack, 2000).

BIFs occur in spatial association with some of the largest base metal sulfide deposits of the world. The most extensive BIFs associated with massive sulfide deposits (MSDs) are found in volcano-sedimentary sequences of continental rift systems, such as those near the giant Paleoproterozoic (~1.69 Ga) Broken Hill deposit, Australia (Fig. 48.3–48.4) and the Ordovician Bathurst deposit, New Brunswick, Canada (Spry, Peter, & Slack, 2000). BIFs appear close to the Broken Hill and Pinnacles deposits in the southern Curnamona Province of Australia, but also extend laterally and intermittently for about 100 km throughout the province (Stanton, 1972; Plimer, 1988; Parr, 1992; Parr & Plimer, 1993; Spry, Peter, & Slack, 2000; Heimann & others, 2009, 2013). Many of these BIFs do not have a clear temporal relationship with the sulfide ores (Spry, Peter, & Slack, 2000). In the Bathurst mining camp, BIFs and sulfide ore

extend for 12 km (Peter & Goodfellow, 1996). Other important occurrences of BIFs associated with large MSDs appear in the Mesoproterozoic Gamsberg and Aggeneys deposits in South Africa and the Bergslagen deposit in Sweden (e.g., Plimer, 1988; Spry, Peter, & Slack, 2000).

Typical lithologies associated with BIFs related to metamorphosed MSDs include metamorphosed clastic sedimentary rocks and felsic volcanic rocks, as well as minor mafic igneous rocks that do not occur within the ore (Spry, Peter, & Slack, 2000). The mineralogy of the BIFs may include carbonates, oxides, silicates, and/or sulfides. Sulfide-bearing iron formation is present at the Gamsberg deposit (South Africa), the carbonate iron formation at the Bathurst deposit (Canada), the oxide-silicate iron formation at the Broken Hill deposit (Australia), and the Bergslagen deposit (Sweden) (Plimer, 1988; Peter & Goodfellow, 1996; Spry, Peter, & Slack, 2000).

SPATIAL AND TEMPORAL DISTRIBUTION OF BIFs

Archean–Paleoproterozoic banded iron formations (BIFs) range in age from ~3.8 Ga to ~1.88 Ga. Recent studies suggest that all Neoproterozoic BIFs may be ~716.5 Ma, although previous studies considered their ages to be ~0.8–0.6 Ga. The oldest BIFs are those (~3.8 Ga) from the Isua Supracrustal Belt of Western Greenland (Appel, 1987; Dymek & Klein, 1988). Other Archean BIFs include the ~3.6–3.2 Ga BIFs from the Sebakwian Group in Zimbabwe and the ~2.8–2.6 Ga BIFs of the Dharwar Supergroup in India (Manikyamba, Balaram, & Naqvi, 1993; Arora & others, 1995; Khan & others, 1996; Kato, Kano, & Kunugiza, 2002). There is some evidence that indicates that the largest peak in Algoma-type BIF deposition is related to a major mantle plume event at 2.75–2.70 Ga (Huston & Logan, 2004). A second peak in BIF deposition occurred at 2.5–2.45 Ga with the deposition of the large Superior-type BIFs of the Ghaap/Chuniespoort Group of the Kaapvaal Craton, South Africa, and the Hamersley Group, Australia (Houston & Logan, 2004; Beukes & Gutzmer, 2008). Another peak in BIF deposition occurred in the late Paleoproterozoic at ~1.88 Ga in the Lake Superior region of the USA and Canada. Studies of BIFs in the Frere Formation of Western Australia, previously thought to be 1.84 Ga, concluded that they are actually ~1.88 Ga, indicating that the deposition of BIFs in the Lake Superior region of North America and those in Western Australia are coeval and likely reflect global ocean chemistry (Rasmussen & others, 2012). These BIFs are coeval with important 1.88 Ga mafic-ultramafic magmatism, a large igneous province (LIP) interpreted to be related to a mantle plume event, juvenile continental and oceanic crust formation, mantle depletion, and volcanogenic MSD formation (Heaman & others, 1986; Condie, 1998; Isley & Abbott, 1999; Condie, 2002; Franklin & others, 2005; Kemp & others, 2006; Parman, 2007; Pearson, Parman, & Nowell, 2007; Hamilton & others, 2009; Heaman, Peck, Toope, 2009; Bekker & others, 2010; Meert & others, 2011). This suggests that BIFs formed as a result of major mantle activity and crustal growth (Rasmussen & others, 2012). After this event, large BIFs disappear from the rock record for more than one billion years (Klein & Beukes, 1993), returning in the Neoproterozoic associated with global glaciations of Snowball Earth distributed on nine separate paleocontinents (Macdonald & others, 2010). After these, BIFs typical of the Precambrian are not present in the rock record.

The present day geographic distribution of BIFs reaches every continent (e.g., Klein, 2005). Algoma-type BIFs are relatively small and commonly less than 10 km in lateral extent (Beukes & Gutzmer, 2008; Bekker & others, 2010). Examples of Algoma-type BIFs occur in India, Singhbhum Group (3.5 Ga) (Mukhopadhyay & others, 2008), and South Africa, Fig Tree Group, Barberton Greenstone Belt (~3.3 Ga) (Hofmann, 2005), among other places.

The largest BIFs (10^5 km^2) are Superior-type BIFs, such as the Brockman Iron Formation of the Hamersley Range of Western Australia (~2.6–2.45 Ga) (Trendall & Blockley, 1970; Trendall, 2002; Trendall & others, 2004); the Quadrilátero Ferrífero of the Itabira Group, Minas Gerais, Brazil (~2.6-2.4 Ga) (Klein, 2005); and the Kuruman, Griquatown, and Penge Iron Formations of the Transvaal Supergroup of South Africa (~2.5–2.3 Ga) (Klein & Beukes, 1989) (Fig. 45.1). Paleogeographic reconstructions and detailed geochronological studies suggest that the Asbestos Hills-Penge Iron Formations, Kaapvaal Craton, South Africa (~2.5–2.45 Ga) and the Brockman Iron Formation, Pilbara Craton, Western Australia, were deposited synchronously in the super continent Vaalbara (Cheney, 1996; Zegers & others, 1998; Beukes & Gutzmer, 2008). However, some scientists have suggested, that the similarities, including the stratigraphy, reflect synchronized events on a global scale (Trendall, 1968; Button, 1976; Nelson, Trendall, & Altermann, 1999). Of the late Paleoproterozoic BIFs, the large Gunflint Iron Formation in the Animikie basin of North America (~1.88 Ga) contains the first undisputed microfossils that offer evidence of life on the early Earth (e.g., Barghoorn & Tyler, 1965; Awramik & Barghoorn, 1977). See *Clues from Microfossils,* p. 116–118, for elaboration. The youngest of the Paleoproterozoic BIFs include the ~1.7 Ga Baraboo BIF from the Freedom Formation, Wisconsin, USA (e.g., Weidman, 1904), which has not been studied in detail.

Examples of Neoproterozoic BIFs occur between 0.8 and 0.6 Ga in the Rapitan Group, Yukon and the Northwest Territory, Canada (~0.716 Ga); Jacadigo Group in the Urucúm District, Brazil and Bolivia (~0.6 Ga); the Damara Supergroup, Chuos Formation, Namibia (~0.75–0.65 Ga); and Arroyo del Soldado Group, eastern Uruguay (~0.6 Ga) (Breitkopf, 1988; Klein & Beukes, 1993; Klein & Ladeira, 2004; Klein, 2005; Pecoits & others, 2008). An integrated mapping, stratigraphic, geo-chemical, and geochronological study of Neoproterozoic BIFs and associated rocks in Namibia and South Africa proposed that all Neoproterozoic iron formations may be of Sturtian age (~716.5 Ma) (Macdonald & others, 2010), instead of some being Marinoan in age (635 Ma) as previously thought (e.g., Frimmel, 2008). An association between Neoproterozoic BIFs and mantle plume events has also been proposed to explain their time-related genesis (e.g., Bekker & others, 2010). See *Hypotheses of BIF Formation,* p. 103–119, for elaboration on this topic.

MINERALOGY AND GEOCHEMISTRY OF BIFs

MINERALOGY AND PRECURSOR PHASES

The main minerals present in banded iron formations (BIFs) include (Table 2): siderite, magnetite, hematite, chert, stilpnomelane, minnesotaite and accessory ankerite, ferroan dolomite, riebeckite, mica (ferri-annite), and chlorite (Klein, 2005). Pyrite may be present as a rare accessory mineral. Some of these minerals, such as siderite and minnesotaite, required low oxygen conditions, whereas others, such as hematite or its precursor Fe oxyhydroxides, clearly required at least some oxygen present in the environment of formation. Some magnetite, siderite, ferrosilicates (minnesotaite), ankerite, and pyrite likely formed during diagenesis and metamorphism (e.g., Ayres, 1972; Perry, Tan, & Morey, 1973). Ankerite, for example, overgrew early, very thin siderite laminations in the carbonate-rich Kuruman Iron Formation, likely evidencing a late diagenetic origin for ankerite and an early diagenetic origin for siderite (Fig. 45.3–45.4; Fig. 46.1–46.2) (Beukes & Klein, 1990; Beukes & others, 1990; Heimann & others, 2010).

The original mineralogy of BIFs has been debated for decades. The original or early diagenetic mineralogy of BIFs likely included the minerals siderite, amorphous or crystalline ferric hydroxides (ferrihydrite,

1

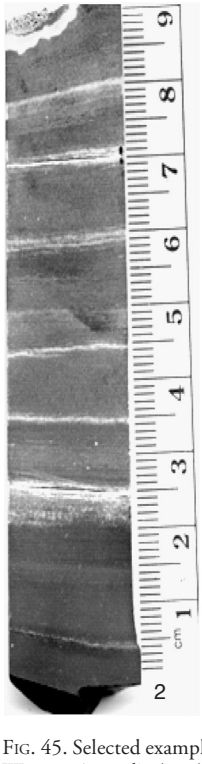

FIG. 45. Selected examples of banded iron formation with different mineralogy from the Brockman Iron Formation, Western Australia (*1–2*) and the Kuruman Iron Formation, South Africa (*3–4*). *1,* View of the Dales Gorge of the giant Brockman Iron Formation (new; image courtesy of Clark M. Johnson). *2,* Core slab sample of banded and laminated oxide and carbonate BIF; magnetite (gray), siderite + stilpnomelane (brown), pure siderite (light tan),

(*continued on facing page*)

TABLE 2. Mineralogy and chemistry of major mineral constituents in Banded Iron Formations.

Mineral Group	Mineral Species	Chemical Composition
Carbonates	Siderite	$FeCO_3$
	Ankerite	$Ca(Fe^{2+},Mg)(CO_3)_2$
	Ferroan dolomite	$(CaMg,Fe^{2+})(CO_3)_2$
Oxides	Magnetite	Fe_3O_4 (or $FeO.Fe_2O_3$)
	Hematite	Fe_2O_3
Silicates	Quartz	SiO_2 (chert or amorphous silica)
	Stilpnomelane	$K(Fe^{2+},Mg,Fe^{3+})_8(Si,Al)_{12}(O,OH)_{27}.n(H_2O)$
	Greenalite	$(Fe^{2+},Fe^{3+})_{2-3}Si_2O_5(OH)_4$
	Minnesotaite	$Fe^{2+}{}_3Si_4O_{10}(OH)_2$
	Riebeckite	$Na_2(Fe^{2+},Mg)_3Fe^{3+}{}_2Si_8O_{22}(OH)_2$
	Ferriannite	$KFe^{2+}{}_3((Fe^{3+},Al)Si_3O_{10})(OH)_2$
	Chlorite	$(Mg,Fe^{2+})_3(Si,Al)_4O_{10}(OH)_2(Mg,Fe^{3+})_3(OH)_6$
	Nontronite	$Na_{0.3}Fe_2(Si,Al)_4O_{10}(OH)_2.nH_2O$
Hydroxides	Ferrihydrite	$Fe^{3+}{}_2O_3.0.5(H_2O)$
	Ferric hydroxide	$Fe^{3+}(OH)_3$
	Goethite	$Fe^{3+}O(OH)$
Sulfides	Pyrite	FeS_2

ferric hydroxide, and goethite), greenalite, nontronite, and amorphous silica (Table 2) (e.g., KLEIN, 2005; BEUKES & GUTZMER, 2008). It has also been suggested that most siderite and pyrite in BIFs precipitated within the water column of anoxic basins, but some also formed during early diagenesis (OHMOTO & others, 2006). Silica was also present in the structure of original clays. Thermodynamic calculations and experiments indicate that ferric hydroxides (ferrihydrite or goethite) can be transformed to hematite by dehydration and recrystallization reactions during early diagenesis (BERNER, 1969; SCHWERTMANN & CORNELL, 1991). Nanoscale hematite inclusions found within siderite in the Kuruman BIF have been interpreted as reflecting the origin of siderite in a reaction involving coupled oxidation of organic matter and reduction of Fe(III) hosted in primary hematite or an original Fe(III) hydroxide by bacterial dissimilatory iron reduction (DIR) (HEIMANN & others, 2010). Similar

FIG 45. (*continued from facing page*)

Dales Gorge Member, Brockman Iron Formation, Western Australia, sample DDH#44-19. *3,* Core sample of banded and finely laminated carbonate BIF with siderite-chert laminations (dark black), pure siderite laminations (light brown), and large, diagenetic ankerite (white), Kuruman Iron Formation, Transvaal, South Africa, sample WB98-815 (*2–3,* core samples, Geology Museum, University of Wisconsin-Madison; new, photos, Adriana Heimann). *4a–b,* Iron-carbonate microlaminations, organic matter remains, and mineralogy typical of the Kuruman Iron Formation; *a,* photomicrograph showing siderite mud microlaminae (*Sid,* dark gray-brown), organic matter remains (*OM,* black), and diagenetic ankerite (*Ank,* white, coarser grained), plane polarized ×10, sample WB98-800A; *b*, back-scattered scanning electron microscope image of same sample showing siderite (almost white), coarser diagenetic ankerite (gray), and organic matter (black) remains (new). Color version available in *Treatise Online* 147 (paleo.ku.edu/treatiseonline).

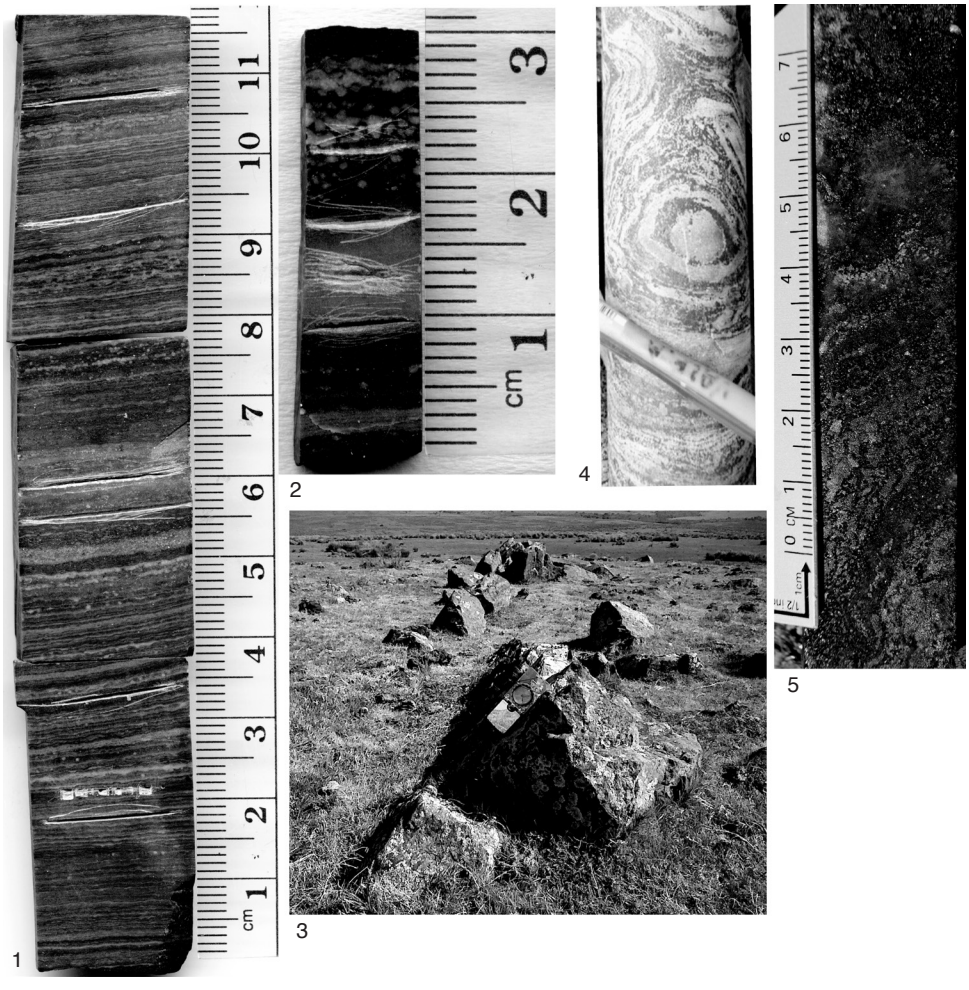

5

FIG. 46. Selected examples of banded iron formations with different mineralogy from various locations worldwide. *1,* Core slab sample showing banded and finely laminated carbonate BIF of the Kuruman Iron Formation, South Africa, pure siderite laminations (light brown/tan), lamination rich in hematite (reddish), sample DI1-213.8 (Geology Museum, University of Wisconsin-Madison). *2,* Core slab sample of banded carbonate BIF of the Kuruman Iron Formation, siderite (dark), large, late, diagenetic ankerite (white areas), sample AD5-161-9A, Geology Museum, University of Wisconsin-Madison (*1–2,* new; photos, Adriana Heimann). *3,* Field photo of the Valentines Iron Formation, Nico Pérez Terrane, Uruguay, compass for scale (new; photo courtesy of Richard Lateulade). *4,* Core sample of deformed and metamorphosed quartz-magnetite iron formation from the Valentines Iron Formation, quartz (white), magnetite (dark, brown). *5,* Core slab sample of deformed banded quartz-magnetite-pyroxene iron formation, magnetite (reddish brown), quartz (dark), pyroxene (greenish), quartz (coarse, whitish spots), Valentines Iron Formation (new; photo, Heather Lancaster). Color version available in *Treatise Online* 147.

hematite microspheroids, dusty hematite, or microcrystalline hematite have been reported from other BIFs, including the Bruno's BIF of the Mount Sylvia Formation, Hamersley Basin (Western Australia), and interpreted to be the result of recrystallization of original ferrihydrite (e.g., BEUKES & GUTZMER, 2008).

BIFs were originally classified based on their dominant mineralogy as carbonate, oxide, silicate, and sulfide facies BIFs (JAMES, 1954). Sulfide facies BIFs were originally defined as pyritic and organic carbon-rich black shales with high iron contents (>15 wt%) (JAMES, 1954), although most authors

do not consider these as BIFs but as shales (e.g., Bekker & others, 2010). These shales commonly occur stratigraphically above, below, or interbedded with oxide or carbonate. More recently, Beukes and Gutzmer (2008) classified BIF facies into oxide-, hematite-, and siderite-facies BIFs. Some BIFs contain more than one dominant type of mineral. Oxide facies BIFs are comprised predominantly of magnetite, hematite, and chert. The large Superior-type ~2.5 Ga Brockman Iron Formation (Fig. 45.1–45.2) is a good example of an oxide facies BIF but also contains carbonate (siderite)-rich bands and silicates (stilpnomelane) (Ewers & Morris, 1981; Pecoits & others, 2009, and herein). The giant ~2.5 Ga Kuruman Iron Formation is an excellent example of a carbonate-rich BIF primarily composed of siderite, ankerite, and minor ferroan dolomite with local laminations of iron oxides (Fig. 45.3–45.4; Fig. 46.1–46.2) (Klein & Beukes, 1989; Beukes & others, 1990; Heimann & others, 2010). It represents the best-preserved, carbonate-rich BIF, as it has only been affected by very low metamorphism and almost no deformation. It is characterized by millimeter-scale laminations of very fine-grained (up to 5 μm) siderite with interstitial organic matter intercalated with very fine-grained chert (Fig. 45.4a–b). Ankerite appears as an accessory, late diagenetic, medium-grained mineral in the fine-grained, siderite-rich laminations (Fig. 45.4a; Fig. 46.1–46.2). Other BIFs also contain oxide and carbonate minerals. Algoma- and Superior-type BIFs are similar mineralogically, whereas Neoproterozoic BIFs have very simple mineralogies, containing mainly iron oxides and silica (Klein & Beukes, 1992; Klein & Ladeira, 2004).

Most Archean BIFs have experienced metamorphism and deformation and only some have very low or low metamorphic grade mineral assemblages (Fig. 47). Many of the large and most-studied late Archean–early Proterozoic BIFs, such as the Kuruman and Brockman BIFs, have undergone only very low-grade metamorphism and even preserve diagenetic mineral assemblages (Fig. 45.4a) (Klein, 2005). In most cases metamorphism was isochemical, except for dehydration and decarbonation reactions. The BIFs of the Hamersley Basin in Australia have been metamorphosed to sub-greenschist to greenschist facies conditions at estimated burial temperatures of 200–300°C and burial pressures of ~1.2 kbar (Klein & Gole, 1981; Kaufman, Hayes, & Klein, 1990). The burial temperatures of the BIFs from the Kaapvaal Basin in South Africa have been estimated to be one of the lowest, at 100–150°C (Miyano & Klein, 1983).

The mineralogy of silicate-rich BIFs depends on the metamorphic grade. At low metamorphic grades of the biotite zone, the minerals can include greenalite, stilpnomelane, minnesotaite, chamosite, ripidolite, riebeckite, and minor ferriannite. At medium and high pressures and temperatures, amphiboles (cummingtonite, grunerite, actinolite, hornblende), pyroxenes, fayalite, and minor garnet form (Fig. 46.3–46.5; 48.3–48.4) (Klein, 2005).

GEOCHEMISTRY

Most researchers agree that original iron-rich minerals in banded iron formations (BIFs), except some Fe silicates, formed by oxidation and direct precipitation of iron dissolved in seawater as Fe(III) oxyhydroxides in large water bodies (Trendall & Blockley, 1970; Ayres, 1972; Ewers & Morris, 1981; Trendall, 2002). If this is the case, the geochemistry of BIFs can help scientists understand the chemistry of the water from which they precipitated. In particular, rare earth elements (REEs) in BIFs could serve as redox proxies (e.g., Bau & Möller, 1993; Planavksy & others, 2010). However, there are still some unknowns regarding the fractionation of elements and isotopes during precipitation and the effects of diagenesis and metamorphism. In addition, some scientists have argued and continue to postulate that the precursor sediments of BIFs were not direct chemical precipitates but microgranular muds or

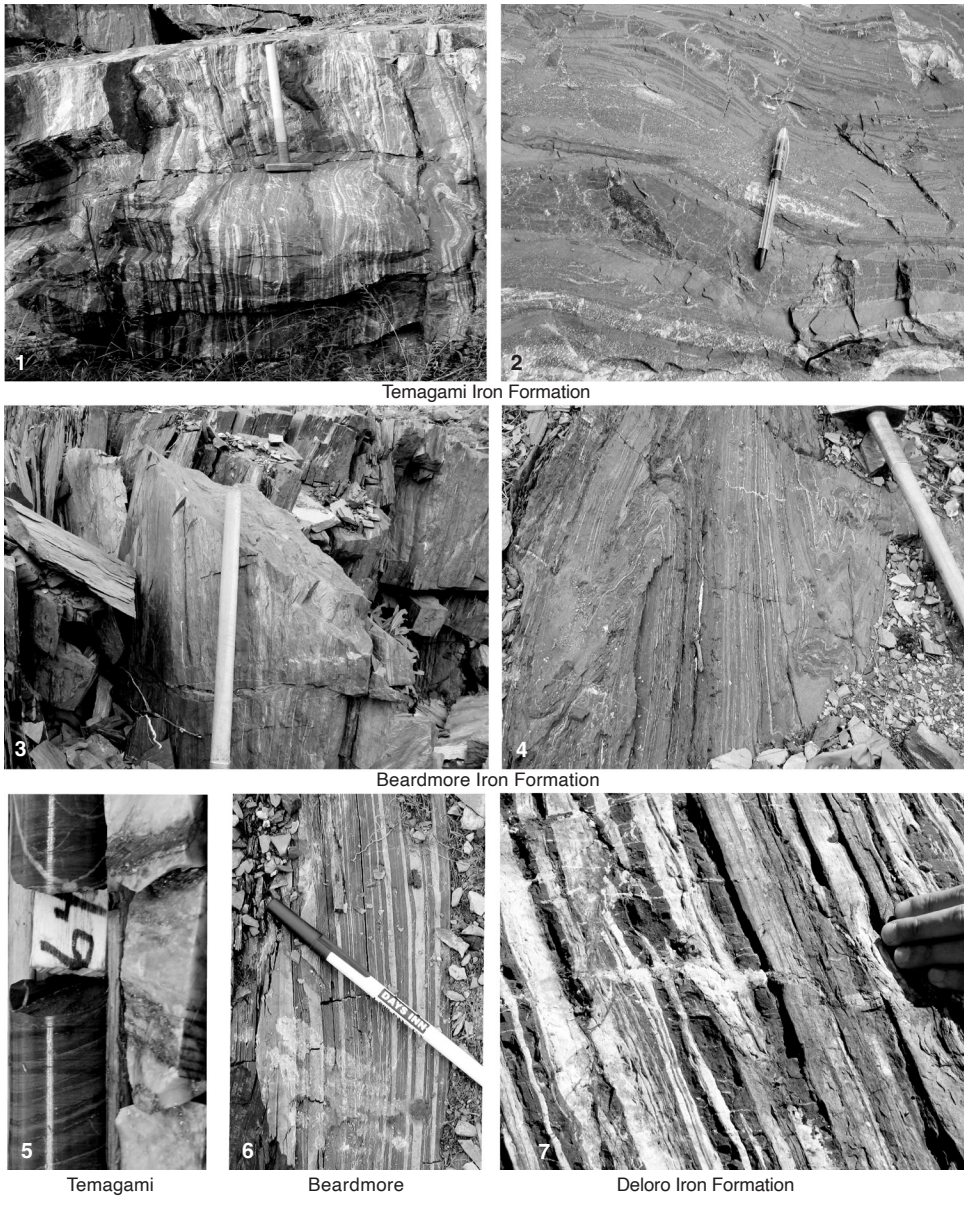

Fig. 47. Photos showing mesoscopic layering and deformation features of various deformed banded iron formations from the southwestern Superior Province, Ontario, Canada (new; all photos, Adriana Heimann). *1,* Outcrop of Neoarchean, Algoma-type, Temagami Iron Formation (2.7 Ga) showing vertical to subvertical layering and minor folding, layers of gray/black hematite (gray), red jasper (chert and hematite), and chert (white); also present, carbonates and iron silicates, Sherman Mine, Cobalt area. *2,* Close-up of outcrop showing deformation features in the Temagami Iron Formation, layers are red jasper (chert with hematite) and black-gray hematite. *3,* Neoarchean BIF (2.7 Ga), Beardmore area, BIF is red and metallic gray and characterized by vertical to subvertical layering of hematite-magnetite (gray) and jasper (red). *4,* Close-up of horizontal face of outcrop of Beardmore iron formation showing thin, deformed, folded layers of specular hematite and magnetite (gray) and chert + hematite (red). *5,* Drill core of laminated Neoarchean (2.7 Ga) Temagami Iron Formation associated with mafic-intermediate volcanic rocks, laminations composed of red hematite, gray magnetite, also a quartz vein with pyrite, Sherman Mine, sample core ORS_1-87, 64 feet. *6,* Outcrop image from the Beardmore area showing vertical laminations of oxide-rich (magnetite-hematite)

(*continued on facing page*)

Fe-rich, Al-poor silicate microgranules that were resedimented by dilute density currents. The granules were originally comprised of greenalite, chamosite, or nontronite and are now present as stilpnomelane (Table 2, see p. 99) (Krapež, Barley, & Pickard 2003; Rasmussen & others, 2013).

The iron content of BIFs typically ranges from 15 to 35 wt% Fe, and their silica content varies from 34 to 56 wt% SiO_2 (James, 1954; Klein, 2005). The concentrations of CaO, MgO, MnO, Al_2O_3, Na_2O, K_2O, and P_2O_5 are typically low. The Ca, Mg, and Mn contents reflect the presence of carbonate (siderite, ankerite, minor calcite), whereas Al, Na, and K are hosted mainly by silicates (riebeckite, greenalite, stilpnomelane; Klein, 2005). The CaO and MgO values range from 1.8 to 9.0 wt%, whereas those for Na_2O and K_2O are very low (<1.5 wt%). The very low-metamorphic-grade, siderite-rich BIF from the Kuruman Iron Formation has organic carbon contents ranging from 0.05 to 0.2 wt% (see Fig. 45.4) (Klein & Beukes, 1989). Magnetite-rich BIFs from the same sequence have even lower organic carbon contents (Klein, 2005), which has been the focus of debate regarding the role of biologic processes in mediating the deposition of BIF minerals.

It is commonly accepted that, under conditions of low fluid/rock ratios, bulk-rock REE contents are not affected by post-depositional processes, such as diagenesis and metamorphism (e.g., Taylor & McLennan, 1986; McLennan & Taylor, 1991; Bau, 1991). The REE contents and the presence of Ce and Eu anomalies in normalized REE patterns of BIFs have been used to understand their origin and the chemical composition and redox state of the Precambrian oceans. Cerium anomalies are defined as $Ce/Ce^* = Ce_N/(\{La_N+Pr_N\}/2)$ (where N refers to the normalization value of shale composites or the Chondrite concentration, and Ce* to the predicted normalized concentration calculated from the equation) and true negative Ce anomalies have Ce/Ce* <1 and Pr/Pr* ($Pr_N/[\{Ce_N+Nd_N\}/2]$) >1 (Bau & Dulski, 1996; Planavsky & others, 2010). Another way of defining the Ce anomaly is using Pr and Nd to avoid utilizing possibly anomalous concentrations of La. Thus, it is defined as $Ce^*_N = Pr^*_N(Pr_N/Nd_N)^2$ (Lawrence & Kamber, 2006). In modern oxygenated seawater, true negative Ce anomalies develop when Ce^{3+} is oxidized and removed as Ce^{4+} by Fe-Mn oxides or hydroxides, organic matter, and clays. Consequently, modern oxic seawater is depleted in Ce and has very large negative Ce anomalies. Suboxic and anoxic waters (0.05–5 μmol O_2 and no dissolved sulfide) lack significant negative Ce anomalies, and some have positive Ce anomalies. These anomalies are the result of reductive dissolution of settling Mn-Fe-rich particles that return Ce back to seawater which is then captured by precipitating Fe-Mn oxides (German & Elderfield, 1990; De Carlo & Green, 2002). Cerium has therefore been used to determine paleooceanic redox conditions. Europium anomalies ($Eu/Eu^*= Eu_N/[\{Sm_N+Gd_N\}/2]$) develop due to an abundance of Eu^{2+} in high-temperature (>250 °C), reduced, hydrothermal fluids and reflect the relative contribution of hydrothermal and riverine influx to the oceans (Klinkhammer, Elderfield, & Hudson, 1983; Sverjensky, 1984; Elderfield, 1988). For further discussion of the significance of REE compositions of BIFs as indicators of paleooceanic redox conditions, see p. 107–108.

HYPOTHESES OF BIF FORMATION

The processes responsible for the generation and precipitation of the vast amounts of iron present in banded iron formations

Fig 47. (*continued from facing page*)
Neoarchean iron formation (dark) with interbedded metapelitic rocks (lighter gray). *7,* Close-up outcrop view of Neoarchean Deloro Iron Formation (2,723 Ma) from the Abitibi Greenstone belt, Canada, exhibiting banded magnetite-hematite (gray/black), siderite (brown), and chert (not visible), with crosscutting veins. Color version available in *Treatise Online* 147 (paleo.ku.edu/treatiseonline).

(BIFs) have been the subject of extensive study during the last ~60 years (e.g., Gross, 1988; Brown, Gross, & Sawicki, 1995). A summary of some of the main ideas about BIF formation is presented here, followed by a more detailed view of the recent thinking about the source of iron and silicon, the origin of the banding in BIFs, the paleoredox ocean structure, and inorganic and biological hypotheses of BIF formation. Table 3 provides a summary of the current thinking of the processes (organic and inorganic) involved in the formation of some well-studied Precambrian BIFs.

The most accepted view of BIF genesis holds that they formed in Archean and Paleoproterozoic oceans that were characterized by extremely low sulfate and sulfide concentrations and oxygen-free deep waters that contained high amounts of dissolved ferrous Fe [$(Fe(II)_{aq}$] (Canfield, Habicht, & Thamdrup, 2000; Canfield, 2005). Most researchers agree that a large reservoir of marine dissolved Fe(II) (~20 ppm; Ewers, 1980; Veizer, 1983) in the Archean and Paleoproterozoic oceans existed due to a high hydrothermal iron flux and a reduced atmosphere, or one that had a low oxidation potential (Holland, 1973; 1984; 2006; Bekker & others, 2004; Kump & Seyfried, 2005). The low sulfate and sulfide contents were necessary to maintain the large amounts of dissolved iron (Habicht & others, 2002). In such an environment, the accumulation of large volumes of iron took place by oxidation of hydrothermally derived Fe(II) and precipitation (Jacobsen & Pimentel-Klose, 1988; Klein & Beukes, 1992; Holland & Petersen, 1995; Isley, 1995). Cloud (1965) was the first to consider the role of bacterial processes for the generation of Fe(III) in BIFs and invoked oxidation of riverine Fe(II) by O_2 produced by oxygenic photosynthesis (cyanobacteria). A contrasting view of BIF genesis, based on the similarity of ancient BIFs and modern chert-hematite deposits associated with volcanogenic massive sulfide deposits (MSDs), considers that BIFs are the result of local discharge of submarine hydrothermal fluids under a fully oxygenated atmosphere and oceans (except in local basins) since ~3.8 Ga (Ohmoto, 1997, 2004; Ohmoto & others, 2006; Kato & others, 2006).

Considerable effort in the study of the origin of BIFs has centered particularly on the mechanisms of oxidation of Fe(II) to Fe(III), the latter estimated to account for 40% of the total Fe in BIFs (Ohmoto & others, 2006; Konhauser & others, 2007; Beukes & Gutzmer, 2008). Most models of BIF formation invoke two stages of Fe cycling. First, hydrothermal Fe(II) is oxidized in the photic zone of the oceans resulting in the crystallization and deposition of Fe(III) oxides or oxyhydroxides on the seafloor. Then, $Fe(II)_{aq}$ reacts with deposited Fe(III) oxides in the sediment or during diagenesis to produce mixed valence minerals or with carbonate or dissolved silica to produce siderite or Fe(II) silicates (Klein, 2005; Beukes & Gutzmer, 2008; Johnson, Beard, & Roden, 2008). Possible mechanisms of Fe oxidation include abiologic and biologically mediated Fe(II) oxidation by oxygen (Cloud, 1965; Konhauser & others, 2002), UV Fe(II) photo-oxidation (Cairns-Smith, 1978; Braterman, Cairns-Smith, & Sloper, 1983), and anoxygenic phototrophic Fe(II) oxidation (or photoferrotrophy) (Widdel & others, 1993; Kappler & others, 2005). It is more than likely that no single mechanism was responsible for the oxidation, precipitation, and generation of the vast amounts of iron present in Precambrian BIFs (Trouwborst & others, 2007). The generation of the Fe(II) present in BIF minerals (magnetite, siderite, Fe silicates) has also been debated and ascribed to either direct inorganic precipitation of Fe(II) (e.g., Beukes & others, 1990) or bacterial DIR (Walker, 1984; Johnson & others, 2003; Johnson & others, 2008; Johnson, Beard, & Roden, 2008).

One of the most striking discoveries is the temporal relationship between the episodic deposition of giant BIFs and major mantle plume events evidenced by the emplace-

TABLE 3. Summary of the current thinking of the processes (organic and inorganic) involved in the formation of some well-studied Precambrian banded iron formations (*ank*, akerite; *cal*, calcite; *goe*, goethite; *hem*, hematite; *mgt*, magnetite; *qtz*, quartz; *sid*, siderite; *stp*, stilpnomelane).

BIF	Mineralogy	Metamorphism	Age	Type	Processes	References
Isua and Akilia, Greenland	Fe silicates, mgt, qtz	Amphibolite-granulite facies	~3.8 Ga	Algoma	Inorganic or organic mediated by anaerobic photosynthetic oxidation	Dauphas & others, 2004; Whitehouse & Fedo, 2007; Czaja & others, 2013
Carajás BIF, Brazil	Hem, ±mgt, goe, qtz, kerogen	Lower greenschist facies	~2.75 Ga	Superior	Inorganic, organic oxidation (from biomats)	Klein & Ladeira, 2002; Fabre & others, 2011; Ribeiro da Luz & Crowley, 2012
Marra Mamba BIF, Australia	Mgt, hem, qtz	Lower greenschist facies	~2.6 Ga	Superior	Organic	Brocks & others, 1999; Summons & others, 1999
Kuruman BIF, South Africa	Sid, ank, mgt, hem, qtz, kerogen	Lower greenschist facies	~2.5 Ga	Superior	Bacterial DIR (siderite); inorganic precipitation from Fe(II) waters	Johnson & others. 2003; Beukes & Gutzmer, 2008; Heimann & others, 2010; Johnson & others, 2013
Dales Gorge Member, Brockman BIF, Australia	Sid, mgt, hem, stp, qtz	Lower greenschist facies	~2.5 Ga	Superior	Bacterial DIR (siderite); chemolithotrophic or photoferrotrophic Fe(II) oxidation (Fe oxides); inorganic (Fe-rich silicates)	Konhauser & others, 2002; Johnson & others, 2003; Pecoits & others, 2009; Cradock & Dauphas, 2011; Li & others, 2013; Rasmussen & others, 2013
Hotazel BIF, South Africa	Mgt, hem, Fe silicates, qtz, ank, cal	Lower greenschist facies	~2.3 Ga	Superior	Inorganic? oxidation	Tsikos & others, 2010
Gunflint BIF, North America	Hem, qtz, carbonates	Lower greenschist facies	~1.88 Ga	Superior	Bacterial oxidation	Planavsky & others, 2009
Rapitan BIF, Canada	Hem, qtz	Lower greenschist facies	~716.5 Ma	Rapitan	Inorganic? oxidation	Halverson & others, 2011

ment of LIPs (KLEIN & BEUKES, 1992; ISLEY, 1995; ISLEY & ABBOTT, 1999). Similarly, a close temporal association of BIFs with volcanogenic MSDs was identified decades ago (e.g., VEIZER, 1976; JAMES, 1983; ISLEY & ABBOTT, 1999; HUSTON & LOGAN, 2004; HUSTON & others, 2010). In a study of BIFs, the association between BIFs of all ages and volcanogenic MSDs was attributed to the interplay among mantle plume events that led to the formation of LIPs, enhanced rates of midocean ridge spreading, high hydrothermal fluxes in the oceans, and changing surface redox states (BEKKER & others, 2010).

The disappearance of large BIFs from the rock record at ~1.8 Ga ago has been attributed to the increase in seawater sulfate concentration as a result of oxic chemical weathering of the continents due to rising atmospheric oxygen contents, the subsequent expansion of bacterial dissimilatory sulfate reduction (DSR), and the formation

of a sulfidic ocean in the Proterozoic, which would have favored iron sulfide precipitation over iron oxidation (Canfield, 1998; Habicht & others, 2002; Poulton, Fralick, & Canfield, 2004). Alternatively, their disappearance has simply been attributed to the complete oxidation of the atmosphere (e.g., Holland, 1984, 2006), but this is also a topic of debate. The hypothesis of a sulfidic ocean transition at ~1.84 Ga implies one of the most significant changes in ocean chemistry throughout Earth's history and is largely based on sulfur isotope compositions and iron speciation data from sedimentary rocks in the Paleoproterozoic Animikie Basin of North America (e.g., Poulton, Fralick, & Canfield, 2004). This transition to a global sulfidic ocean, however, was challenged on the basis of new sulfur isotope data in the context of recent tectonic and sedimentologic models from a correlative section in northern Michigan, USA. These data and models suggest that the Animikie Basin studied to support the hypothesis actually records a basin with restricted water circulation and not open circulation with the global ocean (Pufahl, Hiatt, & Kyser, 2010). However, there is also debate as to whether this basin was a restricted basin or open ocean (Fralick, Poulton, & Canfield, 2011; Pufahl, Hiatt, & Kyser, 2011).

SOURCES OF IRON AND SILICA AND THE ORIGIN OF THE BANDING

The source of iron and silicon in banded iron formations (BIFs) is considered to have been oceanic hydrothermal vents mixed with seawater plus a continentally derived freshwater input (Simonson, 1985; Gross, 1993; Hamade & others, 2003; Delvigne & others, 2012). Most studies have focused on the origin of the iron. Earlier ideas proposed a continental-weathering source for iron and that BIFs formed in continental environments by precipitation of iron and silicon due to evaporation of water (Garrels, 1987). In this model, the banding in BIFs represents cyclic episodes similar to those that produce varves (Garrels, 1987). Later studies agree on a hydrothermal iron source (e.g., Jacobsen & Pimentel-Klose, 1988; Bau & Möller, 1993). More recent studies based on the chemical composition of mesobands of the Dales Gorge Member of the Brockman Iron Formation of Western Australia proposed that metal/Si ratios could help distinguish a continental versus a hydrothermal source for the silica (Hamade & others, 2003). Iron-rich mesobands have Ge/Si ratios that reflect a hydrothermal source for the silicon. In contrast, chert-rich mesobands and mesobands with varved laminations have ratios that fall within the continental end-member range of compositions, which suggests a continental source and weathering of a landmass as the predominant source for the silica.

Precambrian ocean waters were silicon-saturated (~120 ppm Si) due to the absence of silica-secreting microorganisms (e.g., diatoms, radiolarians) at that time, which allowed the precipitation of large quantities of amorphous silica (Siever, 1992). The role of microorganisms in generating the silicon component of BIFs has not received much attention because silicon cannot be metabolized by prokaryotes (archaea and bacteria), the only organisms available during the formation of early BIFs (e.g., Koehler, Konhauser, & Kappler, 2010). However, a biological role for silica precipitation has also been proposed because bacteria are known to promote silicification through their metabolic activity (Birnbaum & Wireman, 1985). Some scientists have suggested that all the chert in BIFs is of early diagenetic origin and not a primary precipitate or diagenetic replacement of earlier silica precipitated from seawater (Krapež, Barkey, & Pickard, 2003; Pickard, Barkley, & Krapež, 2004). In this model, chert was more likely a pore-filling cement and a replacement of sediments.

A later model proposed that silica could have been adsorbed onto the surface of hydrous ferric oxides, which precipitated on the bottom of the ocean along with organic matter (Fischer & Knoll, 2009). Then, once in the sediment pile, reduction of

Fe(III) by bacterial respiration released most of the iron as $Fe(II)_{aq}$ and liberated silica to the sediment pores, which ultimately precipitated as a diagenetic mineral (Fischer & Knoll, 2009). Similarly, based on coupled Ge/Si ratios, REE+Y, and silicon isotope studies, a hypothesis for a two-stage precipitation of silica was proposed by Delvigne and others (2012). They envisioned a first stage of silicon adsorption onto Fe oxyhydroxides followed by early diagenetic release of silica to pore fluids from the Fe oxyhydroxides and consequent silica precipitation upon silica saturation at the sediment-water interface. These ideas have important consequences for the interpretation of oxygen and silicon isotope compositions in chert as indicative of a high seawater temperature in the Archean and Proterozoic (Knauth & Lowe, 2003; Robert & Chaussidon, 2006).

During BIF formation, precipitation of iron probably took place episodically, which caused the development of alternating Fe- and Si-rich bands. The origin of these alternating bands, including their presumed lateral continuity for hundreds of kilometers, has also been the matter of extensive research for more than 50 years (Trendall, 1968; Garrels, 1987; Posth & others, 2008). Based on recent detailed studies including modeling, bacteria incubations, and petrographic studies, the main hypotheses currently being considered to explain the banding include: 1) seasonal stratification or yearly climatic cycles, which would allow for periodic upwelling or pulses of hydrothermal Fe(II)-rich waters interrupted by seasonal evaporation and precipitation of silica (Holland, 1973; Garrels, 1987; Jacobsen & Pimentel-Klose, 1988; Siever, 1992; Morris, 1993); 2) temperature fluctuations, which would allow the maximum biogenic Fe(III) precipitation by iron oxidizing microbes (Fe(II)-oxidizing phototrophs) at 20–25 °C and lower Fe oxide precipitation and abiotic silica precipitation at higher or lower temperatures (Posth & others, 2008); and 3) formation and deposition of silt-size iron-rich silicate microgranules accompanied by alternating seafloor silicification during nondeposition and burial compaction of non-silicified lamina sets (Rasmussen & others, 2013). Based on the first two hypotheses, it seems that temperature could have been an important factor controlling BIF formation in the Archean and Proterozoic oceans. However, because temperature estimates for the Archean and Proterozoic are still a matter of considerable debate, this require further studies.

PALEOOCEANIC REDOX STRUCTURE AND THE FORMATION OF BIFS

Secular variations of cerium (Ce) and europium (Eu) anomalies in banded iron formations (BIFs) have been used to understand the redox state and hydrothermal versus riverine input to the Precambrian oceans and the bio-geochemical evolution of Earth (Klein, 2005; Kato, Yamaguchi, & Ohmoto, 2006; Bekker & others, 2010; Planavsky & others, 2010). In general, the concentration of REEs and the size of the positive Eu anomaly in BIFs seem to decrease with decreasing BIF age (Klein, 2005; Kato, Yamaguchi, & Ohmoto, 2006; Planavsky & others, 2010). Pre-2.7 Ga, Algoma-type BIFs (Isua BIF) have very strong positive Eu anomalies. Middle Archean BIFs (Cleaverville, Australia, and Sargur, India BIFs) have distinct positive Eu anomalies but they are smaller than those in the early Archean BIFs (Rao & Naqvi, 1995; Huston & Logan, 2004; Kato, Yamaguchi, & Ohmoto, 2006). Late Paleoproterozoic BIFs have smaller Eu anomalies. Neoproterozoic BIFs have REE patterns with no or slightly positive Eu anomalies (Fryer, 1976; Klein & Beukes, 1993; Klein & Ladeira, 2004). This trend in Eu anomalies suggests a declining hydrothermal input into the deep ocean from the Eoarchean to the Early Proterozoic, likely linked to falling temperatures of the hydrothermal solutions as a result of lowering upper-mantle temperatures (Bau & Möller, 1993). In addition, no or slightly positive Eu anomalies in Neoproterozoic BIFs indicate

the dilution of local hydrothermal fluids by mixing with mildly oxidized seawater in semi-isolated basins (e.g., Maynard, 2003).

New studies show that bulk Archean and early Paleoproterozoic BIFs lack significant shale-normalized negative Ce anomalies, and that strong positive Ce anomalies are only present in BIFs younger than 1.9 Ga (Planavsky & others, 2010). Some earlier studies of smaller samples have suggested that Ce anomalies were also present in Archean and early Paleoproterozoic BIFs (e.g., Kato, Yamaguchi, & Ohmoto, 2006; Ohmoto & others, 2006). However, bulk-rock studies reflect the overall chemistry of the water mass and the latest findings have been used to propose that late Paleoproterozoic BIFs record the shuttle of metal and Ce oxides from oxic shallow seawater to deeper anoxic waters, similar to the process taking place in modern redox-stratified basins (e.g., Planavsky & others, 2010). In this scenario, as the Ce-bearing oxides (mainly Mn) are transported to the deeper part of the water column, they dissolve under anoxic conditions and release Ce to the water, which is later incorporated in Fe oxides that precipitate at the redoxcline or in the shallow oxygenated water, thus resulting in a positive Ce anomaly (Planavsky & others, 2010; Bekker & others, 2010). In contrast, Archean BIFs do not show the effects of an oxide shuttle, implying the absence of a redoxcline before the rise of atmospheric oxygen (Planavsky & others, 2010; Bekker & others, 2010). This model supports the idea that Archean BIFs formed by metabolic oxidation of iron and not by oxidation of iron by free oxygen in shallow ocean environments (Planavsky & others, 2010; Czaja & others, 2013).

INORGANIC HYPOTHESES FOR BIF FORMATION

UV Photo Oxidation of Fe(II) by Radiation of a Young Sun

An inorganic mechanism to explain Fe(II) oxidation in the Archean is photo oxidation by UV radiation (Cairns-Smith, 1978; Braterman, Cairns-Smith, & Sloper, 1983). This process could have been possible due to the high levels of ultraviolet radiation that reached Earth prior to the formation of the protective ozone layer (Cairns-Smith, 1978). UV photolysis would not have required free oxygen to oxidize dissolved ferrous Fe but instead requires absorption of radiation (wavelengths in the ~200–400 nm range) to form dissolved ferric iron:

$$2Fe^{2+}_{(aq)} + 2H^{+} + h\upsilon = 2Fe^{3+}_{(aq)} + H_{2(g)}$$

Dissolved ferric iron is subsequently hydrolyzed to form solid ferric hydroxide at circumneutral pH (Cairns-Smith, 1978; Braterman, Cairns-Smith, & Sloper, 1983). This mechanism has been demonstrated in laboratory experiments (Braterman, Cairns-Smith, & Sloper, 1983), although only for simple aqueous solutions in which other ions were not available for reactions with original dissolved ferrous iron. Experiments with silica- and calcite-saturated solutions that mimic deep water conditions suggested that the process of photo oxidation would have been slower than and inhibited by the formation of ferrous silicate minerals (such as greenalite) and carbonates (siderite) in the silica-saturated Precambrian ocean waters from which BIF minerals precipitated (Konhauser & others, 2007). In addition, the calculated precipitation rates of ferric iron oxides through photo-oxidation obtained from the earlier experiments yield an annual amount of Fe(II) oxidized from 2.3×10^{13} to 1.8×10^{14} mol/yr (Braterman & Cairns-Smith, 1986; François, 1986). These precipitation rates, however, are faster than sedimentation rates calculated for the Kuruman and Brockman BIFs (compacted sedimentation rates = 22–33 m/myr) (Pickard, 2002, 2003). The consensus seems to be that UV photo oxidation was not likely a dominant process in the formation of ferric oxide minerals in BIFs older than 2.5 Ga (e.g., Koehler, Konhauser, & Kappler, 2010). However, more detailed experiments would help understand the role of this process in the generation of BIFs prior to the rise of atmospheric oxygen.

Abiotic Fe(II) Oxidation by O_2 Produced by Cyanobacteria

A traditional view of Fe(II) oxidation considers inorganic oxidation of dissolved Fe(II) with oxygen produced by photosynthetic cyanobacteria (Cloud, 1965). Prokaryotic microbes, such as oxygenic photosynthesizing cyanobacteria, were likely abundant in the nutrient- and Fe(II)-rich photic zones of nearshore Archean oceans, where Fe(II) and nutrients originated by a combination of continental weathering and upwelling of deep hydrothermal waters (Cloud, 1973). This model envisions an anoxic atmosphere where Fe could have been oxidized by a reaction with O_2 in so-called oxygen oases via oxygenic photosynthesis:

$$CO_2 + H_2O \rightarrow [CH_2O] + O_2$$

followed by:

$$2Fe^{2+}_{aq} + 0.5O_2 + 5H_2O \rightarrow 2Fe(OH)_3 + 4H^+$$

Other studies considered a stratified ocean with a thin upper oxic zone and a lower anoxic ferruginous layer (e.g., James, 1954; Klein & Beukes, 1989). In this model, earlier views considered that Fe^{2+} was provided by continental weathering under an anoxic atmosphere and transported to chemically stratified oceans by rivers (James, 1954), whereas in most modern hypotheses, the Fe^{2+} is derived from hydrothermal alteration of oceanic crust in the deep ocean (e.g., Isley, 1995). Both of these models require the existence of oxygenic photosynthesizers, and several studies have suggested their existence by the Neoarchean (see also *Clues from Molecular Biomarkers,* p. 118). A new model of BIF genesis was recently proposed to explain the formation of BIFs in the ~1.8 Chiall Formation, North America, by inorganic precipitation of Fe oxyhydroxides in riverine systems from Fe derived from terrestrial weathering and coastal upwelling (Pufahl, Pirajno, & Hiatt, 2013).

Low $\delta^{13}C$ values (-57 to -28‰) in preserved organic carbon in ~2.7 to 2.57 Ga shales and carbonates from the Hamersley Province in Western Australia were interpreted as evidence of oxygenated microbial ecosystems comprised of cyanobacteria and aerobic methanotrophs (Eigenbrode & Freeman, 2006; Eigenbrode, Freeman, & Summons, 2008). Additionally, 2.7 Ga stromatolites from the Tumbiana Formation in the same stratigraphic sequence were considered to be evidence of a microbial mat community of cyanobacteria (Buick, 1992). However, this does not explain the formation of earlier BIFs. Further, no single type of bacteria can be assigned unequivocally to the construction of the mats and stromatolites.

In situ observations and quantitative geochemical modeling of oxidation of Fe(II) by cyanobacterial oxygenic photosynthesis in high-Fe(II) anoxic waters buffered by bicarbonate and silica at Chocolate Pots hot springs, Yellowstone National Park, USA, also supported the Cloud (1965, 1973) hypothesis (Parenteau & Cady, 2010). In the Parenteau and Cady study, the contributions to *in situ* Fe(II) oxidation by oxygenic photosynthesis (by cyanobacteria), anoxygenic photosynthesis (by *Chloroflexus* Pierson & Castenholz, 1974, purple bacteria, plus any other bacteriochlorophyll-containing phototrophs), and chemolithotrophy (by e.g., *Gallionella* Ehrenberg, 1838) were assessed, and the results suggest that oxygenic photosynthesis was the sole mechanism of Fe(II) oxidation in the anoxic vent waters. Light intensity was the primary variable affecting the rate of oxygen production and subsequent Fe(II) oxidation in the benthic cyanobacterial mats that are surrounded by anoxic water (Parenteau & Cady, 2010). However, a large body of evidence suggests that molecular oxygen was very scarce before ~2.4 Ga (Farquhar & Johnston, 2008) and this would have made abiotic Fe(II) oxidation extremely slow (Konhauser, Newman, & Kappler, 2005). Biological oxidation of Fe(II) at low oxygen partial pressure is much faster (Søgaard, Medenwaldt, & Abraham-Peskir, 2000), and Fe(II) chemoautotrophic metabolic oxidation is known to occur in modern microaerophilic environments (e.g., Crowe

& others, 2008a, 2008b). However, this mechanism also requires the supply of O_2 (see *Bacterial Metabolic Iron Oxidation,* below, for elaboration).

Direct Precipitation from Seawater

It is possible that some siderite (e.g., spheroidal siderite) formed directly by precipitation from anoxic water by mixing of ferrous iron and bicarbonate originating from a combination of hydrothermal fluids and microbial respiration of sedimented organic carbon (Beukes & others, 1990; Tice & Lowe, 2004; Klein, 2005) via:

$$4Fe^{2+} + 8HCO_3^- \rightarrow 4FeCO_3 + 4H_2O + 4CO_2$$

By this mechanism, siderite precipitates along the chemocline where there is supply of some organic carbon. Magnetite and hematite can precipitate in deeper areas where the organic supply is low and some oxygen is available (Beukes & others, 1990). However, it is difficult to envision enough oxygen to form magnetite and hematite in the deeper parts (below the redoxcline) of the Archean–Paleoproterozoic oceans where BIFs precipitated.

A later petrographic study of the Dales Gorge Member of the Brockman Iron Formation found silt-sized microgranules comprised of stilpnomelane and proposed the inorganic origin of 2.5 Ga BIFs as Fe-rich, Al-poor silicates that formed in the water column or ocean floor (Rasmussen & others, 2013).

BIOLOGICAL HYPOTHESES FOR BIF FORMATION

The hypothesis that biological processes could have an important role in the deposition of iron-rich sediments was first proposed by Ehrenberg (1836). Winogradsky (1888) later showed that a bacterium (*Leptothrix* Kützing, 1843) was able to live and grow only in the presence of ferrous iron in solution. Cloud (1965, 1973), while studying the microfossils of the Paleoproterozoic banded iron formations of the Lake Superior area, suggested that cyanobacteria could have participated in the oxidation and precipitation of Fe. Others proposed that BIF formation was related to carbon-cycling processes in which oxidation of Fe(II) driven by photosynthesis (oxygenic or anoxygenic) led to the contemporaneous deposition of Fe(III) oxides and organic matter. In this model, the formation of BIFs was ultimately the result of coupled organic carbon oxidation and iron reduction by anaerobic bacteria, such as iron-reducing bacteria (Walker, 1984; Konhauser, Newman, & Kappler, 2005; Kappler & others, 2005). Based on new observations of microbes and biofilms living in extreme conditions, such as near hydrothermal vents or deep in boreholes, the realization has occurred that prokaryotes probably also thrived in similar hostile environments in shallow Archean ocean waters and that they also likely utilized iron.

Mechanisms of BIF formation: Fe(II)-oxidizing and Fe(III)-reducing bacteria

Bacterial metabolic iron oxidation. Bacterial microaerophilic (chemolithotrophy) Fe(II) oxidation was likely an important process for the generation of banded iron formations (e.g., Holm, 1989; Konhauser & others, 2002). Iron-metabolic (chemolithotrophy) proteobacteria, such as *Leptothrix* and *Gallionella* are common in iron-rich freshwater streams and groundwater seeps (e.g., Harder, 1919). In addition, microaerophilic Fe(II) oxidizers are widespread in marine environments, including iron-rich hydrothermal vents (Emerson & Moyer, 2002) and at the chemocline of ferruginous lakes, such as Pavin Lake (France), where Fe-rich sediments are being deposited (e.g., Lehours & others, 2007). These bacteria use oxygen, carbon dioxide, and water to form ferric iron hydroxides, possibly by reactions such as:

$$6Fe^{2+} + 0.5O_2 + CO_2 + 16H_2O \rightarrow CH_2O + 6Fe(OH)_3 + 12H^+$$

This microbial Fe(II) oxidation reaction by microaerophilic bacteria could have dominated the redox Fe cycle in the low-oxygen conditions of the Precambrian oceans because its rate can be 60 times

faster than abiotic oxidation reactions (e.g., Søgaard, Medenwaldt, & Abraham-Peskir, 2000). The limitation, however, is that sulfur isotope studies have demonstrated that the oxygen levels of the atmosphere ($<10^{-5}$ present levels) and the surface ocean water layer (<0.003 μmol/liter at 25° C) in the Archean were too low to sustain abiotic oxidation (Farquhar, Bao, & Thiemens, 2000; Pavlov & Kasting, 2002). These low O_2 levels could also have restricted the availability of O_2 for biologic oxidation (Farquhar, Bao, Thiemens, 2000; Pavlov & Kasting, 2002).

Another metabolic Fe(II) oxidation mechanism that has been proposed to explain the origin of Fe(III) deposition in BIFs is anoxygenic photosynthetic oxidation, or photoferrotrophy, in which Fe(II) is used instead of H_2O as an electron donor to produce Fe(III) and biomass (Garrels & Perry, 1974; Ehrenreich & Widdel, 1994; Kappler & others, 2005) via:

$$4Fe^{2+} + 11H_2O + CO_2 \rightarrow CH_2O + 4Fe(OH)_3 + 8H^+$$

The presence of enormous amounts of Fe(II) in Archean seawater suggests that these bacteria could have existed and oxidized ferrous iron to ferric iron within the photic zone of the oceans through photosynthesis involving CO_2 fixation fueled by light energy (Konhauser & others, 2002). Until recently, all Fe(II)-oxidizing anoxygenic phototrophs had been cultured in the laboratory from iron-rich springs, ditches, and other shallow, ephemeral environments (Widdel & others, 1993; Ehrenreich & Widdel, 1994; Heising & Schink, 1998; Heising & others, 1999; Straub, Rainey, & Widdel, 1999). In particular, laboratory cultures of green *Chlorobium ferrooxidans* (Heising & others, 1999) (a green sulfur bacterium) and purple bacteria (α and γ *Proteobacteria*) have shown that they can phototrophically oxidize dissolved Fe(II) for carbon dioxide fixation by using Fe(II) as a reductant (Widdel & others, 1993; Heising & others, 1999; Straub, Rainey, & Widdel, 1999). Later, phototrophic Fe(II)-oxidizing bacteria were found in the photic zone of the water column in two Fe(II)-rich lakes (Lake Matano, Indonesia, and Lake La Cruz, Spain) (Crowe & others, 2008a, 2008b; Walter & others, 2009). Finally, although physical and chemical evidence for the existence of phototrophic Fe(II)-oxidizing bacteria in the Archean is yet to be found, phylogenetic studies of the enzymes that are involved in the biosynthesis of bacteriochlorophyll showed that anoxygenic photosynthetic lineages are more deeply rooted than oxygenic cyanobacterial lineages (Xiong, 2006; Posth, Konhauser, & Kappler, 2011). The main takeaway from these studies is that the anoxygenic photoferrotrophy mechanism of Fe(II) oxidation could have been dominant in the Precambrian oceans when molecular oxygen was absent and could have aided in the formation of BIFs.

Bacterial dissimilatory iron reduction (DIR). Based on evidence from natural observations, a role for DIR in the formation of banded iron formations, such as the Brockman and Kuruman BIFs, has been proposed by several researchers (Walker, 1984; Nealson & Myers, 1990; Lovley, 1991; Coleman & others, 1993; Beard & others, 1999; Johnson & others, 2003; Johnson & others 2008; Johnson, Beard, & Roden, 2008; Konhauser & others, 2002; Konhauser, Newman, & Kappler, 2005). It is known that magnetite and siderite, two abundant Fe minerals present in Archean and Proterozoic BIFs, are common products of DIR (Lovley & others 1987). Under complete reduction of iron oxides, the reaction to form siderite proceeds via:

$$4Fe(OH)_3 + CH_2O + 3HCO_3^- \rightarrow 4FeCO_3 + 3OH^- + 7H_2O$$

This reaction requires two sources of carbon, organic carbon and seawater carbon, to form siderite. If bicarbonate is not present in excess, Fe reduction is incomplete and Fe^{2+}_{aq} is also formed as a product via:

$$4Fe(OH)_3 + CH_2O + 2HCO_3^- \rightarrow 3FeCO_3 + Fe^{2+}_{aq} + 4OH^- + 6H_2O$$

Similar reactions can be written for different organic carbon vs. inorganic carbon ratios. Mass balance considerations using the values of $\delta^{13}C$ for organic matter and carbonate carbon in the ~2.5 Ga Kuruman BIF, estimated Archean–early Paleoproterozoic seawater $\delta^{13}C$ and $\delta^{56}Fe$ values, and the stoichiometric coefficients of these equations show that the predicted C (~-8‰) and Fe (+1‰ to -1‰) isotope compositions for siderite actually match those measured in siderite BIFs (Heimann & others, 2010) (see *Clues from Iron Isotope Investigations,* p. 114–116, for elaboration). By this mechanism, DIR produces aqueous Fe(II), which was likely present in relatively high concentrations in the Fe(III)-reducing precursor sediments to BIFs (e.g., Johnson & others 2008; Johnson, Beard, & Roden, 2008). High concentrations of Fe(III) present in the sedimentary pile along with organic matter would have suppressed DSR and allowed DIR to dominate and generate the Fe(II) present in BIFs (Walker, 1984).

Magnetite present in BIFs could have also formed by the reaction of Fe^{2+}_{aq} generated by DIR with original ferric oxyhydroxides in an anaerobic setting (Lovley & others, 1987; Lovley, 1991; Brown, Gross, & Sawicki, 1995; Johnson & others, 2003, Johnson & others 2008; Johnson, Beard, & Roden, 2008) via:

$$8Fe^{2+} + 16Fe(OH)_3 + 16OH^- \rightarrow 8Fe_3O_4 + 32H_2O$$

In addition, magnetite could have originated during diagenesis (or metamorphism) through oxidation of Fe(II) in siderite by O_2 via:

$$3FeCO_3 + \tfrac{1}{2}O_2 \rightarrow Fe_3O_4 + 3CO_2$$

or by reaction of siderite with hematite via:

$$Fe_2O_3 + FeCO_3 \rightarrow Fe_3O_4 + CO_2$$

The very low organic carbon content of most BIFs, in particular oxide facies, has been used in support of an inorganic origin for BIFs (e.g., Klein, 2005), or to explain the metamorphic origin of magnetite or siderite by a reaction between organic carbon and iron oxides (e.g., Perry, Tan, & Morey, 1973; Trendall, 2002) such as:

$$6Fe_2O_3 + C \rightarrow 4Fe_3O_4 + CO_2$$

Other mechanisms proposed to explain the loss of organic carbon from the sediment pile include transformation by hydrolysis and fermentation and utilization of some of the organic matter by methanogens (Hayes, 1983; Konhauser, Newman, & Kappler, 2005).

Bacterial DIR provides an alternative and consistent explanation for the formation of the large amount of Fe(II) present in BIFs, the formation of mixed-valence minerals, such as magnetite, as well as the negative $\delta^{13}C$ values measured in BIF carbonates (Johnson & others, 2003, 2008; Heimann & others, 2010; Cradock & Dauphas, 2011; Li & others, 2013). This mechanism also explains the low amount of organic carbon present in BIFs if organic carbon was the limiting factor in the reactions (Walker, 1984; Heimann & others, 2010). Moreover, the finding of a variety of deeply branching, presumably very ancient, hyperthermophilic bacteria and archaea that can reduce Fe(III) to Fe(II) reinforces the idea that DIR is a deeply rooted metabolism (Vargas & others, 1998; Lovley, 2004) that was likely active and played a role during the formation of Archean and Paleoproterozoic BIFs.

Clues from Biological Experiments and Cell Calculations

Two studies investigated the size of the bacterial communities and oxidation rates necessary to oxidize Fe(II) to Fe(III) in ancient marine settings and form the vast amounts of Fe oxides in Precambrian BIFs (Konhauser & others, 2002; Kappler & others, 2005). These studies showed that these settings would have had enough nutrients and light to sustain a community large enough to generate the necessary iron. It was also shown, by ecophysiological experiments and quantitatively by modeling, that direct chemolithotrophic or photoferrotrophic Fe(II) oxidation by phototrophic bacteria would have been capable of generating most, if not all, of the original ferric iron hosted in BIFs (Konhauser & others, 2002).

Konhauser and others (2002) calculated the number of metabolizing cells required to form an annual BIF deposit (layer) based on: 1) the Fe content of iron-rich mesobands in the 2.5 Ga Dales Gorge Member of the Brockman Iron Formation; 2) the density of the layers; 3) estimated maximum annual Fe depositional rates for the Hamersley Basin of ~1 m/700 yr (Morris, 1993), or 1 mm of hematite per year; 4) the area of the basin; and 5) cell production from iron oxidation by *Gallionella* and *Chromatium* Perty, 1852. Konhauser and others (2002) showed that bacterial oxidation could account for most, if not all, of the ferric iron present in BIFs. Kappler and others (2005) also demonstrated experimentally using radiation at wavelengths that penetrate to 100 meters depth in the water column at only 1% surface radiance, that photoferrotrophs could have oxidized Fe(II) down to a few hundred meters of water depth and generate enough Fe(III) to account for all the ferric iron in BIFs. This means that photoferrotrophs could have potentially oxidized all the Fe(II) during upwelling before they reached shallow levels and possibly shallow oxygenated waters (Kappler & others, 2005). These studies also calculated the amount of reduced Fe necessary to produce during diagenesis all the magnetite present in BIFs. Finally, they proposed that a complex bacterial community likely existed on the Archean seafloor, including Fe(III) reducers and possibly methanotrophs that could link Fe(III) reduction to methane oxidation (Konhauser, Newman, & Kappler, 2005).

Clues from Carbon Isotope Studies

Numerous studies have investigated the carbon isotope composition of BIFs (expressed as $\delta^{13}C$, in per mil, ‰, relative to Pee Dee Belemnite (PDB)—a standard for carbon) as a way of understanding their genesis. In particular, abundant data exist for the carbonates and organic matter from the low metamorphic grade ~2.5 Ga Kuruman BIF (Klein & Beukes, 1989; Beukes & Klein, 1990; Kaufman, Hayes, & Klein, 1990; Johnson & others, 2003; Heimann & others, 2010), the ~2.5 Ga Brockman BIF (Becker & Clayton, 1972; Baur & others, 1985; Craddock & Dauphas, 2011), and the ~1.88 Ga Gunflint and Biwabik BIFs (Fig. 48.1) (Perty, 1852; Perry, Tan, & Morey, 1973; Winter & Knauth, 1992). Iron formation carbonates have very negative carbon isotope compositions as low as -12‰, and organic carbon isotope values are extremely negative with values as low as -40‰ (Becker & Clayton, 1972; Walker, 1984; Baur & others, 1985; Kaufman, Hayes, & Klein, 1990; Johnson & others, 2003; 2008; Beukes & Gutzmer, 2008; Fischer & others, 2009; Heimann & others, 2010; Craddock & Dauphas, 2011). In contrast, most Ca-Mg-rich carbonates have near-zero $\delta^{13}C$ values (Beukes & others, 1990; Shields & Veizer, 2002; Fischer & others, 2009; Heimann & others, 2010; Craddock & Dauphas, 2011).

The negative carbonate C isotope values in BIF carbonates have been interpreted in various ways as a result of: 1) direct precipitation of siderite from an iron-rich water column that was stratified with respect to the carbon isotope composition of inorganic carbon (e.g., Beukes & Klein, 1990); 2) a fermentative mechanism and anaerobic respiration in the water column (Perry, Tan, & Morey, 1973; Walker, 1984; Fischer & others, 2009; Johnson & others, 2003; Heimann & others, 2010); 3) a hydrothermal flux dominated by mantle-derived carbon (e.g., Beukes & Klein, 1990); and 4) methane oxidation linked to ferric iron reduction (Konhauser, Newman, & Kappler, 2005). Inorganic mechanisms, such as Fischer-Tropsch processes, can also produce large carbon isotope fractionations (between -50 and -100‰), which make it difficult to be certain that the negative $\delta^{13}C$ values measured in BIF carbonates reflect biologic processes. Most researchers, however, interpret the negative $\delta^{13}C$ values of carbonates as reflecting diagenetic siderite precipitation by microbial oxidation of organic matter derived from photosynthesis coupled to reduction of ferric

oxides via DIR (Walker, 1984; Johnson & others, 2003; Heimann & others, 2010; Craddock & Dauphas, 2011).

Clues from Iron Isotope Investigations

Investigations of the iron isotope composition (expressed as δ^{56}Fe in units of per mil, ‰, relative to igneous rocks) of ancient marine sedimentary rocks have been undertaken in the last 20 years to understand the formation of BIFs and the biogeochemical cycling of iron in the early oceans (Beard & others, 1999, 2003; Johnson & others, 2003; Johnson & others, 2008; Johnson, Beard, & Roden, 2008; Dauphas & others, 2004, 2007; Rouxel, Bekker, & Edwards, 2005; Whitehouse & Fedo, 2007; Planavsky & others, 2009, 2012; Heimann & others, 2010; Tsikos & others, 2010; Steinhoefel, Horn, & von Blanckenburg, 2009; Craddock & Dauphas, 2011; Fabre & others, 2011; Halverson & others, 2011; Czaja & others, 2013; Li & others, 2013). This is possible because iron isotopes fractionate during redox changes when iron species are separated, and iron cycling was extensive in the Archean–Proterozoic Earth. In modern marine environments, DSR is the dominant pathway for the oxidation of sediment organic carbon (Thamdrup, 2000). The sulfide produced by this process reacts with sediment or hydrothermal iron with near-zero δ^{56}Fe values to form iron sulfides that have near zero or slightly positive δ^{56}Fe values (e.g., Severmann & others, 2006). In contrast, in the Archean and early Proterozoic oceans, high rates of reactive iron flux and low sulfate and sulfide concentrations, as evidenced by the compositions of BIFs (Klein, 2005), would have favored bacterial DIR over bacterial DSR (e.g., Johnson & others, 2008; Johnson, Beard, & Roden, 2008). This, in turn, would have favored extensive bacterial redox iron cycling and phase separation that resulted in iron isotope fractionation.

Iron isotope studies of millimeter scale samples reveal processes that took place in the sediment pile during the formation of BIFs prior to lithification (Johnson & others, 2003; Heimann & others, 2010). Bulk-rock analyses (e.g., Planavsky & others, 2009, 2012), however, give an average of different processes that possibly operated in various places and at different scales, and provide an estimate of the bulk or average iron isotope composition of BIFs. The record through time of iron isotope compositions of marine sedimentary rocks, including pyrite in shales, bulk BIFs, and BIF minerals, shows a large, slightly positive to highly negative (~ -3‰) excursion at ~2.7–2.5 Ga (Rouxel, Bekker, & Edwards, 2005; Johnson & others, 2008; Johnson, Beard, & Roden, 2008; Planavsky & others, 2012; Li & others, 2013). In contrast, δ^{56}Fe values are mostly near zero to positive in the Eoarchean 3.8 Ga BIFs from Isua in Greenland, the Nuvvuagittuq greenstone belt in northern Quebec, Canada (Dauphas & others, 2004, 2007; Whitehouse & Fedo, 2007; Johnson & others, 2008; Johnson, Beard, & Roden, 2008; Czaja & others, 2013), and the ~1.88 Ga late Paleoproterozoic Gunflint and Biwabik BIFs from the Animikie basin of North America (Planavsky & others, 2009). The majority of younger rocks have near-zero δ^{56}Fe values. These variations in iron isotope compositions have been interpreted as reflecting inorganic processes and direct precipitation of iron-rich minerals from seawater or the dominance of bacterial DIR in the Precambrian oceans and their role during BIF formation. Specifically, the iron isotope variations in Precambrian marine sedimentary rocks have been interpreted by some authors to reflect inorganic oxidation of Fe(II) and precipitation of iron oxides and to record changes in the δ^{56}Fe values of ancient seawater (Rouxel, Bekker, & Edwards, 2005) and not the interplay of biologic and geologic processes in the sedimentary pile prior to lithification (e.g., Yamaguchi & others, 2005). The negative δ^{56}Fe values of minerals (siderite, magnetite, and pyrite) could result from partial abiotic oxidation of near-zero δ^{56}Fe iron in the water column (Rouxel, Bekker,

& Edwards, 2005) or partial Fe(II) utilization during abiotic pyrite precipitation (Guilbaud, Butler, & Ellam, 2011), which would leave behind low-δ^{56}Fe Fe^{2+} to form these minerals. A counter argument to the abiotic partial oxidation hypothesis is that the wide range in δ^{56}Fe values of marine precipitates at small scales cannot directly record the iron isotope composition of seawater due to the large size of the iron pool and its expected long residence time in Archean and early Paleoproterozoic seawater (Johnson & others, 2008). Finally, although abiotic pyrite formation may explain some iron isotope variations, the idea has been questioned for most low-δ^{56}Fe samples on the grounds of detailed studies of the depositional setting, mineralogy, and geologic history of Precambrian sedimentary rocks (Czaja & others, 2012).

The positive δ^{56}Fe values of Eoarchean BIFs from Greenland have been interpreted to reflect incomplete oxidation of near-zero δ^{56}Fe hydrothermal Fe(II), possibly via anaerobic photosynthetic oxidation by bacteria (Dauphas & others, 2004; Johnson, Beard, & Roden, 2008; Czaja & others, 2013), although the Fe isotope fractionations alone could not be taken as a biosignature (Bullen & others, 2001; Dauphas & others, 2004). Similarly, the positive δ^{56}Fe values in the late Paleoproterozoic Gunflint and Biwabik BIFs seem to reflect the cycling of Fe by iron-oxidizing microbial ecosystems in redox-stratified oceans (Planavsky & others, 2009). The excursion in Fe isotope compositions toward negative values at ~2.7–2.5 Ga, as measured in the giant ~2.5 Ga Kuruman and Brockman BIFs, has been interpreted to represent the expansion of DIR bacteria in the Precambrian oceans starting as early as 2.9 Ga (Johnson & others, 2003; Johnson & others, 2008; Johnson, Beard, & Roden, 2008), which points to the antiquity of this anaerobic respiratory pathway. The decrease in iron isotope variations in BIFs after the GOE at ~2.4 Ga (Rouxel, Bekker, & Edwards, 2005) has been interpreted as indicating a change from the peak of DIR activity at 2.7–2.5 Ga to an increase in seawater sulfate and the expansion of DSR bacteria in the oceans with the consequent removal of Fe(II) by pyrite after that (Johnson & others, 2008; Johnson, Beard, & Roden, 2008). This interpretation is also consistent with the change in sulfur isotope composition of sulfides in marine sedimentary rocks toward negative values and disappearance of strong sulfur mass-independent fractionation effects at ~2.4 Ga, which are evident at > ~2.5 Ga (e.g., Canfield, 2001; Ono & others, 2003; Farquhar & Wing, 2003; 2005; Johnson, Beard, & Roden, 2008). Furthermore, this change in isotope compositions also coincides with a shift from extremely negative carbon isotope compositions of kerogens (δ^{13}C down to -60‰) toward less negative values, which all together suggest some major changes in geobiological processes and isotope pathways at this time (Johnson, Beard, & Roden, 2008).

Experimental work on iron isotope fractionation during iron oxidation and reduction with and without bacteria and observations of natural environments provide the needed basis for the interpretation of the large iron isotope excursion toward negative δ^{56}Fe values at 2-7–2.5 Ga. Based on laboratory experiments and evidence from natural environments, the majority of highly negative δ^{56}Fe Fe^{2+}_{aq} is derived from biogenic reduction of Fe(III) by DIR (Beard & others, 1999, 2003; Crosby & others, 2005, 2007; Croal & others, 2004; Johnson & others, 2005; Tangalos & others, 2010; Wu & others, 2012). Experiments show that the iron isotope fractionation factor between Fe^{2+}_{aq} in a simulated Archean seawater analog and Fe(III) in iron-silica co-precipitates (analogous to the ones assumed to have formed BIFs) is up to -4‰ (Wu & others, 2012). These experiments indicate that the highly negative δ^{56}Fe values (~ -2.0 ‰) measured in BIF minerals (magnetite, siderite) and pyrite in black shales could have resulted from a multi-stage process involving the generation of low-δ^{56}Fe Fe^{2+}_{aq} by bacterial DIR

[Reaction: $4Fe(OH)_3 + CH_2O + 2HCO_3^- \rightarrow 3FeCO_3 + Fe^{2+}_{aq} + 4OH^- + 6H_2O$ (see p. 111)] and its mobilization (e.g., Johnson & others, 2003; Johnson & others, 2008; Johnson, Beard, & Roden, 2008; Heimann & others, 2010). In a second stage, the $Fe(II)_{aq}$ produced by DIR would have reacted with bicarbonate to form siderite, or could have been mobilized in the sediment pile and reacted with near-zero $\delta^{56}Fe$ ferric oxides to form magnetite [Reaction: $8Fe^{2+} + 16Fe(OH)_3 + 16OH^- \rightarrow 8Fe_3O_4 + 32H_2O$ (see p. 112)] or reacted with sulfur to form pyrite. These minerals would have retained the negative $\delta^{56}Fe$ value of the $Fe(II)_{aq}$ generated by DIR (Johnson & others, 2003; Johnson & others, 2008; Johnson, Beard, & Roden, 2008; Heimann & others, 2010). In this view, the original Fe(III) oxyhydroxides had near-zero $\delta^{56}Fe$ values that resulted from complete or near-complete oxidation, either biologic or abiologic, of hydrothermal Fe(II) with $\delta^{56}Fe$ values similar to modern-day hydrothermal Fe(II) at ~ 0‰ (Beard & others, 2003; Johnson, Beard, & Roden, 2008).

Near-complete reduction of ~0‰ $\delta^{56}Fe$ Fe(III) oxides by DIR would result in Fe(II) with negative $\delta^{56}Fe$ values, as noted above, and would leave behind ferric oxides enriched in the heavy iron isotopes. A study of coupled iron, carbon, and oxygen isotope compositions of millimeter scale samples of carbonates from the ~2.5 Ga Kuruman BIF found that in laminations where the carbonates (siderite) did not have negative but positive $\delta^{56}Fe$ values, they had micrometric inclusions of hematite, which were interpreted as remains of the original iron oxides (Heimann & others, 2010). All carbonates had negative $\delta^{13}C$ values (> -8‰) indicative of incorporation of oxidized organic matter. The iron and carbon isotope values of these carbonates do not reflect precipitation in equilibrium with ancient seawater but are exactly what is expected from near-complete reduction of Fe(III) in original ferric hydroxides by bacterial DIR coupled to organic matter oxidation (Heimann & others, 2010) (see *Bacterial Dissimilatory Iron Reduction*, p. 111). Furthermore, Sr isotope studies of the same siderite BIF samples also indicate that the carbonates did not precipitate in equilibrium with seawater (Johnson & others, 2013). Therefore, these data point to the likely participation of bacterial DIR in the formation of at least these BIF carbonates.

Clues from Microfossils

Microfossils have been found in chert layers of Precambrian banded iron formations (e.g., Tyler & Barghoorn, 1954), as well as in other older cherts not associated with BIFs (e.g., Schopf, 2006b). This section deals only with the former. The first assemblage of structurally preserved microorganisms was discovered in dense black cherts of the 1.88 Ga Gunflint Iron Formation of southern Ontario, Canada (Fig. 48.1–48.2)(Tyler & Barghoorn, 1954; Barghoorn & Tyler, 1965; Cloud, 1965; Awramik & Barghoorn, 1977). The Gunflint BIF also contains siliceous and calcitic stromatolites of various morphologies (Fig. 48.2) (Hoffman, 1969; Fralick, 1989; Sommers, Awramik, & Woo, 2000; Planavsky & others, 2009). The microorganisms were described in detail in the black cherts that owe their color to the presence of fine-grained pyrite and organic matter (Barghoorn & Tyler, 1965). Spherical structures, filaments, spore-like bodies, and other organic structures are preserved (Barghoorn & Tyler, 1965).

The most abundant microfossils in the Gunflint chert are filaments ranging from 0.5 to 6.0 μm in diameter. The best-preserved filaments appear to be both septate and nonseptate. The grossly septate filaments were placed in a new genus, *Gunflintia* Barghoorn & Tyler, 1965 and divided by the authors into two species (*G. grandis* and *G. minuta*). These are the most abundant microfossils, are characterized by randomly oriented filaments, and occur preferentially in stromatolites (Planavsky & others, 2009).

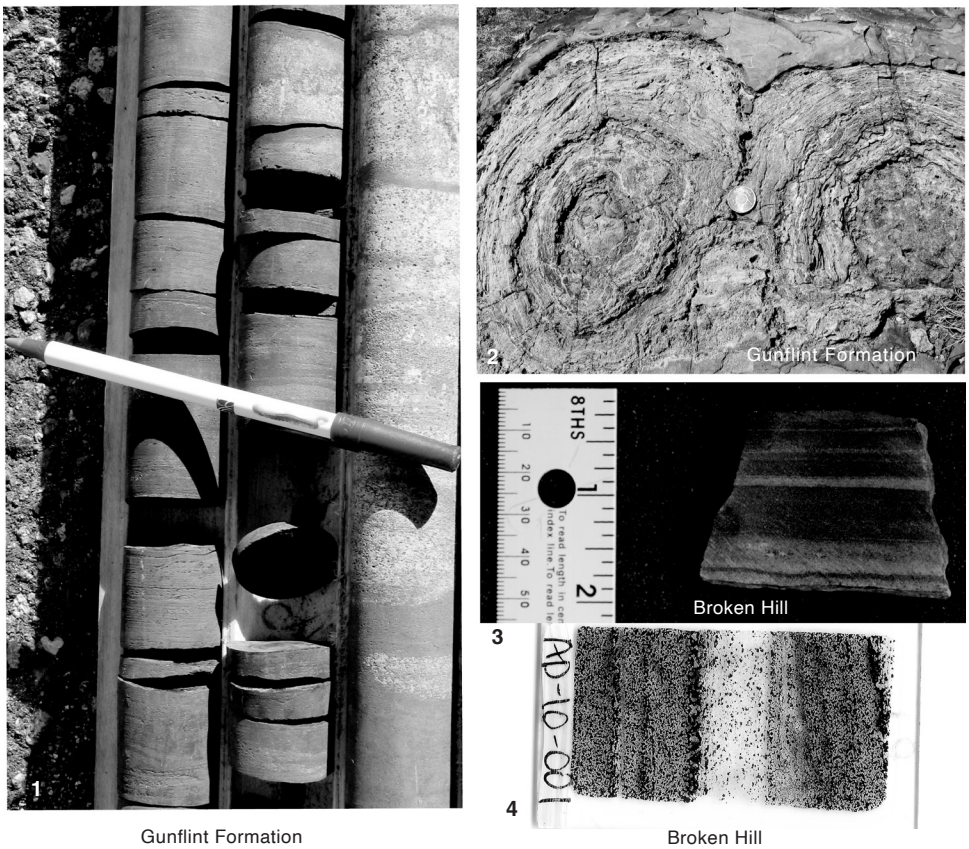

FIG. 48. *1,* Drill core of the Gunflint Formation, Ontario, Canada, showing red, magnetite-rich laminated chemical sediments of the late Paleoproterozoic (1,878 Ma) Gunflint Iron Formation (red/brown) overlaying light color, coarse grained sandstone with magnetite-rich laminations (reddish), drill core 89-mc-1 at ~160 m, Ministry of Northern Development and Mines Core Library (new; photo, Adriana Heimann). *2,* Stromatolites of the Gunflint Formation, coin for scale (new; photo, Adriana Heimann). *3,* Core slab sample of metamorphosed banded iron formation spatially associated with massive sulfide mineralization near the giant late Paleoproterozoic (1.69 Ga) Broken Hill Pb-Zn-Ag deposit, Curnamona Province, Australia, metamorphosed to granulite facies; brown is garnet in quartz, black is magnetite and minor quartz and/or garnet, sample AD-10-010, sample provided by Paul G. Spry (new; photo, Erica Serna). *4,* Scanned polished thin section of BIF near the Broken Hill deposit showing the delicate nature of the magnetite-rich laminations; black is magnetite, clear is quartz, brownish is garnet, sample AD-10-001 (new; image, Erica Serna). Color version available in *Treatise Online* 147 (paleo.ku.edu/treatiseonline).

Some of the finely septate types of filaments exhibit a basic morphology comparable to that present in extant filamentous blue-green algae (cyanobacteria), such as *Oscillatoria* GOMONT, 1892b and *Lyngbya* GOMONT, 1892 and were grouped into a new taxon, *Animikiea septata* by BARGHOORN and TYLER, 1965. Some of the non-septate filaments include very uncommon forms that contain spores and endogonidia and were grouped by the authors into a new taxon, *Entosphaeroides amplus*. These structures have a morphology comparable to a few extant genera of cyanobacteria and the iron bacteria *Crenothrix* COHN, 1870. The spheroidal spore-like organisms that are ubiquitous in the chert exhibit a variety of sizes (1–16 μm), structures, and shapes and were grouped into a new genus, *Huroniospora* BARGHOORN & TYLER, 1965, and subdivided by the authors into three species based on the wall-sculpturing pattern.

Other organisms were also found and assigned to a genus, but these were more rare

and of unclear relationship to any known living group. In particular, some types of organisms are characterized by segmented or septated filaments radiating from a central structure of poorly defined morphology, and are grouped into the new genus *Eoastrion,* defined by Barghoorn and Tyler, 1965. Rare spiral threads (<1 μm in diameter, <35 μm length), either single corkscrew-like filaments or interwoven pairs, have a gross morphology that resembles spiral threads secreted by the living iron bacterium *Gallionella* (see Cloud, 1965). Although some of the biota appear to be planktonic (coccoidal forms), other forms, such as dense intertwined filaments of *Gunflintia,* appear to be benthic (Planavsky & others, 2009).

Earlier studies considered that the microfossils reflected the dominance of oxygenic photosynthesis in the early Precambrian (Barghoorn & Tyler, 1965; Cloud, 1965; Awramik & Barghoorn, 1977). However, a later study concluded that many of the Gunflint-type microfossils that were interpreted as oxygenic photosynthesizers were more likely to be metabolic iron oxidizers (Golubic & Seong-Joo, 1999). A more recent study that combined iron isotope compositions and REEs in microfossil-rich stromatolites from the Gunflint BIF also suggested that the late Paleoproterozoic environment likely hosted an iron-oxidizing microbial ecosystem and not cyanobacteria (Planavsky & others, 2009). It is more likely that the ecosystem present during the formation of the Gunflint BIF was actually quite complex.

Clues from Molecular Biomarkers

Biomarkers are fossil remains of chemically stable organic molecules derived from the carbon skeletons of precursor lipids preserved in the rock record (Waldbauer & others, 2009). They have been found in sedimentary rocks associated with BIFs and in BIFs themselves, and have been used to infer the presence and role of bacteria during their formation (Brocks & others, 1999, 2003a, 2003b; Summons & others, 1999; Waldbauer & others, 2009). For example, fossil hopanes and steranes (biomarkers typically present in eukaryotes) were found in the 2.6 Ga sedimentary rocks of the Transvaal Supergroup, South Africa (Waldbauer & others, 2009). The biosynthesis of steranes requires free oxygen, implying that oxygen was readily available at 2.6 Ga, or about 0.1 Ga before the formation of the Kuruman BIF, one of the largest BIF deposits that occurs in the same Transvaal Supergroup, and 0.2 Ga before the full oxygenation of the atmosphere took place (Noffke, 2009). In another study, 2a-methylhopanes, organic molecules present in membranes of modern cyanobacteria, were extracted from bitumen in the ~2.6 Ga very low metamorphic grade shales of the Marra Mamba Iron Formation and underlying 2.7 Ga rocks of the Hamersley Group, Western Australia (Brocks & others, 1999; Summons & others, 1999). This finding was interpreted as indicative of the existence of cyanobacteria, or oxygen-producing bacteria, 300–200 million years before the rise of atmospheric oxygen. This may also indicate that the BIFs of the Hamersley Group formed as the result of bacterial production of oxygen (Brocks & others, 1999). However, the hopane molecules found in the Marra Mamba shales were also identified in anoxygenic phototrophic Fe(II)-oxidizing bacteria (Rashby & others, 2007) and, therefore, are not an unequivocal fingerprint for the presence of cyanobacteria at the time the rocks formed. Furthermore, it was later found that the carbon isotope composition of pyrobitumen and kerogen extracted from the same rocks is 10–20‰ lighter than the extracted hydrocarbons, providing a strong argument against the indigenous origin of the biomarkers (Rasmussen & others, 2008). Thus, there is much work to be done on molecular biomarkers to determine unequivocally the first appearance of oxygenic photosynthesis and the role of this bacterial metabolism in the formation of BIFs.

The Possible Role of Iron-enriched Biofilms

Iron-enriched biofilms or mats can be considered as possible precursors to the

formation of finely laminated banded iron formation deposits. For example, recent studies of ~2.75 Ga BIFs in the Carajás mining district, Carajás Formation, Grão Pará Group, Brazil, presented evidence (morphology, carbon content, and very negative C isotope compositions) for the biogenicity of stromatolitic structures present in these Neoarchean BIFs that strongly suggests that the BIFs could have originated as biomats (Ribeiro da Luz & Crowley, 2012). The hypothesis is that Fe(III) precipitation would have taken place through Fe oxidation by contact of Fe(II) with bacterial slime and chemical reactions with organic compounds (Ribeiro da Luz & Crowley, 2012). The Fe(III) is considered to have been available later for dissimilatory Fe(III) reduction.

Bacterial processes related to iron oxide deposition in some modern bacterial mats give us clues about similar processes in the Archean–Proterozoic oceans where BIFs formed. In nutrient-limited environments, bacteria form biofilms that preferentially grow as slime-encased microbes on the surface of rocks instead of as free-swimming (planktonic) organisms (ZoBell, 1943). For example, in modern environments, photosynthetic bacteria and filamentous bacteria form laminated mats next to hydrothermal vents and hot springs, where they can be several millimeters thick (Walter, Bauld, & Brock, 1972; Walter & others, 1992; Doemel & Brock, 1977; Brown, Gross, & Sawicki, 1995; Little, Glynn, & Mills, 2004). Bacteria act as substrate or polyionic trap for the precipitation of minerals, promote mineral crystallization by metabolically generating products (e.g., OH^-, CO_2, H^+) that combine with dissolved metallic ions, or mediate enzymatic oxidation of others (e.g., Fe^{2+} to Fe^{3+}) (Konhauser, 1997, 1998; Thompson & Ferris, 1990; Ghiorse & Ehrlich, 1992; Brown, Gross, & Sawicki, 1995).

Modern microbial mats are commonly associated with the formation of iron hydroxides where bacterial biomineralization takes place (Pierson, Parenteau, & Griffin, 1999; Konhauser, 2000; Little, Glynn, & Mills, 2004; Parenteau & Cady, 2010). Studies of hot springs, active black smokers, and deep hydrothermal areas indicate: 1) that the iron-rich mats are mainly comprised of living cells and remains of bacteria (for example, *Gallionella ferruginea* Ehrenberg, 1836) (Boström & Widenfalk, 1984; Holm, 1987); 2) that microbial mats are the favored sites of deposition of iron hydroxides; and 3) that iron oxides form biogenically in areas of low O_2 and slightly acidic pH (Baross & Deming, 1985; Tunnicliffe & Fontaine, 1987; Karl, Brittain, & Tibrook, 1989; Pierson, Parenteau, & Griffin, 1999; Little, Glynn, & Mills, 2004; Parenteau & Cady, 2010).

Earth's possibly oldest fossil cyanobacterial mats found in sandy deposits of a tidal environment in the 2.9 Ga Nhlazatse Section, Pongola Supergroup, South Africa, suggest the existence and diversification of cyanobacteria as early as the Mesoarchean (Noffke, 2010). Therefore, modern microbial mats and biofilms, including relatively young (Pleistocene) fossilized mat-forming prokaryote examples, are possibly one of the keys to understanding ancient benthic microbial communities and their habitats (Brown, Gross, & Sawicki, 1995; Noffke, 2010). Particular examples are described below. The question still remains, however, as to exactly what kind of microbial communities formed these mats, because the mechanism of formation of the mats is not unique to oxygenic photosynthetic bacteria (Tice, 2008).

POSSIBLE PHANEROZOIC AND MODERN ENVIRONMENT ANALOGS

There is no perfect analog for Archean–Proterozoic banded iron formations (BIFs) in chemical composition, environment of formation (physicochemical conditions), and genesis. Paleozoic siliceous iron oxyhydroxide deposits, Phanerozoic hematite-quartz ironstones, and iron-oxide chemical precipitates that form in the modern oceans and deep

lakes from hydrothermal fluids and brines are the closest analogs and are described below. In addition, continental sites where iron oxyhydroxides currently form under somewhat similar environmental conditions (low sulfate, low oxygen) as those in Archean–Proterozoic oceans and where biogenic Fe(III) reduction takes place are also included because even though they are terrestrial environments, they have been considered modern environmental analogs to those in Archean–Proterozoic times where BIFs formed.

MODERN SILICEOUS IRON OXYHYDROXIDE MARINE DEPOSITS

Iron Deposits of Marine Hydrothermal Vents

In modern marine environments, siliceous iron oxyhydroxide deposits commonly form spatially and genetically related to hydrothermal activity; examples occur at the Juan de Fuca Ridge (northeast Pacific Ocean), the Lilliput hydrothermal field on the Mid Atlantic Ridge, Trans-Atlantic Geotraverse (TAG), Loihi seamount hydrothermal vents (Hawaii), Coriolis Troughs (southwest Pacific), Red Sea Mount, and the Jan-Mayen vent fields in the Arctic-Ocean Ridge System (Rona & others, 1986; Alt, 1988; Emerson & Moyer, 2002; Little, Glynn, & Mills, 2004; Toner & others, 2009; Dekov & others, 2010; Moeller & others, 2013). In some of these settings, for example at the Jan-Mayen vent field, iron oxyhydroxides precipitate at depths greater than 1,000 m from diffuse, low-temperature hydrothermal fluids that emanate at the seafloor through fissures and faults distal to high-temperature hydrothermal vents (e.g., Moeller & others, 2013). The siliceous iron oxyhydroxide layers in all these locations consist of iron-rich amorphous phases or ferrihydrite and minor amounts of crystalline iron oxides, such as goethite, with up to 50 wt% Fe_2O_3 in bulk analysis and are intimately associated with filamentous structures of biogenic origin (e.g., Little, Glynn, & Mills, 2004; Moeller & others, 2013). All of the vents, for example at Loihi, are surrounded by microbial mats with a gelatinous texture and are encrusted with iron oxides (Emerson & Moyer, 2002; Little, Glynn, & Mills, 2004).

It has been shown that iron-oxidizing bacteria—for example species similar to *Mariprofundus ferrooxidans* Emerson & others, 2007—play a key role in mediating the oxidation of Fe(II) derived from the low temperature hydrothermal fluids (Emerson & Moyer, 2002; Toner & others, 2009; Moeller & others, 2013). At TAG, the filaments have been described as identical to the iron oxide encrusted stalks of *Gallionella* spp and *Leptothrix ochracea* Kützing 1843 (e.g., Little, Glynn, & Mills, 2004). What is more, studies at Loihi showed that up to 60% of the iron oxyhydroxides occur as filaments or sheaths interpreted to be direct deposition by bacteria (Emerson & Moyer, 2002).

Because of their similarities, modern deep-sea hydrothermal vent iron deposits are considered analogs of Ordovician to late Eocene jaspers, which points to a record of bacteriogenic iron oxide precipitation at marine hydrothermal vent sites of at least 490 million years (Little, Glynn, & Mills, 2004). Even though there are environmental differences between the origin of ancient BIFs and modern siliceous Fe oxyhydroxides, their Si-Fe enrichment and chemical precipitation from hydrothermal fluids makes them the closest modern analogs to ancient BIFs. If we consider the setting near hydrothermal vents, then these Si-Fe precipitates can be considered closer analogs to Algoma-type BIFs, which formed in tectonically active areas and probably close to hydrothermal vents, than to Superior-type BIFs, which formed in stable platforms away from hydrothermal vent sites. The fact that biologic oxidation mediates the precipitation of these iron oxyhydroxides in modern settings also supports the idea of a link between iron precipitation and organic mediation during the formation of BIFs in the ancient oceans.

Iron Deposits of the Red Sea

The Red Sea rift system is characterized by active tectonics and igneous and hydrothermal activities and by a stratified body of water comprised of denser, saline anoxic bottom water overlain by lighter, less saline, cooler, oxic surface water. The deep water that penetrates the sediments achieves a high salinity by leaching of Miocene evaporates and a high temperature by a geothermal gradient and interaction with hot basaltic rocks (e.g., Cocherie, Calvez, & Oudin-Dunlop, 1994). The hot brine that discharges into the basin creates a stratified system with a lower hot (56–67 °C) layer enriched in Fe and Mn (81 mg/kg for each) and with a pH between ~5.5 and 6.4 depending on the location, and an upper, cooler (44°–56 °C) water layer (Taitel-Goldman, Ezrsky, & Mogilyanski, 2009). The Discovery Deep and the Atlantis II Deep are 5 km apart and separated by a sill at a depth of ~1990 m below sea level (Taitel-Goldman, Ezrsky, & Mogilyanski, 2009, and references therein). The lower layer brine flows into various deeps through a fracture and fissure system. The Fe oxyhydroxide minerals crystallize as authigenic minerals and occur at water depths between 2000 and 2216 m.

The mineralogy of the Atlantis II Deep includes Mn-Fe carbonates and rounded particles of Si-associated Fe oxyhydroxides, including well crystallized hematite (α-Fe_2O_3), goethite (α-FeO(OH)), and clusters of ferrihydrite ($Fe_5^{3+}OH_8.4H_2O$), as well as feroxyhyte (δFeO(OH)), lepidocrocite (γ-$Fe^{3+}O(OH)$), and Mn oxyhydroxides (Taitel-Goldman, Ezrsky, & Mogilyanski, 2009). Pure hematite is thought to result from the recrystallization of a former phase, whereas the other oxides are original Si-associated Fe and Mn oxyhydroxides (Taitel-Goldman, Ezrsky, & Mogilyanski, 2009). A lepidocrocite-goethite association crystallizes out of the hot hydrothermal brine with no Mn impurities, whereas the presence of Mn components reflects precipitation from the upper layer or the transition zone. In addition, silicon also discharges from the brine system and precipitates in association with Fe and Mn authigenic phases (Taitel-Goldman, Ezrsky, & Mogilyanski, 2009).

The clusters of hematite, or hematite microspheroids, and the Si-associated rounded particles of Fe oxyhydroxides that form in the Red Sea are similar to fine-grained hematite microspheroids, some containing pore-filling inclusions of early diagenetic silica, present in banded iron formations (Trendall & Blockley, 1970). This similarity suggests that the formation of the Red Sea Fe oxyhydroxides can be considered a close analog to that of BIFs. Because the Fe oxides also coexist with Mn oxides, these modern deposits can be compared with the BIFs and Mn deposits of the 2.4–2.2 Ga Hotazel Formation of South Africa that formed after the Kuruman Iron Formation and close to the timing of the GOE (e.g., Tsikos & others, 2010).

LAKE MATANO, INDONESIA

Lake Matano is located on Sulawesi Island, Indonesia (Crowe & others, 2008a), and is the eighth deepest (>590 m) lake in the world. The steep margins, great depth, and the geographic location, characterized by the lack of strong seasonal temperature changes, allow the existence of a persistent pycnocline at ~100 m depth that separates an oxic surface layer from anoxic bottom waters. Sulfate concentrations are low (<20 μmol/liter) in the surface mixed layer and the rates of sulfate reduction within the anoxic waters of the chemocline are slow (<0.015 μmol/liter/day) (Crowe & others, 2008a). The slow sulfate reduction rates within the chemocline are fast enough to reduce all the sulfate and remove it from the surface waters, which results in deep waters with sulfate concentrations below detection limits. This also results in very low but detectable sulfide concentrations (including free sulfide, sulfide-bearing colloids, and larger particles of NiS and FeS). The low

sulfur results in the accumulation of high concentrations of dissolved ferrous iron (~150 µmol/l). A low, suspended load of inorganic particulate matter, scavenging of phosphate by allogenic and authigenic iron (hydr)oxides, and low primary productivity in the surface mixed layer allows light to penetrate well into the anoxic bottom waters (Crowe & others, 2008a, 2008b).

The presence and abundance peaks with depth of the dominant photosynthetic pigment bacteriochlorophyll *e* (BChl *e*), a light-harvesting pigment used by brown-colored phototrophic green sulfur bacteria (GSB) of the family Chlorobiaceae, which are specially well adapted to low light conditions, indicate that GSB are an important component of the phototrophic bacterial community in Lake Matano (Crowe & others, 2008a). Molecular fingerprinting by Crowe and others (2008a) indicated the existence of an abundant and mixed bacterial community between 110 and 120 m depth, including several phyllogenetically distinct members of Chlorobiaceae. Lake Matano clones have up to 95% sequence similarity to a known photoferrotroph, *Chlorobium ferrooxidans* Heising & others, 1999 (Crowe & others, 2008a). In contrast to most known Chlorobiaceae (obligate photolithoautotrophs that fix carbon using sulfide as an electron donor), *C. ferrooxidans* is an exception that uses ferrous iron as electron donor (Heising & others, 1999).

Unlike other water bodies, such as anoxic sulfidic lakes and euxinic marine basins like the Black Sea, the extremely low dissolved sulfide concentrations in Lake Matano suggest that the community of GSB is sustained by using the abundant concentration of Fe(II) as electron donor (Crowe & others, 2008a). The concentration of free sulfide is considered too low to sustain sulfide-fueled anoxygenic phototrophy by GSB. What is more, calculations of the irradiance in the lake at ~110 m show that the light flux is sufficient to phototrophically oxidize the entire Fe(II) flux through the chemocline (Crowe & others, 2008a). The rates of Fe(II) oxidation are also consistent with the rates of oxidation of known photoferrotrophs. Therefore, the population of GSB is largely sustained by photoferrotrophy, and this mechanism could explain BIF deposition in Archean and Proterozoic oceans. This hypothesis remains to be fully proven, however, because Fe(II) oxidizing GSB have yet to be isolated and cultured in the laboratory (Crowe & others, 2008a). Studies also concluded that iron oxides currently precipitate from the water column in Lake Matano, including the mixed ferrous-ferric mineral green rust, at the oxycline, and that authigenic magnetite formation takes place in the water column and during diagenesis (Poulton, 2011). This has been used to argue that similar processes of formation under anoxic, ferruginous conditions could have formed BIFs in ancient oceans (Poulton, 2011). Further investigations of the paths of formation of these minerals will also help improve our understanding of the cycling of iron in the Archean–Proterozoic oceans and the formations of BIFs.

Because of its high ferrous iron concentration, low sulfate content, deep light penetration, and presence of a mixed upper layer and bottom anoxic layer, as well as other physical and chemical characteristics, Lake Matano is a good modern analog for the chemistry and biology of Archean and early Proterozoic oceans (Crowe & others, 2008a). This setting at Lake Matano can be compared to that of the Archean–Proterozoic oceans where Superior-type BIFs formed in stable basins from a stratified water column. It is important to note, however, that the size of the system is small and the salinity is much lower compared to Archean–Proterozoic marine environments where BIFs formed.

PHANEROZOIC IRONSTONES

Phanerozoic iron-rich sedimentary rocks, called ironstones, are rocks with relatively high iron contents (>15% Fe) and some of them can be considered younger analogs to banded iron formations. Ironstones are rare,

temporally related to marine anoxic events and mainly restricted to the Ordovician–Devonian and Jurassic–Paleogene and to modern local areas of closed to semi-closed basins (Van Houten, 1985; Van Houten & Arthur, 1989; Bekker & others, 2010; Ciobotă & others, 2011; Salama, Aref, & Gaupp, 2012, 2013). Many are temporally associated with peaks in abundance of volcanogenic massive sulfide deposits (MSDs), sea level rise, major anoxic events, and volcanic episodes (Van Houten & Arthur, 1989; Maynard & Van Houten, 1992; Burkhalter, 1995; Taylor & others, 2002; Peter, 2003; Franklin & others, 2005; Garzani, 1993; Bekker & others, 2010; Ciobotă & others, 2011; Salama, Aref, & Gaupp, 2012, 2013). The temporal association between ironstones and volcanogenic MSDs has been used to suggest a hydrothermal origin for the iron and that the deposition of ironstones was linked to global ocean anoxic periods and superplume events (see Bekker & others, 2010 and references therein).

Ironstones are commonly small (most <2 m thick, some 20 m thick) but large examples (>1,000 km) occur along ancient continental margins in Fennoscandia (covers present-day Finland, Norway, Sweden, and the Kola Peninsula in Russia) and the Himalayas (Garzani, 1993; Sturesson, Dronov, & Saadre, 1999; Sturesson, 2003). Large examples of Phanerozoic oolitic ironstones include the Jurassic Minnette deposits of central and western Europe, and the Silurian Clinton ores of North America. Phanerozoic ironstones are comprised of oolites of Fe oxyhydroxides (goethite and limonite), Fe silicates (chamosite and berthierite), and minor amounts of amorphous silica (less chert than BIFs) and are typically enriched in phosphorous. Some ironstones are non-cherty, sandy, fine-grained siliciclastic or siliciclastic-carbonate rocks (e.g., Petránek & Van Houten, 1997).

Even though the genesis of some ironstones is likely different than that of BIFs, others, for example the Phanerozoic deposits from the Løkken ophiolite and the Eocene ironstones of Egypt, have similarities to older jaspers and modern Fe-Si deposits with origins closely linked to Fe(II) oxidation by bacterial processes (Salama, Aref, & Gaupp, 2012; Moeller & others, 2013). This suggests that they can be considered younger equivalents of BIFs. The Phanerozoic Ordovician hematite-quartz deposits from the Løkken ophiolite complex in Norway, which have been metamorphosed to lower greenschist facies, are related to volcanogenic MSDs and associated hydrothermal feeders (e.g., Grenne & Slack, 2005). The rocks consist of fine-grained hematite microspheroids comprised of cryptocrystalline hematite and quartz in a quartz matrix (e.g., Grenne & Slack, 2005). The jasper deposits have soft-sediment deformation structures that along with the presence of the cryptocrystalline hematite reflect their formation as gel-like amorphous iron oxyhydroxides, such as ferrihydrite (Grenne & Slack, 2003). They are interpreted as siliceous ferrihydrite fallout deposits formed from a hydrothermal plume during times of oxic or suboxic conditions in a preponderantly widespread anoxic period (Grenne & Slack, 2005). Therefore, this kind of Phanerozoic ironstone may be somewhat similar to BIFs in its formation. If we take into account the association with volcanogenic MSDs and the occurrence in the ophiolite, the genesis of these ironstones would resemble that of Algoma-type BIFs rather than that of Superior-type BIFs.

Some recent studies also suggest that at least some Phanerozoic ferruginous and stromatolitic ironstones, such as those in the Eocene ironstones of the Western Desert in Egypt, formed by similar processes as those described for hot springs and other hydrothermal venting areas (e.g., Ciobotă & others, 2011; Salama, Aref, & Gaupp, 2013). The Egypt ironstones are interpreted to be genetically linked to iron-oxidizing bacteria and their biofilms, where oxidation of Fe^{2+} in solution by these bacteria in shallow water with near acidic pH and low fO_2 precipitated a hydrous ferric gel that was also colonized by bacteria (Salama,

Aref, & Gaupp, 2013). Ferruginous ooids and oncoids, now comprised of goethite, which coexist with ferruginous stromatolitic microbialites, seem to have been formed *in situ* and later reworked from shallow marine areas during storms to form the ironstones (Salama, Aref, & Gaupp, 2013). Based on the association with stromatolitic rocks, the genesis of these ironstones can be compared with that of Superior-type BIFs, such as the ~2.75 Ga Carajás (Brazil) BIF (Ribeiro da Luz & Crowley, 2012).

IRON MOUNTAIN MINE DRAINAGE SITE, NORTHERN CALIFORNIA

Iron Mountain Mine is a group of mines on Iron Mountain, Shasta County, northern California, USA (Alpers, Nordstrom, & Spitzley, 2003). The acid drainage effluent from Iron Mountain Mine has extremely low pH (-3.6) within the Richmond mine portal, ranging to pH values of +1 to +4 in drainage tributaries, such as Spring Creek (Nordstrom & Alpers, 1999; Edwards, Gihring, & Banfield, 1999; Norstrom & others 2000; Alpers, Nordstrom, & Spitzley, 2003). Concentrations of total dissolved solids in the effluent can exceed 900 g/L, and the waters are iron rich (Nordstrom, 2000). Mixing of neutral pH waters from an upstream reservoir with the iron-rich water of the acid mine drainage from Spring Creek has formed three large surface accumulation piles (>260,000 m^3 total volume) comprised of fine-grained Fe(III) oxide-rich sediment. Minerals present in the piles include ferrihydrite [$Fe(OH)_3$], goethite [α-FeO(OH)], and minerals with structures similar to synthetic schwertmannite [$Fe(III)_8O_8(OH)_6(SO_4)$] (Nordstrom & Alpers, 1999). The concentration of iron in the wet sediments ranges from 4% to 47% and the pore waters have extremely high concentrations of aqueous Fe(II) up to 36 mM (Nordstrom & Alpers, 1999). The pore waters have pH values of 5.5–6.5 and sulfate concentrations of 10 mM (Nordstrom & Alpers, 1999).

Iron Mountain iron-rich sediments represent a potential modern analog to early diagenetic BIF minerals formed in Archean and Proterozoic marine environments (Tangalos & others, 2010). Although the setting where the sediments form is an aerobic continental environment, it is characterized by high concentrations of reactive Fe(III) oxide that result in the dominance of dissimilatory iron reduction (DIR) over dissimilatory sulfate reduction (DSR) in early sediment diagenesis and large quantities of mobile Fe(II) in the pore waters. Additionally, the sediments contain significant concentrations of sulfate (4–23 mM), but there is an absence of acid volatile sulfides and a very low content of Cr(II)-extracted reduced inorganic sulfur (pyrite and/or elemental sulfur) compared with dilute HCl-extractable Fe(II). The sediments also have a relatively high ratio of nonsulfide-associated reactive iron to reduced inorganic sulfur, which are significantly higher than those in most modern marine sediments but similar to oxide and siderite BIFs from the Kuruman BIF and the Dales Gorge Member of the Brockman BIF (Tangalos & others, 2010). These characteristics and the chemical composition of the Iron Mountain sediments make the environment a good analog to study the processes that operated in the sedimentary pile prior to diagenesis and authigenic formation of magnetite and siderite in Archean BIFs (Tangalos & others, 2010). In particular, this site is a natural example of the diagenetic process of bacterial DIR that likely took place in the sedimentary pile during the formation of siderite and magnetite in Superior-type BIFs, such as the Kuruman Iron Formation (Heimann & others, 2010).

Tangalos and others (2010) considered that the high amounts of $Fe(II)_{aq}$ in the Iron Mountain sediment pore water were generated by bacterial DIR of Fe(III) minerals (goethite and ferrihydrite) in the sediments. This is based on the assumption that DIR predominates over DSR due to the high concentration of reactive Fe(III) oxides, which allows dissimilatory iron-reducing microorganisms to outcompete dissimilatory sulfate-reducing bacteria for organic electron

donors (Lovley & Phillips, 1987; Tangalos & others, 2010). The sediments also contain 1.5%–4% (dry weight) particulate organic carbon, derived from primary production in the overlying water or inputs of organic matter from the surrounding terrestrial environment, which is thought to serve as electron donors for DIR. The dominance of DIR was confirmed by gene sequencing of cultures of the material in the sediments and pore waters that showed that the sediments contained gene sequences closely related (97% similarity) to known dissimilatory iron-reducing microorganisms (*Geobacter* Lovley & others 1993 and *Geothrix* Coates & others, 1999). Four different culture isolates of *Geothrix fermentans* Coates & others, 1999 were also obtained, which also confirm that dissimilatory iron-reducing microorganisms are active in the Iron Mountain materials (Tangalos & others, 2010).

Iron isotope analysis indicates that $Fe(II)_{aq}$ from the sediments pore water at Iron Mountain has negative $\delta^{56}Fe$ values (-0.8% to -1.2‰), in contrast to the near-zero $\delta^{56}Fe$ values for the bulk Fe sediments that are isotopically similar to the average crust (Tangalos & others, 2010). The near-zero $\delta^{56}Fe$ values of the bulk sediments indicate that complete oxidation of Fe(II) took place in the near-neutral ~6.5 pH environment prior to the deposition of the Fe(III) oxide sediment. Isotopic fractionations between Fe(II)aq and Fe(III) extractable are similar to those measured in pure culture DIR experiments with Fe(III) oxides that showed the generation of low-$\delta^{56}Fe$ Fe(II) generated by DIR (Crosby & others, 2005, 2007). These *in situ* results were also reproduced in the laboratory with cultured iron oxides (Crosby & others, 2005, 2007). The less negative isotopic composition of $Fe(II)_{aq}$, compared to those measured in modern marine sediments (-1.3‰ to -3‰) (e.g., Severmann & others, 2006; Bergquist & Boyle, 2006) or stratified water bodies (Teutsch & others, 2009), are likely due to differences in the iron redox cycle and redistribution, which are more limited in the Iron Mountain sedimentary piles than they were in Archean and Proterozoic marine environments. At Iron Mountain, therefore, DIR is linked directly to the generation of large quantities of isotopically light, mobile $Fe(II)_{aq}$, which suggests that DIR could have led to the formation of low-$\delta^{56}Fe$ iron-bearing minerals (siderite, magnetite) during early diagenesis of Precambrian BIFs (Tangalos & others, 2010).

CHOCOLATE POTS HOT SPRINGS, YELLOWSTONE NATIONAL PARK

Iron-rich sediments are actively being deposited at Chocolate Pots hot springs, Yellowstone National Park, USA (Pierson, Parenteau, & Griffin, 1999). Colorful, iron-rich phototrophic microbial mats form a boundary layer at the interface between the iron-rich sediment surface and flowing spring water that contains high concentrations (~100 μM) of ferrous iron at the source (Pierson, Parenteau, & Griffin, 1999; Klatt & others, 2013; Wu & others, 2013). The source waters have a near-neutral pH and lack sulfide. Beneath the surface of the microbial mat-water interface the environment is anoxic and rich in Fe(II). Although in a terrestrial surficial location, this site serves as an analog for the extensive anoxic environments of and processes operating in the Precambrian oceans where iron oxides formed (e.g., Pierson, Parenteau, & Griffin, 1999; Wu & others, 2013).

The microbial mats are comprised mainly of filamentous gliding phototrophs that stabilize oxidized iron and enhance the accumulation of sediments that are later compacted to form the iron deposits (Pierson, Parenteau, & Griffin, 1999). The intimate association between the filamentous phototrophs and the iron minerals, as well as the observation that the motility and orientation of the filaments may be important in trapping and stabilizing the sediments to produce the iron formation, is most evident in an olive green-color mat consisting of a narrow (cyanobacteria)

Oscillatoria sp. (Pierson, Parenteau, & Griffin, 1999).

Measurements in the olive mat indicate that both under light and in the dark, ferrous iron stimulates bicarbonate uptake (photosynthesis), with the highest stimulation taking place at Fe contents of 1.0 mM, whereas Fe(II) concentrations of 5 mM inhibited photosynthesis (Pierson, Parenteau, & Griffin, 1999). What is not known with certainty is whether Fe(II)-stimulated photosynthesis in anoxygenic phototrophs (*Chloroflexus* filaments) occurs in the cyanobacterial mat suspensions or only in the cyanobacteria themselves (Pierson, Parenteau, & Griffin, 1999). Isolation of Chocolate Pots mat phototrophs and experiments performed with pure cultures may help resolve which bacteria are stimulated by Fe(II) (Pierson, Parenteau, & Griffin, 1999). Newer studies indicate that the Fe isotope compositions measured at Chocolate Pots could be important to predict those on a limited-oxygen early Earth or on Mars (Wu & others, 2013). This is because the range of Fe isotopic compositions (-1.57‰ to +0.88‰) measured in the iron oxides and hot springs at Chocolate Pots do not reflect simple equilibrium oxidation or Rayleigh oxidation of Fe(II) but rather reflect different extents and rates of Fe(II) oxidation as well as the possible reduction of iron by dissimilatory Fe(III)-reducing bacteria (Wu & others, 2013). Because of the link between iron oxide precipitation, microbial mats, and bacterial iron oxidation, the processes operating at Chocolate Pots hot springs can be considered analogs to those taking place during BIF formation.

FUTURE DIRECTIONS

The following are a few lines of research that will help improve our understanding of the genesis of banded iron formations (BIFs) and the role of various biological processes directly and indirectly involved in their formation. The search for new physical biosignatures in low-metamorphic grade oxide-facies BIFs older than the Gunflint BIF in North America—for example, permineralized cells similar to those present in iron-rich modern microbial mats (e.g., Klein, 2005; Parenteau & Cady, 2010)—will help elucidate the role of bacterial processes in the generation of BIFs (Walter & Hoffman, 1983). Further search for stromatolitic structures and organic matter in BIFs, similar to the ones described from the ~2.75 Carajás BIFs from Brazil (Ribeiro da Luz & Crowley, 2012), will help determine if biomats and BIFs could have a strong genetic link. A common aspect to most, if not all, modern water environments where iron oxide precipitation takes place is their intrinsic association with bacterial mats and biofilms. Further studies of modern environments and BIFs will help to understand the likely role of these bacterial structures in the formation of BIFs, especially the striking extremely fine-scale laminations of iron oxides and chert.

The search in Archean BIFs for chemical fingerprints unique to Fe(II)-oxidizing phototrophs will provide the physical evidence for the existence of these organisms in Archean oceans. For example, the discovery of biomarkers of pigments involved in photosynthesis and radical scavenging (radicals that form during Fe-Fenton reactions), which are two processes important in systems where photosynthetic Fe(II) oxidizers exist, would provide definite clues about their presence during the Archean (Koehler, Konhauser, & Kappler, 2010). Similarly, isolation and culture in the laboratory of Fe(II) oxidizing green sulfur bacteria (GSB) that occur in modern analogs to Archean marine environments, such as the deep Lake Matano, are needed (Crowe & others, 2008a). Culturing of Fe(II)-oxidizing GSB will improve our understanding of the physiology and metabolism of the GSB, help prove that photoferrotrophy is the responsible bacterial process oxidizing iron in the lake (Crowe & others, 2008a), and provide clues as to what bacterial metabolism likely existed and played a role during the formation of BIFs.

Geochemical investigations of iron isotopes to fill the gaps in the iron isotope record through time as well as in modern natural environments will help prove that large variations in iron isotope compositions, observed particularly at ~2.7–2.5 Ga, indicate the expansion of bacterial dissimilatory iron reduction (DIR) in the Precambrian oceans and its likely role during BIF formation. More detailed iron isotope studies similar to the ones conducted at Chocolate Pots, Yellowstone National Park (Wu & others, 2013) will help to understand the processes responsible for the fractionation of iron isotopes in oxygenated and oxygen-limited environments and the implications for the formation of iron deposits on early Earth and Mars. In addition, studies of iron, carbon, and sulfur isotopes on the same rocks in Archean–Proterozoic sequences, including multiple sulfur isotopes to detect mass-independent sulfur isotope effects, will help test the hypothesis that these isotopic records are coupled and reflect photosynthesis and heterotrophic respiration (e.g., Johnson, Beard, & Roden, 2008). Furthermore, basin-wide scale iron isotope studies of BIFs, similar to those undertaken in other sedimentary rocks (mostly shale and carbonate) from Western Australia (e.g., Czaja & others, 2010), will help improve our understanding of the biogeochemical cycling of iron in ancient oceans. Finally, new rare earth element studies of BIFs, coupled with iron and carbon isotopes, as well as isotopes of other redox metals, may also help elucidate the presence or absence of a redoxcline in Archean oceans and the role of bacterial iron oxidation and reduction in the formation of different BIFs in the Archean–Paleoproterozoic and in the late Paleoproterozoic (Planavsky & others, 2010).

ACKNOWLEDGEMENTS

I wish to thank Steve Culver, Terri Woods, Jens Gutzmer, Christopher Fedo, and Nora Noffke for their comments, suggestions, and revisions, which greatly improved this manuscript. I also thank Clark Johnson for kindly providing an image of BIFs.

REFERENCES

Abell, P. I., S. M. Awramik, R. H. Osborne, & S. Tomellini. 1982. Plio-Pleistocene lacustrine stromatolites from Lake Turkana, Kenya: Morphology, stratigraphy and stable isotopes. Sedimentary Geology (32):1–26.

Aharon, Paul. 2000. Microbial processes and products fueled by hydrocarbons at submarine seeps. *In* Robert Riding, S. M. Awramik, eds., Microbial Sediments. Springer. Berlin. p. 270–281.

Aharon, Paul, & Baoshun Fu. 2000. Microbial sulfate reduction rates and sulfur and oxygen isotope fractionations at oil and gas seeps in deepwater Gulf of Mexico. Geochimica et Cosmochimica Acta (64)233–246.

Aitken, J. D. 1967. Classification and environmental significance of cryptalgal limestones and dolomites, with illustrations from the Cambrian and Ordovician of southwestern Alberta. Journal of Sedimentary Research 37:1163–1178.

Aitken, J. D., & G. M. Narbonne. 1989. Two occurrences of Precambrian thrombolites from the Mackenzie Mountains, northwestern Canada. Palaios (4):384–388.

Allen, M. A., B. A. Neilan, B. P. Burns, L. L. Jahnke, & R. E. Summons. 2010. Lipid biomarkers in Hamelin Pool microbial mats and stromatolites. Organic Geochemistry 41(11)1207–1218.

Allwood, A. C., M. T. Rossing, D. T. Flannery, J. A. Hurowitz, & C. M. Heirwegh. 2018. Reassessing evidence of life in 3,700-million-year-old rocks of Greenland. Nature 563:241–244.

Allwood, A. C., M. R. Walter, B. S. Kamber, C. P. Marshall, & I. W. Burch. 2006. Stromatolite reef from the Early Archaean era of Australia. Nature 441:714–718.

Alpers, C. N., D. K. Nordstrom, & John Spitzley. 2003. Extreme acid mine drainage from a pyritic massive sulfide deposit: The Iron Mountain end member. *In* J. L. Jambor, D. W. Blowes, & A. I. M. Ritchie, eds., Environmental Aspects of Mine-Wastes. Mineralogical Association of Canada, Ottawa. p. 407–430.

Alt, J. C. 1988. Hydrothermal oxide and nontronite deposits on seamounts in the eastern Pacific. Marine Geology 81:227–239.

Altermann, Wladyslaw. 2001. The oldest fossils of Africa: A brief reappraisal of reports from the Archean. Journal of African Earth Sciences 33:427–436.

Altermann, Wladyslaw, & J. W. Schopf. 1995. Microfossils from the Neoarchean Campbell Group, Griqualand West Sequence of the Transvaal Supergroup, and their paleoenvironmental and evolutionary implications. Precambrian Research 75:65–90.

Amard, Bertrand, & Janine Bertrand-Sarfati. 1997. Microfossils in 2000 Ma old cherty stromatolites of the Franceville group, Gabon. Precambrian Research 81:197–221.

Amato, S. M., C. H. Fazen, T. C. Henry, W. W. K. Mok, M. A. Orman, E. L. Sandvik, K. G. Volzing, & M. P. Brynildsen. 2014. The role of metabolism in bacterial persistence. Frontiers in Microbiology 5:70 [doi.org/10.3389/fmicb.2014.00070].

Amos, C. L., Alessandro Bergamasco, George Umgiesser, Sergio Cappucci, Danielle Cloutier, Lise DeNat, M. R. Flindt, Maurizio Bonardi, & S. Cristante. 2004. The stability of tidal flats in Venice Lagoon: The results of in-situ measurements using two benthic, annular flumes. Journal of Marine Systems 51:211–241.

Andersen, D. T., D. Y. Sumner, I. Hawes, J. Webster-Brown, & C. P. Mckay. 2011. Discovery of large conical stromatolites in Lake Untersee, Antarctica: Geobiology (9):280–293.

Andres, M. S., & R. P. Reid. 2006. Growth morphologies of modern marine stromatolites: A case study from Highborne Cay, Bahamas. Sedimentary Geology (185):319–328.

Aoki, Shogo, Masanori Shimojo, Shuhei Sakata, Shinji Yamamoto, Akira Ishikawa, Takafumi Hirata, & Tsuyoshi Komiya. 2013. Geology, lithostratigraphy and geochemistry of the oldest Eoarchaean BIFs, northern Labrador. Mineralogical Magazine (Abstract) 77:601.

Appel, P. W. U. 1987. Geochemistry of the early Archean Isua iron-formations, West Greenland. *In* P. W. U. Appel & G. L. LaBerge, eds., Precambrian Iron-formations. Theophrastus Publications. Athens. p. 31–67.

Armbruster, C. R., C. K. Lee, Jessica Parker-Gilham, Jaimede Anda, Xia Aiguo, B. S. Tseng, L. R. Hoffman, Fan Jin, C. S. Harwood, G. C. L. Wong & M. R. Parsek. 2019. Heterogeneity in surface sensing produces a division of labor in Pseudomonas aeruginosa populations. eLife 2019, 8:e45084 [doi.10.7554/eLife.45084].

Armitage, D. W., K. L. Gallagher, N. D. Youngblut, D. H. Buckley, & S. H. Zinder. 2012. Millimeter scale patterns of phylogenetic and trait diversity in a salt marsh microbial mat. Frontiers in Microbiology 3:293 [doi.org/10.3389/fmicb.2012.00293].

Arora, M., P. K. Govil, S. N. Charan, B. Uday Raj, C. Manikyamba, A. K. Chatterjee, & S. M. Naqvi. 1995. Geochemistry and origin of Archean banded iron-formation from the Bababudan schist belt, India. Economic Geology 90:2040–2057.

Arp, Gernot. 2001. Photosynthesis-induced biofilm calcification and calcium concentrations in Phanerozoic oceans. Science (292):1701–1704.

Arp, Gernot, Gert Helms, Klementyna Karlinska, Gabriela Schumann, Andreas Reimer, Joachim Reitner, & Jean Trichet. 2012. Photosynthesis versus exopolymer degradation in the formation of the microbialites on the atoll of Kiritimati, Republic of Kiribati, Central Pacific. Geomicrobiology Journal 29:29–65.

Arp, Gernot, Andreas Reimer, & Joachim Reitner. 1999. Calcification in cyanobacterial biofilms of alkaline salt lakes: European Journal of Phycology (34)393–403.

Arp, Gernot, Andreas Reimer, & Joachim Reitner. 2001. Photosynthesis-induced biofilm calcification

and calcium concentrations in Phanerozoic oceans. Science 292:1071–1074.
Arp, Gernot, Andreas Reimer, & Joachim Reitner. 2004. Microbialite Formation in Seawater of Increased Alkalinity, Satonda Crater Lake, Indonesia: Reply: Journal of Sedimentary Research 74:318–325.
Ashley, B. E. 1937. Fossil algae from the Kundelungu Series of Northern Rhodesia. Journal of Geology 45:332–335.
Astafieva, M. M. 2013. Prokaryotes in the early Precambrian: Paleontological Journal 47(9):973–976.
Aubé, Johanne, Pavel Senin, Patricia Bonin, Olivier Pringault, Celine Jeziorski, Olivier Boiuchez, Christophe Klopp, Remy Guyoneaud, & Marisol Goni-Urriza. 2020. Meta-omics provides insights into the impact of hydrocarbon contamination on microbial mat functioning. Microbial Ecology 80:286–295.
Aubineau, Jérémie, Abderrazak El Albani, Ernest Chi Fru, Murray Gingras, Yann Batonneau, L. A. Buatois, Claude Geffroy, Jérôme Labanowski, Claude Laforest, Laurent Lemée, M. G. Mángano, Alain Meunier, A.-C. Pierson-Wickmann, Philippe Recourt, Armelle Riboulleau, Alain Trentesaux, & K. O. Konhauser. 2018. Unusual microbial mat-related structural diversity 2.1 billion years ago and implications for the Francevillian biota. Geobiology 16:476–497.
Awramik, S. M. 1991. Archaean and Proterozoic Stromatolites. *In* Robert Riding, ed., Calcareous Algae and Stromatolites. Springer. Berlin. p. 289–304.
Awramik, S. M., & E. S. Barghoorn. 1977. The Gunflint microbiota. Precambrian Research 5(2):121–142.
Awramik, S. M., & H. P. Buchheim. 2009. A giant, Late Archean lake system: The Meentheena Member (Tumbiana Formation; Fortescue Group), Western Australia. Precambrian Research 174:215–240.
Awramik, S. M., & H. P. Buchheim. 2012. The quest for microbialite analogs to the South Atlantic Pre-Salt carbonate hydrocarbon reservoirs of Africa and South America. Houston Geological Society Bulletin (55):21–28.
Awramik, S. M., & Kathleen Grey. 2005. Stromatolites: Biogenicity, biosignatures, and bioconfusion. Proceedings of the Society of Photo-optical Instrumentation Engineers (5906):1–9.
Awramik, S. M., L. Margulis, & E. S. Barghoorn. 1976. Chapter 4.4. Evolutionary processes in the formation of stromatolites. Developments in Sedimentology (20):149–162.
Awramik, S. M., & Robert Riding. 1988. Role of algal eukaryotes in subtidal columnar stromatolite formation: Proceedings of the National Academy of Sciences, USA (85):1327–1329.
Awramik, S. M., J. W. Schopf, & M. R. Walter. 1983. Filamentous fossil bacteria from the Archean of Western Australia. Precambrian Research 174:215–240.
Awramik, S. M., & James Sprinkle. 1999. Proterozoic stromatolites: The first marine evolutionary biota. Historical Biology (13):241–253.
Ayres, D. E. 1972. Genesis of iron-bearing minerals in banded iron formation mesobands in the Dales Gorge Member, Hamersley Group, Western Australia. Economic Geology 67:1214–1233.
Baas Becking, L .G. M. 1934. Geobiology. Stockum. Den Haag. The Netherlands. 263 p.
Babilonia, Joany, Ana Conesa, Giorgio Cassaburi, Cecile Pereira, A. S. Louyakis, R. P. Reid, & J. S. Foster. 2018. Comparitive metagneomics provides insight into the ecosystem functioning of the Shark Bay stromatolites, Western Australia. Frontiers in Microcrobiology 9:1359 [doi.10.3389/fmicb.2018.01359].
Bailey, J. V., F. A. Corsetti, S. E. Greene, C. H. Crosby, Pengju Liu, & V. J. Orphan. 2013. Filamentous sulfur bacteria preserved in modern and ancient phosphatic sediments: implications for the role of oxygen and bacteria in phosphogenesis. Geobiology 11:397–405.
Bailey, J. V., S. B. Joye, K. M. Kalanetra, B. E. Flood, & F. A. Corsetti. 2007. Evidence of giant sulphur bacteria in Neoproterozoic phosphorites. Nature 445:198–201.
Bailey, J. V., V. J. Orphan, S. B. Joye, & F. A. Corsetti. 2009. Chemotrophic Microbial Mats and Their Potential for Preservation in the Rock Record. Astrobiology (9):843–849.
Bak, Friedhelm, & Norbert Pfennig. 1987. Chemolithotrophic growth of *Desulfovibrio sulfodismutans* sp. nov. by disproportionation of inorganic sulfur compounds. Archives for Microbiology 147:184–189.
Banks, H. P., K. I. M. Chesters, N. F. Hughes, G. A. L. Johnson, H. M. Johnson, & L. R. Moore. 1967. Chapter 1 Thallophyta–1. Geological Society of London Special Publications 2:163–180.
Bargar, K. E. 1978. Geology and thermal history of Mammoth Hot Springs, Yellowstone National Park, Wyoming. Geological Survey Bulletin (1444). 55 p.
Barghoorn, E. S., & J. W. Schopf. 1965. Microorganisms from the late Precambrian of central Australia. Science 150:337–339.
Barghoorn, E. S., & S. A. Tyler. 1965. Microorganisms from the Gunflint Chert. Science 147:563–577.
Barley, M. E., Robert Kerrich, Bryan Krapež, & D. I. Groves. 1998. The 2.72–2.60 Ga bonanza: Metallogenic and environmental consequences of the interaction between mantle plumes, lithospheric tectonics and global cyclicity. Precambrian Research 91: 65–90.
Barlow, E. V., & M. J. van Kranendonk. 2018. Snapshot of an early Paleoproterozoic ecosystem: Two diverse microfossil communities from the Turee Creek Group, Western Australia. Geobiology 16:445–479.
Barlow, E. V., M. J. van Kranendonk, K. E. Yamaguchi, Minoru Ikehara, & Aivo Lepland. 2016. Lithostratigraphic analysis of a new stromatolite-thrombolite reef from across the rise of atmospheric oxygen in the Paleoproterozoic Turee Creek Group, Western Australia. Geobiology 14(4):317–343.
Bar-On, Y. M., Rob Phillips, & Ron Milo. 2018. The biomass distribution on Earth. Proceedings of the National Academy of Sciences, USA 115:6506–6511.
Baross, J. A., & J. W. Deming. 1985. The role of bacteria in the ecology of black-smoker environments. Hydrothermal vent of the Eastern Pacific: An overview. (M. L. Jones, ed.). Bulletin of the Biological Society of Washington 6:355–371.

Bartley, J. K. 1996. Actualistic taphonomy of cyanobacteria: Implications for the Precambrian fossil record. Palaios 11:571–586.

Basilicii, G., M. V. T. Soares, N. P. Mountney, & Luca Colombera. 2020. Microbial influence on the Accumulation of Precambrian Aeolian Deposits (Neoproterozoic, Venkatpur Sandstone Formation, Southern India): Precambrian Research 347:05–854.

Bates, R. L., & J. A. Jackson. 1987. Glossary of geology, 3rd edition, American Geological Institute, Alexandria. 788 p.

Bateson, M. M., & D. M. Ward. 1988. Photoexcretion and fate of glycolate in a hot spring cyanobacterial mat. Applied and Environmental Microbiology 54(7):1738–1743.

Bau, Michael. 1991. Rare-earth element mobility during hydrothermal and metamorphic fluid-rock interaction and the significance of the oxidation state of europium. Chemical Geology 93: 219–230.

Bau, Michael, & Peter Dulski. 1996. Distribution of yttrium and rare-earth elements in the Penge and Kuruman Iron-Formations, Transvaal Supergroup, South Africa. Precambrian Research 7:37–55.

Bau, Michael, & Peter Möller. 1993. Rare earth element systematics of the chemically precipitated component in Early Precambrian iron-formations and the evolution of the terrestrial atmosphere-hydrosphere-lithosphere system. Geochimica et Cosmochimica Acta 57:2239–2249.

Baud, Aymon, Simonetta Cirilli, & Jean Marcoux. 1997. Biotic response to mass extincion: The lowermost Triassic microbialites. Facies (36):238–242.

Baud, Aymon, Sylvain Richoz, & Sarah Pruss. 2007. The lower Triassic anachronistic carbonate facies in space and time. Global and Planetary Change (55):81–89.

Baumgartner, L. K., Christophe Dupraz, D. H. Buckley, John Spear, N. R. Pace, & P. T. Visscher. 2009. Microbial species richness and metabolic activities in hypersaline microbial mats: Insight into biosignature formation through lithification. Astrobiology 9:861–874.

Baumgartner, L. K., R. P. Reid, Christophe Dupraz, A. W. Decho, D. . Buckley, J. R. Spear, K. M. Przekop, & P. T. Visscher. 2006. Sulfate-reducing bacteria in microbial mats: Changing paradigms, new discoveries. Sedimentary Geology 185:131–145.

Baumgartner, L. K., J. R. Spear, D. H. Buckley, N. R. Pace, R. P. Reid, Christophe Dupraz, N. R. Pace, & P. T. Visscher. 2009. Microbial diversity in modern marine stromatolites, Highborne Cay, Bahamas. Environmental Microbiology 11:2710–2719.

Baur, M. E., J. M. Hayes, S. A. Studley, & M. R.Walter. 1985. Millimeter-scale variations of stable isotope abundances in carbonates from banded iron-formations in the Hamersley Group of Western Australia. Economic Geology 80:270–282.

Bayet-Goll, Aram, & Mehdi Daraei. 2020. Palaeoecological, sedimentological and stratigraphical insights into microbially induced sedimentary structures of the lower Cambrian successions of Iran. Sedimentology 67(6):3199–3235.

Bazylinski, D. A., & R. B. Frankel. 2003. Biologically controlled mineralization in prokaryotes. Reviews in Mineralogy and Geochemistry 54:217–247.

Beam, J. P., H. C. Bernstein, Z. J. Jay, M. A. Kozubal, Ryan deM Jennings, S. G. Tringe, & W. P. Inskeep. 2016. Assembly and succession of iron oxide microbial mat communities in acedici geothermal springs. Frontiers in Microbiology 7:25 [doi.10.3389/fmicb.2016.00025].

Beard, B. L., C. M. Johnson, Lea Cox, Henry Sun, K. H. Nealson, & Carmen Aguilar. 1999. Iron isotope biosignatures. Science 285:1889–1892.

Beard, B. L., C. M. Johnson, K. L. Von Damm, & R. L. Poulson. 2003. Iron isotope constraints on Fe cycling and mass balance in oxygenated Earth oceans. Geology 31:629–632.

Bebout, B. M., & Farran García-Piche. 1995. UV B-induced vertical migration of cyanobacteria in a microbial mat. Applied Environmental Microbiology 6:4215–4222.

Becker, R. H., & R. N. Clayton. 1972. Carbon isotopic evidence for the origin of a banded iron-formation in Western Australia. Geochimica et Cosmochimica Acta 36:577–595.

Bekker, Andrey, H. D. Holland, P.-L. Wang, Douglas Rumble III, H. J. Stein, J. L. Hannah, L. L. Coetzee, & N. J. Beukes. 2004. Dating the rise of atmospheric oxygen. Nature 427:117–120.

Bekker, Andrey, J. F. Slack, Noah Planavsky, Bryan Krapež, Axel Hofmann, K. O. Konhauser, & O. J. Rouxel. 2010. Iron formation: The sedimentary product of a complex interplay among mantle, tectonic, oceanic, and biospheric processes. Economic Geology 105:467–508.

Bengtson, Stefan, Birger Rasmussen, Magnus Ivarsson, Janet Muhling, Curt Broman, Federica Marone, Marco Stampanoni, & Andrey Bekker. 2017. Fungus-like mycelial fossils in 2.4-billion-year-old vesicular basalt. Nature Ecology & Evolution 1:0141 [doi.10.1038/s41559-017-0141].

Bennett, A. C., S. K. Murugapiran, & T. L. Hamilton. 2020. Temperature impacts community structure and function of phototrophic Chloroflexi and Cyanobacteria in two alkaline hot springs in Yellowstone National Park. Environmental Microbiology Reports 12(5):503–513.

Benzerara, Karim, & Nicolas Menguy. 2009. Looking for traces of life in minerals. Comptes Rendus Palevol 8:617–628 [doi.10.1016/j.crpv.2009.03.006].

Benzerara, Karim, Feriel Skouri-Panet, Jinhua Li, Celine Férard, Muriel Gugger, Thierry Laurent, Estelle Couradeau, Marie Ragon, Julie Cosmidis, Nicolas Menguy, Isabelle Margaret-Oliver, Rosaluz Tavera, Purificacion Lopez-Garcia, & David Moreira. 2014. Intracellular Ca-carbonate biomineralization is widespread in cyanobacteria. Proceedings of the National Academy of Sciences, USA 111(30):10933–10938.

Beraldi-Campesi, Hugo. 2013. Early life on land and the first terrestrial ecosystems. Ecological Processes 2(1):1 [doi.org/10.1186/2192-1709-2-1].

Berelson, W. M., F. A. Corsetti, C. Pepe-Ranney, D. E. Hammond, W. Beaumont, & J. R. Spear. 2011. Hot spring siliceous stromatolites from Yellowstone

National Park: Assessing growth rate and laminae formation. Geobiology 9:411–424.

Bergman, Birgitta, Gustaf Sandh, Senjie Lin, John Larsson, & E. J. Carpenter. 2013. *Trichodesmium*: A widespread marine cyanobacterium with unusual nitrogen fixation properties. FEMS Microbiology Reviews 37:286–302.

Bergquist, B. A., & E. A. Boyle. 2006. Iron isotopes in the Amazon River system: Weathering and transport signatures. Earth and Planetary Science Letters 248:54–68.

Berner, R. A. 1969. Goethite stability and the origin of red beds. Geochimica et Cosmochimica Acta 33:267–273.

Bernhard, J. M., V. P. Edgcomb, P. T. Visscher, Anna McIntyre-Wressig, R. E. Summons, M. L. Bouxsein, Leeann Louis & Marleen Jeglinski. 2013. Insights into foraminiferal influences on microfabrics of microbialites at Highborne Cay, Bahamas. Proceedings of the National Academy of Sciences, USA 110:9830–9834.

Bernstein, H. C., J. P. Beam, M. A. Kozubal, R. P. Carlson, & W. P. Inskeep. 2013. In situ analysis of oxygen consumption and diffusive transport in high-temperature acidic iron-oxide microbial mats. Environmental Microbiology 15(8):2360–2370.

Beukes, N. J. 1987. Facies relations, depositional environments and diagenesis in a major early Proterozoic stromatolitic carbonate platform to basinal sequence, Campbellrand Subgroup, Transvaal Supergroup, Southern Africa. Sedimentary Geology 54(1–2):1–5, 7, 9–46.

Beukes, N. J., & Jens Gutzmer. 2008. Origin and paleoenvironmental significance of major iron formations at the Archean-Paleoproterozoic boundary. Reviews in Economic Geology 15:5–47.

Beukes, N. J., & Cornelis Klein. 1990. Geochemistry and sedimentology of a facies transition—from microbanded to granular iron-formation—in the Early Proterozoic Transvaal Supergroup, South Africa. Precambrian Research 47:99–139.

Beukes, N. J., Cornelis Klein, A. J. Kaufman, & J. M. Hayes. 1990. Carbonate petrography, kerogen distribution, and carbon and oxygen isotope variations in an Early Proterozoic transition from limestone to iron-formation deposition: Transvaal Supergroup, South Africa. Economic Geology 85:663–690.

Beukes, N. J., & D. R. Lowe. 1989. Environmental control on diverse stromatolite morphologies in the 3000 Myr Pongola Supergroup, South Africa. Sedimentology (36):383–397.

Bi, Zhen, Deqing Wanyan, Xiang Li, & Yong Huang. 2020. Biological conversion pathways of sulfate reduction ammonium oxidation in anammox consortia. Frontiers of Environmental Science & Engineering 14:38 [doi.10.1007/s11783-019-1217-1].

Biddanda, B. A., A. C. McMillan, S. A. Long, M. J. Snider, & A. D. Weinke. 2015. Seeking sunlight: Rapid phototactic motility of filamentous matforming cyanobacteria optimize photosynthesis and enhance carbon burial in Lake Huron's submerged sinkholes. Frontiers in Microbiology (6):930 [doi.org/10.3389/fmicb.2015.00930].

Birgel, Daniel, Volker Thiel, K. U. Hinrichs, Marcus Elvert, K. A. Campbell, Joachim Reitner, J. D. Farmer, & J. Peckmann. 2006. Lipid biomarker patterns of methane-seep microbialites from the Mesozoic convergent margin of California. Organic Geochemistry (37)1289–1302.

Birnbaum, S. J., & J. W. Wireman. 1985. Sulfate-reducing bacteria and silica solubility: A possible mechanism for evaporate diagenesis and silica precipitation in banded iron formations. Canadian Journal of Earth Sciences 22:1904–1909.

Black, Maurice. 1933. The precipitation of calcium carbonate on the Great Bahama Bank. Geological Magazine (70):455–466.

Blokker, Peter, Pim van Bergen, Rich Pancost, M. E. Collinson, J. W. de Leeuw, & J. S. Sinninghe damsté. 2001. The chemical structure of *Gloeocapsomorpha prisca* microfossils: Implications for their origin. Geochimica et Cosmochimica Acta 65:885–900.

Blumenberg, Martin, Volker Thiel, & Joachim Reitner. 2015. Organic matter preservation in the carbonate matrix of a recent microbial mat: Is there a 'mat seal effect'? Organic Geochemistry 87:25–34.

Bolhuis, Henk, M. S. Cretoiu & L. J. Stal. 2014. Molecular ecology of microbial mats. FEMS Microbiology Ecology 90:335–350.

Bolhuis, Henk, & L. J. Stal. 2011. Analysis of bacterial and archaeal diversity in coastal microbial mats using massive parallel 16S rRNA gene tag sequencing. ISME Journal 5:1701–1712.

Bonilla-Rosso, German, Mariana Peimbert, L. D. Alcaraz, Ismael Hernandez, L. E. Eguiarte, Gabriela Olmedo-Alvarez, & Valeria Souza. 2012. Comparative metagenomics of two microbial mats at Cuatro Ciénegas basin ll: Community structure and composition in oligotrophic environments. Astrobiology 12(7):659–673.

Bonin, P. C., & V. D. Michotey. 2006. Nitrogen budget in a microbial mat in the Camargue (southern France). Marine Ecology Progress Series 322:75–84.

Bonneville, S. C., Frank Delpomdor, Alain Préat, Clément Chevalier, Tohru Araki, M. Kazemian, Andrew Steele, Anja Schreiber, Rainer Wirth, & L. G. Benning. 2020. Molecular identification of fungi microfossils in a Neoproterozoic shale rock. Science Advances 6:eaax7599 [doi.10.1126/sciadv.aax7599].

Bornemann, J. G. 1886. Die Versteinerungen des Cambrischen Schichten-Systems der Insel Sardinien nebst vergleichenden Untersuchungen iiber analoge Vorkommnisse aus andern Landern. Verhandlungen Der Kaiserlich Leopoldinisch-Carolinischen Deutschen Akademie Der Naturforscher 51:1–147.

Bornet, Édouard, & Charles Flahault. 1886a. Revision des Nostocacées hétérocystées contenues dans les principaux herbiers de France (quatrième et dernier fragment). Annales des Sciences Naturelles, Botanique, Septième (série 7):177–262.

Bornet, Édouard, & Charle Flahault. 1886b. Revision des Nostocacées hétérocystées contenues dans les principaux herbiers de France. Annales des Sciences Naturelles, Botanique, Septième (série 3):323–381.

Bornet, Édouard, & Charles Flahault. 1886c. Revision des Nostocacées hétérocystées contenues dans les

principaux herbiers de France (Troisième fragment). Annales des Sciences Naturelles, Botanique, Septième (série 5):51–129.

Bornet, Édouard, & Charles Flahault. 1888. Note sur deux nouveaux genres d'algues perforantes. Journal de Botanique Morot 2:161–165.

Bosak, Tanja, J. W. M. Bush, M. R. Flynn, Biqing Liang, S. Ono, A. P. Petroff, & M. S. Sim. 2010. Formation and stability of oxygen-rich bubbles that shape photosynthetic mats. Geobiology (8):45–55.

Bosak, Tanja, A. H. Knoll, & A. P. Petroff. 2013. The meaning of stromatolites. Annual Review of Earth and Planetary Sciences (41):21–44.

Bosak, Tanja, Biqing Liang, M. S. Sim, & A. P. Petroff. 2009. Morphological record of oxygenic photosynthesis in conical stromatolites. Proceedings of the National Academy of Sciences, USA 106:10939–10943.

Boström, Kurt, & Lennart Widenfalk. 1984. The origin of iron-rich muds at the Kameni Islands, Santorini, Greece. Chemical Geology 42:203–218.

Bottjer, D. J., & J. W. Hagador. 2007. Mat features in sandstones: Mat growth features. *In* Juergen Schieber, P. K. Bose, P. G. Eriksson, S. Banjeree, S. Sarkar, W. Altermann, & O. Catuneau, eds., Atlas of Microbial Mat Features Preserved Within the Clastic Rock Record. Elsevier. Amsterdam. p. 53–71.

Bottjer, D. J., J. W. Hagador, & S. O. Dornbos. 2000. The Cambrian substrate revolution. GSA Today 10:1–7.

Bouougri, E. H., & Hubertus Porada. 2012. Wind-induced mat deformation structures in recent tidal flats and sabkhas of SE-Tunisia and their significance for environmental interpretation of fossil structures. Sedimentary Geology 263–264:56–66.

Bouton, Anthony, Emmanuelle Vennin, Christophe Thomazo, Olivier Mathieu, Fabien Garcia, Maxime Jaubert, & P. T. Visscher. 2020. Microbial origin of the organic matter preserved in the Cayo Coco lagoonal network, Cuba. Minerals 10(2):143 [doi.10.3390/min10020143].

Bouwer, E. J., H. H. M. Rijnaarts, A. B. Cunningham, & Robin Gerlach. 2000. Biofilms in porous media. *In* J. D. Bryers, ed., Biofilms II: Process Analysis and Applications. Wiley-Liss/Wiley & Sons. New York. p. 123–158.

Braga, J. C., J. M. Martin, & Robert Riding. 1995. Controls on microbial dome fabric development along a carbonate-siliciclastic shelf-basin transect, Miocene, SE Spain. Palaios (10):347–361.

Braissant, Olivier, Guillaume Cailleau, Christophe Dupraz, & E. P. Verrecchia. 2003. Bacterially Induced mineralization of calcium carbonate in terrestrial environments: The role of exopolysaccharides and amino acids. Journal of Sedimentary Research 73(3): 485–490.

Braissant, Olivier, A. W. Decho, Christophe Dupraz, Christina Glunk, K. M. Przekop, & P. T. Visscher. 2007. Exopolymeric substances of sulfate-reducing bacteria: Interactions with calcium at alkaline pH and implications for formation of carbonate minerals. Geobiology 5:401–411.

Braissant, Olivier, A. W. Decho, K. M. Przekop, K. M. Gallagher, Christina Glunk, Christophe Dupraz, & P. T. Visscher. 2009. Characteristics and turnover of exopolymeric substances (EPS) in a hypersaline microbial mat. FEMS Microbiology Ecology 67:293–307.

Brasier, M. D., O. R. Green, A. P. Jephcoat, A. K. Kleppe, M. J. V. Kranendonk, J. F. Lindsay, Andrew Steele, & N. V. Grassineau. 2002. Questioning the evidence for Earth's oldest fossils. Nature 416:76–81.

Brasier, M. D., O. R. Green, J. F. Lindsay, Nicola McLoughlin, Andrew Steele, & Cris Stoakes. 2005. Critical testing of Earth's oldest putative fossil assemblage from the 3.5 Ga Apex chert, Chinaman Creek, Western Australia. Precambrian Research 140:55–102.

Brasier, M. D., Nicola McLoughlin, O. R. Green, & David Wacey. 2006. A fresh look at the fossil evidence for early Archaean cellular life. Philosophical Transactions of the Royal Society of London B (Biological Sciences) 361:887–902.

Brasier, M. D., & David Wacey. 2012. Fossils and astrobiology: new protocols for cell evolution in deep time. International Journal of Astrobiology 11:217–228.

Braterman, P. S., & A. G. Cairns-Smith. 1986. Photoprecipitation and the banded iron-formations: Some quantitative aspects. Origins of Life and Evolution of Biospheres 17:221–228.

Braterman, P. S., A. G. Cairns-Smith, & R. W. Slope. 1983. Photooxidation of hydrated Fe^{2+}: Significance for banded iron formations. Nature 303:163–164.

Breitbart, Mya, Ana Hoare, Anthony Nitti, Janet Siefert, Matthew Haynes, Elizabeth Dinsdale, Robert Edwards, Valeria Souza, Forest Rohwer, & David Hollander. 2009. Metagenomic and stable isotopic analyses of modern freshwater microbialites in Cuarto Cienegas, Mexico. Environmental Microbiology 11(1):16–34.

Breitkopf, J. H. 1988. Iron formations related to mafic volcanism and ensialic rifting in the southern margin zone of the Damara orogen, Namibia. Precambrian Research 38:111–130.

Briggs, D. E. G. 2003. The role of decay and mineralization in the preservation of soft-bodied fossils. Science 31:275–301.

Briggs, D. E. G., & Sean McMahon. 2016. The role of experiments in investigating the taphonomy of exceptional preservation. Palaeontology 59:1–11.

Briggs, D. E. G., & R. E. Summons. 2014. Ancient biomolecules: Their origins, fossilization and role in revealing the history of life. Bioessays 36(5):482–490.

Brock, T. D., M. T. Madigan, J. M. Martinko, & Jack Parker. 1994. Biology of Microorganisms. Prentice Hall. Englewood Cliffs, NJ. 909 p.

Brocks, J. J., R. Buick, G.A. Logan, & R. E. Summons. 2003a. Composition and syngeneity of molecular fossils from the 2.78 to 2.45 billion-year-old Mount Bruce Supergroup, Pilbara Craton, Western Australia. Geochimica et Cosmochimica Acta 67:4289–4319.

Brocks, J. J., R. Buick, R. E. Summons, & G. A. Logan. 2003b. A reconstruction of Archean biological diversity based on molecular fossils from the 2.78 to 2.45 billion-year-old Mount Bruce Supergroup, Hamersley Basin, Western Australia. Geochimica et Cosmochimica Acta 67:4321–4335.

Brocks, J. J., G. A. Logan, Roger Buick, & R. E. Summons. 1999. Archean molecular fossils and the early rise of eukaryotes. Science 285:1033–1036.

Brocks, J. J., G. D. Love, R. E. Summons, A. H. Knoll, G. A. Logan, & S. A. Bowden. 2005. Biomarker evidence for green and purple sulphur bacteria in a stratified Palaeoproterozoic sea. Nature 437:866–870.

Brown, D. A., G. A. Gross, & J.A. Sawicki. 1995. A review of the microbial geochemistry of banded-iron formations. Canadian Mineralogist 33:1321–1333.

Brown, M. R. W., D. G. Allison, & Peter Gilbert. 1988. Resistance of bacterial biofilms to antibiotics a growth-rate related effect? Journal of Antimicrobial Chemotherapy 22(6):777–780.

Bryers, J. D. 1988. Modeling biofilm accumulation. *In* M. J. Bazi, & J. I. Prosser, eds., Physiological Models in Microbiology. Volume 2. CRC Press. Boca Raton. p. 109–144.

Buatois, L. A., & M. G. Mángano. 2003. Early colonization of the deep sea: Ichnologic evidence of deep-marine benthic ecology from the Early Cambrian of northwest Argentina. Palaios 18:572–581.

Buatois, L. A., M. G. Mángano, E. D. Brussa, J. L. Benedetto, & J. F. Pompei. 2009. The changing face of the deep: Colonization of the Early Ordovician deep-sea floor, Puna, northwest Argentina. Palaeogeography, Palaeoclimatology, Palaeoecology 280:291–299.

Buatois, L. A., G. M. Narbonne, M. G. Mángano, N. B. Carmona, & Paul Myrow. 2014. Ediacaran matground ecology persisted into the earliest Cambrian. Nature Communications 5:3544 [doi.org/10.1038/ncomms4544].

Buatois, L. A., R. G. Netto, M. G. Mángano, & N. B. Carmona. 2013. Global deglaciation and the re-appearance of microbial matground-dominated ecosystems in the late Paleozoic of Gondwana. Geobiology 11:307–317.

Buck, S. G. 1980. Stromatolite and Ooid deposits within the fluvial and lacustrine sediments of the Precambrian Ventersdorp Supergroup of South Africa. Precambrian Research 12:311–330.

Buckley, D. H., L. K. Baumgartner, & P. T. Visscher. 2008. Vertical distribution of methane metabolism in microbial mats of the Great Sippewissett Salt Marsh. Environmental Microbiology 10:967–977.

Bühn, B., I. G. Stanistreet, & M. Okrusch. 1992. Late Proterozoic outer shelf manganese and iron deposits at Otjosondu (Namibia) related to the Damaran oceanic opening. Economic Geology 87:1393–1411.

Buick, Roger. 1984. Carbonaceous filaments from North Pole, Western Australia: Are they fossil bacteria in Archean stromatolites? Precambrian Research 24:157–172.

Buick, Roger. 1990. Microfossil recognition in Archean rocks: An appraisal of spheroids and filaments from a 3500 My old chert-barite unit at North Pole, Western Australia. Palaios 5:441–459.

Buick, Roger. 1992. The antiquity of oxygenic photosynthesis: evidence from stromatolites in sulfur-deficient Archean lakes. Science 255:74–77.

Buick, Roger & J. S. R. Dunlop. 1990. Evaporitic sediments of early Archaean age from the Warrawoona Group, North Pole, Western Australia. Sedimentology 37:247–277.

Buick, Roger, J. S. R. Dunlop, & D. I. Groves. 1981. Stromatolite recognition in ancient rocks: an appraisal of irregularly laminated structures in an Early Archaean chert-barite unit from North Pole, Western Australia. Alcheringa 5:161–181.

Bullen, T. D., A. F. White, C. W. Childs, D. V. Vivit, & M. S. Schulz. 2001. Demonstration of significant abiotic iron isotope fractionation in nature. Geology 29:699–702.

Burkhalter, R. M. 1995. Ooidal ironstones and ferruginous microbialites: Origin and relation to sequence stratigraphy (Aalenian and Bajocian, Swiss Jura Mountains). Sedimentology 42:57–74.

Burne, R. V., & L. S. Moore. 1987. Microbialites: Organosedimentary deposits of benthic microbial communities. Palaios 2:241–254.

Burne, R. V., L. S. Moore, A. G. Christy, Ulrike Troizsch, P. L. King, A. M. Carnerup, & P. J. Hamilton. 2014. Stevensite in the modern thrombolites of Lake Clifton, Western Australia: A missing link in microbialite mineralization. Geology 42:575–578.

Burrows, E. H., F. W. R. Chaplen, & R. L. Ely. 2011. Effects of selected electron transport chain inhibitors on 24-h hydrogen production by Synechocystis sp. PCC 6803. Bioresources and Technology 102(3):3062–3070.

Butler, A. D., J. A. Cunningham, G. E. Budd, & P. C. J. Donoghue. 2015. Experimental taphonomy of *Artemia* reveals the role of endogenous microbes in mediating decay and fossilization. Proceedings of the Royal Society of London B (Biological Sciences) 282:20150476 [doi.10.1098/rspb.2015.0476].

Butterfield, N. J. 2002. *Leanchoilia* guts and the interpretation of three-dimensional structures in Burgess Shale-type fossils. Paleobiology 28:155–171.

Butterfield, N. J., & F. W. Chandler. 1992. Paleoenvironmental distribution of Proterozoic microfossils, with an example from the Agu Bay Formation, Baffin Island. Palaeontology 35:943–957.

Butterfield, N. J., A. H. Knoll, & Keene Swett. 1994. Paleobiology of the Neoproterozoic Svanbergfjellet Formation, Spitsbergen. Fossils and Strata 34:1–84.

Button, A. 1976. Transvaal and Hamersley Basins-review of basin development and mineral deposits. Minerals Science and Engineering 8:262–293.

Butts, S. H. 2014. Silicification. *In* Marc Laflamme, J. D. Schiffbauer, & S. A. F. Darroch, eds., Reading and Writing of the Fossil Record: Preservational Pathways to Exceptional Fossilization. The Paleontological Society Papers, Volume 20. p. 15–33.

Byerly, G. R., D. R. Lower, & M. M. Walsh. 1986. Stromatolites from the 3,300–3,500-Myr Swaziland Supergroup, Barberton Mountain Land, South Africa. Nature 319:489–491.

Cairns-Smith, A. G. 1978. Precambrian solution photochemistry, inverse segregation, and banded iron formations. Nature 76:807–808.

Callefo, Flavia, Fresia Ricardi-Branco, G. A. Hartmann, Douglas Galante, Fabio Rodrigues, L. M. Cerqueira Peres, Elder Yokoyama, V. C. Teixeira, Nora Noffke, D. M. Bower, E. S. Bullock, A. H. Braga, J. A. H.

Coaquirs, & M. A. Fernandes. 2019. Evaluating iron as a biomarker of rhythmites: An example from the last Paleozoic ice age of Gondwana. Sedimentary Geology 383:1–15.

Callow, R. H. T., & M. D. Brasier. 2009. Remarkable preservation of microbial mats in Neoproterozoic siliciclastic settings: Implications for Ediacaran taphonomic models. Earth-Science Reviews 96:207–219.

Calner, Mikael, & M. E. Eriksson. 2012. The record of microbially induced sedimentary structures (MISS) in the Swedish Paleozoi *In* Nora Noffke & Henry Chafetz, eds., Microbial Mats in Siliciclastic Depositional Systems Through Time: SEPM Special Publication 101:29–35.

Camoin, G. F., Pascale Gautret, L. F. Montaggioni, & Guy Cabioch. 1999. Nature and environmental significance of microbialites in Quaternary reefs: The Tahiti paradox. Sedimentary Geology (126):271–304.

Campbell, K. A., J. D. Farmer, & D. Des Marais. 2002. Ancient hydrocarbon seeps from the Mesozoic convergent margin of California: Carbonate geochemistry, fluids and palaeoenvironments. Geofluids (2):63–94.

Campbell, Matthew, Kliti Grice, P. T. Visscher, Therese Morris, H. L. Wong, R. A. White, B. P. Burns, & M. J. C. Coolen. 2020. Functional gene expression in Shark Bay hypersaline microbial mats: Adaptive responses. Frontiers in Microbiology 11:2741 [doi.10.3389/fmicb.2020.560336].

Canfield, D. E. 1998. A new model for Proterozoic ocean chemistry. Nature 396:450–453.

Canfield, D. E. 2001. Biogeochemistry of sulfur isotopes. Reviews in Mineralogy and Geochemistry 4:607–36.

Canfield, D. E. 2005. The early history of atmospheric oxygen: Homage to Robert Garrels. The Annual Review of Earth and Planetary Sciences 33:1–36.

Canfield, D. E., & D. J. De Marais. 1991. Aerobic sulfate reduction in microbial mats. Science 251:1471–1473.

Canfield, D. E., & D. J. Des Marais. 1993. Biogeochemical cycles of carbon, sulphur, and free oxygen in a microbial mat. Geochimica et Cosmochimica Acta 57:3971–3984.

Canfield, D. E., K. S. Habicht, & B. Thamdrup. 2000. The Archean sulfur cycle and the early history of atmospheric oxygen. Science 288:658–61.

Canfield, D. E., & Rob Raiswell. 1991. Carbonate precipitation and dissolution, its relevance to fossil preservation. *In* P. A. Allison, & D. E. G. Briggs, eds., Taphonomy: Releasing the Data Locked in the Fossil Record, Topics in Geobiology. Vol. 9. Plenum Press. New York. p. 411–453.

Canfield, D. E., & Rob Raiswell. 1999. The evolution of the sulfur cycle. American Journal of Science 299:697–723.

Cao, Ruiji, Xunlai Yuan, & Shuhai Xiao. 2001. On morphogenesis of *Conophyton* stromatolites. Acta Palaeontologica Polonica 40:318–329.

Cardoso, D. C., Anna Sandionigi, M. S. Cretoiu, Maurizio Casiraghi, L. J. Stal & Henk Bolhuis. 2017. Comparison of the active and resident community of a coastal microbial mat. Scientific Reports 7:2969 [doi.10.1038/s41598-017-03095-z].

Carmona, N. B., J. J. Ponce, Andreas Wetzel, C. A. Bournod, & D. G. Cuadrado. 2012. Microbially induced sedimentary structures in Neogene tidal flats from Argentina: Paleoenvironmental, stratigraphic and taphonomic implications. Palaeogeography, Palaeoclimatology, Palaeoecology 353:1–9.

Casanova, Joel. 1994. Stromatolites from the East African Rift: A synopsis. *In* Janine Bertrand-Sarfati & C. L. Monty, eds., Phanerozoic stromatolites II. Springer. Berlin. p. 193–226.

Castellani, Christopher, Andreas Maas, M. E. Eriksson, J. T. Haug, Joachim Haug, & Dieter Waloszek. 2018. First record of Cyanobacteria in Cambrian Orsten deposits of Sweden. Palaeontology 61:855–880.

Castenholz, R. W. 2001. Phylum BX. Cyanobacteria. *In* D. R. Boone, R. W. Castenholz, & G. M. Garrity, eds., Bergey's Manual of Systematic Bacteriology. Volume 1. Springer New York. p. 473–599.

Caumette, Pierre. 1993. Ecology and physiology of phototrophic bacteria and sulfate-reducing bacteria in marine sediments. Experientia 49:473–481.

Censi, Paolo, Marianna Cangemi, Lorenzo Brusca, Paolo Madonia, Filipo Saiano, & Pierpaolo Zuddas. 2015. The behavior of Rare-Earth Elements, Zr and Hf during biologically-mediated deposition of silica-stromatolites and carbonate-rich microbial mats. Gondwana Research 27(1):209–215.

Chafetz, H. S. 1986. Marine peloids: A product of bacterially induced precipitation of calcite. Journal of Sedimentary Research 56(6):812–817.

Chafetz, H. S., P. F. Rush, & N. M. Utech 1991. Microenvironmental controls on mineralogy and habit of $CaCO_3$ precipitates: An example from an active travertine system. Sedimentology 1991 38:107–126.

Chagas, A. A. P., G. E. Webb, R.V. Burne, & Gordon Southam. 2016. Mocern lacustrine microbialites: Towards a synthesis of aqeous and carbonate geochemistry and minerology. Earth-Science Reviews 162:338–363.

Chan, C. S., David Emerson, & G. W. Luther, III. 2016. The role of microaerophilic Fe-oxidizing micro-organisms in producing banded iron formations. Geobiology 14:509–528.

Chan, C. S., S. C. Fakra, David Emerson, E. J. Fleming, & K. J. Edwards. 2011. Lithotrophic iron-oxidizing bacteria produce organic stalks to control mineral growth: implications for biosignature formation. The ISME Journal 5:717–727.

Chan, C. S., S. M. McAllister, A. H. Laevittt, B. T. Clazer, S. T. Krepski, & David Emerson. 2016. The architecture of iron microbial mats reflects the adaptation of chemolithotrophic iron oxidation in freshwater and marine environments. Frontiers in Microbiology 9:796 [doi.10.3389/fmicb.2016.00796].

Chang, S. B. R., & J. L. Kirschvink. 1989. Magnetofossils, the magnetization of sediments, and the evolution of magnetite biomineralization. Annual Review of Earth and Planetary Sciences 17:169–195.

Chang, S. B. R., J. F. Stolz, J. L. Kirschvink, & S. M. Awramik. 1989. Biogenic magnetite in stromatolites. II. Occurrence in ancient sedimentary environments. Precambrian Research 43:305–315.

Chen, Menge, & Kuiwu Liu. 1986. The geological significance of newly discovered microfossils from the upper Sinian (Doushantuo age) phosphorites. Scientia Geologica Sinica 1:46–53.

Chen, Zhe, Chuanming Zhou, Mike Meyer, Ke Xiang, J.D. Schiffbauer, Xunlai Yuan, & Shuhai Xiao. 2013. Trace fossil evidence for Ediacaran bilaterian animals with complex behaviors. Precambrian Research 224:690–701.

Cheney, E. S. 1996. Sequence stratigraphy and plate tectonic significance of the Transvaal succession of southern Africa and its equivalent in Western Australia. Precambrian Research 79:3–24.

Chiang, Wen-Chi, Martin Nilsson, P. Ø. Jensen, Niels Høiby, T. E. Nielsen, Michael Givskov, & Tim Tolker-Nielsen. 2013. Extracellular DNA shields against aminoglycosides in *Pseudomonas aeruginosa* biofilms. Antimicrobial Agents and Chemotherapy 57(5):2352–2361.

Chi Fru, Ernest, Magnus Ivarsson, S. P. Kilias, Stefan Bengtson, Veneta Belivanova, Federica Marone, Danielle Fortin, Curt Broman, & Marco Stampanoni. 2013. Fossilized iron bacteria reveal a pathway to the biological origin of banded iron formation. Nature Communications 4:2050 [doi.10.1038/ncomms3050].

Chisholm, S. W., S. L. Frankel, Ralf Goericke, R. J. Olson, Brian Palenik, J. B. Waterbury, Lisa West-Johnsrud, & E. R. Zettler. 1992. *Prochlorococcus marinus* nov. gen. nov. sp.:An oxyphototrophic marine prokaryote containing divinyl chlorophyll a and b. Archives of Microbiology 157:297–300.

Chivas, A. R., Thomas Torgersen, & H. A. Polach. 1990. Growth rates and Holocene development of stromatolites from Shark Bay, Western Australia. Australian Journal of Earth Sciences (37):113–121.

Chu, Daoliang, Jinnan Tong, Haijun Song, M. J. Benton, D. J. Bottjer, Huyue Song, & Li Tian. 2015. Early Triassic wrinkle structures on land: Stressed environments and oases for life. Scientific Reports 5:10109 [doi.org/10.1038/srep10109].

Ciobotă, Valerian, Walid Salama, Nicolae Tarcea, Petra Rösch, Mourtada El Aref, Reinhard Gauppc, & Jürgen Popp. 2011. Identification of minerals and organic materials in Middle Eocene ironstones from the Bahariya Depression in the Western Desert of Egypt by means of micro-Raman spectroscopy. Journal of Raman Spectroscopy 43:405–410.

Cloud, P. E. 1965. Significance of Gunflint (Precambrian) microflora: Photosynthetic oxygen may have had important local effects before becoming a major atmospheric gas. Science 148:27–35.

Cloud, P. E. 1973. Paleoecological significance of banded iron-formation. Economic Geology 68:1135–1143.

Cloud, P. E., G. R. Licari, L. A. Wright, & B. W. Troxel. 1969. Proterozoic eucaryotes from eastern California. Proceedings of the National Academy of Sciences, USA 623–630.

Cloud, P. E., & Karen Morrison. 1979. On microbial contaminants, micropseudofossils, and the oldest records of life. Precambrian Research 9:81–91.

Cloud, P. E., & M. A. Semikhatov. 1969. Proterozoic stromatolite zonation. American Journal of Science (267):1017–1061.

Coates, J. D., D. J. Ellis, C. V. Gaw, & D. R. Lovley. 1999. *Geothrix fermentans* gen. nov., sp. nov., a novel Fe(III)-reducing bacterium from a hydrocarbon-contaminated aquifer. International Journal Systematic and Evolutionary Microbiology 49:1615–1622.

Cocherie, Alain, J. Y. Calvez, & E.Oudin-Dunlop. 1994. Hydrothermal activity as recorded by Red Sea sediments: Sr-Nd isotopes and REE signatures. Marine Geology 118:291–302.

Cockell, C. S., & Aude Herrera. 2008. Why are some microorganisms boring? Trends in Microbiology 16:101–106.

Coffey, J. M., D. T. Flannery, M. R. Walter, & S. C. George. 2013. Sedimentology, stratigraphy and geochemistry of a stromatolite biofacies in the 2.72 Ga Tumbiana Formation, Fortescue Group, Western Australia. Precambrian Research 236:282–296.

Cohen, Yehuda. 2002. Bioremediation of oil by marine microbial mats. International Microbiology 5: 189–193.

Cohen, Yehuda, & Eugene Rosenberg. 1989. Microbial mats: Physiological ecology of benthic microbial communities. American Society for Microbiology. Washington. 494 p.

Cohn, Ferdinand. 1870. Über den Brunnenfaden (*Crenothrix polyspora*) mig Bemerkungen über die mikroskopische analyse des Brunnenwassers. Beitrage zur Biologie der Pflanzen, Heft 1:108–131.

Cohn, Ferdinand. 1872. Untersuchungen über Bakterien. Beiträge zur Biologie der Pflanzen, Heft 2: 127–224.

Coleman, M. L., D. B. Hedrick, D. R. Lovley, D. C. White, & Kenneth Pye. 1993. Reduction of Fe(III) in sediments by sulphate-reducing bacteria. Nature 361:436–438.

Condie, K. C. 1998. Episodic continental growth and supercontinents: A mantle avalanche connection? Earth and Planetary Science Letters 163:97–108. Condie, K. C. 2002. Continental growth during a 1.9-Ga superplume event. Journal of Geodynamics 34:249–264.

Conley, D. J., P. J. Frings, Guillaume Fontorbe, Wim Clymans, Johanna Stadmark, K. R. Hendry, A. O. Marron, & C. L. De La Roch. 2017. Biosilicification drives a decline of dissolved Si in the oceans through geologic time. Frontiers in Marine Science 4:397 [doi.10.3389/fmars.2017.00397].

Consalvey, Mireille, B. Jesus, R. G. Perkins, Vanda Brotas, G. J. C. Underwood, & D. M. Paterson. 2004. Monitoring migration and measuring biomass in benthic biofilms: The effects of dark/far-red adaptation and vertical migration on fluorescence measurements. Photosynthesis Research 81:91–101.

Corriveau, L., & P. G. Spry. 2014. Metamorphosed hydrothermal ore deposits. *In* S. D. Scott, ed., Geochemistry of Mineral Resources. Treatise on Geochemistry. 2nd Edition. Vol. 13. Elsevier. New York. p. 175–194.

Corsetti, F. A., & M. C. Storrie-Lombardi. 2003. Lossless compression of stromatolite images: A biogenicity index? Astrobiology 3:649–655.

Cosmidis, Julie, Karim Benzerara, Emmanuel Gheerbrant, Imène Estève, Baadi Bouya, & Mbarek Amaghzaz. 2013. Nanometer-scale characterization of exceptionally preserved bacterial fossils in Paleocene phosphorites from Ouled Abdoun (Morocco). Geobiology 11:139–153.

Costerton, J. W., Zbigniew Lewandowski, D. E. Caldwell, D. R. Korber, & H. M. Lappin-Scott. 1995. Microbial biofilms. Annual Review of Microbiology 49(1):711–745.

Costerton, J. W., P. S. Stewart, & E. P Greenberg. 1999. Bacterial biofilms: A common cause of persistent infections. Science 284(5418):1318–1322.

Costerton, J. W., & Paul Stoodley. 2003. Microbial biofilms: Protective niches in ancient and modern geomicrobiology. *In* W. E. Krumbein, D. M. Paterson, & G. A. Zavarzin, eds., Fossil and Recent Biofilms: A Natural History of Life on Earth. Kluwer. Dordrecht. p. 15–21.

Corkeron, Maree, G. E. Webb, Joshua Moulds, & Kathleen Grey. 2012. Discriminating stromatolite formation modes using rare earth element geochemistry: Trapping and binding versus in situ precipitation of stromatolites from the Neoproterozoic Bitter Springs Formation, Northern Territory, Australia. Precambrian Research (212-213):194–206.

Couradeau, Estelle, Karim Benzerara, Emmanuelle Gerard, David Moreira, Sylvain Bernard, G. E. Brown Jr., & Purificación López-García. 2012. An early-branching microbialite cyanobacterium forms intracellular carbonate. Science 336:459–462.

Craddock, P. R., & Nicolas Dauphas. 2011. Iron and carbonisotope evidence for microbial iron respiratio throughout the Archean. Earth and Planetary Science Letters 303:121–132.

Crépeau, Valentin, M-A. Cambon Bonavita, Françoise Lesongeur, Henintsoa Randrianalivelo, Pierre-Marie Sarradin, Jozée Sarrazin, & Anne Godfroy. 2011. Diversity and function in microbial mats from the Lucky Strike hydrothermal vent field. FEMS Microbiology Ecology 76:524–540.

Croal, L. R., C. M. Johnson, B. L. Beard, & D. K. Newman. 2004. Iron isotope fractionation by Fe(II)-oxidizing photoautotrophic bacteria. Geochimica et Cosmochimica Acta 68:1227–1242.

Croft, W. N., & E. A. George. 1959. Blue-green algae from the Middle Devonian of Rhynie, Aberdeenshire. Bulletin of the British Museum (Natural History). Geology Series 3:341–353.

Crosby, C. H., J. V. Bailey, & Mukund Sharma. 2014. Fossil evidence of iron-oxidizing chemolithotrophy linked to phosphogenesis in the wake of the Great Oxidation Event. Geology 42:1015–1018.

Crosby, H. A., C. M. Johnson, B. L. Beard, & E. E. Roden. 2007. The mechanisms of iron isotope fractionation produced during dissimilatory Fe(III) reduction by Shewanella putrefaciens and Geobacter sulfurreducens. Geobiology 5:169–189.

Crosby, H. A., C. M. Johnson, E. E. Roden, & B. L. Beard. 2005. Fe(II)-Fe(III) electron atom exchange as a mechanism for Fe isotope fractionation during dissimilatory iron oxide reduction. Environmental Science and Technology 39:6698–6704.

Crowe, S. A. J., C. Katsev, S. Magen, A. H. O'Neill, A. H. Sturm, D. E. Canfield, G. D. Haffner, A. Mucci, B. Sundby, & D. A. Fowle. 2008. Photoferrotrophs thrive in an Archean ocean analogue. Proceedings of the National Academy of Sciences, USA 105:15937–15943.

Crowe, S. A., A. H. O'Neill, S. Katsev, P. Hehanussa, G. D. Haffner, B. Sundby, A. Mucci, & D. A. Fowl. 2008. The biogeochemistry of tropical lakes: A case study from Lake Matano, Indonesia. Limnology and Oceanography 53:319–331.

Cuadrado, D. G. 2020. Geobiological model to ripple genesis and preservation in a heterolithic sedimentary sequence in a supratidal area. Sedimentology 67:2747–2763.

Cuadrado, D. G., N. B. Carmona, & Constanza Bournod. 2011. Biostabilization of sediments by microbial mats in a temperate siliciclastic tidal flat, Bahia Blanca estuary (Argentina). Sedimentary Geology 237:95–101.

Cuadrado, D. G., & JerÓnimo Pan. 2018. Field observations on the evolution of reticulate patterns in microbial mats in a modern siliciclastic coastal environment. Journal of Sedimentary Research 88:24–37.

Cuadrado, D. G., JerÓnimo Pan, E. A. Gómez, & Lucía Maisano. 2015. Deformed microbial mat structures in a semiarid temperate coastal setting. Sedimentary Geology 325:106–118.

Cuadrado, D. G., G. M. E. Perillo, & A. J. Vitale. 2014. Modern microbial mats in siliciclastic tidal flats: Evolution, structure and role in hydrodynamics. Marine Geology 352(11):367–380.

Cunningham, J. A., C.-W. Thomas, S. Bengtson, F. Marone, M. Stampanoni, F. R. Turner, J. V. Bailey, R. A. Raff, E. C. Raff, & P. C. J. Donoghue. 2012. Experimental taphonomy of giant sulphur bacteria: Implications for the interpretation of the embryo-like Ediacaran Doushantuo fossils. Proceedings of the Royal Society of London B (Biological Sciences) 279:1857–1864.

Cypionka, Heribert, Friedrich Widdel, & Norbert Pfennig. 1985. Survival of sulfate-reducing bacteria after oxygen stress, and growth in sulfate-free oxygen-sulfide gradients. FEMS Microbiology Ecology 27:189–193.

Czaja, A. D., C. M. Johnson, B. L. Beard, J. L. Eigenbrode, K. H. Freeman, & K. E. Yamaguchi. 2010. Iron and carbon isotope evidence for ecosystem and environmental diversity in the ~2.7 to 2.5 Ga Hamersley Province, Western Australia. Earth and Planetary Science Letters 292:170–180.

Czaja, A. D., C. M. Johnson, B. L. Beard, E. E. Roden, W. Li, & S. Moorbath. 2013. Biological Fe oxidation controlled deposition of banded iron formation in the ca. 3770 Ma Isua Supracrustal Belt (West Greenland). Earth Planetary Science Letters 363:192–203.

Czaja, A. D., C. M Johnson, K. E. Yamaguchi, & B. L. Beard. 2012. Comment on 'Abiotic pyrite formation produces a large Fe isotope fractionation'. Science 335(6068):538.

Daddi Oubekka, S., R. Briandet, M. P. Fontaine-Aupart, & Karine Steenkeste. 2012. Correlative time-resolved fluorescence microscopy to assess antibiotic

diffusion-reaction in biofilms. Antimicrobial Agents and Chemotherapy 56(6):3349–3358.

Dahanayake, Kapila. 1977. Classification of oncoids from the upper Jurassic carbonates of the French Jura. Sedimentary Geology (18):337–353.

Dai, Y. D., H. M. Song, & J. Y. Shen. 2004. Fossil bacteria in Xuanlong iron ore deposits of Hebei Province. Science in China Series D (Earth Sciences) 47:347–356.

Darroch, S. A. F., Marc LaFlamme, J. D. Schiffbauer, & D. E. G. Briggs. 2012. Experimental formation of a microbial death masks. Palaios 27:293–303.

Davies, D. G., M. R. Parsek, J. P. Pearson, B. H. Iglewski, J. W. Costerton, & E. P. Greenberg. 1998. The involvement of cell-to-cell signals in the development of a bacterial biofilm. Science 280: 295–297.

Davies, N. S., A. G. Liu, M. R. Gibling, & R. F. Miller. 2016. Resolving MISS conceptions and misconceptions: A geological approach to sedimentary surface textures generated by microbial and abiotic processes. Earth-Science Reviews 154:210–246.

Dauphas, Nicolas, N. L. Cates, S. J. Mojzsis, & Vincent Busigny. 2007. Identification of chemical sedimentary protoliths using iron isotopes in the >3750 Ma Nuvvuagittuq supracrustal belt, Canada. Earth and Planetary Science Letters 254:357–376.

Dauphas, Nicolas, M. van Zuilen, M. Wadhwa, A. M. Davis, B. Marty, & P. E. Janne. 2004. Clues from Fe isotope variations on the origin of Early Archean BIFs from Greenland. Science 306:2077–2080.

De Carlo, E. H., & W. J. Green. 2002. Rare earth elements in the water column of Lake Vanda, McMurdo Dry Valleys, Antarctica. et Cosmochimica Acta 66:1323–1333.

Decho, A. W. 1990. Microbial exopolymer secretions in ocean environments: their role(s) in food webs and marine processes. Oceanography Marine Biology Annual Reviews 28:73–153.

Decho, A. W. 1994. Exopolymers in microbial mats: Assessing their adaptive roles. *In* L. J. Stal & Pierre Caumette, eds., Microbial Mats: Structure, Development and Environmental Significance. NATO ASI Series G35:215–219.

Decho, A. W. 2010. Overview of biopolymer-induced mineralization: What goes on in biofilms? Ecological Engineering 36(2):137–144.

Decho, A. W. 2015. Localization of quorum sensing by extracellular polymeric substances (EPS): Considerations of in situ signaling. *In* S. J. Hagen, ed., The Physical Basis of Bacterial Quorum Communication. Biomedical Engineering book series. Springer. New York. p. 105–121.

Decho, A. W., & Tony Gutierrez. 2017. Microbial extracellular polymeric substances (EPSs) in ocean systems. Frontiers of Microbiology 8:922 [doi.10.3389/fmicb.2017.00922].

Decho A. W., Tomohiro Kawaguchi, M. A. Allison, E. M. Louchard, R. P. Reid, F. C. Stephens, K. J. Voss, R. A. Wheatcroft, & B. B. Taylor. 2003. Sediment properties influencing upwelling spectral reflectance signatures: The "biofilm gel effect." Limnology and Oceanography 48:431–443.

Decho, A. W., R. S. Norman, & P. T. Visscher. 2010. Quorum sensing in natural environments: Emerging views from microbial mats. Trends in Microbiology 18:73–80.

Decho, A. W., P. T. Visscher, & R. P. Reid. 2005. Production and cycling of natural microbial exopolymers (EPS) within a marine stromatolite. Paleogeography, Paleoclimatology, Paleoecology 219:71–86.

Decker, K. L. M., C. S. Potter, B. M. Bebout, D. J. Des Marais, Scott Carpenter, Mykell Discipulo, T. M. Hoehler, S. R. Miller, Bo Thamdrup, K. M. Turk, & P. T. Visscher. 2005. Mathematical simulation of the diel O, S, and C biogeochemistry of a hypersaline mat. FEMS Microbiology Ecology 52:377–395.

Dekov, V. M., Sven Petersen, C.-D. Garbe-Schonberg, G. D. Kamenov, Mirjam Perner, Erno Kuzmann, & Mark Schmidt. 2010. Fe-Si-oxyhydroxide deposits at a slow-spreading centre with thickened oceanic crust: The Lilliput hydrothermal field (9°33′S, Mid-Atlantic Ridge). Chemical Geology 278:186–200.

Delvinge, C., D. Cardinal, A. Hofmann, & L. André. 2012. Stratigraphic changes of Ge/Si, REE+Y and silicon isotopes as insights into the deposition of a Mesoarchean banded iron formation. Earth and Planetary Science Letters 355–356:109–118.

Demoulin, C. F., Y. J. Lara, Luc Cornet, Camille François, Denis Baurain, Annick Wilmotte, & E. J. Javaux. 2019. Cyanobacteria evolution: Insight from the fossil record. Free Radical Biology and Medicine 140:206–223.

Derenne, Sylvie, Peter Metzger, Claude Largeau, P. F. van Bergen, J. P. Gatellier, J. S. Sinninghe Damsté, J. W. de Leeuw, & Claire Berkaloff. 1991. Similar morphological and chemical variations of *Gloeocapsomorpha prisca* in Ordovician sediments and cultured *Botryococcus braunii* as a response to changes in salinity. Organic Geochemistry 19:299–313.

Des Marais, D. J. 1995. The biogeochemistry of hypersaline microbial mats. *In* J.G. Jones, ed., Advances in Microbial Ecology, vol 14. Springer. Boston. p. 251–274.

Des Marais, D. J. 2003. Biogeochemistry of hypersaline microbial mats illustrates the dynamics of modern microbial ecosystems and the early evolution of the biosphere. Biological Bulletin 204:160–167.

Des Marais, D. J., & D. E. Canfield. 1994. The carbon isotope biogeochemistry of microbial mats. Microbial Mats. NATO ASI (Series G)35:289–298.

Desnues, Christelle, V. D. Michotey, Andrea Wieland, Cui Zhizang, Aude Fourçans, Robert Duran, & P. C. Bonin. 2007. Seasonal and diel distribution of denitrifying and bacterial communities in a hypersaline mat (Camargue, France). Water Research 41(15):3407–3419.

Desnues, Christelle, Beltran Rodriguez-Brito, Steve Rayhawk, Scott Kelly, Tuong Tran, Matthew Haynes, Mike Furlan, Linda Wegley, Betty Chau, Yijun Ruan, F. E. Angly, R. A. Edwards, Linlin Li, Rebecca Vega-Thurber, R. P. Reid, Janet Siefert, Valeria Souza, D. L. Valentine, B. K. Swan, Mya Breitbart, & Forest Rohwer. 2008. Biodiversity and biogeography of phages in modern stromatolites and thrombolites. Nature 452:340–343.

De Wit, Rutger, & Hans van Gemerden. 1987. Chemolithotrophic growth of the phototrophic sulfur bacterium *Thiocapsa roseopersicina.* FEMS Microbiology Ecology 3(2):117–126.

De Wit, Rutger, H.M. Jonkers, F. P. van den Ende, & Hans van Gemerden. 1989. In situ fluctuations of oxygen and sulphide in marine microbial sediment ecosystems. Netherlands Journal of Sea Research 23(3):271–281.

De Zwart, J. M. M., & J. G. Kuenen. 1997. Aerobic conversion of dimethyl sulfide and hydrogen sulfide by *Methylophaga sulfidovorans*: Implications for modeling DMS conversion in a microbial mat. FEMS Microbiology Ecology 22(2):155–165.

Diaz, Carolina, M. C. Cortizo, P. L. Scilardi, S. G. Gomez de Saravia, M. A. Fernandez, & Lorenze de Mele. 2007. Influence of the nano-structure of the surface on bacterial adhesion. Materials Research 10(1):11–14.

Diaz, M. R., G. P. Eberli, Patricia Blackwelder, Brian Phillips, & P. K. Swart. 2017. Microbially mediated organomineralization in the formation of ooids. Geology 45(9):771–774.

Dick, G. J., S. L. Grim, & J. M. Klatt. 2018. Controls On O_2 Production In Cyanobacterial Mats And Implications For Earth's Oxygenation. Annual Review Of Earth And Planetary Sciences 46(1):123–147.

Didyk, B. M., B. R. T. Simoneit, S. C. Brassell, & Geoffrey Eglington. 1978. Organic geochemical indicators of paleoenvironmental conditions of sedimentation Nature 272:216–222.

Dill, R. F., E. A. Shinn, A. T. Jones, K. M. Kelly, & R. P. Steinen 1986. Giant subtidal stromatolites forming in normal salinity waters. Nature (324):55.

Dilling, Waltraud, & Heribert Cypionka. 1990. Aerobic respiration in sulfate-reducing bacteria. FEMS Microbiology Letters 71:123–128.

Dillon, M. L., Ian Hawes, A. D. Jungblut, T. J. Mackey, J. A. Eisen, P. T. Doran, & D. Y. Sumner. 2020. Environmental control on the distribution of metabolic strategies of benthic microbial mats in Lake Fryxell, Antarctica. PLOS One 15(4)e0231053 [doi.org/10.1371/journal.pone.0231053].

Djokic, Tara, M. J. van Kranendonk, K. A. Campbell M. R. Walter, & C. R. Ward. 2017. Earliest signs of life on land preserved in ca. 3.5 Ga hot spring deposits. Nature Communications 8:15263 [doi.10.1038/ncomms15263].

Dodd, M. S., Dominic Papineau, Tor Grenne, J. F. Slack, Martin Rittner, Franco Pirajno, J. O. O'Neil, & C. T. Little. 2017. Evidence for early life in Earth's oldest hydrothermal vent precipitates. Nature 543:60–64.

Doemel, W. N., & T. D. Brock. 1977. Structure, growth, and decomposition of laminated algal-bacterial mats in alkaline hot springs. Applied and Environmental Microbiology 34:433–452.

Dong, Lin, Shuhai Xiao, Bing Shen, Chuanming Zhou, Guoxiang Li, & Jinxian Yao. 2009. Basal Cambrian microfossils from the Yangtze Gorges area (South China) and the Aksu area (Tarim Block, northwestern China). Journal of Paleontology 83:30–44.

Donlan, R. M. 2002. Biofilms: microbial life on surfaces. Emerging Infectious Diseases 8(9):881–890.

Dörfelt, Heinrich, A. R. Schmidt, & Jörg Wunderlich. 2000. *Rosaria succina* spec. nov.: A fossil cyanobacterium from Tertiary amber. Journal of Basic Microbiology 40:327–332.

Draganits, Erich, & Nora Noffke. 2004. Siliciclastic stromatolites and other microbially induced sedimentary structures in an early Devonian barrier-island environment (Muth Formation, NW Himalayas). Journal of Sedimentary Research 74:191–202.

Dragoš, Anna, H. T. Kiesewalter, Marivic Martin, Hsu C.-Y., Raimo Hartmann, Tobias Wechsler, Carsten Eriksen, Susanne Brix, Knut Drescher, Nicola Stanley-Wall, Rolf Kümmerli, & Á. T. Kovács. 2018. Division of labor during biofilm matrix production. Current Biology 28(12):1903–1913.

Dravis, J. J. 1983. Hardened subtidal stromatolites, Bahamas. Science (219):385–386.

Driese, S. G., M. A. Jirs, Minghua Ren, S. L. Brantley, N. D. Sheldon, Don Parker, & Mark Schmitz. 2011. Neoarchean paleoweathering of tonalite and metabasalt: Implications for reconstructions of 2.69 Ga early terrestrial ecosystems and paleoatmospheric chemistry. Precambrian Research 189 (1): 1–17.

Duda, J.-P., M. J. van Kranendonk, Volker Thiel, Danny Ionescu, Harald Strauss, Nadine Schäfer, & Joachim Reitner. 2016. A Rare Glimpse of Paleoarchean Life: Geobiology of an Exceptionally Preserved Microbial Mat Facies from the 3.4 Ga Strelley Pool Formation, Western Australia. PLOS One 11(1):e0147629 [doi.10.1371/journal.pone.014629].

Dunn, F. S., A. G. Liu, & P. C. J. Donoghue. 2018. Ediacaran developmental biology. Biological Reviews 93:914–932.

Dupraz, Christophe, Ronny Pattisina, & E. P. Verrecchia. 2006. Translation of energy into morphology: Simulation of stromatolite morphospace using a stochastic model. Sedimentary Geology 185:185–203.

Dupraz, C., R. P. Reid, O. Braissant, A. W. Decho, R. S. Norman, & P. T. Visscher. 2009. Processes of carbonate precipitation in modern microbial mats. Earth-Science Reviews 96(3):141–162.

Dupraz, Christophe, R. P. Reid, & P. T. Visscher. 2011. Modern Microbialites. *In* Joachim Reitner & Volker Thiel, eds., Encylopedia of Geobiology. Springer. Berlin. p. 617–634.

Dupraz, Christophe, & Andre Strasser. 1999. Microbialites and micro-encrusters in shallow coral bioherms (Middle to Late Oxfordian, Swiss Jura mountains). Facies (40):101–129.

Dupraz, Christophe, & Andre Strasser. 2006. Microbialites and micro-encrusters in shallow coral bioherms (Middle to Late Oxfordian, Swiss Jura mountains). Facies (40):101–129.

Dupraz, Christophe, & P. T. Visscher. 2005. Microbial lithification in modern marine stromatolites and hypersaline mats. Trends in Microbiology 13(9):429–438.

Dupraz, Christophe, P. T. Visscher, L. K. Baumgartner, & R. P. Reid. 2004. Microbe-mineral interactions: Early carbonate precipitation in a hypersaline lake (Eleuthera Island, Bahamas). Sedimentology 51:745–765.

Duteil, Thibault, Raphaël Bourillot, Brian Grégoire, Maxime Virolle, Benjamin Brigaud, Julius Nouet, Olivier Braissant, Eric Portier, Hugues Féniès, Patricia Patrier, Etienne Gontier, Isabelle Svahn, & P. T. Visscher. 2020. Experimental formation of clay-coated sand grains using diatom biofilm exopolymers. Geology 48(10):1012–1017.

Dymek, R. F., & Cornelis Klein. 1988. Chemistry, petrology, and origin of banded iron formation lithologies from the 3800 Ma Isua supracrustal belt, West Greenland. Precambrian Research 39:247–302.

Edwards, Dianne, Lindsey Axe, John Parkes, & David Rickard. 2006. Provenance and age of bacteria-like structures on mid-Palaeozoic plant fossils. International Journal of Astrobiology 5:109–142.

Edwards, D. S., & A. G. Lyon. 1983. Algae from the Rhynie chert. Botanical Journal of the Linnean Society 86:37–55.

Edwards, K. J., T. M. Gihring, & J. F. Banfield. 1999. Seasonal variations in microbial populations and environmental conditions in an extreme acid mine drainage environment. Applied and Environmental Microbiology 65:3627–3632.

Ehrenberg, C. G. 1835. Die Akalephen des rothen Meeres und der Organismus der Medusen der Ostsee. Abhandlungen der Königlichen Akademie der Wissenschaften zu Berlin. p. 181–260.

Ehrenberg, D. C. G. 1836. Vorläufige Mittheilungen über das wirkliche Vorkommen fossiler Infusorien und ihre grosse Verbreitung. Annalen der Physik und Chemie 38:213–227.

Ehrenberg, D. C. G. 1838. Die Infusionsthierchen als vollkommene Organismen. L. Voss. Leipzig. 577 p.

Ehrenreich, Armin, & Friedrich Widdel. 1994. Anaerobic oxidation of ferrous iron by purple bacteria, a new type of phototrophic metabolism. Applied and Environmental Microbiology 60:4517–4526.

Ehrlich, H. L., & D. K. Newman. 2009. Geomicrobiology (5th edition). CRC Press/Taylor & Francis. Boca Raton. 606 p.

Eigenbrode, J. L., & K. H. Freeman. 2006. Late Archean rise of aerobic microbial ecosystems. Proceedings of the National Academy of Sciences, USA 103:15759–15764.

Eigenbrode, J. L., K. H. Freeman, & R. E. Summons. 2008. Methylhopane biomarker hydrocarbons in Hammersley Province sediments provide evidence for Neoarchean aerobiosis. Earth and Planetary Science Letters 273(3–4):323–331.

Elderfield, Henry. 1988. The oceanic chemistry of the rare-earth elements. Philosophical Transactions of the Royal Society of London (series A) 325:105–126.

Elias, Sivan, & Ehud Banin. 2012. Multi-species biofilms: Living with friendly neighbors. FEMS Microbiology Reviews 36(5):990–1004.

Elling, F. J., J. D. Hemingway, T. W. Evans, J. J. Kharbush, Eva Spieck, R. E. Summons, & Ann Pearson. 2020. Vitamin B12-dependent biosynthesis ties amplified 2-methylhopanoid production during oceanic anoxic events to nitrification. Proceedings of the National Academy of Sciences, USA 117:32996–33004.

Elmore, R. D. 1983. Precambrian non-marine stromatolites in alluvial fan deposits, Copper Harbor Conglomerate, upper Michigan. Sedimentology 30:829–842.

Emerson, David, E. J. Fleming, & J. M. McBeth. 2010. Iron-oxidizing bacteria: An environmental and genomic perspective. Annual Review of Microbiology 64:561–583.

Emerson, David, & C. L. Moyer. 2002. Neutrophilic Fe-oxidizing bacteria are abundant at the Loihi seamount hydrothermal vents and play a major role in Fe oxide deposition. Applied and Environmental Microbiology 68:3085–3093.

Emerson, David, J. A. Rentz, T. G. Lilburn, R. E. Davis, Henry Aldrich, Clara Chan, & C. L. Moyer. 2007. A novel lineage of Proteobacteria involved in formation of marine fe-oxidizing microbial mat communities. PLOS One 2(8):e667 [doi.10.1371/journal.pone.0000667].

Emerson, David, & N. P. Revsbech. 1994. Investigation of an iron-oxidizing microbial mat community located near Aarhus, Denmark: Field studies. Applied and Environmental Microbiology 60(11):4022–4031.

Erikson, Dagny. 1949. The morphology, cytology, and taxonomy of the Actinomycetes. Annual Review of Microbiology 3:23–54.

Eriksson, P. G., S. Banerjee, Octavian Catuneanu, Subir Sarkar, A. J. Bumby, & M. N. Mtimkulu. 2007. Prime controls on Archaean-Palaeoproterozoic sedimentation: Change over time. Gondwana Research (12):550–559.

Eriksson, P. G., Rajat Mazumder, Octavian Catuneanu, A. J. Bumby, & B. Ountsché Ilondo. 2006. Precambrian continental freeboard and geological evolution: A time perspective. Earth-Science Reviews (79):165–204.

Eriksson, P. G., Subir Sarkar, Paradip Samanta, Santanu Banerjee, Huberus Porada, & Octavian Catuneau. 2010. Paleoenvironmental context of microbial mat-related structures in siliciclastic rocks. *In* Joseph Seckbach & Aharon Oren, eds., Microbial Mats. Cellular Origin, Life in Extreme Habitats and Astrobiology, vol. 14. Springer. Dordrecht. p 71–108.

Eriksson, P. G., E. L. Simpson, K. A. Eriksson, A. J. Bumby, G. L. Steyn, & Subir Sarkar. 2000. Muddy roll-up structures in siliciclastic interdune beds of the ca. 1.8 Ga Waterberg Group, South Africa. Palaios 15:177–183.

Espinosa-Ortiz, Erika J. and Robin Gerlach. 2021. Part B, Chapter 2: Biofilms. Treatise Online 147: 1–12, 3 fig.

Ewers, W. E. 1980. Chemical conditions for the precipitation of banded iron-formations. *In* P. A. Trudinger, M. R. Walter, & B. J. Ralph, eds., Biogeochemistry of Ancient and Modern Environments. Springer-Verlag. Netley, Australia. p. 83–92.

Ewers, W. E., & R. C. Morris. 1981. Studies of the Dales Gorge Member of the Brockman Iron Formation, Western Australia. Economic Geology 76:1929–1953.

Fabre, S., A. Nédélec, F. Poitrasson, H. Strauss, C. Thomazo, & A. Nogueira. 2011. Iron and sulphur

isotopes from the Carajás mining province (Pará, Brazil): Implications for the oxidation of the ocean and the atmosphere across the Archaean–Proterozoic transition. Precambrian Research 289:124–139.

Fadel, Alexandre, Kevin Lepot, Vincent Busigny, Ahmed Addad, & David Troadec. 2017. Iron mineralization and taphonomy of microfossils of the 2.45–2.21 Ga Turee Creek Group, Western Australia. Precambrian Research 298:530–551.

Fan, Haoxin, Henk Bolhuis, & L. J. Stal. 2015. Nitrification and nitrifying bacteria in a coastal microbial mat. Frontiers in Microbiology 6:1367 [doi.103389/fmicb.2015.01367].

Farias, M. E., Manuel Contreras, M. C. Rasuk, Daniel Kurth, R. Flores, J. Maldonado, D. G. Poiré, Fernando Novoa, & P. T. Visscher. 2014. Characterization of bacterial diversity associated with microbial mats, gypsum evaporites, and carbonate microbialites in thalassic wetlands: Tebenquiche and Brava, Salar de Atacama, Chile. Extremophiles 18:311–329.

Farias, M. E., M. C. Rasuk, K. L. Gallagher, M. C. Contreras, Daniel Kurth, A. B. Fernandez, D. G. Poiré, Fernando Novoa, & P. T. Visscher. 2017. Prokaryotic diversity and biogeochemical characteristics of benthic microbial ecosystems at La Brava, a hypersaline lake at Salar de Atacama, Chile. PLOS One 12(11):e0186867 [doi.10.1371/journal.pone.0186867].

Farquhar, James, Huiming Bao, & Mark Thiemens. 2000. Atmospheric influence of Earth's earliest sulfur cycle. Science 289:756–758.

Farquhar, James, & D. T. Johnston. 2008. The oxygen cycle of the terrestrial planets: Insights into the processing and history of oxygen in surface environments. Reviews in Mineralogy and Geochemistry 68:463–492.

Farquhar, James, & B. A. Wing. 2003. Multiple sulfur isotopes and the evolution of the atmosphere. Earth and Planetary Science Letters 213:1–13.

Farquhar, James, & B. A. Wing. 2005. The terrestrial record of stable sulphur isotopes: A review of the implications for evolution of Earth's sulphur cycle. Geological Society Special Publication 248:167–177.

Fedonkin, M. A. 1992. Vendian Faunas and the Early Evolution of Metazoa. *In* J. H. Lipps & P. W. Signor, eds., Origin and Early Evolution of the Metazoa. Springer. Heidelberg. p. 87–129.

Fedorchuk, N. D. 2014. Evaluating the Biogenicity of Fluvial-lacustrine Stromatolites from the Mesoproterozoic Copper Harbor Conglomerate, Upper Peninsula of Michigan, USA. Theses and Dissertations, vol. 403. p. 1–161.

Fedorchuk, N. D., S. Q. Dornbos, F. A. Corsetti, J. L. Isbell, V. A. Petryshyn, J. A. Bowles, & D. T. Wilmeth. 2016. Early non-marine life: Evaluating the biogenicity of Mesoproterozoic fluvial-lacustrine stromatolites. Precambrian Research (275):105–118.

Feng, Xueqian, Z.-Q. Chen, D. J. Bottjer, Siqu Wu, Laishi Zhao, Yaling Xu, G. R. Shid, Yuangeng Huang, Yuheng Fang, & Chenyi Tu. 2019. Unusual shallow marine matground-adapted benthic biofacies from the Lower Triassic of the northern Paleotethys: Implications for biotic recovery following the end-Permian mass extinction. Earth-Science Reviews 189:194–219.

Fenton, C. L. 1946. Algae of the Pre-Cambrian and Early Paleozoic. The American Midland Naturalist 36:259–263.

Fernández, A. B., M. C. Rasuk, P. T. Visscher, M. C. Contreras, Fernando Novoa, Daniel Poiré, M. M. Patterson, Antonio Ventosa, & M. E. Farias. 2016. Microbial diversity in sediment ecosystems (evaporites domes, microbial mats, and crusts) of hypersaline Laguna Tebenquiche, Salar de Atacama, Chile. Frontiers in Microbiology 7:1284 [doi.10.3389/fmicb.2016.01284].

Fernández, D. E., & P. J. Pazos. 2014. Xiphosurid trackways in a Lower Cretaceous tidal flat in Patagonia: Palaeoecological implications and the involvement of microbial mats in trace-fossil preservation. Palaeogeography, Palaeoclimatolology, Palaeoecology 375:16–29.

Ferris, F. G., T. J. Beveridge, & W. S. Fyfe. 1986, Iron-silica crystallite nucleation by bacteria in a geothermal sediment. Nature 320:609–610.

Ferris, F. G., W. S. Fyfe, & T. J. Beveridge. 1987. Bacteria as nucleation sites for authigenic minerals in a metal-contaminated lake sediment. Chemical Geology 63:225–232.

Ferris, F. G., W. S. Fyfe, & T. J. Beveridge. 1988. Metallic ion binding by *Bacillus subtilis*: Implications for the fossilization of microorganisms. Geology 16:149–152.

Ferris, M. J., S. C. Nold, N. P. Revsbech, & D. M. Ward. 1997. Population structure and physiological changes within a hot spring microbial mat community following disturbance. Applied and Environmental Microbiology 63(4):1367–1374.

Findlay, A. J. 2016. Microbial impact on polysulfide dynamics in the environment. FEMS Microbiology Letters 363(11):fnw103 [doi.10.1093/femsle/fnw103].

Finke, Nico, R. L. Simister, A. H. O'Neil, S. Nomosatryo, C. Henny, L. C. MacLean, D. E. Canfield, Kurt Konhauser, S. V. LaLonde, D. A. Fowle, & S. A. Crowe. 2019. Mesophilic microorganisms build terrestrial mats analogous to Precambrian microbial jungles. Nature Communications 10:4323 [doi.10.1038/s41467-019-11541-x].

Fischer, Sadie, & Philip Fralick. 2020. Biological mats in siliciclastic sediments of the Paleoproterozoic Gunflint Formation, northwestern Ontario, Canada. Canadian Journal of Earth Sciences 57(8):947–953.

Fischer, W. W., & A. H. Knoll. 2009. An iron shuttle for deep-water silica in Late Archean and early Paleoproterozoic iron formation. Geological Society of America Bulletin 121:222–235.

Fischer, W. W., S. Schroeder, J. P. Lacassie, N. J. Beukes, T. Goldberg, H. Strauss, U. E. Horstmann, D. P. Schrag, & A. H. Knoll. 2009. Isotopic constraints on the Late Archean carbon cycle from the Transvaal Supergroup along the western margin of the Kaapvaal craton, South Africa. Precambrian Research 169:15–27.

Flannery, D. T., & M. R. Walter. 2011. Archean tufted

microbial mats and the Great Oxidation Event: New insights into an ancient problem. Australian Journal of Earth Sciences 59:1–11.
Flemming, H.-C. 1995. Sorption sites in biofilms. Water Science and Technology 32(8):27–33.
Flemming, H.-C., T. R. Neu, & D. J. Wozniak. 2007. The EPS matrix: The 'house of biofilm cells'. Journal of Bacteriology 189:7945–7947.
Flemming, H.-C., & Jost Wingender. 2010. The biofilm matrix. Nature Reviews Microbiology 8:623–633.
Flemming, H.-C., Jost Wingender, Ulrich Szewzyk, Peter Steinberg, S. A. Rice, & Staffan Kjelleberg. 2016. Biofilms: An emergent form of bacterial life. Nature Reviews Microbiology 14(9):563–575.
Flemming, H.-C., & Stefan Wuertz. 2019. Bacteria and archaea on Earth and their abundance in biofilms. Nature Reviews Microbiology 17:247–260.
Flick, H, H. D. Nesbor, & R. Behnisch. 1990. Iron ore of the Lahn-Dill type formed by diagenetic seeping of pyroclastic sequences: A case study on the Schalstein section at Gänsberg (Weilburg). International Journal of Earth Sciences 79:1401–415.
Flombaum, Pedro, J. L. Gallegos, R. A. Gordillo, José Rincón, L. L. Zabala, Nianzhi Jiao, D. M. Karl, W. K. W. Li, M. W. Lomas, Daniele Veneziano, C. S. Vera, J. A. Vrugt, & A. C. Martiny. 2013. Present and future global distributions of the marine Cyanobacteria *Prochlorococcus* and *Synechococcus*. Proceedings of the National Academy of Sciences, USA 110:9824–9829.
Flügel, Erik. 2004. Microfacies of Carbonate Rocks: Analysis, Interpretation and Application. Springer-Verlag. Berlin & Heidelberg. 976 p.
Flügel, Erik. 2010. Microfacies of Carbonate Rocks: Analysis, Interpretation and Application, second edition. Springer-Verlag. Berlin & Heidelberg. 924 p. .
Flügel, Erik, & T. Steiger. 1981. An Upper Jurassic sponge- algal buildup from the northern Frankenalb, West Germany. *In* Donald F. Toomey., ed., European Fossil Reef Models. Society for Sedimentary Geology, Special Publication 30. Tulsa. p. 371–397.
Folk, R. L. 1987. Detection of organic matter in thin-sections of carbonate rocks using a white card. Sedimentary Geology 54:193–200.
Foster, C. B., J. D. Reed, & Reed Wicander. 1989. *Gloeocapsomorpha prisca* Zalessky, 1917: A new study part I: Taxonomy, geochemistry, and paleoecology. Geobios 22:735–759.
Fralick, P. W. 1989. Microbial bioherms, Lower Proterozoic Gunflint Formation, Thunder Bay, Ontario. *In* H. H. J. Geldsetzer, N. P. James, & G. E. Tebbutt, eds., Reefs: Canada and Adjacent Areas. Memoirs, Canadian Society of Petroleum Geologists. p. 24–29.
Fralick, P. W., S. W. Poulton, & D. E. Canfield. 2011. Does the Paleoproterozoic Animikie Basin record the sulfidic ocean transition? Comment. Geology 39 (5):e241[doi.10.1130/G31747C.1].
Fralick, P. W., & P. K. Pufahl. 2006. Iron formation in Neoarchean deltaic successions and the microbially mediated deposition of transgressive systems tracts. Journal of Sedimentary Research 76:1057–1066.
Fralick, P. W., & Robert Riding. 2015. Steep Rock Lake: Sedimentology and geochemistry of an Archean carbonate platform. Earth-Science Reviews (151):132–175.
François, L. M. 1986. Extensive deposition of banded iron formations was possible without photosynthesis. Nature 320:352–354.
Frankel, R. B., & D. A. Bazylinski. 2003. Biologically induced mineralization by bacteria. Reviews in Mineralogy and Geochemistry. Biomineralization 54:95–114.
Franklin, J. M., H. L. Gibson, I. R. Jonasson, & A. G. Galley. 2005. Volcanogenic massive sulfide deposits. Economic Geology, 100th Anniversary Volume. p. 523–560.
Franks, Jonathan, & J. F. Stolz. 2009. Flat laminated microbial mat communities. Earth-Science Reviews 96:163–172.
Frantz, C. M., V. A. Petryshyn, & F. A. Corsetti. 2015. Grain trapping by filamentous cyanobacterial and algal mats: Implications for stromatolite microfabrics through time. Geobiology 13:409–423.
Frantz, C. M., V. A. Petryshyn, P. J. Marenco, Aradhna Tripati, W. M. Berelson, & F. A. Corsetti. 2014. Dramatic local environmental change during the early Eocene climatic optimum detected using high resolution chemical analyses of Green River Formation stromatolites. Palaeogeography, Palaeoclimatology, Palaeoecology (405):1–15.
French, K. L., C. Hallmann, J. M. Hope, P. L. Schoon, J. A. Zumberge, Yosuke Hoshino, C. A. Peters, S. C. George, G. D. Love, J. J. Brocks, Roger Buick, & R. E. Summons. 2015. Reappraisal of hydrocarbon biomarkers in Archean rocks. Proceedings of the National Academy of Sciences, USA 112:5915–5920.
Freytet, Pierre, & E. P. Verrecchia. 1998. Freshwater organisms that build stromatolites: A synopsis of biocrystallization by prokaryotic and eukaryotic algae. Sedimentology 45:535–563.
Friend, P. L., C. H. Lucas, P. M. Holligan, & M. B. Collins. 2008. Microalgal mediation of ripple mobility. Geobiology 6:70–82.
Frimmel, H. E. 2008. The Gariep Belt. *In* R. M. Miller, ed., The Geology of Namibia. Handbook of the Geological Survey of Namibia, Geological Survey of Namibia. p. 1–39.
Fründ, Claudia, & Yehuda Cohen. 1992. Diurnal cycles of sulfate reduction under oxic conditions in cyanobacterial mats. Applied and Environmental Microbiology 58(1):70–77.
Fryer, B. J. 1976. Rare earth evidence in iron-formations for changing Precambrian oxidation states. Geochimica et Cosmochimica Acta 41:361–367.
Furnes, Harald, N. R. Banerjee, Karlis Muehlenbachs, Hubert Staudigel, & Maarten de Wit. 2004. Early life recorded in Archean pillow lavas. Science 304:578–581.
Gaillard, Christian, & P. R. Racheboeuf. 2006. Trace fossils from nearshore to offshore environments: Lower Devonian of Bolivia. Journal of Paleontology 80:1205–1226.
Gaines, R. P., E. G. Briggs, & Yuanlong Zhao. 2008. Cambrian Burgess Shale Deposits share a common mode of fossilization. Geology 36:755–758.
Gallagher, K. L., Christophe Dupraz, Olivier Braissant,

R. S. Norman, A. W. Decho, & P. T. Visscher. 2011. Mineralization of sedimentary biofilms: Modern mechanistic insights. *In* W. C. Bailey, ed., Biofilms: Formation, Development and Properties. NOVA Publishers. New York. p. 227–258.

Gallagher, K. L., Christophe Dupraz, & P. T. Visscher. 2014. Two opposing effects of sulfate reduction on carbonate precitation in normal marine, hypersaline, and alkaline environments (Comment). Geology 42:313–314.

Gallagher, K. L., T. J. Kading, Olivier Braissant, Christophe Dupraz & P. T. Visscher. 2012. Inside the alkalinity engine: The role of electron donors in the organomineralization potential of sulfate-reducing bacteria. Geobiology 10:518–530.

Gallardo, V. A. 1977. Large benthic microbial communities in sulphide biota under Peru-Chile subsurface counter current. Nature 268:331–332.

Gallardo, V. A., & Carola Espinoza. 2007. New community of large filamentous sulfur bacteria in the eastern South Pacific. International Microbial 10:97-102.

Gan, Tian, Taiyi Luo, Ke Pang, Chuanming Zhou, Guanghong Zhou, Bin Wan, Gang Li, Qiru Yi, A. D. Czaja, & Shuhai Xiao. 2021. Cryptic terrestrial fungus-like fossils of the early Ediacaran Period. Nature Communications 12:641 [doi.10.1038/s41467-021-20975-1].

Garcia-Pichel, Ferran, Jonathan Lombard, Tanya Soule, Sean Dunaj, S. H. Wu, & M. F. Wojciechowski. 2019. Timing the evolutionary advent of cyanobacteria and the later Great Oxidation Event using gene phylogenies of a sunscreen. mBio (American Society for Microbiology) 10:e00561–00519 [doi.10.1128/mBio.00561-19].

García-Ruiz, J. M., S. T. Hyde, A. M. Carnerup, A. G. Christy, M. J. van Kranendonk, & N. J. Welham. 2003. Self-assembled silica-carbonate structures and detection of ancient microfossils. Science 302:1194–1197.

García-Ruiz, J. M., Elias Nakouzi, Electra Kotopoulou, Leonardo Tamborrino, & Oliver Steinbock. 2017. Biomimetic mineral self-organization from silica-rich spring waters. Science Advances 3:e1602285 [doi.10.1126/sciadv.1602285].

Garrels, R. M. 1987. A model for the deposition of the microbanded Precambrian iron formations. American Journal of Science 287:81–106.

Garrels, R. M., & E. A. J. Perry. 1974. Cycling of carbon, sulfur, and oxygen through geologic time. *In* E. A. Goldberg, ed., The Sea. Wiley. New York. p. 303–336.

Garzani, Eduardo. 1993. Himalayan ironstones, "superplumes," and the breakup of Gondwana. Geology 21:105–108.

Gaylarde, C. C., & P. M. Gaylarde. 2005. A comparative study of the major microbial biomass of biofilms on exteriors of buildings in Europe and Latin America. International Biodeterioration & Biodegradation 55(2):131–139.

Gebelein, C. D. 1969. Distribution, morphology, and accretion rate of recent subtidal algal stromatolites, Bermud.: Journal of Sedimentary Petrology (39):49–69.

Gehling, J. G. 1999. Microbial mats in terminal Proterozoic siciliclasts: Ediacaran death masks. Palaios 14(1):40–57.

Gehling, J. G., & Mary Droser. 2009. Textured organic surfaces associated with the Ediacara biota in South Australia. Earth-Science Reviews 96:196–206.

van Gemerden, Hans. 1993. Microbial mats: A joint venture. Marine Geology 113(1–2):3–25.

van Gemerden, Hans, & Jordi Mas. 1995. Ecology of phototrophic sulfur bacteria. *In* R. E. Blankenship, M. T. Madigan, & C. E. Bauer, eds., Anoxygenic Photosynthetic Bacteria (Advances in Photosynthesis and Respiration, Vol 2). Kluwer Academic Publishers. Dordrecht. p. 50–85.

Gerbersdorf, S. U., Thomas Jancke, Bernhard Westrich, & D. M. Paterson. 2008. Microbial stabilization of riverine sediments by extracellular polymeric substances. Geobiology 6:57–69.

Gerbersdorf, S. U., & Silke Wieprecht. 2015. Biostabilization of cohesive sediments: Revisiting the role of abiotic conditions, physiology and diversity of microbes, polymeric secretion, and biofilm architecture. Geobiology 13:68–97.

Gerdes, Gisela. 2007. Structures left by modern microbial mats in their host systems. *In* Jürgen Schieber, P. K. Bose, P. G. Eriksson, S. Banerjee, S. Sarkar, W. Altermann, & O. Catuneau, eds., Atlas of Microbial Mat Features Preserved Within the Clastic Rock Record. Elsevier Science. Amsterdam. p. 5–38.

Gerdes, Gisela, Thomas Klenke, & Nora Noffke. 2000. Microbial signatures in peritidal siliciclastic sediments: A catalogue. Sedimentology 47:279–308.

Gerdes, Gisela, & W. E. Krumbein. 1987. Biolaminated Deposits. Springer. Heidelberg. 193 p.

Gerdes, Gisela, W. E. Krumbein, & Nora Noffke. 2000. Evaporite microbial sediments. *In* Robert Riding & S. M. Awramik, eds., Microbial Sediments. Springer. Berlin. p. 196–208.

Gerdes, Gisela, W. E. Krumbein, & H. E. Reineck. 1985. The depositional record of sandy, versicolored tidal flats (Mellum Island, southern North Sea). Journal of Sedimentary Petrology 55:265–78.

Gerdes, Gisela, W. E. Krumbein, & H. E. Reineck. 1991. Biolaminations: Ecological versus depositional dynamics. *In* G. Einsele, W. Ricken, & A. Seilacher, eds., Cycles and Events in Stratigraphy. Springer. Berlin. p. 592–610.

Gerdes, Gisela, W. E. Krumbein, & H E. Reineck. 1994. Microbial mats as architects of sedimentary surface structures. *In* W. E. Krumbein, D. M. Paterson, & L .J. Stal, eds., Biostabilization of Sediments. BIS-Verlag. Oldenburg. p. 165–182.

German, C. R. & Henry Elderfield. 1990. Application of the Ce-anomaly as a paleoredox indicator: The ground rules. Paleoceanography 5:823–833.

van Gestel, Jordi, Hera Vlamakis, & Roberto Kolter. 2015. From cell differentiation to cell collectives: Bacillus subtilis uses division of labor to migrate. PLOS Biology 13(4):1002141 [doi.org/10.1371/journal.pbio.1002141].

Ghiorse, W. C., & H. L. Ehrlich. 1992. Microbial biomineralization of iron and manganese. *In* H. C. W. Skinner & R. W Fitzpatrick, eds., Biomineraliza-

tion. Processes of iron and manganese. Cremlingen. Catena Supplement 21:75–99.
Gibson, T. M., P. M. Shih, V. M. Cumming, W. W. Fischer, P. W. Crockford, M. S. W. Hodgskiss, Sarah Wörndle, R. A. Creaser, R. H. Rainbird, T. M. Skulski, & G. P. Halverson. 2018. Precise age of *Bangiomorpha pubescens* dates the origin of eukaryotic photosynthesis. Geology 46:135–138.
Ginsburg, R. N. 1991. Controversies about stromatolites: Vices and virtues. *In* D. W. Müller, J. A. McKenzie, & H. Weissert, eds., Controversies in Modern Geology. Academic Press. London. p. 25–36.
Gischler, Eberhard, M. A. Gibson, & Wolfganschmann. 2008. Giant Holocene freshwater microbialites, Laguna Bacalar, Quintana Roo, Mexico. Sedimentology (55):1293–1309.
Glumac, Bosiljka, & K. R. Walker. 1997. Selective dolomitization of Cambrian microbial carbonate deposits: A key to mechanisms and environments of origin. Palaios (2):98–110.
Golubic, Stjepko, & E. S. Barghoorn. 1977. Interpretation of microbial fossils with special reference to the Precambrian. *In* Erik Flügel, ed., Fossil Algae: Recent Results and Developments. Springer-Verlag. Berlin. p. 1–14.
Golubic, Stjepko, & J. W. Focke. 1978. *Phormidium hendersonii* Howe: Identity and significance of a modern stromatolite building microorganism. Journal of Sedimentary Research 48:751–764.
Golubic, Stjepko, & H. J. Hofmann. 1976. Comparison of Holocene and mid-Precambrian Entophysalidaceae (Cyanophyta) in stromatolitic algal mats: Cell division and degradation. Journal of Paleontology 50:1074–1082.
Golubic, Stjepko, & Seong-Joo Lee. 1999. Early cyanobacterial fossil record: Preservation, palaeoenvironments and identification. European Journal of Phycology 34:339–348.
Golubic, Stjepko, R. D. Perkins, & K. J. Lukas. 1975. Boring microorganisms and microborings in carbonate substrates. *In* R. W. Frey, ed., The Study of Trace Fossils. Springer-Verlag. Berlin. p. 229–259.
Golubic, Stjepko, A. M. Pietrini, & Sandra Ricci. 2015. Euendolithic activity of the cyanobacterium *Chroococcus lithophilus* Erc. in biodeterioration of the Pyramid of Caius Cestius, Rome, Italy. International Biodeterioration & Biodegradation 100:7–16.
Golubic, Stjepko, V. N. Sergeev, & A. H. Knoll. 1995. Mesoproterozoic *Archaeoellipsoides:* Akinetes of heterocystous cyanobacteria. Lethaia 28:285–298.
Gomes, M. L., L. A. Riedman, Shane O'Reilly, Usha Lingappa, Kyle Metcalfe, D. A. Fike, J. P. Grotzinger, W. W. Fischer, & A. H. Knoll. 2020. Taphonomy of biosignatures in microbial mats on Little Ambergris Cay, Turks and Caicos Islands. Frontiers in Earth Science 8:576712 [doi.10.3389/feart.2020.576712].
Gomont, M. A. 1892a. Monographie des Oscillariées (Nostocacées homocystées). Annales des Sciences Naturelles, Botanique (Série 7) 15:263–368, pl. 266–214.
Gomont, M. A. 1892b. Monographie des Oscillariées (Nostocacées Homocystées). Deuxième partie. Lyngbyées. Annales des Sciences Naturelles, Botanique (série 7) 16:91–264, pl. 1–7.
Gomont, M. A. 1895. Note sur le *Scytonema ambiguum* Kützing. Journal de Botanique 9:49–52.
Goodwin, A. M. 1956. Facies relations in the Gunflint iron-formation. Economic Geology 51:565–595.
Goodwin, A. M. 1973. Archean iron-formations and tectonic basins of the Canadian Shield. Economic Geology 68:915–933.
Gorbushina, A. A., & Karin Petersen. 2000. Distribution of microorganisms on ancient wall paintings as related to associated faunal elements. International Biodeterioration & Biodegradation 46(4):277–284.
Gorokhov, I. M., A. B. Kuznetsov, M. A. Semikhatov, I. M. Vasil'eva, N. G. Rizvanova, G. V. Lipenkov, & E. O. Dubinina. 2019. Early Riphean Billyakh Group of the Anabar Uplift, north Siberia: C–O isotopic geochemistry and Pb–Pb age of dolomites. Stratigraphy and Geological Correlation 27:514–528.
Gradziński, Michal. 2010. Factors controlling growth of modern tufa: Results of a field experiment. Geological Society, London, Special Publications 336:143–191.
Gradziński, Michal, Jaroslaw Tyszka, Alfred Uchman, & Renata Jach. 2004. Large microbial-foraminiferal oncoids from condensed Lower–Middle Jurassic deposits: A case study from the Tatra Mountains, Poland. Palaeogeography, Palaeoclimatology, Palaeoecology 213:133–151.
Grant, Jonathan, & Giselher Gust. 1987. Prediction of coastal sediment stability from photopigment content of mats of purple sulfur bacteria Nature 330:244–246.
Greco, Carla, D. T. Anderzen, Ian Hawes, A. M. C. Bowles, M. L. Yallop, Gary Baker, & A. D. Jungblut. 2020. Microbial diversity of pinnacle and conical microbial mats in the perennially ice-covered lake Untersee, East Antarctica. Frontiers in Microbiology 11:607251 [doi.10.3389/fmicb.2020.607251].
Greco, Francesco, Barbara,Cavalazzi, Axel Hofmann, & Keyron Hickman-Lewis. 2018. 3.4 Ga biostructures from the Barberton Greenstone belt of South Africa: New insights into microbial life. Bollettino della Societa Palaeontologica Italiana 57:59–74.
Green, J. W., A. H. Knoll, Stjepko Golubic, & Keene Swett. 1987. Paleobiology of distinctive benthic microfossils from the upper Proterozoic Limestone-Dolomite "Series," central East Greenland. American Journal of Botany 74:928–940.
Gregory, K. F. 1956. Hyphal anastomosis and cytological aspects of *Streptomyces scabies*. Canadian Journal of Microbiology 2:649–655. Greinert, Jens, Gerhard Bohrmann, & Marcus Elvert. 2002. Stromatolitic fabric of authigenic carbonate crusts: Result of anaerobic methane oxidation at cold seeps in 4,850 m water depth. International Journal of Earth Sciences 91:698–711. Grenne, Tor, & J. F. Slack. 2003. Bedded jaspers of the Ordovician Løkken ophiolite, Norway: Seafloor deposition and diagenetic maturation of hydrothermal plume-derived silica-iron gels. Mineralium Deposita 38:625–639.
Grenne, Tor, & J. F. Slack. 2005. Geochemistry of jasper beds from the Ordovician Løkken ophiolite,

Norway: Origin of proximal and distal siliceous exhalites. Economic Geology 100:1511–1527.
Grey, Kathleen. 1989. Handbook for the study of stromatolites and associated structures. Stromatolite Newsletter 14:82–171.
Grey, Kathleen. 2005. Ediacaran palynology of Australia. Memoirs of the Association of Australasian Palaeontologists 31:1–439.
Grey, Kathleen, & S. M. Awramik. 2020. Handbook for the study and description of microbialites. Geological Survey of Western Australia Bulletin 14. 290 p.
Grey, Kathleen, A. C. Hill, & Clive Calver. 2011. Chapter 8: Biostratigraphy and stratigraphic subdivision of Cryogenian successions of Australia in a global context. Geological Society, London, Memoirs (36): 113–134.
Grey, Kathleen, & A. M. Thorne. 1985. Biostratigraphic significance of stromatolites in upward shallowing sequences of the early proterozoic duck creek dolomite, Western Australia. Precambrian Research (29):183–206.
Grosch, E. G., & Nicola McLoughlin. 2014. Reassessing the biogenicity of Earth's oldest trace fossil with implications for biosignatures in the search for early life. Proceedings of the National Academy of Sciences, USA 111:8380–8385.
Gross, G. A. 1965. Geology of iron deposits in Canada. Volume I. General Geology and Evaluation of Iron Deposits. Geological Survey of Canada Economic Report 22. 181 p.
Gross, G. A. 1980. A classification of iron-formation based on depositional environments. Canadian Mineralogist 18:215–222.
Gross, G. A. 1983. Tectonic systems and the deposition of iron-formation. Precambrian Research 20:171–187.
Gross, G. A. 1988. A comparison of metalliferous sediments, Precambrian to Recent. Krystalinikum 19:59–74.
Gross, G. A. 1993. Element distribution patterns as metallogenetic indicators in siliceous metalliferous sediments. Resource Geology Special Issue 17: 96–107.
Gross, G. A. 1995. The distribution of rare earth elements in iron-formations. Global Tectonics and Metallogeny 5:63–68.
Grotzinger, J. P. 1990. Geochemical model for Proterozoic stromatolite decline. American Journal of Science (290):80–103.
Grotzinger, J. P., E. W. Adams, & Stefan Schröder. 2005. Microbial-metazoan reefs of the terminal Proterozoic Nama Group (c. 550–543 Ma), Namibia, Geological Magazine 142:499–517.
Grotzinger, J. P., & A. H. Knoll. 1999. Stromatolites in Precambrian carbonates: Evolutionary mileposts or environmental dipsticks? Annual Review of Earth and Planetary Sciences 27:313–358.
Grotzinger, J. P., & D. H. Rothman. 1996. An abiotic model for stromatolite morphogenesis.: Nature 383:423–425.
Gruner, J. W. 1922. The origin of sedimentary iron formations: The Biwabik Formation of the Mesabi Range. Economic Geology 17:407–460.
Gruner, J. W. 1923. Algae believed to be Archean. Journal of Geology 31:146–148.
Gruner, J. W. 1924. Contributions to the geology of the Mesabi Range, with special reference to the magnetites of the iron-bearing formation west of Mesaba. Minnesota Geological Survey Bulletin 19:1–71.
Gruner, J. W. 1925. Discovery of life in the Archean. Journal of Geology 33:151–152.
Gu Huan, Hou Shuyu, Chanokpon Yongyat, Suzanne De Tore, & Dacheng Ren. 2013. Patterned biofilm formation reveals a mechanism for structural heterogeneity in bacterial biofilms. Langmuir 29(35):11145–11153.
Gueneli, Nur, A. M. McKenna, Naohiko Ohkouchi, C. J. Boreham, Jérémie Beghin, E. J. Javaux, & J. J. Brocks. 2018. 1.1-billion-year-old porphyrins establish a marine ecosystem dominated by bacterial primary producers. Proceedings of the National Academy of Sciences, USA 115(30):E6978–E6986.
Guilbaud, Romain, I. B. Butler, & R. M. Ellam. 2011. Abiotic pyrite formation produces a large Fe isotope fractionation. Science 332:1548–1551.
Guitiérrez-Preciado, Ana, Aurélien Saghaï, David Moreira, Yvan Zivanovic, Philippe Deschamps, & Purificación López-García. 2018. Functional shifts in microbial mats recapitulate early Earth metabolic transitions. Nature Ecology & Evolution 2:1700–1708.
Guo, Jun-feng, Yong Li, & De-gan Shu. 2010. Cyanobacteria fossils from the Yanjiahe Formation, Terreneuvian, Cambrian, Yichang, Hubei. Acta Micropalaeontologica Sinica 27:144–149.
Guo, Li, & Robert Riding. 1998. Hot-spring travertine facies and sequences, Late Pleistocene, Rapolano Terme, Italy. Sedimentology (45):163–180.
Habicht, K. S., Michael Gade, Bo Thamdrup, Peter Berg, & D. E. Canfield. 2002. Calibration of sulfate levels in the Archean ocean. Science 298:2372–2374.
Hagadorn, J. W., & D. J. Bottjer. 1997 Wrinkle structures: Microbially mediated sedimentary structures common in subtidal siliciclastic settings at the Proterozoic-Phanerozoic transition. Geology 25: 1047–1050.
Hagadorn, J. W., & D. J. Bottjer. 1999. Restriction of a late Neoproterozoic biotope: Suspect microbial structures and trace fossils at the Vendian-Cambrian transition. Palaios 14:58–72.
Hagadorn, J. W., & D. C. McDowell. 2012. Microbial influence on erosion, grain transport and bedform genesis in sandy substrates under uniflow directions. Sedimentology 5:795–808.
Hagadorn, J. W., Freidrich Pflüger, & D. J. Bottjer. 1999. Unexplored Microbial Worlds. Palaios 14:1–2.
Halverson, G. P., Franck Poitrasson, P. H. Hoffman, Anne Nedelec, J.-M. Montel, & Jason Kirby. 2011. Fe isotope and trace element geochemistry of the Neoproterozoic syn-glacial Rapitan iron formation. Earth and Planetary Science Letters 309:100–112.
Hamade, Tristan, K. O. Konhauser, R. Raiswell, R. C. Morris, & S. Goldsmith. 2003. Using Ge:Si ratios to decouple iron and silica fluxes in Precambrian banded iron formations. Geology 31:35–38.

Hamilton, M. A., K. L. Buchan, R. E. Ernst, & G. M. Stott. 2009. Widespread and short-lived 1870 Ma mafic magmatism along the northern Superior craton margin. EOS Transactions, American Geophysical Union, 2009 Joint Assembly, Toronto, Canada, Abstract GA11A-01.

Hamilton, T. L. 2019. The trouble with oxygen: The ecophysiology of extant phototrophs and implications for the evolution of oxygenic photosynthesis. Free Radical Biology and Medicine 140:233–249.

Handley, K. M., S. J. Turner, K. A. Campbell, & B. W. Mountain. 2008. Silicifying biofilm exopolymers on a hot-spring microstromatolite: Templating nanometer-thick laminae. Astrobiology 8(4):747–770.

Hanson, R. S., & T. E. Hanson. 1996. Methanotrophic bacteria. Microbiological Reviews 60:439–471.

Harder, E. C. 1919. Iron-depositing bacteria and their geological relations. U.S. Geological Survey Professional Paper 113. 89 p.

Hardie, Lawrence, & Peter Garrett. 1977. Sedimentation on the modern carbonate tidal flats of Northwest Andros Island, Bahamas. Johns Hopkins University Press. Baltimore. 202 p.

Härtig, Cornelia, & Britta Planer-Friedrich. 2012. Thioarsenate transformation by filamentous microbial mats thriving in an alkaline, sulfidic hot spring. Environmental Science & Technology 46(8):4348–4356.

Harwood, C. L., & D. Y. Sumner. 2011. Microbialites of the Neoproterozoic Beck Spring Dolomite, Southern California. Sedimentology 58(6):1684–1673.

Hauck, Ferdinand. 1885. Die Meeresalgen Deutschlands und Österreichs. *In* L. Rabenhorst, ed., Kryptogamen-Flora von Deutschland, Österreich und der Schweiz. Zweite Auflage. Vol. 2. Eduard Kummer. Leipzig. p. i-xxiv + 513–575.

Hawkins, A. D., H. P. Liu, D. E. G. Briggs, A. D. Muscente, R. M. McKay, B. J. Witzke, & Shuhai Xiao. 2018. Taphonomy and biological affinity of three-dimensionally phosphatized bromalites from the Middle Ordovician Winneshiek Lagerstätte, northeastern Iowa, USA. Palaios 33:1–15.

Hayes, J. M. 1983. Geochemical evidence bearing on the origin of aerobiosis: a speculative hypothesis. *In* J. W. Schopf, ed., Earth's Earliest Biosphere: Its Origin and Evolution. Princeton University Press. Princeton. p. 291–301.

Heaman, L. M., N. Machado, T. E. Krogh, & W. Weber. 1986. Precise U-Pb zircon ages for the Molson dyke swarm and the Fox River sill: Constraints for Early Proterozoic crustal evolution in northeastern Manitoba, Canada. Contributions to Mineralogy and Petrology 94:82–89.

Heaman, L. M., Dave Peck, & Kimberly Toope. 2009. Timing and geochemistry of 1.88 Ga Molson igneous events, Manitoba: Insights into the formation of a craton-scale magmatic and metallogenic province. Precambrian Research 172:143–162.

Heijs, S. K., J. S. Sinninghe Damste, & L. J. Forney. 2005. Characterization of a deep-sea microbial mat from an active cold seep at the Milano mud volcano in the Eastern Mediterranean Sea. FEMS Microbiology Ecology 54:47–56.

Heim, Arnold. 1916. Monographie der Churrsten-Mattstock-Gruppe. 3: Teil Beitrge zur Geologischen Karte der Schweiz (Neue Folge) (20):369–573. In German.

Heim, Christine, N.-V. Quéric, Danny Ionescu, Nadine Schäfer, & Joachim Reitner. 2017. *Frutexites*-like structures formed by iron oxidizing biofilms in the continental subsurface (Äspö Hard Rock Laboratory, Sweden). PLOS One 12:e0177542 [doi.10.1371/journal.pone.0177542].

Heimann, Adriana. 2021. Part B, Chapter 6: Banded iron formations. Treatise Online 158:1–48, 4 fig.

Heimann, Adriana, C. M. Johnson, B. L. Beard, J. Valley, E. E. Roden, M. J. Spicuzza, & N. J. Beukes. 2010. Fe, C, and O isotope compositions of banded iron formation carbonates demonstrate a major role for dissimilatory iron reduction in ~2.5 Ga marine environments. Earth and Planetary Science Letters 294:8–18.

Heimann, Adriana, P. G. Spry, G. S. Teale, C. H. H. Conor, & W. R. Leyh. 2009. Geochemistry of garnet-rich rocks in the Southern Curnamona Province, Australia, and their genetic relationship to Broken Hill-type Pb-Zn-Ag mineralization. Economic Geology 104:687–712.

Heimann, Adriana, P. G. Spry, G. S. Teale, W. R. Leyh, C. H. H. Conor, Germán Mora, & J. J. O'Brien. 2013. Geochemistry and genesis of low grade metasediment-hosted Zn-Pb-Ag mineralization, southern Proterozoic Curnamona Province, Australia. Journal of Geochemical Exploration 128:97–116.

Heising, Silke, Lothar Richter, Wolfgang Ludwig, & B. Schink. 1999. *Chlorobium ferrooxidans* sp. nov., a phototrophic green sulfur bacterium that oxidizes ferrous iron in coculture with a "Geospirillum" sp. Strain. Archives of Microbiology 172:116–124.

Heising, Silke, & B. Schink. 1998. Phototrophic oxidation of ferrous iron by a *Rhodomicrobium vannielii* strain. Microbiology 144:2263–2269.

Hermann, T. N. 1974. Findings of mass accumulations of trichomes in the Riphean. *In* B. V. Timofeev, ed., Proterozoic and Paleozoic microfossils of the USSR. Nauka. Moscow. p. 6–10.

Heubeck, Christoph. 2009. An early ecosystem of Archean tidal microbial mats (Moodies Group, South Africa, ca. 3.2 Ga). Geology 37:931–934.

Heubeck, Christoph, Saskia Biasing, Mark Grund, Nadja Drabon, Martin Homann, & Sami Nabhan. 2016. Geological constraints on Archean (3.22 Ga) coastal-zone processes from the Dycedale Syncline, Barberton Greenstone Belt. South African Journal of Geology 119:495–518.

Hickman, A. H. 2012. Review of the Pilbara Craton and Fortescue Basin, Western Australia: Crustal evolution providing environments for early life. Island Arc (21):1–31.

Hickman-Lewis, Keyron, Barbara Cavalazzi, Frederic Foucher, & Frances Westall. 2018. Most ancient evidence for life in the Barberton greenstone belt: Microbial mats and biofabrics of the ~3.47 Ga Middle Marker horizon. Precambrian Research 312:45–67 [doi.10.1016/j.precamres.2018.04.007].

Hickman-Lewis, Keyron, Barbara Cavalazzi, Stephanie Sorieul, Pascale Gautret, Frederic Foucher, M. J.

Whitehouse, Heejin Jeon, Thomas Georgelin, C. S. Cockell, & Frances Westall. 2020. Metallomics in deep time and the influence of ocean chemistry on metabolic landscapes of Earth's earliest ecosystems. Scientific Reports 10(1):4965 [doi.10.1038/s41598-020-61774-w].

Hickman-Lewis, Keyron, R. J. Garwood, M. D. Brasier, Tomasz Goral, Haibo Jiang, Nicola McLoughlin, & David Wacey. 2016. Carbonaceous microstructures of the 3.46 Ga stratiform 'Apex chert', Chinaman Creek locality, Pilbara, Western Australia. Precambrian Research 278:161–178.

Hickman-Lewis, Keyron, Pascale Gautret, Laurent Arbaret, Stéphanie Sorieul, Rutger De Wit, Frédéric Foucher, Barbara Cavalazzi, & Frances Westall. 2019. Mechanistic morphogenesis of organo-sedimentary structures growing under geochemically stressed conditions: Keystone to the interpretation of some Archaean stromatolites? Geosciences (9):359 [doi.10.3390/geosciences9080359].

Hickman-Lewis, Keyron, Blandine Gourcerol, Frances Westall, Daniela Manzini, & Barbara Cavalazzi. 2020. Reconstructing Palaeoarchaean microbial biomes flourishing in the presence of emergent landmasses using trace and rare earth element systematics. Precambrian Research 342:105689 [doi.10.1016/j.precamres.2020.105689].

Hickman-Lewis, Keyron, Frances Westall, & Barbara Cavalazzi. 2019. Traces of early life from the Barberton Greenstone Belt, South Africa. in Earth's Oldest Rocks. Elsevier. Amsterdam. p. 1029–1058.

Hickman-Lewis, Keyron, Frances Westall, & Barbara Cavalazzi. 2020. Diverse communities of Bacteria and Archaea flourished in the Paleoarchean (3.5–3.3 Ga) microbial mats. Paleontology 63(6):1007–1033.

Hill, A. C., K. L. Cotter, & Kathleen Grey. 2000. Mid-Neoproterozoic biostratigraphy and isotope stratigraphy in Australia. Precambrian Research (100): 281–298.

Hillier, R. D., & L. B. Morrissey. 2010. Process regime change on a Silurian siliciclastic shelf: Controlling influences on deposition of the Gray Sandstone Formation, Pembrokeshire, UK. Geological Journal 45:26–58.

Hints, Rutt, Sigrid Hade, Alvar Soesoo, & Margus Voolma. 2014. Depositional framework of the East Baltic Tremadocian black shale revisited. GFF 136:464–482.

Hippler, Dorothee, Nanjie Hu, Michael Steiner, Gerhard Scholtz, & Gerhard Franz. 2011. Experimental mineralization of crustacean eggs: New implications for the fossilization of Precambrian–Cambrian embryos. Biogeosciences 9:1765–1775.

Hodgskiss, M. S. W., O. M. J. Dagnaud, J. L. Frost, G. P. Halverson, M. D. Schmitz, N. L. Swanson-Hysell, & E. A. Sperling. 2019. New insights on the Orosirian carbon cycle, early Cyanobacteria, and the assembly of Laurentia from the Paleoproterozoic Belcher Group. Earth and Planetary Science Letters 520:141–152.

Hoeft, S. E., T. R. Kulp, Sukkyun Han, Brian Lanoil, & R. S. Oremland. 2010. Coupled arsenotrophy in a photosynthetic hot spring biofilm from Mono Lake, California. Applied and Environmental Microbiology 76:4633–4639.

Hoeft, S. E., T. R. Kulp, J. F. Stolz, J. T. Hollibaugh, & R. S. Oremland. 2004. Dissimilatory arsenate reduction with sulfide as electron donor: Experiments with Mono Lake water and Isolation of strain MLMS-1, a chemoautotrophic arsenate respirer. Applied and Environmental Microbiology 70(5):2741–2747.

Hoeft McCann, S. E., Alison Boren, Jamie Hernandez-Maldonado, Brendon Stoneburner, C. W. Saltikov, J. F. Stolz, & R. S. Oremland. 2016. Arsenite as an electron donor for anoxygenic photosynthesis: Description of three strains of *Ectothiorhodospira* from Mono Lake, California and Big Soda Lake, Nevada. Life 7(1):1 [doi.10.3390/life7010001].

Hoehler, T. M., B. M. Bebout, & D. J. Des Marais. 2001. The role of microbial mats in the production of reduced gases on early Earth. Nature 412:324–327.

Hoffmann, C. F., C. B. Foster, T. G. Powell, & R. E. Summons. 1987. Hydrocarbon biomarkers from Ordovician sediments and the fossil alga *Gloeocapsomorpha prisca* Zalessky 1917. Geochimica et Cosmchimica Acta 51(10):2681–2697.

Hoffman, P. F., A. J. Kaufman, G. P. Halverson, & D. P. Schrag. 1998. A Neoproterozoic snowball Earth. Science 281:1342–1346.

Hofmann, Axel. 2005. The geochemistry of sedimentary rocks from the Fig Tree Group, Barberton greenstone belt: Implications for tectonic, hydrothermal and surface processes during mid-Archaean times. Precambrian Research 143:23–49.

Hofmann, B. A., J. D. Farmer, Friedhelm von Blanckenburg, & A. E. Fallick. 2008. Subsurface filamentous fabrics: an evaluation of origins based on morphological and geochemical criteria, with implications for exopaleontology. Astrobiology 8: 87–117.

Hofmann, H. J. 1969. Stromatolites from the Proterozoic Animikie and Sibley Groups. Geological Survey of Canada Paper, Geological Survey of Canada. p. 68.

Hofmann, H. J. 1973. Stromatolites: Characteristics and utility. Earth Science Reviews (9):339–373.

Hofmann, H. J. 1974. Mid-Precambrian prokaryotes (?) from the Belcher Islands, Canada. Nature 249:87–88.

Hofmann, H. J. 1976. Precambrian microflora, Belcher Island, Canada: Significance and systematics. Journal of Paleontology 50:1040–1073.

Hofmann, H. J. 2000. Archean Stromatolites as Microbial Archives. *In* Robert Riding & S. M. Awramik, eds., Microbial Sediments. Springer. Berlin. p. 315–327.

Hofmann, H. J., Kathleen Grey, A. H. Hickman, & R. I. Thorpe. 1999. Origin of 3.45 Ga coniform stromatolites in Warrawoona Group, Western Australia. Geological Society of America Bulletin 111:1256–1262.

Hofmann, H. J., & G. D. Jackson. 1987. Proterozoic ministromatolites with radial-fibrous fabric. Sedimentology (34):963–971.

Hofmann, H. J., & G. D. Jackson. 1994. Shale-facies microfossils from the Proterozoic Bylot Supergroup, Baffin Island, Canada. Paleontological Society Memoir 37:1–35.

Høiby, Niels, Thomas Bjarnsholt, Michael Givskov, Søren Molin, & Oana Ciofu. 2010. Antibiotic resistance of bacterial biofilms: International Journal of Antimicrobial Agents, 35(4):322–332.

Holland, H. D. 1973. The oceans: A possible source of iron in iron-formations. Economic Geology 68:1169–1172.

Holland, H. D. 1984. The Chemical Evolution of the Atmosphere and Oceans. Princeton University Press. New York. 582 p.

Holland, H. D. 2006. The oxygenation of the atmosphere and oceans. Philosophical Transactions of the Royal Society of London B (Biological Sciences) 361:903–915.

Holland, H. D., & Ulrich Petersen. 1995. Living dangerously. Princeton University Press. Princeton. 490 p.

Holm, N. G. 1987. Biogenic influences on the geochemistry of certain ferruginous sediments of hydrothermal origin. Chemical Geology 63:45–57.

Holm, N. G. 1989. The $^{13}C/^{12}C$ ratios of siderite and organic matter of a modern metalliferous hydrothermal sediment and their implications for banded iron formations. Chemical Geology 63:45–57.

Homann, Martin. 2019. Earliest life on Earth: Evidence from the Barberton Greenstone Belt, South Africa. Earth-Science Reviews 196:102–108.

Homann, Martin, Christoph Heubeck, Alessandro Airo, & M. M. Tice. 2015. Morphological adaptations of 3.22 Ga-old tufted microbial mats to Archean coastal habitats (Moodies Group, Barberton Greenstone Belt, South Africa). Precambrian Research 266:47–64.

Homann, Martin, Christoph Heubeck, T. R. R. Bontognali, & Alessandro Airo. 2016. Evidence for cavity-dwelling microbial life in 3.22 Ga-old tidal deposits. Geology 44:51–54.

Homann, Martin, Pierre Sansjofre, Mark van Zuilen, Christophe Heubeck, Jian Gong, Bryan Killingsworth, I. S. Foster, Alessandro Airo, M. J. van Kranendonk, Magadali Ader, & S. V. Lalonde. 2018. Microbial life and biogeochemical cycling on land 3,220 million years ago. Nature Geoscience 11:665–671.

Horodyski, R. J., Bonnie Bloeser, & Stephen Vonder Haar. 1977. Laminated algal mats from a coastal lagoon, Laguna Mormona, Baja California, Mexico. Journal of Sedimentary Petrology 47:680–696

Horodyski, R. J., & J. A. Donaldson. 1980. Microfossils from the middle Proterozoic Dismal Lakes Group, Arctic Canada. Precambrian Research 11:125–159.

Hörnlein, Christine, Veronique Confurius-Guns, L. J. Stal, & Henk Bolhuis. 2018. Daily rhythmicity in coastal microbial mats. Nature Partner Journals Biofilms Microbiomes 4:11 [doi.10.1038/s41522-018-0054-5].

Howell, Jason, Jusun Woo, & S. K. Chough. 2011. Dendroid morphology and growth patterns: 3-D computed tomographic reconstruction. Palaeogeography, Palaeoclimatology, Palaeoecology (299): 335–347.

Hunt, A. P., & S. G. Lucas. 2007. Ttrapod ichnofacies: A new paradigm. Ichnos 14(1):59–68.

Huston, D. L., & G. A. Logan. 2004. Barite, BIFs and bugs: Evidence for the evolution of the Earth's early hydrosphere. Earth and Planetary Science Letters 220:41–55.

Huston, D. L., S. Pehrsson, B. M. Eglington, & K. Zaw. 2010. The geology and metallogeny of volcanic-hosted massive sulfide deposits: Variations through geologic time and with tectonic setting. Economic Geology 105:571–591.

Ibarra, Yadira, & F. A. Corsetti. 2016. Lateral Comparative Investigation of Stromatolites: Astrobiological Implications and Assessment of Scales of Control. Astrobiology (16):271–281.

Igisu, Motoko, Yuichiro Ueno, Mie Shimojima, Satoru Nakashima, S. M. Awramik, Hiroyuki Ohta, & Shigenori Maruyama. 2009. Micro-FTIR spectroscopic signatures of bacterial lipids in Proterozoic microfossils. Precambrian Research 173:19–26.

Igisu, Motoko, Tadashi Yokoyama, Yuichiro Ueno, Satoru Nakashima, Mie Shimojima, Hiroyuki Ohta, & Shigenori Maruyama. 2018. Changes of aliphatic C-H bonds in cyanobacteria during experimental thermal maturation in the presence or absence of silica as evaluated by FTIR microspectroscopy. Geobiology 4:412–428.

Ilyn, A. V. 2009. Neoproterozoic banded iron formations. Lithology and Mineral Resources 44:78–86.

Iniesto, Miguel, Candela Blanco-Moreno, Aurora Villalba, Á. D. Buscalioni, M. C. Guerrero, & A. I. López-Archilla. 2018. Plant tissue decay in long-term experiments with microbial mats. Geosciences 8(11):387 [doi.10.3390/geosciences8110387].

Iniesto, Miguel, Á. D. Buscalioni, M .C. Guerrero, Karim Benzerara, David Moreira, & A. I. López-Archilla. 2016. Involvement of microbial mats in early fossilization by decay delay and formation of impressions and replicas of vertebrates and invertebrates. Scientific Reports 6:25716 [doi.10.1038/srep25716].

Iniesto, Miguel, Nina Zeyen, A. I. López-Archilla, Sylvain Bernard, A. D. Buscalioni, M. C. Guerrero, & Karim Benzerara. 2015. Preservation in microbial mats: Mineralization by a talc-like phase of a fish embedded in a microbial sarcophagus. Frontiers in Earth Science 3:51 [doi.10.3389/feart.2015.00051].

Isley, A. E. 1995. Hydrothermal plumes and the delivery of iron to banded iron formation. Journal of Geology 10:169–185.

Isley, A. E., & D. H. Abbott, 1999. Plume-related mafic volcanism and the deposition of banded iron formation. Journal of Geophysical Research 104: 15461–15477.

Ivarsson, Magnus, Henrik Drake, Anna Neubeck, Therese Sallstedt, Stefan Bengtson, N. M. W. Roberts, & Birger Rasmussen. 2020. The fossil record of igneous rock. Earth-Science Reviews 210:103342 [doi.10.1016/j.earscirev.2020.103342].

Jacobsen, S. B., & M. R. Pimentel-Klose. 1988. A Nd isotopic study of the Hamersley and Michipicoten banded iron formations: The source of REE and Fe in Archean oceans. Earth and Planetary Science Letters 87:29–44.

Jaeschke, Andrea, H. J. M. Op den Camp, Harry Harhangi, Adam Klimiuk, E. C. Hopmans, M. S. M.

Jetten, Stefan Schouten, & J. S. Sinninghe Damsté. 2009. 16S rRNA gene and lipid biomarker evidence for anaerobic ammonium-oxidizing bacteria (anammox) in California and Nevada hot springs. FEMS Microbiology Ecology 67(3):343–350.

Jahnke, L. L., V. J. Orphan, T. Embaye, K. A. Turk, M. D. Kubo, R. E. Summons, & D. J. Des Marais. 2008. Lipid biomarker and phylogenetic analyses to reveal archaeal biodiversity and distribution in hypersaline microbial mat and underlying sediment Geobiology 6(4):394–410.

James, H. L. 1954. Sedimentary facies of iron-formation. Economic Geology 49:235–293.

James, H. L. 1983. Distribution of banded iron-formation in space and time. *In* A. F. Trendall & R. C. Morris, eds., Iron-formation: Facts and Problems. Elsevier. Amsterdam. p. 471–490.

Javaux, E. J. 2019. Challenges in evidencing the earliest traces of life. Nature 572:451–470].

Javaux, E. J., A. H. Knoll, & M. R. Walter. 2004. TEM evidence for eukaryotic diversity in mid-Proterozoic oceans. Geobiology 2:121–132.

Javaux, E. J., & Kevin Lepot. 2018. The Paleoproterozoic fossil record: Implications for the evolution of the biosphere during Earth's middle-age. Earth-Science Reviews 176:68–86.

Javaux, E. J., C. P. Marshall, & Andrey Bekker. 2010. Organic-walled microfossils in 3.2-billion-year-old shallow-marine siliciclastic deposits. Nature 463: 934–938.

Jensen, P. Ø., Mette Kolpen, K. N. Kragh, & Michael Kühl. 2017. Microenvironmental characteristics and physiology of biofilms in chronic infections of CF patients are strongly affected by the host immune response. APMIS 125(4):276–288.

Jiang, Ganqing, M. J. Kennedy, & Nicholas Christie-Blick. 2003. Stable isotopic evidence for methane seeps in Neoproterozoic postglacial cap carbonates. Nature 426:822–826.

Johannessen, K. C., Nicola McLoughlin, & P. E. Vullum. 2018. On the biogenicity of Fe-oxyhydroxide filaments in silicified low-temperature hydrothermal deposits: Implications for the identification of Fe-oxidizing bacteria in the rock record. Geobiology 18:31–53.

Johannessen, K. C., Nicola McLoughlin, P. E. Vullum, & I. H. Thorseth. 2020. On the biogenicity of Fe-oxyhydroxide filaments in silicified low-temperature hydrothermal deposits: Implications for the identification of Fe-oxidizing bacteria in the rock record. Geobiology 18:31–53.

Johnson, C. M., B. L. Beard, N. J. Beukes, Cornelis Klein, & J. M. O'Leary. 2003. Ancient geochemical cycling in the Earth as inferred from Fe isotope studies of banded iron formations from the Transvaal craton. Contributions to Mineralogy and Petrology 144:523–547.

Johnson, C. M., B. L. Beard, Cornelis Klein, N. J. Beukes, & E. E. Roden. 2008. Iron isotopes constrain biologic and abiologic processes in banded iron formation genesis. Geochimica et Cosmochimica Acta 72:151–169.

Johnson, C. M., B. L. Beard, & E. E. Roden. 2008. The iron isotope fingerprints of redox and biogeochemical cycling in the modern and ancient Earth. Annual Reviews of Earth and Planetary Sciences 36:457–493.

Johnson, C. M., J. M. Ludois, B. L. Beard, N. J. Beukes, & Adriana Heimann. 2013. Iron formation carbonates: Paleoceanographic proxy or recorder of microbial diagenesis? Geology 41:1147–1150.

Johnson, C. M., E. E. Roden, S. A. Welch, & B. L. Beard. 2005. Experimental constraints on Fe isotope fractionation during magnetite and Fe carbonate formation coupled to dissimilatory hydrous ferric oxide reduction. Geochimica et Cosmochimica Acta 69:963–993.

Johnston, D. T., B. A. Wing, James Farquhar, A. J. Kaufman, Harald Strauss, T. W. Lyons, L. C. Kah, & D. E. Canfield. 2005. Active microbial sulfur disproportionation in the Mesoproterozoic. Science 310:1477–1479.

Jones, Brian, & Xiaotong Peng. 2012. Intrinsic versus extrinsic controls on the development of calcite dendrite bushes, Shuzhishi Spring, Rehai geothermal area, Tengchong, Yunnan Province, China. Sedimentary Geology 249–250:45–62.

Jones, Brian, & Xiaotong Peng. 2014. Signatures of biologically influenced $CaCO_3$ and Mg-Fe silicate precipitation in hot springs: Case study from the Ruidian geothermal area, western Yunnan Province, China. Sedimentology 61:56–89.

Jones, Brian, & R. W. Renaut. 1997. Formation of silica oncoids around geysers and hot springs at El Tatio, northern Chile. Sedimentology (44):287–304.

Jones, Brian, R. W. Renaut, & M. R. Rosen. 1997. Biogenecity of silica precipitation around geysers and hot-spring vents, North Island, New Zealand. Journal of Sedimentary Research 67(1):88–104.

Jones, Brian, R. W. Renaut, & M. R. Rosen. 1998. Microbial biofacies in hot-spring sinters; a model based on Ohaaki Pool, North Island, New Zealand. Journal of Sedimentary Research 68:413–434.

Jones, Brian, R. W. Renaut, & M. R. Rosen. 1999. Actively growing siliceous oncoids in the Waiotapu geothermal area, North Island, New Zealand. Journal of the Geological Society (156):89–103.

Jones, Brian, R. W. Renaut, & M. R. Rosen. 2001. Taphonomy of silicified filamentous microbes in modern geothermal sinters: Implications for identification. Palaios 16:580–592.

Jonkers, H.M, Rebecca Ludwig, Rutger de Wit, Olivier Pringault, Gerard Muyzer, Helge Niemann, Niko Finke, & Dirk De Beer. 2003. Structural and functional analysis of a microbial mat ecosystem from a unique permanent hypersaline inland lake: 'La Salada de Chiprana' (NE Spain). FEMS Microbiology Ecology 44(2):175–189.

Jørgensen, B. B. 2001. Space for hydrogen. Nature 412:286–288.

Jørgensen, B. B., & Antje Boetius. 2007. Feast and famine: Microbial life in the deep-sea bed. Nature Reviews Microbiology 5:770–781.

Jørgensen, B. B., Yehuda Cohen, & D. J. Des Marais.1987. Photosynthetic action spectra and adaptation to spectral light distribution in a benthic

cyanobacterial mat. Applied and Environmental Microbiology 53(4):879–886.

Jørgensen, B. B., Yehuda Cohen, & N. P. Revsbech. 1986. Transition from anoxygenic to oxygenic photosynthesis in a *Microcoleus chthonoplastes* cyanobacterial mat. Applied and Environmental Microbiology 51(2):408–417.

Jørgensen, B. B., & D. J. Des Marais. 1986. Competition for sulfide among colorless and purple sulfur bacteria in a cyanobacterial mat. FEMS Microbiology Ecology 38:179–186.

Jørgensen, B. B., & N. P. Revsbech. 1983. Colorless sulfur bacteria, *Beggiatoa* spp. and *Thiovulum* spp., in O_2 and H_2S Microgradients. Applied and Environmental Microbiology 45(4):1261–1270.

Jørgensen B. B., N. P. Revsbech, & Yehuda Cohen. 1983. Photosynthesis and structure of benthic microbial mats: Microelectrode and SEM studies of four cyanobacterial communities. Limnology and Oceanography 28:1075–1093.

Joye, S. B., & H. W. Paerl. 1994. Nitrogen cycling in microbial mats: Rates and patterns of denitrification and nitrogen fixation. Marine Biology 119:285–295.

Kah, L. C., & J. P. Grotzinger. 1992. Early Proterozoic (1.9 Ga) thrombolites of the Rocknest Formation, Northwest Territories, Canada. Palaios 7(3):305–315.

Kah, L. C., & A. H. Knoll. 1996. Microbenthic distribution of Proterozoic tidal flats: Environmental and taphonomic considerations. Geology 24:79–82.

Kah, L. C., & Robert Riding. 2007. Mesoproterozoic carbon dioxide levels inferred from calcified cyanobacteria. Geology 35:799–802.

Kalkowsky, Ernst. 1908. Oolith und Stromatolith im norddeutschen Buntsandstein. Zeitschrift der deutschen geologischen Gesellschaft p. 68–125.

Kappler, Andreas, Claudia Pasquer, K. O. Konhauser, & D. K. Newman. 2005. Deposition of banded iron formations by anoxygenic phototrophic Fe(II)-oxidizing bacteria. Geology 33:865–868.

Karl, D. M., A. M. Brittain, & B. D. Tibrook. 1989. Hydrothermal and microbial processes at Loihi Seamount, a mid-plate hot-spot volcano. Deep-Sea Research 36:1655–1673.

Karsten, Ulf. 1996. Growth and organic osmolytes of geographically different isolates of *Microcoleus chthonoplastes* (Cyanobacteria) from benthic microbial mats: Response to salinity change. Journal of Phycology 32(4):501–506.

Kato, Yasuhiro, Takashi Kano, & Keitaro Kunugiza. 2002. Negative Ce anomaly in the Indian banded iron formations: Evidence for the emergence of oxygenated deep-sea at 2.9–2.7 Ga. Resource Geology 52:101–110.

Kato, Yasuhiro, K. E. Yamaguchi, & Hiroshi Ohmoto. 2006. Rare earth elements in Precambrian banded iron formations: Secular changes of Ce and Eu anomalies and evolution of atmospheric oxygen. *In* S. E. Kesler & Henry Ohmoto, eds., Evolution of the Early Earth's Atmosphere, Hydrosphere, and Biosphere: Constraints from Ore Deposits. Geological Society of America Memoir 198:269–289.

Kaufman, A. J., J. M. Hayes, & Cornelis Klein. 1990. Primary and diagenetic controls of isotopic compositions of iron-formation carbonates. Geochimica et Cosmochimica Acta 54:3461–3473.

Kawaguchi, Tomohiro, & A. W. Decho. 2000. Biochemical characterization of cyanobacterial extracellular polymers (EPS) from modern marine stromatolites (Bahamas). Preparative Biochemistry and Biotechnology 30:321–330.

Kaye, T. G., Gary Gaugler, & Zbigniew Sawlowicz. 2008. Dinosaurian soft tissues interpreted as bacterial biofilms. PLOS One 3(7):e2808 [doi.10.1371/journal.pone.0002808].

Kelly, D. P. 1982. Biochemistry of the chemolithotrophic oxidation of inorganic sulphur. Philosophical Transactions of the Royal Society of London B (Biological Sciences) 298:499–528.

Kemp, A. I. S., C. J. Hawkesworth, B. A. Paterson, & P. D. Kinny. 2006. Episodic growth of the Gondwana supercontinent from hafnium and oxygen isotopes in zircon. Nature 439:580–583.

Kempe, Stephan, Jozef Kazmierczak, Gunter Landmann, Tosun Konuk, Andreas Reimer, & Andreas Lipp. 1991. Largest known microbialites discovered in Lake Van, Turkey. Nature (349):605.

Kennard, J. M. 1994. Thrombolites and stromatolites within shale-carbonate cycles, middle-late Cambrian Shannon formation, Amadeus Basin, central Australia. *In* Janine Bertrand-Sarfati & C. L. Monty, eds., Phanerozoic Stromatolites II. Springer. Berlin. p. 443–471.

Kennard, J. M., & N. P. James. 1986. Thrombolites and stromatolites: Two distinct types of microbial structures: Palaios (5):492–503.

Kershaw, Stephen, Yue Li, Sylvie Crasquin-Soleau, Qinglai Feng, Xinan Mu, P. Y. Collin, Alan Reynolds, & Li Guo. 2007. Earliest Triassic microbialites in the South China block and other areas: Controls on their growth and distribution. Facies (53):409–425.

Kershaw, Stephen, Tingshan Zhang, & Guangzhi Lan. 1999. A microbialite carbonate crust at the Permian-Triassic boundary in South China, and its palaeoenvironmental significance. Palaeogeography, Palaeoclimatology, Palaeoecology 146(1–4):1–18 [doi.10.1016/S0031-0182(98)00139-4].

Kester, J. C., & S. M. Fortune. 2014. Persisters and beyond: Mechanisms of phenotypic drug resistance and drug tolerance in bacteria. Critical Reviews in Biochemistry and Molecular Biology 49(2):91–101 .

Khan, R. M. K., S. Das Sharma, D. J. Patil, & S. M. Naqvi. 1996. Trace, rare-earth elements, and oxygen isotope systematics for the genesis of banded iron-formations: Evidence from Kushtagi schist belt, Archean Dharwar Craton, India. Geochimica et Cosmochimica Acta 60:3285–3294.

Khohadad, C. L. M., & J. S. Foster. 2012. Metagenomic and metabolic profiling of nonlithifying and lithifying stromatolitic mats of Highborne Cay, The Bahamas. PLOS One 7(5):e38229 [doi.10.1371/journal.pone.0038229].

Kidston, Robert, & W. H. Lang. 1921. On old red sandstone plants showing structure, from the Rhynie chert bed, Aberdeenshire. Part V. The Thallophyta occurring in the peat-bed; the succession of the plants through a vertical section of the bed, and the

conditions of accumulation and preservation of the deposit. Transaction of the Royal Society of Edinburgh 52:855–902.

Kiene, R. P., P. T. Visscher, M. D. Keller, & G. O. Kirst. 1996. Biological and Environmental Chemistry of DMSP and Related Sulfonium Compounds. Plenum Press. New York. 430 p.

Kilias, S. P., Magnus Ivarsson, E. C. Fru, J. E. Rattray, Hakan Gustafsson, Jonathan Naden, & Kleopatra Detsi. 2020. Precipitation of Mn Oxides in Quaternary Microbially Induced Sedimentary Structures (MISS), Cape Vani Paleo-Hydrothermal Vent Field, Milos, Greece. Minerals 10:536 [doi.org/10.3390/min10060536].

Kimberley M. M. 1978. Palaeoenvironmental classification of iron formations. Economic Geology 73:215–229.

King, G. M. 1988. Methanogenesis from methylated amines in a hypersaline algal mat. Applied and Environmental Microbiology 54(1):130–136.

Kinsman-Costello, L. E., C. S. Sheik, N. D. Sheldon, G. Allen Burton, D. M. Costello, D. Marcus, P. A. Uyl, & G. J. Dick. 2017. Groundwater shapes sediment biogeochemistry and microbial diversity in a submerged Great Lake sinkhole. Geobiology 15(2):225–239.

Kirschvink, J. L. 1992. Late Proterozoic low-latitude global glaciation: The Snowball Earth. *In* J. W. Schopf & C. Klein eds, The Proterozoic Biosphere: A Multi-disciplinary Study. Cambridge University Press. New York. p. 51–52.

Klatt, C. G., W. P. Inskeep, M. J. Herrgard, Z. J. Jay, D. B. Rusch, S. G. Tringe, M. N. Parenteau, D. M. Ward, S. M. Boomer, D. A. Bryant, & S. R. Miller. 2013. Community structure and function of high-temperature chlorophototrophic microbial mats inhabiting diverse geothermal environments. Frontiers in Microbiology 4:1–23 [doi.10.3389/fmicb.2013.00106].

Klaveness, Dag. 1999. *Metallogenium*: A microbial enigma. *In* Joseph Seckbach, ed., Enigmatic Microorganisms and Life in Extreme Environments. Springer. Dordrecht. p. 541–548.

Klein, Cornelis. 2005. Some Precambrian banded iron-formations (BIFs) from around the world: Their age, geologic setting, mineralogy, metamorphism, geochemistry, and origin. Presidential Address to the Mineralogical Society of America, Boston. American Mineralogist 90:1473–1499.

Klein, Cornelis, & N. J. Beukes. 1989. Geochemistry and sedimentology of a facies transition from limestone to iron-formation deposition in the early Proterozoic Transvaal Supergroup, South Africa. Economic Geology 84:1733–1774.

Klein, Cornelis, & N. J. Beukes. 1992. Proterozoic iron formations. *In* K. C. Condie, ed., Proterozoic Crustal Evolution. Elsevier. Amsterdam. p. 383–418.

Klein, Cornelis, & N. J. Beukes. 1993. Sedimentology and geochemistry of the glaciogenic late Proterozoic Rapitan Iron-Formation in Canada. Economic Geology 88:542–565.

Klein, Cornelis, N. J. Beukes, & J. W. Schopf. 1987. Filamentous microfossils in the early Proterozoic Transvaal Supergroup: Their morphology, significance, and paleoenvironmental setting. Precambrian Research 36:81–94.

Klein, Cornelis, & M. J. Gole. 1981. Mineralogy and petrology of parts of the Marra Mamba iron-formation, Hamersley Basin, Western Australia. American Mineralogist 66:507–525.

Klein, Cornelis, & E. A. Ladeira. 2002. Petrography and geochemistry of the least altered banded iron-formation of the Archean Carajás Formation, Northern Brazil. Economic Geology 97:643–651.

Klein, Cornelis, & E. A. Ladeira. 2004. Geochemistry and mineralogy of Neoproterozoic banded iron-formations and some selected, siliceous manganese formations from the Urucum district, Mato Grosso do Sul, Brazil. Economic Geology 99:1233–1244.

Klinkhammer, G., Henry Elderfield, & A. Hudson. 1983. Rare-earth elements in seawater near hydrothermal vents. Nature 305:185–188.

Klock, J. H., Andrea Wieland, Richard Seifert, & Walter Michaelis. 2007. Extracellular polymeric substances (EPS) from cyanobacterial mats: Characterisation and isolation method optimisation. Marine Biology 152:1077–1085 [doi.1007/s00227-007-0754-5].

Knauth, L. P., & D. R. Lowe. 2003. High Archean climatic temperature inferred from oxygen isotope geochemistry of cherts in the 3.5 Ga Swaziland Supergroup, South Africa. Geological Society of America Bulletin 115:566–580.

Knittel, Katrin, Tina Lösekann, Antje Boetius, Renate Kort, & Rudolf Amann. 2005. Diversity and distribution of methanotrophic archaea at cold seeps. Microbial Ecology 71:467–479 [doi.10.1128/AEM.71.1.467-479.2005].

Knoll, A. H. 1985a. Exceptional preservation of photosynthetic organisms in silicified carbonates and silicified peats. Philosophical Transactions of the Royal Society of London B (Biological Sciences) 311:111–122.

Knoll, A. H. 1985b. A paleobiological perspective on sabkhas. *In* G. M. Friedman, & W. E. Krumbein, eds., Hypersaline Ecosystems: The Gavish Sabkha. p. 407–425.

Knoll, A. H. 2008. Cyanobacteria and Earth history. *In* Antonia Herrero, & Enrique Flores, eds., The Cyanobacteria: Molecular Biology, Genomics and Evolution. Horizon Scientific. Heatherset. p. 1–19.

Knoll, A. H. 2016. Paleobiological perspectives on early microbial evolution. *In* Howard Ochman, ed., Cold Spring Harbor Perspectives in Biology, Vol. 7. Cold Spring Harbor Laboratory Press. New York. 210 p. (First published online in 2015).

Knoll, A. H., & E. S. Barghoorn. 1974. Ambient pyrite in Precambrian chert: New evidence and a theory. Proceedings of the National Academy of Sciences, USA 71:2329–2331.

Knoll, A. H., & E. S. Barghoorn. 1975. Precambrian eukaryotic organisms: A reassessment of the evidence. Science 190:52–54.

Knoll, A. H., & E. S. Barghoorn. 1977. Archean microfossils showing cell-division from Swaziland System of South Africa. Science 198:396–398.

Knoll, A. H., E. S. Barghoorn, & S. M. Awramik. 1978. New microorganisms from the Aphebian Gunflint Iron Formation, Ontario Journal of Paleontology 52:976–992.

Knoll, A. H., E. S. Barghoorn, & Stjepko Golubic. 1975. *Paleopleurocapsa wopfnerii* gen. et sp. nov.: A late Precambrian alga and its modern counterpart. Proceedings of the National Academy of Sciences, USA 72:2488–2492.

Knoll, A. H., I. J. Fairchild, & Keene Swett. 1993. Calcified microbes in Neoproterozoic carbonates: implications for our understanding of the Proterozoic/Cambrian Transition. Palaios 8:512–525.

Knoll, A. H., & Stjepko Golubic. 1992. Proterozoic and living cyanobacteria. *In* Manfred Schidlowski, Stjepko Golubic, M. M. Kimberley, D. M. McKirdy, & P. A. Trudinger, eds., Early Organic Evolution: Implications for Mineral and Energy Resources. Springer-Verlag. Berlin & Heidelberg. p. 450–462.

Knoll, A. H., E. J. Javaux, David Hewitt, & Phoebe Cohen. 2006. Eukaryotic organisms in Proterozoic oceans. Philosophical Transactions of the Royal Society of London B (Biological Sciences) 361:1023–1038.

Knoll, A. H., & M. A. Semikhatov. 1998. The genesis and time distribution of two distinctive Proterozoic stromatolite microstructures. Palaios 13:408–422.

Knoll, A. H., Keene Swett, & Jonathan Mark. 1991. Paleobiology of a Neoproterozoic tidal flat/lagoonal complex: The Draken Conglomerate Formation, Spitsbergen. Journal of Paleontology 65:531–570.

Koehler, Inga, K. O. Konhauser, & Andreas Kappler. 2010. Role of microorganisms in banded iron formations. *In* L. L. Barton, Martin Mandl, & Alexander Loy, eds., Geomicrobiology: Molecular and Environmental Perspective. Springer Science+Business Media BV. Dordrecht. p. 309–324.

Kohler, T. J., D. J. van Horn, Joshua Darling, & D. M. McKnight. 2016. Nutrient treatments alter microbial mat colonization in two glacial meltwater streams from the McMurdo Dry Valleys, Antarctica. FEMS Microbiology Ecology 92(4):fiw049 [doi.10.1093/femsec/fiw049].

Komiya, Tsuyoshi, Shigenori Maruyama, Toshiaki Masuda, Susumu Nohda, Mamoru Hayashi, & Kazuaki Okamoto. 1999. Plate tectonics at 3.8-3.7 Ga: Field evidence from the Isua accretionary complex, southern West Greenland. Journal of Geology 107:515–554.

Konhauser, K. O. 1997. Bacterial iron biomineralization in nature. FEMS Microbiology Reviews 20:315–326.

Konhauser, K. O. 1998. Diversity of bacterial iron mineralization. Earth-Science Reviews 43:91–121.

Konhauser, K. O. 2000. Hydrothermal bacterial biomineralization: Potential modern-day analogues for banded iron formations. Marine Authigenesis: From Global to Microbial, SEPM Special Publication 66:133–145.

Konhauser, K. O., Larry Amskold, S. V. Lalonde N. R. Posth, Andreas Kappler, & Ariel Anbar. 2007. Decoupling photochemical Fe(II) oxidation from shallow-water BIF deposition. Earth and Planetary Science Letters 258:87–100.

Konhauser, K. O., Tristan Hamade, Rob Raiswell, R. C. Morris, F. G. Ferris, Gordon Southam, & D. E. Canfield. 2002. Could bacteria have formed the Precambrian banded iron formations? Geology 30:1079–1082.

Konhauser, K. O., Brian Jones, V. R. Phoenix, F. G. Ferris, & R. W. Renaut. 2004. The microbial role in hot spring silicification. Ambio: A Journal of the Human Environnment 33(8):552–558.

Konhauser, K. O., Brian Jones, A.-L. Reysenbach, & R. W. Renaut. 2003. Hot spring sinters: Keys to understanding Earth's earliest life forms. Canadian Journal of Earth Sciences 40:1713–1724.

Konhauser, K. O., D. K. Newman, & Andreas Kappler. 2005. Fe(III) reduction in BIFs: The potential significance of microbial Fe(III) reduction during deposition of Precambrian banded iron formations. Geobiology 3:167–177.

Konhauser, K. O., V. R. Phoenix, S. H. Bottrell, D. G. Adams, & I. M. Head. 2001. Microbial-silica interactions in Icelandic hot spring sinter: Possible analogues for some Precambrian siliceous stromatolites. Sedimentology (4):415–433.

Konhauser, K. O., & Robert Riding. 2012. Bacterial biomineralization. *In* A. H. Knoll, D. E. Canfield, & K. O. Konhauser. Fundamentals of Geobiology. Blackwell Wiley. Philadelphia. p. 105–129.

Kopp, R. E., & J. L. Kirschvink. 2008. The identification and biogeochemical interpretation of fossil magnetotactic bacteria. Earth-Science Reviews 86:42–61 [doi.10.1016/j.earscirev.2007.08.001].

Korde, K. B. 1973. Vodorosli kembriya [Cambrian Algae]: Nauka [Science]. Moscow. 349 p. In Russian.

Krajewski, K. P. 1983. Albian pelagic phosphate-rich macrooncoids from the Tatra Mts (Poland). *In* Tadeusz Peryt, ed., Coated Grains. Springer. Berlin. p. 344–357.

Krapež, Bryan, M. E. Barley, & A. L. Pickard. 2003. Hydrothermal and resedimented origins of the precursor sediments to banded iron formations: Sedimentological evidence from the early Palaeoproterozoic Brockman Super-sequence of Western Australia. Sedimentology 50:979–1011.

Kremer, Barbara, Józef Kazmierczak, Maja Łukomska-Kowalczyk, & Stephan Kempe. 2012. Calcification and Silicification: Fossilization Potential of Cyanobacteria from Stromatolites of Niuafo'ou's Caldera Lakes (Tonga) and Implications for the Early Fossil Record. Astrobiology 12:535–548.

Krepski, S. T., David Emerson, P. L. Hredzak-Showalter, G. W. Luther, III, & C. S. Chan. 2013. Morphology of biogenic iron oxides records microbial physiology and environmental conditions: toward interpreting iron microfossils. Geobiology 11:457–471.

Krings, Michael. 2019. *Palaeolyngbya kerpii* sp. nov., a large flamentous cyanobacterium with affinities to Oscillatoriaceae from the Lower Devonian Rhynie chert. Paläontologische Zeitschrift 93 (3):377–386.

Krings, Michael, & C. J. Harper. 2019. A microfossil resembling Merismopedia (Cyanobacteria) from the 410-million-yr-old Rhynie and Windyfield cherts: *Rhyniococcus uniformis* revisited. Nova Hedwigia 108:17–35.

Krings, Michael, Hans Kerp, Hagen Hass, T. N. Taylor, & Nora Dotzler. 2007. A filamentous cyanobacterium showing structured colonial growth from the Early Devonian Rhynie chert. Review of Palaeobotany and Palynology 146:265–276 [doi.10.1016/j.revpalbo.2007.05.002].

Krumbein, W. E. 1983. Stromatolites:The challenge of a term in space and time. Precambrian Research 20:493–531.

Krumbein, W. E., D. M. Paterson, & L. C. Stal. 1994. Biostabilization of Sediments. BIS-Verlag. Oldenburg. 526 p.

Kruse, P. D., & A. Y. Zhuravlev. 2008. Middle–Late Cambrian Rankenella–Girvanella reefs of the Mila Formation, northern Iran. Canadian Journal of Earth Sciences (45):619–639.

Krylov, I. N. 1963. Columnar branching stromatolites of the Riphean deposits of the Southern Ural and their significance for the stratigraphy of the Upper Precambrian. Trudi Geologicheskogo Instituta, Akademija Nauk SSSR (69):133 p. In Russian.

Kühl, Michael, & Thomas Fenchel, 2000. Bio-optical characteristics and the vertical distribution of photosynthetic pigments and photosynthesis in an artificial cyanobacterial mat. Microbial Ecology 40:94–103.

Kühl, Michael, Carsten Lassen, & B. B. Jørgensen. 1994. Light penetration and light intensity in sandy marine sediments measured with irradiance and scalar fiber-optic microprobes. Marine Ecology Progress Series 105:139–148.

Kulp, T. R., S. E. Hoeft, M. Asao, M. T. Madigan, J. T. Hollibaugh, J. C. Fisher, J. F. Stolz, C. W. Culbertson, L. G. Miller, & R. S. Oremland. 2008. Arsenic (III) fuels anoxygenic photosynthesis in hot spring biofilms from Mono Lake, California. Science 312:967–970.

Kump, L. R., & W. E. Seyfried. 2005. Hydrothermal Fe fluxes during the Precambrian: Effect of low oceanic sulfate concentrations and low hydrostatic pressure on the composition of black smokers. Earth and Planetary Science Letters 235:654–662.

Kunin, Victor, Jeroen Raes, H. K. Harris, J. R. Spear, J. J. Walker, Natalie Ivanova, Christian von Mering, B. M. Bebout, N. R. Pace, Peer Bork, & Philip Hugenholtz. 2008. Millimeter-scale genetic gradients and community-level molecular convergence in a hypersaline microbial mat. Molecular Systems Biology 4:198 [doi.10.1038/msb.2008.35].

Kützing, F. T. 1843. Phycologia Generalis oder Anatomie, Physiologie und Systemkunde der Tange. F. A. Brockhaus. Leipzig. xxxii + 458 p.

Kvale, E. P., Jeff Cutright, Douglas Bilodeau, A. W. Archer, H. R. Johnson, & Brian Pickett. 1995. Analysis of modern tides and implications for ancient tidalites. Continental Shelf Research 15(15):1921–1943.

Laflamme, Marc, J. D. Schiffbauer, G. M. Narbonne, & D. E. G. Briggs. 2011. Involvement of microbial mats in early fossilization by decay delay and formation of impressions and replicas of vertebrates and invertebrates. Lethaia 44:203–213.

Lamboy, Michel, V. P. Rao, Ezzat Ahmed, & Nasreddine Azzouzi. 1994. Nannostructure and significance of fish coprolites in phosphorites. Marine Geology 120:373–383.

Lan, Zhongwu, Shujing Zhang, Maurice Tucker, Zhensheng Li, & Zhuoya Zhao. 2020. Evidence for microbes in early Neoproterozoic stromatolites. Sedimentary Geology 398:105589 [doi.10.1016/j.sedgeo.2020.105589].

Latham, Andrew, & Robert Riding. 1990. Fossil evidence for the location of the Precambrian/Cambrian boundary in Morocco. Nature (344):752.

Lauterborn, Robert. 1907. A new genus of sulfur bacteria (*Thioploca schmidlei* nov. gen. nov. spec.). Berichte der Deutschen Botanischen Gesellschaft 25:238–242.

Laval, Bernard, S. L. Cady, J. C. Pollack, C. P. McKay, J. S. Bird, J. P. Grotzinger, D. C. Ford, & H. R. Bohm. 2000. Modern freshwater microbialite analogues for ancient dendritic reef structures. Nature (407):626.

Lawrence, M. G., & B. S. Kamber. 2006. The behaviour of the rare earth elements during estuarine mixing—revisited. Marine Chemistry 100:147–161.

Lee, K. W. K., Saravanan Periasamy, Manisha Mukherjee, Xie Chao, Staffan Kjelleberg, & S. A. Rice. 2014. Biofilm development and enhanced stress resistance of a model, mixed-species community biofilm. The ISME Journal 8(4):894–907.

Lee, S.-J., & Stjepko Golubic. 1998. Multi-trichomous cyanobacterial microfossils from the Mesoproterozoic Gaoyuzhuang Formation, China: Paleoecological and taxonomic implications. Lethaia 31:169–184.

Lehours, A. C., Paul Evans, Corinne Bardot, Keith Joblin, & Gérard Fonty. 2007. Phylogenetic diversity of Archaea and Bacteria in the anoxic zone of a meromictic lake (Lake Pavin, France). Applied and Environmental Microbiology 73:2016–2019.

Leinfelder, R. R., Winfried Werner, Martin Nose, D. U. Schmid, Manfred Krautter, Ralf Laternser, Martin Takacs, & Dorothea Hartmann. 1996. Paleoecology, growth parameters and dynamics of coral, sponge and microbolite reefs from the Late Jurassic. *In* Joachim Reitner, Fritz Neuweiler, & Felix Gunkel, eds., Global and Regional Controls on Biogenic Sedimentation. Göttinger Arbeiten zur Geologie und Paläontologie, Göttingen. p. 227–248.

Lekele Baghekema, S. G., Kevin Lepot, Armelle Riboulleau, Alexandre Fadel, Alain Trentesaux, & Abderrazak El Albani. 2017. Nanoscale analysis of preservation of ca. 2.1 Ga old Francevillian microfossils, Gabon. Precambrian Research 301:1–18.

Leo, R. F., & E. S. Barghoorn. 1976. Silicification of wood. Botanical Museum Leaflets, Harvard University 25:1–47.

Lepot, Kevin. 2020. Signatures of early microbial life from the Archean (4 to 2.5 Ga) eon. Earth-Science Reviews 209:103296 [doi.10.1016/j.earscirev.2020.103296].

Lepot, Kevin, Karim Benzerara, G. E. Brown, & Pascal Philippot. 2008. Microbially influenced formation of 2,724-million-year-old stromatolites. Nature Geoscience (1):118–121.

Lepot, Kevin, K. H. Williford, Pascal Philippot, Christophe Thomazo, Takayuki Ushikubo, K. Kitajima,

Smail Mostefaoui, & J. W. Valley. 2019. Extreme ^{13}C-depletions and organic sulfur content argue for S-fueled anaerobic methane oxidation in 2.72 Ga old stromatolites. Geochimica et Cosmochimica Acta 244:522–547.

Ley, R. E., J. K. Harris, J. Wilcox, J. R. Spear, S. R. Miller, B. M. Bebout, J. A. Maresca, D. A. Bryant, M. L. Sogin, & N. R. Pace. 2006. Unexpected diversity and complexity of the Guerrero Negro hypersaline microbial mat. Applied and Environmental Microbiology 72:3685–3695.

Li, Guoxiang. 1997. Early Cambrian phosphate-replicated endolithic algae from Emei, Sichuan, SW China. Bulletin of the National Museum of Natural Science (Taichung, China) 10:193–216.

Li, Jinhua, Karim Benzerara, Sylvain Bernard, & Oliver Beyssac. 2013. The link between biomineralization and fossilization of bacteria: Insights from field and experimental studies. Chemical Geology 359:49–69 [doi.10.1016/j.chemgeo.2013.09.013].

Li, Jinhua, Nicolas Menguy, A. P. Roberts, Lin Gu, Eric Leroy, Julie Bourgon, Xin'an Yang, Xiang Zhao, Peiyu Liu, H. G. Changela, & Yongxin Pan. 2020. Bullet-shaped magnetite biomineralization within a magnetotactic deltaproteobacterium: Implications for magnetofossil identification. Journal of Geophysical Research: Biogeosciences 125:e2020JG005680 [doi.10.1029/2020JG005680].

Li, Weiqiang, J. M Huberty, B. L.Beard, N T. Kita, J. W. Valley, & C. M. Johnson. 2013. Contrasting behavior of oxygen and iron isotopes in banded iron formations as determined by *in situ* isotopic analysis. Earth and Planetary Science Letters 384:132–143.

Lin,Yitian, Dongjie Tang, Xiaoying Shi, Xiqiang Zhou, & Kangjun Huang. 2019. Shallow-marine ironstones formed by microaerophilic iron-oxidizing bacteria in terminal Paleoproterozoic. Gondwana Research 76:1–18.

van Lith, Yvonne, Crisógono Vasconcelos, Rolf Whathmann, J. C. F. Martins, & J. A. McKenzie. 2002. Bacterial sulfate reduction and salinity: Two controls on dolomite precipitation in Lagoa Vermelha and Brejo do Espinho (Brazil). Hydrobiologia 485: 35–49.

Little, C. T. S., S. E. J. Glynn, & R. A. Mills. 2004. Four-hundred-and-ninety-million-year record of bacteriogenic iron oxide precipitation at sea-floor hydrothermal vents. Geomicrobiology Journal 21:415–429.

Little, C. T. S., K. C. Johannessen, Stefan Bengtson, C. S. Chan, Magnus Ivarsson, J. F. Slack, Curt Broman, I. H. Thorseth, Tor Grenne, O. J. Rouxel, & Andrey Bekker. 2021. A late Paleoproterozoic (1.74 Ga) deep-sea, low-temperature, iron-oxidizing microbial hydrothermal vent community from Arizona, USA. Geobiology 19(3):228-249.

Liu, A. G., & F. S. Dunn. 2020. Filamentous Connections between Ediacaran Fronds. Current Biology 30:1322–1328.

Liu, A. G., Duncan McIlroy, J. B. Antcliffe, & M. D. Brasier. 2011. Effaced preservation in the Ediacara Biota and its implications for the early macrofossil record. Palaeontology 54:607–630.

Liu, Wei, & Xingliang Zhang. 2017. Possible biogenic structures from the Lower Cambrian strata in Yunnan Province, South China. Geological Magazine 154:1285–1293.

Liu, Wenzheng, H. L. Røder, J. S. Madsen, Thomas Bjarnsholt., S. J. Sørensen, & Mette Burmølle. 2016. Interspecific bacterial interactions are reflected in multispecies biofilm spatial organization. Frontiers in Microbiology 7:1366 [doi.org/10.3389/fmicb.2016.01366].

Liu, Zhenfeng, C. G. Klatt, J. M. Wood, D. B. Rusch, Marcus Ludwig, Nicola Wittekindt, L. P. Tomsho, S. C. Schuster, D. M. Ward, & D. A. Bryant. 2011. Metatranscriptomic analyses of chlorophototrophs of a hot-spring microbial mat. ISME Journal 5:1279–1290.

Lloyd, K. G., D. B. Albert, J. F. Biddle, J. P. Chanton, Oscar Pizarro, & Andreas Teske. 2010. Spatial structure and activity of sedimentary microbial communities underlying a *Beggiatoa* spp. mat in a Gulf of Mexico hydrocarbon seep. PLOS One [doi.10.1371/journal.pone.0008738].

Locey, K. J., & J. T. Lennon. 2019. Scaling laws predict global microbial diversity. Proceedings of the National Academy of Sciences, USA 113:5970–5975.

Lockey, M. G., & Kelly Conrad. 1989. The paleoenvironmental context, preservation and paleoecological significance of dinosaur tracksites in the western USA. *In* D. D. Gilette & M.G. Lockey, ed., Dinosaur Tracks and Traces. Cambridge University Press. Cambridge, UK. p 121–134.

LoDuca, S. T., Natalia Bykova, Mengying Wu, Shuhai Xiao, & Yuanlong Zhao. 2017. Seaweed morphology and ecology during the great animal diversification events of the early Paleozoic: A tale of two floras. Geobiology 15:588–616.

Logan, B. W. 1961. Cryptozoon and associate stromatolites from the Recent, Shark Bay, Western Australia. Journal of Geology 69:517–533.

Logan, B. W., Richard Rezak, & R. N. Ginsburg. 1964. Classification and environmental significance of algal stromatolites. Journal of Geology 72:68–83.

Logan, G. A., C. R. Claver, Paul Girjan, R. E. Summons, J. M. Hayes, & M. R. Walter. 1999. Terminal Proterozoic mid-shelf benthic microbial mats in the Centralian Superbasin and their environmental significance. Geochimica et Cosmochimica Acta 63:345–1358.

Lopéz-Lopéz, Arantxa, Michael Richter, Arantxa Peña, Javier Tamames, & R. A. Rosselló-Móra. 2013. New insights into the archaeal diversity of a hypersaline microbial mat obtained by a metagenomic approach. Systematic and Applied Microbiology 36(3)205–214.

Louyakis, A. S., J. M. Mobberley, B. E. Vitek, P. T. Visscher, P. D. Hagan, R. P. Reid, Reinhard Kozdon, I. J. Orland. J. W. Valley, N. J. Planavsky, Giorgio Casaburi, & J. S. Foster. 2017. A study of spatial heterogeneity of Bahamian thrombolites using molecular, biochemical, and stable isotope analyses. Astrobiology 17:413–430.

Lovelock, J. E., R. J. Maggs, & R. A. Rasmussen. 1972. Atmospheric diemthyl sulphide and the

natural sulphur cycle. Nature 237:452–453.
Lovley, D. R. 1991. Dissimilatory Fe(III) and Mn(IV) reduction. Microbiology Reviews 55:259–287.
Lovley, D. R. 2004. Potential role of dissimilatory iron reduction in the early evolution of microbial respiration. *In* J. Seckbach, ed., Origins, Evolution, and Biodiversity of Microbial Life. Kluwer. The Netherlands. p. 301–313.
Lovley, D. R. 2013. Dissimilatory Fe(III)- and Mn(IV)-reducing prokaryotes. *In* Eugene Rosenberg, E. F. DeLong, S. Lory, E. Stackebrandt, & F. Thompson, eds., The Prokaryotes: Prokaryotic Physiology and Biochemistry (4th edition). Springer-Verlag. Berlin Heidelberg. p. 287–308.
Lovley, D. R., S. J. Giovannoni, D. C. White, J. E. Champine, E. J. P. Phillips, Y. A. Gorby, & Steve Goodwin. 1993. *Geobacter metallireducens* gen. nov. sp. nov., a microorganism capable of coupling the complete oxidation of organic compounds to the reduction of iron and other metals. Archives of Microbiology 159:336–344.
Lovley, D. R., & E. J. P. Phillips. 1987. Competitive mechanisms for inhibition of sulfate reduction and methane production in the zone of ferric iron reduction in sediments. Applied and Environmental Microbiology 53:2636–2641.
Lovley, D. R., J. F. Stolz, G. L. Nord, & E. J. P. Phillips. 1987. Anaerobic production of magnetite by a dissimilatory iron-reducing microorganism. Nature 330:252–254.
Lowe, D. R. 1980. Stromatolites 3,400-myr old from the Archean of Western Australia. Nature 284:441–443.
Luo, Genming, Shuhei Ono, N. J. Beukes, D. T. Wang, Shucheng Xie, & R. E. Summons. 2016. Rapid oxygenation of Earth's atmosphere 2.33 billion years ago. Science Advances 2:e1600134 [doi.10.1126/sciadv.1600134].
Lyons, T. W., C. T. Reinhard, & N. J. Planavsky. 2014. The rise of oxygen in Earth's early ocean and atmosphere. Nature 506:307–315.
Lyu, Zhe, & Yuchen Liu. 2018. Diversity and taxonomy of methanogens. *In* A. J. M. Stams, & D. Z. Sousa, eds., Biogenesis of Hydrocarbons: Handbook of Hydrocarbon and Lipid Microbiology. Springer. New York. p. 19–77.
Macdonald, F. A., J. V. Strauss, C. V. Rose, F. O. Dudás, & D. P. Schrag. 2010. Stratigraphy of the Port Nolloth Group of Namibia and South Africa and implications for the age of Neoproterozoic iron formations. American Journal of Science 310:862–888.
MacDonell, Michael, & Rita Colwell. 1985. Phylogeny of the Vibrionaceae, and recommendation for two new genera, *Listonella* and *Shewanella*. Systematic and Applied Microbiology 6:171–182.
Maegaard, Karen, L. P. Nielsen, & N. P. Revsbech. 2017. Hydrogen dynamics in cyanobacteria dominated microbial mats measured by novel combined H_2/H_2S and H_2/O_2 microsensors. Frontiers in Microbiology 8:2022 [doi.10.3389/fmicb.2017.02022].
Maisano, Lucia, D. G. Cuadrado, & E. A. Gómez. 2019. Processes of MISS-formation in a modern siliciclastic tidal flat, Patagonia (Argentina). Sedimentary Geology 381:1–12.
Maliva, R. G., A. H. Knoll, & B. M. Simonson. 2005. Secular change in the Precambrian silica cycle: Insights from chert petrology. Geological Society of America Bulletin 117:835–845.
Mángano, M. G., L. A. Buatois, R. R. West, & C. G. Maples. 2002. Ichnology of Pennsylvanian equatorial tidal flat: The Stull Shale Member at Waverly, Eastern Kansas. Kansas Geological Survey Bulletin 245:133 p.
Manikyamba, C., V. Balaram, & S. M. Naqvi. 1993. Geochemical signatures of polygenetic origin of a banded iron formation (BIF) of the Archaean Sandur greenstone belt (schist belt) Karnataka nucleus, India. Precambrian Research 61:137–164.
Manning-Berg, A. R., & L. A. Kah. 2017. Proteozoic microbial mats and their constraints on environments of silicification. Geobiology 15:469–483.
Manning-Berg, A. R., R. S. Wood, K. H. Williford, A. D. Czaja, & L. C. Kah. 2019. The taphonomy of Proterozoic microbial mats and implications for early silicification. Geosciences 9:1–40.
Marin-Carbonne, Johanna, Laurent Remusat, M. C. Sforna, Christophe Thomazo, Pierre Cartigny, & Pascal Philippot. 2018. Sulfur isotopes signal of nanopyrites enclosed in 2.7 Ga stromatolitic organic remains reveal microbial sulfate reduction. Geobiology 16(2):121–138.
Mariotti, Giulio, S. B. Pruss, J. T. Perron, & Tanja Bosak. 2014. Microbial shaping of sedimentary wrinkle structures. Nature Geoscience 7:736–740.
Martin, Derek, D. E. G. Briggs, & R. J. Parkes. 2003. Experimental mineralization of invertebrate eggs and the preservation of Neoproterozoic embryos. Geology 31:39–42.
Martín-Algarra, A., & A. Sánchez-Navas. 1995. Phosphate stromatolites from condensed cephalopod limestones, Upper Jurassic, Southern Spain. Sedimentology (42):893–919.
Martín-Algarra, A., & J. A. Vera. 1994. Mesozoic Pelagic Phosphate Stromatolites from the Penibetic (Betic Cordillera, Southern Spain). *In* Janine Bertrand-Sarfati & C. L. Monty, eds., Phanerozoic Stromatolites II. Springer. Berlin. p. 345–391.
Martindale, R. C., J. V. Strauss, E. A. Sperling, J. E. Johnson, M. J. Van Kranendonk, David Flannery, Katherine French, Kevin Lepot, Rajat Mazumder, M. S. Rice, D. P. Schrag, Roger Summons, Malcolm Walter, John Abelson, & A. H. Knoll. 2015. Sedimentology, chemostratigraphy, and stromatolites of lower Paleoproterozoic carbonates, Turee Creek Group, Western Australia. Precambrian Research 266:194–211.
Marty, Daniel, André Strasser, & C. A. Meyer. 2009. Formation and taphonomy of human footprints in microbial mats of present-day tidal-flat environments: Implications for the study of fossil footprints. Ichnos 16(1–2):127–142.
Maslov, V .P. 1960. Stromatolity [Stromatolites]. Trudi Geologicheskogo Instituta, Akademija Nauk SSSR, Vol. 41. 188 p. In Russian.
Massé, Astrid, Olivier Pringault, & Rutger de Wit. 2002. Experimental study of interactions between

purple and green sulfur bacteria in sandy sediments exposed to illumination deprived of near-infrared wavelengths. Applied and Environmental Microbiology 68(6):2972–2981.

Mata, S. A., & D. J. Bottjer. 2009. The paleoenvironmental distribution of Phanerozoic wrinkle structures. Earth-Science Reviews 96:181–195.

Mata, S. A., & D. J. Bottjer. 2011. Origin of Lower Triassic microbialites in mixed carbonate-siliciclastic successions: Ichnology, applied stratigraphy, and the end-Permian mass extinction. Palaeogeography, Palaeoclimatology, Palaeoecology 300:158–178.

Mata, S. A., & D. J. Bottjer. 2012. Microbes and mass extinctions: Paleoenvironmental distribution of microbialites during times of biotic crisis. Geobiology 10:3–24.

Mata, S. A., C. L. Harwood, F. A. Corsetti, N. J. Stork, K. Eilers, W. M. Berelson, & J. R. Spear. 2012. Influence of gas production and filament orientation on stromatolite microfabric. Palaios 27:206–219.

Maynard, J. B. 2003. Manganiferous sediments, rocks, and ores. Treatise on Geochemistry 7:289–308.

Maynard, J. B., & F. B. Van Houten. 1992. Descriptive model of oolitic ironstones. U.S. Geological Survey Bulletin 2004:39–40.

McLean, R. J. C., M. Whiteley, D. J. Stickler, & W. C. Fuqua. 1997. Evidence of autoinducer activity in naturally occurring biofilms. FEMS Microbiology Letters 154(2):259–263.

McLennan, S. M., & S. R. Taylor. 1991. Sedimentary rocks and crustal evolution: Tectonic setting and secular trends. Journal of Geology 99:1–21.

McLoughlin, Nicola, David Wacey, Siyolise Phungu-phungu, Martin Saunders, & E. G. Grosch. 2020. Deconstructing Earth's oldest ichnofossil record from the Pilbara Craton, West Australia: Implications for seeking life in the Archean subseafloor. Geobiology 18:525–543.

McMahon, Sean. 2019. Earth's earliest and deepest purported fossils may be iron-mineralized chemical gardens. Proceedings of the Royal Society of London B (Biological Sciences) 286:20192410 [doi.10.1098/rspb.2019.2410].

McMahon, W. J., N. S. Davies, & D. J. Went. 2017. Negligible microbial matground influence on pre-vegetation river functioning: Evidence from Ediacaran-Lower Cambrian Series Rouge, France. Precambrian Research 292:13–34.

Medvedev, P. N., Andrey Bekker, J. A. Karhu, & N. M. Kortelainen. 2005. Testing the biostratigraphic potential of Early Paleoproterozoic microdigitate stromatolites: Revista Espanola de Micropaleontologia (37):41–56.

Meeks, J. C., & R. W. Castenholz. 1971. Growth and photosynthesis in an extreme thermophile, *Synechococcus lividus* (Cyanophyta). Archiv fur Mikrobiologie 78:25–41.

Meert, J. G., M. K. Pandit, V. R. Pradhan, & G. Kamenov. 2011. Preliminary report on the paleomagnetism of 1.88 Ga dykes from the Bastar and Dharwar cratons, peninsular India. Gondwana Research 20:335–343.

Megonigal, J. P., M. E. Hines, & P. T. Visscher. 2003. Anaerobic metabolism and production of trace gases. *In* H. D. Holland & K. K. Turekian, ed., Treatise on Geochemistry, Vol. 8. Elsevier. Amsterdam. p. 317–424.

Mendelson, C. V., & J. W. Schopf. 1992. Proterozoic and selected early Cambrian microfossils and microfossil-like objects. *In* J. W. Schopf, & Cornelis Klein, eds., The Proterozoic biosphere: A Multidisciplinary Study. Cambridge University Press. Cambridge, UK. p. 865–952.

Mendes-Monteiro, Juliana, Ryan Vogwill, Katrl Bischoff, & D. B. Gleeson. 2019. Comparative metagenomics of microbial mats from hypersaline lakes at Rottnest Island (WA, Australia), advancing our understanding of the effect of mat community and functional genes on microbialite accretion. Limnology and Oceanography 65:S293–S309.

Méndez-García, Celicia, Victoria Mesa, R. R. Sprenger, Michael Richter, Maria Suarez-Diez, Jennifer Solano, Rafael Bargiela, O. V. Golyshina, Angel Manteca, J. L. Ramos, Irine Llorente, V. A. P. dos Santos, O. N. Jensen, A. I. Pelaez, Jesus Sanches, & Manuel Ferrer. 2014. Microbial stratification in low pH oxic and suboxic macroscopic growths along an acid mine drainage. ISME Journal 8:1259–1274.

Menon, L. R., Duncan Mcilroy, A. G. Liu, & M. D. Brasier. 2016. The dynamic influence of microbial mats on sediments: Fluid escape and pseudofossil formation in the Ediacaran Longmyndian Supergroup: UK. Journal of the Geological Society, London 173:177–185.

Miyano, Takashi, & Cornelis Klein. 1983. Evaluation of the stability relations of amphibole asbestos in metamorphosed iron-formations. Mining Geology 33:213–222.

Mobberley, J. M., C. L. M. Khodadad, & J. S. Foster. 2013. Metabolic potential of lithifying cyanbacteria-dominated thrombolitic mats. Photosynthetic Research 118(1–2)125–140.

Mobberley J. M., C. L. M. Khodadad, P. T. Visscher, R. P. Reid, Paul Hagan, & J. S. Foster. 2015. Inner workings of thrombolites: Spatial gradients of metabolic activity as revealed by meta-transcriptome profiling. Nature Scientific Reports 5:12601 [doi.10.1038/srep12601].

Moczydłowska, Malgorzata, J. W. Schopf, & Sebastian Willman. 2010. Micro- and nano-scale ultrastructure of cell walls in Cryogenian microfossils: revealing their biological affinity. Lethaia 43:129–136.

Moeller, Kirsten, R. Schoenberg, Tor Grenne, I. H. Thorseth, K. Drost, & R. B. Pedersen. 2013. Comparison of iron isotope variations in modern and Ordovician siliceous Fe oxyhydroxide deposits. Geochimica et Cosmochimica Acta 126:422–440.

Moons, Pieter, C. W. Michiels, & Abram Aertsen. 2009. Bacterial interactions in biofilms. Critical Reviews in Microbiology 35(3):157–168.

Moore, E. S. 1918. The iron-formation on Belcher Islands, Hudson Bay, with special reference to its origin and its associated algal limestones. Journal of Geology 26:412–438.

Moore, K. R., Tanja Bosak, Francis Macdonald, Kimberly Du, S. A. Newman, D. J. G. Lahr, & S. B.

Pruss. 2017. Pyritized Cryogenian cyanobacterial fossils from Arctic Alaska. Palaios 32:769–778.

Moore, K. R., Mihkel Pajusalu, Jian Gong, Victor Sojo, Thomas Matreux, Dieter Braun, & Tanja Bosak. 2020. Biologically mediated silicification of marine cyanobacteria and implications for the Proterozoic fossil record. Geology 48:862–866.

Moore, L. S., & R. V. Burne. 1994. The modern thrombolites of Lake Clifton, western Australia. *In* Janine Bertrand-Sarfati & C. L. Monty, eds., Phanerozoic Stromatolites II. Springer. Berlin. p. 3–29

More, T. T., J. S. S. Yadav, Song Yang, R. D. Tyagi, & R. Y. Surampalli. 2014. Extracellular polymeric substances of bacteria and their potential environmental applications. Journal of Environmental Management 144:1–25.

Morgenroth, Eberhard, & P. A. Wilderer. 2000. Influence of detachment mechanisms on competition in biofilms. Water Research 34(2):417–426.

Morris, R. C. 1993. Genetic modeling for banded iron-formation of the Hamersley Group, Pilbara craton, Western Australia. Precambrian Research 60:243–286.

Morris, T. E., P. T. Visscher, M. J. O'Leary, P. R. C. S. Fearns, & L. B. Collins. 2020. The biogeomorphology of Shark Bay, Western Australia. Earth-Science Reviews 205:102921 [doi.10.1016/j.earscirev.2019.102921].

Moyer, A. E., Wenxia Zheng, E. A. Johnson, M. C. Lamanna, D.-q. Li, K. J. Lacovara, & M. H. Schweitzer. 2014. Melanosomes or microbes: Testing an alternative hypothesis for the origin of microbodies in fossil feathers. Scientific Reports 4:4233 [doi.10.1038/srep04233].

Mukhopadhyay, Joydip, N. J. Beukes, R. A. Armstrong, Udo Zimmermann, Gautam Ghosh, & R. A. Medda. 2008. Dating the oldest greenstone in India: A 3.51-Ga precise U-Pb SHRIMP zircon age for dacitic lava of the southern Iron Ore Group, Singhbhum craton. Journal of Geology 116:449–461.

Müller, Johannes, & Jörg Overmann. 2011. Close interspecies interactions between prokaryotes from sulfureous environments. Frontiers in Microbiology 2:146 [doi.10.3389/fmicb.2011.00146].

Muniz, M. C., & D. W. J. Bosence. 2015. Pre-salt microbialites from the Campos Basin (offshore Brazil): Image log facies, facies model and cyclicity in lacustrine carbonates. Geological Society, London, Special Publications (418):221–242.

Muscente, A. D., A. D. Hawkins, & Shuhai Xiao. 2015. Fossil preservation through phosphatization and silicification in the Ediacaran Doushantuo Formation (South China): A comparative synthesis. Palaeogeography Palaeoclimatology Palaeoecology 434:46–62.

Muscente, A. D., J. D. Schiffbauer, Jesse Broce, Marc Laflamme, Kenneth O'Donnell, T. H. Boag, Michael Meyer, A. D. Hawkins, J. W. Huntley, Maria McNamara, L. A. MacKenzie, G. D. Stanley Jr., N. W. Hinman, M. H. Hofmann, & Shuhai Xiao. 2017. Exceptionally preserved fossil assemblages through geologic time and space. Gondwana Research 48:164–188.

Myshrall, K. L., Christophe Dupraz, & P. T. Visscher. 2014. Patterns in Microbialites throughout Geologic Time: Is the Present Really the Key to the Past? *In* D. I. Hembree, B. F. Patt, & J. J. Smith, eds.,Topics in Geobiology, Vol. 41: Experimental Approaches to Understanding Fossil Organisms. Springer Verlag. Berlin. p. 111–142.

Nägeli, C. 1849. Gattungen einzelliger Algen, physiologisch und systematisch bearbeitet. Neue Denkschriften der Allg. Schweizerischen Gesellschaft für die Gesammten Naturwissenschaften 10(7):i-viii, 1–139, pl. 1–8.

Nealson, K. H., & C. R. Myers. 1990. Iron reduction by bacteria: A potential role in the genesis of banded iron formations. American Journal of Science 290:35–45.

Neu, Thomas. 1994. Biofilms and Microbial Mats. *In* W. E. Krumbein, D. Paterson, & L. J. Stal, eds., Biostabilization of Sediments. BIS-Verlag. Oldenburg. p. 3–6.

Nelson, D. R., A. F. Trendall, & W. Altermann. 1999. Chronological correlations between the Pilbara and Kaapvaal Cratons. Precambrian Research 97:165–189.

Nemati, Mehdi, & Gerrit Voordouw. 2003. Modification of porous media permeability, using calcium carbonate produced enzymatically in situ. Enzyme and Microbial Technology 33(5):635–642.

Newman, S. A., Vanja Klepac-Ceraj, Giulio Mariotti, S. B. Pruss, Nicki Watson, & Tanja Bosak. 2017. Experimental fossilization of mat-forming cyanobacteria in coarse-grained siliciclastic sediments. Geobiology 15:484–498.

Newman, S. A., Giulio Mariotti, Sara Pruss, & Tanja Bosak. 2016. Insights into cyanobacterial fossilization in Ediacaran siliciclastic environments. Geology 44:579–582.

Nicholson, H. A., & Robert Etheridge. 1878. A monograph of the Silurian fossils of the Girvan district in Ayrshire, with special reference to those contained in the 'Gray collection.' Part 1. Blackwood & Sons. Edinburgh & London. 135 p.

Nicholson, J. A., J. F. Stolz, & B. K. Pierson. 1987. Structure of a microbial mat at Great Sippewissett Marsh, Cape Cod, Massachusetts. FEMS Microbiology Letters 45(6):343–364.

Nielsen, Michael, N. P. Revsbech, & Michael Kühl. 2015. Microsensor measurements of hydrogen gas dynamics in cyanobacterial microbial mats. Frontiers in Microbiology 6:726 [doi.10.3389/fmicb.2015.00726].

Nielsen, P. H., Andreas Jahn, & Rikke Palmgren. 1997. Conceptual model for production and composition of exopolymers in biofilms. Water Science and Technology 36(1):11–19.

Nisbet, E. G., & C. M. R. Fowler. 1999. Archaean metabolic evolution of microbial mats. Proceedings of the Royal Society of London B (Biological Sciences) 266:2375–2382.

Noffke, Nora. 1997. Mikrobiell induzierte Sedimentstrukturen (MISS) in siliziklastischen Wattablagerungen. Ph.D. Thesis, University of Oldenburg, Germany. 127 p.

Noffke, Nora. 1998. Multidirectional ripple marks arising from bacterial stabilization counteracting

physical rework in modern sandy deposits (Mellum Island, southern North Sea). Geology 26:879–882.
Noffke, Nora. 1999. Erosional remnants and pockets evolving from biotic-physical interactions in a Recent lower supratidal environment. Sedimentary Geology 123:175–181.
Noffke, Nora. 2000. Extensive microbial mats and their influences on the erosional and depositional dynamics of a siliciclastic cold water environment (Lower Arenigian, Montagne Noire, France). Sedimentary Geology 136:207–215.
Noffke, Nora. 2003. Epibenthic cyanobacterial communities counteracting sedimentary processes within siliciclastic depositional systems (present and past). *In* D. M. Paterson, G. Zavarzin, & W. E. Krumbein, eds., Biofilms Through Space and Time: Congress Proceedings. Kluwer Academic Publishers. Dordrecht. p. 265–280.
Noffke, Nora. 2008. Turbulent lifestyle: Microbial mats on Earth's sandy beaches: Today and 3 billion years ago. GSA Today 18(10):4–9 [doi.10.1130/GSATG7A.1].
Noffke, Nora. 2009. An astrobiologist considers life's oldest oxygen. Nature 457:939.
Noffke, Nora. 2010. Geobiology: Microbial Mats in Sandy Deposits from the Archaean Era to Today. Vol. 9. Springer-Verlag. Berlin & Heidelberg. 194 p.
Noffke, Nora, & S. M. Awramik. 2013. Stromatolites and MISS: Differences between relatives. GSA Today 23(9):4–9.
Noffke, Nora, N. J. Beukes, Jens Gutzmer, & R. M. Hazen. 2006. Spatial and temporal distribution of microbially induced sedimentary structures: A case study from siliciclastic storm deposits of the 2.9 Ga Witwatersrand Supergroup, South Africa. Precambrian Research 146:35–44.
Noffke, Nora, N. J. Beukes, R. M. Hazen, & Nora Swift. 2008. Exceptionally preserved microbial mats of Meso-Archean age: The Sinqueni Formation, Pongola Supergroup, South Africa. Geobiology 6:5–20.
Noffke, Nora, Daniel Christian, David Wacey, & R. M. Hazen. 2013. Microbially induced sedimentary structures recording an ancient ecosystem in the ca. 3.48 billion-year-old Dresser Formation, Pilbara, Western Australia. Astrobiology 13:1103–1124.
Noffke, Nora, A. W. Decho, & Paul Stoodley. 2013, Slime though time: The fossil record of prokaryote evolution. Palaios 28:1–5.
Noffke, Nora, K. A. Eriksson, R. M. Hazen, & E. L. Simpson. 2006. A new window into Early Archean life: Microbial mats in Earth's oldest siliciclastic tidal deposits (3.2 Ga Moodies Group, South Africa). Geology 34:253–256.
Noffke, Nora, Gisela Gerdes, & Thomas Klenke. 2003. Benthic cyanobacteria and their influence on the sedimentary dynamics of peritidal depositional systems (siliciclastic, evaporitic salty, and evaporitic carbonatic): Earth-Science Reviews 62:163–176.
Noffke, Nora, Gisela Gerdes, Thomas Klenke, & W. E. Krumbein. 1996. Microbially induced sedimentary structures-examples from modem sediments of siliciclastic tidal flats. Zentralblatt für Geologie und Paläontologie, Teil 1. 1:307–316.
Noffke, Nora, Gisela Gerdes, Thomas Klenke, & W. E. Krumbein. 1997. A microscopic sedimentary succession indicating the presence of microbial mats in siliciclastic tidal flats. Sedimentary Geology 110: 1–6.
Noffke, Nora, Gisela Gerdes, Thomas Klenke, & W. E. Krumbein. 2001. Microbially induced sedimentary structures indicating climatological, hydrological and depositional conditions within Recent and Pleistocene coastal facies zones (southern Tunisia). Facies 44:23–30.
Noffke, Nora, Gisela Gerdes, Thomas Klenke, & W. E. Krumbein. 2001. Microbially induced sedimentary structures: A new category within the classification of primary sedimentary structures. Journal of Sedimentary Research 71:649–656.
Noffke, Nora, J. W. Hagadorn, & Sam Bartlett. 2019. Microbial structures and dinosaur trackways from a Cretaceous coastal environment (Dakota Group, Colorado, U.S.A.) Journal of Sedimentary Research 89(11):1096–1108.
Noffke, Nora, R. M. Hazen, & Noah Nhleko. 2003. Earth's earliest microbial mats in a siliciclastic marine environment (2.9 Ga Mozaan Group, South Africa). Geology 31:673–676.
Noffke, Nora, A. H. Knoll, & J. P. Grotzinger. 2002. Sedimentary controls on the formation and preservation of microbial mats in siliciclastic deposits: A case study from the Upper Neoproterozoic Nama Group, Namibia. Palaios 17:533–544.
Noffke, Nora, & W. E. Krumbein. 1999. A quantitative approach to sedimentary surface structures contoured by the interplay of microbial colonization and physical dynamics. Sedimentology 46:417–426.
Nordstrom, D. K. 2000. Advances in the hydrogeochemistry and microbiology of acid mine waters. International Geology Review 42:499–515.
Nordstrom, D. K., & C. N. Alpers. 1999. Negative pH, efflorescent mineralogy, and consequences for environmental restoration at the Iron Mountain superfund site, California. Proceedings of the National Academy of Sciences, USA 96:3455–3462.
Nordstrom, D. K., C. N. Alpers, C. J. Ptacek, & D. W. Blowes. 2000. Negative pH and extremely acidic mine waters from Iron Mountain, California. Environmental Science and Technology 34:245–258.
Normington, V. J., E. E. Beyer, J. A. Whelan, C. J. Edgoose, & J. D. Woodhead. 2019. Summary of results. NTGS LA-ICP-MS Hf program: Amadeus Basin, July 2013–June 2015. Northern Territory Geological Survey Record 2019–005:1–34.
Nutman, A. P., V. C. Bennett, C. R. L. Friend, M. J. Van Kranendonk, & A. R. Chivas. 2016. Rapid emergence of life shown by discovery of 3,700-million-year-old microbial structures. Nature 537: 535–538.
Oehler, D. Z., François Robert, M. R. Walter, Kenichiro Sugitani, Abigail Allwood, Anders Meibom, Smail Mostefaoui, Madeleine Selo, Aurélien Thomen, & E. K. Gibson. 2009. NanoSIMS: Insights to biogenicity and syngeneity of Archaean carbonaceous structures. Precambrian Research 173:70–78.
Oehler, J. H., & J. W. Schopf. 1971. Artificial microfossils: Experimental studies of permineralization of blue-green algae in silica. Science 174:1229–1231.

Ohkubo, Satoshi, & Hideaki Miyashita. 2017. A niche for cyanobacteria producing chlorophyll *f* within a microbial mat. ISME Journal 11(10):2368–2378.

Ohmoto, Hiroshi. 1997. When did the Earth's atmosphere become oxic? Geochemical News 93(12-13):26–28.

Ohmoto, Hiroshi. 2004. Archean atmosphere, hydrosphere, and biosphere. *In* P. G. Erickson, Wladyslaw Altermann, D. R. Nelson, W. U. Mueller, & Octavian Catuneanu, eds., The Precambrian Earth: Tempos and Events. Developments in Precambrian Geology. Volume 12. Elsevier. Amsterdam. p. 361–368.

Ohmoto, Hiroshi, Yumiko Watanabe, & Kazumasa Kumazawa. 2004. Evidence from massive siderite beds for a CO_2-rich atmosphere before approximately 1.8 billion years ago. Nature 429:395–399.

Ohmoto, Hiroshi, Yumiko Watanabe, K. E. Yamaguchi, H. Naraoka, M. Haruna, T. Kakegawa, K. Hayashi, & Y. Kato. 2006. Chemical and biological evolution of early Earth: Constraints from banded iron formations. *In* S. E. Kesler & Hiroshi Ohmoto, eds., Evolution of early Earth's atmosphere, hydrosphere, and biosphere: Constraints from ore deposits. Geological Society of America Memoir 98:291–331.

Olsen, Ingar. 2015. Biofilm-specific antibiotic tolerance and resistance. European Journal of Clinical Microbiology & Infectious Diseases 34(5):877–886.

Olson, J. B., R. W. Litaker, & H. W. Paerl. 1999. Ubiquity of heterotrophic diazotrophs in marine microbial mats. Aquatic Microbial Ecology 19:29–36.

Ono, Shuhei, J. L. Eigenbrode, A. A. Pavlov, P. Kharech, D. Rumble, J. F. Kasting, & K. H. Freeman. 2003. New insights into Archean sulfur cycle from mass-independent sulfur isotope records from the Hamersley Basin, Australia. Earth and Planetary Science Letters 213:15–30.

Oremland R. S., P. R. Dowdle, S. E. Hoeft, J. O. Sharp, J. K. Schaefer, L. G. Miller, Jody Switzer Blum, R. L. Smith, N. S. Bloom, & Dirk Wallschlaeger. 2000. Bacterial dissimilatory reduction of arsenate and sulfate in meromictic Mono Lake, California. Geochimica et Cosmochimica Acta 64:3073–3084.

Oremland, R. S., & J. F. Stolz. 2003. The ecology of arsenic. Science 300:939–944.

Oren, Aharon. 1990. Formation and breakdown of glycine betaine and trimethylamine in hypersaline environments. Anthonie van Leeuwenhoek 58: 291–298.

Orphan, V. J., L. L. Jahnke, T. Embaye, A. Pernthaler, R. E. Summons, & D. J. Des Marais. 2008. Characterization and spatial distribution of methanogens and methanogenic biosignatures in hypersaline mats of Baja California. Geobiology 6(4):376–393.

Overmann, Jörg, & Hans van Gemerden. 2000. Microbial interactions involving sulfur bacteria: Implications for the ecology and evolution of bacterial communities. FEMS Microbiology Reviews 24(5):591–599.

Pace, Aurélie, Raphaël Bourillot, Anthony Bouton, Emmanuelle Vennin, Olivier Braissant, Christophe Dupraz, Thibault Duteil, Irina Bundeleva, Particia Patrier, Serge Galaup, Yusuke Yokoyama, Michel Franceschi, Aurélien Virgone, & P. T. Visscher. 2018. Formation of stromatolite lamina at the interface of oxygenic-anoxygenic photosynthesis. Geobiology 16(4):378–398.

Pace, Aurélie, Raphaël Bourillot, Anthony Bouton, Emmanuelle Vennin, Serge Galaup, Irina Bundeleva, Patricia Patrier, Christophe Dupraz, Chirstophe Thomazo, Pierre Sansjofre, Yusuke Yokoyama, Michel Franceschi, Yannick Anguy, Léa Pigot, Aurélien Virgone, & P. T. Visscher. 2016. Microbial and diagenetic steps leading to the mineralisation of Great Salt Lake microbialites. Nature Scientific Reports 6:31495 [doi.10.1038/srep31495].

Paerl, H. W., Matthew Fitzpatrick, & B. M. Bebout. 1996. Seasonal nitrogen fixation dynamics in a marine microbial mat: Potential role of cyanobacteria and microheterotrophs. Limnology and Oceanography 41(3):419–427.

Paerl, H. W., S. B. Joye, & B. M. Bebout. 1993. Evaluation of nutrient limitation of CO_2 and N_2 fixation in marine microbial mats. Marine Ecology Progress Series 101:297–306.

Pagès, Anais, Kliti Grice, T. F. Ertefai, Grzegorz Skrzypek, Ricardo Jahnert, & Peter Greenwood. 2014. Organic geochemical studies of modern microbial mats from Shark Bay: Part 1: Influence of depth and salinity on lipid biomarkers and their isotopic signatures. Geobiology 1(5)469–487.

Palmer, Jon, Sreve Flint, & John Brooks. 2007. Bacterial cell attachment, the beginning of a biofilm. Journal of Industrial Microbiology & Biotechnology 34(9):577–588.

Pang, Ke, Qing Tang, Lei Chen, Bin Wan, Changtai Niu, Xunlai Yuan, & Shuhai Xiao. 2018. Nitrogen-fixing heterocystous cyanobacteria in the Tonian Period. Current Biology 28:616–622.

Parenteau, M. N., & S. L. Cady. 2010. Microbial biosignatures in iron-mineralized phototrophic mats at Chocolate Pots Hot Springs, Yellowstone National Park, United States. Palaios 25:97–111.

Parman, S. W. 2007. Helium isotopic evidence for episodic mantle melting and crustal growth. Nature 446:900–903.

Parr, J. M. 1992. Rare-earth element distribution in exhalites associated with Broken Hill type mineralisation at the Pinnacles deposit, New South Wales, Australia. Chemical Geology 100:73–91.

Parr, J. M., & I. R. Plimer. 1993. Models for Broken Hill-type lead-zinc-silver deposits. Geological Association of Canada Special Paper 40:253–288.

Parsek, M. R., & E. P. Greenberg. 2005. Sociomicrobiology: The connections between quorum sensing and biofilms. Trends in Microbiology 13(1):27–33.

Parsiegla, K. I., & J. L. Katz. 2000. Calcite growth inhibition by copper(II): II. Effect of solution composition. Journal of Crystal Growth 213:368–380.

Paterson, D. M. 1997. Biological mediation of sediment erodibility: Ecology and physical dynamics. *In* Neville Burt, R. Parker, & Jacqueline Watts, eds., Cohesive Sediments. Wiley. London. p. 215–229.

Paterson, D. M., & K. S. Black. 2000. Temporal variability in the critical erosion threshold of saltmarsh and upper intertidal sediments. *In* B. R. Sherwood,

B. G. Gardiner, & T. Harris, eds., British Saltmarshes. p. 51–63.

Paul, B. G., Haibing Ding, S. C. Bagby, M. Y. Kellermann, M. C. Redmond, G. L. Andersen, & D. L. Valentine. 2017. Methane-oxidizing bacteria shunt carbon to microbial mats a marine hydrocarbon seep. Frontiers in Microbiology 8:186 [doi.10.3389/fmicb.2017.00186].

Pavlov, A. A., & J. F. Kasting. 2002. Mass-independent fractionation of sulfur isotopes in Archean sediments: Strong evidence for an anoxic Archean atmosphere. Astrobiology 2:27–41.

Pawlowska, M. M., N. J. Butterfield, & J. J. Brocks. 2012. Lipid taphonomy in the Proterozoic and the effect of microbial mats on biomarker preservation. Geology 41(2):103–106.

Pearl, H. W., J. L. Pinkney, & T. F. Steppe. 2000. Cyanobacterial-bacterial mat consortia: Examining the functional unit of microbial survival and growth in extreme environments. Environmental Microbiology 2:11–26.

Pearson, D. G., S. W. Parman, & G. M. Nowell. 2007. A link between large mantle melting events and continent growth seen in osmium isotopes. Nature 449:202–205.

Pecoits, Ernesto, M. K. Gingras, Natalie Aubet, & K. O. Konhauser. 2008. Ediacaran in Uruguay: Palaeoclimatic and palaeobiologic implications. Sedimentology 55:689–719.

Pecoits, Ernesto, M. K. Gingras, M. E. Barley, Andreas Kappler, N. R. Posth, & K. O. Konhauser. 2009. Petrography and geochemistry of the Dales Gorge banded iron formation: paragenetic sequence, source and implications for palaeo-ocean chemistry. Precambrian Research 172:163–187.

Peeters, Karolien, Elie Verleyen, D.A. Hodgson, Peter Convey, Damien Ertz, Wim Vyverman, & Anne Willems. 2012. Heterotrophic bacterial diversity in aquatic microbial mat communities from Antarctica. Polar Biology 35:543–554.

Peng, Xiaotong, & Brian Jones. 2012. Rapid precipitation of silica (opal-A) disguises evidence of biogenicity in high-temperature geothermal deposits: Case study from Dagunguo hot spring, China. Sedimentary Geology 257–260:45–62.

Perfilev, B. V., & D. R. Gabe. 1961. Capillary methods of investigating micro-organisms (English translation 1969). Oliver and Boyd. Edinburgh. 627 p.

Perillo, V. L., Lucía Maisano, A. M. Martinez, I. E. Quijada, & D. G. Cuadrado. 2019. Microbial mat contribution to the formation of an evaporitic environment in a temperate-latitude ecosystem. Journal of Hydrology 575:105–114.

Perri, Eduardo, Maurice Tucker, Miroslaw Slowakiewicz, Fione Whitaker, Leon Bowen, & I. D. Perrotta. 2017. Carbonate and silicate biomineralization in a hypersaline microbial mat (Mesaieed sabkha, Qatar): Roles of bacteria, extracellular polymeric substances and viruses. Sedimentology 65(4):1213–1245

Perry, E. C., F. C. Tan, & G. B. Morey. 1973. Geology and stable isotope geochemistry of Biwabik Iron Formation, northern Minnesota. Economic Geology 68:1110–1125.

Perty, M. 1852. Zur Kenntnis kleinster Lebensformen. Jent and Reinert. Bern. i–vvv +228 p.

Peryt, T. M. 1981. Phanerozoic oncoids: An overview. Facies (4)197–213.

Pesquero, M. D., Virginia Souza-Egipsy, Luis Alcalá, Carmen Ascaso, & Yolanda Fernández-Jalvo. 2014. Calcium phosphate preservation of faecal bacterial negative moulds in hyaena coprolites. Acta Palaeontologica Polonica 59:997–1005.

Peter, J. M. 2003. Ancient iron formations: Their genesis and use in the exploration for stratiform base metal sulphide deposits, with examples from the Bathurst mining camp. Geological Association of Canada, Geotext 4:145–176.

Peter, J. M., & W. D. Goodfellow. 1996. Mineralogy, bulk and rare earth element geochemistry of massive sulphide-associated hydrothermal sediments of the Brunswick Horizon, Bathurst Mining Camp, New Brunswick. Canadian Journal of Earth Sciences 33:252–283.

Peterffy, Olof, Mikael Calner, & Vivi Vajda. 2016. Early Jurassic microbial mats: A potential response to reduced biotic activity in the aftermath of the end-Triassic mass extinction event. Palaeogeography, Palaeoclimatology, Palaeoecology 464:76–85.

Petránek, J., & F. B. Van Houten. 1997. Phanerozoic ooidal ironstones. Czech Geological Survey Special Paper 7:1–71.

Petrisor, A. I., Sandra Szyjka, Tomohiro Kawaguchi, P. T. Visscher, R. S. Norman, & A. W. Decho. 2014. Changing microspatial patterns of sulfate-reducing microorganisms (SRM) during cycling of marine stromatolite mats. International Journal of Molecular Sciences 15:850–877.

Petryshyn, V. A., & F. A. Corsetti. 2011. Analysis of growth directions of columnar stromatolites from Walker Lake, western Nevada. Geobiology 9:425–425.

Petryshyn, V. A., M. Juarez Rivera, H. Agić, C. M. Frantz, F. A. Corsetti, & A. E. Tripati. 2016. Stromatolites in Walker Lake (Nevada, Great Basin, USA) record climate and lake level changes ~35,000 years ago. Palaeogeography, Palaeoclimatology, Palaeoecology 451:140–151.

Pettijohn, F. J., & P. E. Potter. 1964. Atlas and Glossary of Primary Sedimentary Structures. Springer-Verlag. Berlin. 370 p.

Pflüger, Friedrich. 1999. Matground structures and redox facies. Palaios 14:25–39.

Pflüger, Friedrich, & P. G. Gresse. 1996. Microbial sand chips: A non-actualistic sedimentary structure. Sedimentary Geology 102:263–274.

Phillips, A. J., Robin Gerlach, Ellen Lauchnor, A. C. Mitchell, A. B. Cunningham, & Lee Spangler. 2013. Engineered applications of ureolytic biomineralization: A review. Biofouling 29(6):715–733.

Pia, Julius. 1927. Thallophyta. *In* M. J. Hirmer, ed., Handbuch der Paläobotanik, Band 1: Thallophyta, Bryophyta, Pteridophyta. Oldenbourg. Munich. p. 31–136.

Picioreanu, C., M., C. M. van Loosdrecht, & J. J. Heijnen. 2001. Two-dimensional model of biofilm detachment caused by internal stress from liquid flow. Biotechnology and Bioengineering 72(2):205–218.

Pickard, A. L. 2002. SHRIMP U–Pb zircon ages of tuffaceous mudrocks in the Brockman Iron Formation of the Hamersley Range, Western Australia. Australian Journal of Earth Sciences 49:491–507.

Pickard, A. L. 2003. SHRIMP U-Pb zircon ages for the Palaeoproterozoic Kuruman Iron Formation, Northern Cape Province, South Africa: Evidence for simultaneous BIF deposition on Kaapvaal and Pilbara cratons. Precambrian Research 125:275–315.

Pickard, A. L., M. E. Barley, & Bryan Krapež. 2004. Deep-marine depositional setting of banded iron formation: Sedimentological evidence from interbedded clastic sedimentary rocks in the early Paleoproterozoic Dales Gorge Member of Western Australia. Sedimentary Geology 170:37–62.

Pierson, B. K. 1982. Modern mat-building microbial communities: A key to the interpretation of Proterozoic stromatolitic communities. 6.1 Introduction. *In* J. W. Schopf & Cornelus Klein, eds., The Proterozoic Biosphere. Cambridge University Press. Cambridge, UK. p. 247–252.

Pierson, B. K., & R.W. Castenholz. 1974. A phototrophic gliding filamentous bacterium of hot springs, *Chloroflexus aurantiacus*, gen. and sp. nov. Archives of Microbiology 100:5–24.

Pierson, B. K., M. N. Parenteau, & B. M. Griffin. 1999. Phototrophs in high-iron-concentration microbial mats: Physiological ecology of phototrophs in an iron-depositing hot spring. Applied and Environmental Microbiology 65(12):5474–5483.

Pinckney, James, H. W. Paerl, & Matthew Fitzpatrick. 1995. Impacts of seasonality and nutrients on microbial mat community structure and function. Marin Ecology Progress Series 123:207–216.

Planavsky, Noah, Andrey Bekker, O. J. Rouxel, B. Kamber, A. Hofmann, A. Knudsen, & T. W. Lyons. 2010. Rare earth element and yttrium compositions of Archean and Paleoproterozoic Fe formations revisited: New perspectives on the significance and mechanisms of deposition. Geochimica et Cosmochimica Acta 74:6387–6405.

Planavsky, Noah, & R. N. Ginsburg 2009. Taphonomy of modern marine Bahamian microbialites. Palaios 24:5–17.

Planavsky, Noah, R. P Reid, T. W. Lyons, K. L Myshrall, & P. T. Visscher. 2009. Formation and diagenesis of modern marine calcified cyanobacteria. Geobiology 7(5):566–576.

Planavsky, Noah, O. J. Rouxel, Andrey Bekker, Axel Hofmann, C. T. S. Little, & T. W. Lyons. 2012. Iron isotope composition of some Archean and Proterozoic iron formations. Geochimica et Cosmochimica Acta 80:158–169.

Planavsky, Noah, O. J. Rouxel, Andrey Bekker, Russell Shapiro, P. W. Fralick, & Andrew Knudsen. 2009. Iron-oxidizing microbial ecosystems thrived in late Paleoproterozoic redox-stratified oceans. Earth and Planetary Science Letters 286:230–242.

Playford, P. E. 1980. Devonian. Great Barrier Reef of Canning Basin, Western Australia. AAPG Bulletin 64:814–840.

Plimer, I. R. 1988. Broken Hill, Australia and Bergslagen, Sweden: Why God and Mammon bless the anthipodes! *In* The Bergslagen Province, central Sweden: Structure, stratigraphy and ore-forming processes. Geologie en Mijnbouw. Netherlands Journal of Sciences 67:265–278.

Poinar, G. O., Jr., B. M. Waggoner, & U.-C. Bauer. 1993. Terrestrial soft-bodied protists and other microorganisms in triassic amber. Science 259:222–224.

Porada, Hubertus, Julia Ghergut, & E. H. Bouougri. 2008. *Kinneyia*-type wrinkle structures: Critical review and model of formation. Palaios 23:65–77.

Postgate, J. R. 1979. The sulphate-reducing bacteria. Cambridge University Press. Cambridge, UK. 159 p.

Posth, N. R., Florian Hegler, K. O. Konhauser, & Andreas Kappler. 2008. Alternating Si and Fe deposition caused by temperature fluctuations in Precambrian oceans. Nature Geoscience 1:703–708.

Posth, N. R., K. O. Konhauser, & Andreas Kappler. 2011. Banded iron formations. *In* Volker Thiel & Joachim Reitner, eds., Encyclopedia of Geobiology. Encyclopedia of Earth Science Series. Springer. The Netherlands. p. 92–103.

Potts, Malcolm. 1999. Mechanisms of desiccation tolerance in cyanobacteria. European Journal of Phycology 34:319–328.

Poulton, S. W. 2011. Iron mineralization in anoxic, non-sulphidic systems. Mineralogical Magazine 75.3:1662.

Poulton, S. W., P. W. Fralick, & D. E. Canfield. 2004. The transition to a sulphidic ocean 1.84 billion years ago. Nature 43:173–177.

Preisner, E. C., E. B. Fichot, & R. S. Norman. 2016. Microbial mat compositional and functional sensitivity to environmental disturbance. Frontiers in Microbiology 7:1632 [doi.org/10.3389/fmicb.2016.01632].

Pratt, B. R., & N. P. James. 1982. Cryptalgal-metazoan bioherms of early Ordovician age in the St. George Group, western Newfoundland. Sedimentology 29:543–569.

Prave, A. R. 2002. Life on land in the Proterozoic: Evidence from the Torridonian rocks of northwest Scotland. Geology 30:811–814.

Preiss, W. V. 1976. Chapter 2.1 Basic field and laboratory methods for the study of stromatolites. *In* M. R. Walter, ed., Developments in Sedimentology 20: 1–790.

Prieto-Barajas, C. M., Eduaro Valencia-Cantero, & Gustavo Santoyo. 2017. Microbial mat ecosystems: Structure types, functional diversity, and biotechnological application. Electronic Journal of Biotechnology 31:48–56.

Primc-Habdija, Biserka, Ivan Habdija, & Anđelka Plenkovic-Mora. 2001. Tufa deposition and periphyton overgrowth as factors affecting the ciliate community on travertine barriers in different current velocity conditions. Hydrobiologia 457:87–96.

Pruss, S. B., D. J. Bottjer, F. A. Corsetti, & Aymon Baud. 2006. A global marine sedimentary response to the end-Permian mass extinction: Examples from southern Turkey and the western United States. Earth-Science Reviews 78(3–4):193–206.

Pruss, S. B., F. A. Corsetti, & D. J. Bottjer. 2005. The unusual sedimentary rock record of the Early Triassic: A case study from the southwestern United States.

Palaeogeography, Palaeoclimatology, Palaeoecology 21:33–52.

Pruss, S. B., Margaret Fraiser, & D. J. Bottjer. 2004. Proliferation of Early Triassic wrinkle structures: Implications for environmental stress following the end-Permian mass extinction. Geology 32:461–464.

Pufahl, P. K., & P. W. Fralick. 2004. Depositional controls on Palaeoproterozoic iron formation accumulation, Gogebic Range, Lake Superior region, USA. Sedimentology 51:791–808.

Pufahl, P. K., E. E. Hiatt, & T. K. Kyser. 2010. Does the Paleoproterozoic Animikie Basin record the sulfidic ocean transition? Geology 38.7:659–662.

Pufahl, P. K., E. E. Hiatt, & T. K. Kyser. 2011. Does the Paleoproterozoic Animikie Basin record the sulfidic ocean transition? Reply. Geology 39:e242–243 [doi.org/10.1130/G32187Y.1].

Pufahl, P. K., Franco Pirajno, & E. E. Hiatt. 2013. Riverine mixing and fluvial iron formation: A new type of Precambrian biochemical sediment. Geology 41(12):1235–1238.

Qu, Yuangao, Anders Engdahl, Shixing Zhu, Vivi Vajda, & Nicola McLoughlin. 2015. Ultrastructural heterogeneity of carbonaceous material in ancient cherts: Investigating biosignature origin and preservation. Astrobiology 15:825–842.

Qu, Yuangao, Shixing Zhu, Martin Whitehouse, Anders Engdahl, & Nicola McLoughlin. 2018. Carbonaceous biosignatures of the earliest putative macroscopic multicellular eukaryotes from 1630 Ma Tuanshanzi Formation, north China. Precambrian Research 304:99–109.

Raaben, M. E. 1991. Stolbchatyye mikrostromatity v rannem rifei [Columnar microstromatites in the Early Riphean]. Izvestiya Akademii Nauk SSSR Seriya Geologicheskaya. p. 87–96. In Russian.

Raff, E. C., M. E. Andrews, F. R. Turner, Evelyn Toh, D. E. Nelson, & R. A. Raff. 2013. Contingent interactions among biofilm-forming bacteria determine preservation or decay in the first steps toward fossilization of marine embryos. Evolution & Development 15(4):243–56.

Raff, E. C., K. L. Schollaert, D. E. Nelson, P. C. J. Donoghue, C.-W. Thomas, F. R. Turner, B. D. Stein, Xiping Dong, Stefan Bengtson, Therese Huldtgren, Marco Stampanoni, Chongyu Yin, & R. A. Raff. 2008. Embryo fossilization is a biological process mediated by microbial biofilms. Proceedings of the National Academy of Sciences, USA 105:19360–19365.

Ramette, Alban, Michele Frapolli, Marion Fischer-Le Saux, C. Gruffaz, Jean-Marie Meyer, Geneviève Défago, Laurent Sutra, & Yvan Moënne-Loccoz. 2011. Pseudomonas protegens sp. nov., widespread plant-protecting bacteria producing the biocontrol compounds 2,4-diacetylphloroglucinol and pyoluteorin. Systematic Applied Microbiology 34(3):180–188.

Ramsing, N. B., M. J. Ferris, & D. M. Ward. 2000. Highly ordered vertical structure of *Synechococcus* populations within the one-millimeter thick photic zone of a hot spring cyanobacterial mat. Applied and Environmental Microbiology 6:1038–1049.

Rao, T. G., & S. M. Naqvi. 1995. Geochemistry, depositional environment and tectonic setting of the BIF's of the Late Archaean Chitradurga Schist Belt, India. Chemical Geology 121:217–243.

Rashby, S. E., A. L. Sessions, R. E. Summons, & D. K. Newman. 2007. Biosynthesis of 2-methylbacteriohopanepolyols by an anoxygenic phototroph. Proceedings of the National Academy of Sciences, USA 104:15099–15104.

Rasmussen, Birger. 2000. Filamentous microfossils in a 3,235-million-year-old volcanogenic massive sulphide deposit. Nature 405:676–679.

Rasmussen, Birger, I. R. Fletcher, Andrey Bekker, J. R. Muhling, C. J. Gregory, & A. M. Thorne. 2012. Deposition of 1.88-billion-year-old iron formations as a consequence of rapid crustal growth. Nature 484:498–501.

Rasmussen, Birger, I. R. Fletcher, J. J. Brocks, & M. R. Kilburn. 2008. Reassessing the first appearance of eukaryotes and cyanobacteria. Nature 455:1101–1104.

Rasmussen, Birger, D. B. Meier, Bryan Krapež, & J. R. Muhling. 2013. Iron silicate microgranules as precursor sediments to 2.5-billion-year-old banded iron formations. Geology 4:435–438.

Ratcliffe, K. T. 1988. Oncoids as environmental indicators in the Much Wenlock Limestone Formation of the English Midlands. Journal of the Geological Society 145:117–124.

Reid, R. P., N. P. James, I. G. Macintyre, Christophe Dupraz, & R. V. Burne. 2003. Shark Bay stromatolites: Microfabrics and reinterpretation of origins. Facies 49:299–324.

Reid, R. P., I. G. Macintyre, K. M. Brown, R. S. Steneck, & Timothy Miller. 1995. Modern marine stromatolites in the Exuma Cays, Bahamas: Uncommonly common. Facies 33:1–18.

Reid, R. P., P. T. Visscher, A. W. Decho, J. F. Stolz, B. M. Bebout, Christophe Dupraz, I.G. Macintyre, H. W. Paerl, J. L. Pinckney, L. Prufert-Bebout, T. F. Steppe, & D. J. DesMarais. 2000. The role of microbes in acretion, lamination and early lithification of modern marine stromatolites. Nature 406(6799):989–992.

Reineck, H. E. 1979. Rezente und fossile Algenmatten und Wurzelhorizonte. Natur und Museum 109: 290–296.

Reineck, H. E., Gisela Gerdes, Marianne Claes, Katharina Dunajtschik, Heike Riege, & W. E. Krumbein. 1990. Microbial modification of sedimentary surface structures. *In* Dietrich Heling, Peter Rothe, Ulrich Förstner, & Peter Stoffers, eds., Sediments and Environmental Geochemistry. Springer. Berlin. p. 254–276.

Reitlinger, E. A. 1948. Kembriiskie foraminiferi Yakutii [Cambrian Foraminifera of Yakutia]. Byulletin' Moskovskogo Obshchestva Ispytatelej Prirody, Otdelenie Geologii 23:77–81. In Russian.

Rejmankova, Eliska, & Jaroslava Komárková. 2000. A function of cyanobacterial mats in phosphorous-limited tropical wetlands. Hydrobiologia 431:135–150.

Renault, B. 1896. Recherches sur les Bactériacées fossils. Annales des Sciences Naturelles, Série 8 (Botanique) 2:275–349.

Renaut, R. W., Brian Jones, & J. J. Tiercelin. 1998. Rapid *in situ* silicification of microbes at Loburu hot

springs, Lake Bogoria, Kenya Rift Valley. Sedimentology 45:1083–1103.

Reshetnikov, A. S., O. N. Rozova, Y. A. Trotsenko, S. Y. But, V. N. Khmelenia, & I. I. Mustakhimov. 2020. Ectoine degradation pathway in halotolerant methylotrophs. PLOS One 5(4):e0232244 [doi.10.1371/journal.pone.0232244].

Revsbech, N. P., B. B. Jørgensen, T. H. Blackburn, & Yehuda Cohen. 1983. Microelectrode studies of the photosynthesis and O_2, H_2S and pH profiles of a microbial mat. Limnology and Oceanography 28(6):1062–1074.

Ribeiro da Luz, B., & J. K. Crowley. 2012. Morphological and chemical evidence of stromatolitic deposits in the 2.75 Ga Carajás banded iron formation, Brazil. Earth and Planetary Science Letters 355/356:60–72.

Ricardi-Branco, Fresia, Flavia Callefo, R. A. Cataldo, Nora Noffke, L. C. R. Pessenda, A. C. Vidal, & F. C. Branco. 2018. Microbial biofacies and the influence of metazoans in Holocene deposits of the Lagoa Salgada, Rio De Janeiro State, Brazil. Journal of Sedimentary Research 88:1300–1317.

Rico, K. I., N. D. Sheldon, & L. E. Kinsman-Costello. 2020. Associations between redox-sensitive trace metals and microbial communities in a Proterozoic ocean analogue. Geobiology 18(4):462–475.

Riding, Robert. 1977. Skeletal stromatolites. *In* Erik Flügel, ed., Fossil Algae, Recent Results and Developments. Springer. Berlin. p. 57–60.

Riding, Robert. 1983. Cyanoliths (cyanoids): Oncoids formed by calcified cyanophytes. *In* Coated Grains. Springer. Berlin. p. 276–283.

Riding, Robert. 1991. Classification of Microbial Carbonates. *In* Robert Riding, ed., Calcareous Algae and Stromatolites. Springer. Berlin. p. 21–51.

Riding, Robert. 1991. Calcified cyanobacteria. *In* R. Riding, ed., Calcareous Algae and Stromatolites. Springer-Verlag. Berlin. p. 55–87.

Riding, Robert. 1999. The term stromatolite: Towards an essential definition. Lethaia (32):321–330.

Riding, Robert. 2000. Microbial carbonates: The geological record of calcified bacterial-algal mats and biofilms. Sedimentology 47:179–214.

Riding, Robert. 2006. Cyanobacterial calcification, carbon dioxide concentrating mechanisms, and Proterozoic-Cambrian changes in atmospheric composition. Geobiology 4:299–316.

Riding, Robert. 2008. Authigenic carbonate crusts: Components of Precambrian stromatolites. Geologia Croatica (61):73–103.

Riding, Robert. 2011**a**. Microbialites, stromatolites, and thrombolites. *In* Joachim Reitner & Volker Thiel, eds., Encylopedia of Geobiology. Encyclopedia of Earth Sciences Series. Springer. Dordrecht. p. 635–654.

Riding, Robert. 2011b. The nature of stromatolites: 3,500 million years of history and a century of research. *In* Joachim Reitner, N-V. Quéric, & Gernot Arp, eds., Advances in Stromatolite Geobiology. Lecture Notes in Earth Sciences. Springer. Berlin & Heidelberg. 131:29–74.

Riding, Robert, & S. M. Awramik. 2000. Microbial Sediments. Springer. Berlin. 331 p.

Riding, Robert, & A. Y. Zhuravlev. 1995. Structure and diversity of oldest sponge-microbe reefs: Lower Cambrian, Aldan River, Siberia. Geology 23:649–652.

Rinke, Christian, Patrick Schwientek, Alexander Sczyrba, N. N. Ivanova, I. J. Anderson, J-F. Cheng, Aaron Darling, Stephanie Malfatti, B. K. Swan, E. A. Gies, J. A. Dodsworth, B. P. Hedlund, George Tsiamis, S. M. Hugenholtz, & Tanja Woyke. 2013. Insights into the phylogeny and coding potential of microbial dark matter. Nature 499:431–437.

de los Ríos, Asuncion, Carmen Ascaso, Jacek Wierzchos, W. F. Vincent, & Antonio Quesada. 2015. Microstructure and cyanobacterial composition of microbial mats from the High Arctic. Biodiversity and Conservation 24:841–863.

Rios-Del Toro, E. E., E. I. Valenzuela, N. E. Lopez-Lozano, M. G. Cortés-Martínez, M. A. Sánchez-Rodríguez, Omar Calvario-Martínez, Salvador Sánchez-Carrillo, & F. J. Cervantes. 2018. Anaerobic ammonium oxidation linked to sulfate and ferric iron reduction fuels nitrogen loss in marine sediments. Biodegradation 29:429–442.

Risgaard-Petersen, Nils, Michael Kristiansen, R. B. Frederiksen, A. L. Dittmer, J. T. Bjerg, Daniela Trojan, Lars Schreiber, L. R. Damgaard, A. Schramm, & L. P. Nielsen. 2015. Cable bacteria in freshwater sediments. Applied and Environmental Microbiology 81:6003–6011.

Robert, François, & Marc Chaussidon. 2006. A palaeotemperature curve for the Precambrian oceans based on silicon isotopes in cherts. Nature 443:969–972.

Roberts, A. P., Fabio Florindo, Giuliana Villa, Liao Chang, Luigi Jovane, S. M. Bohaty, J. C. Larrasoaña, David Heslop, & J. D. F. Gerald. 2011. Magnetotactic bacterial abundance in pelagic marine environments is limited by organic carbon flux and availability of dissolved iron. Earth and Planetary Science Letters 310:441–452.

Roche, Adeline, Emmanuelle Vennin, Irina Bundeleva, Antony Bouton, Deidre Payandi-Rolland, Pierre Amiotte-Suchet, E. C. Gaucher, Helene Courvoisier, & P. T. Visscher. 2019. The role of the substrate on the mineralization potential of microbial mats in a modern freshwater river (Villiers-le-Bâcle, France). Minerals 9:359 [doi.10.3390/min9060359].

Roeselers, G., M., C. M. van Loosdrecht, & Gerard Muyzer. 2007. Heterotrophic pioneers facilitate phototrophic biofilm development. Microbial Ecology 54(3):578–585.

Rona, P. A., G. Klinkhammer, T. A. Nelsen, J. H. Trefrey, & Henry Elderfield. 1986. Blacksmokers, massive sulphides and vent biota at the mid-Atlantic ridge. Nature 321:33-37.

Rosing, M. T. 1999. ^{13}C-depleted carbon microparticles in >3700-Ma sea-floor sedimentary rocks from West Greenland. Science 283:674–676.

Rossi, Frederico, & Roberto De Philippis. 2015. Role of cyanobacterial exopolysaccharides in phototrophic biofilms and in complex microbial mats. Life 5(2):1218–1238.

Rouillard, Joti, J. M. García-Ruiz, Jian Gong, & M. A. van Zuilen. 2018. A morphogram for silica-witherite biomorphs and its application to microfossil identi-

fication in the early earth rock record. Geobiology 16:279–296.
Rouillard, Joti, M. A. van Zuilen, Celine Pisapia, & J.-M. Garcia-Ruiz. 2021. An alternative approach for assessing biogenicity. Astrobiology 21(2):151–164.
Rouxel, O. J., Andrey Bekker, & K. J.Edwards. 2005. Iron isotope constraints on the Archean and Paleoproterozoic ocean redox state. Science 307:1087–1091.
Rowland, S. M., & R. S. Shapiro. 2002. Reef patterns and environmental influences in the Cambrian and earliest Ordovician. *In* Wolfgang Kiessling, Erik Flügel, & Jan Golonka., eds., Phanerozoic Reef Patterns. Society for Sedimentary Geology, Special Publication 72. Tulsa. p. 95–128.
Rozanov, A. Yu, & M. M. Astafieva. 2009. The evolution of the early precambrian geobiological systems. Paleontological Journal 43:911–927.
Rozenstein, Offer, Eli Zaady, Itzhak Katra, Arnon Karnieli, Jan Adamowski, Hezi Yizhaq. 2014. The effect of sand grain size on the development of cyanobacterial biocrusts. Aeolian Research 15:217–226.
Runnegar, Bruce. 1985. Early Cambrian endolithic algae. Alcheringa 9:179–182.
Ruvindy, Rendy, R. A. White III, B. A. Neilan, & B. P. Burns. 2015. Unravelling core microbial metabolisms in the hypersaline mats of Shark Bay using high-throughput metagenomics. ISME Journal 10:183–196.
Salama, Walid, M. M. El Aref, & Reinhard Gaupp. 2012. Mineralogical and geochemical investigations of the Middle Eocene ironstones, El Bahariya Depression, Western Desert, Egypt. Gondwana Research 22:717–736.
Salama, Walid, M. M. El Aref, & Reinhard Gaupp. 2013. Mineral evolution and processes of ferruginous microbialite accretion: An example from the Middle Eocene stromatolitic and ooidal ironstones of the Bahariya Depression, Western Desert, Egypt. Geobiology 11:15–28.
Sallstedt, Therese, Stefan Bengtson, Curt Broman, P. M. Crill, & D. E. Canfield. 2018. Evidence of oxygenic phototrophy in ancient phosphatic stromatolites from the Paleoproterozoic Vindhyan and Aravalli Supergroups, India. Geobiology 16:139–159.
Sánchez-Baracaldo, Patricia. 2015. Origin of marine planktonic cyanobacteria. Scientific Reports 5:17418 [doi.10.1038/srep17418].
Sánchez-Román, Monica, Crisogono Vasconcelos, Thomas Schmid, Maria Dittrich, J. A. McKenzie, Renato Zenobi, & M. A. Rivadeneyra. 2008. Aerobic Microbial Dolomite at the Nanometer Scale: Implications for the Geologic Record. Geology 36:879–882.
Sancho-Tomás, Maria, Andréa Somogyi, Kadda Medjoubi, Antoine Bergamaschi, P. T. Visscher, A. E. S. van Driessche, Emmanuelle Gérard, M. E. Farias, M. C. Contreras, & Pascal Philippot. 2020. Geochemical evidence for arsenic cycling in living microbialites of a High Altitude Andean Lake (Laguna Diamante, Argentina), Chemical Geology 549:119681 [doi.10.1016/j.chemgeo.2020.119681].
Sarkar, Subir, Santanu Banerjee, Pradip Samanta, & Silambuchelvan Jeevankumar. 2006. Microbial mat-induced sedimentary structures in siliciclastic sediments: Examples from the 1.6 Ga Chorhat Sandstone, Vindhyan Supergroup, M. P., India. Journal of Earth Systems Science 115:49–60.
Sarkar, Subir, Adrita Choudhuri, Sunipa Mandal, & P. G. Erikson. 2016. Microbial mat-related structures shared by both silicilastic and carbonate formations. Journal of Paleogeography 5(3):278–291.
Schaefer, M. O., Jens Gutzmer, & N. J. Beukes. 2001. Late Paleoproterozoic Mn-rich oncoids: Earliest evidence for microbially mediated Mn precipitation. Geology 29:835–838.
Schieber, Juergen. 1986. The possible role of benthic microbial mats during the formation of carbonaceous shales in shallow Proterozoic basins. Sedimentology 33:521–536.
Schieber, Juergen. 1989. Facies and origin of shales from the Mid-Proterozoic Newland Formation, Belt basin, Montana, USA. Sedimentology 36:203–219.
Schieber, Jürgen. 1999. Microbial mats in terrigenous clastics: The challenge of identification in the rock record. Palaios 14:3–12.
Schieber, Juergen. 2004. Microbial Mats in the Siliciclastic Rock Record: A Summary of Diagnostic Features. *In* P. G. Eriksson, W. Altermann, D. Nelson, W. U. Mueller, O. Catuneanu, & K. Strand, eds., The Precambrian Earth: Tempos and Events. Developments in Precambrian Geology. Elsevier. Amsterdam. p. 663–672.
Schieber, Juergen. 2007a. Ripple patches in the Cretaceous Dakota Sandstone near Denver, Colorado, a classical locality for microbially bound tidal sand flats. *In* Juergen Schieber, P. K. Bose, P. G. Eriksson, S. Banjeree, S. Sarkar, W. Altermann, & O. Catuneau, eds., Atlas of Microbial Mat Features Preserved Within the Clastic Rock Record. Elsevier. Amsterdam. p. 222–224.
Schieber, Juergen. 2007b, Benthic microbial mats as an oil shale component: Green River Formation (Eocene) of Wyoming and Utah. *In* Juergen Schieber, P. K. Bose, P. G. Eriksson, S. Banjeree, S. Sarkar, W. Altermann, and O. Catuneau, eds., Atlas of Microbial Mat Features Preserved Within the Clastic Rock Record. Elsevier. Amsterdam. p. 225–232.
Schieber, Jürgen, Pradip Bose, P. G. Eriksson, Santanu Banerjee, Subir Sarkar, Wladyslaw Altermann, & Octavian Catuneanu, eds. 2007. Atlas of Microbial Mat Features Preserved in the Silicilastic Rock Record. Elsevier. Amsterdam. 324 p.
Schiffbauer, J. D., A. F. Wallace, Jesse Broce, & Shuhai Xiao. 2014. Exceptional fossil conservation through phosphatization. *In* Marc Laflamme, J. D. Schiffbauer, & S. A. F. Darroch, eds., Reading and Writing of the Fossil Record: Preservational Pathways to Exceptional Fossilization. The Paleontological Society Papers, Vol. 20. p. 59–82.
Schiffbauer, J. D., Shuhai Xiao, Yaoping Cai, A. F. Wallace, Hong Hua, Jerry Hunter, Huifang Xu, Yongbo Peng, & A. J. Kaufman. 2014. A unifying model for Neoproterozoic–Palaeozoic exceptional fossil preservation through pyritization and carbonaceous compression. Nature Communications 5:5754 [doi.10.1038/ncomms6754].

Schiffbauer, J. D., Leiming Yin, R. J. Bodnar, A. J. Kaufman, Fanwei Meng, Jie Hu, Bing Shen, Xunlai Yuan, Huiming Bao, & Shuhai Xiao. 2007. Ultrastructural and geochemical characterization of Archean-Paleoproterozoic graphite particles: Implications for recognizing traces of life in highly metamorphosed rocks. Astrobiology 7:684–704.

Schirrmeister, B. E., Muriel Gugger, & P. C. J. Donoghue. 2015. Cyanobacteria and the Great Oxidation Event: Evidence from genes and fossils. Palaeontology 58:769–785.

Schirrmeister, B. E., Patricia Sánchez-Baracaldo, & David Wacey. 2016. Cyanobacterial evolution during the Precambrian. International Journal of Astrobiology 15:187–204.

Schloss, P. D., R. A. Girard, Thomas Martin, Joshua Edwards, J. C. Thrash, & E. F. Delong. 2016. Status of the archaeal and bacterial census: An update. mBio (American Society for Microbiology) 7:e00201-00216 [doi.10.1128/mBio.00201-16].

Schmidt, A. R., & Ursula Schäfer. 2005. *Leptotrichites resinatus* new genus and species: A fossil sheathed bacterium in Alpine Cretaceous amber. Journal of Paleontology 79:175–184.

Schopf, J. W. 1968. Microflora of the Bitter Springs Formation, Late Precambrian, central Australia. Journal of Paleontology 42:651–688.

Schopf, J. W. 1983. Earth's Earliest Biosphere: Its Origin and Evolution. Princeton University Press. Princeton. 543 p.

Schopf, J. W. 1992a. Historical development of Proterozoic micropaleontology. *In* J. W. Schopf, & Cornelis Klein, eds., The Proterozoic Biosphere: A Multidisciplinary Study. Cambridge University Press. New York. p. 179–183.

Schopf, J. W. 1992b. Proterozoic prokaryotes: Affinities, geologic distribution, and evolutionary trends. *In* J. W. Schopf, & Cornelis Klein, eds., The Proterozoic Biosphere: A Multidisciplinary Study. Cambridge University Press. New York. p. 195–218.

Schopf, J. W. 1993. Microfossils of the Early Archean Apex Chert: New evidence of the antiquity of life. Science 260:640–646.

Schopf, J. W. 1994. Disparate rates, differing fates: Tempo and mode of evolution changed from the Precambrian to the Phanerozoic. Proceedings of the National Academy of Sciences, USA 91:6735–6742.

Schopf, J. W. 2006a. Fossil evidence of Archaean life. Philosophical Transactions of the Royal Society of London B (Biological Sciences) 361:869–885.

Schopf, J. W. 2006b. The first billion years: When did life emerge? Elements 2:229–233.

Schopf, J. W. 2012. The fossil record of cyanobacteria. *In* B. A. Whitton, ed., Ecology of Cyanobacteria II: Their Diversity in Space and Time. Springer. Dordrecht. p. 15–36.

Schopf, J. W., & E. S. Barghoorn. 1967. Alga-like fossils from the early Precambrian of South Africa. Science 156:508–512.

Schopf, J. W., & E. S. Barghoorn. 1969. Microorganisms from the late Precambrian of South Australia. Journal of Paleontology 43:111–118.

Schopf, J. W., & J. M. Blacic. 1971. New microorganisms from the Bitter Springs Formation (Late Precambrian) of the north-central Amadeus Basin, Australia. Journal of Paleontology 45:925–960.

Schopf, J. M., E. G. Ehlers, D. V. Stiles, & J. D. Birle. 1965. Fossil iron bacteria preserved in pyrite. Proceedings of the American Philosophical Society 109:288–308.

Schopf, J. W., J. D. Farmer, I. S. Foster, A. B. Kudryavtsev, V. A. Gallardo, & Carola Espinoza. 2012. Gypsum-permineralized microfossils and their relevance to the search for life on Mars. Astrobiology 7:619–633 [doi.10.1089/ast.2012.0827].

Schopf, J. W., Kouki Kitajima, M. J. Spicuzza, A. B. Kudryavtsev, & J. W. Valley. 2017. SIMS analyses of the oldest known assemblage of microfossils document their taxon-correlated carbon isotope compositions. Proceedings of the National Academy of Sciences, USA 115(1):53–58.

Schopf, J. W., & Cornelis Klein. 1992. The Proterozoic Biosphere: A Multidisciplinary Study. Cambridge University Press. Cambridge, UK. 1348 p.

Schopf, J. W., A. B. Kudryavtsev, D. G. Agresti, A. D. Czaja, & T. J. Wdowiak. 2005. Raman imagery: A new approach to assess the geochemical maturity and biogenicity of permineralized Precambrian fossils. Astrobiology 5:333–371.

Schopf, J. W., A. B. Kudryavtsev, D. G. Agresti, T. J. Wdowiak, & A. D. Czaja. 2002. Laser-Raman imagery of Earth's earliest fossils. Nature 416:73–76.

Schopf, J. W., A. B. Kudryavtsev, K. Sugitani, & M. R. Walter. 2010. Precambrian microbe-like pseudofossils: A promising solution to the problem. Precambrian Research 179:191–205.

Schopf, J. W., A. B. Kudryavtsev, M. R. Walter, M. J. Van Kranendonk, K. H. Williford, R. Kozdon, J. W. Valley, V. A. Gallardo, Carola Espinoza, & D. T. Flannery. 2015. Sulfur-cycling fossil bacteria from the 1.8-Ga Duck Creek Formation provide promising evidence of evolution's null hypothesis. Proceedings of the National Academy of Sciences, USA 112:2087–2092.

Schopf, J. W., & B. M. Packer. 1987. Early Archean (3.3-billion to 3.5-billion-year-old) microfossils from Warrawoona group, Australia. Science 237:70–73.

Schroeter J. 1872. Über einige durch Bacterien gebildete Pigmente. *In* F. Cohan, ed., Beitrage zur Biologie der Pflanzen. J. U. Kern's Verlag. Breslau & Berlin. p. 109–126.

Schubert, J. K., & D. J. Bottjer. 1992. Early Triassic stromatolites as post-mass extinction disaster forms. Geology 20:883–886.

Schubert, J. K., D. L. Kidder, & D. H. Erwin. 1997. Silica-replaced fossils through the Phanerozoic. Geology 25:1031–1034.

Schultze-Lam, Susanne, F. G. Ferris, K. O. Konhauser, & R. G. Wiese. 1995. In situ silicification of an Icelandic hot spring microbial mat: Implications for microfossil formation. Canadian Journal of Earth Sciences 32:2021–2026.

Schultze-Lam, Susanne, Danielle Fortina, B. S. Davisa, & T. J. Beveridgea. 1996. Mineralization of bacterial surfaces. Chemical Geology 132:171–181.

Schulz, H. N., Thorsten Brinkhoff, T. G. Ferdelman, M. H. Mariné, Andreas Teske, & B. B. Jørgensen. 1999. Dense populations of a giant sulfur bacterium in Namibian shelf sediments. Science 284:493–495.

Schwertmann, Udo, & R. M. Cornell. 1991. Iron oxides in the laboratory; Preparation and characterization. Wiley-VCH, Weinheim, Federal Republic of Germany. 137 p. [Second revised and enlarged edition. 2000. Wiley-VCH. Weinheim. 204 p.]

Seckbach, Joseph, & Aharon Oren. 2010. Microbial mats: Modern and ancient microorganisms in stratified systems. Springer. The Netherlands. 606 p.

Seilacher, Adolf. 1999. Biomat-related lifestyles in the Precambrian. Palaios 14:86–93. <5>

Seilacher, Adolf, L. A. Buatois, & M. G. Mangano. 2005. Trace fossils in the Ediacaran-Cambrian transition: Behavioural diversification, ecological turnover and environmental shift. Palaeogeography, Palaeoclimatology, Palaeoecology 227:323–356.

Semikhatov, M. A., & M. E. Raaben. 2000. Proterozoic stromatolite taxonomy and biostratigraphy. *In* Robert Riding & S. M. Awramik, eds., Microbial Sediments. Springer. Berlin. p. 295–306.

Sergeev, V. N. 1994. Microfossils in cherts from the Middle Riphean (Mesoproterozoic) Avzyan Formation, southern Ural Mountains, Russian Federation. Precambrian Research 65:231–254.

Sergeev, V. N., A. H. Knoll, & J. P. Grotzinger. 1995. Paleobiology of the Mesoproterozoic Billyakh Group, Anabar Uplift, northern Siberia. The Paleontological Society Memoir 39:1–37.

Sergeev, V. N., J. W. Schopf, & A. B. Kudryavtsev. 2020. Global microfossil changes through the Precambrian-Cambrian phosphogenic event: The Shabakta Formation of the phosphorite-bearing Maly Karatau Range, South Kazakhstan. Precambrian Research 349:105386 [doi.10.1016/j.precamres.2019.105386].

Sergeev, V. N., Mukund Sharma, &Yogmaya Shukla. 2012. Proterozoic fossil cyanobacteria. The Palaeobotanist 61:189–358.

Severmann, Silke, C. M. Johnson, B. L. Beard, & James McManus. 2006. The effect of early diagenesis on the Fe isotope compositions of porewaters and authigenic minerals in continental margin sediments. Geochimica et Cosmochimica Acta 70:2006–2022.

Sforna, M. C., M. Daye, Pascal Philippot, Andrea Somogyi, M. A. van Zuilen, Khadda Medjoubi, Emmanuelle Gerard, Frederic Jamme, Christophe Dupraz, Olivier Braissant, Christina Glunk, & P. T. Visscher. 2017. Patterns of metal distribution in hypersaline microbialites during early diagenesis: Implications for the fossil record. Geobiology 15:259–279.

Sforna, M. C., Pascal Philippot, Andrea Somogyi, M. A. van Zuilen, Kadda Medjoubi, Barbara Schoepp-Cothenet, Wolfgang Nitschke, & P. T. Visscher. 2014. Evidence for arsenic metabolism and cycling by microorganisms 2.7 billion years ago. Nature Geosciences 7:811–815.

Shapiro, R. S. 2000. A comment on the systematic confusion of thrombolites. Palaios 15:166–169.

Shapiro, R. S. 2004a. Recognition of fossil prokaryotes in Cretaceous methane seep carbonates: Relevance to astrobiology. Astrobiology 4:439–449.

Shapiro, R. S. 2004b. Neoproterozoic-Cambrian microbialite record. The Paleontological Society Papers 10:5–16.

Shapiro, R. S. 2007. Stromatolites: A 3.5-billion-year ichnologic record. *In* William Miller III, ed., Trace Fossils. Elsevier. Amsterdam. p. 382–390.

Shapiro, R. S., K. R. Aalto, R. F. Dill, & Ray Kenny. 1995. Stratigraphic setting of a subtidal stromatolite field, Iguana Cay, Exumas, Bahamas. *In* H. A. Curran & B. White, eds., Terrestrial and Shallow Marine Geology of the Bahamas and Bermuda, Geological Society of America Special Papers, Denver. p. 139–156.

Shapiro, R. S., & S. M. Awramik. 2000. Microbialite morphostratigraphy as a tool for correlating Late Cambrian–Early Ordovician sequences. The Journal of Geology (108):171–180.

Shapiro, R. S., & S. M. Awramik. 2006. *Favosa-maceria cooperi* new group and form: A widely dispersed, time-restricted thrombolite. Journal of Paleontology (80):411–422.

Shapiro, R. S., H. C. Fricke, & Kelly Fox. 2009. Dinosaur-bearing oncoids from ephemeral lakes of the Lower Cretaceous Cedar Mountain Formation, Utah. Palaios (24):51–58.

Shapiro, R. S., & J. K. Rigby. 2004. First occurrence of an in situ Anthaspidellid sponge in a dendrolite mound (Upper Cambrian; Great Basin, USA): Journal of Paleontology 78:645–650.

She, Zhenbing, Yantao Zhang, Wei Liu, Jingjing Song, Yaguan Zhang, Chao Li, Paul Strother, & Dominic Papineau. 2016. New observations of Ambient Inclusion Trails (AITs) and pyrite framboids in the Ediacaran Doushantuo Formation, South China. Palaeogeography, Palaeoclimatology, Palaeoecology 461:374–388.

Sheldon, N. D. 2012. Microbially Induced Sedimentary Structures in the ca. 1100 Ma Terrestrial Midcontinent Rift of North America. *In* Nora Noffke & H. S. Chafetz, eds., Microbial Mats in Silicilastic Depositional Systems Through Time. SEPM Special Publication 101:153–162.

Shepard, R. N., K. Alexander, M. A. Murphy, & D. Y. Sumner. 2005. Development of complex morphology in a cyanobacterial laboratory system: Implications for the interpretation of fossil microbialites (abstract). Geological Society of America, Earth System Processes. Calgary. Alberta. p. 42–46.

Shepard, R. N., & D. Y. Sumner. 2010. Undirected motility of filamentous cyanobacteria produces reticulate mats. Geobiology 8:179–190.

Shen, Yanan, & Roger Buick. 2004. The antiquity of microbial sulfate reduction. Earth-Science Reviews 64:243–272.

Shi, Min, Qinglai Feng, M. Z. Khan, & Shixing Zhu. 2017. An eukaryote-bearing microbiota from the early Mesoproterozoic Gaoyuzhuang Formation, Tianjin, China and its significance. Precambrian Research 303:709–726.

Shields, Graham, & Ján Veizer. 2002. Precambrian marine carbonate isotope database: version 1.1. Geochemistry. Geophysics. Geosystems 3(6):1–12

Shih, P. M., James Hemp, L. M. Ward, N. J. Matzke, & W. W. Fischer. 2017. Crown group Oxypho-

tobacteria postdate the rise of oxygen. Geobiology 15:19–29.

Shimojo, M., S. Yamamoto, S. Aoki, S. Sakata, K. Maki, K. Koshida, A. Ishikawa, T. Hirata, K. D. Collerson, & T. Komiya. 2013. Occurrence of >3.9 Ga "Nanok" gneiss from Saglek Block, northern Labrador, Canada. Mineralogical Magazine (abstract) 77:2202.

Shiraishi, Fumito, Andrew Bissett, Dirk de Beer, A. Reimer, & Gernot Arp. 2008. Photosynthesis, respiratio and exopolymer calcium-binding in biofilm calcification (Westerhöfer and Deinschwanger Creek, Germany). Geomicrobiology Journal 25(2):83–94.

Sholar, E. M. & W. B. Pratt. 2000. The Antimicrobial Drugs. Oxford University Press. New York. 2nd edition, 607 p.

Siever, Raymond. 1992. The silica cycle in the Precambrian. Geochimica et Cosmochimica Acta 56:3265–3272.

Sigalevich, P. A., Eran Meshorer, Yael Helman, & Yehuda Cohen. 2000. Transition from anaerobic to aerobic growth conditions for the sulfate-reducing bacterium *Desulfovibrio oxyclinae*: Results in flocculation. Applied and Environmental Microbiology 66(11):5005–5012.

Sim, M. S., Biqing Liang, A. P. Petroff, A. Evans, V. Klepac-Ceraj, D. T. Flannery, M. R. Walter, & T. Bosak. 2012. Oxygen-dependent morphogenesis of modern clumped photosynthetic mats and implications for the Archean stromatolite record. Geosciences 2:235–529.

Simonson, B. M. 1985. Sedimentological constraints on the origins of Precambrian iron-formations. Geological Society of America Bulletin 96:244–252 .

Simonson, B. M. 2003. Origin and evolution of large Precambrian iron formations. Geological Society of America Special Paper 370:231–244.

Simonson, B. M., & K. E. Carey. 1999. Roll-up structures: Evidence of in situ microbial mats in Late Archean deep shelf environments. Palaios 14:13–24.

Simonson, B. M., & S. W. Hassler. 1996. Was the deposition of large Precambrian iron formations linked to major marine transgressions? Journal of Geology 104:665–676.

Skyring, G. W., R. M. Lynch, & G. D. Smith. 1988. Acetylene reduction and hydrogen metabolism by a cyanobacterial/sulfate-reducing bacterial mat ecosystem. Geomicrobiology Journal 6:25–31 [.

Slack, J. F., Tor Grenne, & Andrey Bekker. 2009. Seafloor-hydrothermal Si-Fe-Mn exhalites in the Pecos greenstone belt, New Mexico, and the redox state of the ca. 1720 Ma deep seawater. Geosphere 5:302–314.

Slowakiewicz, Miroslaw, Andrej Borkowski, M. C. Syczewski, I. D. Perrotta, Filip Owczarek, Anna Sikora, Anna Detman, Eduardo Perri, & Maurice Tucker. 2021. Newly discovered interactions between bacteriophages and the process of calcium carbonate precipitation. Geochimica et Cosmochimica Acta 292:482–498.

Smith, A. M., & T. R. Mason. 1991. Pleistocene, multiple-growth, lacustrine oncoids from the Poacher's Point Formation, Etosha Pan, northern Namibia. Sedimentology (38):591–599.

Smith, M. D., S. E. Goater, E. S. Reichaldt, Brenton Knott, & Anas Ghadouni. 2010. Effects of recent increases in salinity and nutrient concentrations on the microbialite community of Lake Clifton (Western Australia): Are the thrombolites at risk? Hydrobiologia 649:207–216.

Søgaard, E. G., Robin Medenwaldt, & J. V. Abraham-Peskir. 2000. Conditions and rates of biotic and abiotic iron precipitation in selected Danish freshwater plants and microscopic analysis of precipitate morphology. Water Research 34:2675–2682.

Sohm, J. A., E. A. Webb, & D. G. Capone. 2011. Emerging patterns of marine nitrogen fixation. Nature Reviews Microbiology 9:499–508.

Sommers, M. G., S. M. Awramik, & K. S. Woo. 2000. Evidence for initial calcite-aragonite composition of Lower Algal Chert Member ooids and stromatolites, Paleoproterozoic Gunflint Formation, Ontario, Canada. Canadian Journal Earth Sciences 37:1229–1243.

de Souza Carvalho, Ismar, Leonardo Borghi, & Giuseppe Leonardi. 2013. Preservation of dinosaur tracks induced by microbial mats in the Sousa Basin (Lower Cretaceous), Brazil. Cretaceous Research 44:112–121.

Spang, Anja, J. H. Saw, S. L. Jørgensen, Katarzyna Zaremba-Niedzwiedzka, Joran Martijn, A. E. Lind, Roel van Eijk, Christa Schleper, Lionel Guy, & T. J. G. Ettema. 2015. Complex archaea that bridge the gap between prokaryotes and eukaryotes. Nature 521:173–179.

Spears, B. M., L. Carvalho, R. Perkins, & D. M. Paterson. 2008. Effects of light on sediment nutrient flux and water column nutrient stoichiometry in a shallow lake. Water Research 42(4):977–986.

Spears, B. M., J. E. Saunders, I. Davidson, & D. M. Paterson. 2008. Microalgal sediment biostabilisation along a salinity gradient in the Eden Estuary, Scotland: Unravelling a paradox. Marine and Freshwater Research 59(4):313–321.

Spry, P. G., J. M. Peter, & J. F. Slack. 2000. Metaexhalites as exploration guides to ore. Reviews in Economic Geology 11:163–201.

Stal, L. J. 2012. Cyanobacterial mats and stromatolites. *In* B. A. Whitton, ed., Ecology of Cyanobacteria II: Their Diversity in Space and Time. Springer. London. p. 65–125,

Stal, L. J., & P. Caumette. 1994. Microbial Mats: Structure, Development and Environmental Significance. Springer Verlag. Heidelberg. 463 p.

Stal, L. J., H. van Gemerden, & W. E. Krumbein.1985. Structure and development of a benthic marine microbial mat. FEMS Microbiology Ecology 31 (2):111–125.

Stal, L. J., & R. H. Reed. 1987. Low-molecular mass carbohydrate accumulation in cyanobacteria from a marine microbial mat in response to salt. FEMS Microbiology Ecology 3(5):305–312.

Stanton, R. L. 1972. A preliminary account of chemical relationships between sulfide lode and "banded iron formation" at Broken Hill, New South Wales. Economic Geology 67:1128–1145.

Stanton, R. L. 1976. Petrochemical studies of the ore

environment at Broken Hill, N.S.W.: 3- banded iron formations and sulphide ore bodies: constitutional and genetic ties. Transactions of the Institution of Mining and Metallurgy 85:B132–B141.

Stasiuk, L. D., & K. G. Osadetz. 1990. The life cycle and phyletic affinity of *Gloeocapsomorpha prisca* Zalessky 1917 from Ordovician rocks in the Canadian Williston Basin. Geological Survey of Canada Paper 89–1D:123–137.

Staudigel, Hubert, Harald Furnes, N. R. Banerjee, Yildirim Dilek, & Karlis Muehlenbachs. 2006. Microbes and volcanoes: A tale from the oceans, ophiolites, and greenstone belts. GSA Today 16(10):4–10.

Staudigel, Hubert, Harald Furnes, Nicola McLoughlin, N. R. Banerjee, L. B. Connell, & Alexis Templeton. 2008. 3.5 billion years of glass bioalteration: Volcanic rocks as a basis for microbial life? Earth-Science Reviews 89:156–176.

Steiner, Michael, & Oldrich Fatka. 1996. Lower Cambrian tubular micro- to macrofossils from the Paseky Shale of the Barrandian area (Czech Republic). Paläontologische Zeitschrift 70(3/4):275–299.

Steinhoefel, Grit, Ingo Horn, & F. von Blanckenburg. 2009. Micro-scale tracing of Fe and Si isotope signatures in banded iron formation using femtosecond laser ablation. Geochimica et Cosmochimica Acta 73:5343–5360.

Steppe, T. F., J. B. Olson, H. W. Paerl, R. W. Litaker, & J. Belnap. 1996. Consortial N_2 fixation: A strategy for meeting nitrogen requirements for marine and terrestrial microbial mats. FEMS Microbiology Ecology 21:149–156.

Steppe, T. F., & H. W. Paerl. 2002. Potential N_2 fixation by sulfate-reducing bacteria in a marine intertidal microbial mat. Aquatic Microbial Ecology 28(1):1–12.

Steudel, R., G. Holdt, P. T. Visscher, & Hans van Gemerden. 1990. Search for polythionates in cultures of *Chromatium vinosum* after sulfide incubation. Archives of Microbiology 153:432–437.

Stewart, P. S. 1993. A model of biofilm detachment. Biotechnology and Bioengineering 41(1):111–117.

Stewart, P. S., & M. J. Franklin. 2008. Physiological heterogeneity in biofilms. Nature Reviews Microbiology 6(3):199–210.

Stimson, M. R., R. F. Miller, R. A. Macrae, & S. J. Hinds. 2017. An ichnotaxonomic approach to wrinkled microbially induced sedimentary structures. Ichnos 24:291–316.

Stolz, J. F. 2000. Structure of microbial mats and biofilms. *In* Robert Riding & S. M. Awramik, eds., Microbial Sediments. Springer-Verlag. Berlin, Heidelberg. p. 1–8.

Stoodley, Paul, I. Dodds, Dirk De Beer, Hilary Lappin Scott, & J. D. Boyle. 2005. Flowing biofilms as a transport mechanism for biomass through porous media under laminar and turbulent conditions in a laboratory reactor system. Biofouling 21:161–168.

Stoodley, Paul, Karin Sauer, D. G. Davies, & J. W. Costerton. 2002. Biofilms as complex differentiated communities. Annual Reviews in Microbiology 56:187–209.

Strader, B. D., Penelope Boston, Jane Curnutt, E. A. Gomez, & K. E. Schubert. 2009. Patterned growth in extreme environments. Third IEEE International Conference on Space Mission Challenges for information Technology. Citeseer. p. 221–226.

Straub, K. L., F. A. Rainey, & Friedrich Widdel. 1999. *Rhodovulum iodosum* sp. nov. and *Rhodovulum robiginosum* sp. nov., two new marine phototrophic ferrous-iron-oxidizing purple bacteria. International Journal of Systematic Bacteriology 49:729–735.

Stueken, E. E., Roger Buick, R. E. Anderson, J. A. Baross, N. J. Planavsky, & T. W. Lyons. 2017. Environmental niches and metabolic diversity in Neoarchean lakes. Geobiology 15:767–783.

Sturesson, Ulf. 2003. Lower Palaeozoic iron oolites and volcanism from a Baltoscandian perspective. Sedimentary Geology 159:241–256.

Sturesson, Ulf, Andrei Dronov, & Tönis Saadre. 1999. Lower Ordovician iron ooids and associated oolitic clays in Russia and Estonia: A clue to the origin of iron oolites? Sedimentary Geology 123:63–80.

Suarez-Gonzales, P. A., M. I. Benito, I. E. Quijada, Ramón Mas, & Sonia Campos-Soto. 2019. 'Trapping and binding': A review of the factors controlling the development of fossil agglutinated microbialites and their distribution in space and time. Earth-Science Reviews 194:182–215.

Sugitania, Kenichiro, Koichi Mimura, Tsutomu Nagaoka, Kevin Lepot, & Makoto Takeuchi. 2013. Microfossil assemblage from the 3400 Ma Strelley Pool Formation in the Pilbara Craton, Western Australia: Results form a new locality. Precambrian Research 226:59–74.

Summers Engel, Annette, L. R. Johnson, & M. L. Porter. 2013. Arsenite oxidase gene diversity among *Chloroflexi* and *Proteobacteria* from El Tatio Geyser Field, Chile. 2013. FEMS Microbiology Ecology 83(3):745–756.

Summers, Engel, Anette, M. L. Porter, L. A. Stern, Sarah Quilan, & P. C. Bennett. 2004. Bacterial diversity and ecosystem function of filamentous microbial mats from aphotic (cave) sulfidic springs dominated by chemolithoautotrophic "Epsilonproteobacteria". FEMS Microbiology Ecology 51:31–53. \

Summons, R. E., L. L. Jahnke, J. M. Hope, & G. A. Logan. 1999. 2-Methylhopanoids as biomarkers for cyanobacterial oxygenic photosynthesis. Nature 400:554–557.

Summons, R. E., & M. R. Walter. 1990. Molecular fossils and microfossils of prokaryotes and protists from Proterozoic sediments. American Journal of Science 290A:212–244.

Sumner, D. Y. 1997. Late Archean calcite-microbe interactions: Two morphologically distinct microbial communities that affected calcite nucleation differently. Palaios 12:302–318.

Sumner, D. Y. 2000. Microbial vs environmental influences on the morphology of Late Archean fenestrate microbialites. *In* Robert Riding & S. M. Awramik, eds., Microbial Sediments. Springer-Verlag. Berlin, Heidelberg. p. 307–314.

Sumner, D. Y., Ian Hawes, T. J. Mackey, A. D. Jungblut, & P. T. Doran. 2015. Antarctic microbial mats: A modern analog for Archean lacustrine oxygen oases. Geology 43(10):887–890.

Sun, Funing, Wenxuan Hu, Xiaolin Wang, Jia Cao, Bin Fu, Haiguang Wu, & Shengchao Yang. 2020. Methanogen microfossils and methanogenesis in Permian lake deposits. Geology 49:13–18.

Sutherland, I. W. 2001. Biofilm exopolysaccharides: A strong and sticky framework. Microbiology (Readings) 147(1):3–9.

Sverjensky, D. A. 1984. Europium equilibria in aqueous solution. Earth and Planetary Science Letters 67:70–78.

Taffs, Reed, J. E. Aston, Kristen Brileya, Zackary Jay, C. G. Klatt, Shawn McGlynn, Natasha Mallette, Scott Montross, Robin Gerlach, W. P. Inskeep, D. M. Ward, & R. P. Carlson. 2009. In silico approaches to study mass and energy flows in microbial consortia: A syntrophic case study. BMC Systems Biology 3:114 [https://doi.org/10.1186/1752-0509-3-114].

Taher, A. G. 2014. Microbially induced sedimentary structures in evaporite-siliciclastic sediments of Ras Gemsa sabkha, Red Sea coast, Egypt. Journal of Advanced Research 5:577–586.

Taher, A. G., & A. Abdel-Motelib. 2014. Microbial stabilization of sediments in a recent salina, Lake Aghormi, Siwa Oasis, Egypt. Facies 60:45–2.

Taher, A. G., & A. Abdel-Motelib. 2015. New insights into microbially induced sedimentary structures in alkaline hypersaline El Beida Lake, Wadi El Natrun, Egypt. Geo-Marine Letters 35:341–353.

Taher, A. G., & A. A. Soliman. 1999. Heavy metals concentrations in surficial sediments from Wadi El-Natrun saline lakes, Egypt. International Journal Salt Lake Research 8:75–92.

Taher, A. G., Saad Abdel Wahab, W. E. Krumbein, George Philip, & A. M. Wali. 1994. On heavy metal concentrations and biogenic enrichment in microbial mats. Mineralogica Deposita 29:427–429.

Taitel-Goldman, Nurit, Vladimir Ezrsky, & Dimitry Mogilyanski. 2009. High-resolution transmission electron microscopy study of Fe-Mn oxides in the hydrothermal sediments of the Red Sea deeps system. Clay and Clay Minerals 57:465–475.

Takahashi, Yoshio, Xavier Châtellier, K. O. Hattori, Kenji Kato, & Danielle Fortin. 2005. Adsorption of rare earth elements onto bacterial cell walls and its implication for REE sorption onto natural microbial mats. Chemical Geology 219:53–67.

Talbot, M. R. 1990. A review of the palaeohydrological interpretation of carbon and oxygen isotopic ratios in primary lacustrine carbonates. Chemical Geology: Isotope Geoscience Section 80:261–279.

Tang, Ruikang, G. H. Nancollas, & C. A. Orme. 2001. Mechanism of dissolution of sparingly soluble electrolytes. Journal of Americal Chemical Society 123:5437–5443.

Tang, Qing, Ke Pang, Shuhai Xiao, Xunlai Yuan, Zhiji Ou, & Bin Wan. 2013. Organic-walled microfossils from the early Neoproterozoic Liulaobei Formation in the Huainan region of North China and their biostratigraphic significance. Precambrian Research 236:157–181.

Tang, Qing, Ke Pang, Xunlai Yuan, Bin Wan, & Shuhai Xiao. 2015. Organic-walled microfossils from the Tonian Gouhou Formation, Huaibei region, North China Craton, and their biostratigraphic implications. Precambrian Research 266:296–318.

Tangalos, G. E., B. L. Beard, C. M. Johnson, C. N. Alpers, E. S. Shelobolina, Xu H., H. Konishi, & E. E. Roden. 2010. Microbial production of isotopically light iron(II) in a modern chemically precipitated sediment and implications for isotopic variations in ancient rocks. Geobiology 8:197–208.

Tarhan, L. G., M. L. Droser, & J. G. Gehling. 2015. Depositional and preservational environments of the Ediacara Member, Rawnsley Quartzite (South Australia): Assessment of paleoenvironmental proxies and the timing of 'ferruginization'. Palaeogeography, Palaeoclimatology, Palaeoecology 434:4–13.

Tarhan L. G., N. J. Planavsky, C. E. Laumer, J. F. Stolz, & R. P. Reid. 2013. Microbial mat controls on infaunal abundance and diversity in modern marine microbialites. Geobiology 11:485–497.

Tarhan, L. G., Ashleigh Vs Hood, M. L. Droser, J. G. Gehling, & D. E. G. Briggs. 2016. Exceptional preservation of soft-bodied Ediacara Biota promoted by silica-rich oceans. Geology 44(11):951–954.

Taylor, B. F., & R. P. Kiene. 1989. Microbial metabolism of dimethyl sulfide. In Eric Salzman & W. J. Cooper, eds., Biogenic Sulfur in the Environment. American Chemical Society Symposium Series. 393:202–221.

Taylor, K. G., J. A. Simo, D. Yakum, & D. A. Leckie. 2002. Stratigraphic significance of ooidal ironstones from the Cretaceous western interior seaway: The Peace River Formation, Alberta, Canada, and the Castlegate Sandstone, Utah, U.S.A. Journal of Sedimentary Research 72:316–327.

Taylor, T. N., & Michael Krings. 2005. Fossil microorganisms and land plants: Associations and interactions. Symbiosis 40:119–135.

Taylor, T. N., E. L. Taylor, & Michael Krings. 2009. Paleobotany: The Biology and Evolution of Fossil Plants (Second Edition). Academic Press. Amsterdam. 1252 p.

Taylor, S. R., & S. M. McLennan. 1986. The chemical composition of the Archaean crust. *In* The Nature of the Lower Continental Crust. Geological Society Special Publications 24:173–178.

Tebbut, G. E., C. D. Conley, & D. W. Boyd. 1965. Lithogenesis of a distinctive carbonate rock fabric. Rocky Mountain Geology 4(1)1–13.

Teutsch, Nadya, Martin Schmid, Beat Müller, A. N. Halliday, Helmut Bürgmann, & Bernhard Wehrli. 2009. Large iron isotope fractionation at the oxic–anoxic boundary in Lake Nyos. Earth and Planetary Science Letters 285:52–60.

Thamdrup, Bo. 2000. Bacterial manganese and iron reduction in aquatic sediments. Advances in Microbial Ecology 16:41–84.

Thompson, J. B., & F. G. Ferris. 1990. Cyanobacterial precipitation of gypsum, calcite, and magnesite from natural alkaline lake water. Applied and Environmental Microbiology 62:1458–1460.

Thomas, Katherine, Stephan Herminghaus, Herbertus Porada, & Lucas Goehring. 2013. Formation of *Kinneyia* via shear-induced instabilities in microbial mats. Philosophical Transactions of the Royal Society

for Mathematical, Physical and Engineering Sciences 371:201–203.
Tice, M. M. 2008. Paleontology: Modern life in ancient mats. Nature 452:40–41.
Tice, M. M. 2009. Environmental controls on photosynthetic microbial mat distribution and morphogenesis on a 3.42 Ga clastic-starved platform. Astrobiology 9:989–1000.
Tice, M. M., & D. R. Lowe. 2004. Photosynthetic microbial mats in the 3,416-Myr-old ocean. Nature 431:549–552.
Tice, M. M., & D. R. Lowe. 2006. Hydrogen-based carbon fixation in the earliest known photosynthetic organisms. Geology 34:37–40.
Tice, M. M., D. C. O. Thornton, M. C. Pope, T. D. Olszewski, & Jian Gong. 2011. Archean microbial mat communities. Annual Review of Earth and Planetary Sciences 39:297–319.
Tice, M. M., Kimbra Quezergue, & M. C. Pope. 2017. Microbialite Biosignature Analysis by Mesoscale X-ray Fluorescence (μXRF) Mapping. Astrobiology 17:1161–1172.
Timofeev, B. V., T. N. Hermann, & N. S. Mikhailova. 1976. Microphytofossils of the Precambrian, Cambrian and Ordovician. Nauka. Leningrad. 106 p.
Tomitani, Akiko, A. H. Knoll, C. M. Cavanaugh, & Terufumi Ohno. 2006. The evolutionary diversification of cyanobacteria: Molecular–phylogenetic and paleontological perspectives. Proceedings of the National Academy of Sciences, USA 103:5442–5447.
Toner, B. M., C. M. Santelli, M. A. Marcus, R. Smith, C. S. Chan, T. McCollom, Wolfgang Bach, & K. J. Edwards. 2009. Biogenic iron oxyhydroxide formation at mid-ocean ridge hydrothermal vents; Juan de Fuca Ridge. Geochimica et Cosmochimica Acta 73:388–403.
Toomey, D. F., & J. M. Cys. 1979. Community succession in small bioherms of algae and sponges in the Lower Permian of New Mexico. Lethaia (12):65–74.
Toporski, J. K. W., Andrew Steele, Frances Westall, K. L. Thomas-Keprta, & D. S. McKay. 2002. The simulated silicification of bacteria: New clues to the modes and timing of bacterial preservation and implications for the search for extraterrestrial microfossils. Astrobiology 2:1–26.
Trendall, A. F. 1968. Three great basins of Precambrian banded iron formation deposition: A systematic comparison. Geological Society of America Bulletin 79:1527–1544.
Trendall, A. F. 2002. The significance of iron-formation in the Precambrian stratigraphic record. Special Publication International Association of Sedimentologists 33:33–66.
Trendall, A. F., & J. G. Blockley. 1970. The iron formations of the Precambrian Hamersley group, Western Australia; with special reference to the crocidolite. Bulletin, Geological Survey of Western Australia 119:1–366.
Trendall, A. F., W. Compston, D. R. Nelson, J. R. De Laeter, & V. C. Bennett. 2004. SHRIMP zircon ages constraining the depositional chronology of the Hamersley Group, Western Australia. Australian Journal of Earth Sciences 51:621–644.
Trevisan, Vittore. 1842. Prospetto della Flora Euganea. Coi Tipi Del Seminario. Padova. 68 p.
Trevisan, Vittore. 1887. Sul micrococco della rabbia e sulla possibilita di riconoscere durante il periode d'incubazione, dall'essame del sangue della persona moricata, se ha contratta l'infezione rabbica. Rendiconti Istituto Lombardo (Series 2) 20:88–105.
Trevors, J. T. 2011. Hypothesized origin of microbial life in a prebiotic gel and the transition to a living biofilm and microbial mats. Comptes Rendus Biologies 334(4):269–272.
Trewin, N. H. 1996. The Rhynie cherts: An early Devonian ecosystem preserved by hydrothemal activity: Ciba Foundation Symposium [doi. 10.1002/9780470514986.ch8].
Trewin, N. H., S. R. Fayers, & Ruth Kelman. 2003. Subaqueous silicification of the contents of small ponds in an Early Devonian hot-spring complex, Rhynie, Scotland. Canadian Journal of Earth Sciences 40:1697–1712.
Trompette, R., C. J. S. Alvarenga, & D.de Walde. 1998. Geological evolution of the Neoproterozoic Corumbá graben system (Brazil): Depositional context of the stratified Fe and Mn ores of the Jacadigo Group. Journal of South American Earth Sciences 11:587–597.
Trouwborst, R. E., Anne Johnston, Gretchen Koch, G. W. Luther, & B. K. Pierson. 2007. Biogeochemistry of Fe(II) oxidation in a photosynthetic microbial mat: Implications for Precambrian Fe(II) oxidation. Geochimica et Cosmochimica Acta 71:4629–4643.
Trower, E. J., & D. R. Lowe. 2016. Sedimentology of the ~3.3 Ga upper Mendon Formation, Barberton Greenstone Belt, South Africa. Precambrian Research 281:473–494.
Tsikos, Harilaos, Alan Matthews, Yigal Erel, & J. M. Moore. 2010. Iron isotopes constrain biogeochemical redox cycling of iron and manganese in a Palaeoproterozoic stratified basin. Earth and Planetary Science Letters 298:125–134.
Tuchman, T. L., & R .J. Stevenson. 1980. Comparison of clay tile, sterilized rock, and natural substrate diatom communities in a small stream in Southeastern Michigan, USA. Hydrobiologia 75:73–79.
Tunnicliffe, Verena, & A. R. Fontaine. 1987. Faunal composition and organic surface encrustations at hydrothermal vents on the southern Juan de Fuca Ridge. Journal of Geophysical Research 92:11303–11314.
Turner, E. C., N. P. James, & G. M. Narbonne. 2000. Taphonomic control on microstructure in Early Neoproterozoic reefal stromatolites and thrombolites. Palaios (15):87–111.
Turner, E. C., & B. Jones. 2005. Microscopic calcite dendrites in cold-water tufa: Implications for nucleation of micrite and cement. Sedimentology 52:1043–1066. <
Turner, E. C., G. M. Narbonne, & N. P. James. 1993. Neoproterozoic reef microstructures from the Little Dal Group, northwestern Canada. Geology 21: 259–262.
Tyler, S. A., & E. S. Barghoorn. 1954. Occurrence of structurally preserved plants in pre-Cambrian rocks

of the Canadian Shield. Science 119(3096):606–608.
Tyler, S. A., & E. S. Barghoorn. 1963. Ambient pyrite grains in Precambrian cherts. American Journal of Science 261:424–432.
Uyeda, J. C., L. J. Harmon, & C. E. A. Blank. 2016. A comprehensive study of cyanobacterial morphological and ecological evolutionary dynamics through deep geologic time. PLOS One 11:e0162539. [doi.10.1371/journal.pone.0162539].
Vai, G. B., & F. R. Lucchi. 1977. Algal crusts, autochthonous and clastic gypsum in a cannibalistic evaporite basin: a case history from the Messinian of Northern Apennines. Sedimentology 24:211–244.
Van den Ende, F. P., & Hans van Gemerden. 1993. Sulfide oxidation under oxygen limitation by a *Thiobacillus thioparus* isolated from a marine microbial mat. FEMS Microbiology Ecology 19:141–151.
Van den Ende, F. P., A. M. Laverman, & Hans van Gemerden. 1996. Coexistence of aerobic chemotrophic and anaerobic phototrophic sulfur bacteria under oxygen limitation. FEMS Microbiology Ecology 19:141–151.
Van den Ende, F. P., Jutta Meier, & Hans van Gemerden. 1997. Syntrophic growth of sulfate-reducing bacteria and colorless sulfur bacteria during oxygen limitation. FEMS Microbiology Ecology 23(1):65–80.
Van der Meer, M. T., Stefan Schouten, M. M. Bateson, Ulrich Nübel, Andrea Wieland, Michael Kühl, J. W. de Leeuw, J. S. Sinninghe Damsté, & D. M. Ward. 2005. Diel variations in carbon metabolism by green nonsulfur-like bacteria in alkaline siliceous hot spring microbial mats from Yellowstone National Park. Applied and Environmental Microbiology 71(7):3978–3986.
Van Houten, F. B. 1985. Oolitic ironstones and contrasting Ordovician and Jurassic paleogeography. Geology 13:722–724.
Van Houten, F. B., & M. A. Arthur. 1989. Temporal patterns among Phanerozoic oolitic ironstones and oceanic anoxia. Geological Society Special Publication 46:33–49.
Van Kranendonk, M. J. 2006. Volcanic degassing, hydrothermal circulation and the flourishing of early life on Earth: A review of the evidence from c. 3490–3240 Ma rocks of the Pilbara Supergroup, Pilbara Craton, Western Australia. Earth-Science Reviews 74:197–240.
Van Kranendonk, M. J., G. E. Webb, & B. S. Kamber. 2003. Geological and trace element evidence for a marine sedimentary environment of deposition and biogenicity of 3.45 Ga stromatolitic carbonates in the Pilbara Craton, and support for a reducing Archaean ocean. Geobiology 1:91–108.
Vargas, M. M., Kazem Kashefi, E. L. Blunt-Harris, & D. R. Lovley. 1998. Microbiological evidence for Fe(III) reduction on early Earth. Nature 395:65–67.
Varin, Thibault, Connie Lovejoy, A. D. Jungblut, W. F. Vincent, & Jacques Corbeil. 2011. Metagenomic analysis of stress genes in microbial mat communities from Antarctica and the high Arctic. Applied and Environmental Microbiology 78(2):549–559.
Vasconcelos, Crisógono, Rolf Warthmann, J. A. McKenzie, P. T. Visscher, A. G. Bittermann, & Yvonne van Lith. 2006. Lithifying microbial mats in Lagoa Vermelha, Brazil: Modern Precambrian relics? Sedimentary Geology 185(3–4):175–183.
Veizer, J. 1976. Evolution of ores of sedimentary affiliation through geologic history: Relations to the general tendencies in evolution of the crust, hydrosphere, atmosphere, and biosphere. *In* K. H. Wolf, ed., Handbook of Strata-bound and Stratiform Ore Deposits. Elsevier. Amsterdam. 3:1–41.
Veizer, J. 1983. Geologic evolution of the Archean-early Proterozoic earth. *In* J. W. Schopf, ed., Earth's Earliest Biosphere: Its Origin and Evolution. Princeton University Press. Princeton. p. 240–259.
Vert, Michel, Yoshiharu Doi, K. H. Hellwich, Michael Hess, Philip Hodge, Przemyslaw Kubisa, Marguerite Rinaudo, & François Schué. 2012. Terminology for biorelated polymers and applications (IUPAC Recommendations). Pure and Applied Chemistry. 84:377–410.
Vidal, Gonzalo. 1976. Late Precambrian microfossils from the Visingso beds in southern Sweden. Fossils and Strata 9:1–57.
Vidal, Gonzalo. 1981. Micropalaeontology and biostratigraphy of the upper Proterozoic and Lower Cambrian sequences in East Finnmark, northern Norway. Norges Geologiske Undersokelse Bulletin 362:1–53.
Vinther, Jakob. 2015. Fossil melanosomes or bacteria? A wealth of findings favours melanosomes. BioEssays 38:220–225.
Visscher, P. T., L. K. Baumgartner, D. H. Buckley, D. R. Rogers, M. E. Hogan, C. D. Raleigh, K. A. Turk, & D. J. Des Marais. 2003. Dimethyl sulfide and methanethiol formation in microbial mats: Potential pathways for biogenic signatures. Environmental Microbiology 5:296–308.
Visscher, P. T., Jan Beukema, & Hans van Gemerden. 1991. In situ characterization of sediments: Measurements of oxygen and sulfide profiles with a novel combined needle electrode. Limnology and Oceanography 36:1476–1480.
Visscher, P. T., Christophe Dupraz, Olivier Braissant, K. L. Gallagher, Christina Glunk, Lilliam Casillas-Martinez, & R. E. S. Reed. 2010. Biogeochemistry of carbon cycling in hypersaline mats: Linking the present to the past through biosignatures. *In* Josef Seckbach & Aharon Oren, eds., Cellular Origin, Life in Extreme Habitats and Astrobiology. Vol. 14. Microbial Mats. Springer-Verlag. Berlin. p. 443–468.
Visscher, P. T., F. P. van den Ende, B. E. M. Schaub, & Hans van Gemerden. 1992. Competition between anoxygenic phototrophic bacteria and colorless sulfur bacteria in a microbial mat. FEMS Microbiology Ecology 101:51–58.
Visscher P. T., K. L. Gallagher, Anthony Bouton, M. E. Farias, Daniel Kurth, B. P. Burns, M. R. Walter, Maria Sancho-Tomas, Pascal Philippot, Andrea Somogyi, Khadda Medjoubi, Emmanuelle Vennin, Raphael Bourillot, Marco Contreras, & Christophe Dupraz. 2020. Modern arsenotrophic microbial mats provide an analogue for life in the anoxic Archean. Nature Communications Earth & Environment 1:24 [doi.10.1038/s43247-020-00025-2].
Visscher, P. T., & Hans van Gemerden. 1991. Produc-

tion and consumption of dimethyl-sulfoniopropionate in marine microbial mats. Applied and Environmental Microbiology 57:3237–3242.

Visscher P. T., & H. van Gemerden. 1993. Sulfur cycling in laminated marine microbial ecosystems. *In* R. S. Oremland, ed., Biogeochemistry of Global Change. Springer. Boston. p. 672–690.

Visscher, P. T., & R. P. Kiene. 1994. Production and consumption of volatile organosulfur compounds in microbial mats. *In* L. J. Stal & Pierre Caumette, eds., Microbial Mats: Structure, Development and Environmental significance. Springer-Verlag. Berlin. p. 279–284.

Visscher, P. T., R. A. Prins, & Hans van Gemerden. 1992. Rates of sulfate reduction and thiosulfate consumption in a marine micrsobial mat. FEMS Microbiology Ecology 86:283–294.

Visscher, P. T., R. P. Reid, & B. M. Bebout. 2000. Microscale observation of sulfate reduction: Evidence of microbial activity forming lithified micritic laminae in modern marine stromatolites. Geology 28(10):919–922.

Visscher, P. T., R. P. Reid, B. M. Bebout, S. E. Hoeft, I. G. Macintyre, & J. A. Thompson, Jr. 1998. Formation of lithified micritic laminae in modern marine stromatolites (Bahamas): The role of sulfur cycling. American Mineralogist 83:1482–1494.

Visscher, P. T., & J. F. Stolz. 2005. Microbial mats as bioreactors: Populations, processes, and products. Paleogeography, Paleoclimatology, Paleoecology 219:87–100.

Visscher, P. T., T. M. Surgeon, S. E. Hoeft, B. M. Bebout, J. A. Thompson Jr., & R. P. Reid. 2002. Microelectrode studies in modern marine stromatolites: unraveling the Earth's past? *In* Martial Taillefert & T. Rozan, eds., Environmental Electrochemistry: Analyses of Trace Element Biogeochemistry. American Chemical Society Symposium Series 811. Oxford University Press. New York. p. 265–282.

Visscher, P. T., & B. F. Taylor. 1993. Organic thiols as organolithotrophic substrates for phototrophic bacteria. Applied and Environmental Microbiology 59:93–96.

Visscher, P. T., B. F. Taylor, & R. P. Kiene. 1995. Microbial consumption of dimethyl sulfide and methanethiol in coastal marine sediments. FEMS Microbiology Ecology 18:145–154.

Vlamakis, Hera, Claudio Aguilar, Richard Losick, & Roberto Kolter. 2008. Control of cell fate by the formation of an architecturally complex bacterial community. Genes & Development 22(7):945–953.

Vogt, Christian, Andreas Rabenstein, Jorg Rethmeier, & Ulrich Fischer. 1998. Alkali-labile precursors of dimethyl sulfide in marine benthic cyanobacteria. Archives of Microbiology 169:263–266.

Vologdin, A. G. 1932. Arkehotsiaty Sibiri, II. [The Archaeocyathinae of Siberia, Vol. 2]. State Science Technical Publishing. Moscow & Leningrad. 106 p. In Russian.

Vologdin, A.G., 1962. Drevneishie vodorosli SSSR [The oldest algae of the USSR]. Academy of Sciences of the USSR. Moscow. 116 p. In Russian.

Wacey, David, Kate Eiloart, & Martin Saunders. 2019. Comparative multi-scale analysis of filamentous microfossils from the c. 850 Ma Bitter Springs Group and filaments from the c. 3460 Ma Apex chert. Journal of the Geological Society of London 176:1247–1260.

Wacey, David, M. R. Kilburn, Nicola McLoughlin, John Parnell, C. A. Stoakes, C. R. Grovenor, & M. D. Brasier. 2008. Use of NanoSIMS in the search for early life on Earth: ambient inclusion trails in a c. 3400 Ma sandstone. Journal of the Geological Society of London 165:43–53.

Waggoner, B. M. 1994. An aquatic microfossil assemblage from Cenomanian amber of France. Lethaia 27:77–84.

Waksman, S. A., & A. T. Henrici. 1943. The nomenclature and classification of the actinomycetes. Journal of Bacteriology 46:337–341.

Walcott, C. D. 1914. Cambrian Geology and Paleontology III: Pre-Cambrian Algonkian Algal Flora. Smithsonian Miscellaneous Collections 64 (2):77–156.

Walcott, C. D. 1915. Discovery of Algonkian bacteria. Proceedings of the National Academy of Sciences, USA 1:256–257.

Walcott, C. D. 1919. Cambrian Geology and Paleontology IV: Middle Cambrian algae. Smithsonian Miscellaneous Collections 67:217–260.

Waldbauer, J. R., L. S. Sherman, D. Y. Sumner, & R. E. Summons. 2009. Late Archean molecular fossils from the Transvaal Supergroup record the antiquity of microbial diversity and aerobiosis. Precambrian-Research 169:28–47.

Walker, J. C. G. 1984. Suboxic diagenesis in banded iron formations. Nature 309:340–342.

Wallace, M. W., R. R. Keays, & V. A. Gostin.1991. Stromatolitic iron oxides: Evidence that sea-level changes can cause sedimentary iridium anomalies. Geology (19):551–554.

Walsh, M. M. 1992. Microfossils and possible microfossils from the Early Archean Onverwacht Group, Barberton Mountain Land, South Africa. Precambrian Research 54:271–293.

Walsh, M. M., & D. R. Lowe. 1999. Modes of accumulation of carbonaceous matter in the early Archean: A petrographic and geochemical study of the carbonaceous cherts of the Swaziland Supergroup. Geological Society of America Special Papers 329:115–132.

Walter, M. R., ed. 1976. Stromatolites: Developments in Sedimentology. Vol. 20. Elsevier. Amsterdam. 790 p.

Walter, M. R., & S. M. Awramik. 1979. Frutexites from stromatolites of the Gunflint Iron Formation of Canada, and its biological affinities. Precambrian Research 9(1–20):23–33.

Walter, M. R., John Bauld, & T. D. Brock. 1972, Siliceous algal and bacterial stromatolites in hot spring and geyser effluents of Yellowstone National Park. Science 178:402–405.

Walter, M. R., John Bauld, & T. D. Brock. 1976. Microbiology and morphogenesis of columnar stromatolites (Conophyton, Vacerrilla) from Hot Springs in Yellowstone National Park. *In* M. R. Walter, ed., Stromatolites: Develoments in Sedimentology. Vol. 20. Elsevier. Amsterdam. p. 273–310.

Walter, M. R., R. Buick, & J. S. R. Dunlop. 1980. Stromatolites 3,400–3,500 Myr old from the North

Pole area, Western Australia. Nature 284:443–445.
Walter, M. R., John Bauld, D. J. Des Marais, & J. W. Schopf. 1992. A general comparison of microbial mats and microbial stromatolites: Bridging the gap between the modern and the fossil. *In* J. W. Schopf & C. Klein, eds., The Proterozoic Biosphere. Cambridge University Press. Cambridge, UK. p. 335–338.
Walter, M. R., & G. R Heys. 1985. Links between the rise of the Metazoa and the decline of stromatolites. Precambrian Research 29:14–174.
Walter, M. R., & H. J. Hoffman. 1983. The palaeontology and palaeoecology of Precambrian iron-formations. *In* A. F. Trendall & R. C. Morris, eds., Iron-Formation: Facts and Problems. Elsevier. Amsterdam. p. 373–400.
Walter, X. A., Antonio Picazo, R. M. Miracle, Eduardo Vicente, Antonio Camacho, Michel Aragno, & Jakob Zopfi. 2009. Anaerobic microbial iron oxidation in an iron-meromictic lake. Geochimica et Cosmochimica Acta 73(Supplement 1):A1405.
Wang, Jiasheng, Ganqing Jiang, Shuhai Xiao, Qing Li, & Qing Wei. 2008. Carbon isotope evidence for widespread methane seeps in the ~635 Ma Doushantuo cap carbonate in South China. Geology 36:347–350.
Wang, Yangeng, Gongzheng Yin, Shufang Zheng, Shourong Qin, Shuncai Zhu, Yulin Chen, Qiling Luo, Shixing Zhu, Fuxing Wang, Yi Qian. 1984. The Upper Precambrian and Sinian-Cambrian Boundary in Guizhou. The People's Publishing House of Guizhou. Guiyang. 170 p.
Ward, D. M., M. J. Ferris, S. C. Nold, & M. M. Bateson. 1998. A natural view of microbial biodiversity within hot spring cyanobacterial mat communities. Applied and Environmental Microbiology 62(4):1353–1370.
Warren, John. 1999. Evaporites: Their Evolution and Economics. Blackwell Science. Philadelphia. 483 p.
Watanabe, Yumiko, J. E. J. Martini, & Hiroshi Ohmoto. 2000. Geochemical evidence for terrestrial ecosystems 2.6 billion years ago. Nature 408 (6812):574–578.
Waters, C. M., & B. L. Bassler. 2005. Quorum sensing: Cell-to-cell communication in bacteria: Annual Review of Cell and Developmental Biology 21:319–346.
Webb, G. E. 2002. Latest Devonian and Early Carboniferous reefs: Depressed reef building after the Middle Paleozoic collapse. *In* Wolfgang Kiessling, Erik Flügel, & Jan Golonka., eds., Phanerozoic Reef Patterns. Society for Sedimentary Geology, Special Publication 72. Tulsa. p. 239–269.
Webb, J. A., & E. Spence. 2008. Glaciomarine Early Permian strata at Bacchus Marsh, central Victoria: The final phase of Late Palaeozoic glaciation in southern Australia. Proceedings of the Royal Society of Victoria 120:373–388.
Weed, W. H. 1889. On the formation of siliceous sinter by the vegetation of thermal springs. American Journal of Science (1880–1910) (37):351.
Weidman, Samuel. 1904. The Baraboo iron-bearing district of Wisconsin. Wisconsin Geological and Natural History Survey Bulletin 13:1–190.
Weiner, Steve, & P. M. Dove. 2003. An overview of biomineralization processes and the problem of the vital effect. Biomineralization, Reviews in Mineralogy and Geochemistry (54):1–29.
Wellman, C. H., & P. K. Strother. 2015. The terrestrial biota prior to the origin of land plants (embryophytes): A review of the evidence. Palaeontology 58:601–627.
Welsh, D. T., Y. E. Lindsay, Pierre Caumette, R. A. Herbert, & J. Hannan. 1996. Identification of trehalose and glycine betaine as compatible solutes in the moderately halophilic sulfate reducing bacterium *Desulfovibrio halophilus.* FEMS Microbiology Letters 140:203–207.
West, S. A., & G. A. Cooper. 2016. Division of labour in microorganisms: An evolutionary perspective. Nature Reviews Microbiology 14(11):716–723.
Westall, Frances, Laurita Boni, & Elisabetta Guerzoni. 1995. The experimental silicification of microorganisms. Palaeontology 38:495–528.
Westall, Frances, Barbara Cavalazzi, Laurence Lemelle, & Yves Marrocchi. 2011. Implications of in situ calcification for photosynthesis in a ~3.3 Ga-old microbial biofilm from the Barberton Greenstone Belt, South Africa. Earth and Planetary Science Letters 310:468–479.
Westall, Frances, C. E. J. De Ronde, Gordon Southam, Nathalie Grassineau, Maggy Colas, C. H. Cockell, & Helmut Lammer. 2006. Implications of a 3.472–3.333 Gyr-old subaerial microbial mat from the Barberton greenstone belt, South Africa for the UV environmental conditions on the early Earth. Philosophical Transactions of the Royal Society of London B (Biological Sciences) 361(1474):1857–1876.
Westall, Frances, M. J. De Witt, Jesse Dann, Sjerry Van Der Gaast, Cornel De Ronde, & Dane Gerneke. 2001. Early Archean fossil bacteria and biofilms in hydrothermally-influenced sediments from the Barberton Greenstone Belt, South Africa. Precambrian Research 106:93–116.
Westall, Frances, & R. L. Folk. 2003. Exogenous carbonaceous microstructures in Early Archaean cherts and BIFs from the Isua Greenstone Belt: implications for the search for life in ancient rocks. Precambrian Research 126:313–33.
Westall, Frances, Frederic Foucher, Nicolas Bost, Marylene Bertrand, Damien Loizea, J. L. Vago, Gerhard Kmine, Frederic Gaboyer, K. A. Campbell, J-G. Bréhéret, Pascale Gautret, & C. S. Cockell. 2015. Biosignatures on Mars: What, where, and how? Implications for the search for martian life. Astrobiology 15:998–1028.
Westall, Frances, & Y. Rince. 1994. Biofilms, microbial mats and microbe-particle interactions: Electron microscope observations from diatomaceous sediments.Sedimentology 41:147–162.
Westall, Frances, Andrew Steele, Jan Toporski, Maud Walsh, Carlton Allen, Sean Guidry, David McKay, Everett Gibson, & Henry Chafetz. 2000. Polymeric substances and biofilms as biomarkers in terrestrial materials: Implications for extraterrestrial samples. Journal of Geophysical Research, Planets 105(E10):24511–24527.

de Wet, C. C. B., & J. F. Hubert. 1989. The Scots Bay formation, Nova Scotia, Canada, a Jurassic carbonate lake with Silica-rich hydrothermal springs, Sedimentology (36):857–873.

Whalen, M. T., Jed Day, G. P. Eberli, & P. W. Homewood. 2002. Microbial carbonates as indicators of environmental change and biotic crises in carbonate systems: Examples from the Late Devonian, Alberta basin, Canada. Palaeogeography, Palaeoclimatology, Palaeoecology (181):127–151.

White, R. A. III, A. M. Chan, G. S. Gavelis, B. S. Leander, A. L. Brady, G. F. Slater, D. S. S. Lim, & C. A. Suttle. 2016. Metagenomic analysis suggests modern freshwater microbialites harbor a distinct core microbial community. Frontiers in Microbiology 6:1531 [doi.10.3389/fmicb.2015.01531].

White, R. A. III, P. T. Visscher, & B. P. Burns. 2021. Between a rock and a soft place: Viral role in stromatolite formation. Trends in Microbiology 29(3):204-213.

White, R. A. III, H. L. Wong, Rendy Ruvindy, B. A. Neilan, & B. P. Burns. 2018. Viral communities of Shark Bay modern stromatolites. Frontiers in Microbiology 9:1223 [doi.10.3389/fmicb.2018.01223].

Whitehouse, M. J., & C. M. Fedo. 2007. Microscale heterogeneity of Fe isotopes in >3.71 Ga banded iron formation from the Isua greenstone belt, southwest Greenland. Geology 35:719–722.

Whitman, W. B., D. C. Coleman, & W. J. Wiebe. 1998. Prokaryotes: The unseen majority. Proceedings of the National Academy of Sciences, USA 95:6578–6583.

Widdel, Friedrich, Sylvia Schnell, Silke Heising, Armin Ehrenreich, Bernhard Assmus, & Bernhard Schink. 1993. Ferrous iron oxidation by anoxygenic phototrophic bacteria. Nature 362:834–836.

Wieland, Andrea, Jacob Zopfi, M. Benthien, & Michael Kühl. 2005. Biogeochemistry of an iron-rich hypersaline microbial mat (Camargue, France). Microbial Ecology 49:34–49.

Wignal, P. B., D. P. G. Bond, S. E. Grasby, S. B. Pruss, & Jeffrey Peakall. 2020. Controls on the formation of microbially induced sedimentary structures and biotic recovery in the Lower Triassic of Arctic Canada. GSA Bulletin 132(5–6):918–930.

Wilby, P. R., & D. E. G. Briggs. 1997. Taxonomic trends in the resolution of detail preserved in fossil phosphatized soft tissues. Geobios, Memoire special No. 20:493–502.

Wilmeth, D. T., F. A. Corsetti, N. J. Beukes, S. M. Awramik, V. A. Petryshyn, J. R. Spear, & A. J. Celestian. 2019. Neoarchean (2.7 Ga) lacustrine stromatolite deposits in the Hartbeesfontein Basin, Ventersdorp Supergroup, South Africa: Implications for oxygen oases. Precambrian Research 320:291–302 .

Wilmeth, D. T., F. A. Corsetti, Nemanja Bisenic, S. Q. Dornbos, Tatsuo Oji, & Sersmaa Gonchigdorj. 2015. Punctuated growth of microbial cones within early Cambrian oncoids, Bayan Gol Formation, Western Mongolia. Palaios (30):836–845.

Wilmeth, D. T., S. Q. Dornbos, J. I. Isbell, & Andrew Czaja. 2014. Putative domal microbial structures in fluvial siliciclastic facies of the Mesoprotrozoic (1.09 Ga) Copper Harbor Conglomerate, Upper Peninsula of Michigan, USA. Geobiology 12:99–108.

Winogradsky, S. J. 1888. Ueber Eisenbacterien. Botanische Zeitschrift 46:261–270.

Winsborough, B. M., J. S. Seeler, Stjepko Golubic, R. L. Folk, & Bassett Maguire. 1994. Recent freshwater lacustrine stromatolites, stromatolitic mats and oncoids from northeastern Mexico. *In* Janine Bertrand-Sarfati & C. L. Monty, eds., Phanerozoic stromatolites II. Springer. Berlin. p. 71–100.

Winter, B. L., & L. P. Knauth. 1992. Stable isotope geochemistry of cherts and carbonates from the 2.0 Ga Gunflint Iron Formation: Implications for the depositional setting, and the effects of diagenesis and metamorphism. Precambrian Research 59:283–313.

Wong, H. L., A. Ahmed-Cox, & B. P. Burns. 2016. Molecular ecology of hypersaline microbial mats: current insights and new directions. Microorganisms 4(1):6 [doi.10.3390/microorganisms4010006].

Wong, H. L., D. Lee-Smith, P. T. Visscher, & B. P. Burns. 2015. Niche differentiation of bacterial communities at a millimeter scale in Shark Bay microbial mats. Nature Scientific Reports 5:15607 [doi.10.1038/srep15607].

Wong H. L., I. F. MacLeod, R. A. White III, P. T. Visscher, & B. P. Burns. 2020. Microbial dark matter filling the niche in hypersaline microbial mats. Microbiome 8:135 [doi.10.1186/s40168-020-00910-0].

Wong, H. L., R. A. White III, P. T. Visscher, J. C. Charlesworth, X. Vázquez-Campos, & B. P. Burns. 2018. Disentangling the drivers of functional complexity at the metagenomic level in Shark Bay microbial mat microbiomes, ISME Journal 12:2619–2639.

Woo, K. S., B. K. Khim, H. S. Yoon, & K. C. Lee. 2004. Cretaceous lacustrine stromatolites in the Gyeongsang Basin (Korea): Records of cyclic change in paleohydrological condition. Geosciences Journal 8:179–184.

Wood, Alan. 1957. The type-species of the genus *Girvanella* (calcareous algae). Palaeontology 1:22–28.

Wood, Rachel. 2000. Palaeoecology of a Late Devonian back reef: Canning Basin, Western Australia. Palaeontology (43):671–703.

Wood, T. K., S. J. Knabel, & B. W. Kwan. 2013. Bacterial Persister Cell Formation and Dormancy. Applied and Environmental Microbiology 79(23):7116.

Worden, R. H., Joshua Griffiths, L. J. Wooldridge, J. E. P. Utley, A. Y. Lawan, D. D. Muhammed, N. Simon, & P. J. Armitage. 2020. Chlorite in sandstones. Earth-Science Reviews 204:103–105.

Wright, V. P. 1983. Morphogenesis of Oncoids in the Lower Carboniferous Llanelly Formation of South Wales. *In* Tadeusz Peryt, ed., Coated Grains. Springer. Berlin. p. 424–434.

Wu, Lingling, R. P. Brucker, B. L. Beard, E. E. Roden, & C. M. Johnson. 2013. Iron isotope characteristics of hot springs at Chocolate Pots, Yellowstone National Park. Astrobiology 13:1091–1101.

Wu Lingling, E. M. Percak-Dennett, B. L. Beard, E. E. Roden, & C. M. Johnson. 2012. Stable iron isotope fractionation between aqueous Fe(II) and model Archean ocean Fe–Si coprecipitates and implications for iron isotope variations in the ancient rock record. Geochimica et Cosmochimica Acta 84:14–28.

Xiao, Shuhai, Natalia Bykova, Alex Kovalick, & B. C. Gill. 2017. Stable carbon isotopes of sedimentary kerogens and carbonaceous macrofossils from the Ediacaran Miaohe Member in South China: Implications for stratigraphic correlation and sources of sedimentary organic carbon. Precambrian Research 302:171–179.

Xiao, Shuhai, Zhe Chen, Chuanming Zhou, & Xunlai Yuan. 2019. Surfing in and on microbial mats: Oxygen-related behavior of a terminal Ediacaran bilaterian animal. Geology 47(11):1054–1058.

Xiao, Shuhai, & M. F. Hochella, Jr. 2017. Why and how do phosphatic minerals replicate soft tissues at the highest resolution? Geological Society of America Abstracts with Programs 49(6) [doi.10.1130/abs/2017AM-299804].

Xiao, Shuhai, & A. H. Knoll. 1999. Fossil preservation in the Neoproterozoic Doushantuo phosphorite Lagerstätte, South China. Lethaia 32:219–240.

Xiao, Shuhai, & J. D. Schiffbauer. 2009. Microfossil phosphatization and its astrobiological implications. *In* J. Seckbach, & M. Walsh, eds., From Fossils to Astrobiology. Springer-Verlag. New York. p. 89–117.

Xiao, Shuhai, & Qing Tang. 2018. After the boring billion and before the freezing millions: Evolutionary patterns and innovations in the Tonian Period. Emerging Topics in Life Sciences 2:161–171.

Xiao, Shuhai, Xunlai Yuan, Michael Steiner, & A. H. Knoll. 2002. Macroscopic carbonaceous compressions in a terminal Proterozoic shale: A systematic reassessment of the Miaohe biota, South China. Journal of Paleontology 76:347–376.

Xiao, Shuhai, Yun Zhang, & A. H. Knoll. 1998. Three-dimensional preservation of algae and animal embryos in a Neoproterozoic phosphorite. Nature 391:553–558.

Xiao, Shuhai, Chuanming Zhou, & Xunlai Yuan. 2007. Undressing and redressing Ediacaran embryos. Nature 446:9–10.

Xing, Yusheng, & Zhuizhi Liu. 1973. Sinian micropaleoflora in the Yan-Liao area and its geological significance. Acta Geologica Sinica 1973:1–31.

Xiong, Jin. 2006. Photosynthesis: What color was its origin? Genome Biology 7:245.

Yallop, M. L., Ben de Winder, D. M. Paterson, & L. J. Stal. 1994. Comparitive structure, primary production and biogenic stabilization of cohesive and non-cohesive marine sediments inhabited by microphytobenthos. Estuarine, Coastal and Shelf Science 39(6):565–582.

Yamaguchi, K.E., C. M. Johnson, B.L. Beard, & Hiroshi Ohmoto. 2005. Biogeochemical cycling of iron in the Archean-Paleoproterozoic Earth: Constraints from iron isotope variations in sedimentary rocks from the Kaapvaal and Pilbara Cratons. Chemical Geology 218:135–169.

Yang, X.-G., Jian Han, Xing Wang, J. D. Schiffbauer, Kentaro Uesugi, Osamu Sasaki, & Tsuyoshi Komiya. 2017. Euendoliths versus ambient inclusion trails from Early Cambrian Kuanchuanpu Formation, South China. Palaeogeography, Palaeoclimatology, Palaeoecology 476:147–157.

Yao, Jinxian, Shuhai Xiao, Leiming Yin, Guoxiang Li, & Xunlai Yuan. 2005. Basal Cambrian microfossils from the Yurtus and Xishanblaq formations (Tarim, north-west China): Systematic revision and biostratigraphic correlation of *Micrhystridium*-like acritarchs from China. Palaeontology 48:687–708.

Yee, Nathan, Vernon Phoenix, K. O. Konhauser, L. G. Benning, & F. G. Ferris. 2013. The effect of cyanobacteria on silica precipitation at neutral pH: Implications for bacterial silicification in geothermal hot springs. Chemical Geology 199:83–90.

Yuan, Xunlai, Shuhai Xiao, & T. N. Taylor. 2005. Lichen-like symbiosis 600 million years ago. Science 308:1017–1020.

Zalessky, M. D. 1917. O morekom sapropelit siluriiskago vozrasta, obrazovannom sinnezelenoyu vodoroslyu. [On marine sapropelite of Silurian age, formed by blue-green alga.] Izvestiya Imperatorskoi Akademii Nauky 1:3–18. In Russian.

Zavarzin, G. A. 1981. The Genus *Metallogenium*. *In* M. P. Starr, H. Stolp, H. G. Truper, A. Balows, & H. G. Schlegel, eds., The Prokaryotes: A Handbook on Habitats, Isolation, and Identification of Bacteria. Vol.1. Springer-Verlag. Berlin. p. 524–528.

Zegers, T. E., M. J. de Wit, J. Dann, & S. H. White. 1998. Vaalbara, Earth's oldest assembled continent? A combined structural, geochronological, and palaeomagnetic test. Terra Nova 10:250–259.

Zeyen, Nina, Karim Benzerara,Jinhua Li, Alexis Groleau, Etienne Balan, J. L. Robert, Imène Estève, Rosaluz Tavera, David Moreira & Purificación López-García. 2015. Formation of low-T hydrated silicates in modern microbialites from Mexico and implications for microbial fossilization. Frontiers in Microbiology 3:64 [doi.10.3389/feart.2015.00064].

Zhang, Xiaoqi, P. L. Bishop, & M. J. Kupferle. 1998. Measurement of polysaccharides and proteins in biofilm extracellular polymers. Water Science and Technology 37(4):345–348.

Zhang, Yun, & Stjepko Golubic. 1987. Endolithic microfossils (Cyanophyta) from early Proterozoic stromatolites, Hebei, China. Acta Micropalaeontologica Sinica 4:1–12.

Zhang, Yun, Leiming Yin, Shuhai Xiao, & A. H. Knoll. 1998. Permineralized fossils from the terminal Proterozoic Doushantuo Formation, South China. Journal of Paleontology 72 (supplement to No. 4):1–52.

Zhou, Xiqiang, Daizhao Chen, Dongjie Tang, Shaofeng Dong, Chuan Guo, Zenghui Guo, & Yanqiu Zhang. 2015. Biogenic iron-rich filaments in the quartz veins in the uppermost Ediacaran Qigebulake Formation, Aksu Area, northwestern Tarim Basin, China: Implications for iron oxidizers in subseafloor hydrothermal systems. Astrobiology 15:523–537.

Zhu, Tingting, & Maria Dittrich. 2016. Carbonate precipitation through microbial activities in natural environment, and their potential in biotechnology: A review. Frontiers in Bioengineering and Biotechnology 4:4 [doi.org/10.3389/fbioe.2016.00004].

ZoBell, C. E. 1943. The effect of solid surfaces upon bacterial activity. Journal of Bacteriology 46: 39–56.

INDEX

Below is a selective list of words and phrases used in the volume. Page numbers listed refer to key explanations or applications of the term.